The Measurement Of The Complexation Of Heavy Metals And Radionuclides With Natural Humic Substances

Eleanor Margaret Logan

Submitted For The Degree Of Doctor Of Philosophy

Department Of Environmental Chemistry
University Of Glasgow

October 1995

ProQuest LLC.
789 East Eisenhower Parkway
P.O. Box 1346
Ann Arbor, MI 48106 – 1346

"It requires great love of it deeply to read
The configuration of a land,
Gradually grow conscious of fine shadings,
Of great meanings in slight symbols....."

from "Scotland" by Hugh MacDiarmid

ACKNOWLEDGMENTS

As with any such work there are volumes of family, friends and colleagues to thank. I could not have undertaken the degree if it hadn't been for the love and support of my mother and sister and I certainly wouldn't have finished it without their belief in me.

Professional support and guidance was always on tap from my three supervisors, Ian Pulford, Gus Mackenzie, and Gordon Cook - many thanks for both and for not letting me give up!

At both Glasgow University and SURRC, technical support was invaluable. Well done Michael for not losing your temper too often and for keeping me supplied in pipettes, volumetric flasks, centrifuges, etc..... Thanks also go to Alison, Bob and Colin for all the counting undertaken and for assistance in the ins and outs of Gamma Spectroscopy and Neutron Activation Analysis. I am indebted to Dr Bob Hill for his guidance in interpreting infra-red spectra and to George for guidance in achieving readable spectra. The ion selective electrode work was made possible through the kind loan of a copper electrode from the Electrochemistry Department of Glasgow University, as well as advice on their usage. Thanks also go to Mr Gordon Caskie of South Drumboy Farm for allowing us access to his land for the field studies.

I wouldn't have started all of this if it hadn't been for Ian B. planting the seed - look how it grew! In getting there I appreciated all the moral support, advice and good times supplied by the following - Jackie, Gawen, Phil, Fiona, Elaine, Kenna, Alison S, Petra, Lesley, Ian, Juan and all the wardening staff at Dalrymple Hall and Horselethill House (1992-1994). Many thanks also go to Richard for all the proof reading, who never realised just how many commas I could insert in a sentence, and will probably never offer to help me ever again!

Lastly, the whole project would not have been possible without a research grant from the Natural Environment Research Council (reference number 4/91/AAPS/22).

SUMMARY OF THE WORK CARRIED OUT IN THIS THESIS

Ombrotrophic (rain-water fed) peat bogs have been used to study the contents and distributions of heavy metals and radionuclides. If these systems are dated, a chronology of atmospheric deposition can be assigned to the profiles. Humic substances are an integral, characteristic and substantial component of organic soils such as peats, and complexation of metals with these substances plays an integral role in the dynamics of their interactions in peat soils.

Studies on the complexation of metals to humic substances have centred around monitoring the interaction of metals with humic or fulvic acids. These are operationally-defined fractions which are extracted in order to reduce the heterogeneity of humic substances, and remove contaminants such as silicates or polysaccharide materials. The main problem with such an approach is the question of whether isolation of humic acid leads to chemical or structural changes which may invalidate any results from complexation studies. This question was addressed in this thesis by carrying out all analyses on both humic acid and unextracted peat. The results indicated that isolation of humic acid led to a change in the functional group content and reactivity as well as an increased capacity to bind with metals, as a result of chemical and structural changes. The effect of isolation of humic acid on the stability of interaction depended on the metal being studied, but still demonstrated a difference between unextracted peat and humic acid.

The binding of a range of elements with humic substances was studied, with particular emphasis on the difference in reactions between Cu^{2+}, Pb^{2+} and Cs^{+}. Qualitative studies on the nature of binding were carried out using infra-red analysis and highlighted how Cs^{+} binds through predominantly ionic-type linkages, whilst Pb^{2+} and Cu^{2+} show evidence of more covalent linkages. The stability of these interactions was investigated using three different methods: the Base Titration method, Scatchard analysis of titration data and based on this, an Incremental Addition Method. Each had its own set of limitations and advantages, and analysis of how accurately these methods quantify metal binding was carried out.

These studies on the nature and stability of metal binding to humic substances are laboratory based, questioning whether or not they reflect the interactions of metals in the environment. Field-based studies were also carried out, looking at the distributions and contents of metals and radionuclides in undisturbed peat cores under differing conditions. Interpretation of these data was carried out with the knowledge gained from the laboratory-based studies.

Peat cores were collected from a site to the south west of Glasgow on the Fenwick Moor. This site was chosen since it was affected by the Chernobyl accident, and previous studies had recorded significant levels of radiocaesium on the site. Accordingly, six cores were collected from the site, at different aspects and altitudes in order to investigate more fully the contamination of the site by Chernobyl-derived caesium. In addition, the effects of changes in geochemistry, water content and table, peat type, altitude and aspect on the distribution and content of radiocaesium, ^{210}Pb, Cu, Br, Pb, Mn, Fe, Ta, La, Hf, Sm, Sc, Se, Ce, Th, Hg, Sb, As & Co were investigated.

Where no redeposition of ^{210}Pb was observed the ^{210}Pb profiles were used to provide a chronology for the core, using the constant initial concentration model. Consequently, if no redeposition of the pollutant metals was observed, changes in the fluxes of these metals to the profile could then be dated. In addition, analysis of the changes in the $^{206}Pb/^{207}Pb$ ratios over time was carried out in order to attribute different sources to the total content of Pb within each core.

The results produced from the different studies all demonstrated the importance of humic substances on the behaviour of heavy metals and radionuclides in the environment, as well as the complexity of their interactions.

TABLE OF CONTENTS

INDEX OF FIGURES

INDEX OF TABLES

DECLARATION

Except where specific reference is made to other sources, the work presented in this thesis is the original work of the author. It has not been submitted, in part or in whole, for any other degree. Certain of the results have been published elsewhere.

Eleanor M Logan

October 1995

CHAPTER 1

THE AIMS OF AND BACKGROUND TO THE RESEARCH

1.1 INTRODUCTION TO THE MAIN OBJECTIVES AND AIMS OF THE RESEARCH

In studying the interaction of metals and radionuclides in organic soils, two main approaches can be adopted - namely laboratory-based studies where interactions are modelled on a microsite scale with purified materials, or field-based studies where interactions are studied on raw, unpurified materials. Both adopt quite separate stances, making quite different assumptions, and can ultimately often show quite different conclusions. One of the main aims of the research presented here was to use both approaches in the study of the interactions of caesium, copper and lead with humic substances and to investigate whether there was any parallel in the conclusions made. Of particular interest was the stability of their interactions and how this affected their mobility and consequently bioavailability in the environment.

The laboratory-based studies generally focus on the reactions between a metal or radionuclide with a purified, operational fraction of organic matter, such as humic acid. A variety of methods can be used to extract and fractionate the humic substances from the organic matter, which can also lead to ambiguity in the results obtained. The humic or fulvic acids are extracted from the organic matter in an effort to reduce the inherent heterogeneity of the materials, allowing the specific reaction between the metal and humic acid to be studied. However, to extract these fractions the organic matter is subjected to a rigorous and caustic extraction and fractionation procedure, involving strong alkali and concentrated acid. In many cases it is also subjected to further purificaton, as will be discussed further in the chapter. The effects of the extraction and fractionation procedures on the chemical nature of the organic matter has yet to be established conclusively, with conflicting results reported in the literature. Few studies have also focussed on the interaction of metals with unextracted, unpurified materials and how these differ to the purified extracts. Accordingly, little information has been gained on how the interactions between metals and organic matter varies with the extracted materials and the consequences on the conclusions on stability or nature of interaction. Thus, one of the main aims of the research was to investigate how the extraction and fractionation processes have affected the nature and reactivity of humic substances and their interactions with metals and radionuclides through carrying out all investigations on both humic acid and unextracted peat.

It has been suggested that organic soils such as peats be used to globally monitor the effects of atmospheric pollution, providing the peat is ombrotrophic. This is of course dependent on the pollutant materials being complexed by the organic matter and not subject to any post-depositional movement.

The study site chosen for the field-based studies had been significantly affected by the Chernobyl accident and therefore provided an ideal site for the investigation of the interactions of radiocaesium from both weapons testing fallout and Chernobyl in organic soils. Previous work has established that radiocaesium is inherently mobile in such systems and therefore one of the aims of the research was to investigate the nature of the mobility, with knowledge gained from the laboratory studies.

The potential mobility of Pb is of interest due to its prevalence in environmental systems to pollutant levels. Again conflicting results of Pb mobility are published in the literature, as also for Cu. Should Pb be mobile under certain conditions then this will potentially invalidate any ^{210}Pb dating, making it unwise to assign a chronology through this method.

In order to fully investigate the mobility of Pb, Cu and Cs a series of cores were extracted to allow the investigation of changes in topography and geochemistry on the behaviour of the elements.

1.2 SUMMARY OF THE AIMS OF RESEARCH

1. To investigate the effects of the extraction and fractionation process on the characteristics and interactions of humic substances.

2. To investigate the process of complexation of metals with humic substances and its effect on the bioavailability of the metals.

3. To investigate the capacity of unextracted and extracted humic substances to complex various metals, utilising different techniques.

4. To study the interaction of metals with humic substances in natural systems, with particular emphasis on their potential mobility and bioavailability, relating the results to knowledge gained from complexation studies.

5. To evaluate the validity of dating peat profiles with ^{210}Pb.

6. To study the impact of Chernobyl on the content and movement of radiocaesium in organic soils.

7. To potentially evaluate a chronology of past atmospheric deposition of metals within undisturbed peat cores.

1.3 THE ORIGIN OF HUMIC SUBSTANCES

The natural organic matter component of soils, sediments and waters is a dynamic system composed of live organisms and their undecomposed, partially decomposed and transformed remains. It is highly complex and can be subdivided into groups of species which have similar morphological or chemical characteristics. One such subdivision is the separation of humic from non humic substances:

(a) **Non-humic substances.**
These include the soil mineral matter, fresh animal and plant debris, and breakdown products of plant matter such as polysaccharides and proteins.

(b) **Humic substances.**
These are amorphous, polydisperse, polyelectrolytic, yellow to black coloured polymers which bear no resemblance to the soil components from which they are derived.

Humic substances are the most widely distributed natural products on the earth's surface, occurring in soils, rivers, lakes, sediments and the sea (Schnitzer & Khan, 1972) and comprise a significant proportion of the total organic carbon in the global carbon cycle. In addition, they have the capacity for diverse chemical and physical interactions in the environment (Horth *et al.*, 1988) and are often viewed as highly complex biopolymers. It is convenient to describe polymers in terms of primary, secondary and tertiary structures, e.g. in proteins, primary structure can be defined as the sequence of amino acids, the secondary structure the helical conformations that the chains form via intramolecular bonding, and the tertiary structure the folding of the macromolecule. By knowing these, it is possible to predict the behaviour of the polymer in different environments. This is not possible with humic substances since synthesis does not appear to be under any kind of control resulting in a highly irregular structure (Hayes, 1991).

Humic substances are considered to be formed from constituents in the soil by two main processes - degradation and synthesis. In degradation, organic macromolecules such as lignins, paraffins, waxes and polysaccharides are broken down biologically by the soil micro-organisms, to produce humic substances directly or building blocks for the second main process, synthesis. Synthetic processes involved include the Maillard reaction of reducing sugars and amino acids, and polymerisation and polycondensation reactions of quinones (Stevenson, 1982). The

predominant reaction which occurs, and the rate of this reaction, is controlled by the soil environment, and this can vary on a microsite basis. This, along with the heterogeneity of substrates, results in humic substances being highly heterogeneous and complex materials. Malcolm and McCarthy (1991) sum up this heterogeneity by stating that:

"*each humic component in each environment possesses an individuality that distinguishes it from other components in the same environment and from the same component in different environments.*"

1.4 STRUCTURAL INVESTIGATIONS

As yet no chemical or molecular structure for humic substances has been elucidated although many theories exist. Flaig *et al.* (1964) proposed that it was not possible to write a chemical structure for humic substances because such a structure would represent a temporary state only.

Degradation studies have been used extensively in an attempt to characterise the structural building blocks of humic substances. These studies showed that humic substances contain a variety of aromatic groupings including bound phenolic groupings, quinone structures, and COOH groups variously placed on aromatic rings. Many workers then concluded that humic substances consisted of an aromatic core with branches of aromatic and aliphatic groupings arranged and linked in various ways, often with nitrogen and oxygen ligands acting as bridge units (Stevenson, 1982).

One example of such a theory on structure came from electron spin resonance studies. Haworth (1971) concluded that humic acid contained or readily gave rise to a complex aromatic core responsible for the electron spin resonance signal and to which the following are attached chemically and physically:

(a) polysaccharides
(b) proteins
(c) simple phenols
(d) metals.

More recently Curie-point mass spectrometry was used to show that the structural network of humic substances consists of aromatic rings joined by long alkyl structures, through covalent bonds, to give a flexible network. The oxidative

degradation of the structure would produce the benzene carboxylic acids which have been isolated repeatedly as major oxidation products of humic acids (Schulten, 1991).

This **chemical network** theory is similar to that of Khan and Schnitzer (1971) who suggested that fulvic acid was composed of phenolic and benzene-carboxylic acids joined by hydrogen bonds to form a stable polymeric structure which can adsorb organic and inorganic compounds. The proposed structure also has voids or holes of different dimensions which can trap or fix molecules, and this was also a feature of the **chemical network** structure.

A slightly different theory was proposed by Wershaw *et al.* (1977) who suggested that humic substances are composed of a hierarchy of structural elements. The lowest level consists of simple phenolic, quinoid and benzene-carboxylic acid groups joined by covalent bonds onto smaller species with molecular weights of a few thousand or less. Groups of these species are linked together by weak covalent and non-covalent bonds into aggregates, with the degree of aggregation being controlled by the pH, the amount of metal ions present and the oxidation state of the system. Humic substances are then formed by mixtures of aggregates combining randomly, and these can then bind to the mineral matter to form larger aggregates within the soil.

Cross polarisation magic angle spinning ^{13}C nuclear magnetic resonance (CPMAS ^{13}C NMR) is now widely used to study humic substances and the spectra produced are highly resolved. One of the main advantages of the technique is that it is non-destructive unlike previous structural investigations which include highly degradative procedures. The most striking conclusion to result from these studies is that humic substances are highly aliphatic in composition.

Ikan *et al.*. (1992) used a combination of methods including ^{13}C NMR and concluded that humic substances were composed of various heterocyclic components as building blocks rather than the aromatic benzenoid structures as previously proposed.

This clearly contrasts with the conclusion from the degradative studies that most humic substances were predominantly aromatic in composition, indicating that the degradative studies were chemically changing the materials. This conclusion can be supported by studies on the hydrolysis of humic substances in 6M HCl, which results in losses of mass amounting to as much as 40-50% of the starting material. The non-hydrolysable residues then give high values for aromaticity (Hayes, 1991).

Current research is leading to many advances in structural investigations of humic substances, although a definite structure for these materials will probably never be attained due to their heterogeneous nature. However, it is not necessary to know the structure of humic substances when studying their dynamics and interactions with

pollutants. It is more important to understand and characterise their behaviour and properties.

1.5 THE EXTRACTION AND FRACTIONATION OF HUMIC SUBSTANCES

Due to the heterogeneity of humic substances and the complexity of the organic matter with which they are associated, it is desirable firstly to extract the humic substances from the organic matter, and then fractionate them into less heterogeneous components. This then provides a more suitable starting material for studies of structure, composition and metal binding.

1.5.1 EXTRACTION

The extraction step is concerned with removing the humic substances from the other components of the soil organic matter e.g. polysaccharides and proteins as well as the mineral matter. Humic substances are bound in the soil in the following ways:

1. As insoluble macromolecular complexes

2. As macromolecular complexes bound together by polyvalent cations, such as Ca^{2+}, Fe^{3+}, and Al^{3+}

3. Bound to clay minerals and sesquioxides through bridging by polyvalent cations, hydrogen bonding, and Van Der Waals forces.

The extractant must interfere with the binding mechanisms to release the humic substances and the ideal extraction method would satisfy the following objectives:

(a) The isolation of unaltered material

(b) The extraction of humic substances free of contaminants such as silicates and polysaccharides

(c) A complete extraction

(d) A method universally applicable to all soils.

(Stevenson, 1982).

However, these objectives are not met by any of the current extraction methods. The most commonly used method of extraction is alkali extraction using sodium hydroxide (NaOH) or sodium carbonate (Na_2CO_3) solutions of 0.1 to 0.5M and a soil to solution ratio of 1:2 to 1:5 (g ml^{-1}). NaOH was the first extractant used in the attempt to isolate humic substances from soil (Aiken *et al.*, 1985). The alkali is

effective in removing the humic substances from the soil since raising the pH results in the acidic groupings becoming ionised causing repulsion of charges and an opening up of the structure. The dissociated sites can then be readily solvated. But alkali extraction has associated problems:

(a) Alkali solutions dissolve silica from the mineral matter

(b) Alkali solutions also dissolve protoplasmic and structural components from organic tissues which can become fixed on humic substances

(c) In alkaline conditions autoxidation of some organic constituents can occur in contact with air

(d) Chemical changes can also occur in alkaline solutions, such as condensation between amino acids and the carbonyl groups of aromatic aldehydes or quinones to form humic type compounds

(e) Carbohydrates and proteins may be covalently bound to the humic substances and therefore difficult to remove.

(Stevenson, 1982).

To alleviate the problems of autoxidation extraction of humic materials with NaOH under a nitrogen atmosphere was proposed (Choudri & Stevenson, 1957). Swift and Posner (1972) confirmed that autoxidation of extracted humic acid can occur under alkaline conditions and showed that under nitrogen the effect was markedly reduced. However, recently a comparative study between NaOH extraction in air and a nitrogen atmosphere produced only small differences in composition and spectral characteristics of the humic compounds and failed to show that extraction in an inert atmosphere was superior to extraction in air (Tan *et al.*, 1991). In order to standardise the extraction procedure the International Humic Substances Society (IHSS), recommend that humic substances from the soil be extracted using 0.1M NaOH under nitrogen and can provide reference materials extracted with the recommended procedure.

Investigations on the alkaline extraction method have given conflicting conclusions as to whether or not the humic substances are altered.

Chemical, spectroscopic and gel filtration studies have previously failed to provide evidence that extraction with alkali causes modification of the organic matter (Schnitzer & Skinner, 1968), and more recently solid state ^{13}C NMR studies have shown no significant change in the distribution of functional groups after chemical treatment with acid or base (Krosshavn, 1992). In a similar study Alberts *et al.* (1992) isolated humic and fulvic acids from bulk humic substances using NaOH extraction followed by purification with XAD resin, and showed that the materials produced

were similar to each other in elemental composition, FTIR and ^{13}C NMR spectra, as well as copper-binding capacities.

However, differences have been seen between alkali-extracted material and resin-extracted material when they were oxidised with alkaline permanganate after methylation. The alkali-extracted humic acid was less condensed and degraded than the resin-extracted humic acid, yet as observed in the above studies the functional group and spectroscopic analyses were similar. The alkaline extraction process has also been shown to lead to increases in molecular complexity and can increase the amount of aromatic groupings in the extracted material (Campanella & Thomasseti, 1990). Gregor and Powell (1987) also reported changes in the physical properties of humic substances after alkali extraction as well as increasing the ability to form stable complexes with copper.

This conflicting evidence could be due to the different sources of the humic substances and differing reaction times in alkali. The incorporation of a standard method of extraction and reference materials from the IHSS in all analyses may result in this ambiguity being reduced.

Since amide groups and some amino groups are labile in alkaline solutions, extraction can result in losses of nitrogen. The ammonia which is liberated in this process can react with other components, particularly quinones at high pH, to give artefacts (Parsons, 1988). In an attempt to stop degradation of structure and the formation of artefacts on extraction, some milder extractants have been used as an alternative to the classical extraction with strong alkali. Sodium pyrophosphate at pH 7 and pH 10 has been used to extract humic substances (Swift & Posner, 1972). At pH 7, the oxidative effects of the alkali are reduced and the bridging cations are complexed by the pyrophosphate allowing the acidic groups to become ionised and expand and solvate.

Other extractants include EDTA, acetylacetone, and various organic solvents. These may cause less alteration of the organic material but are conversely less effective, producing lower yields of material which are less representative of the organic matter (Stevenson, 1982). Marley *et al.* (1992) used ultrafiltration to separate out aquatic humic substances on the basis of molecular weight and proposed that this method can be used to give a milder extraction process which can extract a sufficient amount of material.

Pre-extraction treatments can also be used to increase effectiveness e.g. organic solvents can be used to remove waxy materials and mineral acids can remove carbonates, silicates and cations (Hayes & Swift, 1978). HCl/HF mixtures can be used

to remove carbonates, silicates and adsorbed materials but can result in weight losses and chemical changes (Stevenson, 1982).

It may be necessary to alter the extraction procedure depending on the study being carried out, as in some studies chemical changes will be less desirable than others. A sequence of extractants may also be used to give a more complete and effective extraction.

1.5.2 FRACTIONATION AND PURIFICATION

Extracted humic substances are still highly heterogeneous and it is often desirable to further reduce this through fractionation into groups of substances with similar characteristics or properties. This can help purification and characterisation, although it is often necessary to further purify the samples to remove contaminants such as proteins. A wide range of techniques exist for fractionation and purification and these generally exploit differences in solubility, adsorption behaviour, molecular weight or charge characteristics.

1.5.2.1 FRACTIONATION AND PURIFICATION OF HUMIC SUBSTANCES BASED ON SOLUBILITY DIFFERENCES

The earliest and most commonly used method of fractionation of humic substances is based on the difference in acid solubility of the alkali-extracted material. The procedure gives rise to three main fractions, fulvic acids, which are soluble in alkali and acid, humic acids which are soluble in alkali but insoluble in acid and humin, which is insoluble in acid and alkali (Figure 1.1). The same nomenclature is often used even when neutral salts or organic solvents replace the alkali.

Humic acid is usually precipitated at pH 1, but the pH can be manipulated in order to decrease the effects of the acidic conditions on the extracted material. Flaig *et al.* (1975) used pH values of 1.5 or 2.

The fractionation procedure can result in contamination in particular fractions. The fulvic acid fraction is often contaminated with polysaccharide material or other low molecular weight organic substances, whereas the humic acid fraction is more commonly contaminated by lignified materials (Hayes & Swift, 1978). Humic extracts from mineral soils are generally contaminated with silicates and salts. The salts can be removed by dialysis whereas the silicates are often removed by further treatment with HF or HF-HCl mixtures which may result in some chemical modifications of the humic substances (Mortensen & Schendinger, 1963).

The removal of polysaccharide material by hydrolysis with 6M HCl can also give weight losses and chemical changes. Lipids and other fat soluble contaminants can be removed by treatment with solvents such as ether (Stevenson, 1982).

The three fractions produced are not individual chemical components but can be seen as gross mixtures of similar properties and composition spanning a range of molecular weights (Stevenson & Butler, 1969).

Parsons (1988) questioned the validity of the procedure when he pointed out, that for the majority of soils, dilute acid extraction fails to dissolve much fulvic material, yet, once an alkaline extract has been acidified a significant proportion remains in acid solution.

Figure 1.1 Extraction and fractionation of humic susbtances utilising solubility differences.

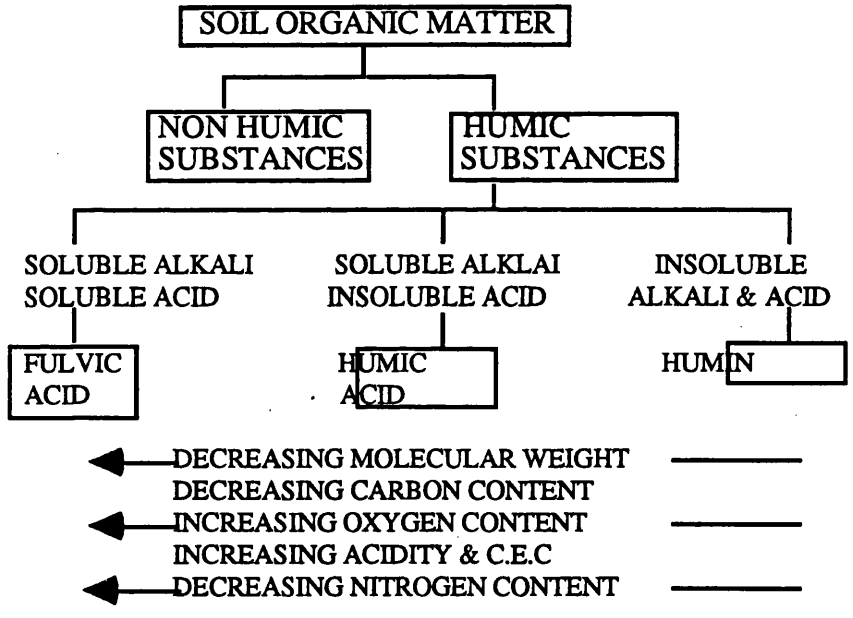

1.5.2.2 FRACTIONATION AND PURIFICATION BASED ON MOLECULAR SIZE DIFFERENCES

Humic substances can be viewed as a system of polymers varying in molecular weight between several hundred and 1,500,000. The carbon and oxygen contents, acidity and degree of polymerisation all vary systematically with molecular weight, with the lower molecular weight fulvic acids having higher oxygen contents and lower carbon contents, (Figure 1.1), than the higher molecular weight humic acids (Kononova, 1966). Thus humic substances can be fractionated into fractions of similar molecular weight or further fractionation and purification of extracted humic and fulvic acids can be carried out utilising the differences.

Gel permeation chromatography can be used to fractionate, purify and characterise humic substances on the basis of molecular size. The method does have some problems associated with it, the most important being gel/solute interactions. However, these problems can be minimised by manipulating the gel and buffer types (Swift & Posner, 1971).

Ultrafiltration has been used to isolate humic substances from aquatic systems but has not been used as commonly with soil humic substances. The method involves the use of membrane filters of known pore size with nominal cut off values ranging from 50 to 1,000,000. One problem with the method is that the cut off values supplied by the manufacturers may not be as sharp as published and they should be interpreted with caution (Swift, 1985). The method is not as suitable for determining molecular weights as gel permeation chromatography, but is useful for preparative fractionation of aquatic humic substances and removal of small molecular weight materials.

1.5.2.3 FRACTIONATION AND PURIFICATION OF HUMIC SUBSTANCES ON THE BASIS OF CHARGE

One of the most fundamental properties of humic substances is their polyelectrolytic nature, resulting from the presence of ionised functional groupings.

Electrophoresis has been used to give a gradation of fractions by utilising the charge on humic substances. This procedure has recently been combined with gel permeation chromatography to give PAGE (polyacrylamide gel electrophoresis). The polyacrylamide gel, e.g. XAD-8, is used as the support medium and the sample is simultaneously subjected to fractionation on the basis of charge by electrophoresis and on the basis of molecular weight by gel permeation chromatography. The procedure is most applicable to purification of the fulvic acid fraction produced by alkali extraction, since this is present in a soluble form. Humic acids can be dissolved in dimethyl sulphoxide (DMSO) before passing into XAD-8 columns and once the contaminants and DMSO have passed through the humic substances can be recovered by raising the pH and then precipitating the fractions which are produced with acid (Hayes, 1991).

Anion exchange can also be used to fractionate humic substances via their charge characteristics, as well as providing a means for purification. However, the fractionation obtained is rather crude (Swift, 1985).

1.6 THE CHARACTERISATION OF HUMIC SUBSTANCES

Even after extraction and fractionation, humic substances are highly heterogeneous materials and their properties can vary on a microsite basis. When working with these substances, it is important that their nature and properties be characterised as far as current procedures allow. The characterisation procedures described here are primarily concerned with determining the number and nature of the reactive functional groups since these are particularly relevant to metal binding studies.

1.6.1 ELEMENTAL ANALYSIS

Elemental or ultimate analysis involves the determination of the elements present in a compound and this is an important chemical property of humic substances, potentially providing information on their nature and source.

Schnitzer and Khan (1978) carried out elemental analysis for a large number of humates extracted from arctic, temperate, subtropical, and tropical soils. The values centred around 54-56% carbon, 4-5% hydrogen and 34-36% oxygen. However, the simplest way to express the results of elemental analysis is to use atomic ratios. The ratios of H/C,O/C, and N/C can prove useful in the following ways:

1. To identify types of humic substances.
2. To monitor structural changes of humic substances in soils and sediments.
3. To devise structural formulae for humic substances.

(Steelink, 1985).

In the identification of the type of humic substance the O/C ratio is particularly instructive and soil and aquatic humic acids tend to show ratios of around 0.5. Soil fulvic acids centre around 0.7 with aquatic fulvic acids showing lower ratios of around 0.6 which could reflect the lower carbohydrate content of the waters (Thurman and Malcolm, 1983). The H/C ratios can also be used to identify the type of humic substance with lake and marine humic substances extracted from the sediment having higher H/C ratios than their soil counterparts (Steelink, 1985).

The elemental composition of humic substances varies with the extractant used, so comparisons can only be made between humic substances extracted with the same extractant and procedure (Hayes & Swift, 1978).

Steelink (1985) proposed that the elemental analysis of a humic substance could be used to give a potential structural formula or chemical structure. However, he

also pointed out that fulvic acid and wood share the same empirical formula, and as such to write a structural formula for any humic substance other information such as titration results and functional group contents should be utilised.

One inherent problem in the study of humic substances is the lack of reproducibility of results due to the heterogeneity of the materials. This also affects elemental analysis leading to variability in the results, even with the same sample and extraction procedure (MacCarthy, 1976).

1.6.2 SPECTROSCOPIC INVESTIGATIONS OF HUMIC SUBSTANCES

1.6.2.1 UV-VISIBLE SPECTROSCOPY

Absorption in the ultraviolet and visible region is caused by atomic and electronic vibrations, and involves the elevation of electrons in orbitals from the ground state to higher energy levels. Systems containing conjugated C=C bonds and unbonded electrons on oxygen are capable of showing absorption. Humic substances, since they contain aromatic groupings, such as phenolic groups, as well as conjugated aliphatic groupings, can show absorption in the visible and ultraviolet regions of the electromagnetic spectrum and these groupings are usually referred to as chromophores. However, the spectra recorded for humic substances tend to be featureless, lacking the well defined peaks which are seen in simple organic compounds (Hayes & Swift, 1978).

Absorption near 465nm has been used for quantitative analysis since it is simple, non-destructive and requires very small amounts of material. Extinction coefficients obtained increase with an increase in molecular weight, degree of condensation, percentage carbon, and the ratio of carbon in aromatic structures to carbon in aliphatic structures (Kononova, 1966). However the results obtained vary between soils and within the same soil extract and are ultimately related to the molecular weight of the humic acid fractions (Swift *et al.*, 1970). Therefore, as with any analysis, the results can only be compared when components from the same or different soils are subjected to the same isolation and fractionation techniques.

As well as these differences in extinction coefficients, humic substances display differences in colour which can be recorded by changes in the gradient of the UV/VIS spectrum. The gradient is measured between 400 and 600nm and is known as the E_4/E_6 ratio. This ratio decreases with increasing molecular weight and condensation and has been used to give an indication of the degree of humification (Stevenson, 1982).

1.6.2.2 ELECTRON SPIN RESONANCE

When molecules containing unpaired electrons are placed in a magnetic field, the energy of each electron is split into two discrete states through interaction of the magnetic moment of the electrons with the applied field. These molecules can be excited from the lower to the higher energy level by absorption of electromagnetic radiation in the microwave region. This is called electron spin resonance spectroscopy and is used to study species which contain free radicals. Humic substances have been found to contain high concentrations of free radicals and these may influence many of the reactions which they are involved in, e.g. metal complexing. Free radicals are also important in the synthesis and degradation procedures in the soil which result in the formation of humic substances (Stevenson, 1982). Steelink & Tollin (1967) proposed that the sources of free radicals in humic acids could include hydroxyquinone, semiquinone polymer, adsorbent complexes, trapped radicals and polynuclear hydrocarbons.

The ESR spectrum of humic acid or fulvic acid consists of a single line identified by its position and width and, on its own, contains very little information on the nature of these materials since the signal comes from only a small fraction of the total number of molecules that comprise the humic or fulvic acid.

1.6.2.3 INFRA-RED SPECTROMETRY

Infra-red analysis can be used to provide information on the reactivity, nature and structural arrangement of the oxygen containing functional groups as well as information on the occurrence of protein and carbohydrate constituents and impurities such as metal ions and mineral material. It is primarily a qualitative method of analysis which is non-destructive and requires minimal sample preparation.

The development of Fourier Transform Infra-Red Spectroscopy (FTIR) has led to increased resolution in the spectra produced. Fourier transformation is a way of computing mathematically the spectrum of radiation passing through an interferometer from an interferogram. It results in high resolution spectra and observes the radiation of all wavenumbers all the time (Griffiths, 1975). A more recent development is Diffuse Reflectance Infra-Red Spectroscopy (DRIFT) which does not incorporate the problems of hygroscopic moisture encountered in normal FTIR (Baes and Bloom, 1989).

The infra-red spectra of humic substances have broad bands due to the heterogeneous nature of the materials. In order to try to elucidate chemical structure,

humic substances have been modified by chemical treatment such as methylation or acetylation. Wood *et al.* (1961) found infra-red bands characteristic of cyclic anhydrides in lignite humic acid that had been refluxed with acetic anhydride, indicating that many of the carboxylic acid groupings occupied positions sufficiently close together to form anhydrides. Wagner and Stevenson (1965) subjected humic acid to methylation, acetylation and saponification in an attempt to determine the number and arrangement of functional groups. They found that about one third of the carboxylic acid groupings could form cyclic anhydrides and also that about two thirds of the hydroxyl groupings were phenolic in nature. However the results of such studies can be ambiguous due to non-specificity of the reactions and side reactions as well as the destructive nature of the treatments.

Infra-red spectroscopy has been used to provide information on the effects of differing geochemistry and source on the composition of humic substances and a combination of chemical and spectroscopic investigations is often used.

Deina *et al.* (1990) studied humic acids extracted from sewage sludges, manure and worm compost. The humic acids from the sewage sludge were more akin to aquatic humic substances whereas those extracted from worm and manure compost were akin to soil derived humic acids. The spectra of fungal melanins were also shown to be similar to those of soil humic polymers indicating that they play a role in the formation of humic substances (Paim *et al.*, 1990).

Stevenson and Goh (1971) studied humic and fulvic acids from several different sources and separated the materials into three main spectral types according to their absorption characteristics. They also studied the humification process and how it affects the spectra. Humification was seen to result in a loss of carboxyl groupings and a change in the environment of the carbonyl group from free or weakly bonded states to strongly adsorbed forms. Humification has also been seen to result in a decrease in the polysaccharide content of humic substances with an increase in amide content as fatty acids are converted into bound forms (Hempfling *et al.*, 1988).

FTIR has also been used for quantitative analysis of the carboxyl content of fulvic acid. Interference from water was corrected for by spectral subtraction. The results were then compared to those calculated by potentiometry and were found to be comparable to the spectroscopic method (Cabaniss, 1991).

Studies of unextracted organic matter have become more frequent in an attempt to overcome the problems of alkaline extraction. Humification of peat samples resulted in a decrease in the polysaccharide intensity, as seen in humic acids, whilst the intensity of carbonyl groupings and aromatic bands increased on humification (Niemeyer *et al.*, 1992). This study utilised DRIFT spectroscopy which was also

utilised by Holmgren and Norden (1988) to characterise *Sphagnum* and *Carex* peat. They observed differences in the spectra due to the plant origin and also showed that DRIFT spectroscopy can be used to give a quantitative determination of amino acids and sugars in peat. The results were in excellent agreement with values calculated by Kjeldahl measurements.

DRIFT spectroscopy will undoubtedly become more important in infra-red studies, not only for quantitative determinations, but also in the study of unextracted humic substances.

1.6.2.4 NUCLEAR MAGNETIC RESONANCE

The nuclei of certain atoms (e.g. ^{1}H and ^{13}C) can exhibit magnetic spin momentum when placed in a magnetic field, causing energy transitions to occur. The spectrum produced can provide valuable information regarding the immediate chemical environment of the atom under study and is seen as a powerful new tool for the determination of functional groups in humic substances providing more information on the functional groups. But, the measurement of the functional group concentration of humic substances by both ^{13}C and ^{1}H NMR spectroscopy in both liquid and solid samples is at best semi-quantitative (Hatcher *et al.*, 1983).

Baldock *et al.* (1991) also highlighted another major problem when using solid state ^{13}C NMR in mineral soils, namely, the low carbon content coupled with the low natural abundance of ^{13}C nuclei. Therefore long scan periods are necessary to give adequate signal resolution, unless the soil is incubated with a ^{13}C-labelled substrate. Organic soils, with their higher carbon content, are not affected as much by this disadvantage.

The development of cross polarisation magic angle spinning (CPMAS) ^{13}C NMR has improved the resolution of the method and it is now widely used in structural and chemical investigations. In particular greater understanding of the role of aliphatic carbon in humic substances has been gained through CPMAS ^{13}C NMR studies. This aliphatic material would have previously been hydrolysed in the degradation procedures used in earlier structural investigations. Thus, concepts of the compositional nature of humic substances were challenged.

The method has been utilised to identify different chemical forms of carbon in mor and mull humus as well as other variations in the types of humus (Hopkins & Shiel, 1991). ^{13}C NMR has also been instrumental in confirming that humic acids from each environment are very different in composition from the fulvic acids from the same environment (Malcolm & MacCarthy, 1991).

Baldock *et al.* (1991) showed that organics in whole soil samples could be characterised without resorting to lengthy extraction and/or fractionation procedures, thus minimising changes within the humic substances. They showed that combining ^{13}C NMR with pyrolysis had far greater potential than a single technique and they proposed that applying combinations of techniques such as NMR, IR and MS to unextracted organic matter in soils and waters could lead to significant advances in the understanding of the behaviour of these materials in the natural environment.

1.6.3 FUNCTIONAL GROUP ANALYSIS

The acidity of humic substances and their reactivity towards heavy metals and radionuclides is ultimately related to their content of oxygen-containing functional groups, although the involvement of other functional groups cannot be discounted. The qualitiative determination of parameters such as total acidity or carboxyl group content is complicated by the heterogeneity of the humic substances. Many of the analytical techniques used lack specificity in reaction or result in undesirable oxidation, reduction or derivatisation reactions which can affect the results. In addition, the reactions are often non-stoichiometric. Consequently, comparison of the results produced with published results can be ambiguous due to a lack of standardisation of methods for extraction, fractionation and purification (Stevenson, 1982).

Dubach and Mehta (1963) concluded that the following could easily result in contradictory results being published:

(a) Divergent origin of humic substances.

(b) Lack of adequate criteria for purity.

(c) Variable molecular weights, leading to incomplete reactions, adsorption of reagents and undesirable fractionation during manipulation.

(d) The proximity of many and different functional groups which influence the reactivity of the groups and the specificity used for their detection and measurement.

1.6.3.1 DETERMINATION OF THE TOTAL ACIDITY

Determination of the total acidity is one of the most commonly used methods of chemical characterisation. Since it is based on the acidity of the reactive groupings it has its own set of problems, one of the most important being the complex nature of the humic substances resulting in the overlapping acidities of various groups (Stevenson, 1982).

One method of determining the total acidity involves reacting the humic substances with barium hydroxide and then determining the amount of bound barium by titrating the unused base with standard acid. The main advantage of the method is its simplicity, although it does suffer some interferences, one being associated with the filtration step. If any weakly ionised groups remain in solution they will be re-titrated and consequently lower the value. If a coloured filtrate is obtained, ultrafiltration should be employed (Davis, 1982). Oxygen can also interfere with the method, and all measurements should consequently be carried out under nitrogen.

Regardless of the potential interferences, Perdue (1985) reported that the barium hydroxide method is potentially an accurate method of analysis if the filtration step is approached with care, and all measurements are carried out under nitrogen.

Potentiometric titration with dilute alkali can also be used to calculate the total acidity. The sample is equilibriated with a reagent at very high pH so that even the weakest acids will react. This can pose problems in that it is difficult to determine accurately how much base has reacted in the presence of the extreme excess of base which is required to give a high pH.

Humic acids are viewed as complex polyelectrolytes. Their acidic properties are complicated by electrostatic charge accumulation on the polymer as neutralisation proceeds, resulting in the remaining acidic groups becoming weaker in acidity (Stevenson, 1982). Thus a continuous distribution of pKa values is seen, resulting in no recognisable end point. To compensate for this, Posner (1966) used the end point where the rate of change of pH became a maximum to calculate the end point. Stevenson (1977) also calculated the total acidity from the titration curve in this way, as well as defining a value for the amount of available reactive groups present at any pH value. It is also preferable to have equilibrium achieved as soon as possible to avoid base-catalysed side reactions, such as the hydrolysis of esters and peptides which may lead to releases of carboxylic acids (Perdue, 1985).

Piccolo & Camici (1990) compared the two methods and found that the barium hydroxide method always gave higher results than the potentiometric method due to the precipitation of humic subtances before measurement, which led to an underestimation of the total acidity. However, potentiometric titration gave better precision and did not suffer from the interferences that affect the barium hydroxide method.

1.6.3.2 DETERMINATION OF THE CARBOXYL CONTENT

Due to the abundance of carboxyl groupings and their importance in the reactivity of the materials, determination of the carboxyl content of humic substances is often carried out. Bonn & Fish (1991) suggested that the carboxyl content provided a better indication of the complexing potential of humic matter that the total acidity measurements, since it excludes the phenolic groupings which will not be dissociated at most soil pH values.

The calcium acetate method has been widely used for determining the carboxyl content of humic substances. The method yields fractionally defined carboxyl contents and is based on the release of acetic acid when humic substances react with calcium acetate (Schnitzer & Khan, 1972). It is a simple method which yields accurate results when compared to direct decarboxylation. However, as with the determination of the total acidity, interferences can occur. Calcium acetate (0.1M) is poorly buffered and the equilibrium pH, which determines the extent to which acidic functional groups react, is dependent on the amount of humic substances added. Also, additional protons can be released in the reaction with calcium acetate (Perdue, 1990). There is also a problem with groups other than the carboxyl groups reacting with the calcium acetate leading to an over-estimation of the carboxyl content. In addition, functional groups less acidic than carboxyl groups which do not react with calcium acetate could still react with the sodium hydroxide on titration.

As with calculation of the total acidity, the filtration step can also cause problems, which led Holtzclaw & Sposito (1978) to modif the method accordingly. However, they could not avoid the other interferences described above.

Bonn & Fish (1991) studied the method using laboratory experiments with humic acids, as well as computer stimulations with hypothetical acids. From these studies they concluded that unless the exact reactions are known, individual carboxyl content measurements cannot be compared. Also, no titration method can be assumed to quantify the acidic group content for humic acids which have a continuous pK distribution.

1.6.3.3 DETERMINATION OF THE METAL BINDING CAPACITY

In determining the content of reactive functional groups for metal binding, the maximum binding capacity (MBC) of a humic substance for that metal may be calculated, and this can give information on the availability and movement of the metal in the environment. Van Dijk (1970) proposed that the capacity of humic acids

to bind metal ions was at most equal to the number of titratable hydrogen ions divided by the valency of the metal. However, it is preferable to titrate the humic substance with the metal being studied until no further metal can be bound, since the interaction of a metal with the humic substance varies between different metals. This approach was suggested to be the most accurate for determining the total ligand concentration of humic substances for metal binding studies (Fish *et al.*, 1986).

Perdue (1989) proposed that the MBC is a compositional rather than thermodynamic parameter, unlike the conditional stability constant for the reaction of a metal with a humic substance. Thus it should not be dependent on pH, ionic strength, nature of the metal or concentration of ligand. Yet, the MBC appears to vary with reaction conditions and appears highest at near-neutral pH, low ionic strength, high ligand concentration and with highly polarisable metals such as Cu^{2+}. The MBC of such a humic substance is a weighted average of the complexation capacities of the individual ligands present in the mixture and these ligands in binding energy or log K. It is this binding energy which is affected by changes in pH, ionic strength, etc., and thus it makes it more difficult to realise the MBC under less than optimum conditions (Perdue, 1989). Therefore, the MBC should always be assessed for the reaction conditions being employed in the study.

Interpretation of the titration data and calculation of the MBC has involved using the Langmuir equation (Zunino & Martin, 1977, McLaren & Crawford, 1973), a mathematical expression originally developed by Langmuir (1918, cited in Mott, 1988) to describe the adsorption of a gas on a clean solid. The equation assumes that the complexing strength remains constant as the proportion of complexing sites increases, and that only one type of complexing site is present.

Zunino & Martin (1977) studied copper complexing by colloidal organic matter and achieved linear Langmuir plots. They concluded that many small successive Langmuir responses may be happening as different strengths or classes of binding site are occupied. These cannot be detected but combine to give an overall Langmuir response.

Sanders (1980) also studied organic matter-copper complexes and found that humified organic matter gave curved graphs instead of a linear relationship. This could be indicating that not all binding sites have the same strength. Alternatively, the presence of adsorbed metal ions could be making further adsorption more difficult. Indeed both effects could be contributing to the lack of linearity and many authors have proposed the existence of more than one class of binding site (Buffle *et al.*, 1977: Mantoura & Riley, 1977). Therefore, many researchers utilise the double surface Langmuir isotherm which assumes two distinct classes of binding site whose

complexing strength remains constant as they become filled (Sposito, 1982). Sanders (1980) found that the data which gave a curved Langmuir response fitted the double surface Langmuir well and this was reinforced by Fitch and Stevenson (1984), who also showed that the Langmuir plots gave an underestimation of the MBC as calculated from the double surface isotherm. Since the functional groups on humic substances are dominated by weak acid sites such as carboxylic acids, the optimum conditions for saturating these sites with a metal often result in flocculation. This process could give ambiguous results, and resulted in Perdue (1989) proposing that the total acidity could instead be utilised to give an estimate of the MBC of a humic substance.

The values for the MBC are conditional, yet provide information on the reactivity of the humic substance towards a particular metal. Zunino & Martin (1977) proposed that the MBC is more important in the study of natural systems than studies on structure or the calculation of stability constants.

1.7 THE INTERACTION OF METALS WITH HUMIC SUBSTANCES

The ability of humic substances to react with cations via the negatively charged functional groups has long been recognised (Stevenson, 1982). They therefore play a significant role in controlling the behaviour of pollutant metals in the environment. The reactions involved are highly complex and differ depending on the metal, humic material and pH. However, in terms of the environmental implications of metal binding the following effects can be seen:

1. Metal ions which would normally form insoluble precipitates may form a soluble organic complex, with the potential to contaminate groundwater systems or be available for plant uptake. Mierle and Ingram (1991) reported that Hg can be remobilised into water systems through soluble organic complexes, and the mobility of Pb in organic soils under reducing conditions is correlated with the contents of dissolved organic matter (Urban *et al.*, 1990).

2. Alternatively, insoluble complexes can be formed which result in a reduction in bioavailability and consequently ecotoxicity of metals as they become immobilised by the complexation process (Dissanayake, 1983). Copper and cadmium have been shown to react with humic substances in this way (Brennan *et al.*, 1983).

1.7.1 THE NATURE OF THE INTERACTION BETWEEN METALS AND HUMIC SUBSTANCES

1.7.1.1 CLASSIFYING COMPLEXATION

The interaction of a metal with a humic substance can be called coordination or complexation and the metal complexes formed can be grouped into two main types of interaction:

(1) OUTER SPHERE COMPLEXES.

These have a purely electrostatic nature and both the ligand and the metal retain their hydration sphere (Figure 1.2). The alkali metals and group 2 elements tend to favour this ionic type of interaction where the metal is also seen to be held in an ionic, exchangeable form.

Figure 1.2. The interaction of a metal to form an outer sphere complex.

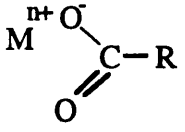

Bonn and Fish (1993), demonstrated that this effect was indeed occurring for Li^+, Na^+ and K^+.

(2) INNER SPHERE COMPLEXES.

These result in the formation of a covalent bond between the coordinating ligand(s) and the metal ion, with partial or total dehydration breakdown of the hydration sphere of the metal. The transition metal elements tend to favour this more covalent type of interaction which can be called coordination, chelation or bridging.

Figure 1.3. The different types of inner sphere complexes.

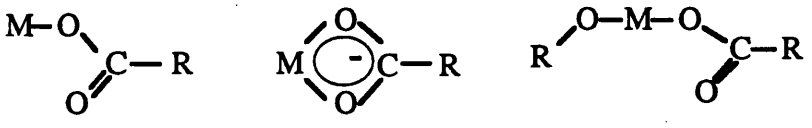

COORDINATION CHELATION BRIDGING

(Buffle, 1988).

In a study on the metal ion binding of unextracted organic matter, Bloom and McBride (1979) showed that divalent ions such as Ca^{2+}, Mn^{2+}, Co^{2+} and Ni^{2+} were

all bound as hydrated ions in outer sphere complexes whilst Cu^{2+} was able to form inner sphere complexes. However, the formation of more stable inner sphere complexes does not always guarantee immobilisation of metals in the environment. Piccolo (1989) showed that the complexing of cadmium, zinc and nickel did reduce the plant availability of these metals, but, particularly with lower molecular weight humic substances, the inner sphere complexes can be soluble, resulting in the enhanced mobility of a metal (Tipping & Woof, 1991).

The ability of metal ions to react with specific ligand atoms can also be classified, and this is governed by the number of electrons in their outer electron shell.

Class A metal cations have the inert gas type (d^0) electron configuration and as such the electron shells are not easily deformed under the influence of an electric field. These cations prefer to complex with F^-, O^- or Cl^- containing ligands and include Na^+, K^+, Mg^{2+}, Al^{3+}, and Sr^{2+}. Class B metal cations have electron shells which are easily deformed and they prefer to react with ligands containing I, S, P or N. These cations include Ag^+, Au^+, Zn^{2+}, Pb^{2+}, Cd^{2+} and Hg^{2+}.

Pearson (1963) noted that the class A metal cations, or acids, were small compact and not very polarisable and that they consequently preferred ligands, or bases, which were less polarisable. He called these acids and bases "hard". In turn the class B metal cations tend to be larger and more polarisable and thus prefer ligands which are more polarisable. These are known as soft acids and bases. The interactions can be summed up with the statement that:

"hard acids prefer hard bases and soft acids prefer soft bases."

(Pearson, 1963).

The hard acid-hard base interaction will contribute towards the outer sphere complexes described by Buffle (1988), where the interaction is ionic or electrostatic in nature and the metal is held by the humic substance in an exchangeable form. Conversely, the soft acid-soft base interaction will contribute towards the formation of inner sphere complexes which are more covalent in nature.

1.7.1.2 HUMIC SUBSTANCES AS LIGANDS

Humic substances possess a large number and variety of functional groups, and can be viewed as polyfunctional ligands (Buffle, 1988).

Oxygen-containing functional groups are the most abundant and are ultimately the most important to metal binding. However, the involvement of other groups in metal binding cannot be discounted. Sikora and Stevenson (1988) correlated the maximum binding capacities of humic acids for silver with their nitrogen contents and

Ephraim *et al.* (1986) proposed the existence of a linkage between copper and an amino-carboxylic acid group.

Infra-red studies have not only been integral in elucidating the prescence of these groups, but have also been used to observe the changes which occur on metal binding. The main changes in the infra-red spectrum on metal binding occurs in the 1720-1600 cm^{-1} region, where the carboxylic acids, quinone and ketonic groups absorb. Changes in the hydroxyl groupings can be difficult to interpret (Piccolo & Stevenson, 1982).

Although the importance of the carboxyl groupings has been established, the exact nature of this linkage has yet to be elucidated. Stevenson (1977) suggested that salicylate or phthalate type ligands could be responsible. Cu^{2+} has been used extensively to study metal humic interactions, often with salicylic and phthalic acids as model compounds. From these studies it appears that salicylate and phthalate type linkages alone do not provide a model for Cu^{2+} binding and are weaker than humic metal interactions (Livens, 1991).

It is accepted that metals such as Cu^{2+} can complex with more than one binding site, often forming 2:1 linkages (Buffle *et al.*, 1977: Stevenson *et al.*, 1993). Polydentate linkages, involving up to 3 or 4 donor ligands have also been proposed and these could potentially be any combination of phthalate or salicylate type groupings (Bresnahan *et al.*, 1978). Gregor *et al.* (1989) alternatively postulated that the donor ligands came from malonate, peptide and citrate type groupings, with a possible contribution from nitrogen containing heterocycles. This was also observed by Town & Powell (1993) in a study of soil-derived humic and fulvic acids.

Certainly the polyfunctional nature of humic acid substances will encourage such chelation reactions, and it should be remembered that the irregular structure of these materials means that no two functional groups will be chemically identical (Gamble *et al.*, 1980).

1.7.2 QUANTIFYING METAL BINDING

With humic substances being important metal binding agents in the environment it would be desirable to quantify their reactions and therefore be able to predict their behaviour. Quantification of metal binding generally involves the calculation of a formation or equilibrium constant for the metal-humate complex, e.g. for the reaction,

$$\mathbf{M + L \Leftrightarrow ML}$$

the thermodynamic equilibrium constant, by the law of mass action, is:

$$K = \frac{\{ML\}}{\{M\}\{L\}}$$

Here the constant is expressed in terms of activities, and since it is more convenient to measure concentrations these must be converted by means of the activity coefficient. The formation constant calculated is also highly conditional, and depends on temperature, pressure, ionic strength, pH, concentration of competing metals and ligand concentration.

Humic substances are not as simple as this, since there are a large number of ligands of various types with varying affinities. Thus the equation can then be rewritten to give a cumulative formation constant for m cations M, with l ligands L:

$$K = \frac{\{M_m L_l\}}{\{M\}^m \{L\}^l}$$

(Buffle, 1988).

In quantifying metal binding it is more important to achieve a valid thermodynamic description of metal binding than to define binding chemically (Turner *et al.*, 1986). However, defining binding thermodynamically is complicated by secondary effects which affect the environment of the ligand or binding site before and during complexation. There are three main categories of secondary effects:

(1) CHANGES DUE TO POLYFUNCTIONAL PROPERTIES.
Humic substances have a diversity in chemical nature, electronic environment and steric environment of the functional groups, which alter on metal binding.

(2) CONFORMATIONAL CHANGES ON COMPLEXATION.
On complexation the ionic strength, pH and complexable ion content all alter, and the degree of conformational alteration depends in particular on the hydration-dehydration process and the formation of hydrogen bonds and metallic bridges within the humic substance.

(3) POLYELECTROLYTE CHANGES.
On metal binding the remaining groups become weaker in acidity and fewer in amount. Thus the overall negative charge on the humic substance will decrease and binding will become increasingly more difficult.

Buffle, (1988).

Accounting for these effects within the mass balance equations would lead to the inclusion of an unpheasible number of parameters, and in practical terms this is not

possible since several of the effects can occur at once, and they cannot be measured and quantified. Even when the pH and ionic strength are constant K can still vary since, as described above, when the metal/ligand ratio increases K decreases resulting in K constantly changing. Therefore, as Perdue (1989) states,

"formation constants for metal-humic substance complexation are not actually constant and should be viewed with skepticism."

In modelling the metal-humate interactions it is therefore necessary to make several assumptions, the most important and universally relevant being that thermodynamic equilibrium has been achieved. The formation constants generated from such models should also be interpreted with caution.

1.7.2.1 MODELS OF METAL BINDING

In modelling metal binding it must be remembered that the equilibrium constants obtained are highly conditional and are only valid within the range of conditions employed within the titration reaction.

The relative merits of each of the following models are hard to ascertain, since they all appear to fit the data equally well. In terms of using the models to calculate constants from data, careful consideration should be made of the uses of the model, the quality and quantity of titration data, and the available computational resources (Fish *et al.*, 1986). The four main types of model will be outlined in turn as follows, and the relevant papers can be consulted for more detailed information.

(1) DISCRETE LIGAND MODELS.

These models will be discussed in most detail, since they were utilised most in the research. They are multiligand models which require only a few ligands to fit the data and ignore the effects of variations in humic charge which occur on binding, and changes in the conformation of the humic molecule. The ligands expressed in the models do not represent actual types of functional groups, since humic materials are so complex, but instead represent distinct classes of binding site which have similar binding affinities. The number of ligands required can be estimated as one ligand for each order of magnitude of bound-metal concentration observed in metal-humate titration data (Dzombak *et al.*, 1986).

The first discrete ligand model developed was the **multisite model** (Dzombak *et al.*, 1986). Binding of a metal to the humic macromolecule is characterised by a formation function, which can be regarded as the average number of metal ions

associated with each humic macromolecule. The humic macromolecule is assumed to be the central group, with the metal interacting with sites on it. If more than one class of binding site is present, then treatment of the titration data results in a curve. Thus, further treatment of the titration data is required to determine the formation constant for that class of binding site. This approach has been utilised by Bresnahan *et al.* (1978), Saar & Weber (1979) and Sikora & Stevenson (1988) in the determination of formation constants for the reaction of various cations with humic substances, and generally two distinct classes of binding site were identified.

The **multidentate model**, developed by Buffle *et al.* (1977) is mathematically similar to the Scatchard approach, in that a degree of complexation function is determined, and treatment of the data can result either in a linear relationship suggesting one class of binding site, or a curve indicating the existence of more than one class of binding site. Formation constants can then be calculated by manipulation of the titration data accordingly. However, in this approach the metal ion is the central group, and more than one humic acid molecule can potentially interact with the metal.

Stevenson (1976) utilised the modified Bjerrum approach, developed by Gregor (1955) for the analysis of metal polyacrylate titration curves. In this approach complex formation is regarded as a competitive reaction between the metal ion and protons for the ligand sites, with the metal acting as the central group in binding. The reactions between the ligand and the metal are expressed by two successive formation constants, one for each ligand group reacting with the metal, and these are combined to give an overall constant B_2. The method was developed further to incorporate the assumption that the metal interacts with a dissociated ligand site, with the protons being released from the re-establishment of ionisation equilibrium (Stevenson, 1977).

The most recent discrete ligand model, the **fixed-k model,** adopts a slightly different approach by having pre-decided equilibrium constants. The experimental data is then fitted to these constants to provide values for the discrete ligands present on the humic substance, and also to assess the goodness of fit of the titration data when the reaction conditions varies (Tao, 1992).

(2) CONTINUOUS DISTRIBUTION MODELS.

Due to the complexity of humic materials and the variety in type and affinity of the binding sites, continuous distribution models were developed. These models assume that a stability constant K, represents a continuum of binding sites on the humic substances, rather than discrete classes of binding site (Dzombak *et al.*, 1986), and that the continuum is produced from the above secondary effects, which alter the affinities of the binding sites as binding proceeds. The ligand frequency distributions are then integrated over the distribution of log K. Examples of these include the affinity spectrum approach (Thakur *et al.* 1980), the constant stability function model Gamble *et al.* (1983) and the normal distribution model (Perdue and Lytle, 1983).

Stevenson and Chen (1991) adapted the Scatchard **multi site** approach from a discrete model into a continuous distribution model with the **Incremental Stability Constant** model. In this model, instead of graphically calculating a log K value for a distribution of binding sites, a continuum of average stability constants is calculated for each increment of metal added.

(3) THE ELECTROSTATIC MODEL.

This approach to modelling attempts to take into account the electrostatic effects which affect metal binding, particularly as a titration proceeds. The **electrostatic model** was developed by Wilson & Kinney (1977) and assumes that all binding sites are chemically the same, with variations in apparent log K being ascribed to the effects of electrostatic interactions resulting from the change in humic charge on metal binding. This was also the basis of a model developed by Backes and Tipping (1987) for the study of aluminium and proton binding. No parameters are included for the heterogeneity of the humic substances.

(4) DISCRETE SITE/ELECTROSTATIC MODELS.

These models take the ideas developed by Wilson & Kinney (1977) further by including parameters for more than one binding site and ionic strength, and are the most advanced models for metal binding. Ephraim *et al.* (1986) were the first to consider such an approach through the developement of the **polyelectrolyte gel model**. Tipping and co-workers further developed these ideas with a series of models, with the integral concept that metal and proton binding take place at a number of chemically discrete binding sites, with electrostatic secondary effects being accounted for (Tipping & Hurley, 1992: Tipping & Woof, 1990: Tipping *et al.*, 1991: Tipping & Hurley, 1988: Backes & Tipping, 1987) .

No single approach can be regarded as being superior, each has its own set of limitations. Fish *et al.* (1986) and Turner *et al.* (1986) independently reviewed the various discrete and continuous models using both synthetic and experimental data. Both groups of workers concluded that the discrete ligand models, although conceptually and mathematically the simplest, were the most useful as well as accurate way of fitting titration data. In particular, the discrete ligand models can be used to predict competitive interactions among metal ions. However, the ligands classes are also easily incorporated into chemical equilibrium computer programmes such as MINEQL, and can successfully predict metal ion binding by humic material in the absence of competing ions and within the range of calibrating titrations (Dzombak *et al.*, 1986).

Turner *et al.* (1986) found the **multi-site model** most able to fit the experimental data and cope with the heterogeneity of fulvic acid. But, the Scatchard plots used in the discrete models to analyse the data and provide equilibrium constants do suffer from errors, one in particular being the curvilinearity of the plots. Two discrete lines are then fitted to the plots to give two discrete binding zones and equilibrium constants. The fitting of these lines is arbitrary and often unfounded (Saar & Weber 1980: Perdue & Lytle 1983). In addition the approach relies on an accurate measure of total ligand concentration, since all other parameters in the model rely on this. This cannot be measured unambiguously due to the nature of humic substances and the secondary effects that they suffer from (Fish *et al.*, 1986).

The discrete models have also been critiscised since they do not take into account the electrolytic nature of humic substances and consequently cannot be applied at salt concentrations different from those used in the formulation of the models (Marinsky & Ephraim, 1986). Also, the discrete models are producing equilibrium constants which are fitting parameters, and not actually representing distinct classes of binding site (Tao, 1992). As Masini (1993) demonstrates, if the electrolytic nature of humic susbtances and the corresponding secondary effects are ignored then 2 to 3 distinct classes of binding site do give a good mathematical fit.

Stevenson *et al.* (1993) recognised the value of the Scatchard approach, as well as its limitations. Therefore they used the **Incremental Technique** where the Scatchard slopes are used to calculate a continuum of average stability constants, which reflect variations in the binding energies of humic substances. The constants that they calculated from this model were in good agreement with those calculated from the **Bjerrum approach.** They also found that the **Normal Distribution Model,** a continuous distribution model, did not model copper humic acid binding well since to

calculate the constants a linear effect is needed and a linear effect can only occur with a single class of binding sites where electrostatic effects are negligible.

Marinsky & Ephraim (1986) proposed that the continuous distribution models can overestimate the complexity of the polyelectrolytic nature of the humic substances. The **polyelectrolyte gel model** was the first model to attempt to account for both the secondary effects of heterogeneity and polyelectrolytic properties. Ephraim *et al.* (1986) were able to demonstrate that the polyelectrolytic nature was more significant in metal binding than heterogeneity, since it directly affected the accessibility of metal binding sites. The inherent problem with this approach is its complexity, no attempts were made to simplify the model and instead the aim was to attempt to understand more fully the humic-proton-metal equilibria.

Backes & Tipping (1987) found that the **polyelectrolyte gel model** was able to fit the data, but they preferred to adapt the model and its philosophy to give a more simplified model, with fewer parameters which could then be utilised in a more practical way. As Tipping and Hurley (1992) point out:

"there is no justification for increasing the complexity of the model as long as it can describe the observed behaviour satisfactorily. The key is to find the minimum degree of complexity that has to be assumed"

Tipping and co-workers have undoubtedly approached the modelling of metal binding in the most comprehensive and advanced way, with compensations for secondary effects and attempts at modelling the competition reactions of protons and metals with humic substances, as well as the competition reactions of different types of metals. In particular, their **model V** interprets the competition effects between trace metal species such as copper and alkaline earth cations such as Mg and Ca. It also allows for sites with different relative affinities for different metals, mono- and bidentate binding sites and the effect on alkaline earth binding of the contribution of non-specific counterion accumulation on the charge.

Their models do suffer from errors in fitting the experimental data. In two of the models, namely **Model IV** and **CHAOS**, there is an underestimation of binding at low pH values and an overestimation at high pH values. This could be due to many factors, the most likely being analytical error, although a deficiency in the model which is neglecting competition effects from other cations cannot be discounted. After all, in the environment metal binding will be complicated by many factors including competition. These factors though can never be quantified since they are so numerous and would require more parameters than could be effectively computed. Also, they are highly conditional and in the environment will deviate on a microscopic basis. From

this it is easy to see the attraction of the simple discrete type models which have also been shown to be accurate in fitting data.

All of the above studies have been carried out using humic or fulvic acids, apart from Tipping & Hurley (1988), who used alkali-extracted humic substances with no acid precipitation. However, as Baes & Bloom (1988a) pointed out, soil organic matter is a solid phase cation binder, not an operationally-derived extract. Bloom and McBride (1979) suggested, from studies on the metal binding of peat, that modelling the metal binding of organic matter need not take into account the secondary effects of heterogeneity. Instead these materials can be modelled well by assuming a cross-linked polycarboxylic acid type structure. Baes and Bloom developed this idea (1988a, 1988b) in modelling the exchange of alkaline earth cations in soil organic matter. They used a model developed by Eisenman (1962; cited in Baes and Bloom 1988a), originally developed to model exchange in aluminosilicate glasses. From these studies it was seen that the organic matter can exchange cations and that the material acts as a weak field exchanger, due to the distance between fixed anionic sites. By increasing the ionic strength, swelling of the structure was reduced and binding sites were brought closer together, enhancing bidentate interactions. Gamayunov & Maslennikov (1992) also studied the interaction of cations with peat soil and concluded that interaction depends on the overall charge of the material, and again heterogeneity did not seem as important a factor as it is in the modelling of humic and fulvic acid interactions.

Allen *et al.* (1992) modelled the interaction of cations with peat and found that the equilibrium data conformed to a linear Langmuir plot, whereas humic acids tend to give curvilinear Langmuir plots (Sanders, 1980).

From the few studies on metal binding with unextracted organic matter such as peat it can be seen that the interactions are quite different and consequently modelling has been approached in a different way. To understand further the behaviour of metals, in particular pollutant metals, in the environment it may be necessary to develop this approach.

1.8 NATURAL HUMIC SUBSTANCES AND THEIR ROLE IN MONITORING THE DEPOSITION OF HEAVY METALS AND RADIONUCLIDES FROM THE ATMOSPHERE

1.8.1 PEAT AS A SOURCE OF NATURAL HUMIC SUBSTANCES

Humic substances are an integral, characteristic and substantial constituent of organic soils and consequently play a vital role in the dynamics of these systems.

Peat soils are highly organic soils which contain up to 97% organic matter in the solid phase, with the moisture content often 90% by weight. Globally they cover around 500 million hectares and have a carbon content of 67 billion x 10^{12} metric tons (Bramryd, 1980). Thus they play a significant role in the regulation of climate since they are a sink for carbon dioxide, but as a consequence of human activity, they are also increasingly a source of carbon dioxide due to practices such as the drainage of large areas of peatlands (Moore & Bellamy, 1974).

Peat soils are formed by the accumulation of organic matter due to seasonal or continual waterlogging which limits degradation and humification. They vary in their botanical origin, extent of humification, present flora, and physical and chemical properties, with these differences being utilised in their classification (Mathur & Farnham, 1985). An important classification system is based on the nutrient content of the peat and leads to the distinction between ombrotrophic or nutrient deficient peats and minerotrophic or nutrient rich peats (Gore, 1983). Ombrotrophic peats are also assumed to be rainwater fed, being raised above the mineral groundwater limit and two major hydromorphological types exist, namely raised bogs and blanket bogs. Blanket bogs are the most extensive type of peat ecosystem in Britain. They "blanket" large areas of land with a cover of peat, and can occur at a wide variety of topographical locations. However, they can often be minerotrophic in part (Wheeler, 1993). Raised bogs occur in the bottom of broad valleys or in basins, and can be distinguished by shallow domes of peat formed when *Sphagnum* moss begins to colonise the nutrient poor, acidic peat surface. The *Sphagnum* mosses lower the pH of the system discouraging colonisation by other bog species, and producing an even more dense matt of vegetation cover on the bog surface. *Sphagnum* mosses also have a high water holding capacity. Their colonisation results in the hydraulic conductivity of the peat being lowered, further removing the peat from groundwater influences (Shotyk, 1988).

Since ombrotrophic peats are rainwater dependent they are able to retain a record of the past atmospheric deposition of heavy metals and radionuclides, and are particularly useful due to the following properties:

1. All inputs are from the atmosphere, via wet or dry deposition.

2. Long term records of deposition can be provided in deeper cores giving information on changes in atmospheric content throughout the Holocene period.

3. The profile can be dated utilising a variety of techniques, depending on the time period being studied.

4. They are abundant and easily sampled.

(Barber, 1993).

These properties led to the proposal that ombrotrophic peats could be used as a global pollution monitoring system, since they are present in every continent of the world (Markert & Thornton, 1990). Obviously, there are problems associated with using ombrotrophic peats as a monitoring system, with a major one being establishment that the peat system is in fact ombrotrophic and removed from groundwater influences. There is no clear botanical or chemical fingerprint for ombrotrophicity, and the chemistry of ombrotrophic substrates formed under different environmental regimes will vary. Therefore, in order to establish ombrotrophicity data on the chemistry of the peat profile, water chemistry and plant species present are needed (Karlin & Bliss, 1984). The other problems surrounding utilisation of these systems as records of deposition, are discussed in greater detail in sections 1.8.3 and 1.8.4.

1.8.2 SOURCES OF HEAVY METALS AND RADIONUCLIDES IN THE ATMOSPHERE

1.8.2.1 SOURCES OF POLLUTANT METALS

To avoid confusion, in the following sections the term heavy metal will be replaced by metal. Heavy metal usually refers to metal ions which have a relative density greater than 5 g cm^{-3} (Morgan & Stumm, 1991). However, the term has been used indiscriminately in the past to include both ferrous and non-ferrous metals, and even non-metals and metalloids (Niebor & Richardson, 1980). Pollution is easier to define than heavy metals, and the following definition by Holdgate (1979) is widely accepted. This states that pollution is: *"the introduction by man into the environment of substances or energy liable to cause hazards to human health, harm to living resources and ecological systems, damage to structure or amenity, or interference with legitimate uses of the environment"*.

Metals are released into the atmosphere from a variety of industrial and domestic activities, with the principle sources of metals being as shown in Table 1.1.

Table 1.1 Industrial sources of atmospheric chemicals

Process	Metals Released
Combustion Fossil Fuels	Be, Co, Mo, Sb, Se, Cd, Zn, Ni, V
Mining & Smelting:	
Lead Industry	Pb, Cu, Zn, Cd
Ni & Cu Smelting	Ni, Cu, Co, Pb, Mn
Zn Smelting	Zn, Cd, Cu, Pb
Iron & Steel Industry	Cr, Mn
Car Exhaust Emissions	Pb, Br

(Adriano, 1986: Hardman *et al.*, 1993).

However, there are also natural sources of metals which give rise to background concentrations of metal. The natural sources include windblown dusts, sea salt sprays, volcanic emissions, forest fires, and other biogenic sources (Nriagu, 1989). The natural fluxes of metals from these sources are small for some of the pollutant metals when compared to industrial activities, as Table 1.2 demonstrates:

Table 1.2 Worldwide emissions of metals to the atmosphere from natural and anthropogenic sources (as 10^9 g y^{-1}).

Element	Natural sources	Anthropogenic sources
Antimony	2.6	3.5
Arsenic	12	19
Cadmium	1.4	7.6
Chromium	43	31
Copper	28	35
Lead	12	332
Mercury	2.5	3.6
Molybdenum	3.0	6.3
Nickel	29	52
Selenium	10	5.1
Vanadium	28	86
Zinc	45	132

(Nriagu, 1991)

In order to assess the importance of industrial processes on the release of metals into the atmosphere, and their consequent incorporation into the biosphere, enrichment

factors can be calculated. Zoller *et al.* (1974) proposed the use of such factors to quantify enrichments, and defined the enrichment factor of an element as:

$$\frac{(C_{x,p} / C_{Al,p})}{(C_{x,c} / C_{Al,c})}$$

where $C_{x,p}$ and $C_{x,c}$ are the element concentrations in the atmospheric particulates and crustal rock respectively.
$C_{Al,p}$ and $C_{Al,c}$ are the aluminium concentrations in these fractions respectively.

Elements with atmospheric enrichment factors of 10 or less are not considered to be significantly enriched in atmospheric particulates relative to a crustal source, whereas if the enrichment factor is in the range $10\text{-}10^4$, the elements are considered to be enriched. The majority of metals present in the atmosphere are associated with particulate material and size governs the atmospheric half-life of a particle. Settlement velocity is a complicated function of particle diameter and because large particles settle more rapidly, dry metal deposition from such particles will occur close to the source of pollution. Metals associated with smaller particles will become dispersed over greater distances, and removal by wet deposition becomes more important (Hardman *et al.* 1993). This explains the observed long-range transport of pollutant metals (Renberg *et al.*, 1994). Galloway *et al.* (1982) illustrated the importance of proximity to sources of pollution on the inventory, with the highest concentrations of metals being recorded in urban areas.

In the United Kingdom, the Department of the Environment monitors the air quality at sites around the country. A summary of the results for 1990/1991 is presented in Table 1.3 and the data reflects the influence of proximity to industry on the concentrations of many metals:

Table 1.3. Average concentrations of metals at selected sites around the United Kingdom, for 1990/1991, in ng m^{-3}.

Site	Cd	Cr	Cu	Fe	Mn	Ni	Pb	Zn
London[1]	1.3	4.3	28	1687	25	8.6	120	139
Leeds[2]	0.7	4.8	21	657	24	10	120	66
Motherwell[3]	1.3	3.9	64	1780	58	19	160	212
Glasgow[4]	1.4	2	27	539	13	8.3	92	95

1= Minster House, Vauxhall Bridge Road 2= Market Builidngs, Vicar Lane
3=Civic Centre 4=St. Mungos Academy

The high concentrations of the metals at the Motherwell site are due to the presence, at that time, of the Ravenscraig Steel Works and can be seen as an example of a point source of pollution.

Changes in the atmospheric concentrations of metals have been studied using ombrotrophic peat profiles, and these reflect the environmental impact of industrial activity over the last 1,500 years (Livett 1988). Lee & Tallis (1973) reported short but distinct increases in metal deposition in a peat core collected from Snake Pass in Derbyshire, dated to between 1500 and 2000 BP. It was concluded that Roman smelting operations close to the site had produced measurable fluxes of the metals. Renberg *et al.* (1994) in a study of pre-industrial atmospheric lead contamination in Swedish lake sediments demonstrated the importance of these pre-industrial events, not only at a local level, but globally. They reported that the cumulative deposition from anthropogenic sources in pre-industrial times (600 BC to AD 1800), was at least as large as the cumulative deposition during the industrial period (AD 1800 to present).

The latter part of the eighteenth century marked the beginning of a major period of prosperity of the lead industry in the United Kingdom, with the metal profiles at sites close to the smelters showing corresponding fluctuations (Livett *et al.*, 1979: Sugden et *al.*, 1991). Fluctuations were also recorded in remote sites, indicating that the lead smelters caused widespread contamination (Livett *et al.*, 1979: Livett, 1982). The Industrial Revolution, which began in the eighteenth century, also resulted in widespread increases in atmospheric metal content, which have been recorded in peat profiles (Livett *et al.*, 1979: Martin *et al.*, 1979: Markert & Thornton, 1990) and sediment profiles (Farmer *et al.*, 1980).

Ruhling & Tyler (1968) and Lee & Tallis (1973) investigated the twentieth century trends in atmospheric contents of heavy metals, suggested a lowering in the deposition rates of metals in certain localities of the United Kingdom and Scandinavia over the last 50-60 years. However, Livett (1988) in a summary of all the stratigraphic evidence produced from studies in Britain and Scandinavia concluded that these reductions were confined to specific rural sites, where the decline in local industries had led to an improvement in air quality. Recent reports do, however, suggest that the levels of metals in the atmosphere are being reduced and airborne concentrations of metals in the United Kingdom do not at present exceed internationally accepted guidelines (Harrison *et al.*, 1993).

Studies in North America have shown the dependence of the atmospheric Pb content on car exhaust emissions, and car exhausts have been described as the greatest single source of air contamination in the United States (Adriano, 1986). Pb alkyls were

first introduced to petrol as anti-knock additives in the 1920s, and led to significant increases in the output of lead from cars which peaked in the 1960s. Decreases in Pb fluxes by up to 80% between 1979 and 1983 have been proposed to be due to decreases in the Pb content of petrol (Eisenreich *et al.*, 1986). Miller & Friedland (1991) also reported decreases in the atmospheric Pb flux in North American forest soils, with the atmospheric fluxes measured in the 1990s being 90% less than those in the 1980s. They proposed that this was due to a combination of a reduction in heavy industry, as well as a reduction in the use of leaded petrol.

The source of atmospheric Pb can be studied by utilising the stable Pb isotope ratios. Elemental Pb is composed of four stable isotopes. ^{204}Pb is a primordial radionuclide whereas ^{206}Pb, ^{207}Pb and ^{208}Pb are the products of the U/Th radioactive decay series (Figure 1.4), with ^{206}Pb being the stable daughter product of the ^{238}U series, ^{207}Pb the stable product of the ^{235}U series, and ^{208}Pb the stable daughter product of the ^{232}Th series. Isotopic ratios of natural Pb vary considerably throughout the world. Uranium bearing minerals and ores contain a greater amount of ^{206}Pb, whereas thorium bearing minerals will be enriched in ^{208}Pb. Thus the isotopic ratio of mined Pb will depend on the uranium content of the ore, which determines the contribution of the radiogenic isotopes (Ault *et al.*, 1970).

Most Pb ores have $^{206}Pb/^{207}Pb$ ratios less than natural Pb of soils and soil-related components, since the accumulation of ^{206}Pb due to radioactive decay stops when lead is separated from U in the formation of ore bodies. Since virtually all Pb now present in the atmosphere originates from industrial sources, its isotopic composition is determined mainly by that of the ores which are used in the industrial processes or manufacture of petrol. The residence time of Pb particulates in the atmosphere is around 1-2 weeks, so the isotopic composition of the atmosphere will change accordingly (Shirahata *et al.*, 1980). The major contemporary source of Pb pollution is from car exhaust emission and interpretation of atmospheric isotopic Pb data is often complicated by temporal variations in the types of ore used in the manufacture of petrol Pb additives world-wide. Therefore, to accurately identify the source of deposited Pb in environmental systems it is necessary to establish the isotopic compositions of Pb ores and petrol in the region being studied (Sturges & Harrison, 1986). However, stable Pb isotopes have been used successfully in a variety of different studies, including the identification of the sources of childhood exposure to Pb, studies on Pb contamination in aquatic systems (Shirahata, *et al.*, 1980) and the study of the effect of the source of Pb on the Pb signatures of aquatic and terrestrial systems (Sugden *et al.*, 1991).

Isotopic ratios of a ^{210}Pb-dated sediment core from a rural pond in North America showed a decrease in value at the surface when compared to natural values at depth. This effect was explained by inputs of Pb from industrial sources which have been steadily increasing into the remote system over the last 100 years (Shirahata *et al.*, 1980). The input of pollutant lead into isolated systems was also demonstrated by Chow & Johnstone (1965) in a study of the isotope ratios of freshly fallen snow in an isolated region of California. The $^{206}Pb/^{207}Pb$ ratios of the snow closely matched those of petrol sold in the region. Sugden *et al.* (1991) demonstrated the importance of car exhaust emissions on the $^{206}Pb/^{207}Pb$ ratios of ombrotrophic peat cores in the United Kingdom. Decreases in the $^{206}Pb/^{207}Pb$ ratios were observed over the last 40-50 years due to the input into the atmosphere of particulate Pb with a low ^{206}Pb content from car exhausts. In the United Kingdom, the alkyl Pb compounds in petrol are manufactured from a mixture of Australian and Canadian ores, which give a lower $^{206}Pb/^{207}Pb$ ratio (~1.037), than industry and coal combustion (~1.170).

The Br/Pb ratio has also been utilised in an attempt to assign the importance of industry and car exhaust emission to the content of atmospheric particulate Pb, since bromine is also added to petrol. However, there are a number of problems with the method. Firstly, the Br/Pb content of petrol can be variable, and the specific ratio of the petrol in the area being studied must therefore be established. Also in order to assess the importance of industry on the ratios, suitable "background" or pre-industrial levels must be established (Harrison & Sturges, 1983). Sturges & Harrison (1986) were able to demonstrate the effect of industrial Pb from a lead smelter in West Yorkshire on the atmospheric Br/Pb ratio, and were also able to establish consistent pre-industrial background ratios.

The isotope signature studies reinforce the importance of car exhaust emissions on the atmospheric Pb content. In urban areas the influence of exhaust Pb is balanced by contributions from industrial and domestic emissions. But in rural and isolated regions, car emissions have predominated over industrial emissions for the last 40 years (Shirihata *et al.*, 1980: Sturges & Harrison, 1986: Sugden *et al.*, 1991).

1.8.2.2 SOURCES OF RADIONUCLIDES IN THE ENVIRONMENT

The sources of atmospherically-derived radionuclides, like atmospherically-derived metals, can be divided into two main groups - natural radionuclides, and anthropogenically-derived radionuclides produced as a consequence of human activities. Both sources result in the exposure of the public to ionising radiation.

Natural radioactivity in the environment comes from terrestrial and cosmic sources. Terrestrial radiation from the earth's crust accounts for the majority of natural radiation and is due partly to primordial radionuclides which have half-lives great enough relative to the age of the earth (estimated as 4.5×10^9 yr) to remain in detectable amounts. There are at least 22 primordial radionuclides which occur singly, not being part of a decay series. The majority of these have such long half-lives, small isotopic and elemental abundances and low biological uptake and concentration factors, that they are of little significance in terms of environmental dose. Terrestrial radionuclides are also present as decay series. Three of these series are found in nature (Figure 1.4), each headed by a primordial radionuclide with a half-life that is long relative to the age of the earth and they account for most of the terrestrial radioactivity. Within these series some of the most environmentally important radionuclides are produced. The ^{238}U series includes ^{230}Th ($t_{1/2}$ = 75,400y), which may be the most significant contributor to the lung dose from inhaling uranium bearing dusts, ^{226}Ra ($t_{1/2}$ = 1600y) and its gaseous daughter ^{222}Rn ($t_{1/2}$ = 3.83d). The ^{232}Th series also produces a gaseous isotope ^{220}Rn ($t_{1/2}$ = 55s) (Kathren, 1984). These gaseous short-lived radionuclides diffuse out of the rocks and soils where they are produced and enter the atmosphere, contributing to the content of radionuclides in the environment. ^{222}Rn ($t_{1/2}$ = 3.83d), due to its gaseous nature, is the largest single contributor to the natural radiation dose. The content of radon isotopes in the air depends on the rock type which determines the concentrations of precursers in the soil, and also soil porosity and grain size. Snow cover or ice cover and high soil moisture result in limited diffusion of radon from the soil surface (Kathren, 1984).

Cosmic radiation includes both primary ionising radiation of extraterrestrial origin, and secondary radiations which result from their interactions with the atmosphere. These radionuclides generally have low atomic weights and half-lives ranging from 32 min (^{34m}Cl), to 2.5×10^6 y (^{10}Be). The shorter lived ones usually decay before settling to earth and entering the biosphere (Kathren, 1984). The short lived cosmogenic radionuclides can be used as tracers of various atmospheric processes, e.g. precipitation scavenging (Olsen *et al.*, 1985). Of all the cosmogenic radionuclides ^3H ($t_{1/2}$ = 12.3y) and ^{14}C ($t_{1/2}$ = 5730y), are the most important biologically. The role of ^{14}C in the carbon cycle is discussed in section 1.8.4. As a result of its role in the carbon cycle it becomes incorporated into the biosphere, ultimately through fixation by photosynthesis.

Figure 1.4 The uranium and thorium natural decay series.

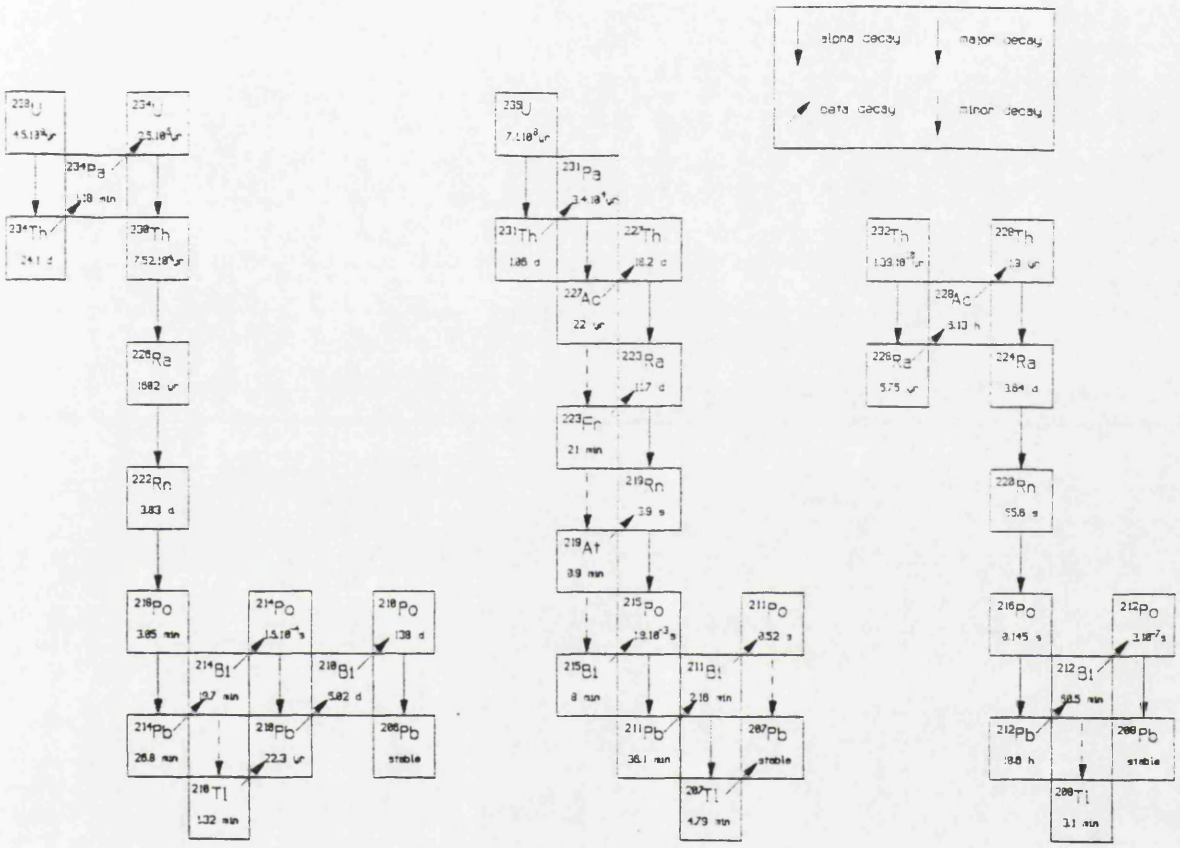

In addition to the cosmic and terrestrial radiation sources, atmospheric radionuclides may come from artificially produced sources. These anthropogenically induced radiation sources can be attributed to three main processes: fallout from nuclear weapons testing, routine emissions from nuclear installations, and accidental emissions from nuclear installations.

The advent of nuclear weapons testing in the years following the second world war resulted in major inputs of radionuclides into the atmosphere (Table 1.4). As with the atmospheric deposition of metals, weapons testing resulted in global and point source fallout. After detonation the larger particles settle to the earth, being deposited within a hundred miles of the point of detonation. The smaller particles which contain most of the volatile fission products remain suspended for longer periods of time and fall out over a larger area mainly in the same hemisphere, giving a global pollution pattern (Kathren, 1984). Of the more than 200 fission products produced by nuclear explosions, only a relatively small number have half-lives sufficiently long to be environmentally important.

Table 1.4 Radionuclides introduced into the atmosphere as a consequence of weapons testing.

Nuclide	Half - life
^{239}Pu	24360y
^{240}Pu	6540y
^{241}Pu	15y
^{241}Am	433y
^{89}Sr	50.5d
^{90}Sr	28y
^{106}Ru	369d
^{131}I	8.85d
^{137}Cs	30.3y
^{140}Ba	12.8d
^{144}Ce	284d

It has been estimated that 1.26×10^6 TBq of ^{137}Cs had been introduced to the environment prior to 1970 by nuclear weapons testing (Joseph, 1971), as a result of a total of 200 megatons of atomic and H-bomb tests. Due to the Atmospheric Test Ban Treaty of 1963, little bomb testing is still carried out, however some countries are still developing their nuclear capabilities and are still carrying out weapons testing. As a

consequence of this it is estimated that another 9.6 x 10^5 TBq have been introduced into the atmosphere since 1970 (UNSCEAR, 1982). Widespread global fallout of ^{137}Cs derived from weapons testing occurred during the early 1960s, when weapons testing was at its maximum. In the middle stratosphere ^{137}Cs has a residence time of 6-12 months (Joseph, 1971), and due to its 30y half life, ^{137}Cs is environmentally persistent. ^{137}Cs can be immobilised by the clay fraction of soils, resulting in reduced bioavailability (Segal & Morris, 1991) however, in some organic soils it can be mobile, and this will be discussed further in section 1.8.3.

As far as other radionuclides are concerned, 10^8 MBq of ^{131}I, 10^6 MBq of $^{89,90}Sr$ and 10^5 MBq of $^{239,240}Pu$ were released (Santschi & Honeyman, 1989). Of these ^{239}Pu is the most important due to its long half-life, and persistence in the environment. Most of the Pu injected into the atmosphere has fallen out onto the soil surface and is present in the soil as an oxide, resulting in potential immobility (Kathren, 1984). However, as discussed in section 1.8.3, Pu has some mobility in organic soils.

Two cosmogenic radionuclides, ^3H and ^{14}C, have had their atmospheric content increased due to neutron activation induced by atmospheric weapons testing. This led to increases in the content of ^3H in the atmosphere, and during 1962 it was estimated that 3 x 10^7 TBq of ^3H were added to the atmosphere (Kathren, 1984). In addition, approximately 2.2 x 10^5 TBq of ^{14}C was introduced to the atmosphere through weapons testing (UNSCEAR, 1982), which along with the contradictory Suess effect has significantly distorted the natural ^{14}C levels, thus affecting radiocarbon dating.

The atmospheric discharge of radionuclides from nuclear reactors represents a point source of pollution. It does not contribute to the global radionuclide loadings produced from weapons testing. However, longer range transport of radionuclides cannot be discounted. Radioactive noble gases, along with tritium are the main source of activity released from operating nuclear power reactors, with the quantity and constituents of release varying from plant to plant (Table 1.5).

The most important radiological effects of nuclear power, apart from accidental discharges such as Chernobyl, are connected to the mining of uranium, which can also result in the localised release of radionuclides to the environment. To remove the build-up of radioactive dusts and ^{222}Rn gas, uranium mines are well ventilated, with the exhausted air discharged directly to the atmosphere. Uranium mines exhaust 10^3-10^6 cubic feet of air per minute, containing 650-2600 Bq/m^3. For an estimated 200 days per year production, this would give a release of 3 TBq of ^{222}Rn into the atmosphere annually (Kathren, 1984).

Table 1.5 Radioactive atmospheric discharges for 1991, in TBq.

Site	Noble Gases[1]	Tritium
Sellafield	40200	621
Power stations[2]	9842	1900[4]
AEA Technology[3]	586	58

1. Main concentrations of noble gases at each site are as follows:
Sellafield, ^{85}Kr and ^{41}Ar. Power stations, ^{41}Ar. AEA technology, ^{85}Kr, ^{41}Ar, and other isotopes of Kr and Xn.
2. Includes all Nuclear Electric plc, Scottish Nuclear Ltd and Chapelcross power stations.
3. Trading name of UKAEA (sites at Winfrith, Dounreay & Harwell).
4. Only Chapelcross data available.

(D.O.E. 1992).

The most important and environmentally significant releases of radionuclides to the atmosphere from nuclear power are associated with reactor accidents. The first of these occurred in October 1957 at Windscale, in Cumbria. An estimated 740 TBq of ^{131}I, 46 TBq of ^{137}Cs, 3 TBq of ^{89}Sr and 3.3 GBq of ^{90}Sr were released. The release of this quantity of ^{131}I to the environment resulted in widespread contamination of milk, as well as exposure to radiation through inhalation (Kathren, 1984).

The accident at the Chernobyl nuclear power station in the Ukraine, on the 26 April 1986, was the world's most serious nuclear power accident. The No.4 reactor exploded, releasing a plume of radioactive gas which was initially transported in a north-westerly direction towards the Baltic, where it split into three major parts. In section 1.8.2.1 long-range transport of pollutant metals released from point sources was discussed, and the accident at Chernobyl resulted in widespread contamination of western Europe due to movement of the radioactive plume released (Livens *et al.*, 1992). ^{131}I from Chernobyl was also recorded in North America, from a section of the plume which arrived on 9-10 May, possibly by a circumpolar route (Schell & Tobin, 1990), and a snow layer in Greenland containing fission products was found in the ice sheet (Davidson *et al.*, 1987). Thus, to some extent the accident at Chernobyl has resulted in global contamination, although not to the same degree as weapons testing.

One section of the plume moved to the south-west towards central Europe, and then turned north-west towards the U.K. This section of the plume reached the south of England on 2 May, moving north over the following days (Livens *et al.*, 1992). Due to heavy rainfall in Wales, Cumbria, and south west Scotland, high levels of fallout of ^{134}Cs, ^{137}Cs, ^{131}I and ^{103}Ru occurred (Smith & Clark, 1989: Livens *et al.*, 1992). The levels of individual radionuclides emitted at one and ten days after the explosion are shown below:

Table 1.6 Radionuclides emitted during the Chernobyl accident in PBq

Radionuclide	Activity After 1 Day	Activity After 10 Days
^{131}I	170	440
^{137}Cs	10	50
^{134}Cs	5	25
^{90}Sr	0.5	9
$^{239, 240}Pu$	0.01	0.07

(Smith & Clark, 1989: Sumner, 1987)

Weapons testing had produced a total global concentration of 19.6 x 10^{17} Bq ^{137}Cs, which gave a surface activity of 1.9 x 10^{2} Bq m^{-2}. The Chernobyl accident resulted in an atmospheric activity of 1 x 10^{17} Bq of ^{137}Cs which gave a surface activity of 0.1 - 1.0 x 10^{2} Bq m^{-2} for western Europe alone (Santschi & Honeyman, 1989). Rainfall samples collected in Cumbria during the period 4-19 May 1986 showed considerable activties of ^{137}Cs, ^{134}Cs, and ^{131}I. Maximum activities of ^{131}I in the rainfall reached 34 Bq l^{-1}. In Cumbria, the levels of ^{137}Cs in soils increased from approximately 100 Bq m^{-2} before the accident, to approximately 7000 Bq m^{-2} after the accident (McDonald *et al.*, 1992). Due to the release of ^{134}Cs, which was not present in weapons testing fallout, the relative contribution of Chernobyl to the levels of ^{137}Cs in the environment can be assessed utilising the Chernobyl $^{134}Cs/^{137}Cs$ activity ratio which was around 0.55 at the time of release (Horrill *et al.*, 1988).

The radionuclides present in the Chernobyl plume were deposited by wet and dry deposition as described below, and were then incorporated into the aquatic and terrestrial environment. The influence of Chernobyl on environmental systems has been studied and of particular importance is the mobility of radiocaesium in the upland systems affected by the accident (Coughtrey *et al.*, 1990: Horrill *et al.*, 1990) as discussed further in section 1.8.3.

Radionuclides in the atmosphere are potentially harmful to human's since they are sources of ionising radiation. Radiation of the skin and inhalation of nuclides can give direct exposure to radiation and are especially important for short-lived nuclides which decay before exposure by other pathways. The direct radiation pathway results from the exposure of man from a plume of fallout, and the noble gases released from nuclear power plants are associated with this pathway (Kathren, 1984). Cosmic radiation can also result in direct exposure of the body to ionising radiation, with altitude being important in assessing the contribution from this source (Burkhart,

1991). Inhalation is also a direct pathway, and this is particularly important for the gaseous natural radionuclides ^{222}Rn and ^{220}Rn, which then become deposited in the lung giving direct irradiation of the tissue by alpha particles (Burkhart, 1991).

Deposition on soil and plants, and inhalation by animals, can be seen as indirect pathways, since the radionuclide becomes incorporated within the food chain before being transferred to man. One exception to this pathway is the inhalation of contaminated soil (Kathren, 1984). The potential pathways of entry into the food chain are many and complex, and the major routes are summarised in Figure 1.5.

Figure 1.5 Radionuclide transfer in the food chain.

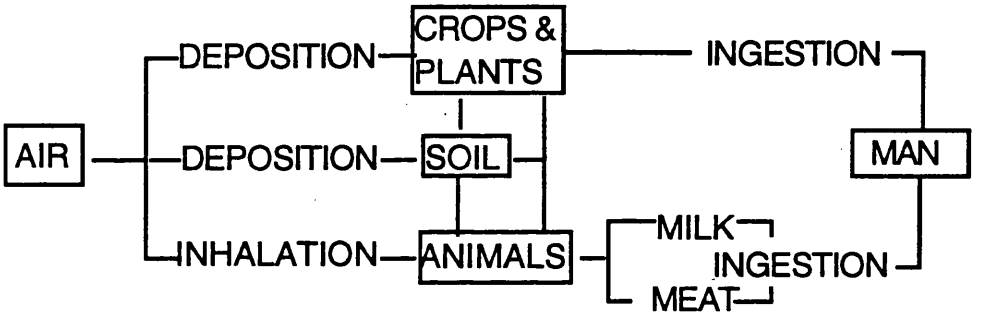

(Segal & Morris, 1991).

The movement of radionuclides through the food chain results in the radioactivity passing through one or more organisms before it reaches man. Radionuclides can potentially concentrate in any one part of this food chain, and the concentration ratio (C.R.), or concentration factor, can be calculated as:

$$C.R. = \frac{(\text{CONCENTRATION IN CONSUMER})}{(\text{CONCENTRATION IN ENVIRONMENT})}$$

Concentration or bioaccumulation occcurs if this ratio is greater than 1. These ratios are useful in predicting the rates and routes of transfer of radionuclides through the food chain to man, and are necessary for the calculation of radiation doses. The ratios are affected by many factors including the chemical and physical form of the radionuclide in the environment, the biological need for the element by the plant and animal, climatic factors, the specific tissue or organs affected and the age of the organism (Kathren, 1984).

Kirkton *et al.* (1990) measured plant concentration ratios for ^{134}Cs transfer from upland soils to upland plant species and observed ratios extending from 2 to 14. Thus bioaccumulation was occurring, with the different species exhibiting different abilities

to accumulate ^{134}Cs. An interesting observation from the study was that ^{134}Cs from Chernobyl was more available for uptake than pre-Chernobyl ^{137}Cs.

1.8.3 FACTORS AFFECTING THE DISTRIBUTION OF DEPOSITED METALS AND RADIONUCLIDES IN PEAT PROFILES

Heavy metals and radionuclides can become incorporated in peat profiles either directly through the exposed surface peat, or indirectly via the vegetation cover. Once incorporated within the peat profile a number of factors can affect their distribution.

One such factor is the vegetation itself. First of all this plays an important role in trapping the pollutants and conveying them to the peat profile, and unvegetated sites have been shown to give lower inventories of ^{210}Pb than vegetated sites (Olsen, 1985). In addition, the type of vegetation is also important in this transfer process.

Sphagnum spp. have been shown to be particularly efficient at trapping metals since they have no vascular system and can allow unrestricted exchange of solutes between the plant tissue and the atmosphere (Livett, 1988). The metals then accumulate in the cell wall and intracellular membranes, and the ability of these species to retain metals is attributed to their high polyuronic acid content, which can complex the metals (Clymo, 1963). However, *Sphagnum* mosses are not the only plant species present in bog ecosystems. Vascular plants such as *Eriophorum* spp. or *Carex* spp. are often predominant, and do not take up metals across the leaf surface like the *Sphagnum* spp. Instead, metals are captured on the leaf surface and incorporated within the peat profile on leaf fall. The turnover rate of the plant litter can therefore affect the residence time of these metals in the vegetation. Therefore, a time lapse could occur before incorporation of a metal into the peat profile, and erosion could remove significant amounts of the metal from the surfaces of the litter (Livett, 1988).

Remobilisation of metals within the peat profile can be caused by the vegetation. The root systems of vascular plants are involved in the active uptake of the pore water, and therefore any element which is present in that water. Downward movement of metals within the profile can also be facilitated by the root channels which penetrate the peat (Clymo, 1983). Most species root systems concentrate within the top 20 cm of peat profiles, but some root systems, e.g. *Eriophorum* spp., can extend to 60 cm (Livett, 1988). Metals which are essential for plant growth could be recycled within the surface peat by the above processes, and the distribution of ^{137}Cs in peat profiles has been proposed to occur in this way (Oldfield *et al.*, 1979: Clymo, 1983: Mitchell, *et al.*, 1992). Damman (1978) was able to demonstrate that K and Na were actively

taken up from surface peat by the vegetation, in particular the vascular plants. The *Sphagnum* mosses were also showing some active uptake of K, challenging the hypothesis that they were obtaining all of their nutrients from the atmosphere. Pakarinen (1978) also demonstrated small scale redistribution of metals by *Sphagnum* mosses. *Sphagnum spp.* and *Calluna vulgaris* have also been shown to have higher ^{137}Cs concentrations than other vascular plants (Horrill *et al.*, 1990: Colgan *et al.*, 1990).

K, Na and Cs will favour this kind of cycling because of their chemistry. They tend to form outer sphere complexes (for full classification refer to section 1.7.1.1.), and thus are retained in exchangeable forms within the peat. Tipping & Hurley (1988) in a model of metal complexation processes in acid soils were able to demonstrate that Na was held by electrostatic interactions, whereas Al was predominately complexed with the humic substances. The Na was then in direct contact with the soil solution making it readily exchangeable.

Cs is however less mobile in soils with higher clay content, in particular micaceous clays, which can trap the Cs in interstitial layers, thus removing it from the soil solution. However, in organic soils this occurs only to a limited extent depending on the clay content, and the Cs is predominately present in the soil solution (Maguire, 1993).

The rate of incorporation of plant material into the peat profile is affected by the temperature, water supply, oxygen supply, the nature of the plant material, and the microbiological environment (Clymo, 1983). All of these factors are highly interactive and affect the rate of accumulation of the peat profile. Peat accumulation depends on the amount of plant material produced at the surface and the rate at which this is decayed and compacted (Johnson *et al.*, 1990). Therefore a more waterlogged peat profile will result in a low rate of decay and low degree of humification, low oxygen content, reducing conditions at depth, specialised plant species and a higher accumulation rate. A more aerated, humified system will result in the breakdown of the organic matter with a loss of structure of the plant material, a change in chemical state of the peat, an increase in bulk density, and a lower accumulation rate (Clymo, 1984).

The difference in peat type caused by the different moisture regime can affect the distribution of metals within a profile by affecting:

(1) COMPACTION & DECOMPOSITION PROCESSES
(2) THE REDOX ENVIRONMENT
(3) THE MOVEMENT OF WATER IN THE PROFILE.

Urban *et al.* (1990) commented on the distortion of metal profiles due to compaction and decomposition processes. As with all the processes which affect these profiles, the processes also affect the relationship between the depth and age, and therefore the chronology of the system (Damman, 1978).

Decomposition is most likely to occur in aerated, humified profiles, such as peat colonised by *Eriophorum* spp., and this results in loss of structure and a greater bulk density. The loss of carbon gives accumulation of metals at that point in the profile (Urban *et al.*, 1990). In waterlogged systems, decomposition is reduced and as plant matter accumulates compaction can occur. Partial decay weakens the structure of the plant material, usually *Sphagnum* mosses, until eventually the weakened moss can no longer support the weight of the waterlogged system giving collapse and compaction. This is illustrated in the profile by a sudden increase in bulk density (Clymo, 1983). Compaction can cause increases in metal content at the point of compaction and causes irregularities when assessing accumulation rates in a profile (Appleby & Oldfield, 1978).

The redox environment is ultimately controlled by the water content of the peat. In many peat systems there is a surface zone of aerobic decay overlying a subsurface anoxic zone. The surface zone is often referred to as the acrotelm, and is distinguished by its high hydraulic conductivity, as compared to the anoxic catotelm (Ingram, 1978). The depth of each layer is dependent on the depth of the water table, and the distinction between the oxic and anoxic conditions is often not clear cut, giving a zone of water table fluctuation with a fluctuating redox environment (Clymo, 1991: Damman, 1978).

Aaby & Jacobsen (1979) observed that enrichment of metals in peat profiles, which is often assumed to be due to increases in deposition often coincides with the junction between well and poorly humified peat, at the zone of water table fluctuation. Damman (1978) studied the distribution of Na, K, Mg, P, Ca, Al, Fe, Mn, Pb, and Zn in ombrotrophic peat cores and showed that the redox environment can affect the distribution of Al, Fe, Mn, Pb, and Zn, whereas biological and hydrological effects accounted for the distribution of the other elements. Fe and Mn were removed from waterlogged, anoxic profiles, and were retained in the aerated profiles. Al, Pb and Zn were removed from the anoxic, permanently waterlogged profiles, but were shown to accumulate at the zone of water table fluctuation. Glooschenko *et al.* (1986) observed secondary peaks for Cu and Pb at depth in peat profiles and proposed that this could be due to fluctuation at the zone of water table fluctuation. The loss of Fe and Mn from peat profiles was also observed by Sugden (1993), with no loss of Pb, indicating that

water saturation had been transitory and only caused enough of a redox change to influence the Mn and Fe.

Urban *et al.* (1990) also observed loss of Pb from permanently saturated profiles, and enhancement at the zone of water table fluctuation. However, here, the enhancement was proposed to be due to the combination of decomposition of organic matter in the aerobic zone, and leaching effects in the anaerobic zone. No relationship between the redox environment and redistribution of Al, Pb and Zn was seen in peat cores analysed by Jones & Hao (1992), although the three metals did show similar distribution profiles.

The redistribution of deposited metals in peat profiles is also catalysed by the movement of water through the peat profile. Dumontet *et al.* (1990) proposed that chemical diffusion was involved in the downward migration of Cu and Zn, although Clymo (1983) proposed that diffusion was of less importance to metal migration than biological cycling or mass flow. Vertical and lateral flow of water can occur, and in the aerated surface layers of the peat hydraulic conductivity tends to be high favouring vertical flow. Olsen (1985) demonstrated that rainwater can penetrate to depths of 10 cm in unsaturated surface peat and move easily due to the high hydraulic conductivity. However, if the profile was saturated little penetration and movement could occur. Clymo (1983) proposed that once the water table is reached, and hydraulic conductivity is reduced, lateral flow becomes more important to metal movement than vertical flow. Oldfield *et al.* (1979), El-Daoushy (1988) and Urban *et al.* (1990) proposed that the loss of metals from peat cores was due to lateral flow. Vertical mobility of Cs was reported by Mitchell *et al.* (1992), and up to 50% of Cs was estimated to be lost from a peatland through a combination of vertical and lateral flow (Clymo, 1978). Coughtrey *et al.* (1990) found that ^{137}Cs was moving predominantly through lateral flow in upland pasture.

Although ombrotrophic peats are assumed to be removed from groundwater influences, the effect of the groundwater on the profile cannot always be discounted. Hill & Siegel (1991) demonstrated that major variations in the concentrations of the cations Ca, Mg, Sr, Fe, and Na were due to groundwater discharge only, whereas the concentrations of Cu, Ni, Pb, and Zn in the profile were related to groundwater discharge combined with atmospheric loadings. The hydraulic conductivity at depth is often assumed to be low due to waterlogging and compaction effects, yet if macrostructures such as buried wood exist, the hydraulic conductivity could be enhanced.

From the above studies it can be seen that the assumption that metals are immobilised on incorporation into peat profiles through complexation processes is

often unfounded. As well as the conditions within the peat profile, and the peat type, metal type appears to play an important role in the interaction of the metal with the peat, and its diagenesis within the profile. The Class A metal cations, such as Na, K, Mg and Cs which bind through outer sphere complexes show considerable mobility since they are held in readily exchangeable forms (Bonn & Fish 1993) and are unaffected by redox transformations within the peat profile (Damman 1978). The Class B metal cations, such as Pb, Zn and Cu, however, can form inner complexes with the soil organic matter, and the formation constants of these complexes are often high (Stevenson, 1982) so movement of these metals through a profile is not expected. However, Shotyk *et al.* (1992) proposed that complexation by organic matter was not the main process controlling the behaviour of these metals in peatlands, with the redox environment being a more important control. Fe and Mn were shown to be present as aqueous species illustrating their solubility in reducing conditions, whereas Cu was present in an insoluble form in reducing conditions. Jones (1987) utilised sequential extraction to study the chemical forms of Cu, Zn, Pb, Fe and Mn in peats. Cu was found to be associated with the organic matter fraction, giving predominantly insoluble forms, particularly at depth in the profile, indicating that incorporation of deposited Cu from particulate to organic form can take time. Mn and Fe were found to occur largely in oxide form whereas Pb and Zn were found to occur in high proportions in exchangeable, soluble forms, as well as in the residual fraction. In particular higher proportions of Pb and Zn were found in soluble forms in waterlogged peat profiles. There was evidence to suggest that the Fe and Mn oxides were scavenging Pb and Zn, perhaps when in association with low molecular weight organic matter. The oxides, when coming into solution in reducing conditions, released Pb and Zn and gave increases in soluble forms of Pb and Zn in waterlogged systems. Harrison et al. (1981), in a study of the chemical associations of Pb, Cd, Cu and Zn in soils, found that Pb and Zn were again present predominantly in oxide form, with Cu being predominantly associated with the organic material. The solubility of Zn and Pb in acidic peat profiles was also demonstrated by Shotyk *et al.* (1992), but in this study these metals did not have a redox dependency.

The solubility and movement of metals has also been proposed to be due to the concentration of dissolved organic matter. Urban *et al.* (1990) showed that the leaching of Pb from waterlogged profiles was correlated with the concentration of dissolved organic matter. The formation of dissolved organic matter, or the release of soluble humic substances from the organic matter, is dependent on the pH and metal content which controls humic charge (Tipping & Woof, 1990). At pH values below 5, Tipping and Woof (1991) found that the majority of Al in solution was in inorganic

form, whilst at higher pH values soluble organic complexes were more important for the movement of Al.

The profiles of metal concentration with depth, should therefore, always be interpreted with caution since as Jones and Hao (1992) point out:

"there is insufficient evidence to support the assumption that all metal deposition records retain their chronological integrity"

1.8.4 DATING THE PEAT PROFILE: ESTABLISHING A HISTORY OF DEPOSITION

In calculating the chronology of a peat profile, a relationship is established between depth and age, which can be applied to the profiles of metal concentration versus depth to give the deposition history of the profile. Problems do exist in establishing these relationships due to variations in the accumulation rates, the remobilisation of elements, and the decay and compaction processes discussed in section 1.8.3, which upset the chronological integrity of the profile. Consequently, care must be taken in the interpretation of these profiles.

A variety of dating mechanisms can be used to establish a chronology in a peat, and the mechanism used depends on the time scale being studied. Since the vegetation of ombrotrophic peat systems is dominated by *Sphagnum* mosses, the annual growth increments of these can be used to provide a chronology of deposition over the last 50 years (Pakarinen & Tolonen, 1977). The method involves utilising the seasonal growth periodicity which is reflected by a cyclic zonation in branching patterns and pigmentation in straightened *Sphagnum* stems. From this, the annual increments are calculated, by dividing the mean stem length with the mean increment length (El-Daoushy *et al.*, 1982). The technique is particularly useful in dating surface peat horizons where other methods cannot be used. However, it requires a well established colony of *Spagnum* and its application is limited to poorly humified, waterlogged systems where the structure of the vegetation is maintained (Livett, 1988).

One of the most widely applied dating mechanisms is a radiometric technique, which utilises ^{210}Pb. In rocks and soils the decay of ^{226}Ra (half life 1600y) generates the gaseous daughter isotope ^{222}Rn (half life 3.83d), which diffuses into the atmosphere and decays to give ^{210}Pb (half life 22.26y). The ^{210}Pb is then removed from the atmosphere by wet and dry deposition with a mean atmospheric residence time of 5 days (Nozaki *et al.*, 1978). Thus, there is a direct input of unsupported ^{210}Pb

onto the surface of the peat, as well as the *in situ* production of supported ^{210}Pb from the mineral material within the profile (Robbins, 1978).

There are two ^{210}Pb dating schemes which can be utilised to give chronologies spanning 100-150 years, namely the constant initial concentration model (c.i.c.) and constant rate of supply model (c.r.s.) (Appleby & Oldfield, 1978). These have been extensively applied to the dating of aquatic sediments, and have since been applied to ombrotrophic peat systems (Oldfield *et al.*, 1979: Schell, 1986: Cole *et al.*, 1990).

The c.i.c. model is based on the assumption that there is a constant initial concentration of unsupported ^{210}Pb falling on the surface of the peat, and that the sedimentation rate is constant, giving the following relationship:

$$\frac{dA}{dM} = \frac{\lambda A_o}{S_r} e - \lambda\left(\frac{m}{S_r}\right)$$

where A_O is the cumulative inventory of unsupported ^{210}Pb, m is the cumulative dry mass, $\lambda = \frac{\ln 2}{22.26}$ and S_r is the accumulation rate.

To calculate a chronology the unsupported ^{210}Pb is plotted on a logarithmic scale against cumulative dry mass. If a linear profile is produced the accumulation rate (S_r) can be obtained from the gradient of the line, $\frac{-\lambda}{Sr}$,

A chronology is calculated by dividing the cumulative weight to various depth intervals by the accumulation rate (Robbins, 1978). Non-linear profiles can occur when there are changes in the accumulation rate and due to this effect the c.r.s. model was developed (Appleby & Oldfield, 1978).

In the c.r.s. model a date is calculated for each increment in the profile using the following equations:

$\varnothing = \lambda \times A_o$ where $\varnothing$ is the annual unsupported ^{210}Pb flux, λ is the decay constant, and A_o is the cumulative inventory of unsupported ^{210}Pb, in the profile. The age of a depth increment, where the total inventory of ^{210}Pb has decayed to A, can then be calculated as follows:

$t = \frac{1}{\lambda} \ln \frac{A_0}{A}$ The c.r.s. ages are then used to calculate an accumulation rate (El-Daoushy, 1988).

The inventory of ^{210}Pb in a profile should always be based on, or related to depths, expressed in mass equivalent units, rather than length units, since this removes any effects of changes in the core due to compaction or decomposition processes (Clymo *et al.*, 1990).

Cole *et al.* (1990) observed changes in the accumulation rate in the surface of ombrotrophic peat, and therefore utilised the c.r.s. model to determine the chronology, and resultant deposition history. El-Daoushy *et al.* (1982) applied both models and compared the results to dates derived from the moss increment method. They found that the dates calculated using the c.i.c. model were underestimated in comparison to the moss increment dates. The c.r.s.-derived dates gave good agreement with the moss increment dates, but with higher statistical uncertainties at depth. Urban *et al.* (1990) found that the c.r.s. model was underestimating ages of ombrotrophic peat, when the dates were compared to those derived from pollen diagrams and horizons of trace organics, and they proposed that this was due to leaching of ^{210}Pb from the profiles. However, they also proposed that in some profiles sporadic leaching could result in errors which may cancel each other out, resulting in the model appearing valid. The leaching of Pb from profiles was discussed in depth in section 1.8.3., and can be seen to be a potential disadvantage to the method. ^{210}Pb can cycle within the surface peat, causing fluctuations in the dates. As a result, Malmer & Holm (1984) proposed that the method could not be used as a dating technique for the surface peat. Robbins & Herche (1993) pointed out that the c.r.s. model is a point transform model, rather than a true process model and therefore it cannot be used to predict profiles and carries no test of validity. As a result the c.r.s. model can potentially fit any profile and give a reasonable depth profile.

Another radiometric dating technique is radiocarbon dating, which can be used to date profiles older than 200 years. ^{14}C is produced continually in the upper atmosphere by the irradiation of atmospheric nitrogen by neutrons from cosmic radiation. After formation ^{14}C quickly combines with oxygen to form $^{14}CO_2$ which mixes with the CO_2 in the biosphere and becomes incorporated into the carbon cycle through photosynthesis and the oceans as dissolved carbonate. In organic matter which is no longer exchanging carbon, there is loss of ^{14}C by radioactive decay with no subsequent replenishment (Aitken, 1990).

Radiocarbon dating has been important in assigning timescales for studies of pre-industrial atmospheric deposition (Renberg *et al.*, 1994), and is also used to assign dates which validate pollen diagrams (Aitken, 1990).

Pollen diagrams can be utilised to derive a chronology, providing a series of independent dating features are present which reinforce each other. Some dating features may be reasonably specific e.g., the increase in cereal cultivation during the Napoleonic Wars period 1790-1815 A.D., whereas other pollen features have more diffuse limits e.g., the cessation of hemp cultivation, sometime between 1730-1770 A.D. (Livett *et al.*, 1979). The use of pollen diagrams to date profiles has been

significantly reduced by the advent and development of radiocarbon dating and instead is mainly used to reconstruct past climatic changes (Aitken, 1990). However, it is often used in combination with other dating mechanisms to give independent verification of a chronology (Oldfield *et al.*, 1979: Clymo *et al.*, 1990: Cole *et al.*, 1990: Gorres & Frenzel, 1993).

Another group of radiometric dating mechanisms utilises the distribution of fission-product radionuclides in the profile, based on the history of radioactive fallout. In particular, the atmospheric testing of nuclear weapons began in 1954, and the period of peak fallout was 1963-1964. ^{137}Cs was originally used to date lake sediments, and has also been applied to the dating of peat profiles (Aaby & Jacobsen, 1979: Oldfield *et al.* 1979). From the discussions on the redistribution of elements in peat profiles, in particular the mobility of ^{137}Cs, this nuclide is no longer utilised as a dating mechanism (Schell, 1986: Clymo, 1984). Other products of weapons testing such as ^{239}Pu and ^{241}Am have also been shown to be remobilised in peat profiles (Oldfield *et al.*, 1979), with this movement being proposed to be due to the movement of dissolved organic matter (Mitchell *et al.*, 1992).

CHAPTER 2

THE ISOLATION OF AND CHARACTERISATION OF HUMIC SUBSTANCES

2.1 INTRODUCTION

In this chapter the effect on the functional group arrangement and content of the extraction and fractionation procedure used to isolate humic acid will be considered.

As discussed in section 1.7, there is controversy over whether the extraction and fractionation procedure does alter the humic substances in any way. In particular, the alkali extraction step is seen as potentially the most destructive step due to the oxidative properties of the alkali and the long reaction times used (Stevenson, 1982). The aim of the extraction procedure is to extract humic acid from the soil free of contaminants such as polysaccharides or ash, with minimal disturbance to the material. In this study NaOH was used as an extractant since it is highly efficient at extracting humic substances from the soil. It acts by raising the pH, causing the acidic groups to ionise giving an opening up of the structure. The ionised groups are also soluble and result in the humic substances coming into solution (Hayes, 1991). It was also chosen in order to investigate whether or not any changes in the functional group contect could be detected after alkali extraction. Protonation of the humic acid and unextracted peat was also carried out. Protonation is a common purification procedure aimed at removing further any existing metals on humic substances (Piccolo & Stevenson, 1982).

A diagram of the extraction and fractionation procedure is presented in Figure 2.2. 0.5M NaOH was chosen since it is a stronger extractant than the 0.1M recommended by the I.H.S.S., and can potentially give a lower ash content. Therefore, no further purification step was required to remove the ash (Schnitzer & Khan, 1972). In order to minimise any possible auto-oxidation effects, the extraction process was carried out in a nitrogen atmosphere, as recommended by Swift & Posner (1972).

The functional groups are the reactive constituents of the humic substances and any potential alteration of these groupings has consequences for the reactivities of the substances towards metals. To investigate changes in the functional group content, several different methods were utilised, which collectively gave a more representative investigation than one method. The total acidity and carboxyl content determinations are well established characterisation procedures (Schnitzer & Khan, 1972: Stevenson, 1982), which have been used extensively to characterise humic and fulvic acids, but little information on these contents in unextracted humic substances exists in the literature.

Infra-red spectroscopy was also utilised since it was readily accessible and can give information on the functional group content. Unlike the total acidity and carboxyl

group determinations, is a non-destructive estimation which requires no further chemical treatment (Stevenson, 1982).

The characterisation procedures used are summarised in Figure 2.1, and with the exception of elemental analysis were carried out for both unextracted peats, their protonated forms, their humic acids and the protonated forms of the humic acids.

Figure 2.1 The characterisation procedures utilised in the study of the isolation of humic acid.

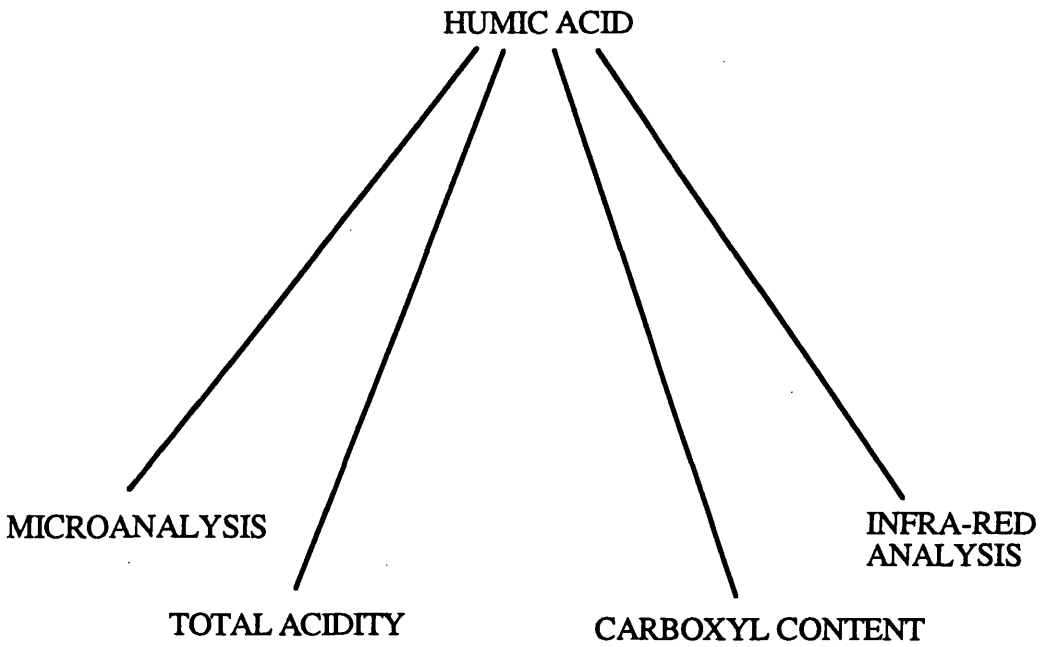

The phenolic content of the humic substances was not estimated, although it can be estimated from the difference in values between the total acidity and carboxyl values. However, this can result in the errors associated with both methods being carried directly into the phenolic estimation (Bonn & Fish, 1991). The modified Ubaldini procedure (Stevenson, 1982) can be used to calculate the phenol content, but cannot be viewed as satisfactory with materials which exhibit a wide range of pKa values (Hayes & Swift, 1978). Therefore it was not a parameter which was viewed as useful in this study.

2.2 METHODS

2.2.1 EXTRACTION, FRACTIONATION AND PURIFICATION OF HUMIC ACID

The origin of a humic substance, and in particular the vegetational background, can affect the composition and reactivity of the substance (Bonnet and Cousins, 1987 : Krosshavn, 1992). Therefore, two peats and their corresponding humic acids were characterised, in order to investigate the relationship between origin and functional group content.

Both peat samples came from the Shetland Islands. Huxter peat was black in colour and contained only a few roots. The peat was sticky to touch and appeared to be highly humified. Lunga Water peat, by contrast, was light brown in colour and had a high content of root material.

Prior to extraction, the peat samples were air dried for 24 hours before being macerated in a blender. 100g of the macerated peat was then suspended in 1l of 0.5M NaOH and stirred for 24 hours to give maximum extraction of humic substances. The suspension was then centrifuged at 5,000 rpm for 30 minutes to separate the humin from the humic substances. The supernatant was decanted off and stored under nitrogen whilst the precipitate was re-extracted with NaOH for a further 24 hours. The remaining precipitate was washed with 0.5M NaOH and the washings combined with the supernatants.

In order to fractionate the humic acid the humic substances were acidified to pH 1 using concentrated HCl. This was left stirring for 2 hours to allow complete precipitation of the humic acid, which was then isolated by centrifugation at 5,000 rpm for 30 minutes. The supernatant, or fulvic acid, was discarded and the precipitate of humic acid was washed with dilute HCl. The humic acid was then dialysed against distilled water to remove Cl^- and an aliquot of the unprotonated humic acid was removed and freeze dried.

The humic acid suspension was titrated to pH 8 with 0.1M NaOH to bring it into solution before applying to the column of cation exchange resin for protonation. Dowex 50W-X8 resin was prepared by swelling in 2M HCl for 24 hours to convert it to the hydrogen form, before being washed with distilled water to remove any Cl^- ions, which could potentially cause precipitation of humic acid on the column. Columns of 10 cm length, 2 cm diameter plugged with glass wool were used. Care was taken to ensure a slow and regular flow rate which would allow a complete and uniform protonation of the humic acid, and the optimum flow rate used was 1 ml min$^-$

[1]. The solution of protonated humic acid was then rotary evaporated to remove excess water before being freeze dried.

Figure 2.2 The isolation and protonation of humic acid.

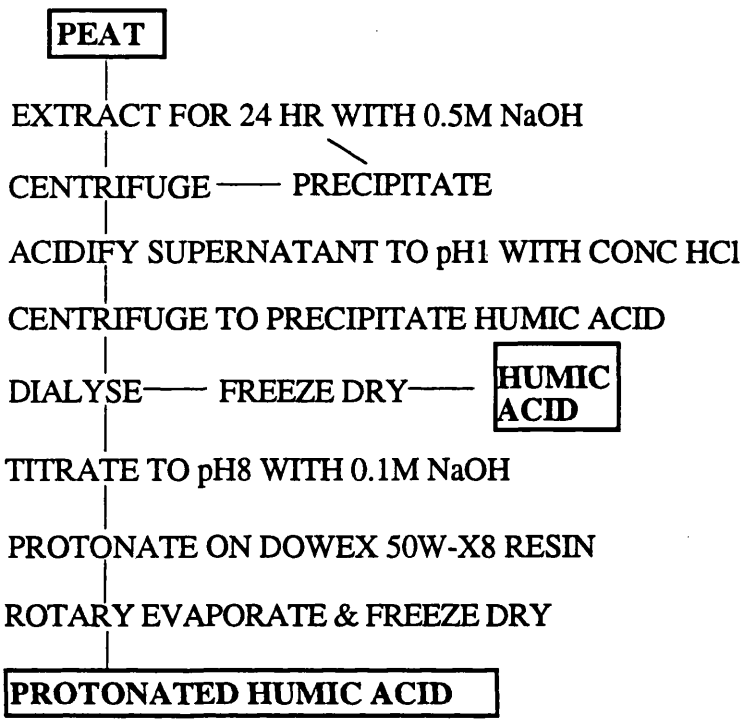

2.2.2 PROTONATION OF PEAT

The air-dried peat was freeze dried to ensure complete dehydration of the material in preparation for further procedures. The freeze-dried material was then stirred for two hours in 2M HCl with a soil solution ratio of 1:20. The protonated peat was then thoroughly washed with distilled water to remove all traces of excess acid, before being freeze dried.

2.2.3 ELEMENTAL ANALYSIS

A Carlo Erba Elemental Analyser, model 1106, was used to determine the content of carbon, hydrogen and nitrogen in the unprotonated peats and their unprotonated humic acids.

2.2.4 INFRA-RED CHARACTERISATION

2.2.4.1 PELLET PREPARATION

In order to analyse the samples, they first have to pelleted with anydrous KBr, and consequently care has to be taken in the preparation of the pellets since moisture can become incorporated in the pellet causing interference in the spectra produced (Stevenson & Goh, 1974). To minimise hygroscopic moisture the materials were always freeze dried and stored in a desiccator containing silica gel before pelleting.

0.7 mg of humic substance was ground with 300 mg of anhydrous KBr powder and pelleted under vacuum. The quantity of humic substance used is important since too much, or too little, can result in poor spectra which are difficult to interpret. The pellets produced were then desiccated under vacuum with silica gel before analysis in a Phillips PU9800 Spectrophotometer in the single-beam mode.

2.2.4.2 IONISATION STUDIES

To investigate the effects of alkali on the infra-red spectra of humic substances the protonated samples were titrated to pH 5 and pH1 0 with 0.05M KOH.

10 mg of the peat samples were suspended in 10 ml of de-ionised water and titrated to the required pH. After equilibration had been achieved the peat samples were washed with de-ionised water to remove any residual salt. The peats were then freeze dried before pelleting.

The protonated humic acid was titrated to pH 5 and pH 10, after the protonation step on the Dowex column. Thus it had not been freeze dried before titration and was still in a suspension. After titration and equilibration to the required pH value the humic acids were rotary evaporated to dryness and freeze dried before pelleting.

2.2.5 DETERMINATION OF THE TOTAL ACIDITY

The barium hydroxide method was used, which involved reacting the humic substances with barium hydroxide and then determining the amount of barium bound by titrating the unused base with standard acid (Piccolo & Camici, 1990).

The first step in the procedure involves the preparation of the 0.1M barium hydroxide used in the method. Contamination by CO_2 was minimised by preparing the solution using 1l of CO_2 free distilled water to which 36 g of $Ba(OH)_2$ was added. This was then sealed, taking care to displace all air with N_2, and the solution was

stirred for 24 hours, whilst gently heating. The solution was then cooled and settled before checking the concentration with standard 0.1M HCl.

50-100 mg of the humic substances were shaken for 24 hours with 20 ml of the $Ba(OH)_2$ under nitrogen. A blank sample containing only $Ba(OH)_2$ was also run. On completion of shaking the samples were filtered and washed with CO_2 free distilled water. The filtrate and the washings were combined and stored under N_2 until being titrated potentiometrically with standard acid to pH 8.4. An Orion pH meter was used to record the pH, and to obtain an accurate measurement of the end point a microburette was used. The blank sample was also titrated and is included in the calculation below.

Initially the acid used was 0.5M HCl (Schnitzer & Khan, 1972). Since the end point was too sharp with this acid 0.1M HCl was standardised against 1M NaOH and used in all measurements. The calculation used is as follows:

$$\frac{(\text{end point blank} - \text{end point sample}) \times \text{M acid} \times 1000}{\text{mg of sample}} = \text{mmolc / g total acidity}$$

- where $mmol_c$ = millimoles of charge on the humic substance.

2.2.6 DETERMINATION OF THE CARBOXYL CONTENT

The method used involved reacting the humic substances with calcium acetate to give acetic acid and calcium humate. The released acetic acid is then titrated with standard base to determine how many groups have reacted (Schnitzer & Khan, 1972).

As with the total acidity determination care must be taken to avoid interference from CO_2 and all determinations were carried out under nitrogen. Again between 50-100 mg of humic substance is required.

The humic substances were shaken with 10 ml of 1M calcium acetate, and 40 ml of CO_2 free distilled water for 24 hours, along with a blank sample. The suspensions and blanks were then filtered and washed with CO_2 free distilled water and the filtrates and washings combined. These were titrated potentiometrically with standard 0.1M sodium hydroxide to pH 9.8. The carboxyl content is determined through the following equation:

$$\frac{(\text{end point sample} - \text{end point blank}) \times \text{M base} \times 1000}{\text{mg of sample}} = \text{mmolc / g COOH}$$

2.3 RESULTS AND DISCUSSION

2.3.1 ELEMENTAL ANALYSIS

Table 2.1 Results of elemental analysis.

Sample	%Carbon	%Hydrogen	%Nitrogen
Huxter Peat	54.3	6.3	1.2
Huxter Humic Acid	52.0	5.5	2.2
Lunga Water Peat	51.5	5.7	1.4
Lunga Water Humic Acid	51.3	5.2	2.3

Table 2.2 Molar ratios of elements for Lunga Water and Huxter humic acids.

Ratio	Huxter Humic Acid	Lunga Water Humic Acid
H/C	1.27	1.22
N/C	0.04	0.04

The Lunga Water samples had a lower carbon content than the Huxter samples, indicating a lower degree of aromaticity and molecular weight (Hayes & Swift, 1978). The H/C molar ratios for the two humic acids are similar, as are the N/C molar ratios and reflect their source as being peat (Ishiwatari, 1975).

Extraction and fractionation has resulted in a slight reduction in the carbon and hydrogen content for the Huxter samples. This is consistent with the loss of carbon observed by Flaig *et al.* (1975) on alkali extraction and losses in molecular weight observed on extraction and fractionation of humic acid (Swift & Posner, 1972: Gregor & Powell, 1987). The increase in nitrogen content has also been previously reported by Flaig *et al.*. (1975), who proposed that it was due to protein and other nitrogen containing compounds being dissolved in the alkali. Krosshavn (1992) also reported that most of the nitrogen from organic matter is concentrated in the humic acid fraction after the same extraction procedure utilised in this study.

2.3.2 INFRA-RED CHARACTERISATION

2.3.2.1 GENERAL FEATURES OF THE SPECTRA

The most striking feature of any infra-red spectrum of a humic substance is the broadness of the bands. This occurs due the heterogeneity of the humic substances, where there is a wide diversity in the types of functional group present as well as the diversity in the chemical environment of each functional group.

Table 2.3 The main absorption bands observed in infra-red spectra of humic substances.

Wavenumber (cm^{-1})	**Functional Group**
3400	O-H stretching and N-H stretching.
2920 &2860	Aliphatic C-H stretching.
1720	C=O stretching, mainly from carboxyl groupings
1650-1600	C=C vibrations, conjugated with C=O or COO^-. H-bonded C=O from quinones.
1590	COO^- symmetric stretching.
1400	COO^- antisymmetric stretching.
1250	C-O stretching, & OH deformation of COOH groups.
1100-1020	Si-O stretching (intense).
1040	C-O stretching of polysaccharides.

2.3.2.2 EFFECT OF PEAT TYPE ON THE SPECTRA

In comparing the different types of humic substance only the unprotonated materials will be discussed, since similar changes were observed in the unprotonated and protonated materials.

The Huxter and Lunga Water samples showed differences in functional group content and arrangement. In Figure 2.3, the Lunga Water peat and the Huxter Peat are overlayed and the Lunga Water peat shows a smaller absorption at 1720cm^{-1}, which could indicate that there is a smaller contribution from carbonyl groupings in this peat. However, this effect could also be due to a high degree of ionisation of the carboxyl groupings, especially since the band at 1600cm^{-1} is showing strong absorption. The same effect is seen in the humic acids,(Figure 2.4) and this indicates that the isolation procedure did not disrupt the functionality which expresses peat type. The Huxter humic substances had a significant proportion of carboxyl groupings present in the structure as well as a high degree of hydrogen bonding through the OH groups, as indicated by the downwards broadening of the band at 3400cm^{-1}. There was less deformation of the OH band at 3400cm^{-1} in the Lunga Water humic acid, suggesting a lower degree of hydrogen bonding. The Lunga Water peat also showed a far greater contribution from polysaccharide material, at 1050cm^{-1}, than the Huxter peat.

The Huxter humic acid can be seen to be similar to the type I humic acids, as classified by Stevenson & Goh (1971), exhibiting strong bands near 3400, 2900, 1720, and 1600 cm^{-1}, with the intensity of the bands at 1720 and 1600cm^{-1} being almost equal. Type I humic acids are typical of soil humic acids.

The Lunga Water humic acid corresponds to the Type III spectra recorded by Stevenson & Goh (1971), which are typical of lake humic acids, where little humification has taken place, and a large amount of aliphatic carbon is present, in particular polysaccharides. Podzolic humic acids also show this type of spectra where the functional group content is dominated by phenolic constituents. In addition the podzolic humic acids have also been shown to give a splitting of the carbonyl stretch at 1720cm^{-1}, resulting in absorptions at 1709cm^{-1} and 1686cm^{-1} (Flaig *et al.* 1975), and this could account for the lack of absorption of the carbonyl groups at 1720cm^{-1}.

Figure 2.3 Infra-red spectra of untreated Lunga water and Huxter peat.

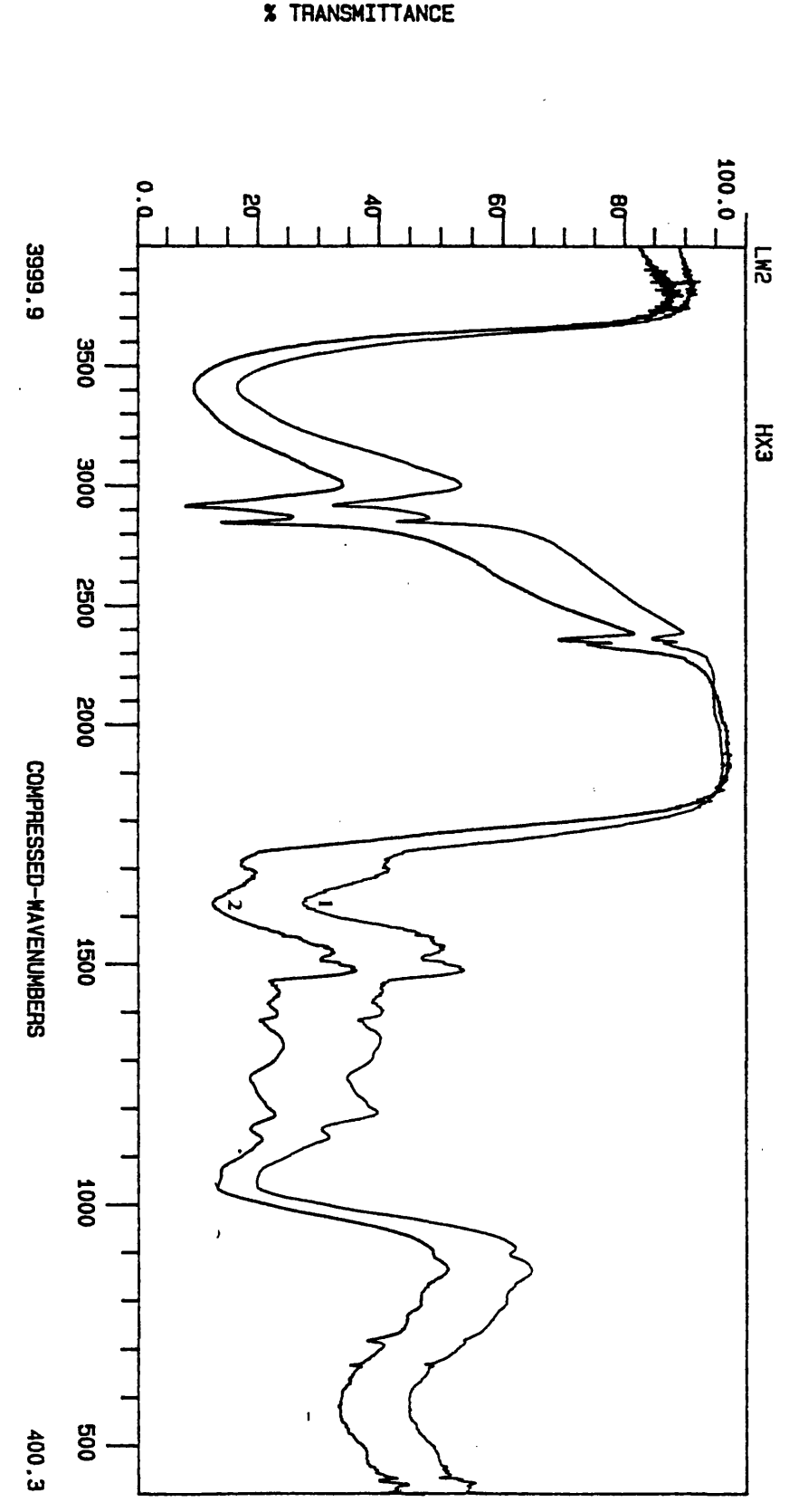

1 = Untreated Lunga Water peat

2 = Untreated Huxter peat

Figure 2.4 Infra-red spectra of untreated Lunga water and Huxter humic acids.

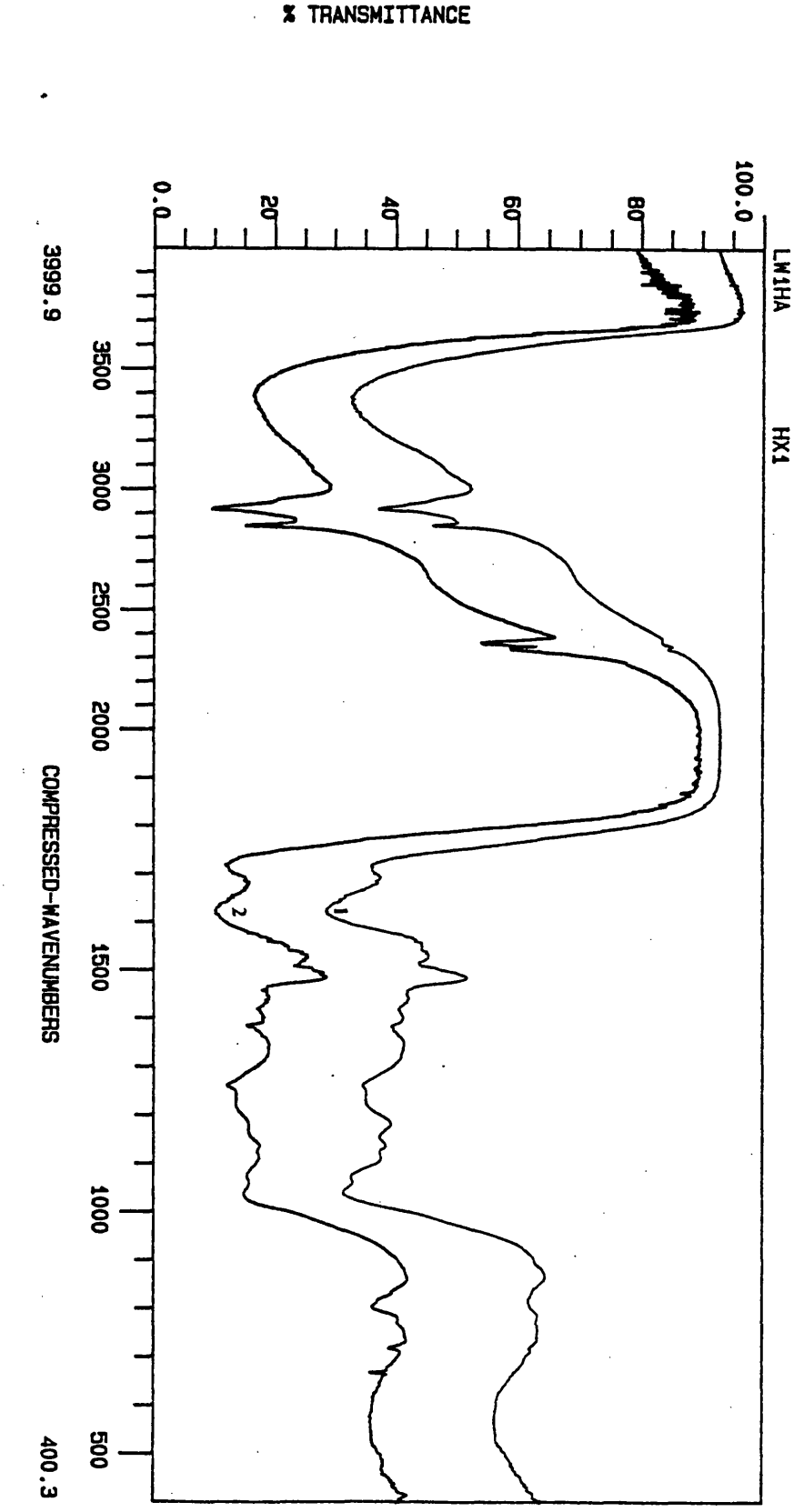

2.3.2.3 INFLUENCE OF EXTRACTION AND FRACTIONATION ON THE SPECTRA

Extraction and fractionation have resulted in changes in the spectra of the humic acids as compared to the spectra of the peats, and again only unprotonated materials are discussed.

In Figure 2.5 the Huxter peat spectrum overlays the Huxter humic acid, and on initial inspection the spectra do not appear significantly different. Since the aim of the extraction procedure is to reduce the heterogeneity of the humic substances we can conclude that no significant reduction has been made. Broad bands are still present, indicating that the diversity in the types of functional group, and their chemical environment was still present in the humic acid. The same effect was seen in the Lunga Water peat and humic acid spectra in Figure 2.6.

On closer inspection of the spectra some very interesting differences can be observed. The extraction and fractionation process has resulted in a loss of absorption at $1050cm^{-1}$, indicating a reduction in the polysaccharide content of the humic substances. This is particularly pronounced in the Lunga Water samples, where the polysaccharide content was observed in section 2.3.2.2 to be highest. In this respect the isolation process is a success since one of the aims of extraction is to isolate humic acid free of contaminants such as polysaccharides (Dubach & Mehta, 1963).

However, extraction and fractionation has resulted in a downwards broadening of the band at $3400cm^{-1}$. This has been suggested to indicate an increase in hydrogen bonding of the OH groupings (MacCarthy & Rice, 1985), and this broadening effect was also observed by Tomar *et al.* (1992). In the humic acids there was also an increase in the absorption at $1720cm^{-1}$, indicating an apparent increase in the content of carbonyl groupings. This increase in carbonyl absorption along with the downward broadening of the OH band was also noted by Swift & Posner (1972) in humic acids which had been incubated in 1M NaOH for 30 days under air and they proposed that this effect was due to autoxidation of the humic acid which also resulted in an overall reduction in molecular weight. Even though these samples were extracted under nitrogen to minimise any autoxidation effect, some chemical alteration of the humic substances occurred during the extraction and fractionation process, which resulted in a similar effect in the humic substances. One possible chemical alteration, other than autoxidation, is alkaline catalysed hydrolysis of esters, since an increase in the carbonyl absorption at $1720cm^{-1}$ is observed (Gregor and Powell, 1987).

Polyphenols have also been shown to be oxidised to quinones in the presence of Fe^{3+} salts in acidic conditions (Gregor & Powell 1987), and this would also contribute to the slight broadening of the $1600cm^{-1}$ peak. Conjugation of aromatic

C=C bonds with C=O bonds on alkali treatment, or hydrogen bonding of conjugated ketones and quinones could also contribute to this broadening. Tomar *et al.* (1992) observed that the carbonyl absorption band for quinones shifted downwards when hydrogen bonding occurred.

However, the results must be interpreted with caution due to the possibility of adsorbed moisture causing interferences in the 3300 to 3000cm^{-1} and 1720 to 1500cm^{-1} regions (Stevenson 1982).

Figure 2.5 Infra-red spectra of untreated Huxter peat and humic acid.

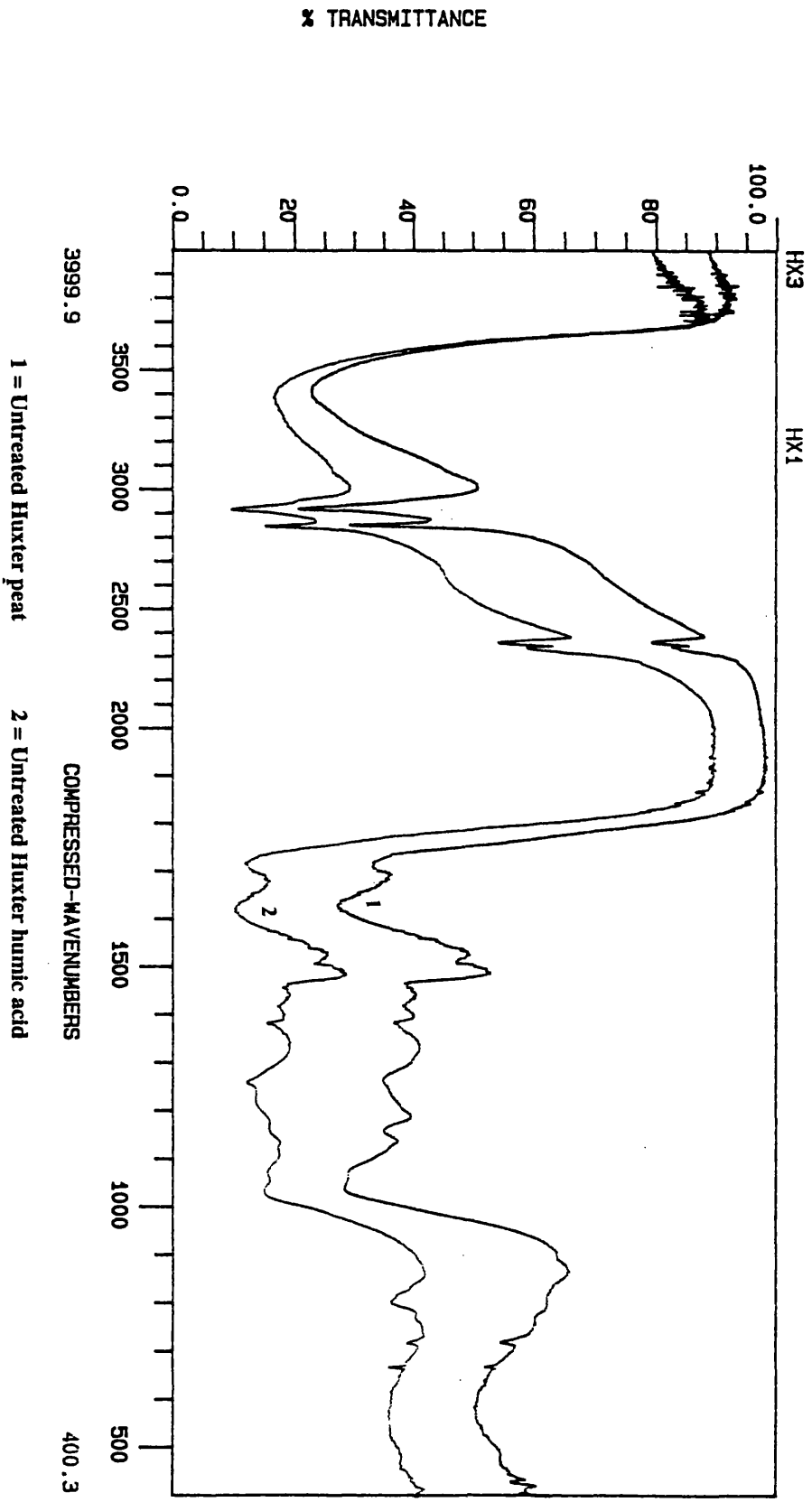

Figure 2.6 Infra-red spectra of untreated Lunga Water peat and humic acid.

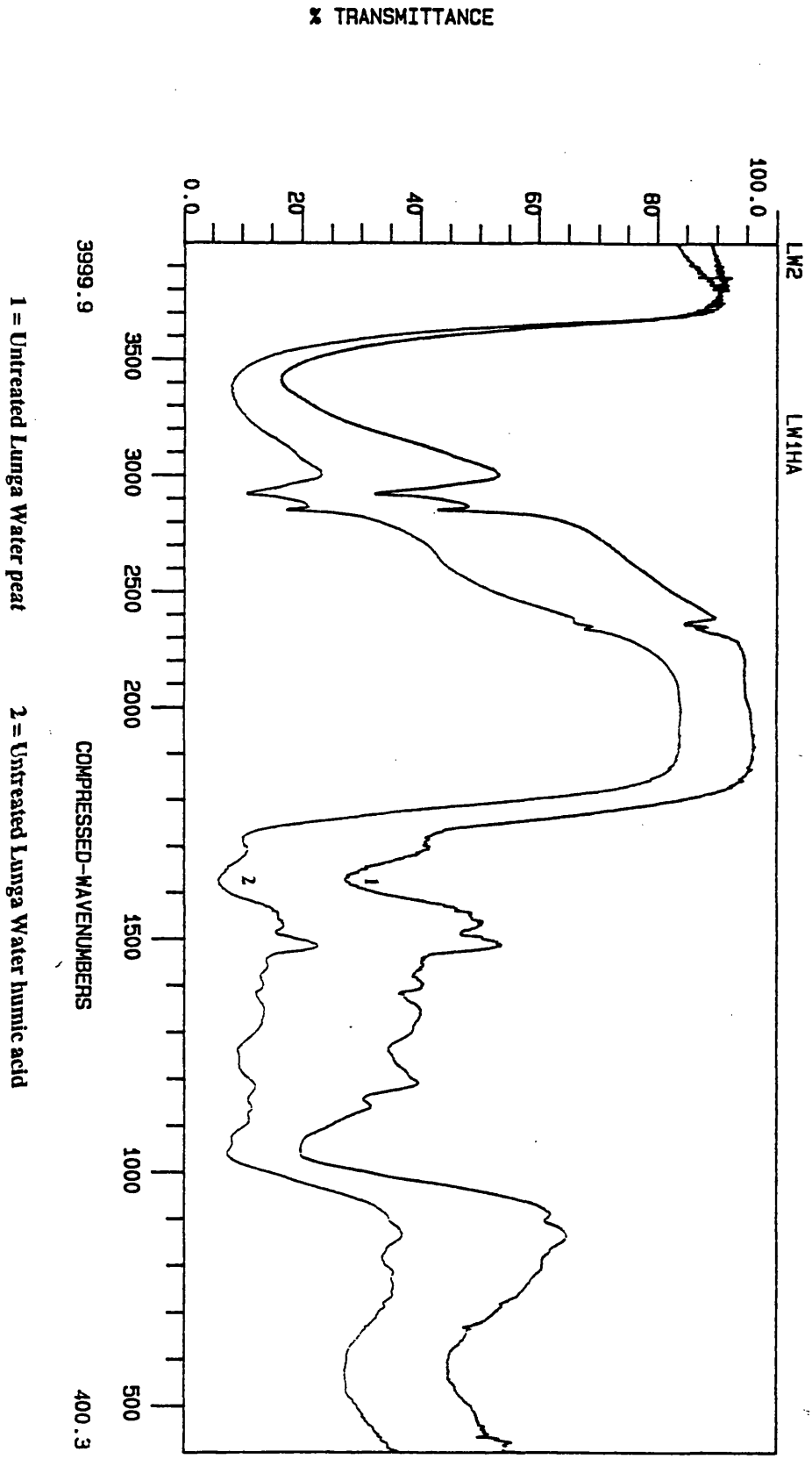

2.3.2.4 EFFECT OF PROTONATION AND TITRATION ON THE SPECTRA.

The spectra for the humic substances and their treatments are presented in Figures 2.7 - 2.10.

Protonation resulted in an increase in absorption at 1720cm^{-1} in all of the materials and indicates that the protonation procedure was effective. This effect was also observed by Stevenson & Goh (1971), after acid hydrolysis of humic acid. The increase in absorption in the humic acids also demonstrates that there are still ionised carboxyl functional groups present after acid fractionation, as observed by Alberts *et al.* (1992). They proposed that steric hindrance resulted in groups still being present in salt form, even after acid precipitation and dialysis.

The protonation procedure resulted in an expected sharpening of the peak at 1600cm^{-1}, as the contribution from the carboxylate salt at 1590cm^{-1} was reduced. The remaining absorption at 1600cm^{-1} is a reflection of the aromatic character and ketone content of the substances.

Titration of the protonated peats to pH 5 and pH 10 gave slightly different spectra than the titrated humic acids. Firstly, in the peat samples (Figures 2.7 & 2.9), titration to pH 5 did not dissociate the groups protonated by treatment with acid. Since the pH of the untreated peat samples was 4.4, we would expect dissociation of the untreated samples at pH 5. Only at pH 10, when the peat sample is beginning to come into solution, was any significant ionisation observed, and this resulted in a broadening of the peak at 1600cm^{-1}.

Titration of the humic acids to pH 5 (Figures 2.8 and 2.10) had a more significant effect on the spectra, especially in the Huxter humic acid (Figure 2.10), where the material was fully ionised at pH 5 and titration to pH 10 had no further effect. In the Lunga Water humic acid (Figure 2.8) some further ionisation was observed at pH 10, but the majority of the changes had occurred at pH 5. Since the pKa of humic acids has been reported as 4.6 (Stevenson, 1982), it is not unrealistic to observe full ionisation at pH 5.

Differences were observed therefore between the behaviours of the humic acids and the peats. The humic acids were more easily ionised than the peat samples, where ionisation did not occur until pH 10 when the material was starting to come into solution. This would indicate that the reactive groupings were in a more accessible arrangement for reaction with alkali, and potentially metals, than would occur in the unextracted material.

Titration and ionisation of the peats and the humic acids also gave a broadening of the band at 1600cm^{-1} which point to chemical and/or structural changes

in the peat samples on protonation and alkali treatment. On ionisation the carboxyl groupings become negatively charged and repulsion of the like charges may occur, giving an opening of structure (Stevenson 1982). Consequently, not only will different functional groupings become exposed, but the environment of the functional groupings will alter, resulting in the broadening effect seen. However, the alkali treatment itself may be causing chemical changes to the groups, resulting in broadening of the 1600cm^{-1} peak, with hydrogen bonding being a distinct possibilty. Extraction and fractionation of humic acid has previously been shown in section 2.3.2.3 to give this effect, along with a broadening of the OH peak which is also seen in the titrated peat samples, further indicating that the alkali treatment caused the changes observed in the humic acids.

The remaining absorption at 1720cm^{-1} seen in the samples at pH 10, could indicate that some COOH groupings were structurally not available for ionisation. In addition ketonic and quinone carbonyl groupings will also contribute to absorption in this region, and will not be ionised by alkali (Piccolo &Stevenson, 1982).

On protonation, the Lunga Water peat (Figure 2.7) and its humic acid (Figure 2.9) showed greater increases in absorption at 1720cm^{-1} than the Huxter samples indicating that there was a greater content of ionisable groupings present. This also points to a higher metal content of the peat, since these will be present as counter ions to the negtively charged groups. The Lunga Water samples were also more responsive to the effect of titration, indicating there was a higher content of oxygen containing functional groups in these samples.

Figure 2.7 Infra-red spectra of Lunga Water peat after various treatments.

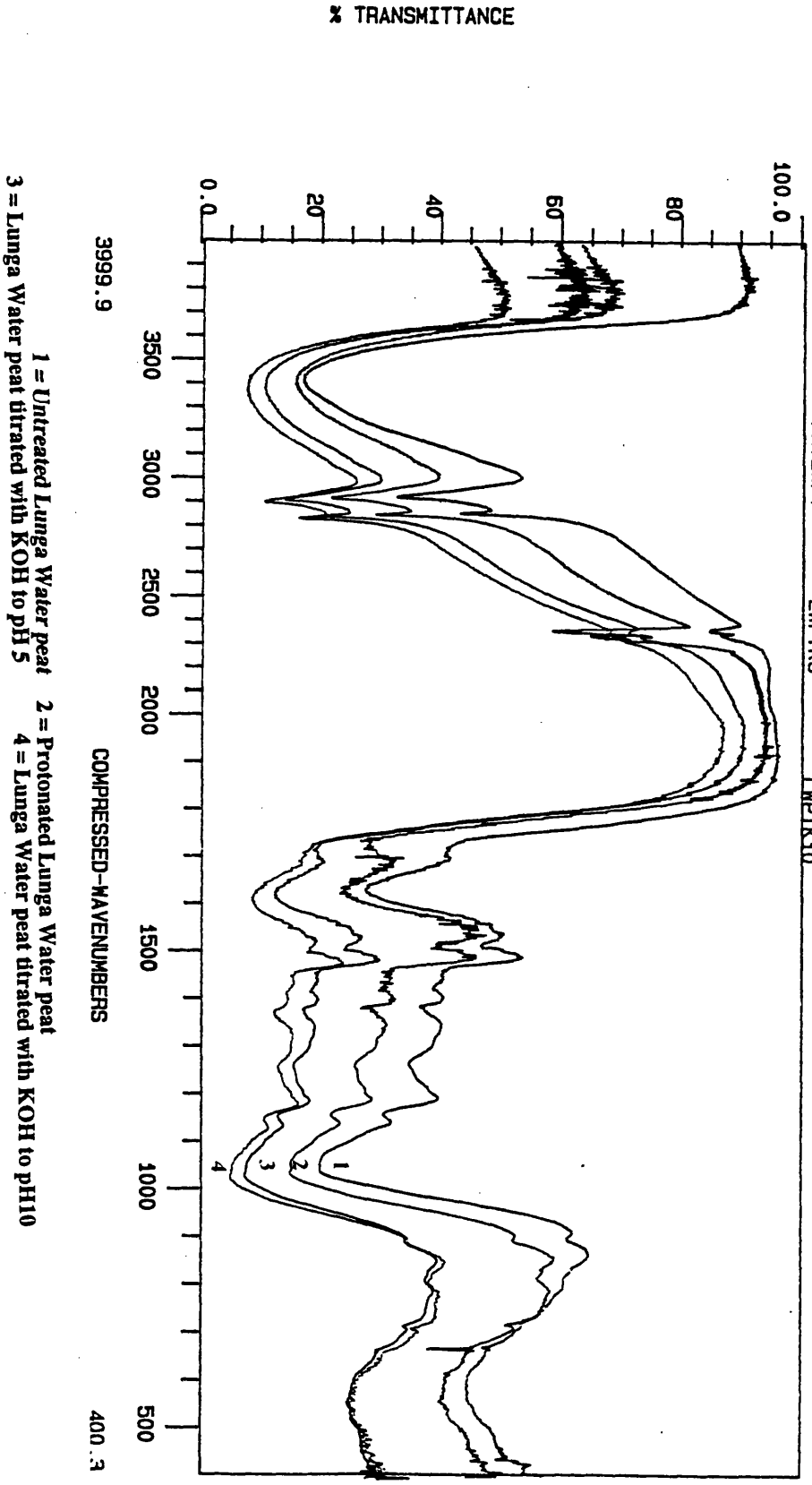

1 = Untreated Lunga Water peat 2 = Protonated Lunga Water peat
3 = Lunga Water peat titrated with KOH to pH 5 4 = Lunga Water peat titrated with KOH to pH10

Figure 2.8 Infra-red spectra of Lunga Water humic acid after various treatments.

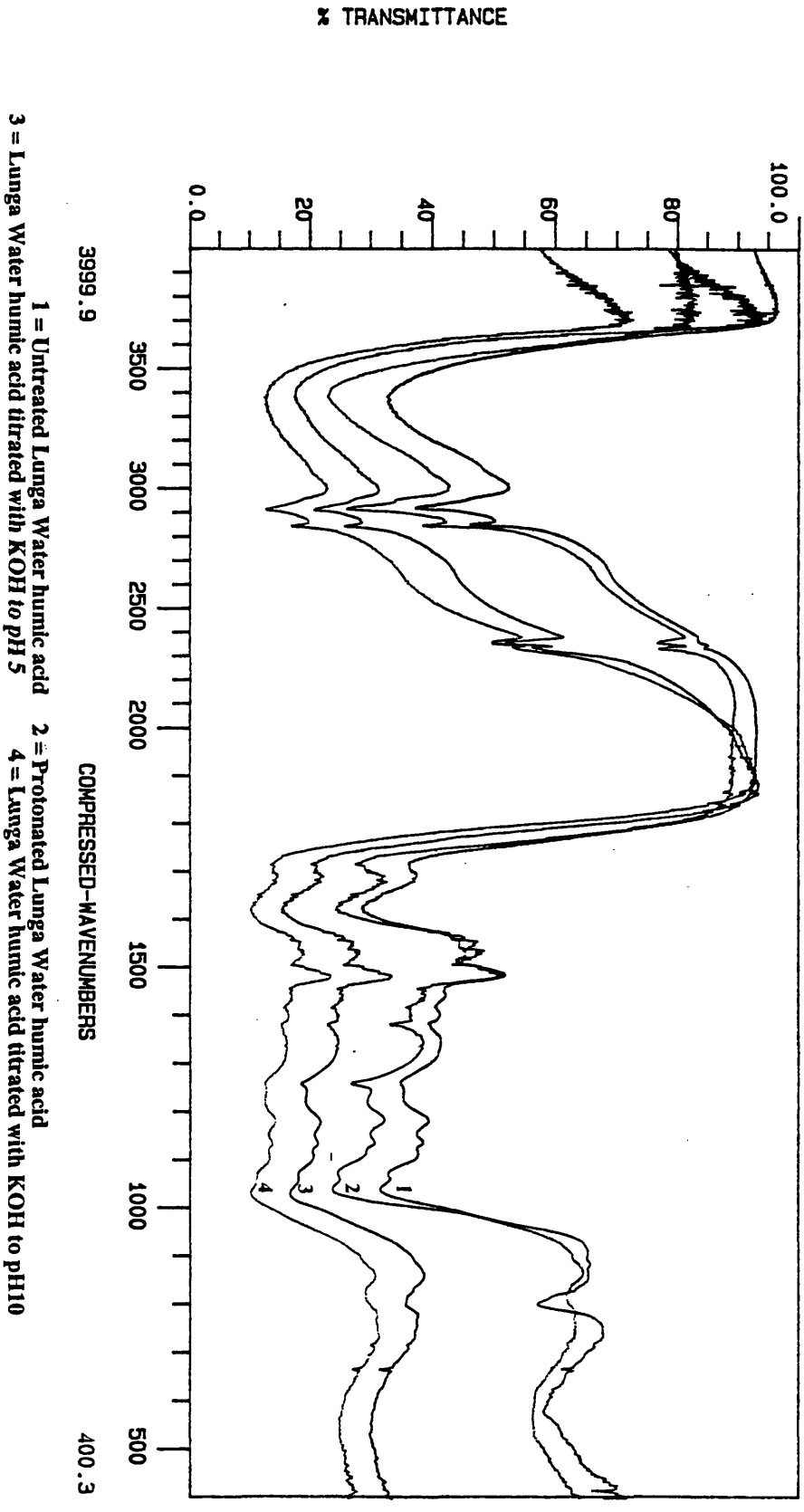

1 = Untreated Lunga Water humic acid 2 = Protonated Lunga Water humic acid
3 = Lunga Water humic acid titrated with KOH to pH 5 4 = Lunga Water humic acid titrated with KOH to pH10

Figure 2.9 Infra-red spectra of Huxter peat after various treatments.

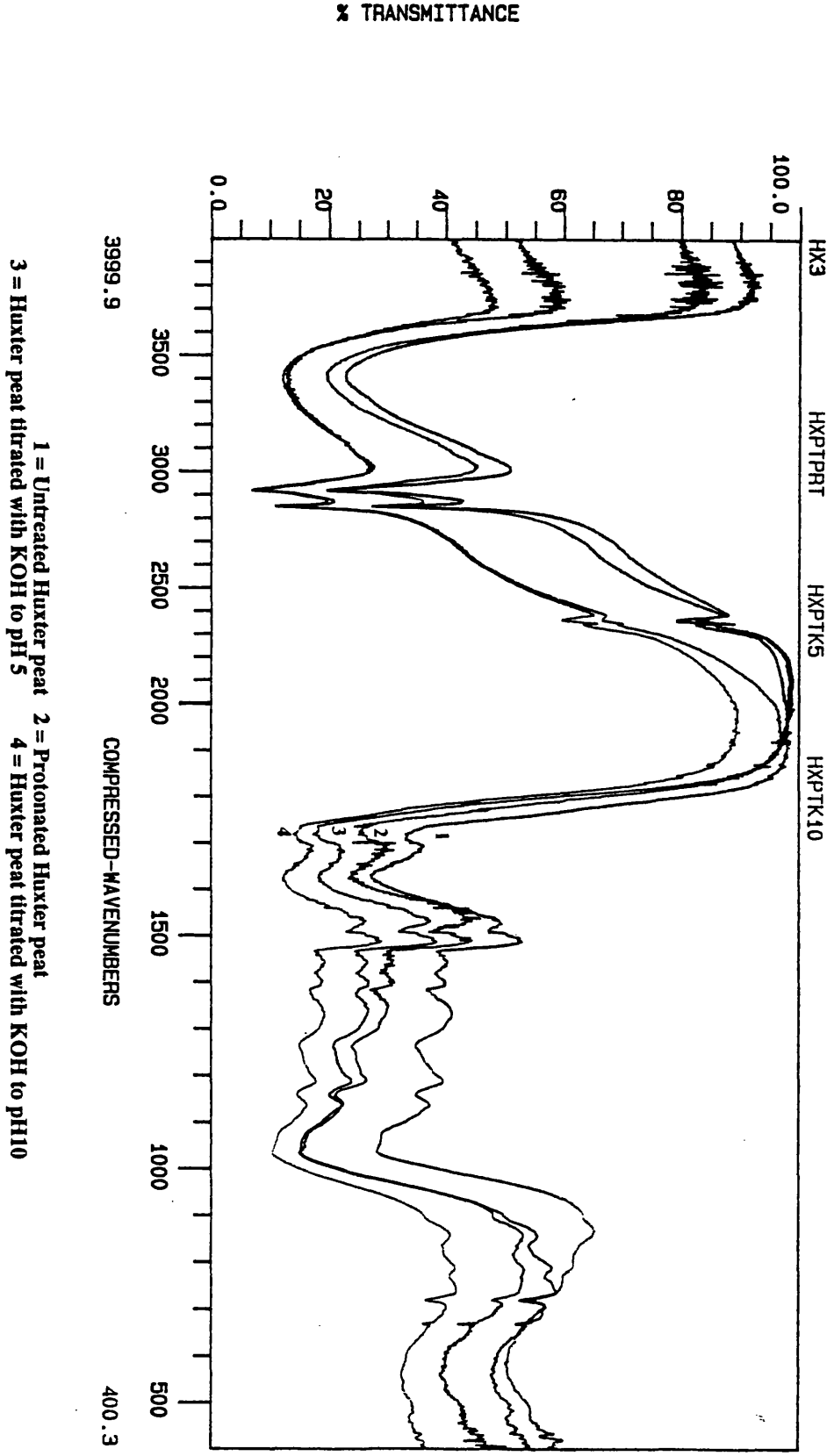

Figure 2.10 Infra-red spectra of Huxter humic acid after various treatments.

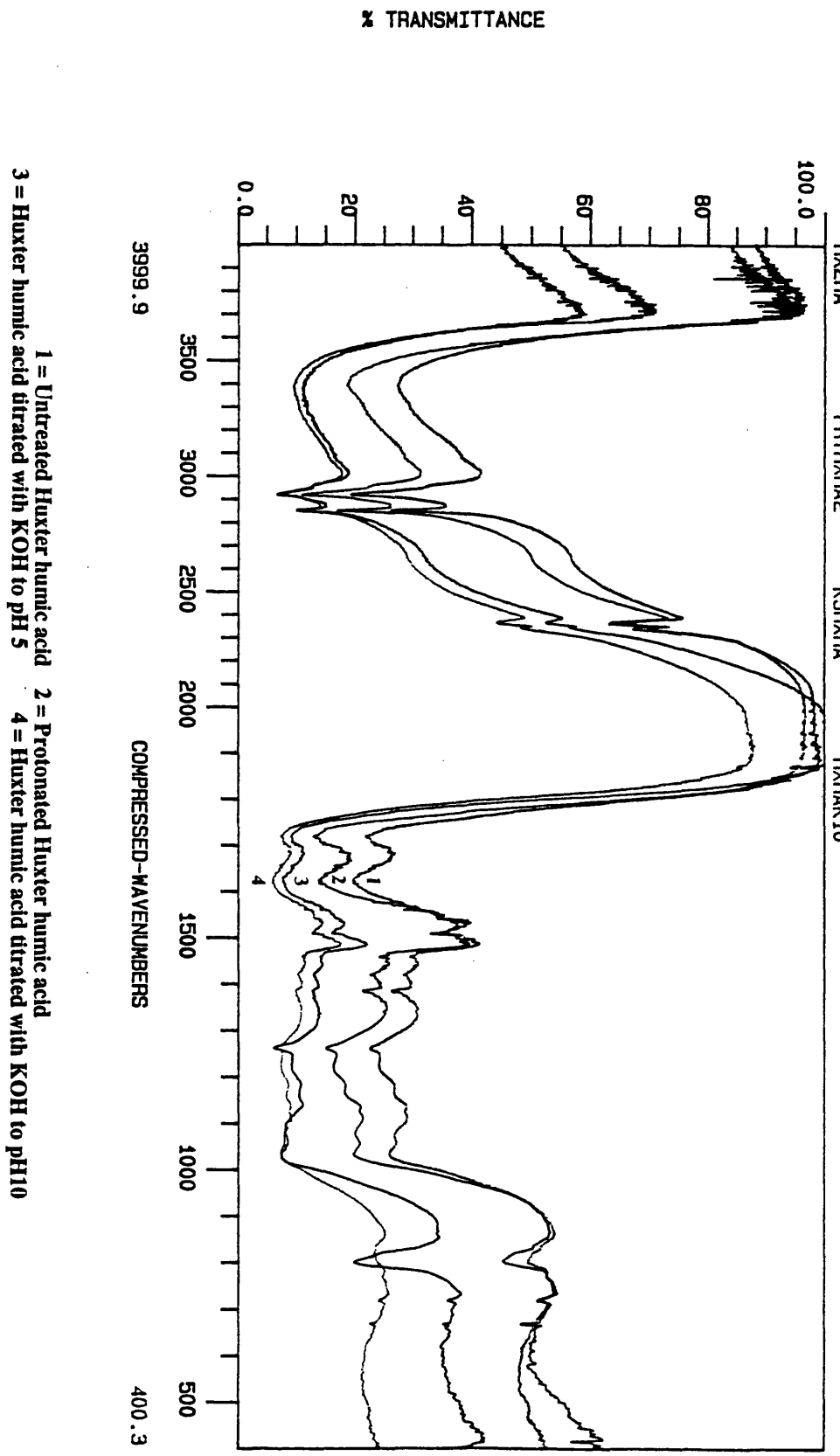

1 = Untreated Huxter humic acid 2 = Protonated Huxter humic acid
3 = Huxter humic acid titrated with KOH to pH 5 4 = Huxter humic acid titrated with KOH to pH10

2.3.3 TOTAL ACIDITY DETERMINATIONS OF HUMIC SUBSTANCES

In order to obtain an estimate of the precision of the method, and to obtain a representative value of the total acidity, up to six replicates were run and a sample titration is shown below in Figure 2.11.

Figure 2.11 Sample total acidity titration.

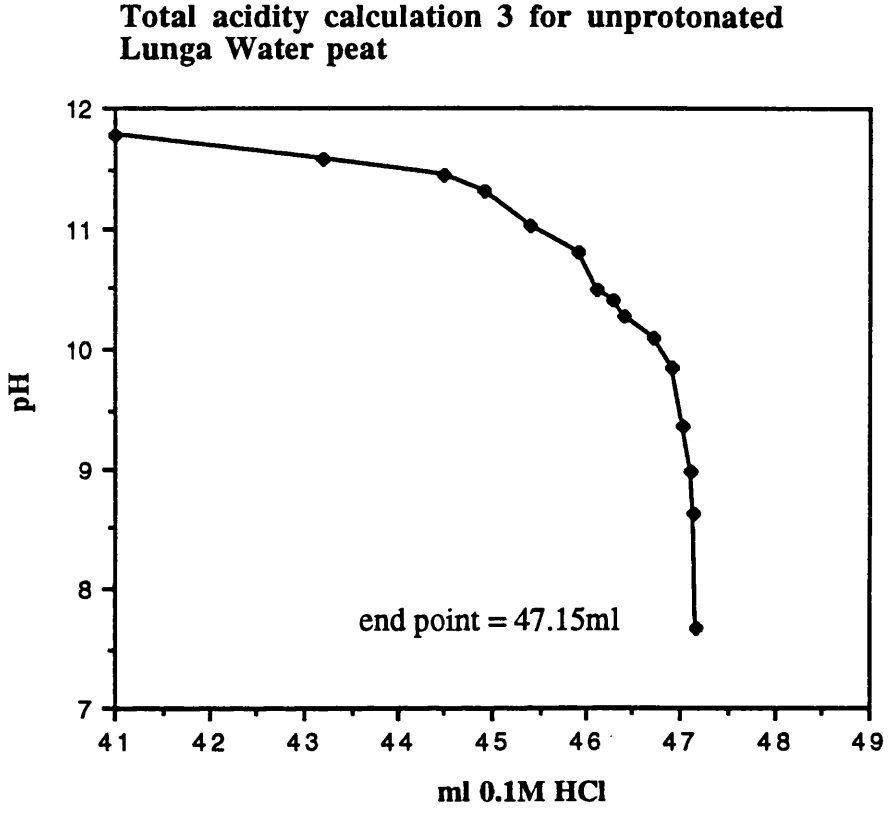

The volume of standardised 0.1M acid required to attain the end point of pH 8.4 was 47.15 ml, and the corresponding blank titration of barium hydroxide gave an end point of 49.95 ml. Therefore, since 65.2 mg of peat was used, the total acidity was calculated as:

$$\frac{(49.95 - 47.15) \times 0.1 \times 1000}{65.2} = 3.74 \text{ mmolc / g total acidity}$$

The remainder of the data and calculations can be found in Appendix 1.1, and the results are summarised below in Table 2.4.

The values for the total acidities agreed well with previously recorded values. Stevenson (1982) stated that humic acids from cool, temperate acid soils usually show total acidities of between 5.7-8.9 $mmol_c\ g^{-1}$, and all the humic acids except the unprotonated Huxter humic acid fall within this range. The Lunga Water peat and its

humic acid had higher total acidity values than the corresponding Huxter samples, reflecting the lower degree of humification of the Lunga Water peat (Hempfling *et al.*, 1988).

Protonation of the peats and humic acids acted to raise the total acidity values. The protonation procedure was aimed at removing any cations which may be complexed onto the oxygen containing functional groups, replacing them with hydrogen ions and thus converting the groups to their protonated forms. Therefore from the total acidity determinations it can be seen that the protonation procedure was successful.

The extraction and fractionation of humic acid from the peat samples resulted in an overall increase in the total acidity values e.g. the unprotonated Lunga Water peat had a mean total acidity of 3.97 $mmol_C\ g^{-1}$ whereas the Lunga Water humic acid has a mean total acidity of 5.64 $mmol_C\ g^{-1}$. Therefore, the process of extraction and fractionation resulted in an increase in acidic functional groupings which can react with the barium hydroxide, either chemically or through a change in structure. Gregor & Powell (1987) previously reported an increase in the titratable acidity on extraction in alkali.

The standard deviations show that the precision of the method was poor and this can be attributed to the formation of insoluble barium carbonate during filtration. This has previously been reported to give poor precision in calculating the total acidity in this way, however the method has also been shown to be more accurate than other methods of calculating total acidity (Piccolo & Camici, 1990).

Table 2.4 Summary of the results for the determination of the total acidities.

Sample	**Mean Of Replicates $mmol_C\ g^{-1}$** (6 determinations run)	**Standard Deviation of mean**
Unprotonated Huxter peat	2.19	1.02
Unprotonated Lunga Water peat	3.97	0.971
Protonated Huxter peat	5.25	0.603
Protonated Lunga Water peat	6.09	0.339
Unprotonated Huxter humic acid	4.05	0.634
Unprotonated Lunga Water humic acid	5.64	0.811
Protonated Huxter humic acid	6.22	0.696
Protonated Lunga Water humic acid	7.18	0.275

2.3.4 CARBOXYL GROUP CONTENT DETERMINATION

As with the total acidity, up to six replicates of the determinations were run and the resulting means and standard deviations of the results were determined and can be found in Appendix 1.2, but are summarised in Table 2.5. A sample titration (Figure 2.12) and calculation are shown below:

Figure 2.12 Sample carboxyl content titration.

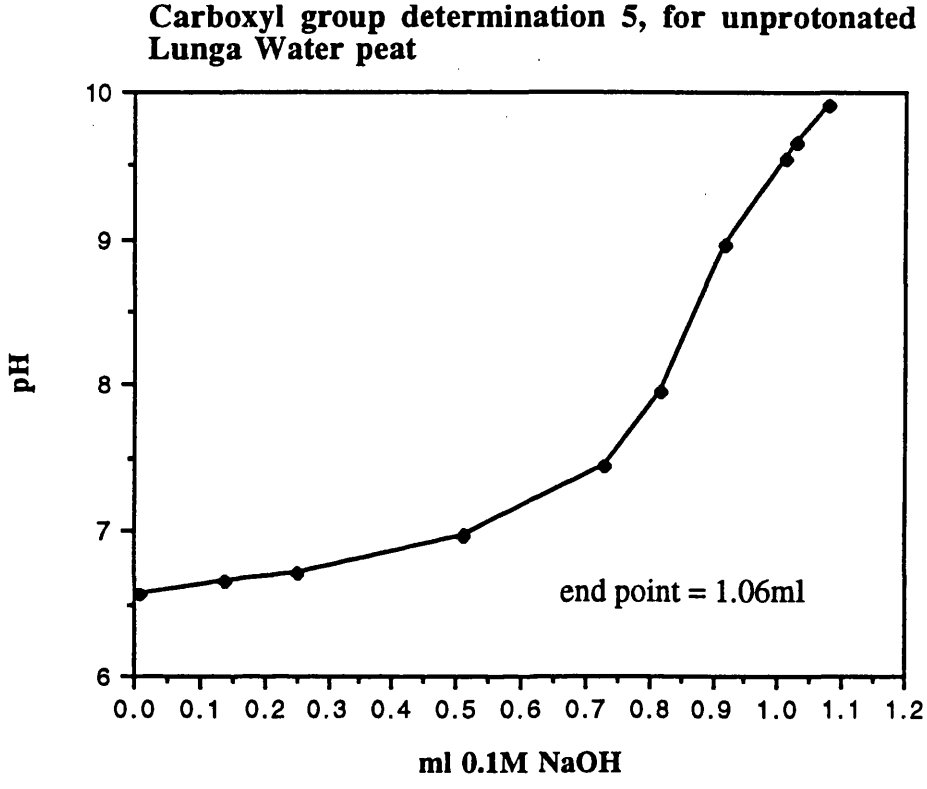

The weight of peat used was 67.2 mg, and the molarity of the base was standardised as 0.0955M. The end point was determined from the amount of base consumed at pH 9.8. The blank titration gave an end point of 0.31 ml. Therefore the carboxyl content was calculated as:

$$\frac{(1.06-0.31) \times 0.0955 \times 1000}{67.2} = 1.07 \text{mmolc} / \text{g}$$

The values for the carboxyl group content of the humic acids agree well with those quoted by Stevenson (1982) for cool, temperate, acid soils which have a range of 1.5-5.7 $\text{mmol}_c\ g^{-1}$ for humic acids. The values themselves are far lower than the corresponding values for the total acidities and have been proposed to reflect the available groups present in humic substances at most soil pH values (Bonn & Fish, 1991). As with the total acidity results, the Huxter peats and its humic acids had lower

values than the Lunga Water peats and humic acids, reflecting the degree of humification of the materials. This corresponds with the infra-red spectra of these materials where the Huxter humic acid showed a lower degree of reactivity towards protonation and titration.

Protonation resulted in an *increase* in the carboxyl content of the humic acids. Since protonation aims to remove any existing cations from the humic substances and replace them with hydrogen ions it can be concluded that this has occurred. The calcium ions were not able to compete with the existing cations on the humic structure. However, protonation of the peat samples resulted in a *decrease* in the carboxyl content. Since 6M HCl is used to hydrolyse polysaccharides and amino acids from humic acids (Stevenson, 1982), and treatment with dilute HCl has been shown to give a decrease in carbon content of soil (Flaig *et al.*, 1975), it can be concluded that the 2M HCl used in the protonation step hydrolysed adsorbed polysaccharide and peptide materials.

Like the total acidity, the carboxyl results have increased on extraction and fractionation suggesting that there has been either a chemical or structural change in the humic substances giving an increase in the calcium acetate derived carboxyl content. The hydrolysis of esters to give carboxylic acids has been previously established and also acts to give a reduction in the molecular weight of humic substances (Gregor & Powell, 1987). In addition, the extraction process could be causing structural changes, which would expose carboxyl groupings for titration.

The precision of the method was variable, and can be attributed to the interferences from sulfonic acid groupings and carbon dioxide, as well as the filtration of dissolved humate material which can lead to over-estimations of the carboxyl content (Bonn & Fish, 1991).

Table 2.5 Summary of the results for the determination of carboxyl contents.

Sample	**Mean of replicates** $mmol_C\ g^{-1}$ (6 determinations run)	**Standard Deviation of mean**
Unprotonated Huxter peat	0.74	0.082
Unprotonated Lunga Water peat	1.01	0.108
Protonated Huxter peat	0.54	0.131
Protonated Lunga Water peat	0.67	0.096
Unprotonated Huxter humic acid	1.50	0.093
Unprotonated Lunga Water humic acid	1.71	0.251
Protonated Huxter humic acid	2.26	0.083
Protonated Lunga Water humic acid	2.74	0.135

2.4 CONCLUSIONS

One of the aims of the project was to investigate the nature of humic acid and whether it is a representative fraction of the soil humic substances, since controversy surrounds whether or not its properties are affected by the extraction and fractionation process. The characterisation studies utilised here show clearly that humic acid does show differences from unextracted materials.

The total acidity and carboxyl contents, even though they were operationally defined (Perdue, 1985) indicated that the reactivity of the humic acid was increased by the extraction and fractionation process, since increases in both of these parameters were observed. These changes could be due to structural effects, since on extraction the humic acid was removed from the other components of the soil and the complexity of the structure was broken down, making groups more available for reaction, and/or chemical changes. The titration of the samples showed how reactivity to alkali was affected by these changes. The humic acid was able to attain full ionisation at pH 5, whereas the peat did not achieve any degree of ionisation until pH 10, when the material was beginning to come into solution and more groups could be exposed for reaction. The infra-red and elemental analysis results reinforce the theory of chemical changes occurring. The infra-red spectra of the humic acids indicated that hydrogen bonding was occurring and the elemental analysis showed an increase in nitrogen content in the humic acid after extraction and fractionation.

The characterisation procedures clearly demonstrate the differences in the nature and reactivity of the two peats and their humic acids. The Lunga Water samples had greater total acidity, carboxyl content, lower carbon content, a greater polysaccharide content and in the infra-red spectra showed a greater reaction towards alkali. Conversely, the Huxter peat had a greater degree of aromatic carbon and a higher carbon content.

The study also demonstrated the potential of the procedures to give useful information on the nature of humic substances, in particular unextracted materials. The values for the total acidity and carboxyl contents can also be utilised in metal binding studies, and indeed the total acidity was used in this way, as will be discussed in Chapter 3.

Since the behaviour and reactivity of extracted humic substances is dependent on the functional group content, and from the results presented here this parameter is affected by extraction, the effect of the extraction on behaviour and reactivity will be discussed further in Chapter 3 and Chapter 4.

CHAPTER 3

INFRA-RED STUDIES OF THE INTERACTION OF METALS WITH HUMIC SUBSTANCES

3.1 INTRODUCTION

The isolation of humic acid from peat was shown to give alterations in the amount of reactive functional groupings, their distribution and possibly even the type of functional group present. In the work presented in this chapter the reactivity of metals to humic substances, before and after isolation is investigated qualitatively, as well as the nature of the reaction between a humic substance and a metal.

Infra-red spectroscopy is used to study the interaction of metals with humic substances, since changes can be observed in the arrangements of the oxygen containing functional groups, in particular the degree of complex formation (Piccolo & Stevenson, 1982). The main changes which are observed occur in the region between 1750-1350cm^{-1}, where the carboxyl groupings absorb. On formation of a carboxylate salt the carbonyl absorption is reduced significantly due to formation of the carboxylate anion, which is resonance stabilised. Correspondingly, two characteristic frequencies for the antisymmetric and symmetric carboxylate stretch are formed and occur at ~1590cm^{-1} and ~1390cm^{-1} accordingly. The exact position of these bands depends on the nature of the linkage between the carboxylic acid grouping and the metal. It was demonstrated that the difference in frequency between these two bands, Δ ($\nu_a CO_2^-$ - νCO_2^-), can be used to characterise complexes.

A carboxylate grouping can complex with a metal ion through chelation, coordination or bridging reactions (see Figure 1.3). The formation of coordinate complexes gave Δ values which were greater than ionic complexes, whilst chelate complexes gave Δ values which were significantly lower than ionic values. The bridging complexes were intermediate between the chelate and ionic Δ values (Nakamoto, 1986).

Vinkler *et al.* (1976) utilised these differences in the Δ values to determine complex formation between humic substances and various metals. They found that the alkaline metals, such as Cs^+, Na^+ and K^+ were showing frequencies of antisymmetric stretch characteristic of ionic linkages. By contrast Mn^{2+}, Fe^{2+}, Cu^{2+}, Mg^{2+}, Al^{3+}, Cr^{2+} and Zn^{2+} all showed shifts towards lower frequencies, with Al^{3+} and Cr^{2+} showing the greatest shifts and correspondingly the greatest degrees of covalency. In a later study, Piccolo and Stevenson (1982) proposed that this type of study could lead to ambiguous conclusions, due to the possibility of the metals interacting with groupings which also absorb in the 1600-1660cm^{-1} region. They demonstrated that Cu^{2+}, Pb^{2+} and Ca^{2+} were able to interact with groupings that K^+ was not able to, and proposed that the reactive groupings could be conjugated ketonic structures which absorb in the range 1660-1600cm^{-1} when weakened by resonance. Mg^{2+}, Sr^{2+} and

Zn^{2+} have also been shown to give this effect, particularly at high degrees of metal loading, indicating again that they can form more covalent inner sphere complexes, perhaps with conjugated ketones (Maguire *et al.*, 1991). Conversely Cs^{+} and K^{+} react to give more ionic, outer sphere complexes (Piccolo & Stevenson, 1982: Maguire *et al.*, 1991).

The ability of metals to form covalent coordinate linkages is related to their hard or soft character, with the softer Class B metal cations such as Pb^{2+} and Zn^{2+} being more polarisable and amenable to coordination reactions. The Class A metal cations such as Na^{+}, K^{+} and Sr^{2+} are less polarisable and participate more in ionic interactions (Pearson, 1963). Thus, in the work presented here a range of metals which incorporated both groups of cations were chosen in order to investigate the potential of different cations to undergo coordination reactions with humic substances, providing valuable information on their potential mobility and bioavailabilty in the environment. The metals were also chosen for their environmental importance as contaminating metals in many systems e.g. Pb, Cu, Zn and Cs. This is of particular importance since they were reacted with the humic substances at levels which would be contaminating in environmental systems.

The effect of metal additions to salicylic and phthalic acids were studied in order to investigate the covalency of interaction in simple compounds which have a known chemical structure. These acids were also chosen since they have been proposed to be the main arrangement of the oxygen-containing functional groupings on humic substances (Stevenson, 1977).

3.2 METHODS

3.2.1 THE ADDITION OF METALS TO HUMIC ACID AND PEAT

Metal additions were carried out to both the peats and their corresponding humic acids which were characterised in Chapter 2. Thus, the investigation on the effects of peat type on reactivity could be continued.

The levels of metal addition were based on the values for the total acidity presented in section 2.3.3, with additions being made at half the total acidity, total acidity and twice the total acidity. All metals were added as 0.02M chloride salts, except for Pb^{2+} and Ag^{+} which were added as 0.02M nitrate salts. Cs^{+}, Pb^{2+}, Sr^{2+}, Zn^{2+}, Cu^{2+} and Ag^{+} were added to the humic acids, and the effects in the spectra investigated. In the peats, only the effects of additions of Cs^{+}, Pb^{2+} and Sr^{2+} were studied.

Metal additions were made to the protonated peats and humic acids, with the pH being recorded as being between pH 2.5 and 3. Metal additions were also made to the peats and humic acids after titration with 0.05M KOH to pH 5, and KOH was also used to re-adjust the pH to 5 after metal addition. Thus the effect of ionisation on the reactivity of the humic substances could also be investigated. The addition of alkali was made utilising a Gilsen microburrete and the pH was recorded with an Orion pH meter. After metal addition all materials were washed with de-ionised water to remove excess salt before freeze drying and stored in a vacuum desiccator until analysis. The metal-humate complexes were analysed as KBr pellets, as outlined in section 2.2.4.1.

3.2.2 THE ADDITION OF METALS TO PHTHALIC AND SALICYLIC ACIDS

The addition of CsCl, $SrCl_2$, $Pb(NO_3)_2$, and $AgNO_3$ to phthalic and salicylic acids was also studied. The metals were added to the total titratable acidity, as calculated from the end point of the titration of the acids with 0.5M KOH. The buffer curves and the calculation of their end points are in Appendix 1.3, and gave a mean value of 8.15 $mmol_c\ g^{-1}$ titratable acidity for salicylic acid and 14.52 $mmol_c\ g^{-1}$ titratable acidity for phthalic acid. A sample buffer curve and calculation are shown in Figure 3.1.

As with the metal additions to humic substances, metal additions were made to the compounds with no pH adjustment and with the pH adjusted before and after

addition of metal to pH 4.5. The acids were then rotary evaporated and freeze dried before pelleting. All materials were stored in a vacuum desiccator until analysis.

Figure 3.1

Titration of salicylic acid with 0.5M KOH, titration 2

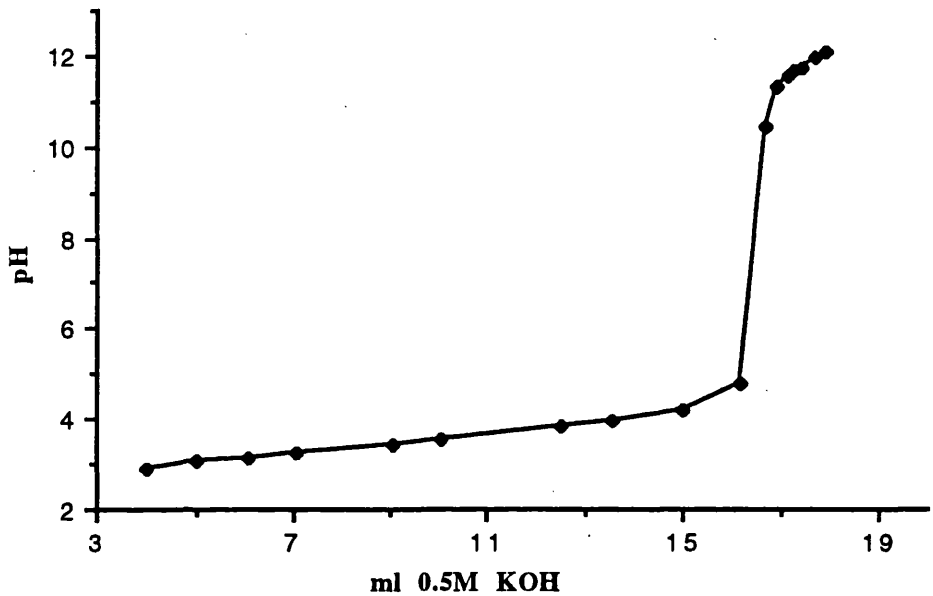

CALCULATION OF TOTAL TITRATABLE ACIDITY

The end point of the titration was 16.4 ml, and the weight of salicylic acid used was 1.031g. Since the molarity of the alkali was 0.5 M, the titratable acidity can be calculated as:

$$\frac{16.4 \times 0.5}{1.031} = 7.95 \text{ mmolc } g^{-1}$$

3.3 RESULTS AND DISCUSSION

3.3.1 COMPARISON OF THE REACTIVITY OF HUXTER AND LUNGA WATER HUMIC SUBSTANCES

The addition of metals to both peats and their respective humic acids was carried out. However, only the results for the Pb^{2+} treated samples will be discussed here, since the Pb^{2+} treated humic substances show the most significant changes in the infra-red, illustrating the differences caused by peat type most effectively.

Addition of metals to the humic acids (Figures 3.4 and 3.5) resulted in similar changes occurring in the infra-red, and no obvious difference in reactivity was seen in these samples. However, the metal-treated peat samples did show differences. The metal treated Lunga Water peat samples (Figure 3.2) showed distinct changes in the bands at $1720cm^{-1}$ and $1600cm^{-1}$ at twice the total acidity, (the significance of these changes as far as complex formation is concerned will be discussed further in section 3.3.3.3). Conversely, the Huxter peat samples showed very little changes in these bands on metal treatment (Figure 3.3), with this being seen in all the replicates carried out.

This qualitative study of the reactivity of humic substances to metals is therefore demonstrating two significant effects. Firstly, the Huxter peat is less reactive towards metals than the Lunga Water peat. The characterisation procedures previously discussed in Chapter 2 showed that the Lunga Water peat, and its humic acid, contained a higher content of reactive functional groupings through higher values for the total acidity and carboxyl group contents, and therefore this increased reactivity towards metals is not unexpected. However, the humic acids do not show any significant differences in the infra-red in reactivity towards metals and from this it can also be concluded that the peat samples are less responsive to metal treatments than the humic acids. This was also mirrored in the total acidity and carboxyl content results, and will be discussed further in section 3.3.3.

Figure 3.2 Lunga Water peat treated with Pb^{2+} to different levels of addition at pH 3.

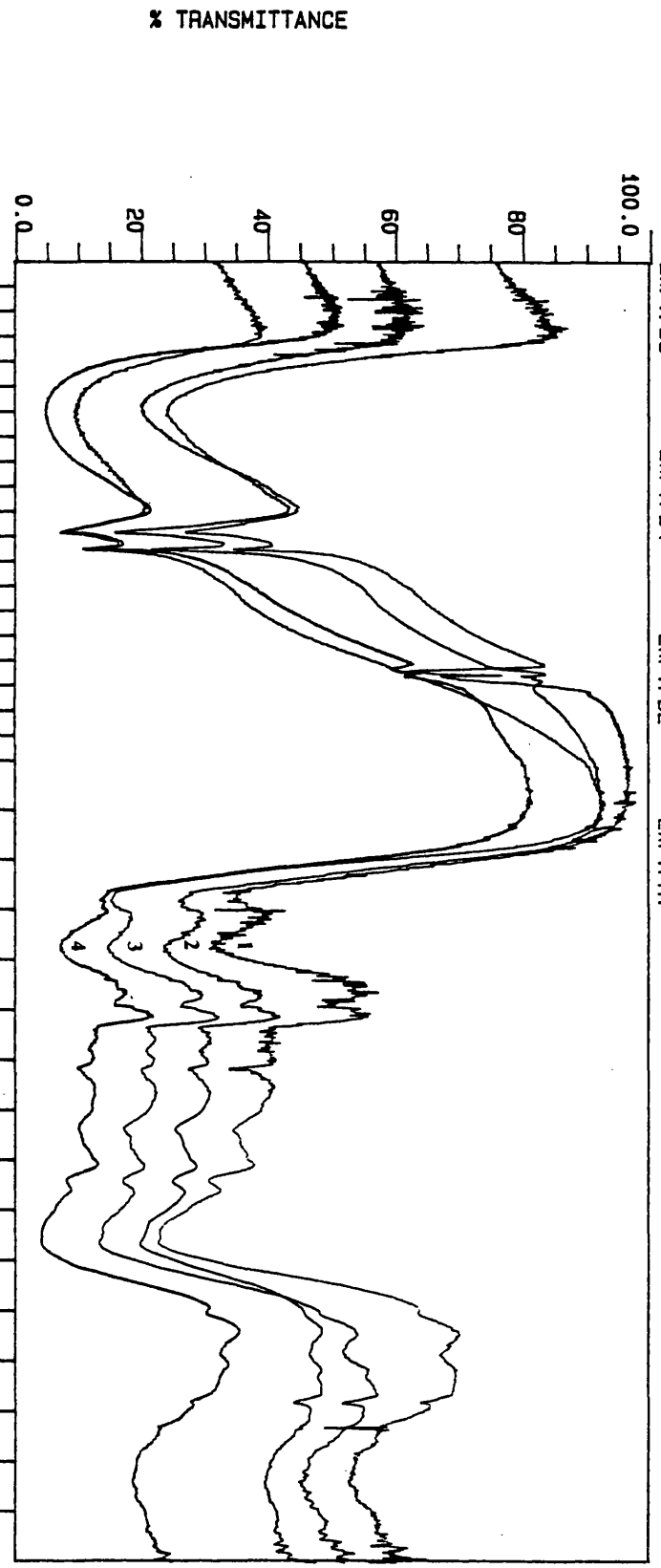

1 = Protonated Lunga Water peat 2 = Lunga Water peat treated with Pb^{2+} to half binding capacity at pH 3

3 = Lunga Water peat treated with Pb^{2+} to binding capacity at pH 3

4 = Lunga Water peat treated with Pb^{2+} to twice binding capacity at pH 3

Figure 3.3 Huxter peat treated with Pb^{2+} to different levels of addition at pH 3.

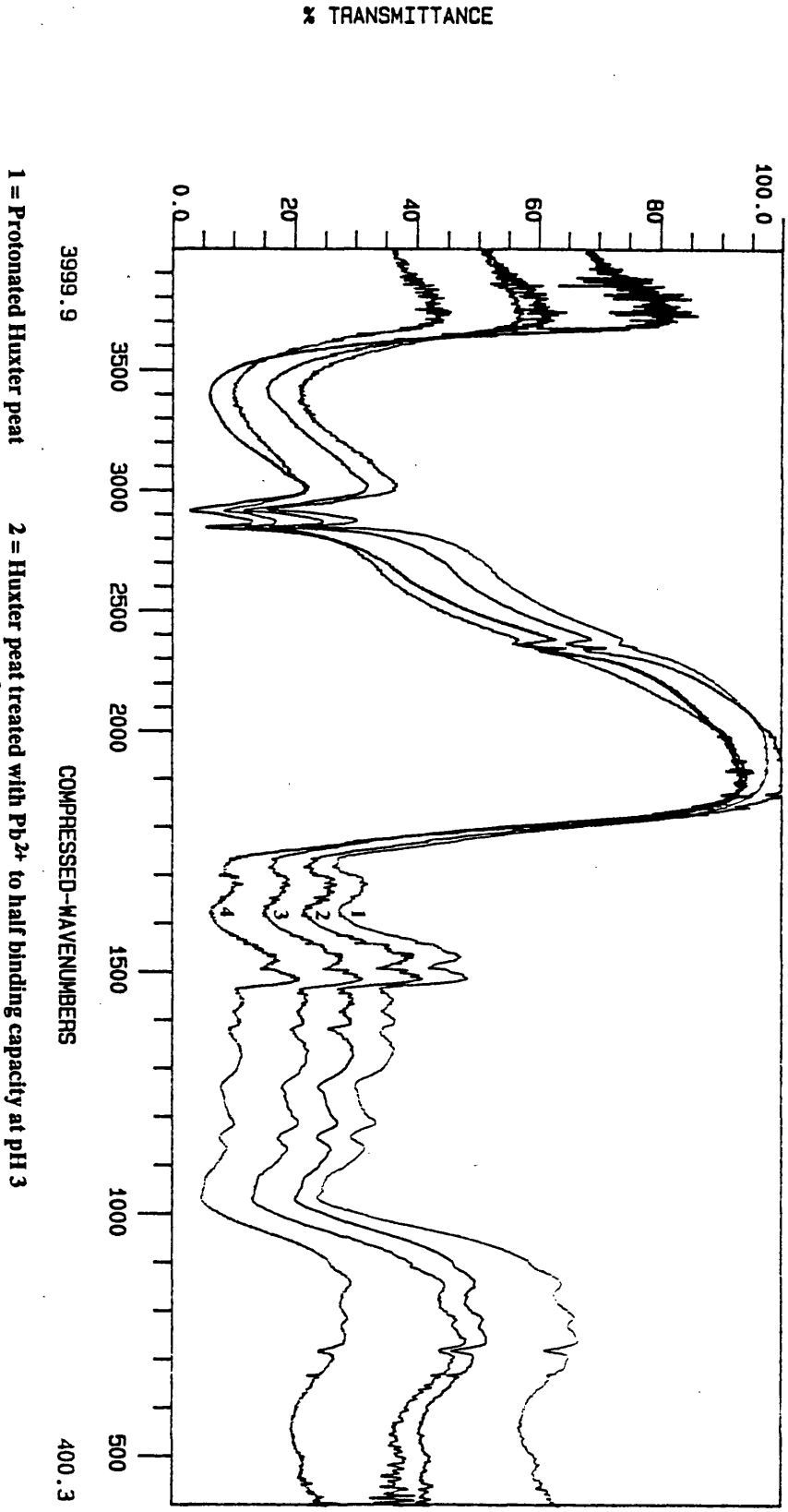

1 = Protonated Huxter peat 2 = Huxter peat treated with Pb^{2+} to half binding capacity at pH 3
3 = Huxter peat treated with Pb^{2+} to binding capacity at pH 3
4 = Huxter peat treated with Pb^{2+} to twice binding capacity at pH 3

Figure 3.4 Lunga Water humic acid treated with Pb^{2+} to different levels of addition at pH 3.

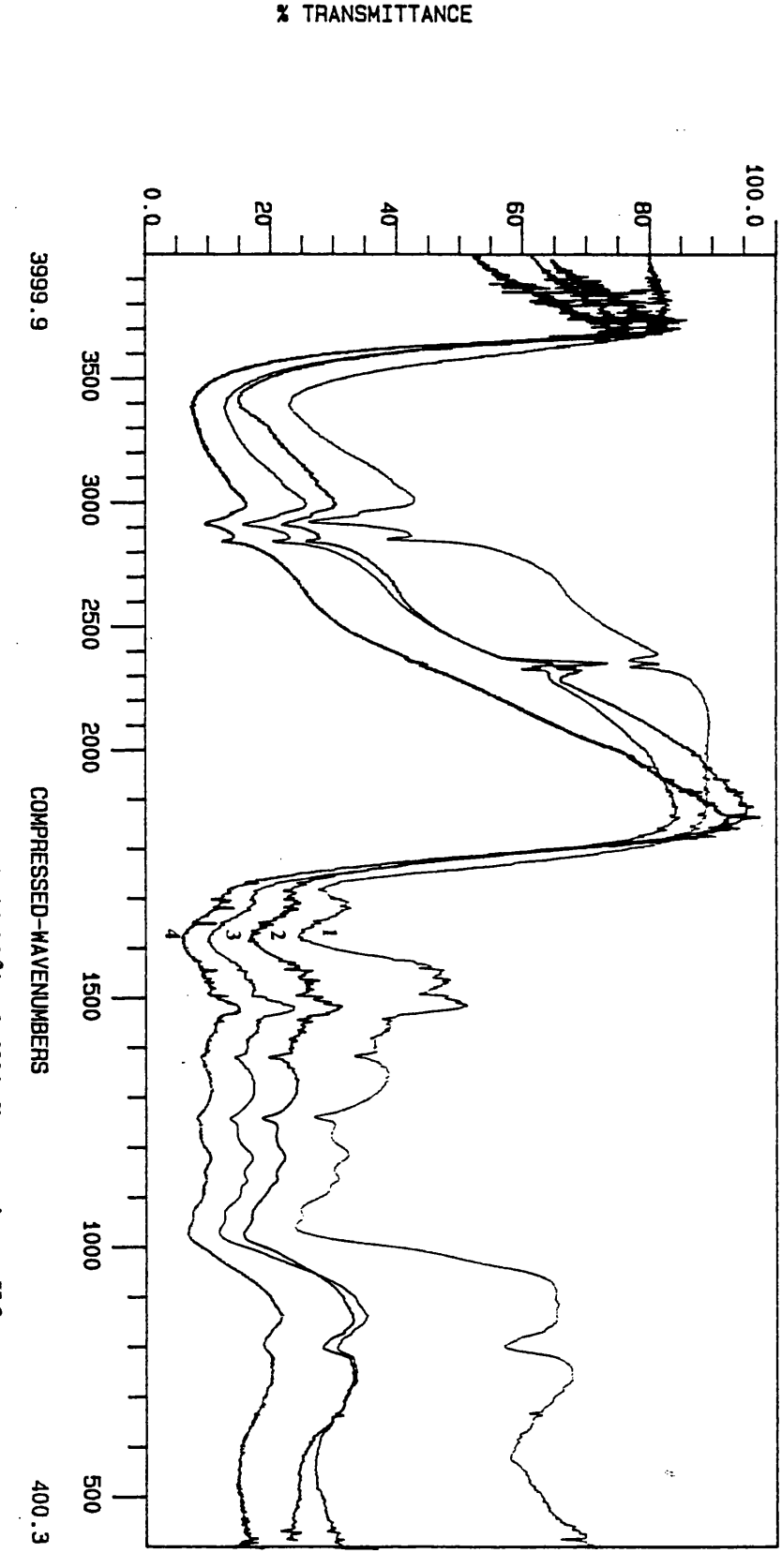

1 = Protonated Lunga Water humic acid 2 = Lunga Water humic acid treated with Pb^{2+} to half binding capacity at pH 3
3 = Lunga Water humic acid treated with Pb^{2+} to binding capacity at pH 3
4 = Lunga Water humic acid treated with Pb^{2+} to twice binding capacity at pH 3

Figure 3.5 Huxter humic acid treated with Pb^{2+} to different levels of addition at pH 3.

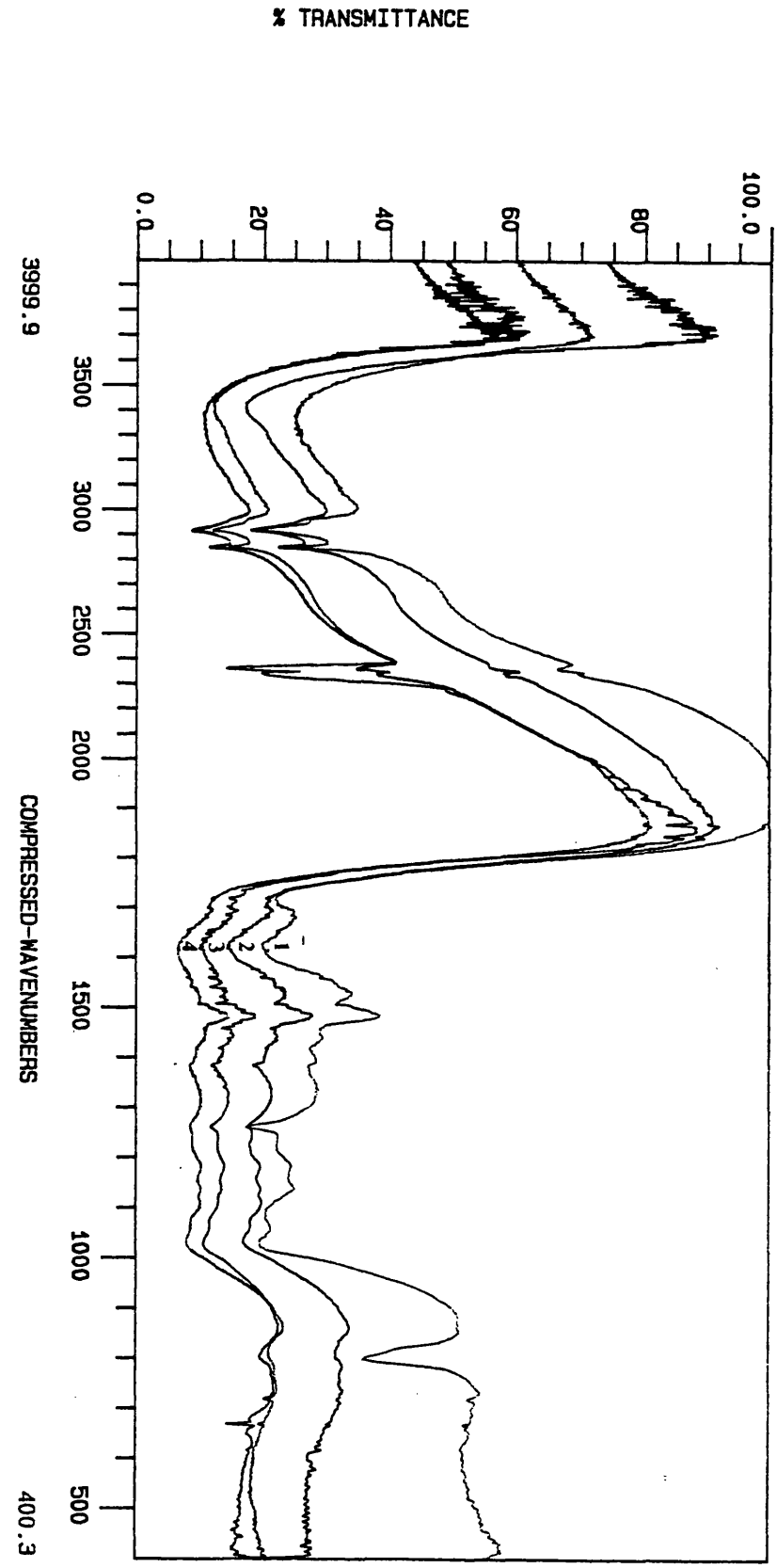

1 = Protonated Huxter humic acid 2 = Huxter humic acid treated with Pb^{2+} to half binding capacity at pH 3
3 = Huxter humic acid treated with Pb^{2+} to binding capacity at pH 3
4 = Huxter humic acid treated with Pb^{2+} to twice binding capacity at pH 3

3.3.2 THE EFFECT OF METAL ADDITIONS TO HUMIC ACID

In order to simplify interpretation only the Lunga Water humic acid treatments will be discussed, since as demonstrated in section 3.3.1., the effect of metal treatment was the same in both humic acids.

3.3.2.1 Cs^+-TREATED HUMIC ACID

The effect of Cs^+ additions to humic acid at different levels of metal addition was investigated in protonated humic acid, at pH 3, and also humic acid which had been titrated to pH 5.

In the protonated humic acid (Figure 3.6), treatment with Cs^+ resulted in changes in the spectra which indicate that ionisation of carboxyl groupings is occurring. As outlined in section 3.1, this gives a loss of the carbonyl absorption at $1720cm^{-1}$, with a corresponding appearance of bands at $\sim 1590cm^{-1}$ and $\sim 1400cm^{-1}$. This effect is clearly seen in the Cs^+ treated samples in Figure 3.6, and also results in a slight broadening of the band at $1600cm^{-1}$. In addition, at twice the total acidity, the band at 3400^{-1} shows downward broadening which is indicative of formation of water of crystallisation on formation of the salt (Kemp, 1991).

The Cs^+ additions at pH 5 are displayed in Figure 3.7, and can be compared to the corresponding K^+ salt at pH 5. From the spectra it can be seen that both Cs^+ and K^+ are binding in a similar manner through an ionic interaction, as demonstrated by previous infra-red studies (Vinkler et *al.*, 1976; Maguire *et al.*, 1991). Bonn and Fish (1993) also showed through adsorption studies that K^+ binds as a hydrated ion, forming ionic complexes with humic acid.

In both Figures 3.6 and 3.7, level of addition has little effect on the changes seen at $1720cm^{-1}$ and $1600cm^{-1}$, with only slight increases in reaction at twice the total acidity, indicating that the maximum binding capacity of the humic acid for Cs^+ was reached at half the total acidity. There is also a remaining carbonyl absorption which is due to ketonic and aldehydic groupings present in the humic substances (Piccolo & Stevenson, 1982). There may also be the interacting effect of some groupings being sterically hindered, and therefore unavailable for reaction.

Figure 3.6 Lunga Water humic acid treated with Cs^+ to different levels of addition at pH 3.

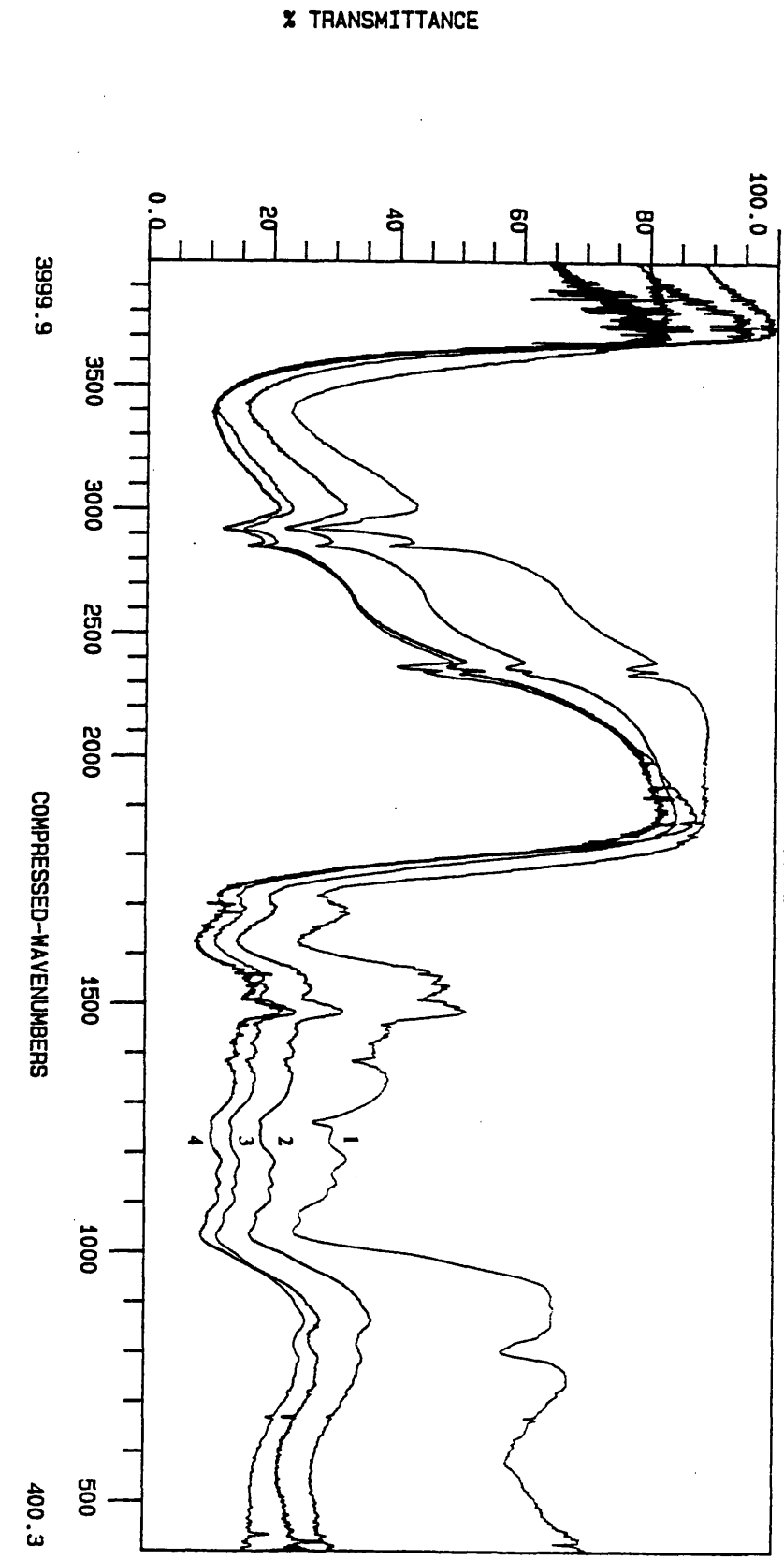

1 = Protonated Lunga Water humic acid 2 = Lunga Water humic acid treated with Cs^+ to half binding capacity at pH 3
3 = Lunga Water humic acid treated with Cs^+ to binding capacity at pH 3
4 = Lunga Water humic acid treated with Cs^+ to twice binding capacity at pH 3

Figure 3.7. Lunga Water humic acid treated with Cs^+ to different levels of addition at pH 5.

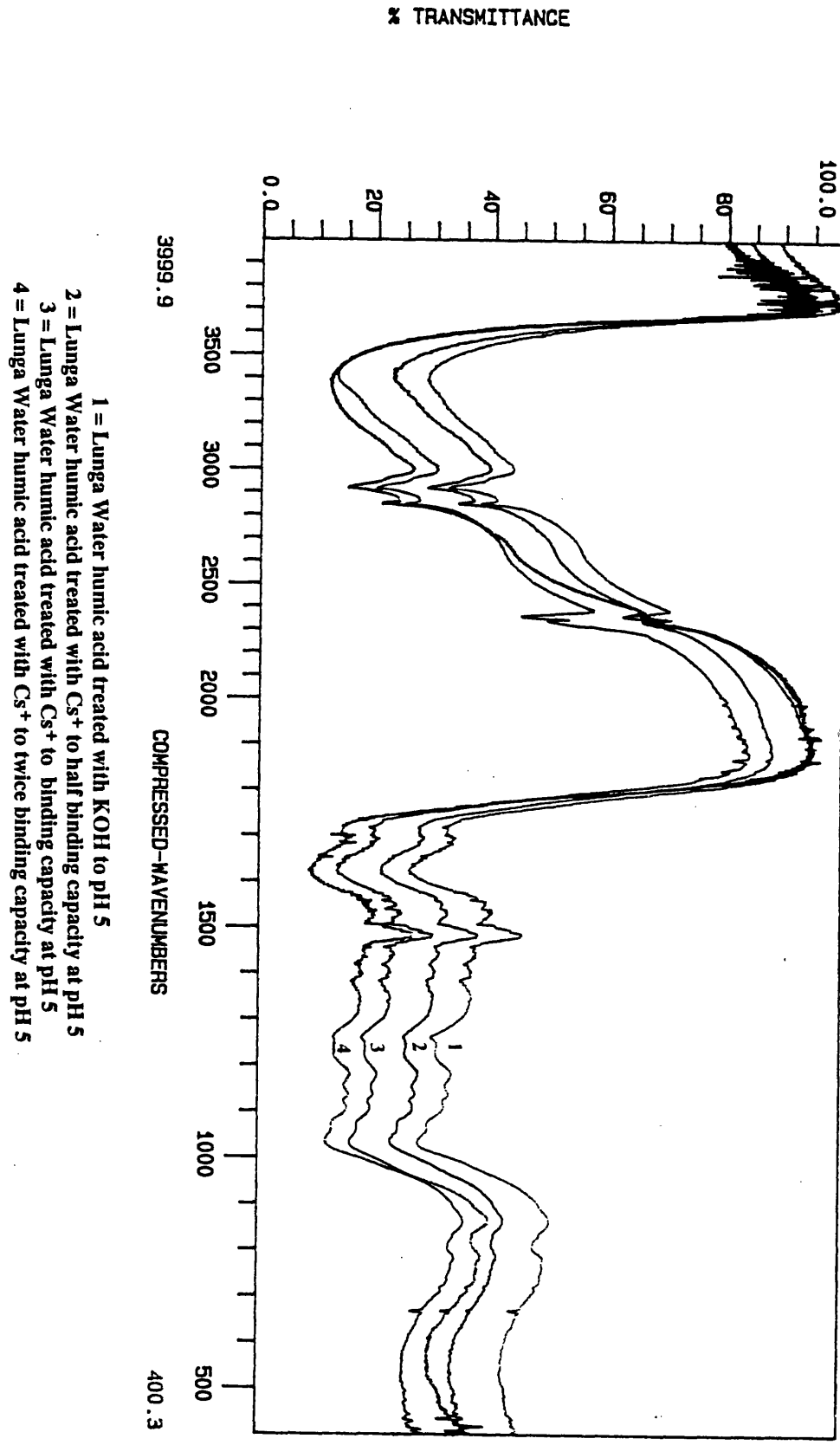

1 = Lunga Water humic acid treated with KOH to pH 5
2 = Lunga Water humic acid treated with Cs^+ to half binding capacity at pH 5
3 = Lunga Water humic acid treated with Cs^+ to binding capacity at pH 5
4 = Lunga Water humic acid treated with Cs^+ to twice binding capacity at pH 5

3.3.2.2 Sr^{2+} AND Pb^{2+}-TREATED HUMIC ACID

Sr^{2+} and Pb^{2+} are presented together since both metals display similar changes in their spectra. The additions of Sr^{2+} and Pb^{2+} at pH 3 are presented in Figures 3.9 and 3.11 respectively, whilst the additions at pH 5 are displayed in figures 3.10 and 3.12. In all of the spectra, the main change which is observed is a broadening of the band at 1600cm^{-1}, with a concurrent loss of absorption at 1720cm^{-1}. The effect in all of the spectra becomes more significant with level of addition. The effect is also more enhanced at pH 5 (Figures 3.10 and 3.12), where the degree of ionisation of the humic acid is increased. Therefore, on ionisation the Pb^{2+} and Sr^{2+} can interact more easily since they do not have to compete with protons for the binding sites. Also, ionisation has been proposed to give an opening up of structure as the negatively-charged groups repel, giving an increase in reactive groupings (Stevenson, 1982). This may also result in more sterically favourable arrangements for complexation reactions.

The changes in the Sr^{2+} and Pb^{2+} spectra are also significantly different from their respective K^{+} treated spectra at pH 5 (Figures 3.10 & 3.12), indicating that in these metals, binding does not occur through an ionic arrangement. Vinkler *et al.* (1976) demonstrated that Sr^{2+} interactions with humic acid were less ionic in character than K^{+} or Cs^{+}, and previous work on the binding of Pb^{2+} and Sr^{2+} to humic acid indicated that the binding was covalent in character (Maguire *et al.*, 1991). Piccolo & Stevenson (1982) demonstrated that the interaction of Pb^{2+} with humic acid resulted in similar changes to those observed in Figure 3.12, with the effect also being more enhanced at high degrees of metal loading.

Broadening of the band at 1600cm^{-1} indicates that a variety of effects are occurring. One such effect could be the interaction of Sr^{2+} and Pb^{2+} with conjugated ketones, which can potentially form complexes with metal ions in the following way:

Figure 3.8 Coordination of a metal with conjugated ketones.

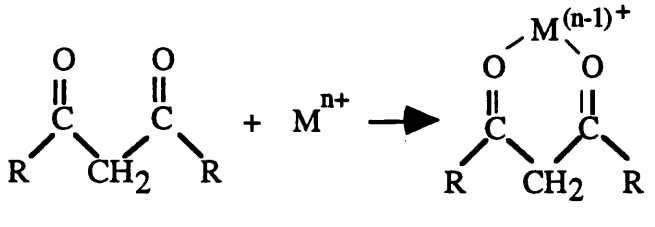

The carbonyl groupings become weakened by this resonance and the frequency of absorption is correspondingly reduced (Bellamy, 1975). This interaction thus explains the observed reduction in absorption at 1720cm^{-1}, which is not observed in the K^+ spectra, and would also contribute to the broadening seen in the spectra of Pb^{2+} and Sr^{2+} humates. The frequency of absorption is also affected by the arrangement of the metal-ketone interaction. Nakamoto (1986) showed that if the metal was bound in the keto form (as shown above), then absorption of the carbonyl group centres around 1700cm^{-1}. However, if the enol form occurs, then absorption is shifted to around 1627cm^{-1}. In humic acid where a variety of ketonic groupings could be present, with different environments, then a mixture of enol and keto arrangements could occur.

In addition, the variety in type and arrangement of functional groupings present could also contribute to the broadening effect. In section 1.7.1.1 the different forms of coordinate covalent complex which a metal could potentially form were presented. As explained in section 3.1 each type of complex, i.e. bridging, coordination and chelation, will result in different frequencies of carbonyl absorption. Therefore, since potentially a combination of effects can occur on binding, it is not surprising that broadening is observed in this region of the spectra. This is best summed up in the following statement:

" given the variety of functional groups in humic molecules, and the various ways in which they can interact with metals, a near infinite number of metal-humic complexes is possible in principle" (Livens, 1991).

Broadening of the band at 1600 cm^{-1} was also observed on titration of humic substances (section 2.3.2.4) and was attributed in this instance to structural changes. On binding, the configuration of the humic acid could alter, causing exposure of previously unreactive groupings. As Sr^{2+} and Pb^{2+} bind, a pH drop was observed, indicating that in order to re-establish ionisation equilibrium, protons had been displaced from adjacent acid groupings, as was also observed by Perdue *et al.* (1980) in a study of Ca-humate binding. This generation of negative charges would also result in an opening of structure due to the charges repelling, and may explain why increases in the level of binding are still being observed at twice the total acidity, since this parameter is effectively operationally defined.

Figure 3.9 Lunga Water humic acid treated with Sr^{2+} to different levels of addition at pH3.

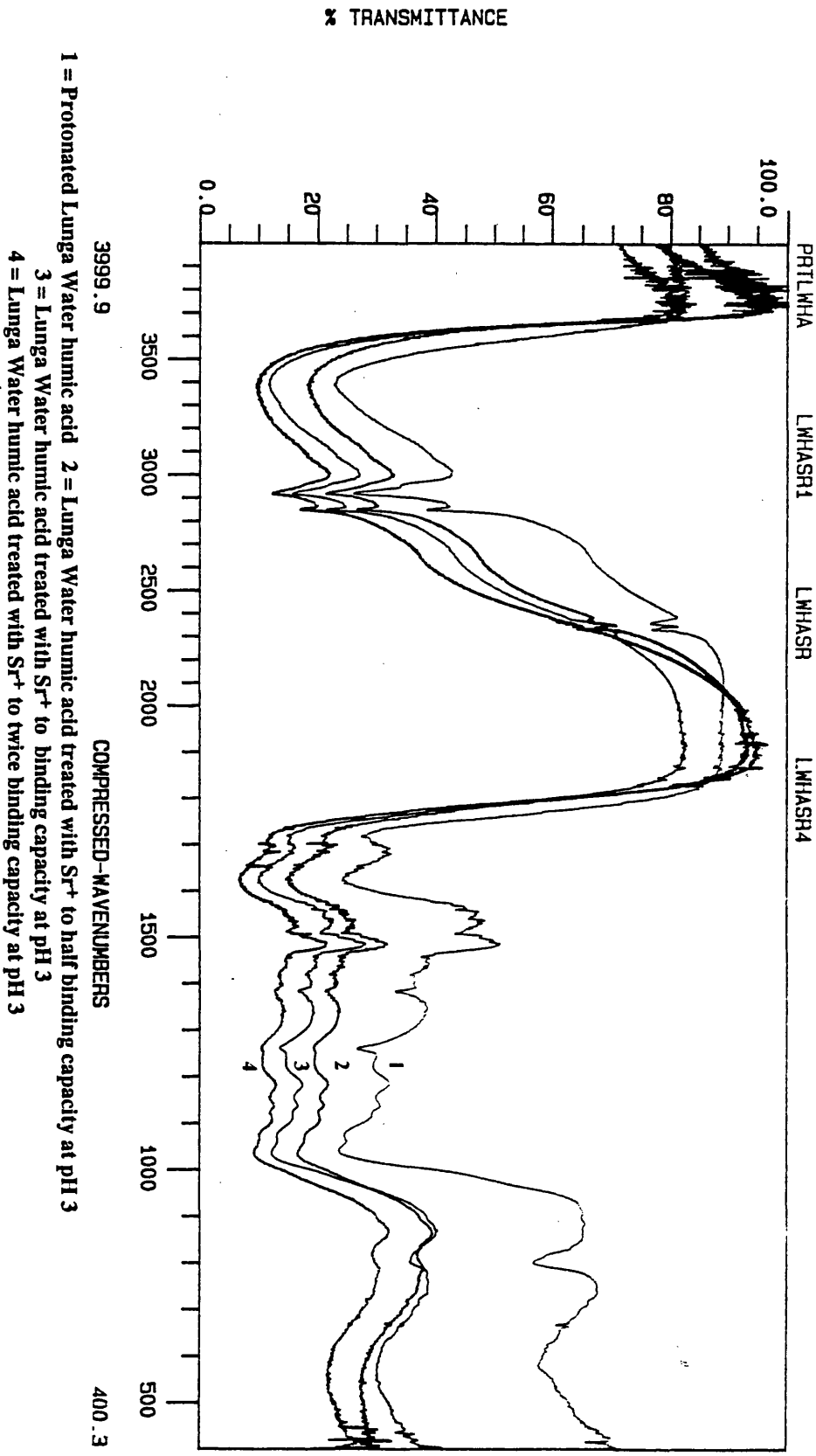

1 = Protonated Lunga Water humic acid 2 = Lunga Water humic acid treated with Sr^{+} to half binding capacity at pH 3
3 = Lunga Water humic acid treated with Sr^{+} to binding capacity at pH 3
4 = Lunga Water humic acid treated with Sr^{+} to twice binding capacity at pH 3

Figure 3.10 Lunga Water humic acid treated with Sr^{2+} to different levels of addition at pH 5.

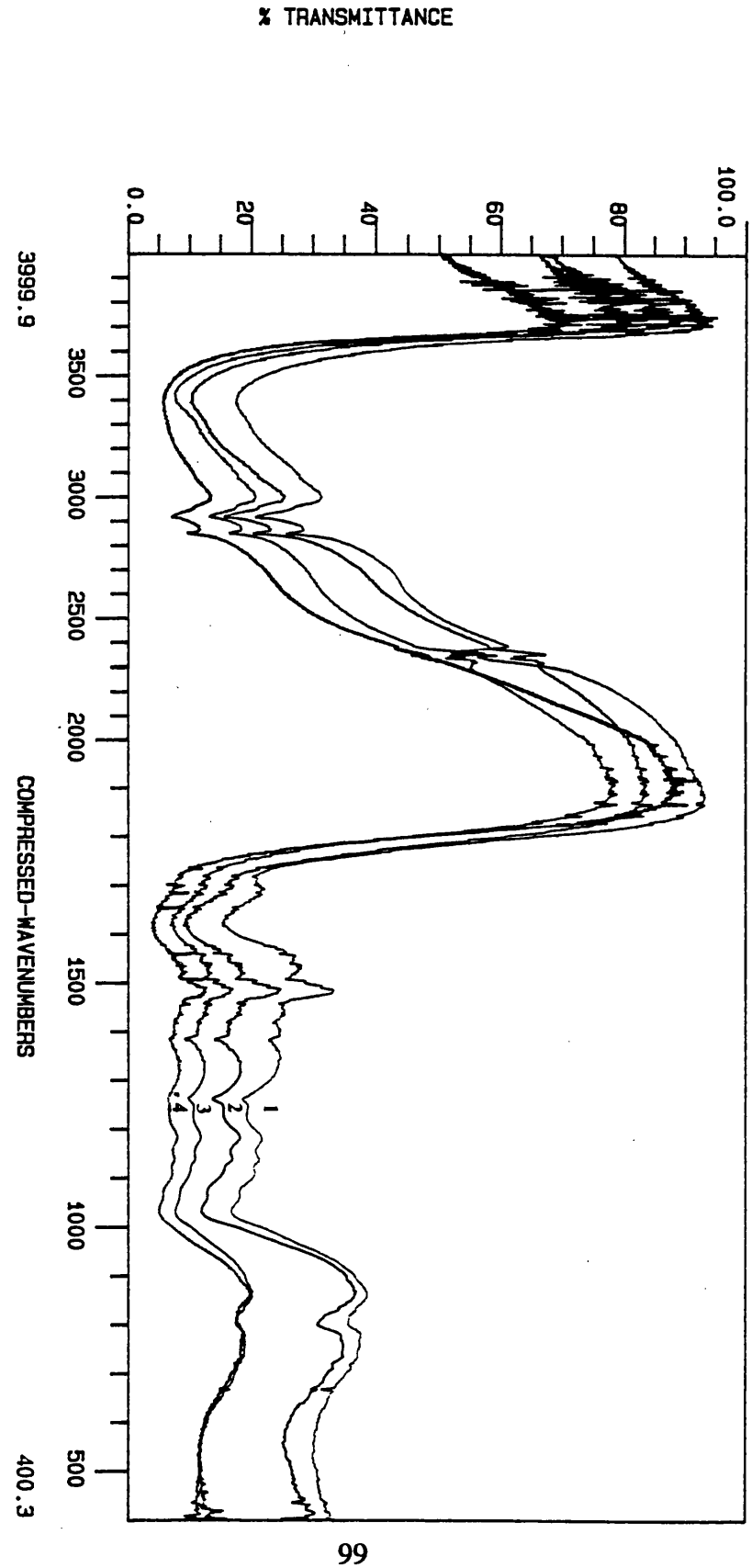

1 = Lunga Water humic acid treated with KOH to pH 5
2 = Lunga Water humic acid treated with Sr^{+} to half binding capacity at pH 5
3 = Lunga Water humic acid treated with Sr^{+} to binding capacity at pH 5
4 = Lunga Water humic acid treated with Sr^{+} to twice binding capacity at pH 5

Figure 3.11 Lunga Water humic acid treated with Pb^{2+} to different levels of addition at pH 3.

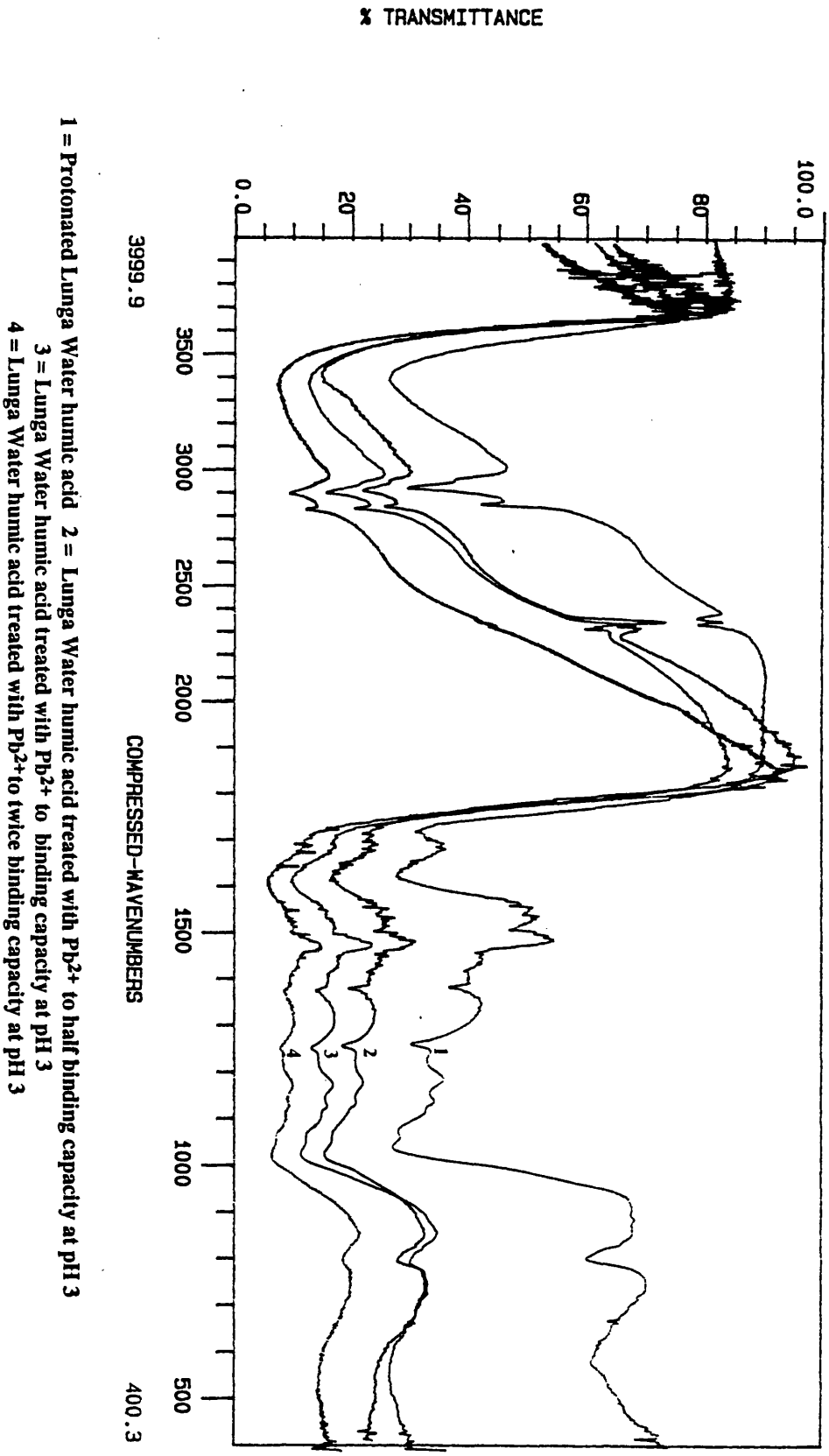

1 = Protonated Lunga Water humic acid 2 = Lunga Water humic acid treated with Pb^{2+} to half binding capacity at pH 3
3 = Lunga Water humic acid treated with Pb^{2+} to binding capacity at pH 3
4 = Lunga Water humic acid treated with Pb^{2+} to twice binding capacity at pH 3

Figure 3.12 Lunga Water humic acid treated with Pb^{2+} to different levels of addition at pH 5.

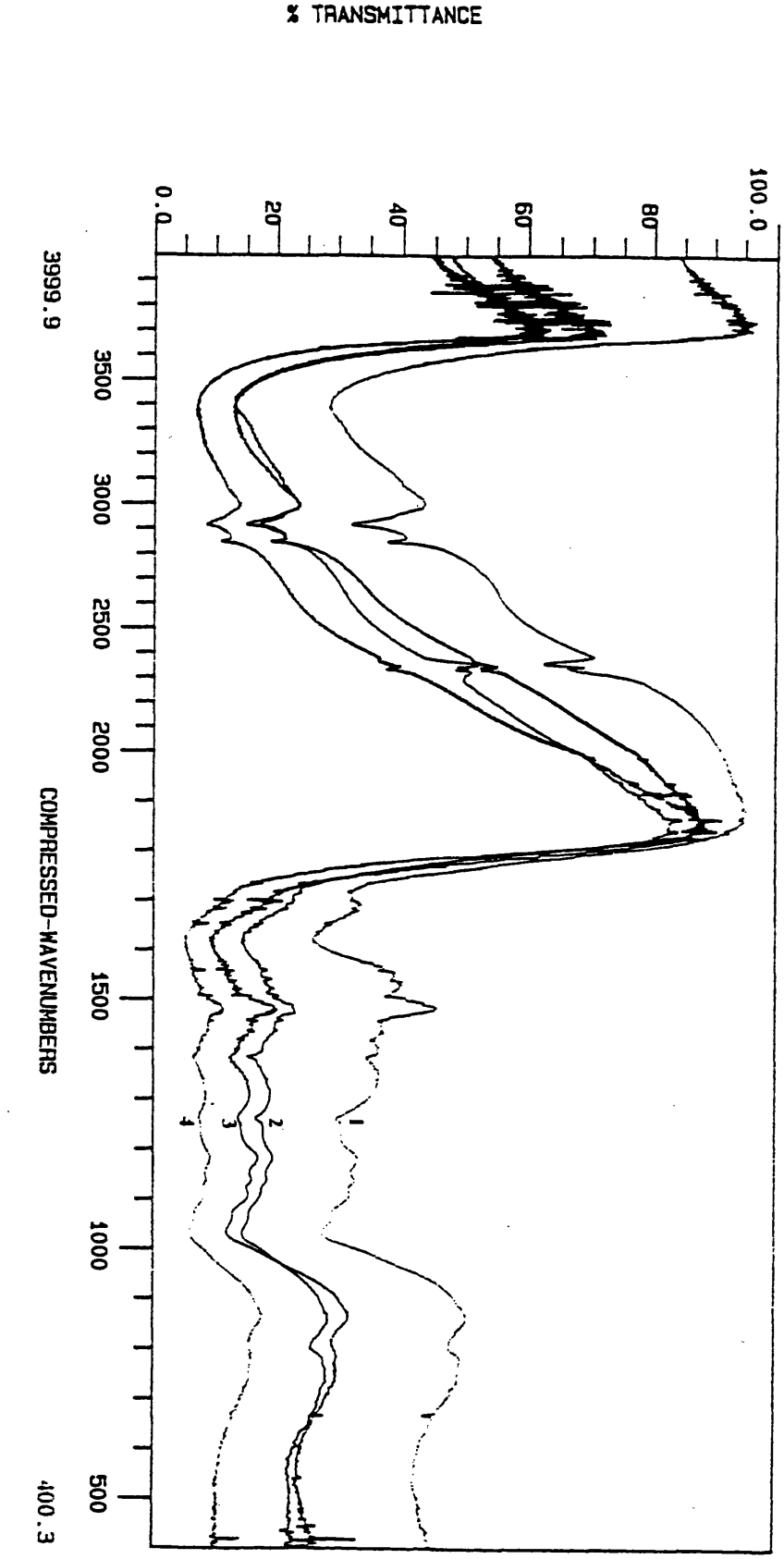

1 = Lunga Water humic acid titrated with KOH to pH 5
2 = Lunga Water humic acid treated with Pb^{2+} to half binding capacity at pH 5
3 = Lunga Water humic acid treated with Pb^{2+} to binding capacity at pH 5
4 = Lunga Water humic acid treated with Pb^{2+} to twice binding capacity at pH 5

3.3.2.3 Cu^{2+} AND Zn^{2+}-TREATED HUMIC ACID

The addition of Cu^{2+} and Zn^{2+} to humic acid was carried out at pH 5 only, since the effect of metal addition to unionised samples had been clearly established with Cs^{+}, Pb^{2+} and Sr^{2+}.

The Cu^{2+}-treated humic acid (Figure 3.13) and the Zn^{2+}-treated humic acid (Figure 3.14) show similar effects. Both are reacting to give pronounced changes in the infra-red, particularly at high levels of metal addition, with total loss of absorption at $1720cm^{-1}$ and significant downward broadening and increase in absorption at $1600cm^{-1}$. This effect is similar to that seen in the Sr^{2+} and Pb^{2+} treated humic acids, but is more enhanced. Therefore, Cu^{2+} and Zn^{2+} are also reacting to form coordinate covalent complexes, perhaps with the conjugated ketones as outlined in section 3.3.2.2. The ability of Cu^{2+} and Zn^{2+} to form stable complexes has previously been demonstrated for organic acids, where Cu^{2+} and Zn^{2+} had the highest stability constants (Buffle, 1988). Cu^{2+} was also seen to give more enhanced changes in the infra-red when compared to Pb^{2+} (Piccolo & Stevenson, 1982).

The reactivity of Cu^{2+} and Zn^{2+} is due partly to their polarisability, and therefore their ability to form inner sphere complexes (see section 1.71.1). Senesi & Calderoni (1987) were able to demonstrate through ESR that Cu^{2+} was binding through inner sphere complexes in humic acids, and that the oxygen containing functional groups were involved in the complexation process. In particular, Cu^{2+} has been proposed to be involved in 2:1 complexes with oxygen containing functional groups on humic acid (Buffle *et al.*, 1977: Stevenson *et al.*, 1993). Stevenson & Chen (1991) studied the binding of Cu^{2+} to humic acid and found that humic acid with higher nitrogen contents formed stronger complexes with Cu^{2+}. This could be due to the binding of Cu^{2+} with porphoryn rings in the humic molecule, which have been previously shown to be involved in Cu^{2+} complexing (Goodman & Cheshire, 1976), and could explain the increased reactivity of humic acid towards Cu^{2+}.

The level of addition also affects the level of reaction to a greater degree in these metals. This could indicate that the total acidity is not expressing the maximum binding capacity of the humic acids for these metals, since a significant effect is only seen at twice the total acidity, or it could be due to the reaction of Cu^{2+} and Zn^{2+} with functional groups other than the oxygen containing groups.

Figure 3.13 Lunga Water humic acid treated with Cu^{2+} at different levels of addition at pH 5.

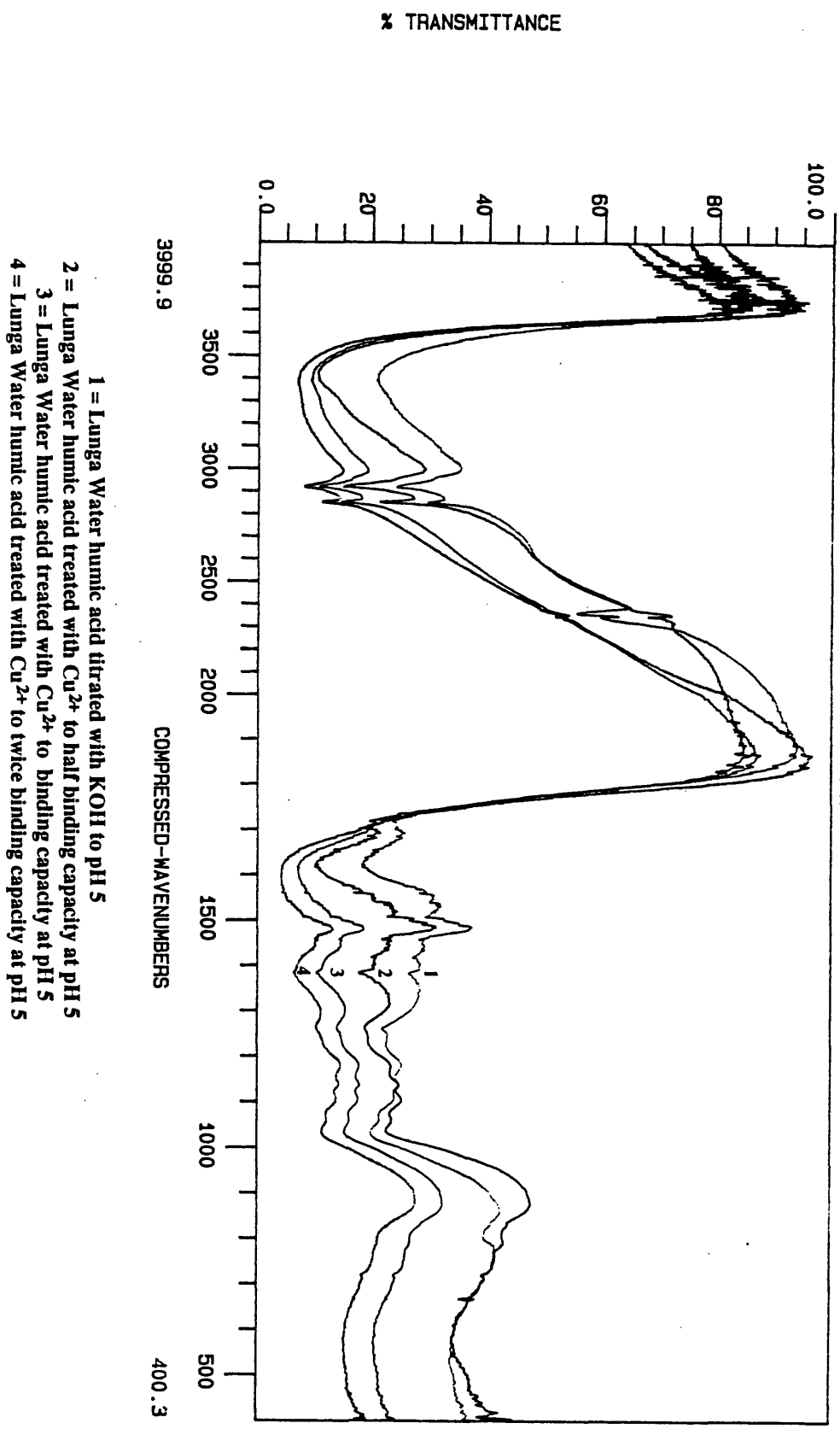

1 = Lunga Water humic acid titrated with KOH to pH 5

2 = Lunga Water humic acid treated with Cu^{2+} to half binding capacity at pH 5

3 = Lunga Water humic acid treated with Cu^{2+} to binding capacity at pH 5

4 = Lunga Water humic acid treated with Cu^{2+} to twice binding capacity at pH 5

Figure 3.14 Lunga Water humic acid treated with Zn^{2+} at different levels of addition at pH 5.

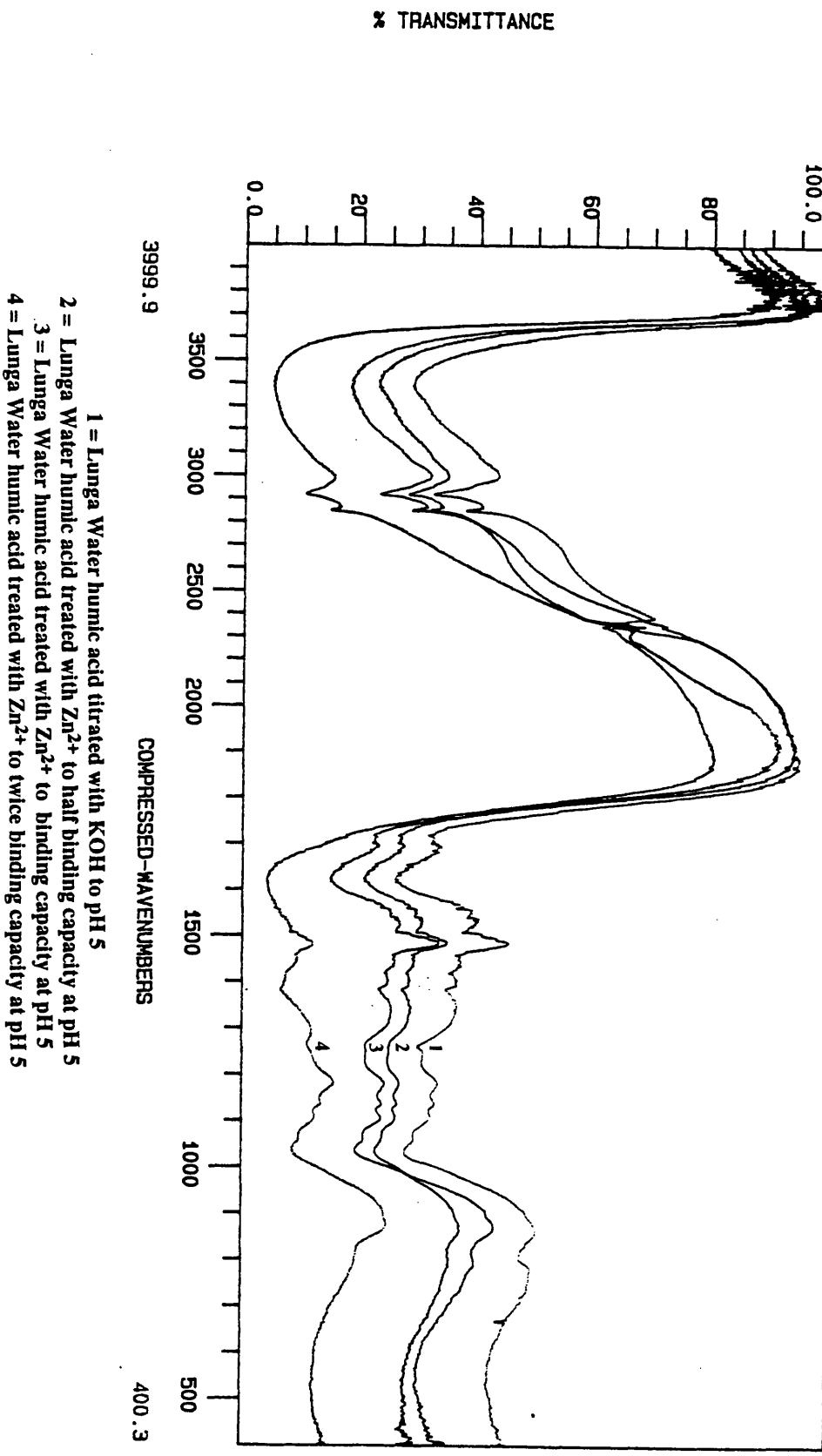

1 = Lunga Water humic acid titrated with KOH to pH 5
2 = Lunga Water humic acid treated with Zn^{2+} to half binding capacity at pH 5
3 = Lunga Water humic acid treated with Zn^{2+} to binding capacity at pH 5
4 = Lunga Water humic acid treated with Zn^{2+} to twice binding capacity at pH 5

3.3.2.4 Ag^+ TREATED HUMIC ACID

Humic acid was treated with Ag^+ at pH 5 only, to investigate the effect of the metal on ionised humic acid.

As with Pb^{2+}, Sr^{2+}, Cu^{2+} and Zn^{2+}, Ag^+ (Figure 3.15) was also able to show a different type of binding than K^+, indicating that the metal was able to form coordinate covalent complexes. This was demonstrated again by a loss of absorption at $1720cm^{-1}$, with a concurrent broadening at $1600cm^{-1}$. However, the level of change in the arrangement of the functional groups in the humic acid was less than for the other metals, suggesting that the humic acid was not as reactive towards Ag^+ as for the other divalent metals.

The ability of Ag^+ to react to form a covalent interaction is also due to its soft character, making it more polarisable and able to coordinate (see section 1.7.1.1). Soft acids react best with soft ligands, such as nitrogen, and Sikora & Stevenson (1988) reported that the maximum binding capacity of humic acid for Ag^+ was related to the nitrogen content of the material. Since there is nitrogen present in the humic acid, the possibility of binding to nitrogen containing groups cannot be discounted. However, since loss of absorption at $1720cm^{-1}$ is also noted, the carbonyl groups must also be involved.

Figure 3.15 Lunga Water humic acid treated with Ag^+ to different levels of addition at pH 5.

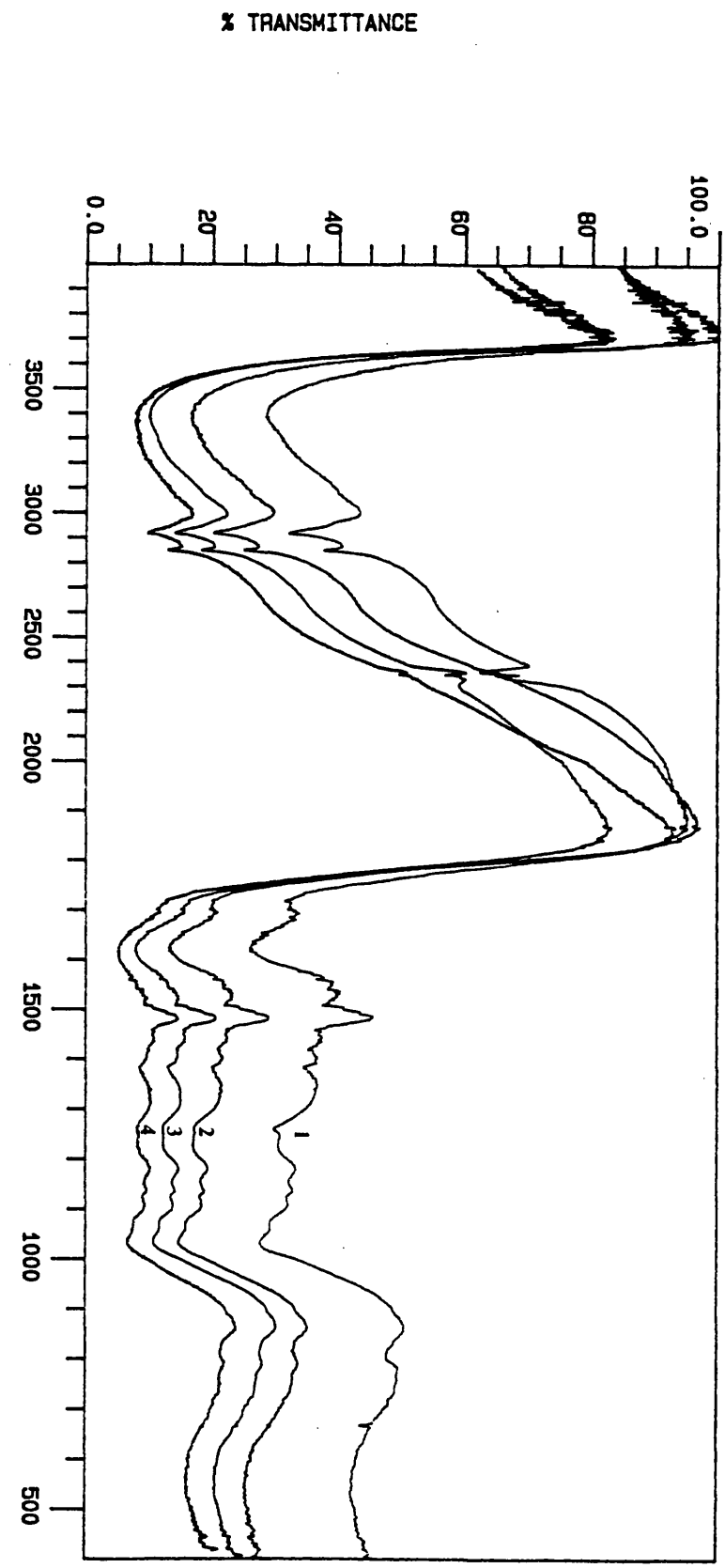

1 = Lunga Water humic acid titrated with KOH to pH 5

2 = Lunga Water humic acid treated with Ag^+ to half binding capacity at pH 5

3 = Lunga Water humic acid treated with Ag^+ to binding capacity at pH 5

4 = Lunga Water humic acid treated with Ag^+ to twice binding capacity at pH 5

3.3.3 METAL ADDITIONS TO UNEXTRACTED PEAT

3.3.3.1 Cs^+-TREATED PEAT

Cs^+ additions were made to protonated peat at pH 3 and to peat which had been titrated to pH 5 with KOH. Figure 3.16 shows the spectra obtained when Cs^+ is added to protonated peat. The level of addition has little effect on the extent of reaction, with the changes which occur in the spectra being evident at half the total acidity. The changes involved are a slight loss of absorption at $1720cm^{-1}$, with a slight broadening at $1600cm^{-1}$ which, as explained in section 3.3.2.1, are indicative of the formation of the carboxylate salt on ionisation. These effects were also observed in the Cs^+ treated humic acid (Figure 3.6), but to a greater degree.

In the samples which have been titrated to pH 5 before and after addition of metal, the same changes are observed. These are displayed in Figure 3.17, and the Cs^+ treated spectra are similar to the K^+ treated spectra, indicating that again the Cs^+ is binding in an ionic arrangement, but with a lower degree of reaction than in the humic acid (Figure 3.7). This reduced reaction of unextracted organic matter towards metals was also observed by Warwick *et al.* (1992), where humic acid showed higher binding capacities.

Figure 3.16 Lunga Water peat treated with Cs^+ to different levels of addition at pH 3.

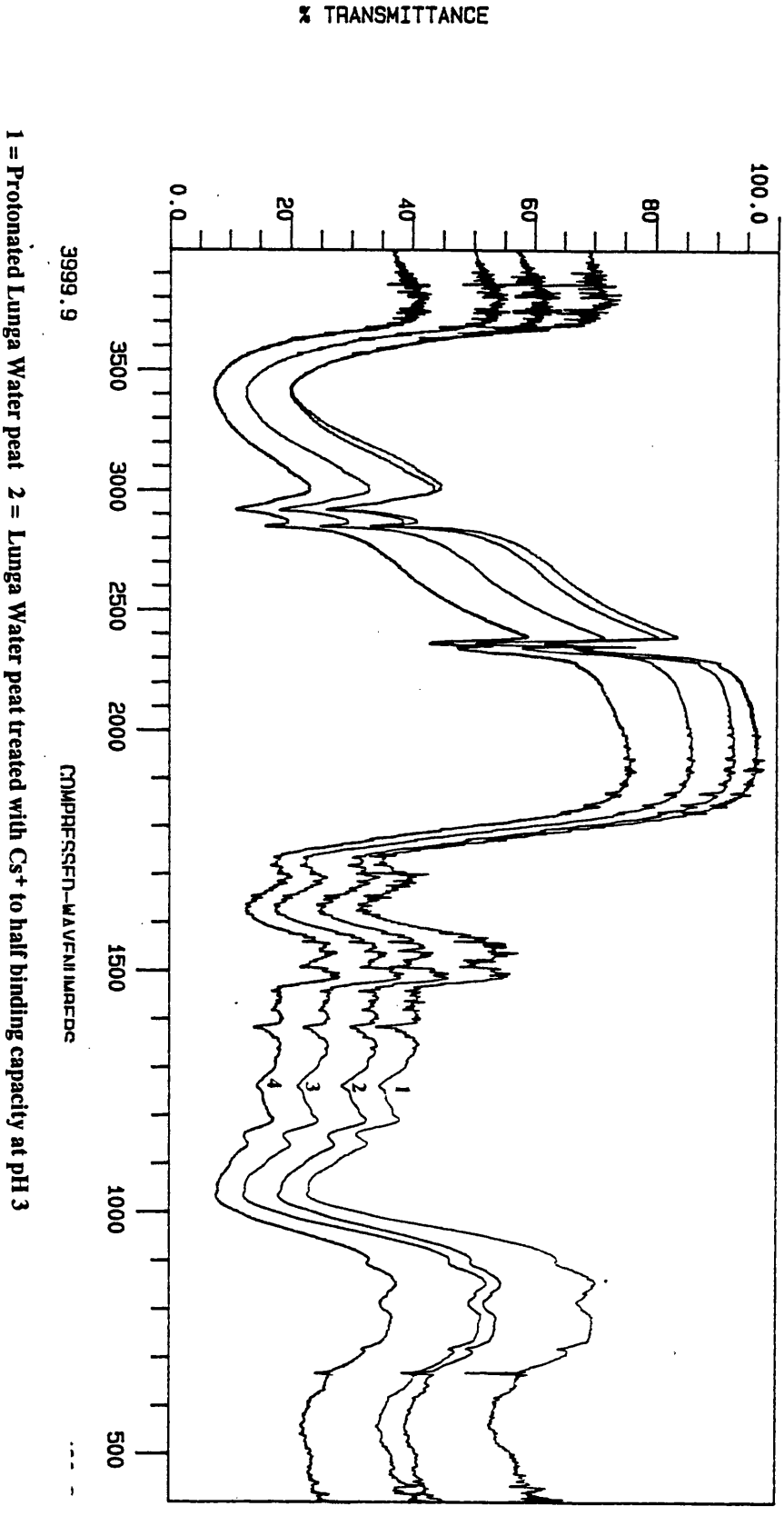

1 = Protonated Lunga Water peat 2 = Lunga Water peat treated with Cs^+ to half binding capacity at pH 3
3 = Lunga Water peat treated with Cs^+ to binding capacity at pH 3
4 = Lunga Water peat treated with Cs^+ to twice binding capacity at pH 3

Figure 3.17 Lunga Water peat treated with Cs^+ to different levels of addition at pH 5.

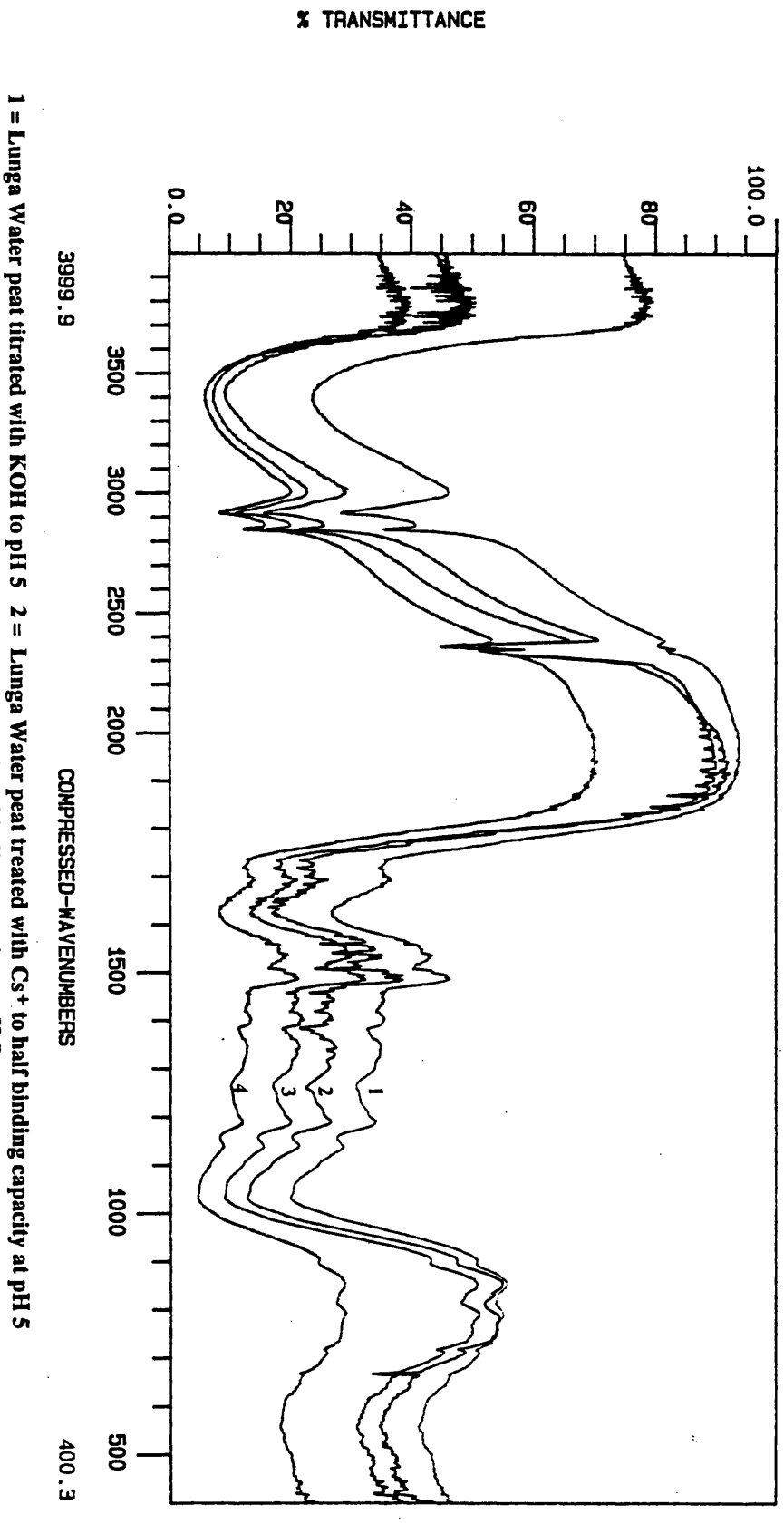

1 = Lunga Water peat titrated with KOH to pH 5 2 = Lunga Water peat treated with Cs^+ to half binding capacity at pH 5
3 = Lunga Water peat treated with Cs^+ to binding capacity at pH 5
4 = Lunga Water peat treated with Cs^+ to twice binding capacity at pH 5

3.3.3.2 Sr^{2+}-TREATED PEAT

As with Cs^+, Sr^{2+} additions were made to protonated peat at pH 3, and peat which had been titrated to pH 5. In Figure 3.18, the Sr^{2+} additions at pH 3 are displayed and show similar changes to Cs^+, with only slight loss of absorption at $1720cm^{-1}$, with a corresponding slight broadening at $1600cm^{-1}$. In Figure 3.9, the Sr^{2+} additions to protonated humic acid are displayed and show a different reaction than in the peat, with a marked loss at $1720cm^{-1}$ and a significant broadening of the $1600cm^{-1}$ peak.

The additions to titrated peat at pH 5 are displayed in Figure 3.19, and again a significantly reduced reaction is seen when compared to the corresponding additions to humic acid (Figure 3.10). The Sr^{2+} spectra are similar to the spectra for the K^+ treated peat and indicate that in peat the Sr^{2+} is binding in an ionic arrangement, whereas in the humic acid Sr^{2+} was able to undergo complexation reactions.

This lack of complexation is consistent with the observations of Bloom and McBride (1979), who showed that Ca^{2+} was able to retain its water of hydration and bind in an ionic arrangement to unextracted peat. They viewed unextracted peat as a solid phase cation exchanger. In humic acid, which is an operationally-derived extract, Ca^{2+} has been shown to participate in complexation reactions (Perdue *et al.*, 1980) as the Sr^{2+} does in the Lunga Water humic acid.

Figure 3.18 Lunga Water peat treated with Sr^{2+} to different levels of addition at pH 3.

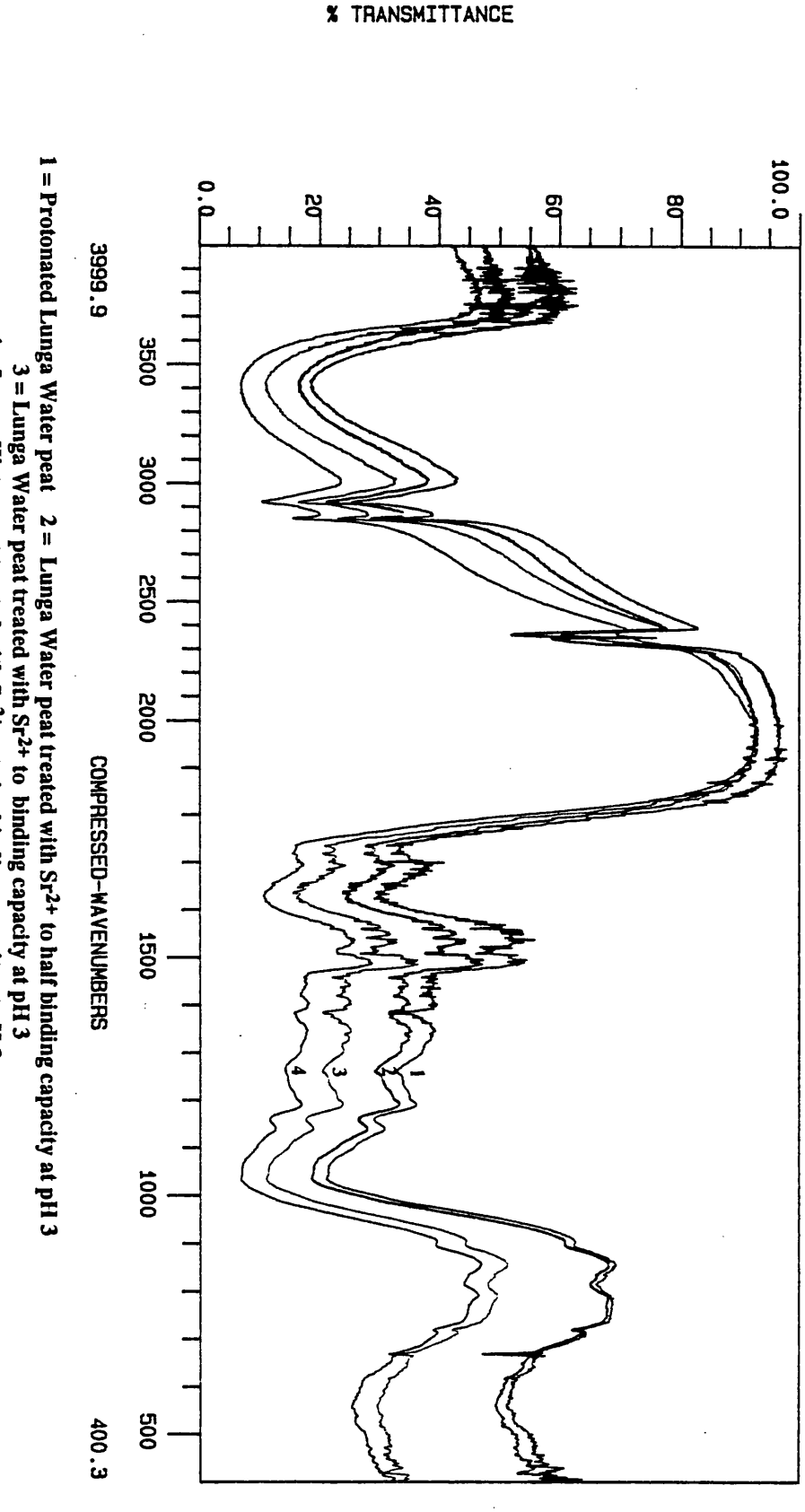

1 = Protonated Lunga Water peat 2 = Lunga Water peat treated with Sr^{2+} to half binding capacity at pH 3
3 = Lunga Water peat treated with Sr^{2+} to binding capacity at pH 3
4 = Lunga Water peat treated with Sr^{2+} to twice binding capacity at pH 3

Figure 3.19 Lunga Water peat treated with Sr^{2+} to different levels of addition at pH 5.

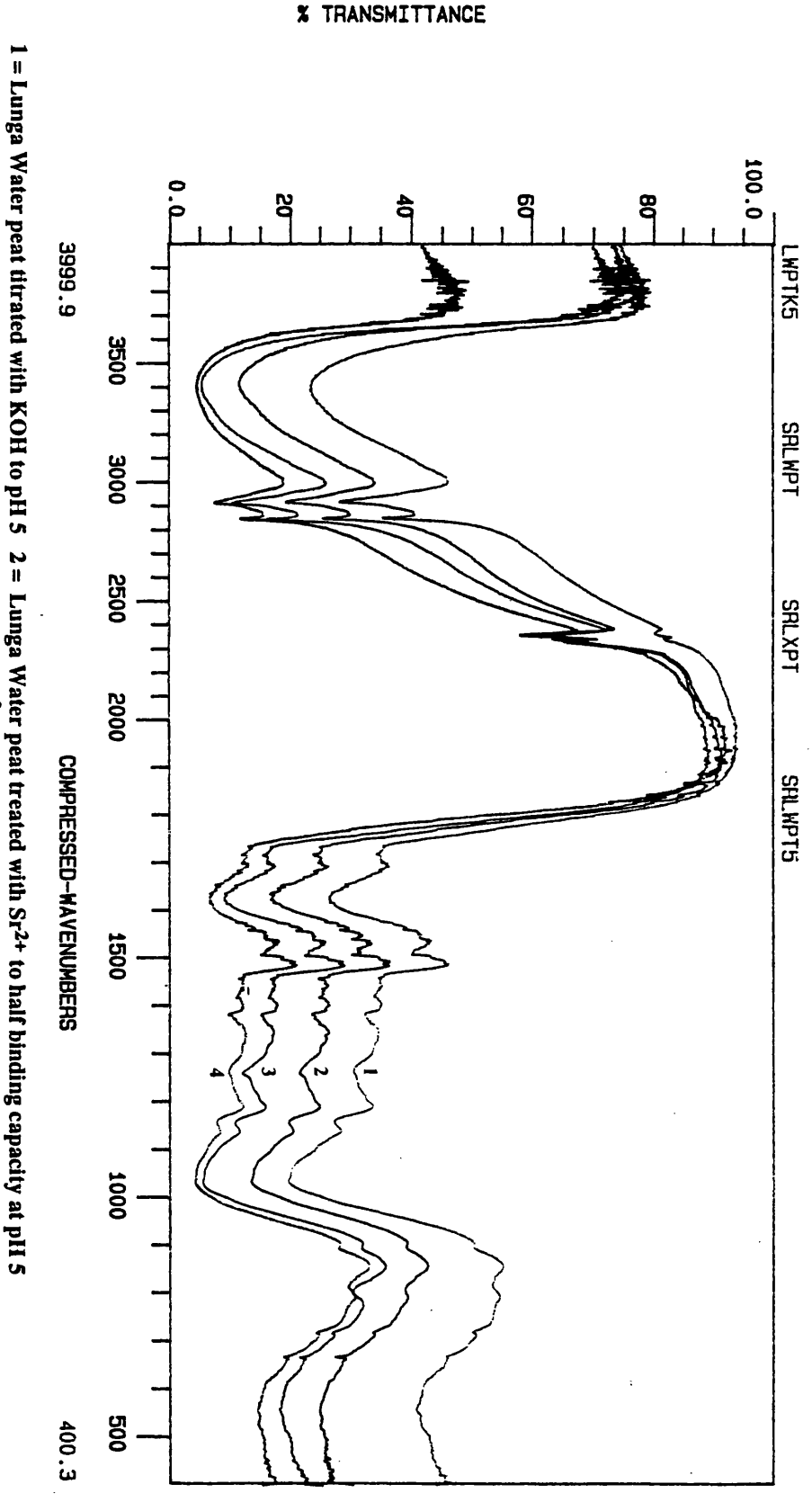

1 = Lunga Water peat titrated with KOH to pH 5 2 = Lunga Water peat treated with Sr^{2+} to half binding capacity at pH 5
3 = Lunga Water peat treated with Sr^{2+} to binding capacity at pH 5
4 = Lunga Water peat treated with Sr^{2+} to twice binding capacity at pH 5

3.3.3.3 Pb^{2+}-TREATED PEAT

The Pb^{2+} additions to peat at pH 3 (Figure 3.20) and pH 5 (Figure 3.21) show the greatest alteration in functional group arrangement for all the metal-treated peat spectra. However, this change is still significantly reduced when compared to the corresponding metal additions to humic acid (Figures 3.11 and 3.12) again indicating that the functional groups are not as available for reaction in unextracted peat, as in isolated humic acid.

The changes in the Pb^{2+} spectra are also dependent on the level of metal addition, with the most significant changes occurring at twice the total acidity in both sets of spectra. At these levels of addition the loss of absorption at $1720cm^{-1}$ was most pronounced, especially when compared to the K^+ treated spectra in Figure 3.21. Thus, at twice the total acidity, the Pb^{2+} treated peat is starting to show some degree of covalency in its interaction, with ionic arrangements predominating at lower levels of addition, where only a few groups are involved in ionic-type linkages. Since the ability of the total acidity to provide a measure for the maximum binding capacity has previously been questioned (section 3.3.2.3), it is possible that in the peats also the total acidity is not an adequate estimate of the maximum binding capacity. This would provide some explanation of the lack of reaction in these materials.

Figure 3.20 Lunga Water peat treated with Pb^{2+} to different levels of addition at pH 3.

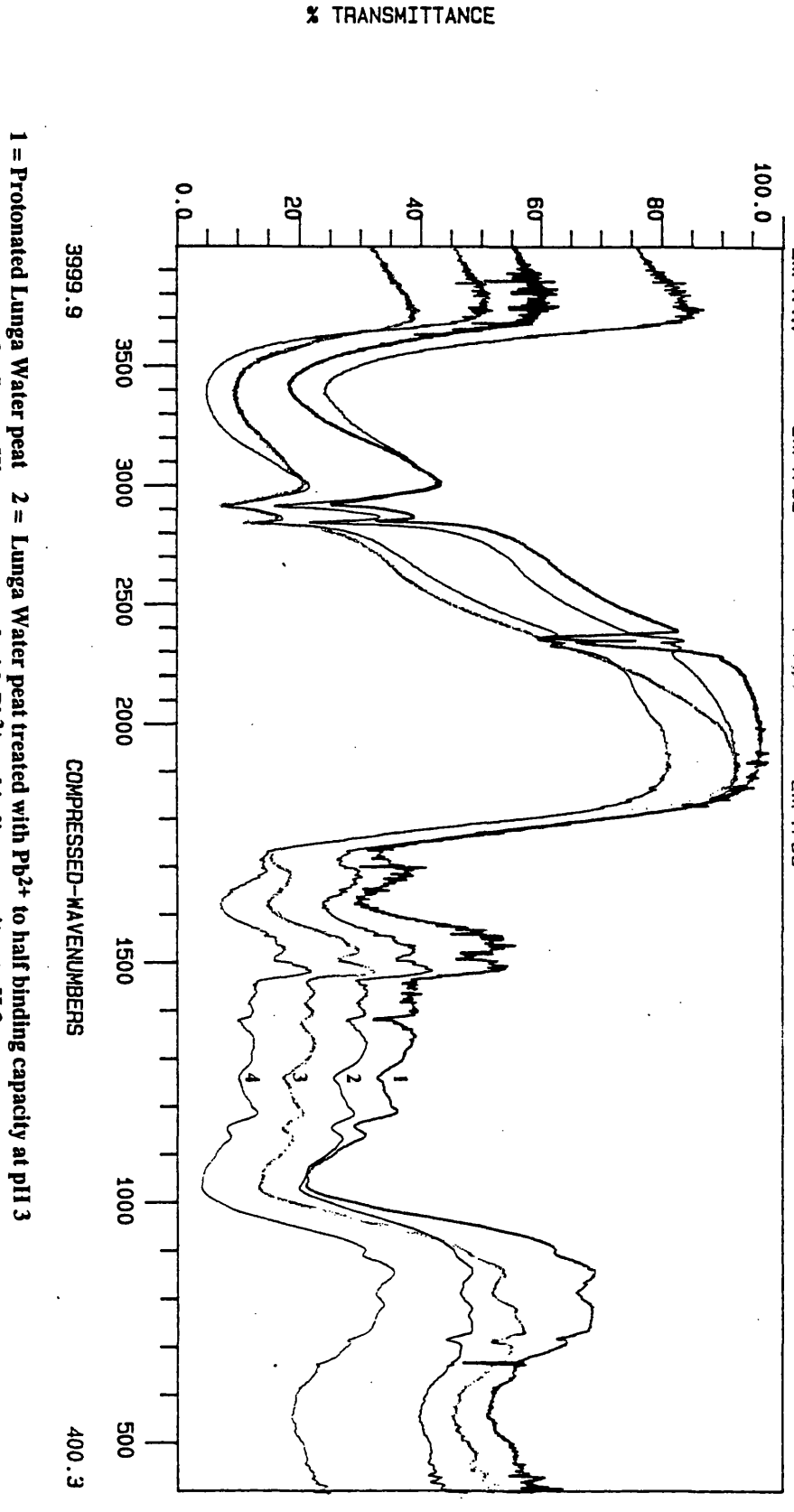

1 = Protonated Lunga Water peat 2 = Lunga Water peat treated with Pb^{2+} to half binding capacity at pH 3
3 = Lunga Water peat treated with Pb^{2+} to binding capacity at pH 3
4 = Lunga Water peat treated with Pb^{2+} to twice binding capacity at pH 3

Figure 3.21 Lunga Water peat treated with Pb^{2+} to different levels of addition at pH 5.

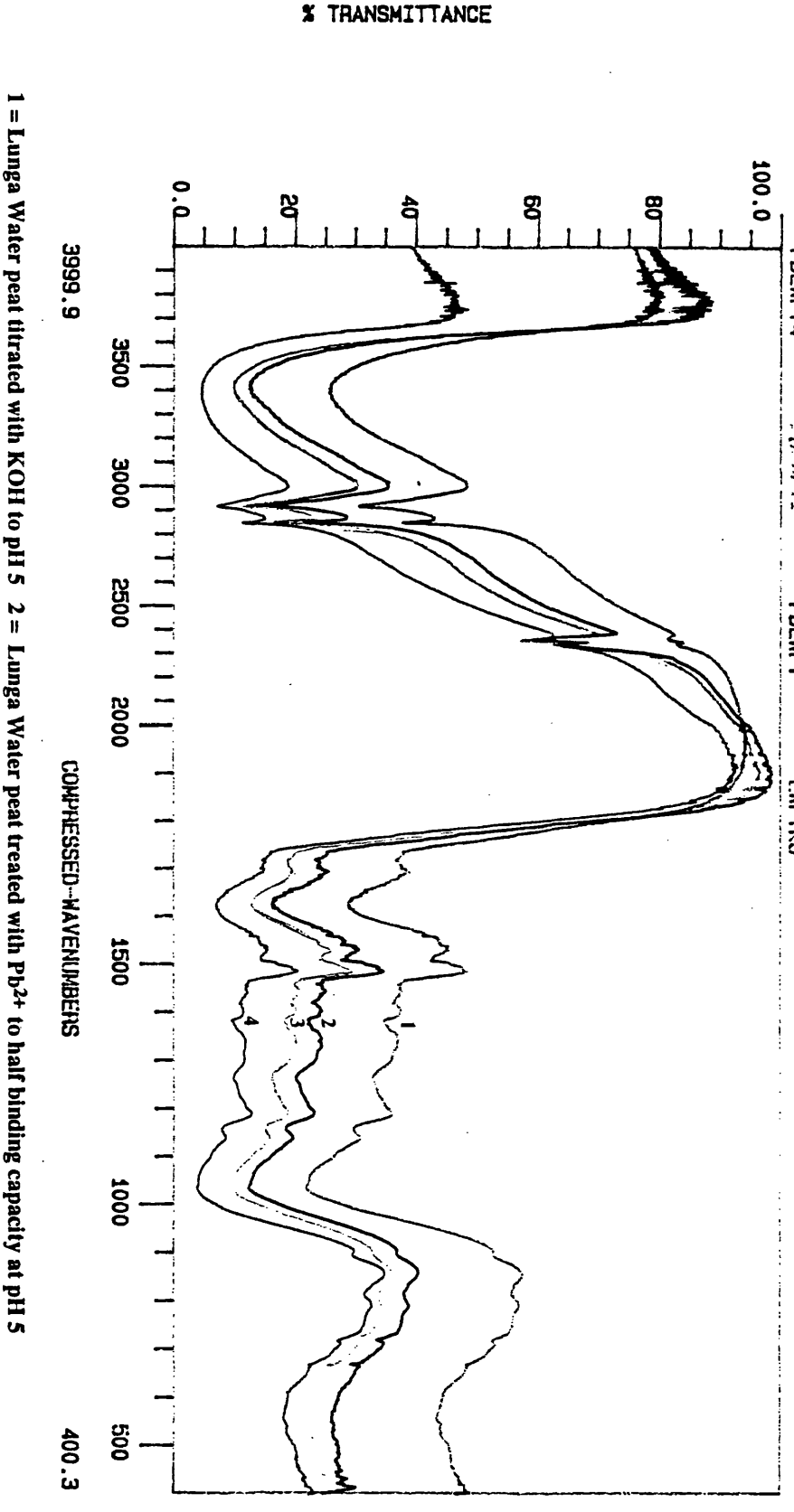

1 = Lunga Water peat titrated with KOH to pH 5 2 = Lunga Water peat treated with Pb^{2+} to half binding capacity at pH 5
3 = Lunga Water peat treated with Pb^{2+} to binding capacity at pH 5
4 = Lunga Water peat treated with Pb^{2+} to twice binding capacity at pH 5

3.3.4 METAL ADDITIONS TO MODEL COMPOUNDS

3.3.4.1 CHANGES IN THE SPECTRA ON SALT FORMATION

Both the untreated salicylic acid and phthalic acids (Figures 3.22 & 3.23 respectively), show evidence of intramolecular hydrogen bonding, indicating that they exist mostly in the dimeric form (Bellamy, 1975). This is most clearly seen from the arrangements of the OH band at 3400-2600cm^{-1}. In these spectra the OH band is seen as a jagged series of bands, which results from the lowering in frequency caused by hydrogen bonding (Williams & Flemming, 1989). The sharp band at 3400cm^{-1} can be attributed to a high frequency OH stretching vibration (Socrates, 1980). This arrangement, along with the carbonyl frequency, is characteristic of carboxylic acids, and is often utilised in their identification.

Intramolecular hydrogen bonding also lowers the frequency of the carbonyl stretch at 1720cm^{-1}. ó-hydroxy carbonyl compounds are particularly affected by this effect, and this is reflected in the salicylic acid (ó-hydroxy benzoic acid), where in Figure 3.22 the carbonyl stretch can be found at 1650cm^{-1}. In Figure 3.23, the carbonyl frequency of phthalic acid (1,2-benzenedicarboxylic acid) is not as affected by hydrogen bonding, and the carbonyl stretch can be found at 1690cm^{-1}. This is consistent with the observations made by previous workers on the positions of the carbonyl groupings in these acids (Bellamy, 1975).

Conversion to the K^+ salt causes characteristic changes in the spectra of the acids. As discussed in section 3.1, ionisation of a carboxylic acid results in the formation of the carboxylate anion, which is resonance stabilised. The anion has two characteristic frequencies for the antisymmetric stretch (~1600cm^{-1}) and the symmetric stretch (~1400cm^{-1}). In salicylic acid (Figure 3.22), the antisymmetric peak is present at 1580cm^{-1}, with a peak superimposed at 1600cm^{-1} which can be attributed to aromatic C=C stretching. The peak for the symmetric stretch is located at 1380cm^{-1}. In phthalic acid (Figure 3.23), the antisymmetric peak is present at 1555cm^{-1} and is broader than the salicylic acid. This broadness is again due to aromatic C=C stretching. The symmetric stretch is located at 1380cm^{-1}.

Both of the salts are contaminated by water, which can be detected by the OH stretch at 3500cm^{-1}, and the band at 1640cm^{-1}, for the HOH bending vibration which can be clearly detected in salicylic acid, but if present, is not resolved in the phthalic acid.

Figure 3.22 Salicylic acid at pH 2.8 and the K^+ salt of salicylic acid at pH 4.5.

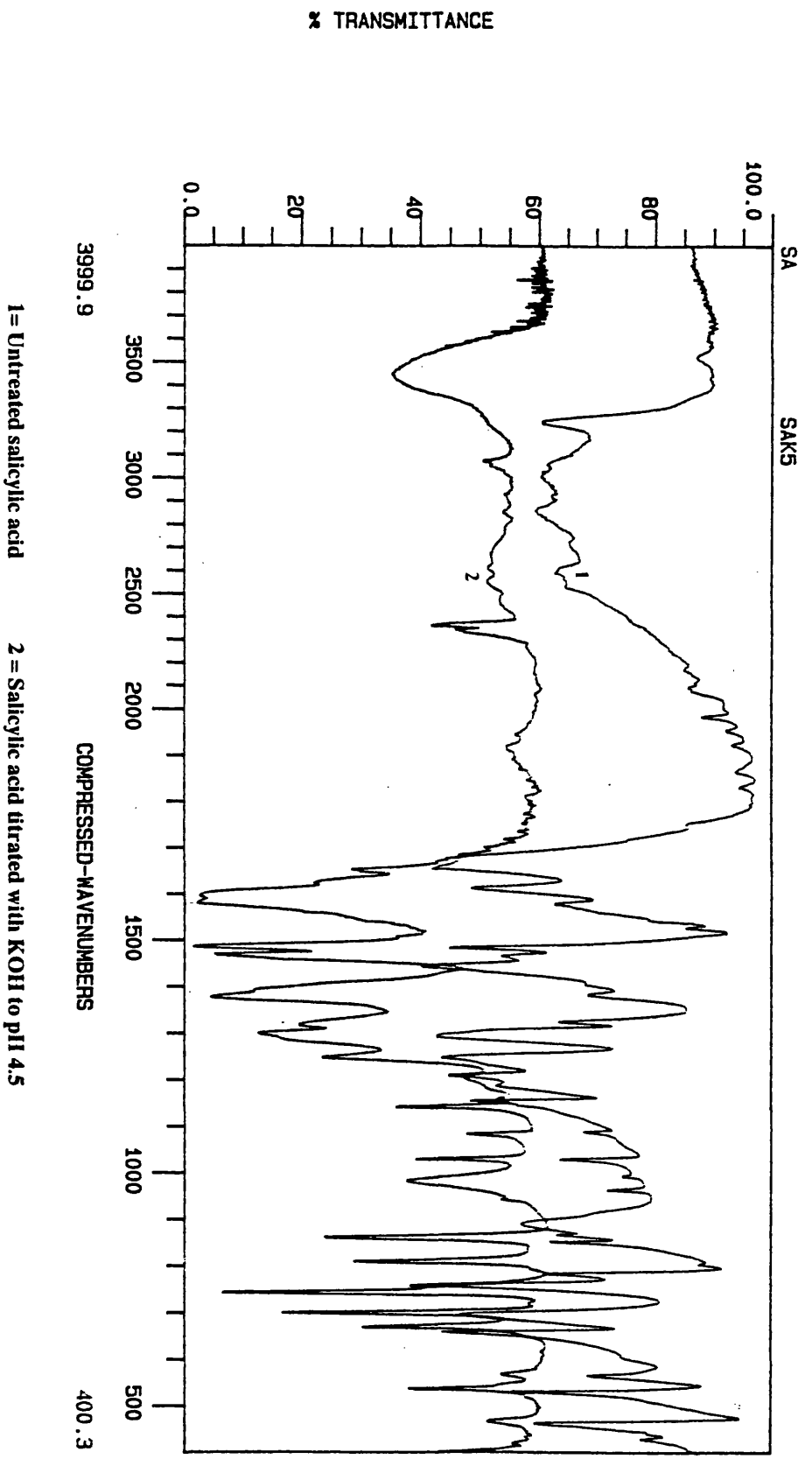

Figure 3.23 Phthalic acid at pH 2.2 and the K^+ salt of phthalic acid at pH 4.5.

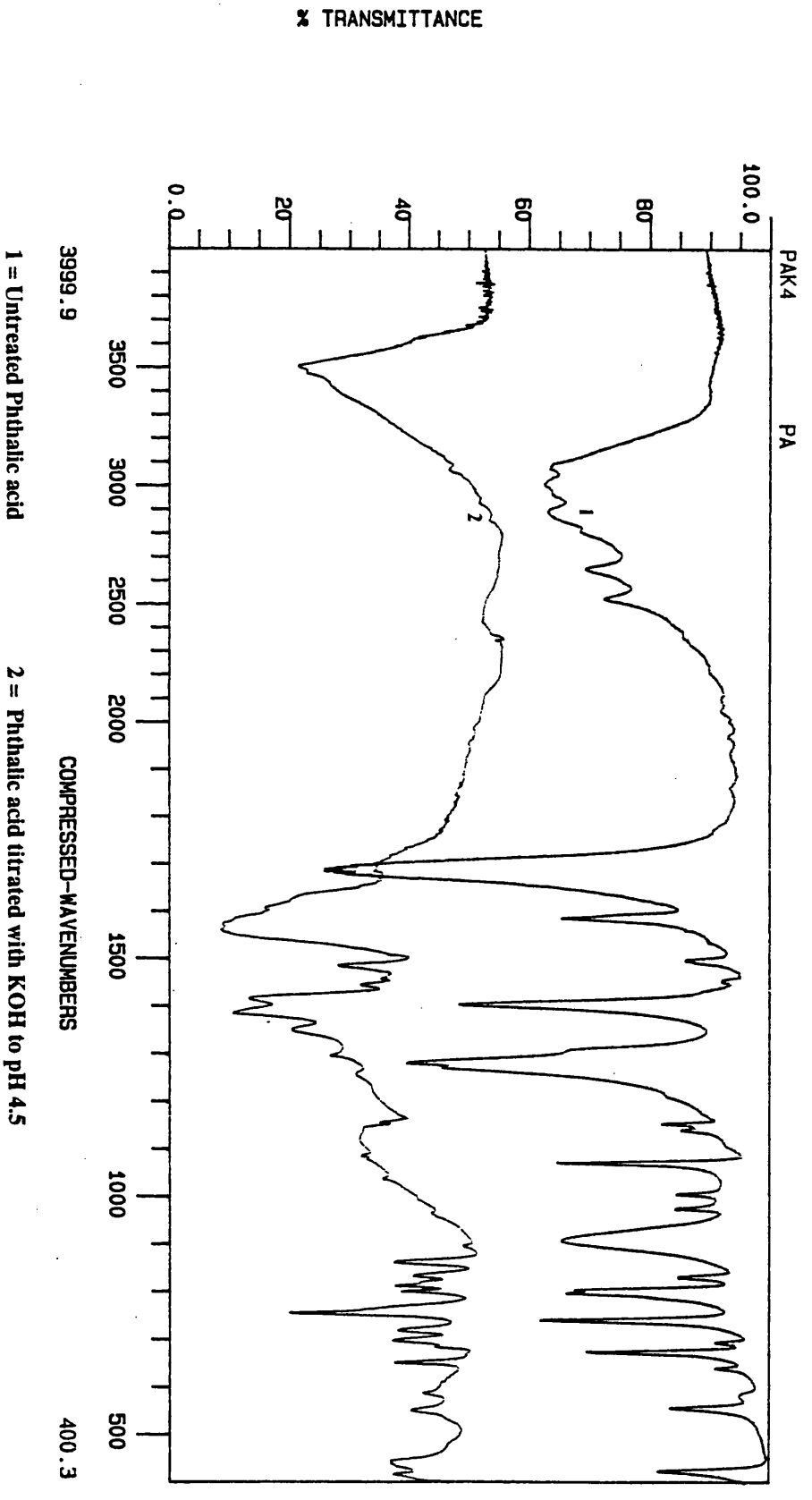

3.3.4.2 Cs^+ AND Ag^+-TREATED PHTHALIC AND SALICYLIC ACID

Both the Cs^+ and Ag^+ additions were made at pH 4.5, and the pH was returned to this value after reaction.

Cs^+ additions to phthalic acid (Figure 3.24) and salicylic acid (Figure 3.25) have resulted in the formation of the ionised form of these acids, and the spectra are virtually identical to the K^+ treated spectra, showing no shift in the frequencies of the carbonyl frequencies. Thus, as in the humic acids and peats, Cs^+ is reacting to give ionic linkages. In the Cs^+ treated salicylic acid the spectrum is more significantly affected by contamination from water, which may be trapped in the crystalline lattice by a combination of weak hydrogen bonds to the anion, or weak ionic bonds to the metal (Bellamy, 1975).

Ag^+ additions to phthalic acid (Figure 3.26) and salicylic acid (Figure 3.27), have also resulted in the formation of the ionised forms of these acid, showing very similar spectra to the K^+ treated salt, with no shifts in the carbonyl frequencies. In the Ag^+ spectra, there is also a broadening of the band at 1390cm^{-1}, which is due to the presence of ionic nitrates, which absorb at 1380cm^{-1}. These are present since Ag^+ was added as the nitrate salt. This is different to the treatment of the humic acid with Ag^+ where some degree of covalent interaction was detected, and would again indicate that Ag^+ is reacting with nitrogen-containing groupings in the humic acid, since these are not present in the model compounds studied here.

Figure 3.24 Phthalic acid treated with Cs^+ at pH 4.5.

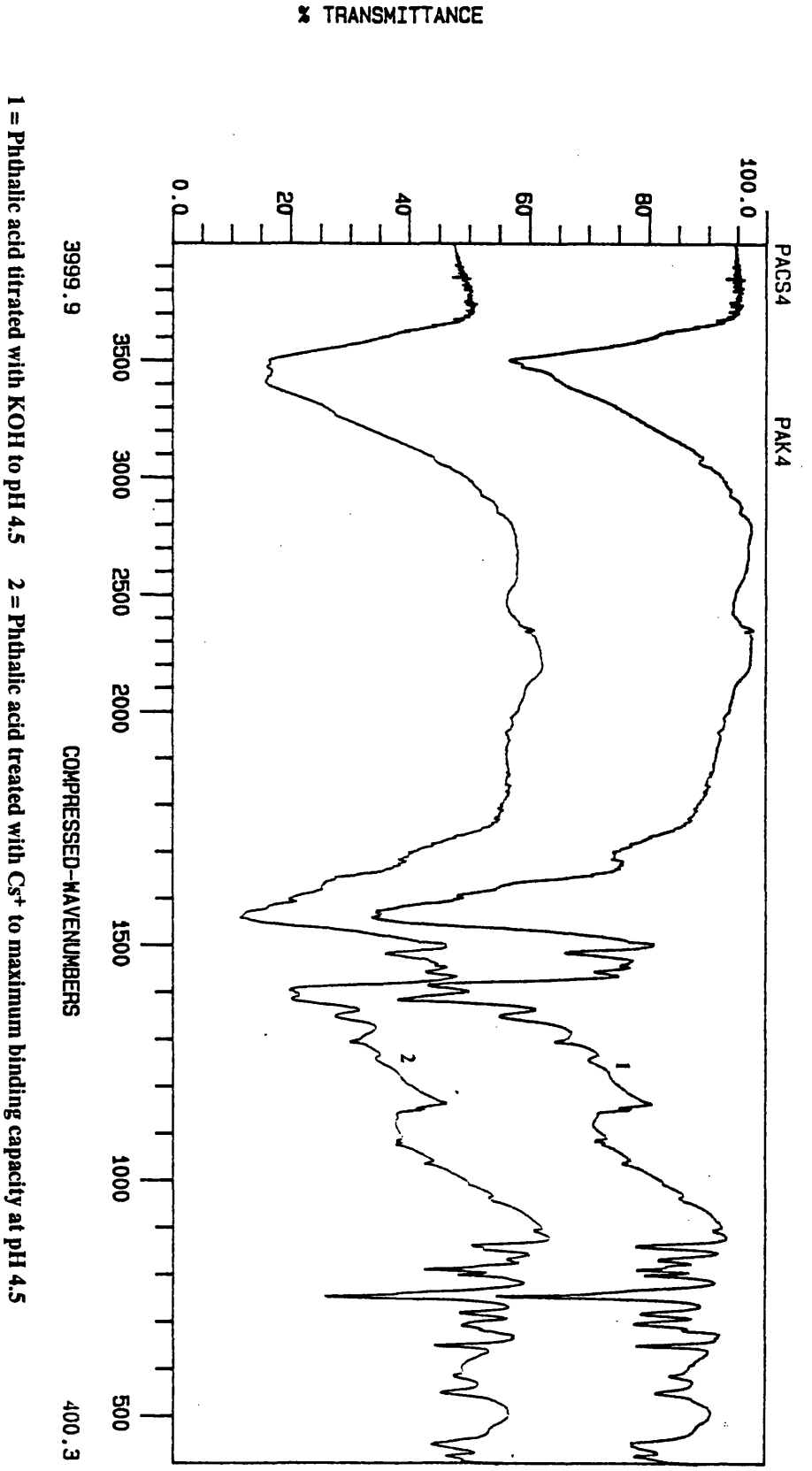

Figure 3.25 Salicylic acid treated with Cs^+ at pH 4.5

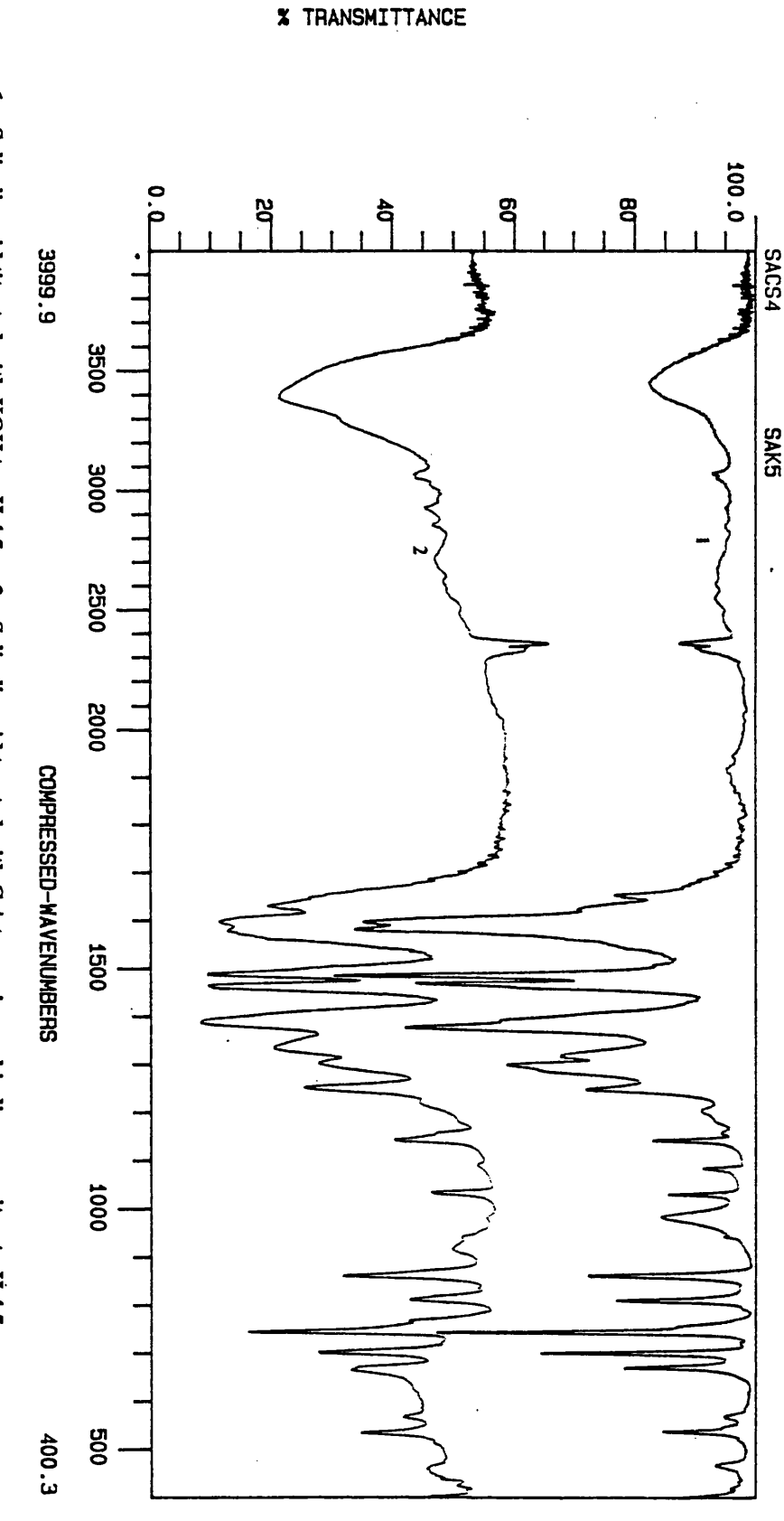

1 = Salicylic acid titrated with KOH to pH 4.5 2 = Salicylic acid treated with Cs^+ to maximum binding capacity at pH 4.5

Figure 3.26 Phthalic acid treated with Ag^+ at pH 4.5.

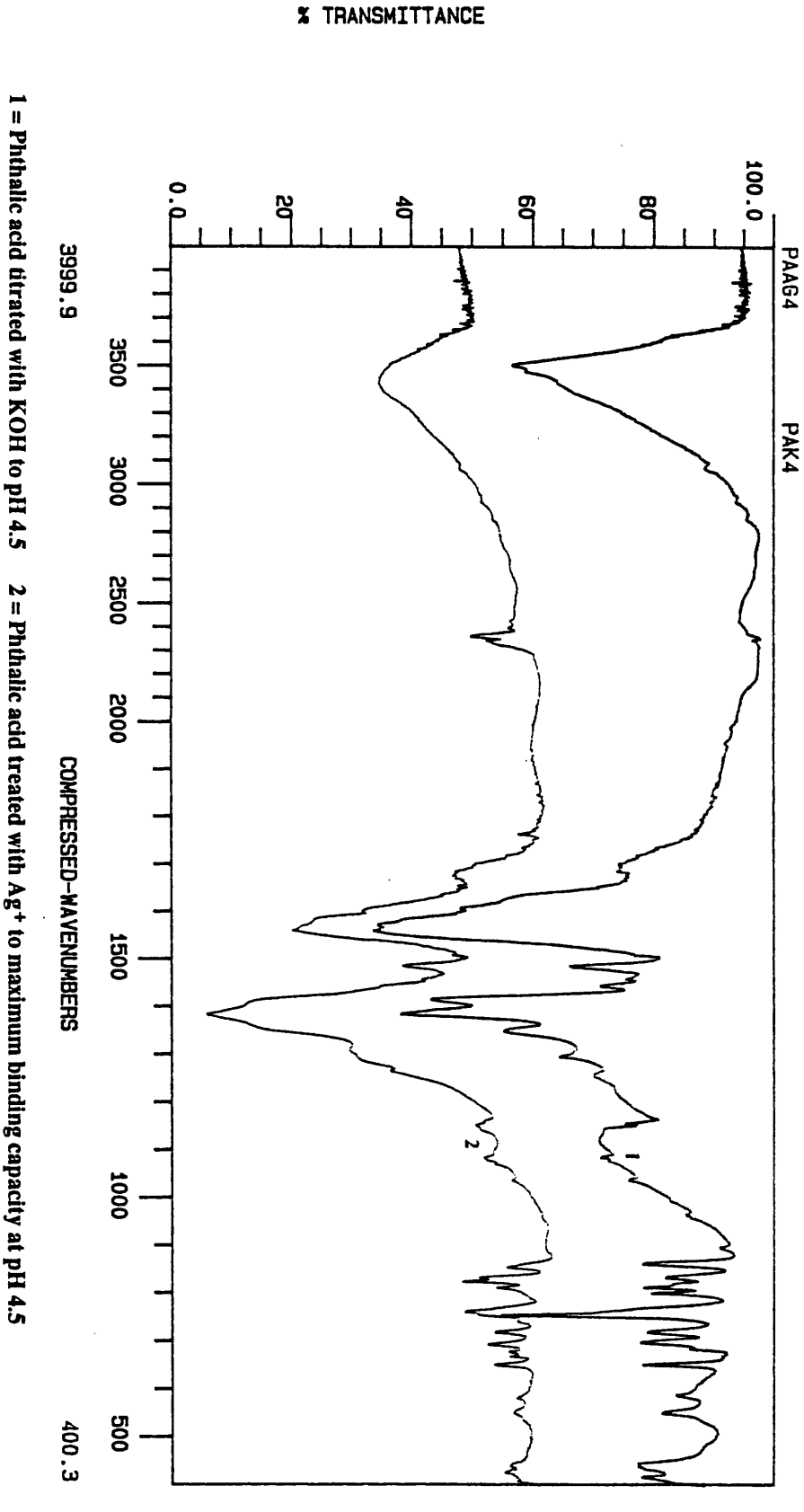

Figure 3.27 Salicylic acid treated with Ag^+ at pH 4.5.

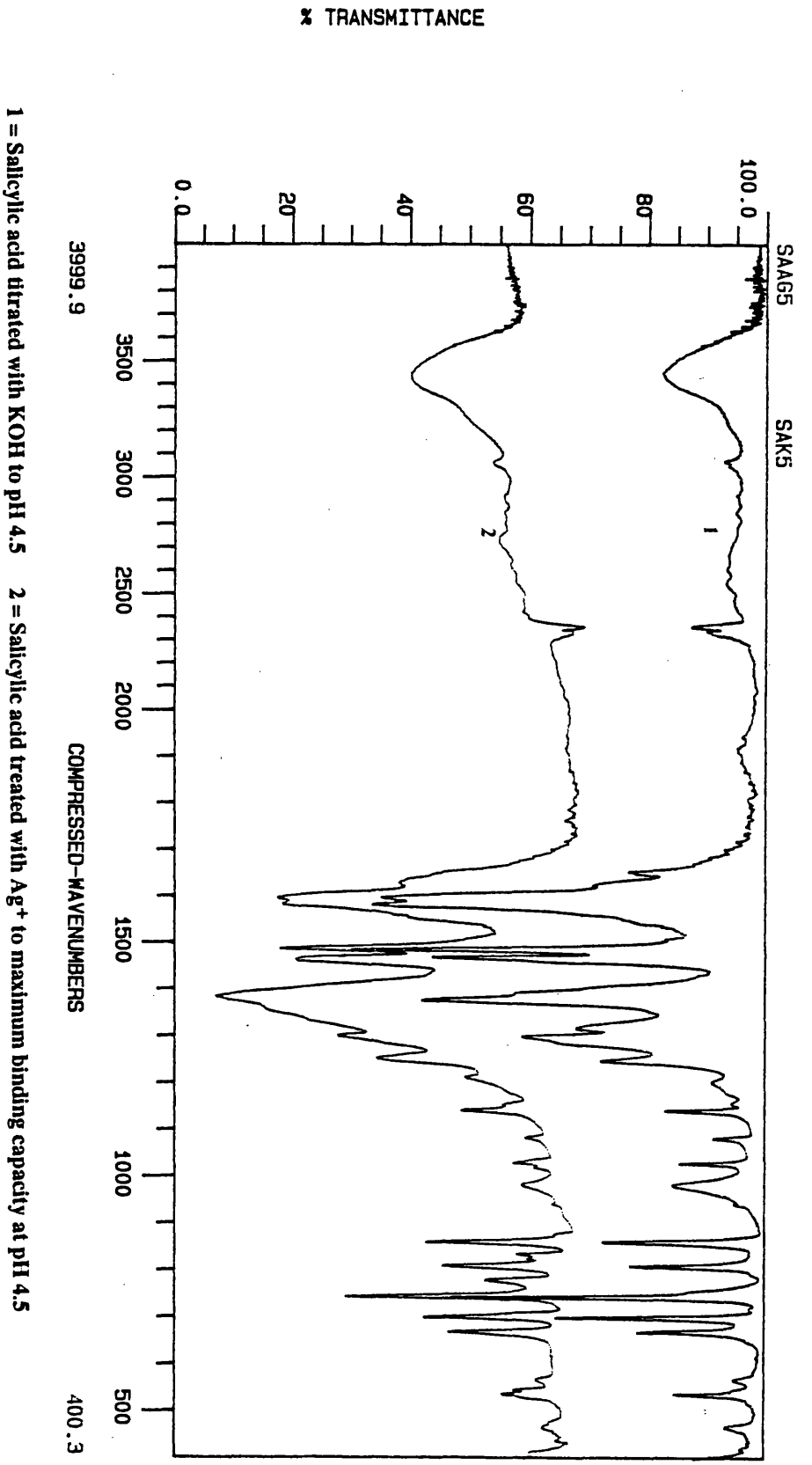

1 = Salicylic acid titrated with KOH to pH 4.5 2 = Salicylic acid treated with Ag^+ to maximum binding capacity at pH 4.5

3.3.4.3 Pb^{2+} AND Sr^{2+}-TREATED PHTHALIC AND SALICYLIC ACID

The interaction of Pb^{2+} and Sr^{2+} with the model compounds has resulted in significant changes in the bands associated with the carboxyl anion when compared to the K^+ salts of these compounds.

In the Sr^{2+}-treated salicylic acid (Figure 3.28) and the Pb^{2+}-treated salicylic acid (Figure 3.30), three sharp peaks can be observed at around 1550cm^{-1}, 1600cm^{-1}, and 1620cm^{-1}. These can be identified as the antisymmetric carboxylate stretch, aromatic C=C stretch, and HOH bending vibration respectively. These peaks vary from the K^+ treated salt in their resolution and their position. These peaks are not as resolved in the Sr^{2+} (Figure 3.29) and Pb^{2+} (Figure 3.31) phthalic acids.

The main frequency shift is observed in the peak for the antisymmetric carboxylate stretch, which has shifted downwards on binding with Sr^{2+} and Pb^{2+}. In the K^+ salt of salicylic acid the antisymmetric carboxylate stretch is present at 1585cm^{-1}, and the symmetric stretch is present at 1380cm^{-1}. On binding with Sr^{2+} these peaks shift to 1550cm^{-1} and 1400cm^{-1} respectively (Figure 3.28). On binding with Pb^{2+} the antisymmetric stretch shifts to 1540cm^{-1} (Figure 3.30). The shift in the symmetric stretch is masked by the presence of a broad band for ionic NO_3^-.

In the K^+ salt of phthalic acid the antisymmetric stretch can be found at 1555cm^{-1}, and the symmetric stretch at 1380cm^{-1}. On binding with Sr^{2+} (Figure 3.29), the antisymmetric stretch shifts downwards to 1530cm^{-1} with the symmetric stretch shifting to 1395cm^{-1}. In the Pb^{2+} treated phthalic acid (Figure 3.31), the antisymmetric stretch shifts to 1520cm^{-1}.

These changes are consistent with the formation of chelate-type linkages, as outlined in section 3.1, indicating that Pb^{2+} and Sr^{2+} are able to interact with the carboxyl groupings to form covalent linkages. From the above frequency shifts of the antisymmetric stretch Pb^{2+} is showing the greatest degree of covalency, which is in accordance with its soft character.

In the Pb^{2+} and Sr^{2+} treated spectra, for both acids, the prescence of lattice water is far more significant than in the K^+ treated spectra. This is reflected in the increase in the HOH bending vibration at 1620cm^{-1} on binding, and in the band for the OH stretch at 3400cm^{-1}.

Figure 3.28 Salicylic acid treated with Sr^{2+} at pH 4.5.

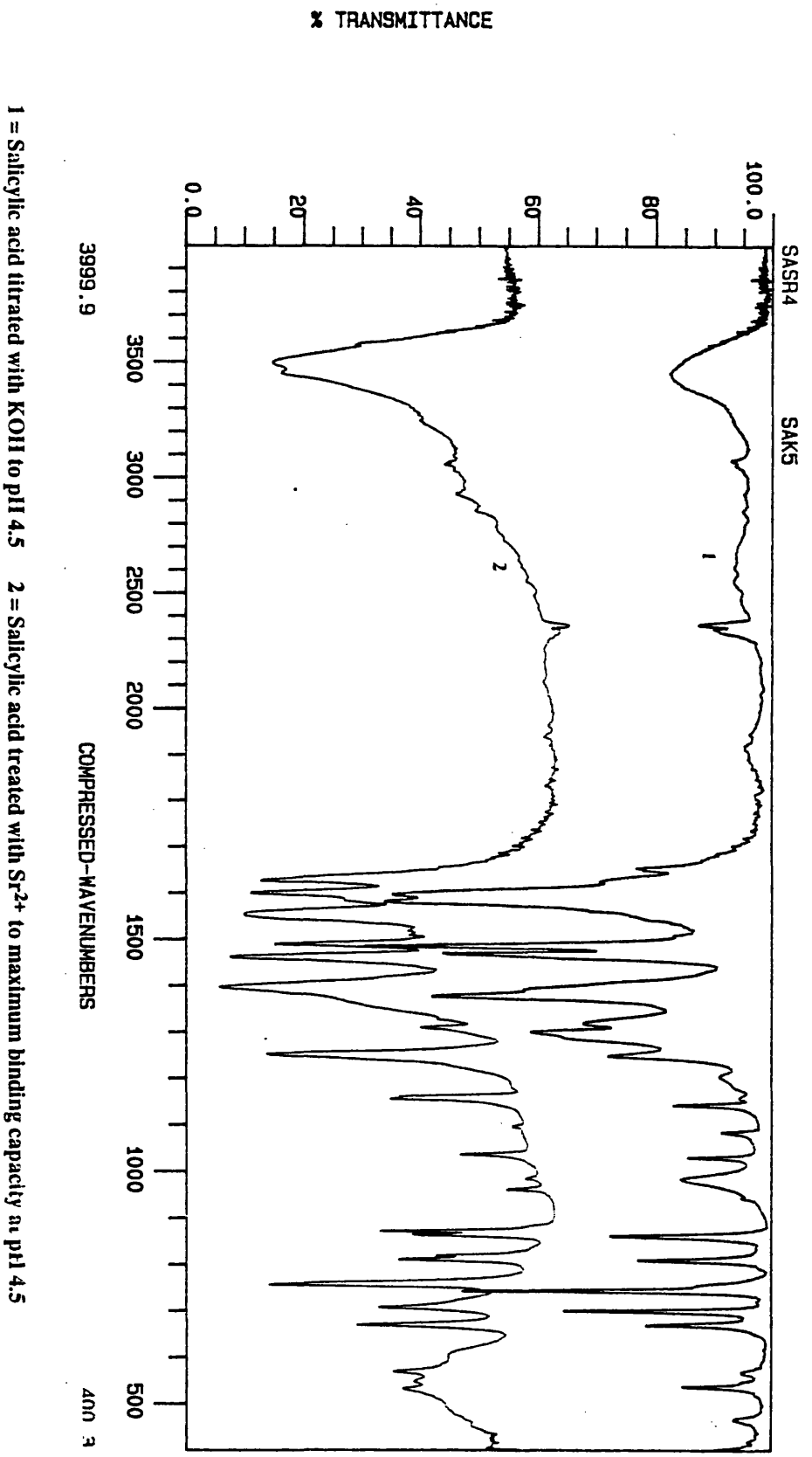

1 = Salicylic acid titrated with KOH to pH 4.5 2 = Salicylic acid treated with Sr^{2+} to maximum binding capacity at pH 4.5

Figure 3.29 Phthalic acid treated with Sr^{2+} at pH 4.5.

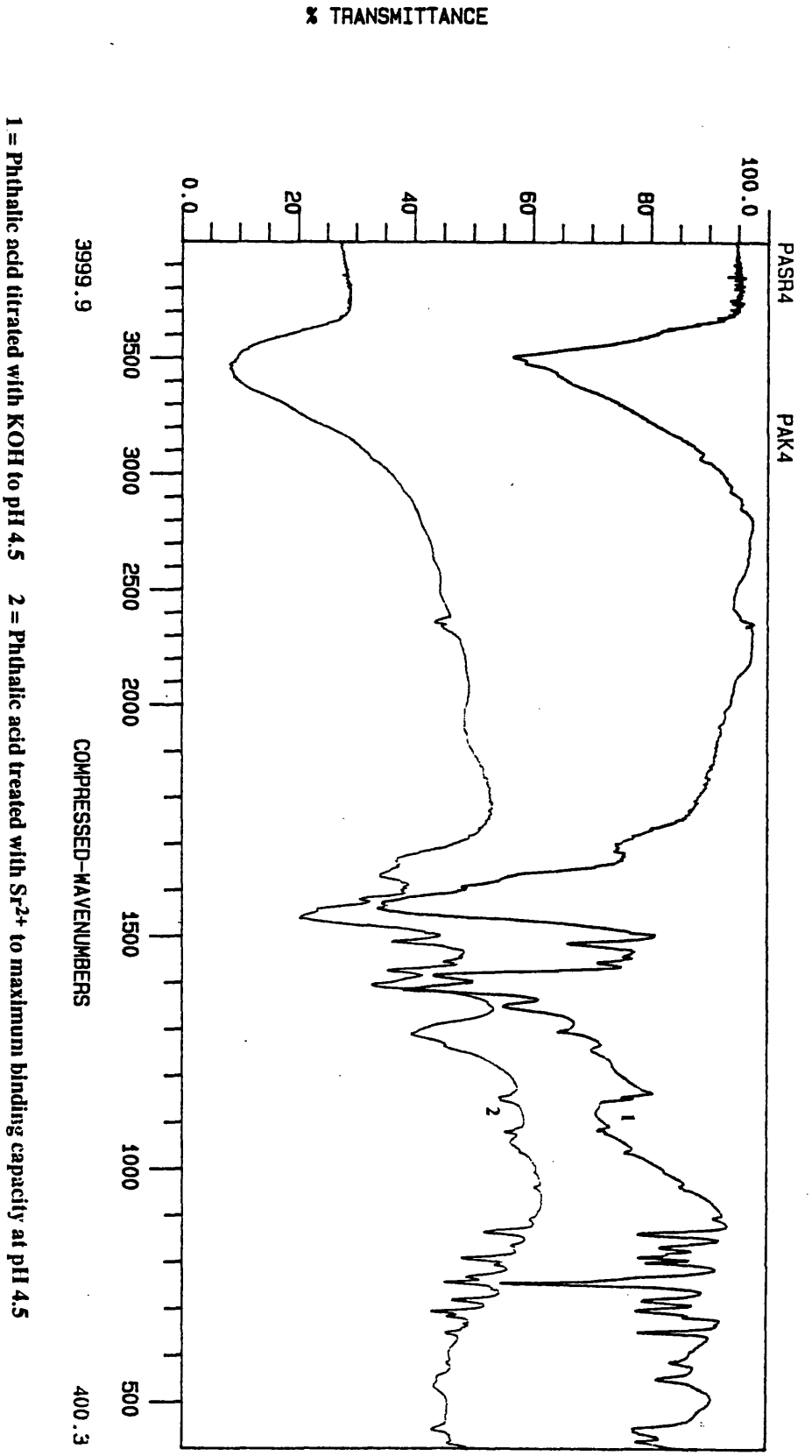

1 = Phthalic acid titrated with KOH to pH 4.5 2 = Phthalic acid treated with Sr^{2+} to maximum binding capacity at pH 4.5

Figure 3.30 Salicylic acid treated with Pb^{2+} at pH 4.5.

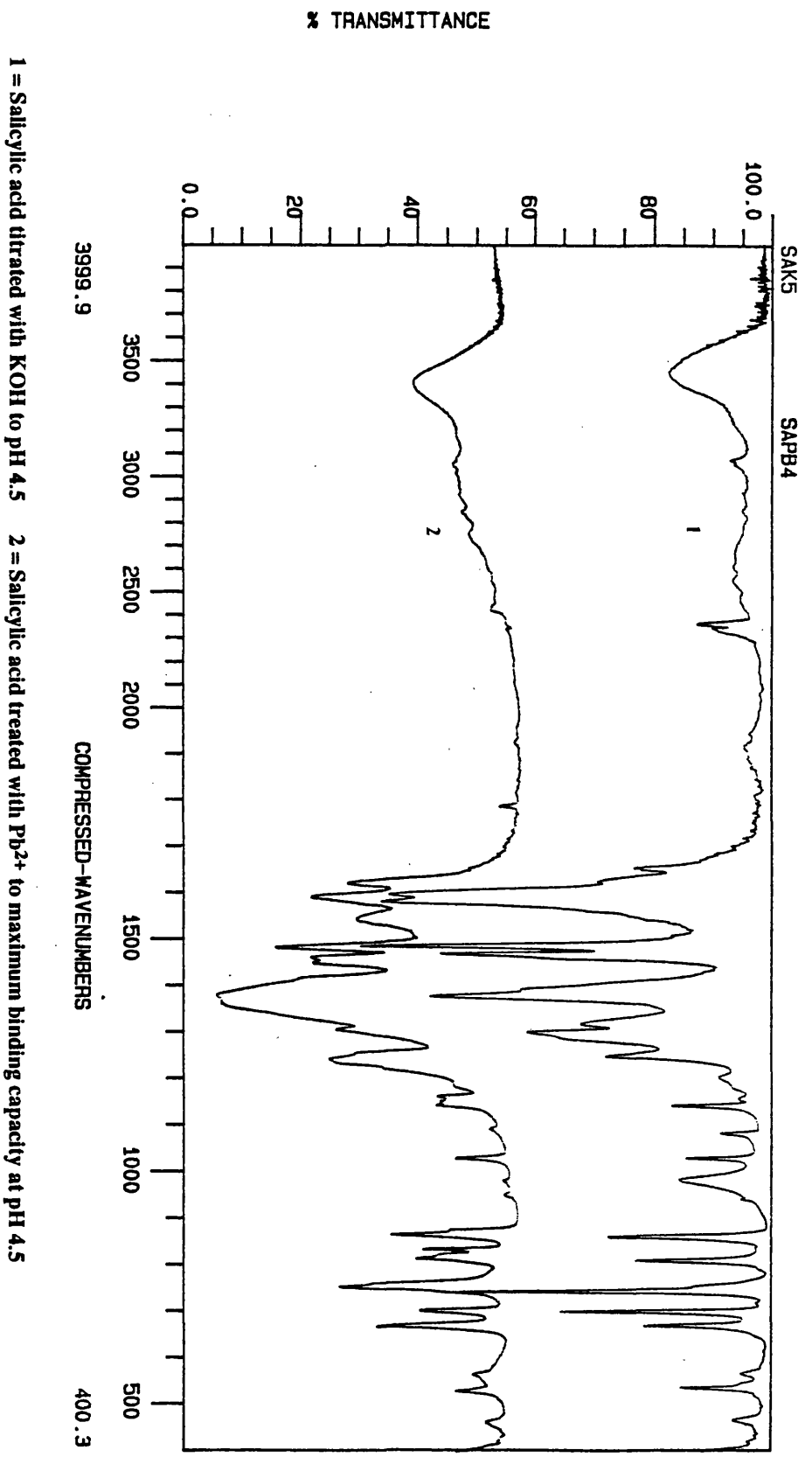

1 = Salicylic acid titrated with KOH to pH 4.5 2 = Salicylic acid treated with Pb^{2+} to maximum binding capacity at pH 4.5

Figure 3.31 Phthalic acid treated with Pb^{2+} at pH 4.5

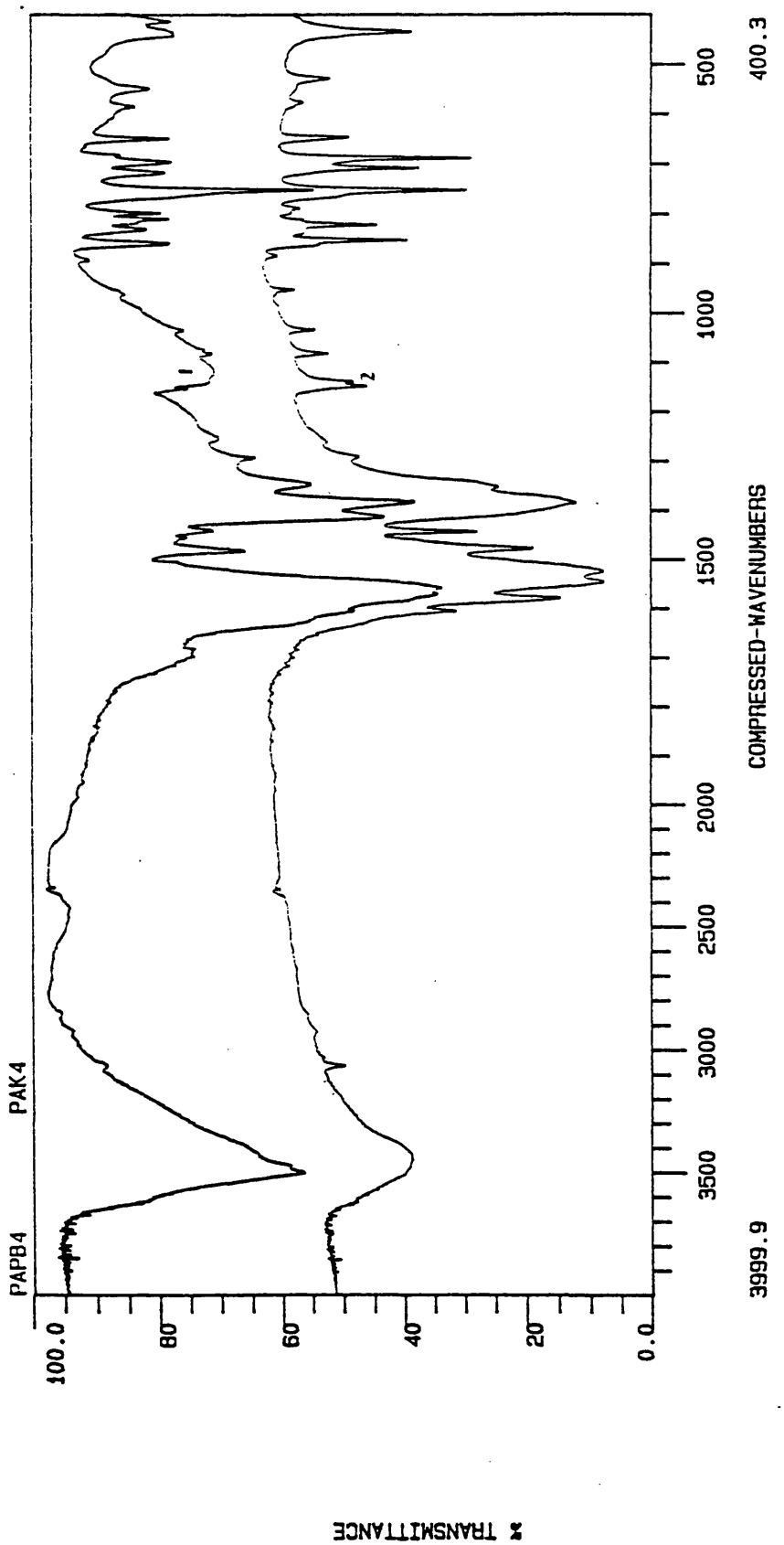

1 = Phthalic acid titrated with KOH to pH 4.5 2 = Phthalic acid treated with Pb^{2+} to maximum binding capacity at pH 4.5

3.4 CONCLUSIONS

The metal-treated spectra are giving information on the nature of the interaction of metals with humic substances. From all of the studies, it is clear that Cs^+ is binding through ionic linkages only, making it potentially available in the environment. Conversely, Cu^{2+}, Zn^{2+}, Pb^{2+} and Sr^{2+} are binding through coordinate covalent linkages in humic acid, with Cu^{2+} and Zn^{2+} giving the most significant change at high levels of metal loading.

In salicylic and phthalic acid, Pb^{2+} and Sr^{2+} were also shown to form coordinate covalent linkages, with the results pointing to the formation of chelate-type complexes. With the functional groupings of humic acid being proposed to be formed from salicylate and phthalate type repeating units, (Gamble *et al.*, 1980) it is not surprising that reaction with metals results in a broadening of the peak at $1600cm^{-1}$ in the humic acid. In the model compounds, which have simple structures in comparison to humic substances, metal treatment resulted in significant changes in the arrangements of the bands associated with the carboxylic groupings, yet in humic substances these effects will be magnified due to the complexity of structure.

In unextracted peat, only Pb^{2+} was able to show any evidence of coordination reactions and showed less of an effect than in the humic acid. This would indicate that for both Pb^{2+} and Sr^{2+}, the total acidity was not an adequate estimation of the maximum binding capacities of these metals with unextracted peat, since the extent of reaction was greatly reduced. The increased reactivity of humic acid compared to unextracted peat was also observed in the infra-red spectra of titrated peat and humic acid samples in section 2.3.2.4. This was proposed to be due to structural changes on extraction, which allow the reactive groupings to be more exposed for reaction, instead of being bound up in the peat matrix. After all, this is the aim of the extraction procedure. In addition, chemical changes were also proposed to occur on isolation.

The increase in reactivity of humic substances after isolation of humic acid has implications for the use of such operationally-defined extracts in the study of metal interactions in environmental systems, if, in the environment, the humic substances have quite different reactivities and behaviours.

CHAPTER 4

THE MEASUREMENT OF THE DEGREE OF COMPLEXATION OF METALS WITH HUMIC SUBSTANCES

4.1 INTRODUCTION

In the infra-red studies presented above it was evident that different metals reacted quite differently with humic substances, showing the potential to participate in complex formation. From these qualititative observations only, assumptions can be made regarding the stability of the interactions, but it is this feature which will govern their behaviour, in particular their bioavailablity, in environmental systems.

In contrast, the formation constant of a metal-humic complex can provide a quantitative measure of the affinity of a humic substance for a metal, therefore providing information on stability of the interaction. The use of formation constants in providing information on the potential environmental behaviour of a metal is complicated by the conditional nature of the constants, as outlined in section 1.7.2. In addition several assumptions must be made:

(a) There is a single homologous complexant with polyelectrolytic properties.

(b) Only one ion or complex compound reacts with the ligand.

(c) Chemically-specific reactions occur between the metal and the ligand.

(d) Thermodynamic equilibrium is achieved.

(Buffle, 1988).

These conditions may not hold, especially when secondary reactions such as those outlined in section 1.7.2 are taking place. As yet no model exists which can compensate for these effects, since this would involve an inordinate number of parameters. Instead, a series of different models exists, which compensate in different ways for particular secondary effects (see section 1.7.2.1.).

In this study of the stability of metal-humic interactions three different approaches were utilised: the Base Titration Method, the Scatchard approach and an Incremental Technique with the theoretical basis of each method being discussed in greater detail in section 4.2. The Base Titration and Scatchard approaches were chosen since they are very different kinds of discrete ligand model, which have been demonstrated to model the interactions better than continous distribution models (Turner *et al.*, 1986). The incremental constants were calculated in order to investigate how binding changes with extent of reaction.

The majority of such quantitative studies have been carried out on humic and fulvic acids which are operationally-defined fractions. Isolation of humic acid from peat has been shown in Chapter 2 to increase the reactive functional group content of the humic substances, an effect also demonstrated by Gregor & Powell (1987) for fulvic acid. In particular, there was an increase in the total acidity and carboxyl group content on extraction, as well as an increase in reactivity towards alkali. The infra-red

studies in Chapter 3 showed that the extracted materials had a greater reactivity towards metals, and revealed the existence of coordinate covalent complexes, which were not so apparent in the unextracted materials. Therefore, in order to provide further information on the effect of isolation on the properties of humic substances, unextracted peat samples were also incorporated into some of the quantitative studies of metal binding. The use of unextracted materials in parallel with the conventional humic acid will also investigate the validity of using the operationally-defined fraction for such studies.

4.2 METHODS

4.2.1 THE BASE TITRATION METHOD - THE BJERRUM APPROACH

This approach is a discrete ligand model which assumes that metal ions and protons compete for complexing sites on humic substances, and that the metal ion is regarded as the central group forming ML_n complexes. It is based on a method developed by Gregor (1955), who modified the Bjerrum approach for calculating stepwise formation constants for metal complexes to polyacrylic acids.

4.2.1.1 THEORETICAL CONSIDERATIONS OF THE BASE TITRATION METHOD

The reactions between a weak acid polyelectrolyte such as humic acid, and a divalent metal ion can be illustrated as follows:

$$HA + M^{2+} \overset{b1}{\Leftrightarrow} MA^{+} + H^{+} \qquad (4.1)$$

$$HA + MA^{+} \overset{b2}{\Leftrightarrow} MA2 + H^{+} \qquad (4.2)$$

where HA represents an acidic functional group, MA_2 the complex formed and b_1 and b_2 the stepwise formation constants for each reaction. The reactions represented by equations 4.1 and 4.2 show interactions with protonated groupings, yet the method assumes interactions between dissociated functional groupings as follows, with protons being released from re-establishment of ionisation equilibrium:

$$M^{2+} + A^{-} \overset{k1}{\Leftrightarrow} MA^{+} \qquad (4.3)$$

$$HA \Leftrightarrow A^{-} + H^{+} \qquad (4.4)$$

which combine to give,

$$M^{2+} + HA \Leftrightarrow MA^{+} + H^{+} \qquad (4.1)$$

However, in equation 4.3, there will be a net change in humic charge, which is not accounted for in this method, being a discrete ligand model and therefore equations 4.1 and 4.2 are utilised. Gregor (1955) proposed that the stepwise formation constants arising from equations 4.1 and 4.2 should be utilised in preference to the constant k_1

arising from equation 4.3, and therefore developed the Bjerrum approach around this assumption.

The two stepwise formation constants (b_1 and b_2) which arise from equations 4.1 and 4.2 can be combined to give an overall constant B_2, which is defined as:

$$B_2 = b_1 b_2 = \frac{(MA_2)(H^+)^2}{(HA)^2(M^{2+})} \qquad (4.5)$$

The average number of ligand molecules bound per metal ion is expressed by the formation function ñ, which provides an estimate of the number of complexing sites bound per mole of metal ion and this can be expressed as :

$$\tilde{n} = \frac{(At) - (HA) - (A^-)}{(Mt)} \qquad (4.6)$$

where A_t is the overall concentration of binding site or ligand, and M_t is the overall concentration of metal ion. ñ is related to the formation constant B_2 through the following relationship:

$$\sum_{n=0}^{n=N} (\tilde{n} - n)\, Bn \left(\frac{HA}{H^+}\right)n = 0 \qquad (4.7)$$

For divalent metals, reacting as in equations 4.1 and 4.2, equation 4.7 can be solved using the method of least squares to give:

$$\frac{\tilde{n}}{(\tilde{n}-1)\left(\frac{HA}{H^+}\right)} = \frac{(2-\tilde{n})\left(\frac{HA}{H^+}\right)}{(\tilde{n}-1)} \times B2 - b1 \qquad (4.8)$$

B_2 can then be computed graphically from equation 4.8.

Should a monovalent ion react with a humic substance, then the reaction can be written as:

$$HA + M^+ \Leftrightarrow MA + H^+ \qquad (4.9)$$

and the formation constant for the reaction can be calcuated from solving equation 4.7 to give:

$$B_1 = \frac{\tilde{n}}{(1-\tilde{n})} \times \frac{H^+}{(HA)} \qquad (4.10)$$

4.2.1.2 ESTABLISHING THE POTENTIAL OF THE HUMIC ACID TO IONISE

Huxter humic acid was isolated and protonated as in section 2.2.1, and used in all measurements in the Base Titration Method.

The total content of reactive functional groups A_t was determined by titrating the protonated humic acid with CO_2 free 0.01M KOH, with the ionic strength adjusted to 0.1M with 5M KNO_3. All subsequent measurements were also carried out at 0.1M, with KNO_3 as the supporting electrolyte. The protonated humic acid was in solution, and had not been freeze dried. Titration was carried out under nitrogen, in a closed cell, with the solution being constantly stirred. All additions of alkali were made using a Gilsen microburette, inserted through an inlet in the cell, and the pH was recorded with a Corning Ion Analyser 250 pH meter. The titrated humic acid or humate salt, KA, was retained for the next step in the method.

4.2.1.3 MONITORING AND MEASURING METAL BINDING

The same closed cell system used in section 4.2.1.2 for the titration of humic acid with KOH, was utilised in the recording of the pH drop on metal addition. The metals were added with a calibrated automatic pipette and the levels of addition were determined from the estimated total content of reactive functional groups. For the divalent ions, sequential additions of 0.2 $mmol_c$ were made and for the monovalent ions this was reduced to 0.1 $mmol_c$.

To achieve the required starting pH aliquots of protonated humic acid (with the ionic strength adjusted to 0.1M) and humate salt were combined. The total volume of pH adjusted humic acid used in the titration was always 50ml for the divalent metals and 30ml for the monovalent metals.

To this equilibrated solution, successive aliquots of metal were then added, with the pH being returned to the starting pH between additions using CO_2 free 0.01M

KOH added through a microburette as described in section 4.2.1.2. Additions were continued until no further drop in pH was detected. Cu^{2+} and Pb^{2+} were added as 0.02M acetates, with the pH of the salt buffered with CH_3COOH to the pH value of the humic acid. Cs^{+} was added as 0.02M CsCl, and Ag^{+} was added as 0.02M $AgNO_3$, both with no correction for the pH of the salts.

The pH was recorded with a combination electrode and Corning Ion Analyser 250 pH meter. The limit of detection of the pH electrode was defined as +/-0.04pH, from a combination of the specified acid and alkaline errors.

4.2.2 THE SCATCHARD AND INCREMENTAL TECHNIQUES

4.2.2.1 THEORETICAL CONSIDERATIONS OF THE SCATCHARD AND INCREMENTAL TECHNIQUES

In the approaches outlined below, the macromolecule is assumed to be the central group, with the metal reacting to give LM, LM_2 and LM_n complexes, with the formation constants being described by:

$$k_1 = \frac{(LM)}{(L)(M)} \qquad k_2 = \frac{(LM2)}{(LM)(M)}$$

and,

$$k_n = \frac{(LMn)}{(LMn-1)(M)} \qquad (4.11)$$

The extent of binding, or the formation function Ø, is then described by:

$$\emptyset = \frac{(LM) + 2(LM2) + ..n(LMn)}{(L) + (LM) + ...(LMn)} = \frac{Mb}{Lt} \qquad (4.12)$$

where M_b is the amount of metal bound and L_t is the total ligand concentration. For binding at identical and independent sites, Ø is described by Adairs equation:

$$\emptyset = \frac{nKo(M)}{1 + Ko(M)} \qquad (4.13)$$

where K_o is the microscopic formation constant and n is the number of binding sites per macromolecule. Equation 4.13 can be rearranged to give:

$$\frac{\emptyset}{M} = nKo - \emptyset Ko \qquad (4.14)$$

Equation 4.14 is known as the Scatchard approach and a Scatchard plot of Ø/M vs Ø yields K_o as the slope (Stevenson *et al.*, 1993).

The Scatchard approach has been utilised by a number of workers in the study of metal binding to humic substances (Bresnahan *et al.*, 1978: Saar & Weber, 1979: Sahu & Banerjee, 1990: Stevenson & Chen, 1991). All workers reported a non-linearity in the plots obtained, and therefore the plots were divided into two straight line segments, from which two constants K_1 and K_2 were calculated, according to equation 4.14. Binding was therefore assumed to occur at two discrete classes of binding site, each represented by these constants. However, Bresnahan *et al.* (1978),

preferred to correct the curvature by further through calculating $\emptyset'$ ($\emptyset$ - n_1). n_1 is the total number of binding sites of the first type and if there are two classes of binding site are present, then a plot of $\emptyset'/M$ vs $\emptyset'$ will give a straight line, from which K_2 the constant for the second class of binding site, can be assessed.

Stevenson & Chen (1991) recognised the arbitary nature of the curve fitting procedure and the errors which it introduced into the K values. In addition, Perdue & Lytle (1983) proposed that the curvilinearity was not due to two distinct classes of binding site, but was due to the polyelectrolytic nature of the humic acid which would result in binding becoming increasingly difficult at higher metal loadings. Therefore, Stevenson & Chen (1991) adapted the discrete ligand Scatchard approach into a continuous distribution model by calculating incremental formation constants from each point in the Scatchard plot. These incremental constants change with $\emptyset$, and an intrinsic constant K_{int} was calculated by extrapolating $\emptyset$ to 0, when these parameters are plotted against one another. Stevenson *et al.* (1993) proposed that this approach was scientifically more sound than the two component Scatchard approach, since it expresses the heterogeneity of the humic substances and how this varies with extent of metal binding.

Therefore, in the titrations carried out here, in addition to the Scatchard approach, a series of incremental formation constants was calculated for each incremental addition of metal. To investigate the nature of the complexes being formed and the stability of the resulting interaction, two constants were calculated:

$$M^{2+} + A^- \overset{k3}{\Leftrightarrow} MA^+ \quad k3 = \frac{(MA^+)}{(M^{2+})(A^-)}$$

$$M^{2+} + 2A^- \overset{k4}{\Leftrightarrow} MA_2 \quad k4 = \frac{(MA_2)}{(M^{2+})(A^-)^2} \qquad (4.15)$$

Integral to the Scatchard approach, and the above estimation of k_3 and k_4 is the calculation of the metal binding capacity (MBC).

Adsorption of a cation onto a surface can be expressed by the Langmuir equation:

$$x = \frac{kKc}{1 + Kc} \qquad (4.16)$$

where c is the concentration of solute at equilibrium, x is the concentration of solute adsorbed per unit weight, k is a constant which represents the maximum binding capacity and K is also a constant which represents the affinity between the adsorbate

and the adsorbant. By plotting c/x vs c, k or the MBC can be calculated from the slope of the line (Zunino & Martin, 1977). However, a linear response may not be observed since the binding energy is not uniform amongst sites and the Langmuir equation is representing binding at a single layer of binding sites. Instead, a two-surface Langmuir plot may be assessed which can be calculated from the following equation:

$$x = \frac{k_1 K_1 c}{1 + K_1 c} + \frac{k_2 K_2 c}{1 + K_2 c} \qquad (4.17)$$

By plotting x/c vs c the MBC can be determined by extrapolating the line to the x axis.

In the work presented here, both techniques were used to calculate the MBC, and the results averaged to give a more representative estimate, since Fitch & Stevenson (1984) observed slight discrepancies in the values calculated by both methods.

4.2.2.2 THE THEORY OF ION SELECTIVE ELECTRODE MEASUREMENTS

When an ion selective electrode is exposed to a sample solution of ions for which it is sensitive, a potential develops across the surface of the membrane, which can be directly related to the activity of the ion being determined. In order to measure this potential, a second, unvarying potential is used in the form of a reference electrode. A filling solution completes the electrical circuit between the sample solution and the reference electrode, and the point of contact between the sample and filling solutions is the liquid junction.

The voltage difference between the ion selective electrode and the reference electrode is a measure of the activity of the metal being studied. This electrode response can be described by the Nernst equation:

$$E = E^0 + k \log(a) \qquad (4.18)$$

where E is the measured voltage, E^0 is a combination of constants within the system, a is the activity of the ion being measured, k = RT/nF (or the slope), R is the gas constant, T is the temperature, F is Faraday's constant and n is the number of electrons discharged. However, in order to relate the voltage difference or potential directly to concentration, the following relationship is utilised:

$$a = cf \qquad (4.19)$$

Since the activity coefficient, *f*, is a measure of the interaction of an ion with other ions present, and depends on the total ionic composition of the solution, by maintaining it at a constant value with a swamping concentration of electrolyte, the activity can be directly related to concentration.

The liquid junction potential should also be included in the Nernst equation, but when the ion selective electrode and the reference electrode are in the same cell this is not necessary. However, certain conditions must be made, and accounted for, namely:

(a) The ionic strength adjuster added to the sample must not introduce any contamination with it.

b) The sample solution must not contain any substance which will interfere with the reference electrode.

(c) The sample itself must not interfere with the reference electrode.

(d) Neither the reference nor the ion selective electrode must release substances into solution which are likely to interfere with each other.

(Midgely & Torrance, 1991)

4.2.2.3 ION SELECTIVE ELECTRODE CONDITIONING AND CALIBRATION

The ion selective electrodes utilised in this work were solid state membranes composed of crystalline solids, of which the determinant is also a component. The electrodes used, their reference electrodes, and their composition, operational limits, interferences and ionic strength adjusters (I.S.A.), are displayed in Table 4.1.

Each ion selective electrode was conditioned before use by polishing with the supplied polishing strip, and then immersing it in 10^{-6}M standard solution overnight. The reference electrodes were also conditioned by soaking them in 0.1M solutions of the I.S.A. The electrodes were stored in their respective conditioning solutions. A calibration curve relating e.m.f (electro-motive force) with concentration of metal was prepared before each experiment, to ensure that the electrode was giving a Nernstian response in the correct range. Standards in the range of 10^{-1}M to 10^{-7}M with the ionic strength adjusted to 0.1M were used. Analar $Cu(NO_3)_2$ was used to generate the Cu^{2+} standard solutions and $Pb(ClO_4)_2$ was used to generate the Pb^{2+} standard solutions. Drift was also assessed and readings were only taken when the drift was less than 0.1mV over 2 minutes.

All ion selective electrode measurements were carried out in an enclosed container since the Ag/AgCl single junction reference electrode is sensitive to U.V. light. The temperature was constant at 25^0C and a magnetic stirrer and stirrer bar were

used to help mixing of the solutions. All measurements were carried out in the same closed cell system outlined in section 4.2.1.2, with inlets for the ion selective electrode, the reference electrode and the pH electrode. The e.m.f was recorded with a Radiometer pH 64 research meter which could discriminate to 0.1mV, and pH was recorded with a Corning Ion Analyser 250 pH meter.

Table 4.1 Ion Selective Electrode specifications.

Electrode	**Composition**	**Reference Electrode**	**Concentration Range (M)**	**Interferences**	**I.S.A**
Copper	CuS & Ag_2S	Single Junction	10^{-8} - 10^{-1}	Hg^{2+}, Ag^{+}, Cu^{+}	5M $NaNO_3$
Lead	PbS & Ag_2S	Double Junction	10^{-6} - 10^{-1}	Hg^{2+}, Ag^{+}, Cu^{2+}	10% KNO_3

4.2.2.4 I.S.E. MEASUREMENT OF METAL BINDING IN HUMIC ACID

Due to a lack of sufficient Lunga Water and Huxter peat, peat was collected from South Drumboy farm (grid ref. NS 502 482) and humic acid was isolated and protonated as outlined in section 2.2.1. The protonated humic acid was titrated to pH 4 and pH 5 with 0.01M KOH, with I.S.A. added to give an ionic strength of 0.1M. 10 ml aliquots of the humate salt were then pipetted into 4 oz glass bottles. To these aliquots, successive increments of 0.01M standard metal solution were added with a calibrated automatic dispenser and stirred. After 15 minutes, the e.m.f was recorded with the relevant ion selective electrode and reference electrode. A blank determination was also carried out for humic acid alone.

4.2.2.5 I.S.E. MEASUREMENT OF METAL BINDING IN PEAT

In addition to the humic acid studies, metals were added to unextracted South Drumboy peat. The peat was protonated as in section 2.2.1, and then titrated to pH4 or pH5 with 0.01M KOH, with the ionic strength also adjusted to 0.1M. Once equilibriated, the K^{+} treated peat was washed with de-ionised water to remove excess salt before freeze drying. Aliquots of 0.5 g of pH adjusted peat were then measured into 4 oz jars. Ionic strength adjusted solutions with increasing concentrations of metal were added to the jars which were then shaken on an orbital shaker for 4 hours, before having the e.m.f. recorded with the relevant ion selective electrode.

4.3 RESULTS AND DISCUSSION

4.3.1 THE BASE TITRATION METHOD

4.3.1.1 CALCULATION OF A_t

As outlined in section 4.2.1.2, this value, which represents the total content of titratable functional groups, can be calculated from the titration curve of humic acid with KOH. A sample titration curve is displayed in Figure 4.1. The end point of the titration is difficult to determine due to the polyelectrolytic nature of the humic substances, and is therefore taken as the point in the titration where the rate of change of pH, with added alkali, reached a maximum (Posner, 1964). Calculating the values for the change in pH with volume of alkali added highlights the overlapping end points which give humic acids their polyelectrolytic nature. Two distinct regions of dissociation can be identified, with the first one being attributed to the dissociation of the more acidic carboxyl groupings, and the second being attributed to the less acidic groupings, such as alcoholic and phenolic hydroxyl groupings (Stevenson, 1982). The end point for the latter was chosen as the value for A_t in the metal additions, since on metal binding and complex formation, conformational changes could occur which would lead to the exposure of more groups for reaction, not just the dissociated groups present at that pH value (Underdown, 1985: Tuschall & Brezonik, 1984).

Figure 4.1

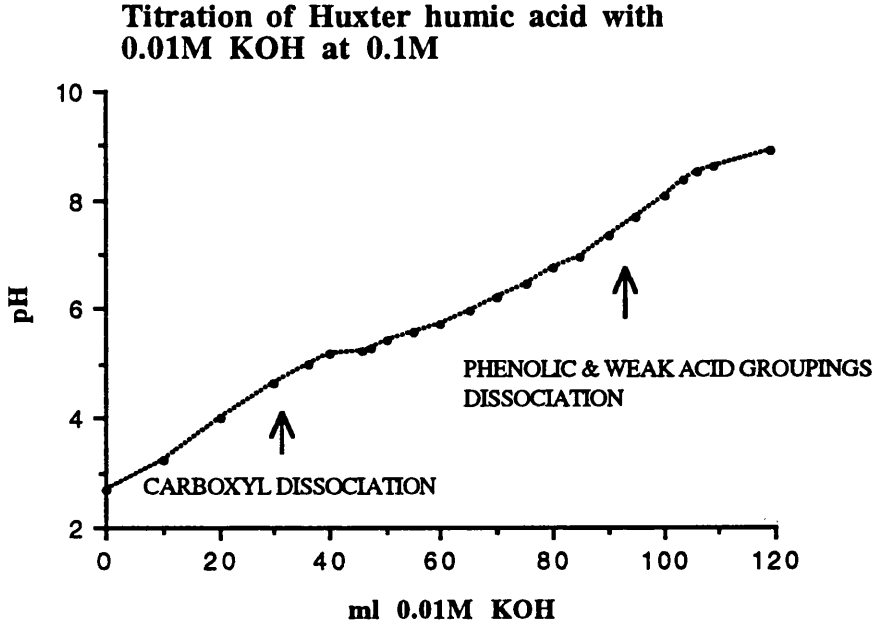

Since the end point of the titration was taken as 95 ml, and the alkali used was 0.01M KOH, the calculation of A_t is as follows:

$$\frac{95 \text{ ml} \times 0.01 \text{ mmol ml}^{-1}}{30 \text{ ml}} = 0.032 \text{ mmol}_c \text{ ml}^{-1}$$

With 150 ml of protonated humic acid yielding approximately 1 g of humic acid, this translates into a value of 4.76 $\text{mmol}_c \text{ g}^{-1}$, which is slightly lower than the 6.22 $\text{mmol}_c \text{ g}^{-1}$ recorded for the same humic acid using the barium hydroxide method. Piccolo and Camici (1990) compared the two methods and found that the barium hydroxide method always gave higher results than the potentiometric method, although it potentially gave more accurate estimates of the total acidity.

The ionisation of humic acid in the above titration can be represented by the following equation:

$$HA \overset{Ki}{\Leftrightarrow} H^+ + A^- \qquad (4.20)$$

Therefore, the ionisation constant K_i can be expressed as:

$$K_i = \frac{(H^+)(A^-)}{(HA)} \qquad (4.21)$$

This constant is required in the calculation of the formation constants and was assessed for each determination, since the starting pH was always slightly different, and as such the ionisation constant would also differ. HA and A^- were calculated using the following equations:

$$At = (HA) + (KOH) + (H^+) - (OH^-) \qquad (4.22)$$

$$A^- = (KOH) + (H^+) - (OH^-) \qquad (4.23)$$

4.3.1.2 FORMATION CONSTANT RESULTS

The results of the sequential additions of metal are displayed in Figures 4.2 to 4.5. In all graphs each successive addition of metal depressed the pH to a lesser extent and accordingly less base was required to neutralise the liberated protons. Therefore, it can be assumed that it was becoming increasingly difficult for each addition of metal to react as binding sites are progressively filled. Tuschall & Brezonik (1983) proposed

that on binding a build up of positive charge on the macromolecule could occur which would result in subsequent binding being more difficult to achieve.

The additions of Cu^{2+} resulted in the greatest release of protons, followed by Pb^{2+}, then Ag^{+}, with Cs^{+} showing the least effect. The significant release of protons by addition of Cu^{2+} and Pb^{2+} was also recorded by Stevenson (1977), and was not unexpected since these metals have previously been demonstrated to participate in complexation reactions (Bresnahan *et al.*, 1977: Gamble *et al.*, 1980: Stevenson *et al.*, 1993). In the Cu^{2+} additions at pH 5, more protons were liberated than can be accounted for by the total content of acidic functional groupings, as determined by titration. Stevenson (1977) also observed this effect for Cu^{2+} and Pb^{2+} and proposed that it was due to the release of protons from dissociation of the hydration water of the metal ion when held in 1:1 complexes. Also, since binding of Cu^{2+} has been shown to give significant changes in the arrangements of the acidic functional groupings (section 3.3.2.3), it is reasonable to assume that these changes could result in the exposure of previously unavailable functional groupings. These conformational changes are also one of the secondary effects, which are proposed to occur on metal binding (Buffle, 1988). Tuschall & Brezonik (1984) in a later paper on the study of Cu^{2+} binding to organic ligands, proposed that conformational changes could occur on metal binding, which may be resulting in the exposure of previously unavailable groupings which have a stronger affinity for the metal than would be expected.

In addition, for Cu^{2+} and Pb^{2+} (Figures 4.2 and 4.3 respectively), significantly fewer protons were released at pH 4 than pH 5, indicating that there was greater competition between the proton and the metal at that pH, due to the reduced ionisation of the materials. With Cs^{+} (Figure 4.4) little difference was observed in proton release between pH 4 and pH 5. However, the pH drops recorded after addition of Cs^{+} at both pH values were bordering on the limit of detection of the pH electrode and therefore are interpreted with caution. Ag^{+} additions were achieved only for pH 5, and they show greater release of protons than observed with Cs^{+}, indicating that Ag^{+} can participate to a greater extent in complexation reactions than Cs^{+}. However, these results should also be interpreted with caution, since the salts were added in the unbuffered form which can affect the results. For the monovalent ions, lower A_t values were used since less humic acid was used in the titration and thus a different scale on the X-axis is recorded. This has no effect on the formation constants recorded, since it is incorporated into the calculations.

Figure 4.2

The sequential additions of buffered copper acetate to Huxter humic acid at pH4 and pH5

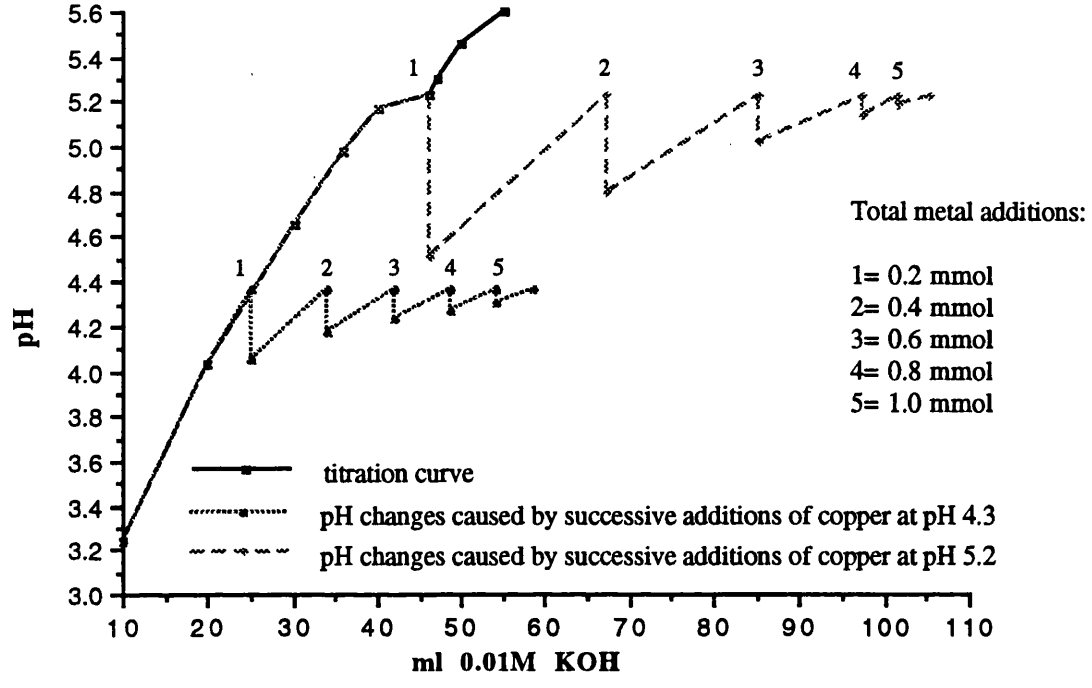

Figure 4.3

The sequential additions of buffered lead acetate to Huxter humic acid at pH4 and pH5.

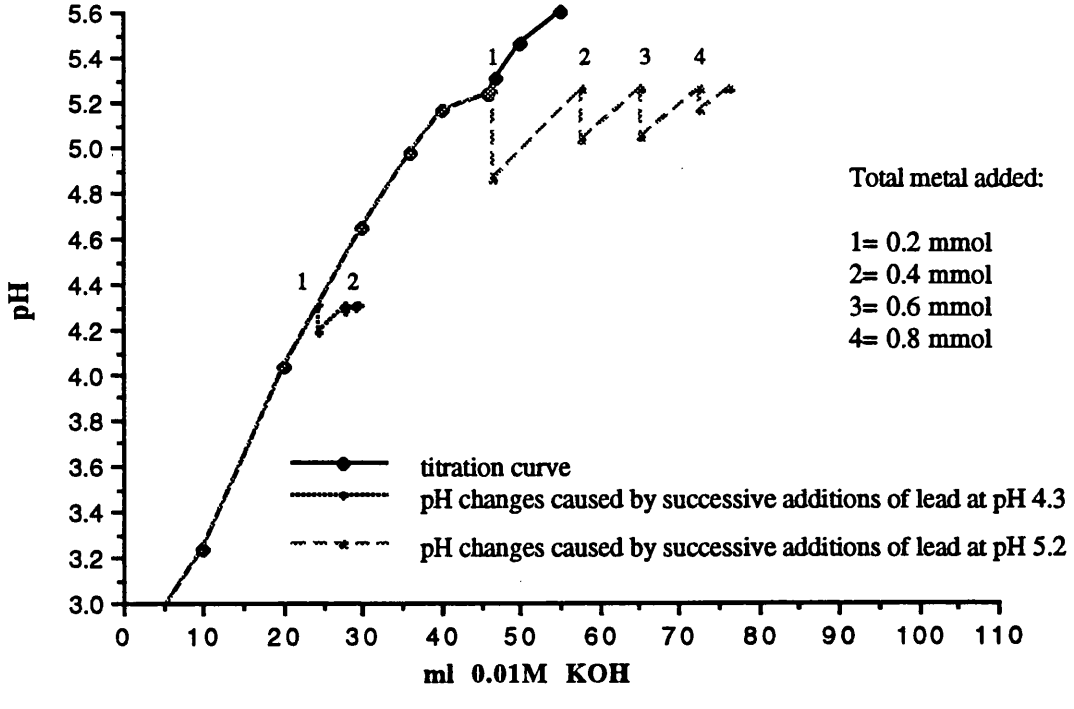

Figure 4.4

The sequential additions of unbuffered caesium chloride to Huxter humic acid at pH4 and pH5.

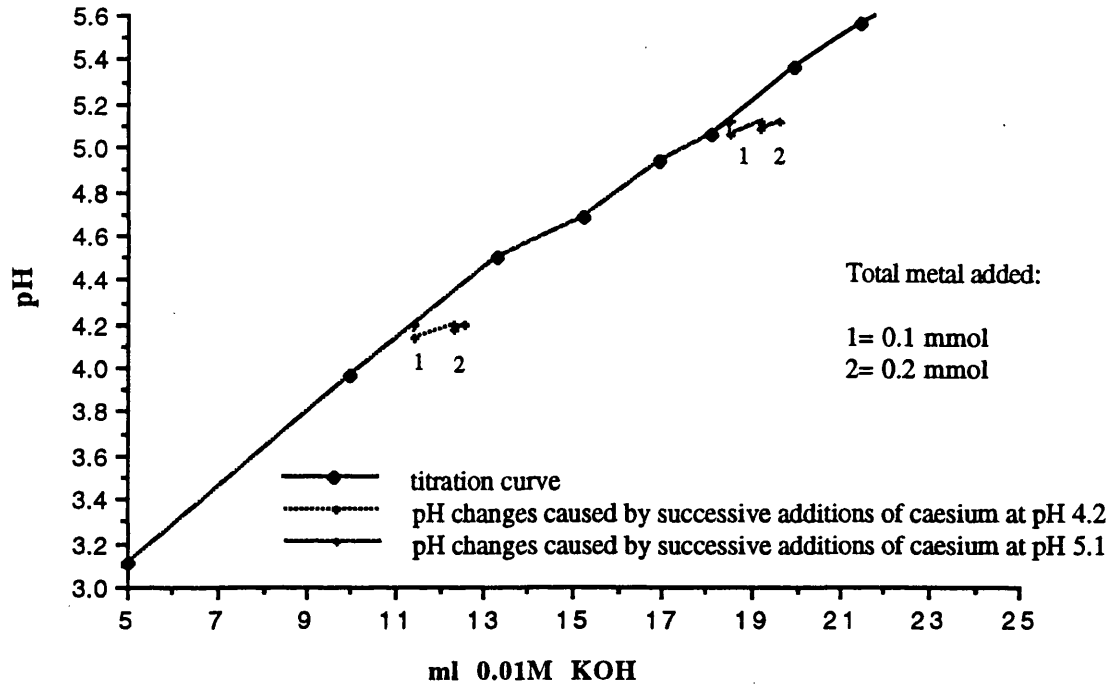

Figure 4.5

The sequential additions of unbuffered silver nitrate to Huxter humic acid at pH 5.4

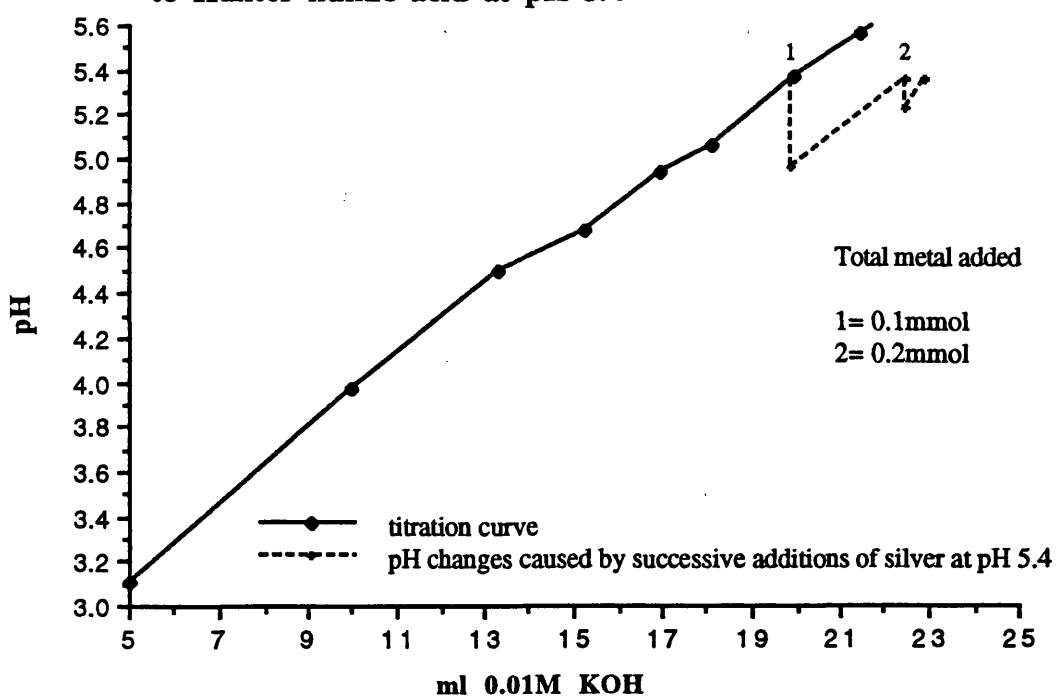

Stevenson (1976) calculated the average formation constants for the metal additions by plotting ñ (the number of complexing sites per mole of metal ion) vs

p(HA/H^+), with b_1 and b_2 being assessed from interpolating at ñ values of 0.5 and 1.5. Since the ñ values can exceed 0.5, an average formation constant has been determined by interpolating at ñ = 1.0 (Stevenson *et al.*, 1973). Stevenson *et al.* (1993) developed this approach further to calculate average formation constants from Bjerrum plots. In the humic acid used here, the ñ values ranged from around 1 to 0.2, making interpolation in the above way difficult, and highly speculative. Instead, the average formation constants for the divalent ions were determined graphically from equation 4.8 and samples of the graphs obtained are presented in Figures 4.6 & 4.7 with the remainder of the data in Appendix 2.1.

From Figure 4.6 a value of B_2 is calculated as 1.0873×10^{-10}, which gives a log B_2 value of -9.96 for the additions of Cu^{2+}, to Huxter humic acid at pH 5. Slight curvature of the graph is observed, and this was also seen in the graphs for buffered $Cu(Ac)_2$ additions at pH 4 (see Appendix 2.1). The lack of linearity comes from the excess of protons which are released, requiring excess base to return the pH to its previous value. This could be a consequence of the release of protons from the water of hydration in 1:1 complexes. Alternatively, it could be due to the release of protons from groups which were previously unavailable for reaction, but were exposed on binding due to conformational changes.

The $Pb(Ac)_2$ additions at pH 5 (Figure 4.7), show a more sigmoidal shape, perhaps indicating that two distinct classes of binding site are present for Pb^{2+} in the humic acid, with the second class of binding site perhaps being these previously unavailable sites which are exposed on binding (Buffle, 1988: Underdown *et al.*, 1985: Tuschall & Brezonik, 1984).

Figure 4.6

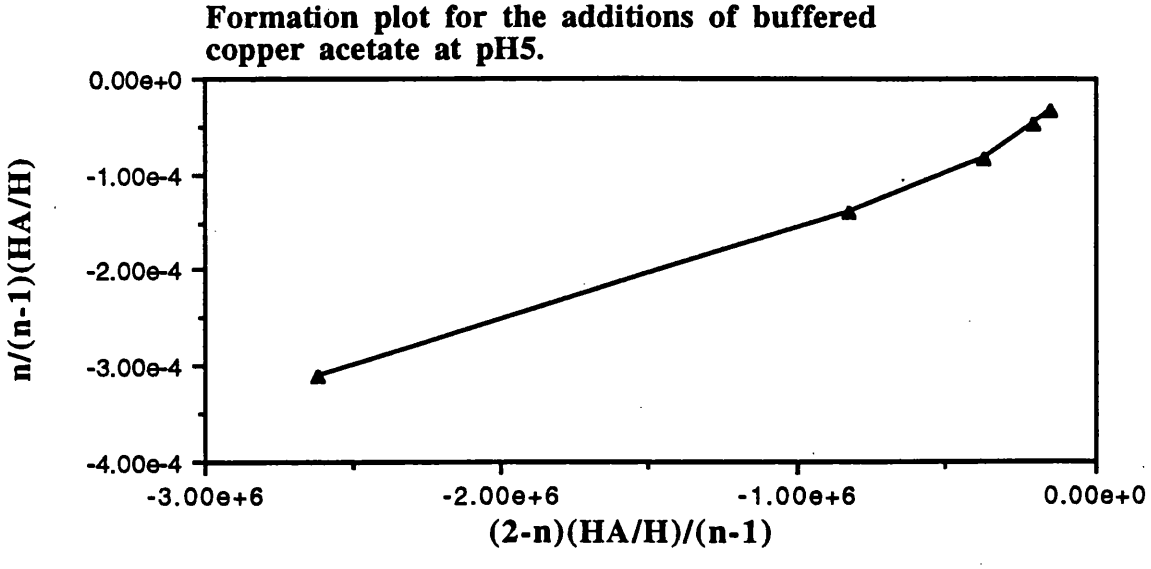

Figure 4.7

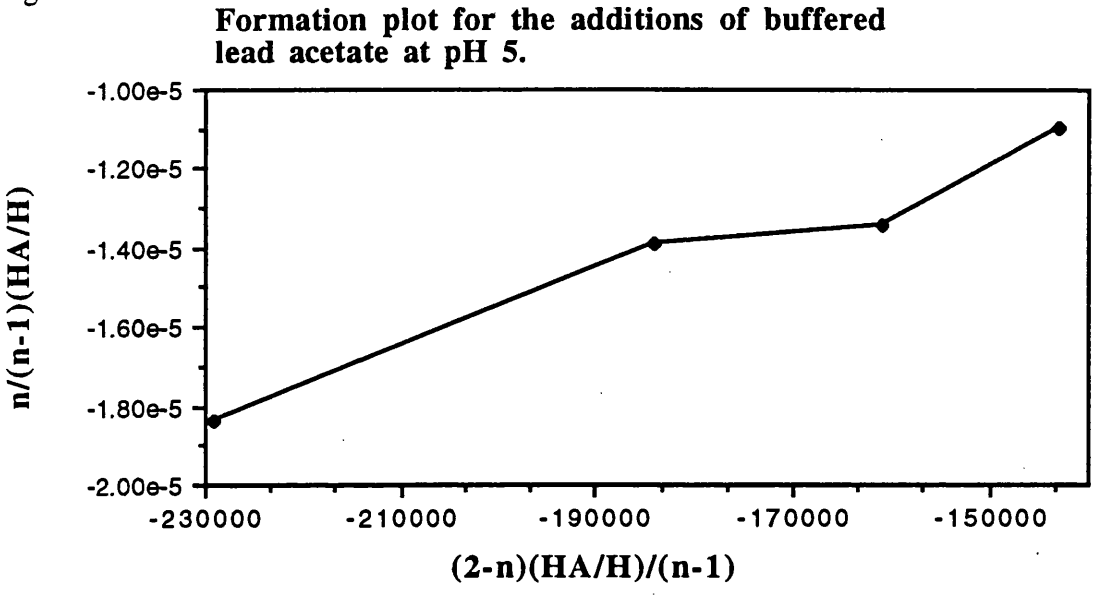

The B_1 values for the monovalent ions were calculated from equation 4.10, for which no graphical treatment is required. When more than one pH drop was observed, the stepwise stability constants were averaged to give the overall formation constant B_2. The average formation constants for each metal are presented in Table 4.2 and are mean values for replicate titrations.

Table 4.2 Mean Log B values (of 3 calculations) and their standard deviations.

Metal Salt	pH	Mean	Standard Deviation
$Cu(Ac)_2$	4	-8.99	0.369
$Cu(Ac)_2$	5	-9.66	0.162
$Pb(Ac)_2$	4	-8.62	0.147
$Pb(Ac)_2$	5	-10.23	0.123
$Ag(NO_3)$	5	-5.04	0.075
CsCl	4	-4.55	0.085
CsCl	5	-5.44	0.045

The log B_2 values are lower than anticipated, indicating that very little metal was binding, with low stability of reaction. Yet, from the pH drops observed, considerable amounts of Cu^{2+} and Pb^{2+} interacted with the humic acid, giving significant drops in pH, but presumably with lower stability. This lower stability was also observed in the constants recorded at pH 5, where again more metal interacted,

releasing more protons. The low constants obtained can be partly explained by the relatively large quantities of metal added, compared to the number of available sites. The levels of addition were chosen to follow on from the infra-red studies, where correspondingly high levels of metal addition were used. In this way, the qualititative and quantitative effects of metal binding could be compared, in addition to the behaviour of these metals at pollutant levels. The high levels of metal added have resulted in significant amounts of protons being released, even though this is not expressed in the constants, and in some cases this amount is greater than the total content of reactive sites. At all pH values the number of protons released as a result of the Cu^{2+} and Pb^{2+} additions, was greater than the amount of available groups at that pH value, as determined from the titration curve. This again indicates that, as well as the possibility of metal oxide formation, conformational changes occurred which resulted in the release of protons and encouraged further metal binding. The use of the total functional group content, to calculate the constants rather than the amount of sites available at that pH will also contribute to the low value of the constants obtained.

With Cs^{+}, this difference in values with pH was less enhanced, but the errors for the additions will be higher due to the very low pH drops recorded, which bordered on the limit of detection of the pH electrode. In addition, with Cs^{+} and Ag^{+}, the values cannot be utilised without consideration of the pH drop caused by the unbuffered salt.

Stevenson (1977) also recorded low B_2 values for divalent metals and these low values could be due to a limitation of the method to express complex formation in humic substances. In addition, Gregor (1955) pointed out that ideal Bjerrum plots are often not obtained even for simple monomeric substances, and therefore they should be interpreted with caution in polymeric substances.

Stevenson (1976, 1977) converted the log B_2 values to log K_2 values which represent the interactions betwen the metal and the ionised groupings, as in equation 4.3. Stevenson (1977) proposed that these two constants were related to each other through the equation:

$$B_2 = K_i K_2 \qquad (4.24)$$

where K_i is the dissociation constant for the pH value at which the additions were carried out. Yet, from equation 4.5, B_2 represents the following relationship:

$$B_2 = \frac{(MA2)(H^+)^2}{(HA)^2(M^{2+})} \qquad (4.25)$$

and K_2 accordingly represents the following equation:

$$K_2 = \frac{(MA2)}{(M^{2+})(A^-)^2} \quad (4.26)$$

since the acid dissociation constant represents the reaction:

$$K_i = \frac{(A^-)(H^+)}{(HA)} \quad (4.27)$$

the relationship between B_2 and K_2 should be represented as:

$$B_2 = (K_i)^2 K_2 \quad (4.28)$$

and not as in equation 4.24.

As well as the mathematical considerations above, the theoretical validity of carrying out such conversions in humic substances was questioned by Perdue (1988). He proposed that such relationships are only valid in simple sytems with one metal and one ligand, not in humic substances where a combination of unquantifiable secondary reactions occur on metal binding. Therefore, log K_2 values were not calculated for the log B_2 values produced here. The formation constants represent average values for the stepwise constants produced from successive metal additions, and express the competition of the metal and proton for the reactive sites on the humic acid. They are also conditional constants, being a function of ionic strength, pH, ligand concentration, and temperature (Perdue, 1988). The effect of changing the pH can be seen clearly from the results. Therefore, because of the conditional nature of the values, comparison with previously published values should be undertaken with caution. Stevenson (1977) used the same method as the one outlined here, yet direct comparison cannot be made with the constants produced in that paper since different ligand to metal ratios, different humic acids, A_t values, type of salt, etc., were utilised.

The constants indicate that Pb^{2+} and Cu^{2+} competed with the protons to give a similar stability of interaction, regardless of the mechanism of reaction. Cs^+ and Ag^+ gave a similar stability of interaction, yet Ag^+ showed more significant pH drops on metal addition. However, interpretation of these values should be undertaken with caution, since these salts were not buffered. The pH of the CsCl was 6.6 and the pH of the $AgNO_3$ was 4.8. Thus, the small pH drops recorded by the Cs^+ could be due to the pH of the salt and not the behaviour of the Cs^+ metal.

Stevenson (1976, 1977) added the metals as chloride salts, with no buffering of the pH of the salt. In this study, Cu^{2+} was originally added as $CuCl_2$ and Pb^{2+} as $Pb(NO_3)_2$ and the sequential additions of Cu^{2+} and Pb^{2+} from these salts are displayed in Figures 4.8 and 4.9 respectively.

When the pH drops with these salts are compared with the previous pH drops obtained on the addition of the buffered salts (Figures 4.2 and 4.3) it is clear that the unbuffered salts gave markedly enhanced pH drops, particularly at pH 5. With the pH

of the $CuCl_2$ being 4.32, and the pH of the $Pb(NO_3)_2$ being 4.73, it is not surprising that this effect is observed. Both metals showed a release of protons which was greater than their corresponding total reactive group contents (A_t) at pH 5. This could be due to the salts artificially depressing the pH, as well as the other effects discussed above.

Figure 4.8

The sequential additions of unbuffered copper chloride to Huxter Humic acid at pH 4 and pH 5.

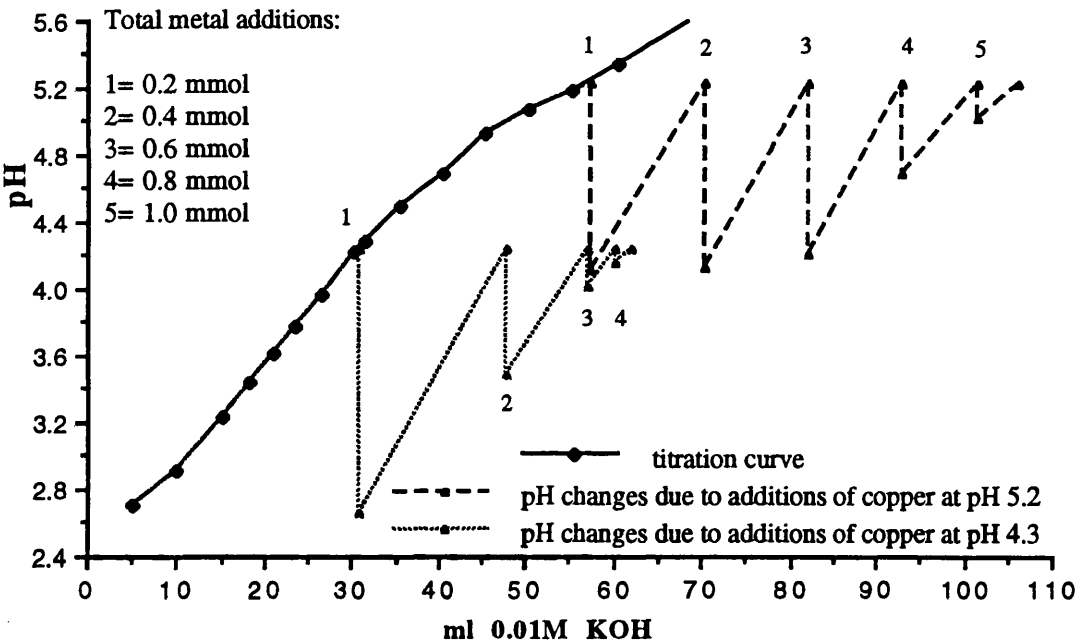

Figure 4.9

The sequential additions of unbuffered lead nitrate to Huxter humic acid at pH 4 and pH 5.

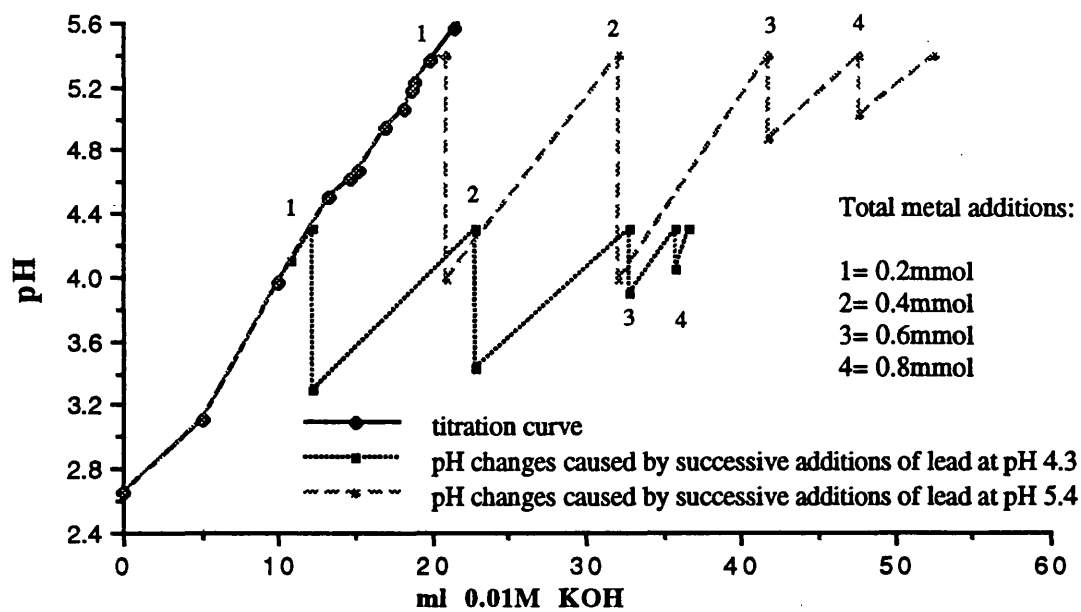

The formation plots for these metal salts are displayed in Figures 4.10 and 4.11 and, because of the non-linear effect, no formation constant can be calculated. The shape of the graphs is due to the non-linear reduction of ñ, the formation function, with increasing metal addition. The formation function is directly related to the amount of base which is required to return the pH to the starting point, and since this amount is artificially enhanced by the pH of the salt, a non-linear relationship is observed. Clearly, any future work of this kind, where pH drop is the parameter which is utilised to measure the extent of metal binding, requires that a buffered salt be used.

Figure 4.10

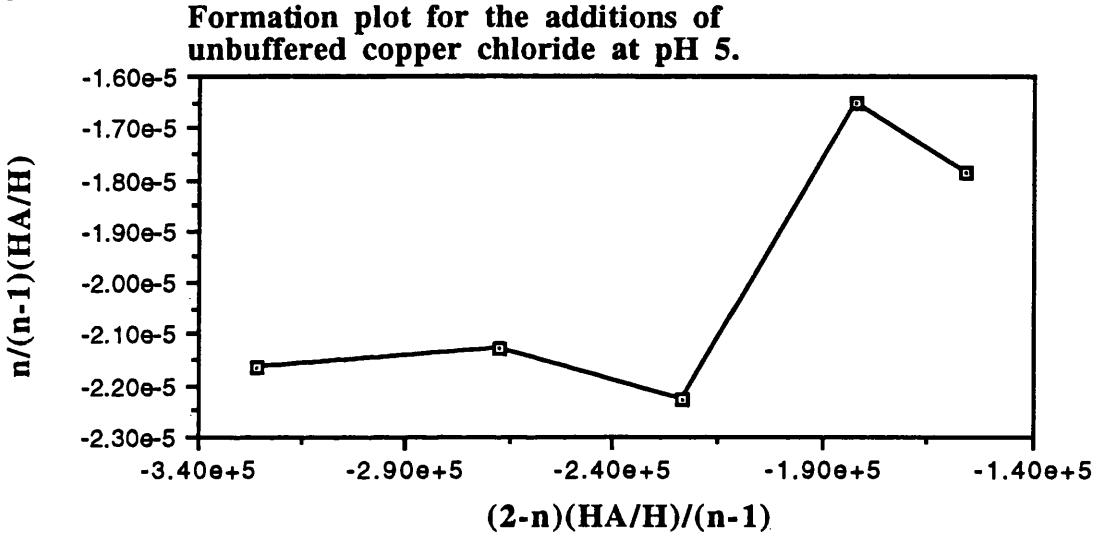

Figure 4.11

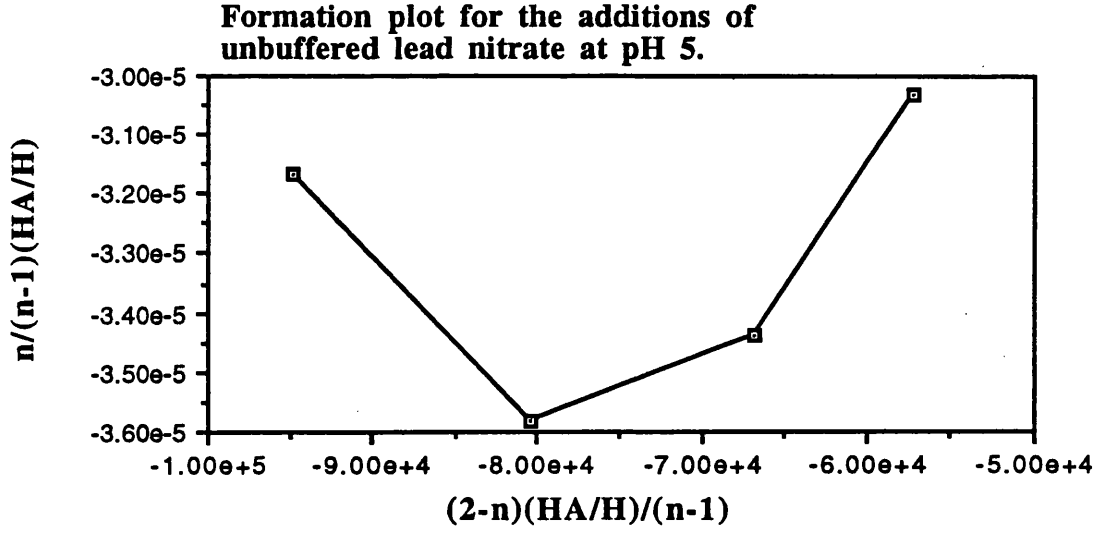

4.3.2 INCREMENTAL ADDITIONS RESULTS

4.3.2.1 CALIBRATION OF THE ION SELECTIVE ELECTRODES

Samples of the calibration lines for the cupric and lead ion selective electrodes are displayed in Figures 4.12 and 4.13 respectively. Due to the possibility of drift occurring, a calibration line relating emf to metal concentration was prepared before each titration, and used to calculate the free metal at each step in the titration. In the concentration range studied, both calibrations exhibit a Nernstian response, according to equation 4.29.

$$E = E^0 + k \log(a) \qquad (4.29)$$

Figure 4.12

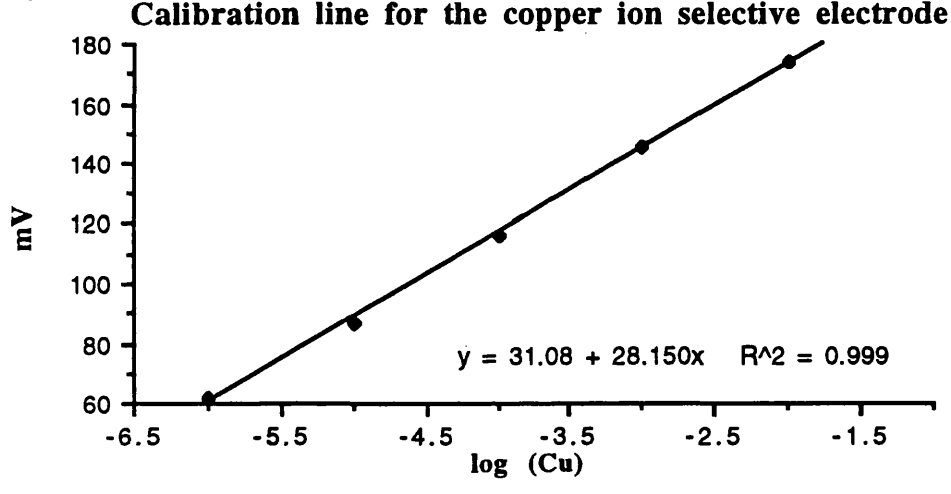

Figure 4.13

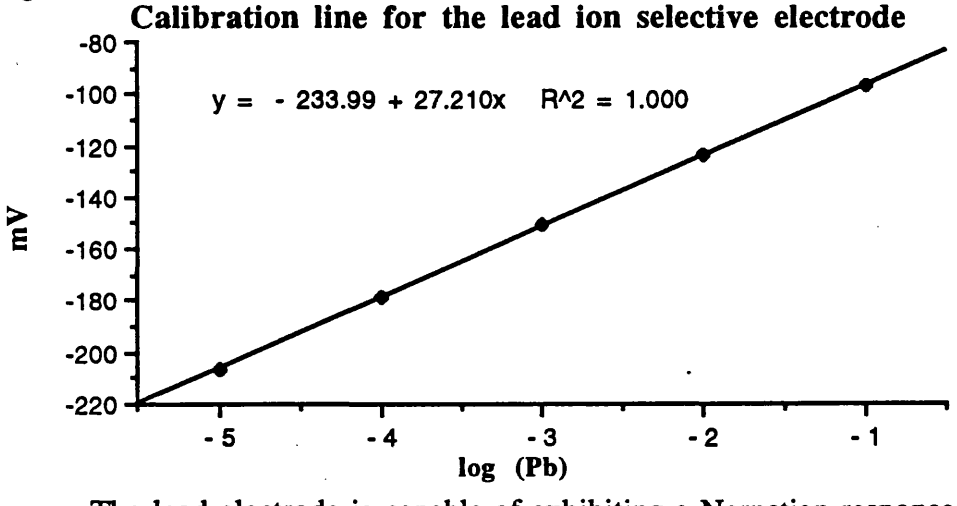

The lead electrode is capable of exhibiting a Nernstian response only within the range 10^{-1}M to 10^{-5}M, whereas the cupric electrode can detect copper to 10^{-6}M.

Therefore, the lead electrode has a higher limit of detection, which decreased the range of the metal-binding studies. One major limitation of ion selective electrodes is that they can only detect levels of metal which are above the concentrations of Cu^{2+} and Pb^{2+} normally found in unpolluted systems, and are therefore only applicable for modelling the behaviour of metals at pollutant levels (Fish & Morel, 1985).

4.3.2.2 CONSIDERATIONS ON ERROR CALCULATIONS

Calculation of the formation constant requires knowledge of the ionic activity of the metal (M), the amount of bound metal (MA) and the total ligand concentration or M.B.C. Only the ionic activity of the free metal is determined directly, with the amount of bound metal being determined from the difference between this value and the total amount of metal added. The M.B.C gives rise to the largest single error in the calculation of formation constants, since it is dependent on the error associated with calculating the amount of bound metal (Fish & Morel, 1985). Bound metal errors increase greatly near the end of the titration (Figure 4.14), where the calculation of this value involves subtracting two large numbers (Fish & Morel, 1985: Cabaniss & Shuman, 1986).

Figure 4.14

Relationship between amount of metal bound and the % error for copper binding to humic acid at pH 4

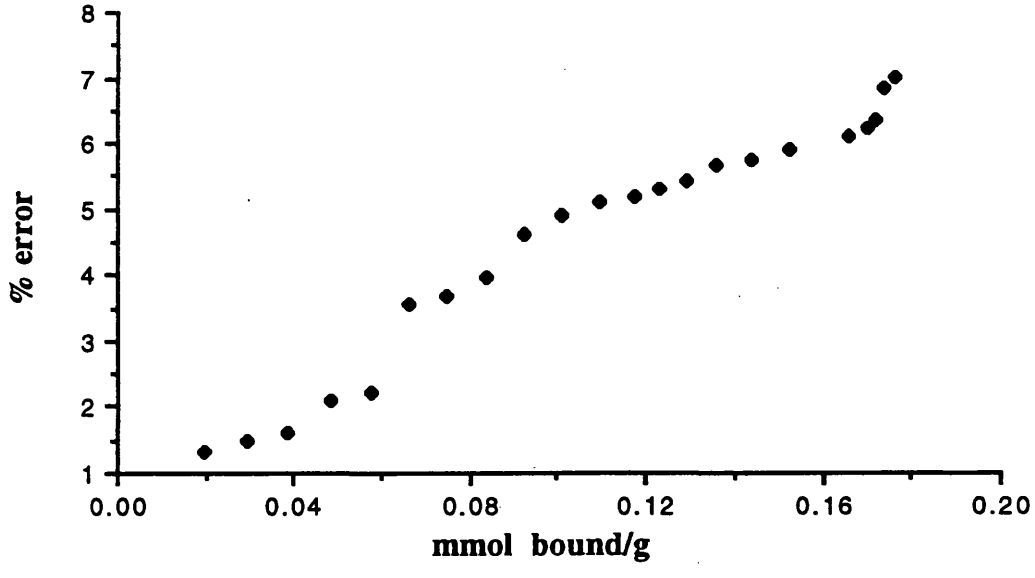

This effect was observed in all the metal additions, to both the peat and the humic acid. Each titration was replicated twice and the results for the amount of bound metal at each level of addition were averaged to give a mean value, from which the

standard deviation was calculated. This was then divided by the mean to give the % error. Cabaniss & Shuman (1986) used this method of error calculation and showed a similar effect.

However, very few of the titration studies which utilise ion selective electrodes to produce the parameters for the subsequent calculations of the formation constants make any reference to the errors associated with such measurements and even fewer include any error calculation. Fish & Morel (1985) studied the error associated with various methods of titration and quantified the propagation of error for each of the methods which can be utilised if no replicate titrations are employed. Should replicate titrations be employed then the error associated in the method can be calculated using the standard error of the mean values.

Bresnahan *et al.* (1978) attributed the lack of error analysis in their analysis and calculations to the interdependence of the variables in the Scatchard approach, in particular the normalisation of bound metal to the M.B.C. In addition, the plots obtained are often curvilinear and division of the plots into two straight line segments is often arbitrary (Fitch & Stevenson, 1984). The problems associated with the Scatchard plots are discussed further in section 4.3.2.4.

4.3.2.3 CALCULATION OF THE MAXIMUM BINDING CAPACITY

The maximum binding capacity (M.B.C.) not only gives an estimation of the capacity of the material to adsorb metal, but is also integral to the measurement of formation constants and therefore it is important that this parameter be determined as accurately as possible. In section 4.3.2.2, it was demonstrated how a large error on this value can occur, and will then propagate throughout the rest of the calculations.

Since controversy exists as to the best method of calculating the M.B.C., both Langmuir and two-surface Langmuir isotherms were utilised and examples of these are displayed in Figures 4.15 and 4.16 respectively. The remainder of the graphs can be found in Appendix 2.2.

Figure 4.15

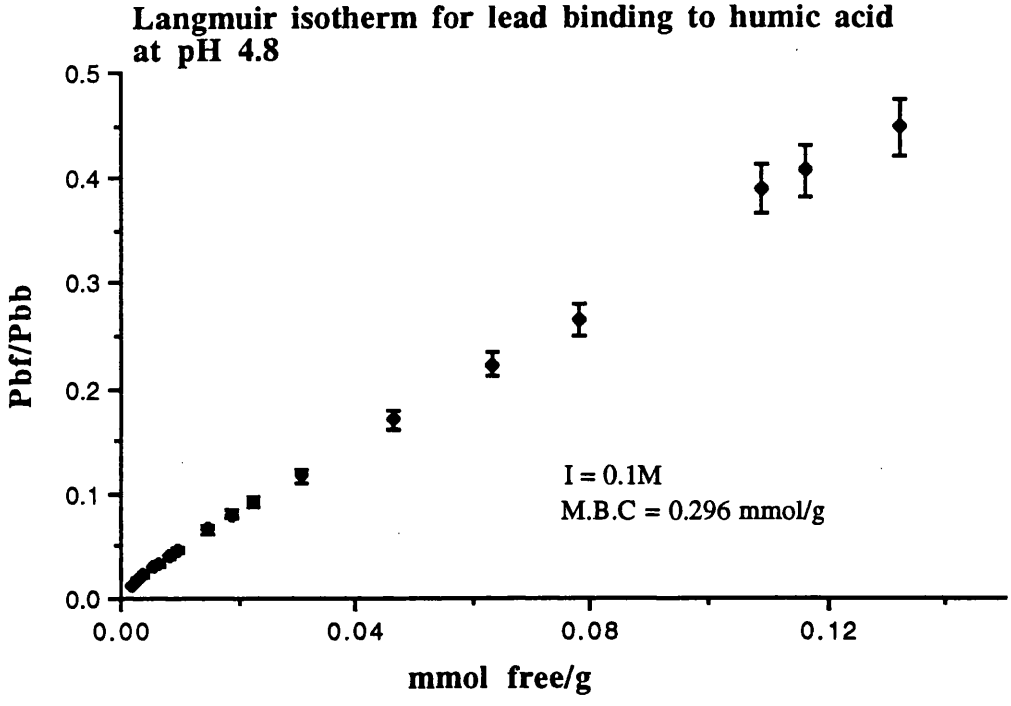

This isotherm assumes that the complexing stength remains constant throughout the titration, and that only one class of binding site exists (Zunino & Martin, 1977). For most of the titrations, a linear Langmuir response was achieved, with slight curvature towards the lower part of the graph in some of the titrations. Zunino & Martin (1977) proposed that any linear response with polyfunctional materials was due to a combination of many small, linear Langmuir responses for a succession of binding sites. However, Fitch & Stevenson (1984) also reported curvature of these isotherms and proposed that this made them unsuitable for the estimation of the M.B.C. They preferred to use the two-surface Langmuir isotherm, which assumes two distinct classes of binding site. This isotherm (Figure 4.16) gives a slightly higher value for the M.B.C., which was consistent for all of the titrations carried out, and mirrors the effect observed by Fitch & Stevenson (1984). Therefore, by combining the two values achieved from the two methods, an M.B.C. of 0.300 mmol g^{-1} for Pb^{2+} binding to humic acid at pH 4.8 was calculated.

Figure 4.16

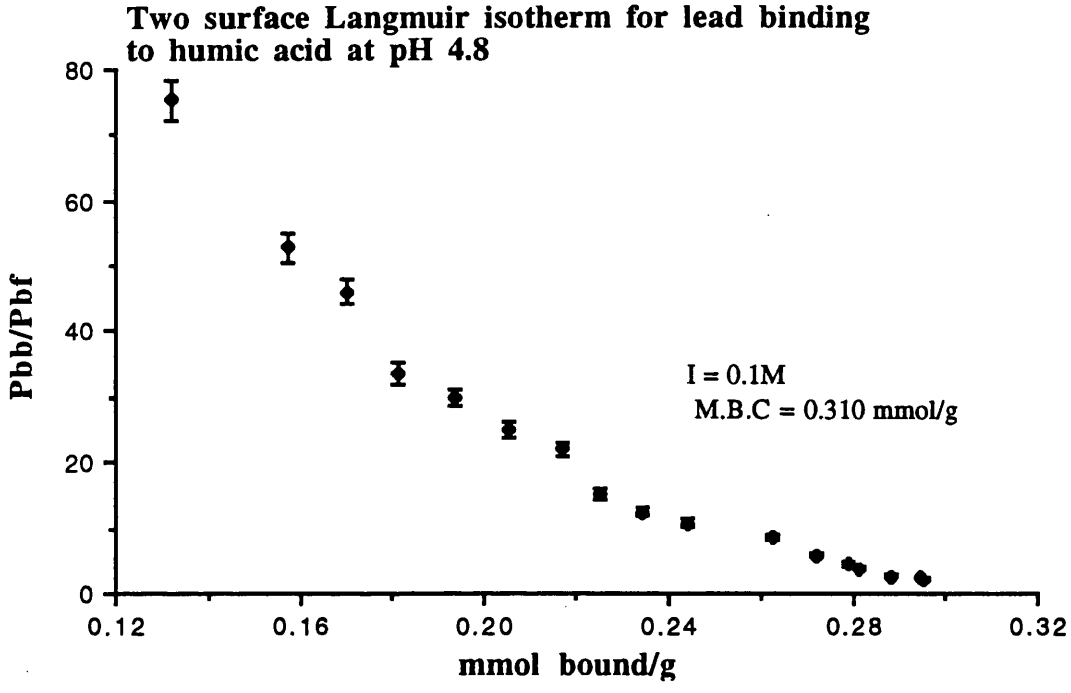

The remaining results for the M.B.C. estimations are presented in Table 4.3 and represent an average of values collected from the two isotherms.

Table 4.3 Mean M.B.C. values (mmol g^{-1}) for Cu^{2+} and Pb^{2+} binding to humic acid and peat.

	Humic acid			**Peat**	
	pH 4.8	pH 5.12	pH 5.8	pH 4	pH 5
Cu^{2+}	0.161 ± 0.008	0.188 ± 0.013	0.290 ± 0.021	0.083 ± 0.004	0.111 ± 0.007
Pb^{2+}	0.300 ± 0.023	0.564 ± 0.036	0.832 ± 0.065	0.207 ± 0.013	0.391 ± 0.027

The M.B.C. values clearly indicate that the humic substances have different capacities for the two metals being studied. In all determinations, the M.B.C. is markedly higher for Pb^{2+} than for Cu^{2+}. Saar & Weber (1980) studied Pb^{2+} and Cu^{2+} binding and observed that fulvic acid had a greater capacity to complex Pb^{2+} than Cu^{2+}. They also observed that at high metal loadings, precipitation of fulvic acid occurred in the Pb^{2+} treated samples, but was not observed in the Cu^{2+} treated samples. This precipitation often occurred before the M.B.C. was attained and they proposed that it would result in the entrapment of Pb^{2+} within the precipitated materials, thereby increasing the amount of Pb^{2+} apparently bound. In addition, sites

would still be available on the surface of the precipitate for further binding. In the Base Titration method, it was observed that Pb^{2+} resulted in the release of fewer protons than Cu^{2+} and this could also be due to a precipitation effect since entrapment, which increases the M.B.C., would not result in a release of protons. However a different humic acid was used in these studies, so direct comparison is perhaps unjustified.

The I.S.E. measures the activity of the free ion in solution and cannot discriminate betweeen the processes of complexation or precipitation. However, if this effect is acting to increase the M.B.C. of the humic substances for Pb^{2+}, then it is doing so in a uniform way, over all pH values, and in both the humic acid and the peat, and can therefore be considered to be a significant effect which would affect the behaviour of Pb^{2+} in the environment.

The conditional nature of the M.B.C. has been demonstrated by the difference in values for each metal, but it is also reflected in the different values obtained at each pH value. For both metals, in both materials, the M.B.C. increased with pH. This is consistent with the increase in reactivity to metals observed in the Base Titration method, and can be attributed to increased ionisation of the materials, giving increased reactivity of the functional groups towards metals. This increased reactivity is partly due to less competition from protons, but also to an opening up of the structure on ionisation (Underdown *et al.*, 1985: Stevenson, 1982). The increase with pH in the peat is a little more unexpected. When unextracted peat was titrated to pH 5 and studied in the infra-red, very little change in the ionisable functional groupings was observed (Chapter 2), yet here clear increases in the M.B.C. were observed. This could again reflect the conditional nature of such measurements, since a different peat was used in the measurements.

The isolation of humic acid from peat has acted to increase the M.B.C. for both metals, an effect also observed by Warwick *et al.* (1992). This increase could be due to an opening up of the structure on extraction, leading to exposure of the reactive functional groups. Since the aim of the extraction process is to isolate humic acid from the other soil constituents, this is highly likely. In addition, chemical changes could be occurring which lead to the formation of reactive functional groups (Gregor & Powell, 1987). This effect is also consistent with the reduced total acidity and carboxyl contents of unextracted peat which were previously demonstrated (Chapter 2), and also the reduced reactivity towards metals observed in the infra-red (Chapter 3). The ability of humic substances such as humic acid to change conformation and aggregate on metal binding (Underdown *et al.*, 1985) could act to increase the M.B.C. of these materials through the exposure of new sites for binding, since the infra-red studies indicate that on metal binding significant changes in the functional groups occur,

which are not seen in the unextracted peat. The unextracted peat is present as a suspension of soil particles in the titration mixture, and binding is effectively taking place at solid surfaces, whereas the humic acid is a colloidal polyelectrolytic suspension, where the structure is less defined and flexible than in the unextracted materials.

4.3.2.4 SCATCHARD ANALYSIS OF METAL BINDING DATA

All of the Scatchard plots produced, irrespective of metal or humic substance, were curvilinear (e.g. Figure 4.17). Some previous workers proposed that this effect indicated that binding was taking place at two distinct classes of binding site (Sahu & Banerjee, 1990), whereas other workers proposed that the curvilinearity was due to a continous distribution of binding sites, with varying binding energies (Bresnahan *et al.*, 1978: Saar & Weber, 1980: Perdue & Lytle, 1983: Stevenson & Chen, 1991). Since the Scatchard method also assumes that binding occurs in a 1:1 stoichiometry, plots of this type have been proposed to indicate a 2:1 stoichiometry of metal binding (Sahu & Banerjee, 1990: Town & Powell, 1993).

Buffle *et al.* (1977) proposed that curvilinearity could be due to a mixture of 1:1 complexes with different formation constants. The curvilinearity is probably also due to a variety of secondary effects occurring on metal binding, which includes electrostatic and conformational changes on binding as well as variations in the binding affinities of ligand sites (Tuschall & Brezonik, 1983, 1984). Town & Powell (1993) also proposed that the formation of colloidal precipitates and aggregation could contribute to the shape of the plots and the constants produced.

Whatever the reasoning, the fitting of two straight-line segments to these plots (e.g. Figure 4.17) is highly uncertain due to the continuous distribution of binding sites and often more than two lines could easily be fitted. Thus, the calculation of the formation constants from these lines can produce ambiguous results (Fitch & Stevenson, 1984) and makes the K values subject to large errors. Log K values were calculated from the Scatchard plots, purely to see how they would compare to the incremental contstants, but as values they merely represent an average stability for a class of binding site. What is perhaps more significant is that there are clear changes in the energies of the binding sites, as represented by the curvilinearity of the relationship.

Figure 4.17.

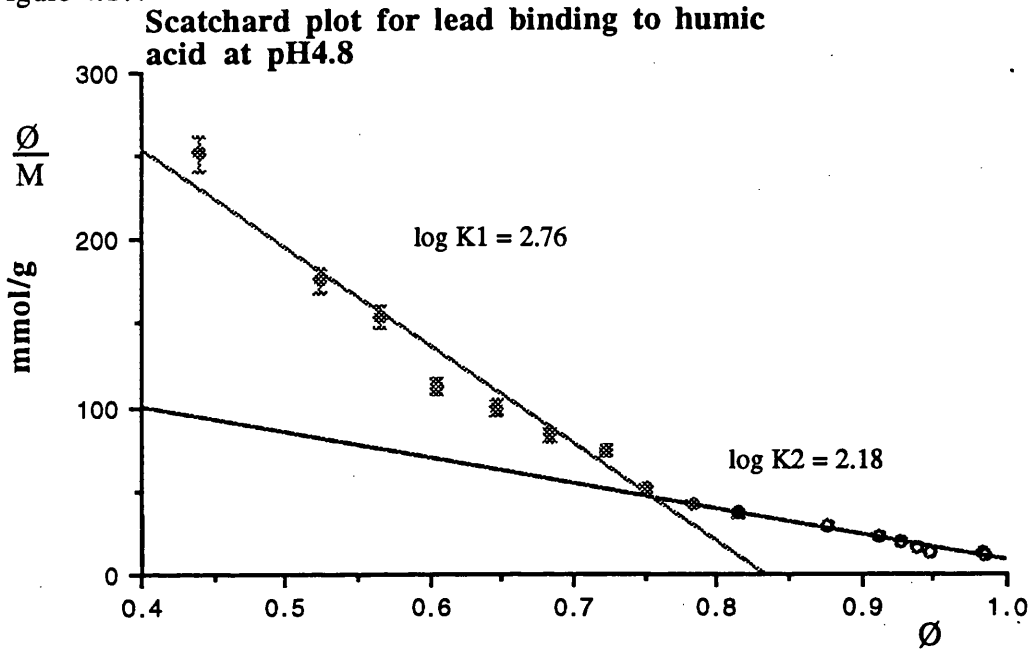

Scatchard plots of Cu^{2+} binding to peat at pH 4 (Figure 4.18) and Cu^{2+} binding to humic acid at pH 4.8 and 5.12, showed interesting effects at low levels of metal binding. At the beginning of the titration, when the metal:humate ratio was low, a small increase in the formation function/free metal value and the incremental formation constants was observed.

Figure 4.18.

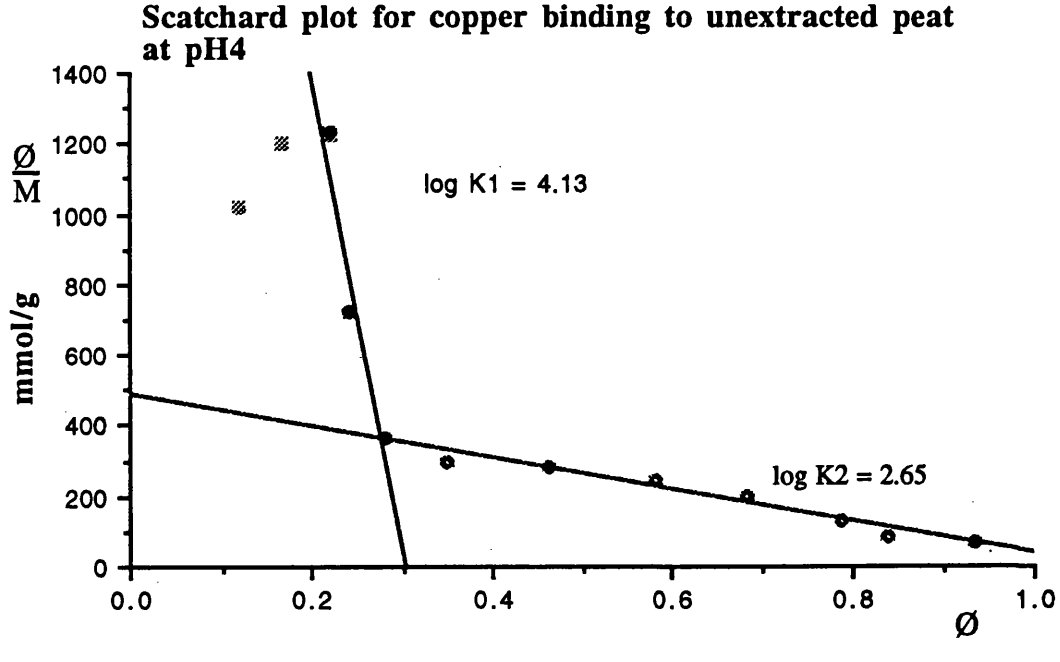

Therefore, at the start of the titration, instead of the proportion of binding sites to metal available decreasing, along with the energy of the binding sites and stability of interaction, an increase was observed. Underdown *et al.* (1985) observed that at very low Cu^{2+} concentrations, the metal was able to undergo highly-specific chelation reactions on one fulvic acid molecule only. Binding of Cu^{2+} by nitrogen containing groups has also been proposed (Stevenson *et al.*, 1993). At the start of the titration, when the binding sites are unfilled and chelation with more than one site is more favourable stereochemically, specific chelation of Cu^{2+} could be occurring which does not inhibit further metal binding or affect the energy of other binding sites. Infra-red analysis of Cu^{2+} complexes (section 3.3.2.3) indicated that especially in humic acid, binding was occurring in quite a specific manner, different to Pb^{2+}.

It is interesting to note that this effect was confined to the lower metal additions and is seen only at pH 5 in humic acid. On metal binding, the greatest pH drop was observed at the start of the titration. This pH drop could be due to the re-establishment of ionisation equilibrium, which could result in significant conformational changes allowing the exposure of new reactive sites for metal binding (Tuschall & Brezonik, 1984). At higher pH values the effect was less significant due to the higher availability of sites in the ionised materials. This effect could also be combined with the chelation of Cu^{2+} at low levels of metal addition.

At the highest pH values, for both metals binding to humic acid and to peat, the Scatchard plots gave three distinct gradients to which lines were fitted and the tentative formation constants calculated (e.g. Figure 4.19).

Figure 4.19

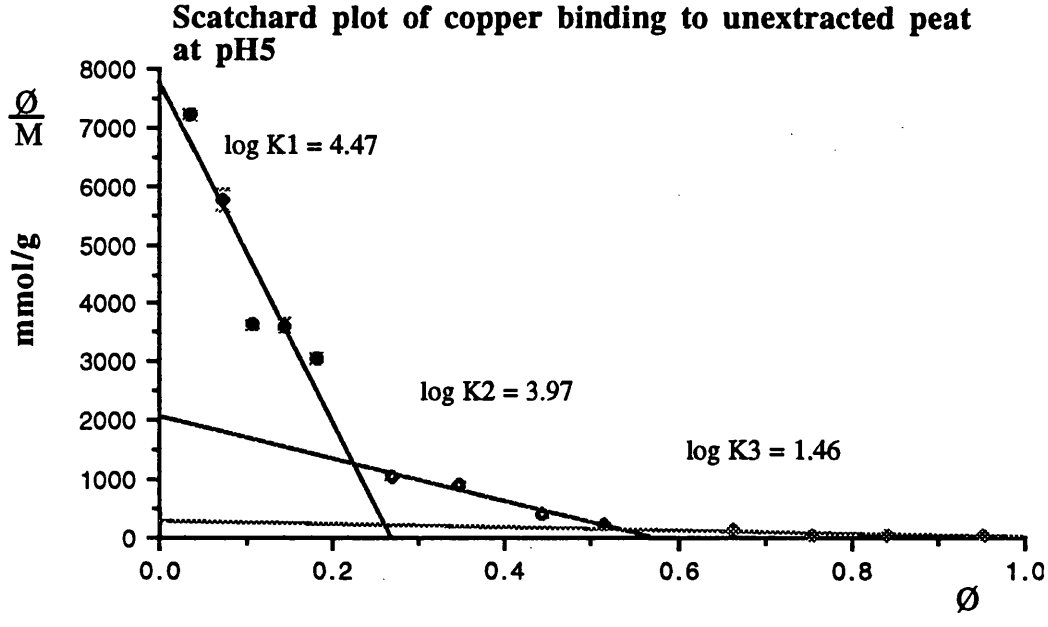

Therefore, at the higher pH values, a third distinct class of binding site was present, which was available due to the increased ionisation of these materials at these pH values. Since the M.B.C. was also higher at these values and in the region of the plot corresponding to this third class, the increased amount of binding could be resulting in conformational changes which lead to the exposure of this class of site.

Aggregation of the humic substances at these high metal loadings could also be occurring and this would lead to changes in the binding energy of sites (Underdown *et al.*, 1985). Precipitation would also lead to enhanced metal binding, as the metal becomes trapped in the flocculating structures and cannot be discounted at these pH values and metal loadings (Saar & Weber, 1980).

The log K values calculated from assigning slopes to the plots are presented in Table 4.4, and the remaining Scatchard plots can be found in Appendix 2.2.

Table 4.4 Log K values calculated from Scatchard plots.

Metal			**Humic Acid**		**Peat**	
log K		**pH 4.8**	**pH 5.12**	**pH 5.8**	**pH 4**	**pH 5**
Cu^{2+}	K_1	1.95	2.63	4.85	4.13	4.47
	K_2	0.34	2.12	3.14	2.65	3.97
	K_3			2.48		1.46
Pb^{2+}	K_1	2.76	3.03	3.07	2.99	3.00
	K_2	2.18	2.61	2.65	1.65	1.38
	K_3					0.55

As also indicated in the Base Titration method, there are differences between the two metals. The formation constants for Cu^{2+} are quite clearly different for each pH value in the humic acid, as expected, since the M.B.C. values increase with each pH value. As more sites become ionised, the chance of chelation occurring increases since more sites are available in favourable conformations. Also, in the humic acid, the structure opens up upon ionisation allowing easier access to sites (Underdown *et al.*, 1985). In the Cu^{2+} treated peat, there is less of a difference in the log K values with pH, since the above conformational changes will not be so enhanced due to the nature of the substance. As Bloom & McBride (1979) pointed out, peat can be viewed as a solid phase ion exchanger, rather than a complex polyelectrolyte.

There is also a difference between the log K values for Cu^{2+} binding calculated for the humic acid and those calculated for the peat. The unextracted peat shows

higher values for each pH value and each constant, indicating that in this material binding is taking place in a more stable arrangement than in the humic acid. Firstly, there is less Cu^{2+} binding to the peat, as demonstrated in the M.B.C. values, and this will promote a more stable arrangement, as the first binding sites to react will have the highest binding energies (Tuschall & Brezonik, 1983). In addition, the Cu^{2+} could also be interacting with other components of the peat, such as the mineral matter and other organic materials such as amines and polysaccharides, which would be removed on isolation of the humic acid. Cu^{2+} has previously been shown to associate strongly with nitrogen containing materials, in particular porphoryn-based structures (Cheshire *et al.*, 1977), and these could be contributing to the stability of the interaction. The ability of Cu^{2+} to form inner sphere complexes with unextracted peat was shown by Bloom & McBride (1979) whereas other metals such as K^{+} and Mn^{2+}, were only able to interact as outer sphere complexes.

The log K values for Pb^{2+} differ from those for Cu^{2+}, in that they show little change with pH, and with isolation of humic acid, indicating that Pb^{2+} is reacting with a similar stability of reaction, in both humic acid and unextracted peat for all pH values. Warwick *et al.* (1991) found no difference in formation constants for the binding of Ni^{2+} with isolated and non-isolated materials.

In the humic acid in particular, the Scatchard plots for Pb^{2+} showed less curvilinearity than for Cu^{2+}, (e.g. Figure 4.20), compared to the unextracted peat, and this is reflected in the similarity in the log K_1 and log K_2 values in the humic acid. The Scatchard plot was originally developed to calculate formation constants in systems with 1:1 stoichiometry, with one or two ligands (Falck, 1988). Since curvilinearity reflects heterogeneity in binding sites and energies, the Pb^{2+} could be binding with predominantly 1:1 arrangements in humic acid, which have little difference in binding energy. Conversely, in the Cu^{2+} binding to humic acid, the binding sites are more distinct. Stevenson *et al.* (1993) studied the stability of Cu^{2+} binding using a variety of methods and concluded that, in humic acid, Cu^{2+} binds in a mixture of 1:1 and 2:1 arrangements.

It must also be remembered that the limit of detection of the Pb^{2+} electrode was poorer than for the Cu^{2+}, and binding at higher energy sites which were detected in Cu^{2+} could not be detected in Pb^{2+} due to this limitation.

Figure 4.20

Scatchard plot of lead binding to humic acid at pH 5.8

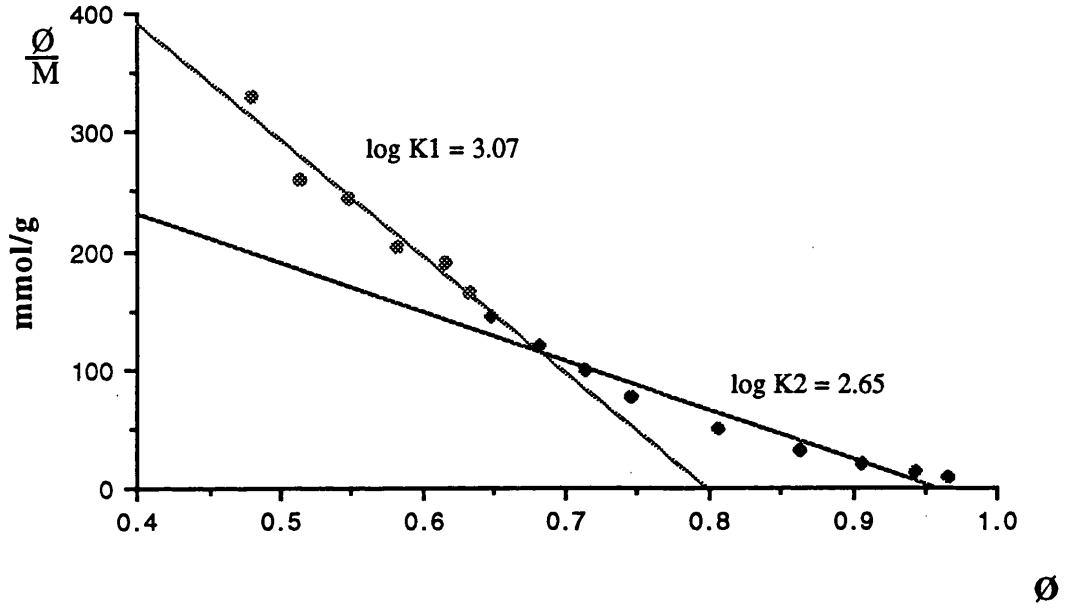

4.3.2.5 CALCULATION OF INCREMENTAL FORMATION CONSTANTS

The incremental constants, calculated from the titration data, reflect the continuous distribution of binding energies which are shown in the curvilinear Scatchard plots (Stevenson *et al.*, 1993). The formation constants were calculated from the titration data, using the following two equations, and the relevant stability of each arrangement could then be analysed:

$$M^{2+} + A^{-} \overset{k3}{\Leftrightarrow} MA^{+} \qquad k3 = \frac{(MA^{+})}{(M^{2+})(A^{-})}$$

$$M^{2+} + 2A^{-} \overset{k4}{\Leftrightarrow} MA_2 \qquad k4 = \frac{(MA_2)}{(M^{2+})(A^{-})^2} \qquad (4.15)$$

The complete set of log k values for all of the titrations can be found in Appendix 2.2, with only examples being displayed here.

The incremental values obtained also reflect the variations between the metals which were expressed in the Scatchard values, as well as the differences between the humic acid and unextracted peat in Cu^{2+} binding. This is expected since the same titration data were used in the calculation of both sets of constants. However, in

calculating the incremental constants, a value for binding is obtained at each step in the titration, thus directly reflecting any changes which occur on metal binding at each step in the titration. In addition, there is less error associated with the value, since in calculating K_1 and K_2 there is considerable ambiguity in where the slope should be assigned.

A plot of the variation in the log k values with extent of reaction is displayed in Figure 4.21. For all of the metals and humic substances, as the titration proceeds, the formation constants decreases (the initial increase in constant observed for Cu^{2+} binding to peat at pH 4 has already been discussed). The continual decrease in constant was also observed by Tuschall & Brezonik (1983) in the study of Cu^{2+} binding to dissolved organic matter. They proposed that complexation with Cu^{2+} decreased the tendency of neighbouring functional groups to complex subsequent metal ions, due to a build up of charge on the material. In addition to this effect, at higher levels of addition fewer sites will be available for binding and these sites will have lower binding energies and less favourable stereochemical arrangements for chelate formation.

Figure 4.21.

Variation in log k values with extent of binding of copper to unextracted peat at pH 4

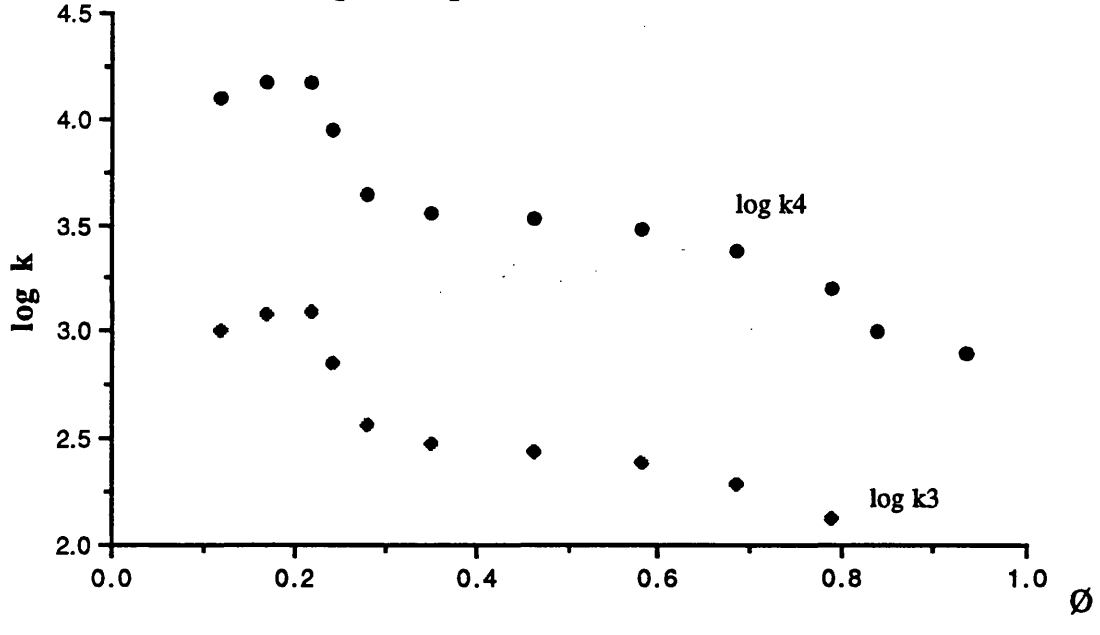

In all of the titrations, modelling the data as k_4 values gave a higher stability of complex, as would be expected for a 2:1 arrangement. The log K_1 values from the Scatchard plots fall within the range of the log k_4 values and often the log K_1 are at the top range of the log k_4 values (Table 4.5). This would indicate that the K_1 values are

expressing binding of metals in a 2:1 arrangement and this has been proposed as one explanation for the curvilinearity of the plots (Sahu & Banerjee, 1990: Falck, 1988). Similarly, the log K_2 values for the Scatchard plots fall within the range of the 1:1 complexes expressed by the incremental log k_3 values, indicating that, at this extent of reaction, 1:1 complexes predominate.

Table 4.5 Formation Constants for Cu^{2+} binding to peat at pH 4.

Ø	log k_3	log k_4	Scatchard values
0.119	3.01	4.10	log K_1 = 4.13
0.168	3.08	4.17	
0.220	3.09	4.18	
0.241	2.86	3.95	log K_2 = 2.65
0.281	2.56	3.65	
0.350	2.47	3.56	
0.464	2.45	3.53	
0.583	2.39	3.48	
0.683	2.29	3.38	
0.787	2.29	3.21	
0.839	2.12	3.00	
0.934	1.91	2.91	

The remainder of the incremental log k values can be found in Appendix 2.2 along with the relevant Scatchard plots.

4.4 CONCLUSIONS

The Base Titration method was not able to model the complexation of metals to humic substances as well as the other methods and the constants obtained should be interpreted with caution. The log B_2 values express the competition of a metal and a proton for a reactive site and, in this sense, the model demonstrated well the differences between metals, provided buffered salts are used. In addition, the graphs of proton release gave valuable information on the behaviours of the different metals. In later papers, Stevenson and co-workers adapted the Bjerrum approach further and instead of modelling the competition of the metal and proton, modelled the interaction at the ionised sites, regardless of the charge differences (Stevenson *et al.*, 1993). This method does give more realistic measurements of metal-humate stability but again the method relies on a secondary effect to provide a quantitative estimate of the amount of metal bound.

The ion selective electrodes, by measuring the amount of free metal directly, provide a more scientifically sound way of measuring the amount of bound metal with their limitations being their relatively high limits of detection and selectivity, making them applicable to only one metal. Analysis of the data by the Scatchard approach can lead to errors in the calculation of the K values, due to the curvilinearity of the plots, but calculation of the incremental K values overcomes this problem well. Where the Scatchard plots are so curvilinear, this method should be used in preference to the Scatchard approach in calculating formation constants.

From the results of the two methods, it is evident that Cu^{2+} and Pb^{2+} are binding by quite different mechanisms with both the peat and the humic acid and this has consequences for the stability of these interactions. In the Base Titration method, binding of Cu^{2+} resulted in a significantly greater release of protons from the humic acid than with Pb^{2+} binding. Although this could be due to release of protons from the hydration of oxides on 1:1 binding, this effect was also seen at pH 4, where hydration of the oxides would not normally be expected to occur. Therefore, it is more likely, that on Cu^{2+} binding, conformational changes are occurring, which result in the release of excess protons, greater than the amount expected from the titration curve.

In the Scatchard plots, the addition of small increments of Cu^{2+} was observed to increase the formation constant at the start of the titrations of humic acid and peat. This would also indicate conformational changes, exposing new reactive sites of considerable binding energy. This effect was not seen at pH 5.8, where the increased ionisation of the materials had probably already resulted in the exposure of these sites, and due to the more open structure of the materials, secondary conformational changes

would be less likely to occur. The Scatchard plots and the Incremental Formation Constants also implied that Cu^{2+} was more able to interact via 2:1 complexes than Pb^{2+}, where 1:1 complexes predominate, and significantly more metal was being bound.

However, it should be remembered that different peats were used to extract the humic acids used in the Base Titration method and the Scatchard method. It was unfortunate that South Drumboy peat could not have been used throughout all the research, as this would have made the comparison between methods, reactivities and the laboratory and field studies easier to evaluate.

The isolation of humic acid from peat had an effect on how the metals interacted and the constants which were produced. Significantly less metal was bound to the unextracted peat than to the humic acid, as reflected in the M.B.C. values for both the metals indicating again that isolation either exposed the reactive sites, or chemically altered the material to give formation of reactive groupings. The formation constants for the metals reacting with the unextracted peat also showed differences between the behaviour and stability of the interactions. Cu^{2+} reacts to form more stable complexes with unextracted peat than humic acid, indicating that in the unextracted material, Cu^{2+} can interact with other components of the soil, not just the humic substances to give stable interactions. However, Pb^{2+} showed little difference in stability between the two materials, regardless of the lower amounts being bound in the peat, as reflected in the M.B.C. values and in the infra-red studies. Therefore, again it can be concluded that the use of humic acid to model the interactions of metals in environmental systems is of dubious value, and further work should centre on the interactions of metals with unextracted peat, rather than an operationally defined fraction. In addition, the competition of cations for binding sites in unextracted materials would be more realistic than these one metal studies.

CHAPTER 5

THE STUDY OF THE HEAVY METAL AND RADIOCAESIUM CONTENTS OF ORGANIC SOILS FROM AN UPLAND HILL FARM IN SOUTH WEST SCOTLAND

5.1 INTRODUCTION

The laboratory-based experiments illustrated that the isolation of humic acid from peat led to changes in the characteristics of the humic substances, in particular the reactive functional group contents. Accordingly, the nature of the interaction of the metals and the stability of this interaction was altered. In the environment metals interact with the unaltered, unextracted material and being a multicomponent system many metals are present at one time, unlike the one-component systems studied in the metal complexation experiments. In parallel to the laboratory based experiments, field-based experiments were therefore carried out in which the interaction of Pb, Cu and Cs with humic substances within peats could be studied further.

Ombrotrophic or rainwater-fed peats have been used to provide a record of past atmospheric deposition of heavy metals and radionuclides (Oldfield *et al.* 1979:: Glooschenko *et al.*, 1986: Markert & Thornton, 1990: Mitchell *et al.*, 1992). The use of such systems in providing a historical record of deposition requires that all inputs of these metals are from the atmosphere, either through wet or dry deposition and that they are immobilised on contact with the peat and not subject to post depositional movement. As discussed in section 1.8.3, post-depositional movement of metals has been shown to occur in some peat deposits and therefore in the field-based study one of the aims was to investigate whether any such movement occurred in the peats studied and if so, what conditions promote remobilisation. To aid this, in addition to Pb, Cu and Cs a suite of elements were studied, which encompassed the rare earth elements and transition metals. These were studied to give information on the redox environment and generally how the geochemistry changed throughout the profiles.

Providing no remobilisation is occurring, a chronology of past atmospheric deposition of metals can be established. Many dating mechanisms exist (section 1.8.4) and which one is utilised depends ultimately on the time scale being studied. One such method utilises the radionuclide ^{210}Pb and results in a chronology spanning approximately the last 150 years. The method requires that once ^{210}Pb becomes incorporated into the peat it is immobilised, not being subject to any post-depositional movement which could distort the dates. Since Pb has been shown to be mobile within peat deposits (Damman, 1978: Aaby & Jacobsen, 1979: Urban *et al.*, 1990), under certain conditions (section 1.8.3), the validity of using this technique in dating peat cores has been questioned (Urban *et al.*, 1990). Therefore, the method was studied here, in order to investigate whether or not it can reliably be used to establish chronologies for peat cores, and where possible to utilise the dates in establishing the chronology.

5.2 DESCRIPTION OF SAMPLING SITES CHOSEN FOR THE STUDY

South Drumboy Farm (grid ref. NS 502 482) is situated to the South West of Glasgow (Figure 5.1) and is affected by the deposition of Chernobyl radiocaesium, with movement of lambs from the farm still being restricted when the first cores were collected. A series of cores was collected (Figure 5.2) from positions selected to investigate the effects of topography and the proximity of the A77 road on metal content. South Drumboy farm is 200-300 m above sea level and receives an annual precipitation of around 1400 mm. Drumboy Hill and the areas surrounding it are covered by extensive hill peat, formed due to the high levels of precipitation and the impermeability of the underlying basaltic till. In addition to the peat, a diverse range of soil types is found within the farm, and this led to variations in the characteristics of the 6 cores collected. One section of the farm had been drained, giving an area of improved grassland. These areas were not sampled directly, since the profiles would be obviously disturbed. Instead, as outlined below sampling took place around these areas to establsh whether there was any indirect effect of drainage on the profiles.

The peats were similar to those used to determine the incremental formation constants in Chapter 4.

CORE 1, NS 502482

This core, of length 70 cm, was collected in October 1992, from a position close to Kingswell Burn. The sampling site was south-easterly facing, at an altitude of 237m, making this the lowest sampling site on the farm and was directly below the improved grassland. The main vegetation comprised various types of grass with *Sphagnum* beginning to colonise the surface. On sampling, the core was extremely wet and black in colour with, at depth, large amounts of undecomposed birch remains.

CORE 2, NS 502485

This core (length 55 cm) was collected in October 1992 and was taken from a site 400m further up Drumboy Hill (altitude 247 m) from the position of Core 1, beyond the improved grassland. The vegetation was composed of grasses and sedges, and the core was characterised by a darkly coloured surface horizon of 20cm, overlying grey material which turned light brown on exposure to the air. This indicated reducing conditions within the core. The gleyed horizon became progressively more mineral with depth from 20 cm downwards.

CORE 3, NS 504493

This core (length 70 cm), was collected in June 1993, close to the summit of Drumboy Hill and was the highest sampling point, at an altitude of 267 m. The vegetation was predominantly composed of grasses and the peat was oxygenated, with a uniform degree of humification throughout the core.

CORE 4, NS 504493

This core (length 65 cm) was collected in June 1993 from the boundary of the farm, at an altitude of 257 m, close to a land-use change from farming to forestry. The sampling site was westerly facing, and was downslope from the ridge of Drumboy Hill. The site was extremely wet and *Sphagnum* mosses were the predominant vegetation. The core was characterised by a significant amount of mineral material in the middle section.

CORE 5, NS 504489

This core (length 50 cm) was collected in June 1993 from the ridge of Drumboy Hill, directly down from Core 1 on the south-westerly facing slope at an altitude of 247 m. The peat was black in colour, indicating a high degree of humification, and again *Sphagnum* mosses were beginning to colonise the surface vegetation.

CORE 6, NS 501488

Core 6 was sampled in June 1993 and was the lowest sampling point on the ridge of Drumboy Hill, directly below cores 3 and 5 on the south-westerly facing slope (altitude 240 m). Again, the peat was black in colour, indicating a high degree of humification, with *Sphagnum* mosses being the predominant vegetation. The peat could only be sampled to a depth of 40 cm since the bedrock was present at this depth.

Figure 5.1 Map of Scotland showing the location of the study site.

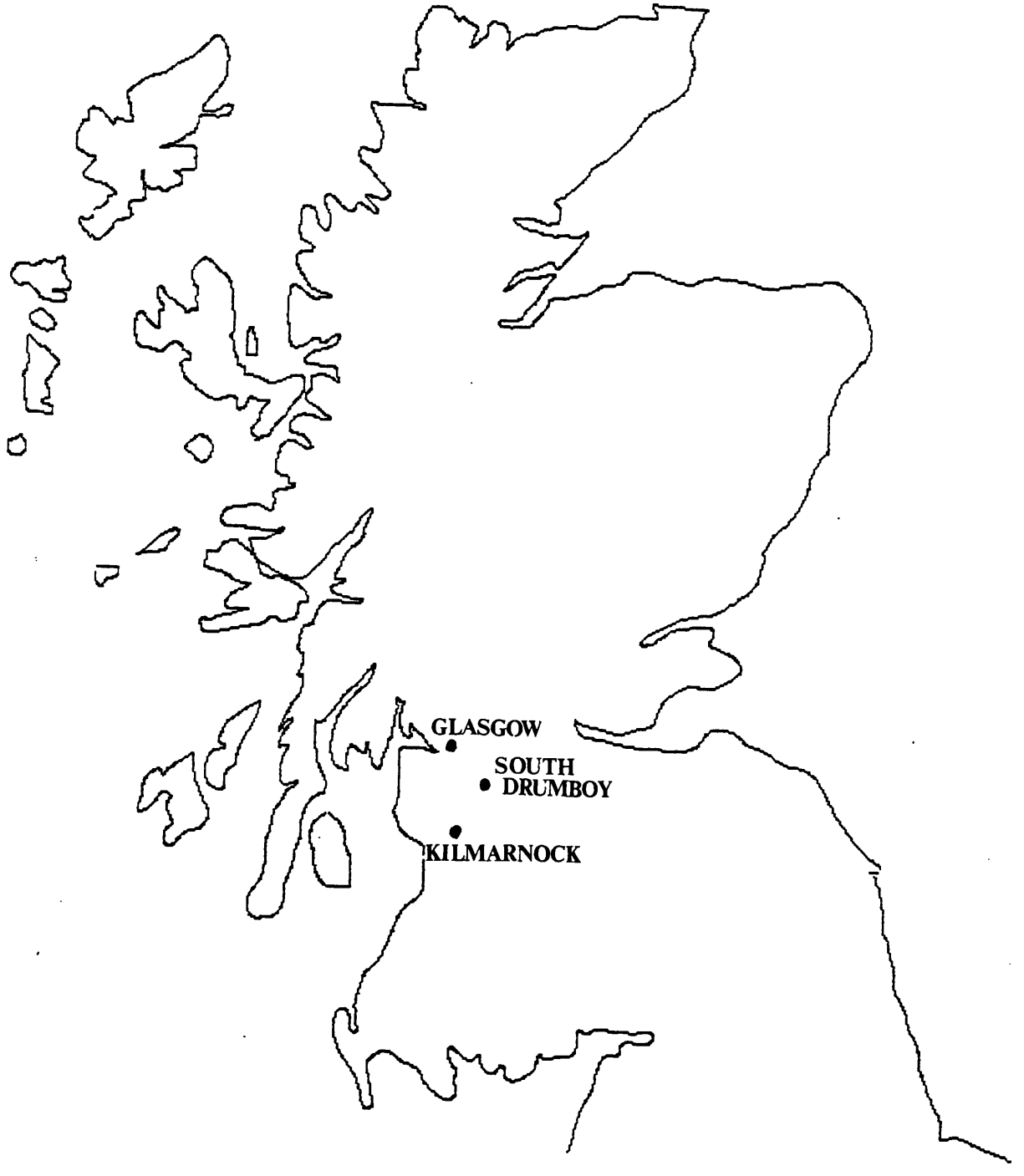

Figure 5.2 The relationships between the sampling sites on Drumboy Hill.

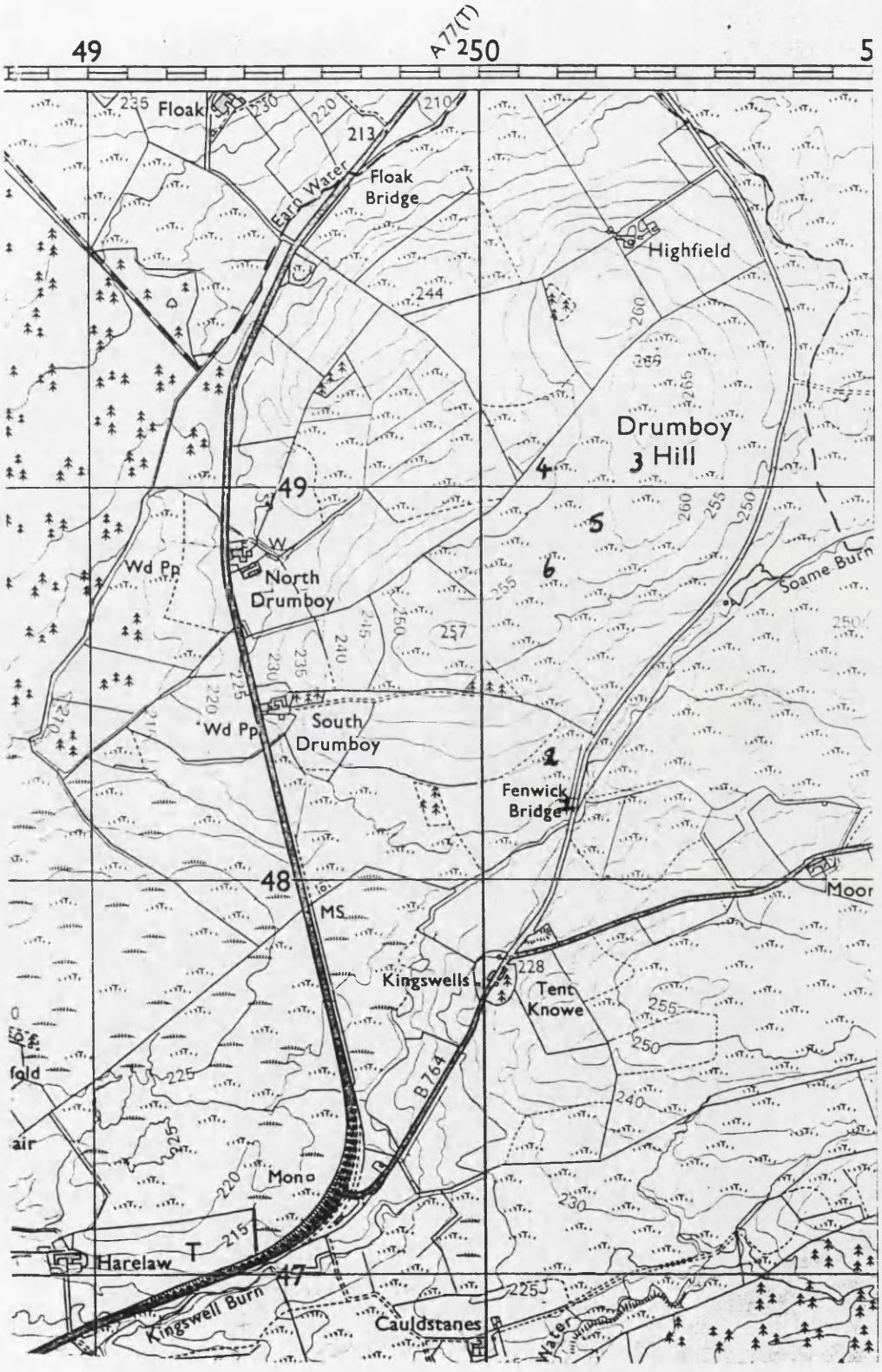

5.3 METHODS

5.3.1 SAMPLING PROCEDURES

The cores were collected by digging a pit and extracting consecutive blocks of approximately 20 cm x 20 cm x 20 cm with a clean spade. Cores were either sampled to a depth of approximately 60 cm, or until the bedrock was reached. The blocks were wrapped carefully in polyethylene for transportation, taking care to minimise disturbance and compaction, and were stored at 4 ^{0}C until processing.

The blocks were sectioned into 3 cm slices, taking care to remove the outer layer which could contain organic matter from further down or up the core. Before the sections were air dried, samples were removed for determination of bulk density, water content and organic matter content. The air-dried peat was then ground.

5.3.2 DETERMINATION OF THE PROPERTIES OF THE PEATS

The methods utilised to characterise the peat samples are all standard procedures, as outlined by MAFF (1986). Each section of each core had the % loss on ignition, moisture content, bulk density and pH determined.

5.3.3 γ - SPECTROMETRY

γ - spectrometry was used to measure the activities of ^{134}Cs, ^{137}Cs, ^{226}Ra and ^{210}Pb in the samples.

5.3.3.1 INTERACTION OF γ RADIATION WITH MATTER

γ radiation consists of high energy photons of electromagnetic radiation, which are emitted as nuclei undergo transitions from higher energy states to lower excited states or the ground state. The γ photons have a low probability of interaction with atoms encountered and the initial energy of the photon is retained until interaction with an absorber (or detector) occurs, by one of the following processes:

(a) THE PHOTOELECTRIC EFFECT. This process transfers all of the photon energy to a bound electron in an atom of the absorber and results in ejection of the electron as an energetic photoelectron and complete disappearance of the γ ray. The photoelectric effect is more efficient at lower photon energies, and the efficiency of the process is

proportional to approximately $E^{-7/2}$ when E (energy) is less then 1 MeV. At higher energies, the efficiency of the effect is proportional to 1/E. The probability of the photoelectric effect increases with the Z value (atomic number) of the material, and is approximately in proportion to Z^5.

(b) COMPTON SCATTERING. In this process the photon transfers only part of its energy to an electron, which may be bound or free. As well as being degraded in energy, the photon is also deflected from its original path. Compton Scattering gives rise to electrons with a continuous distribution of energies absorbed in the detector with the probability of scattering depending on the number of electrons available, and is therefore proportional to the Z value of the absorber. For energies below 0.5 MeV, the probability of Compton scattering is approximately proportional to E^{-1}. Thus the efficiency of the effect falls off more slowly than the photoelectric effect with increasing energy up to approximately 2 MeV.

(c) PAIR PRODUCTION. This effect is less common than the preceding two processes, and occurs when γ rays are transformed, upon interaction with matter, into an electron-positron pair. The probability of pair production is proportional to Z^2 of the absorber, and increases with photon energy above 1.022 MeV.

In summary, all three processes produce moving electrons (or positrons) in matter, which can either be detected directly, or can initiate other electron processes to obtain an electric charge pulse which is utilised in the detection of these processes in γ spectrometry.

5.3.3.2 DETECTION OF γ RADIATION

High purity semi-conductor germanium (Ge) crystals are widely used as detectors for γ spectrometry. Semiconductor detectors have a P-I-N diode structure in which the intrinsic (I) region is extended by application of reverse bias across the diode. When photons interact with the Ge in the depletion region, charge carriers (holes and electrons) are produced and are swept to their respective collecting electrode by the electric field. The resulting charge pulse is collected by application of a high voltage to the crystal and this is integrated by a charge sensitive preamplifier and converted to a voltage pulse with an amplitude proportional to the photon energy. The signal is converted to a digital pulse by an analogue to digital convertor (ADC)

and is then stored in a multi-channel analyser or buffer where it may be accessed by computer on demand (Figure 5.3).

Figure 5.3. Outline of a typical γ detection system.

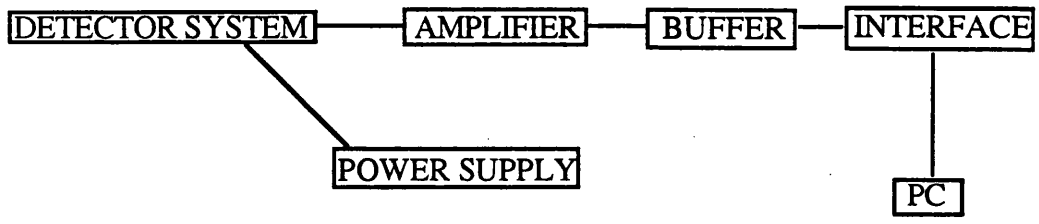

5.3.3.3 SPECIFICATIONS OF THE γ DETECTION SYSTEMS UTILISED

γ spectra were recorded using two different detectors, detectors A and B. Detector A was a Canberra co-axial, n-type intrinsic HPGe detector with a carbon epoxy window. It has 25% relative efficiency, a resolution (full width half maximum) of 2 keV at 1333 keV and an energy range of 10-2000 keV. Detector B was a Canberra reverse electrode co-axial, n-type intrinsic Ge detector with a thin Be window. The detector has a 25% relative efficiency and a resolution (full width half maximum) of 2 keV at 1333 keV, with an energy range of 5-2000 keV.

Both detectors were surrounded by 10 cm of Pb to shield them from background radiation, with a Cd-Cu lining to shield the detector from fluorescent x-rays produced from γ interactions with the Pb shielding. Background count rates were continually assessed over a period of one to two weeks throughout the research (Table 5.3). The analysis system comprised a Canberra ADC Multiplexer unit (model 8535), interfaced with an IBM-compatible PC. Spectra were analysed using the Canberra Spectran-AT v4.0 software package.

5.3.3.4 ENERGY CALIBRATION OF THE γ DETECTION SYSTEM

The detection system was energy calibrated using a ^{152}Eu calibration source which generates a series of peaks at certain channel numbers, to which energies can be assigned. A calibration file was created within the software package using the linear regression analysis of the channel number versus energy of peak.

5.3.3.5 EFFICIENCY CALIBRATION OF THE γ DETECTION SYSTEM

THEORETICAL COSIDERATIONS

The efficiency of the detector is a measure of how many pulses occur for a given number of γ rays. The absolute count rate, A, of the source is related to the observed count rate C, through the following equation,

$$A = \frac{C}{D} \quad \text{where D is the detection efficiency.} \qquad (5.1)$$

The detection efficiency is equal to the product of a number of factors:

$$D = f_g * f_{bs} * f_{sa} * f_e \qquad (5.2)$$

f_g is the geometry factor, f_{bs} is the backscatter factor, f_{sa} is the self-absorption factor and f_e is the intrinsic efficiency factor.

Of most importance to the detection efficiency of γ detection systems is the geometry factor, f_g. Each arrangement of source and detector has its own geometry factor and any change in the position, volume or distribution of the activity will change the geometry factor, and consequently affect the efficiency as the detection efficiency is proportional to $1/d^2$, where d is the distance from the detector. In order to minimise variations in the geometry factor it is desirable to determine the detection efficiency experimentally using standard sources of identical size and volume as the samples.

The self-absorption factor can be significant in γ determinations, particularly when analysing low activity samples, where thick samples are often required to give a measurable counting rate. The self absorption of γ radiation follows the law:

$$T = I e^{-\mu p x} \qquad (5.3)$$

where T is the attenuated-beam intensity, I is the unattenuated-beam intensity, u is the total-attenuation coefficient, p is the density of the material and x is the path length. u is a function of the photon energy E and of the atomic number Z. It increases for a given Z with decreasing E and the energy dependence of u is generally greater the higher the Z value. Therefore, self absorption is more significant the lower the photon energy and heavier the element and is particularly relevant to the detection of ^{210}Pb (E_γ = 46.5 keV).

Coppola & Reiniger (1973) observed that the chemical composition of soils caused variations in the mass attenuation coefficients which were particularly significant when detecting γ ray energies below 300 keV. Cutshall *et al.* (1983)

calculated a correction factor for self absorption of ^{210}Pb in sediment samples, where composition or mineralogy also affects the attenuation coefficient, by combining the above equation for the self absorption of γ radiation with the self absorption equation

$$O = A\frac{1-e^{(-\mu px)}}{T/I-1} \qquad (5.4)$$

(where O is the attenuated sample output and A is the sample photon emission rate). The correction factor was then calculated as:

$$\frac{A}{O} = \frac{\ln(T/I)}{T/I-1} \qquad (5.5)$$

This correction factor was calculated for each sample measured, and a wide range of transmissions (T/I) was recorded for the different samples.

STANDARD AND SAMPLE PREPARATION

In the preparation of samples and standards for the determination of detection efficiencies, due care was taken to minimise the effects of geometry and self absorption variation.

To give a standard geometry and minimise sample height, an aliqout of known weight was taken from each section and pelletised in a metal die (diameter 4.8cm) under a pressure of 8 tonnes. Care was taken in cleaning the equipment between samples to minimise contamination. The height of each pellet was then recorded with a micrometer.

To calculate detection efficiency, as outlined below, it is necessary to minimise any changes in sample height and Z value which would give an invalid estimate of efficiency. In order to mimic the Z value of the sample pellets, standard pellets were made from excess peat from the bottom of Core 1. The count rate for the radionuclides being investigated within the peat was recorded before spiking to ensure that it was minimal with only background levels of ^{210}Pb and ^{226}Ra being recorded (Table 5.3). Relevant amounts (Table 5.1) of standard radionuclide solutions of ^{210}Pb and ^{134}Cs and ^{137}Cs were added to 100g of the bulk peat. Before addition, the peat was wetted with 5 ml of 50:50 (v/v) methanol: water solution. The standards were added dropwise in 10 ml of this solution, whilst stirring the suspension to give even mixing. The spiked peat was then throughly stirred, before drying at 50^0 C. Once dry the spiked peat was further mixed by shaking on an orbital shaker for 6 hours. From this 100g sample, sub-samples of 20g, 15g, 10g, and 5g were removed and pelleted, before gamma spectroscopy to determine the detection efficiency. Three 10g pellets were

prepared and counted to determine the degree of homogenisation and reproducibility in standard preparation. Pellets for determination of the detection efficiency of ^{226}Ra were prepared using DH1A ore, which has a specified ^{226}Ra content, by taking the required amount of peat, and mixing it with the required amount of ore followed by shaking on an end-over-end shaker for 12 hours before pelleting and counting. The activity of ^{226}Ra was determined from the ^{214}Pb peak at 352 keV to avoid the intereference from ^{235}U in the ^{226}Ra peak. It was assumed that ^{214}Pb was in secular equilibrium with ^{210}Pb, and that loss of ^{222}Ra was insignificant.

Table 5.1 Specifications of standard solutions (Amersham International) and DH1A ore used to prepare the standard pellets, and the amount of activity used in standard preparation.

Radionuclide	**Date of initial preparation**	**Certified Activity (A_o)**	**Activity added**
^{210}Pb (46.5 keV)	23.10.89	63.1 Bq ml^{-1}	63.1 Bq per 100g peat
^{226}Ra (352 keV)	1991	31.5 Bq g^{-1}	3.15 Bq per 5g peat
^{134}Cs (604.7 keV)	16.03.89	18.65 x 10^2 Bq ml^{-1}	1.86 kBq per 100g peat
^{137}Cs (661.6 keV)	14.10.89	3.54 x 10^2 Bq ml^{-1}	5.23 kBq per 100g peat

Variations in the heights of the sample pellets were observed, and since the detection efficiency is proportional to $1/d^2$ this could affect the geometry factor and accordingly the efficiency. The variations in pellet heights were correlated with changes in the organic matter content and consequently Z value (R^2 = 0.96) and demonstrated that as the organic matter content was lowered, the height of the pellets were also lowered. Thus, three efficiency calibrations were established which encompassed the range in organic matter content and consequently pellet height (see Figure 5.4 & Table 5.2). Three different samples of bulk peat were utilised, which encompassed the changes in organic matter content, to calculate the detection efficiency.

Absolute efficiency was calculated using equation 5.1. The standard count rates were corrected for bulk peat count rates, or if no radionuclide was detected in the bulk peat the detectors background count rates.

Correction for the decay of the spike since preparation was made by:

$$A_t = A_o e^{-\lambda t} \qquad (5.6)$$

where A_t was the activity at the time of analysis, A_0 was the activity at the time of the preparation of the spike, λ is $\frac{\ln 2}{t_{1/2}}$ ($t_{1/2}$ = half life of radionuclide) and t was the time elapsed since standardisation of the spike solution. The detection efficiencies for the three calibrations are displayed in Figures 5.5 - 5.7, with the data being displayed in Tables 5.4 - 5.6.

Table 5.2 Specifications of bulk peats used to prepare pellets for efficiency calibrations.

Efficiency Calibration	Sample	% loss on ignition	Calibration Range
1	R19	92.74	90 - 98% loss on ignition
2	3.19	53.23	40 - 90% loss on ignition
3	2.13	15.74	14 - 40% loss on ignition

Figure 5.4

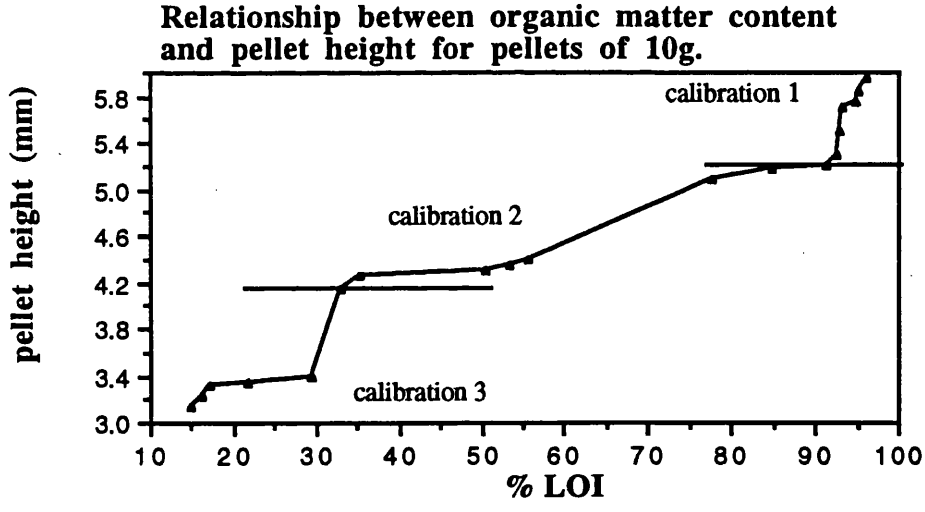

Table 5.3 Background levels of radionuclides present in bulk peat samples used to make standard pellets of 20g, counted over 4 days.

Effic Calib	Detector	% LOI	cps ^{210}Pb	1σ (%)	cps ^{137}Cs	1σ (%)	cps ^{226}Ra	1σ (%)
1	B	98-90	9.12×10^{-4}	20.4	1.86×10^{-2}	9	1.74×10^{-2}	13.7
2	B	90-40	1.09×10^{-3}	39.3	4.30×10^{-3}	6.3	4.60×10^{-3}	7.3
3	A	40-15	1.53×10^{-3}	29.7	1.24×10^{-3}	17.6	5.07×10^{-3}	7.2

Table 5.4 % Detection Efficiency for Calibration 1 Detector B.

weight (g)	^{210}Pb 46.5 keV	1 σ (%)	^{226}Ra 352 keV	1 σ (%)	^{134}Cs 604.7 keV	1 σ (%)	^{137}Cs 661.6 keV	1 σ (%)
5	0.98	3.15	1.85	1.97	2.35	2.82	3.15	0.3
10	0.95	2.89	1.67	1.53	2.17	2.54	2.89	0.2
15	0.80	2.55	1.48	1.13	2.02	2.31	2.55	0.2
20	0.74	2.12	1.38	0.89	1.89	1.89	2.12	0.2

Table 5.5 % Detection Efficiency for Calibration 2 Detector B.

weight (g)	^{210}Pb 46.5 keV	1 σ (%)	^{226}Ra 352 keV	1 σ (%)	^{134}Cs 604.7 keV	1 σ (%)	^{137}Cs 661.6 keV	1 σ (%)
5	1.11	3.92	2.12	3.12	3.23	4.27	2.97	0.3
10	1.04	3.74	1.89	2.89	2.82	3.19	2.62	0.3
15	0.93	3.44	1.71	2.75	2.68	2.61	2.50	0.3
20	0.89	2.86	1.65	2.15	2.48	2.32	2.44	0.2

Table 5.6 % Detection efficiency for Calibration 3, Detector A.

weight (g)	^{210}Pb 46.5 keV	1 σ (%)	^{226}Ra 352 keV	1 σ (%)	^{134}Cs 604.7 keV	1 σ (%)	^{137}Cs 661.6 keV	1 σ (%)
5	0.83	2.92	1.75	2.72	3.01	3.2	2.87	0.3
10	0.76	2.83	1.68	2.53	2.85	2.9	2.62	0.3
15	0.67	1.61	1.54	2.44	2.70	2.6	2.50	0.2
20	0.63	1.77	1.51	1.88	2.56	1.1	2.44	0.2

Figure 5.5 Detector Efficiencies for Calibration 1, Detector B, % LOI values of 98-90%.

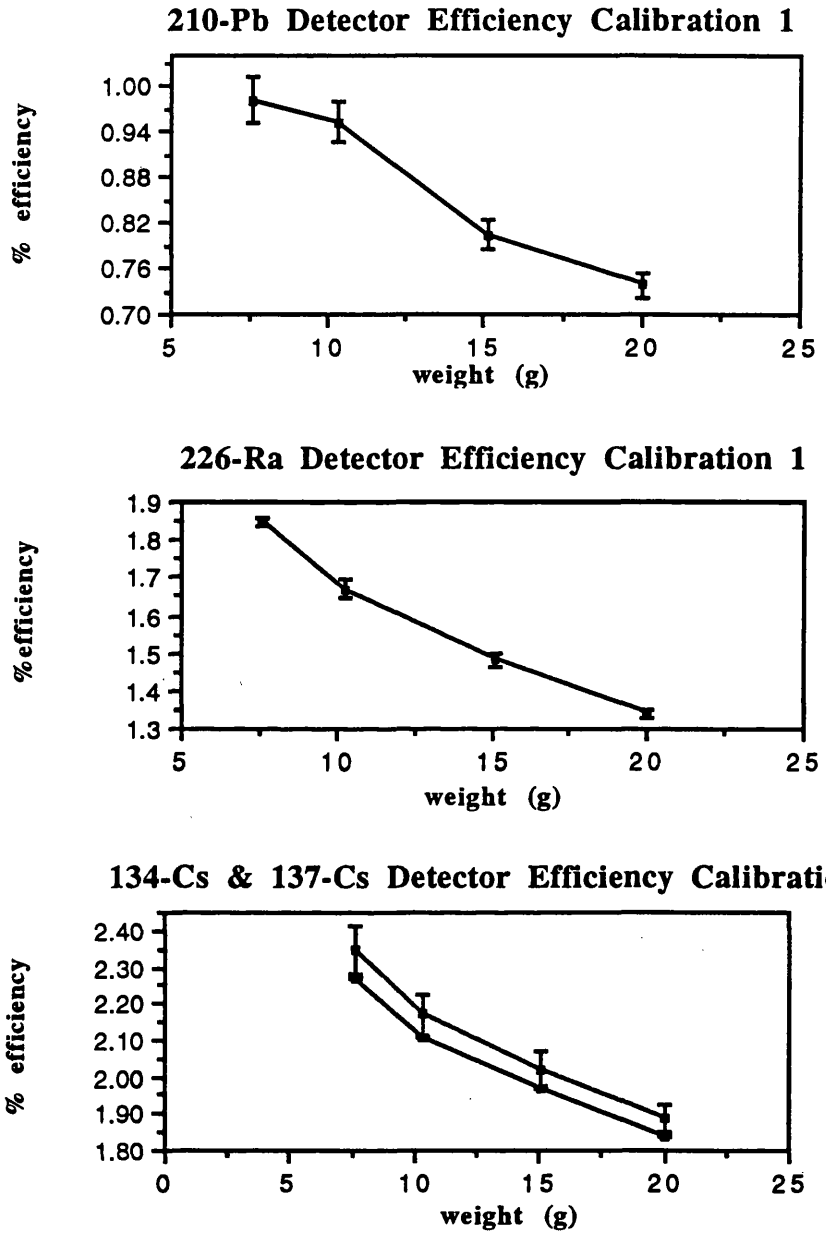

Figure 5.6 Detector Efficiencies for Calibration 2, Detector B, % LOI values of 90-40%.

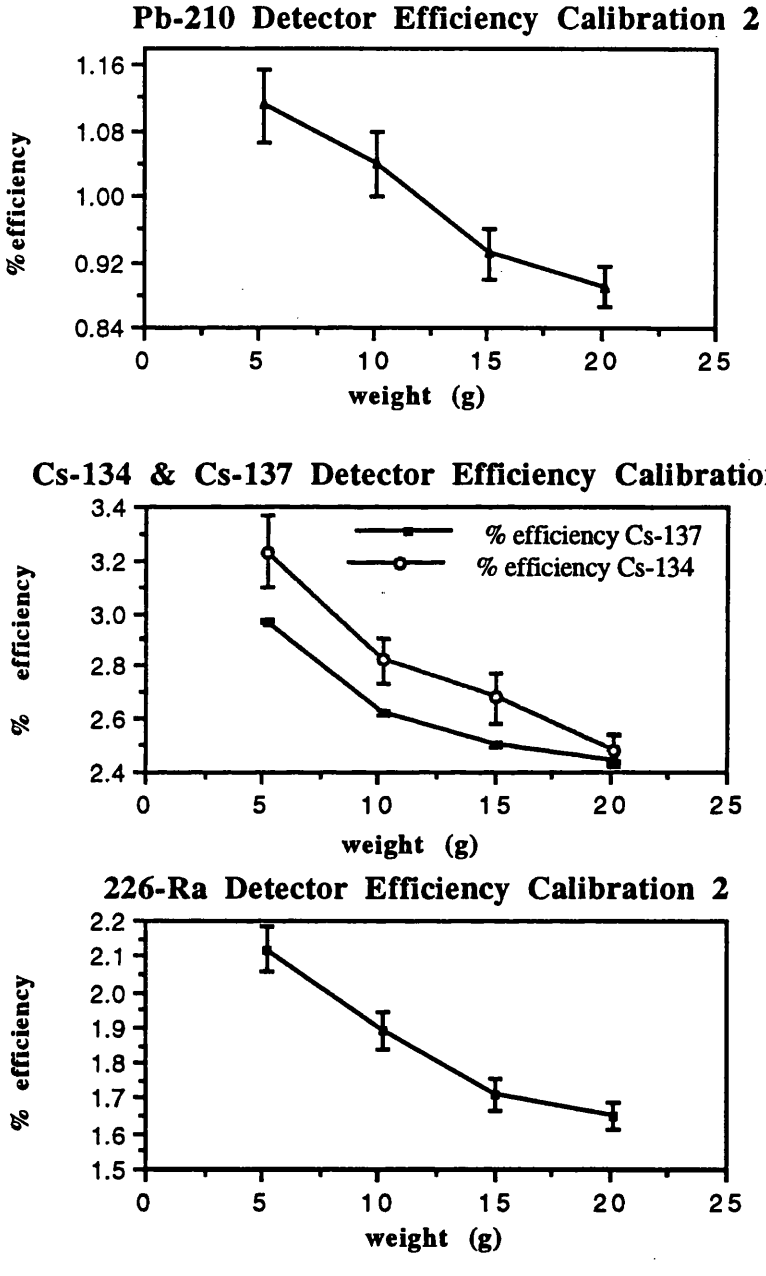

Figure 5.7 Detector Efficiencies for Calibration 3, Detector A, % LOI values of 40-15%.

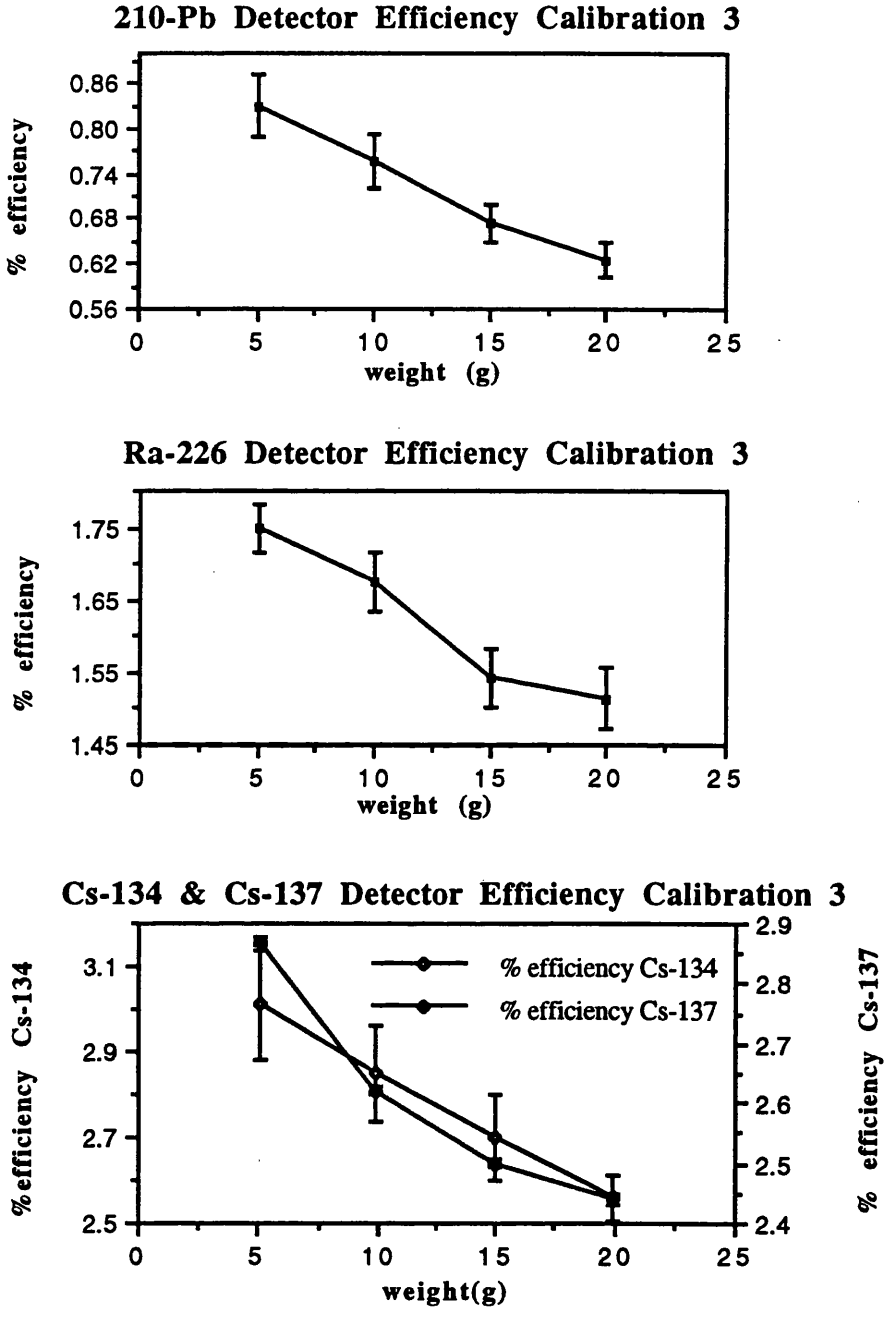

The mean detection efficiencies and their standard deviations for the three replicate 10g standards are presented in Table 5.7 and in all cases the reproducibility is acceptable.

No determination of accuracy could be carried out due to the lack of certifiable reference materials for peats.

Table 5.7 Reproducibility of standard pellets.

	% Detection Efficiency			
	^{210}Pb	^{226}Ra	^{134}Cs	^{137}Cs
	46.5 keV	352 keV	604.7 keV	661.6 keV
Calibration 1	0.947±0.0189	1.664±0.051	2.176±0.091	2.114±0.0145
Calibration 2	1.055±0.0222	1.893±0.066	2.819±0.089	2.619±0.0162
Calibration 3	0.758±0.0228	1.672±0.042	2.482±0.071	2.562±0.0202

Correcting for self-absorption effects is relevant mainly to low-energy photons so only ^{210}Pb was corrected for self absorption using a method based on that developed by Cutshall *et al.*. (1983). A standard ^{210}Pb source was held at a set height above the detector and the unattenuated and attenuated count rate, I and O respectively, were determined over two hours. The correction factors were then calculated for each pellet using equation 5.5 and are summarised in Tables 5.8 - 5.12.

Table 5.8 The correction factors, sample heights and bulk densities for pellets of 5g.

sample	effic calib	weight (g)	pellet height (mm)	bulk density (g cm^{-3})	% transmission	correction factor
1.1	1	5.01	4.00	0.095	92.6	1.04
4.1	1	5.21	4.30	0.099	88.6	1.06
4.2	1	5.14	3.20	0.087	95.6	1.03
mg1	1	5.25	2.93	0.027	93.0	1.04
mg2	1	5.11	2.91	0.061	96.8	1.03
calib 1	***	5.19	2.51	0.299	97.3	1.03
calib 2	***	4.95	3.56	0.141	92.7	1.03

Table 5.9 The correction factors, sample heights and bulk densities for pellets of 10g.

sample	effic. calibrtn	weight (g)	pellet height (mm)	bulk density	% transmission	correction factor
1.2	1	9.94	5.95	0.186	92.6	1.04
1.3	1	10.06	5.70	0.236	86.1	1.08
1.4	1	10.07	5.90	0.175	83.5	1.09
1.5	1	9.99	5.70	0.176	86.8	1.08
1.6	1	10.10	5.31	0.225	84.9	1.08
1.7	1	10.07	5.25	0.261	80.4	1.11
1.8	1	9.93	5.42	0.202	94.9	1.02
1.9	1	10.06	5.25	0.206	86.6	1.07
4.3	1	10.06	6.65	0.129	89.0	1.06
4.4	1	10.10	5.85	0.112	91.2	1.05
4.6	1	10.18	6.31	0.139	89.2	1.06
4.11	2	10.01	4.25	0.371	87.4	1.07
4.12	2	10.06	4.45	0.320	79.2	1.12
mg3	1	10.23	5.65	0.083	88.4	1.06
mg4	1	10.12	5.70	0.087	85.3	1.08
mg5	1	10.21	5.45	0.091	88.6	1.06
mg6	1	10.15	5.71	0.074	90.3	1.06
mg7	1	10.06	5.01	0.096	92.3	1.04
mg8	1	9.99	5.32	0.097	91.8	1.04
mg9	1	10.07	5.29	0.166	89.1	1.06
mg10	1	10.10	5.22	0.166	94.3	1.03
mg11	1	10.03	5.25	0.091	87.8	1.07
3.1	1	10.06	7.01	0.134	89.1	1.06
3.2	1	10.10	5.20	0.133	85.7	1.08
3.5	1	10.04	5.30	0.159	90.8	1.05
3.6	1	10.08	5.05	0.179	91.7	1.04
3.7	1	10.07	5.15	0.204	89.1	1.06
3.8	1	10.15	5.25	0.254	91.9	1.04
3.9	1	10.11	5.25	0.187	90.3	1.05
3.10	1	10.01	5.05	0.174	91.7	1.04
calib 1	*****	10.03	5.85	0.141	84.8	1.08
calib 2	*****	10.15	4.76	0.299	89.9	1.06

Table 5.10 The correction factors, sample heights and bulk densities for pellets of 15g.

sample	effic. calibrtn	weight (g)	pellet height (mm)	bulk density (g cm^{-3})	% transmission	correction factor
SD1	1	14.97	8.65	0.194	86.9	1.07
SD2	1	15.58	8.35	0.295	81.9	1.10
SD3	1	15.16	9.15	0.195	71.3	1.18
SD4	1	15.06	9.45	0.183	76.1	1.15
K2	1	15.27	8.89	0.162	86.4	1.08
K3	1	15.30	8.91	0.161	87.8	1.08
K4	1	15.14	8.72	0.212	85.2	1.09
K5	1	15.06	8.54	0.179	81.2	1.12
K6	1	15.27	8.25	0.391	84.4	1.12
K7	1	15.30	8.15	0.252	82.5	1.11
3.4	1	15.08	9.46	0.181	75.8	1.17
3.5	1	15.03	9.62	0.256	72.9	1.17
4.11	2	14.95	5.85	0.371	74.2	1.16
MB1	2	15.02	7.65	0.224	72.5	1.17
MB2	2	15.12	7.09	0.527	78.2	1.13
MB3	2	15.32	6.52	0.433	74.8	1.15
MB4	2	15.02	6.25	0.371	71.3	1.18
MB5	2	15.04	6.15	0.548	71.7	1.18
calib 1	*****	15.13	9.50	0.141	70.9	1.18
calib 2	*****	15.09	6.99	0.299	75.1	1.15

Table 5.11 The correction factors, sample heights and bulk densities for pellets of 20g.

sample	effic. calibrtn	weight (g)	pellet height (mm)	bulk density (g cm^{-3})	% transmission	correction factor
R1	1	20.49	13.15	0.11	85.5	1.08
R2	1	21.67	11.32	0.19	79.4	1.12
R3	1	19.98	10.72	0.31	69.4	1.20
R4	1	20.01	10.23	0.26	74.2	1.16
calib 1	*****	20.12	10.15	0.299	68.2	1.20
calib 2	*****	20.25	12.35	0.141	73.2	1.16

The results clearly show that as pellet weight, and accordingly pellet height (d) increases, % transmission of the γ rays is reduced and self absorption becomes more significant. The standard deviations for the correction factor within each pellet weight series show a systematic increase with pellet weight (Table 5.12).

Table 5.12 Standard deviations of correction factors.

	standard deviation of values	**% error of values**
5g pellets	0.015	1.44
10g pellets	0.023	2.16
15g pellets	0.037	3.25
20g pellets	0.046	3.99

The standard deviations of the 5 g and 10 g pellets are close to the precision of the method (Table 5.13) and indicate that the variation in values for these pellets is within experimental error and therefore not significant.

The variation in values for the 15 g and 20 g pellets is more significant. For the 15 g pellets no clear correlation with the pellet height or bulk density is observed (see Figure 5.8). However, for the 20 g pellets, there is a more significant correlation between these parameters and the correction factor (Figure 5.9), although there were fewer 20 g sample pellets measured.

Table 5.13 Precision of the method, calculated using a 10g pellet.

sample	**% transmission**	**correction factor ($g\ cm^{-2}$)**	
1.4	83.5	1.09	
1.4	89.1	1.06	**standard deviation**
1.4	87.1	1.07	0.0195
1.4	81.5	1.11	
1.4	84.3	1.09	

Figure 5.8 Correlation of bulk density and pellet height with correction factor for 15 g pellets.

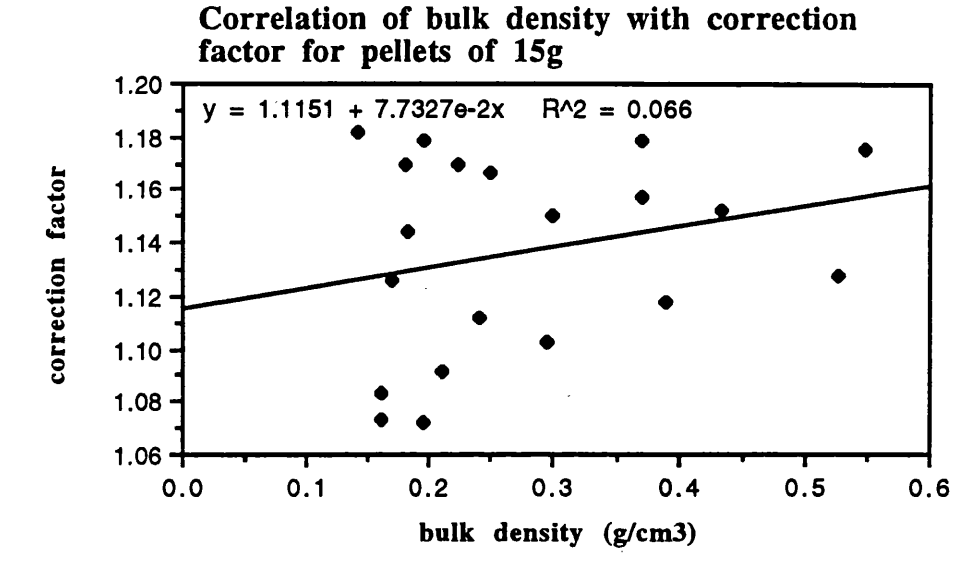

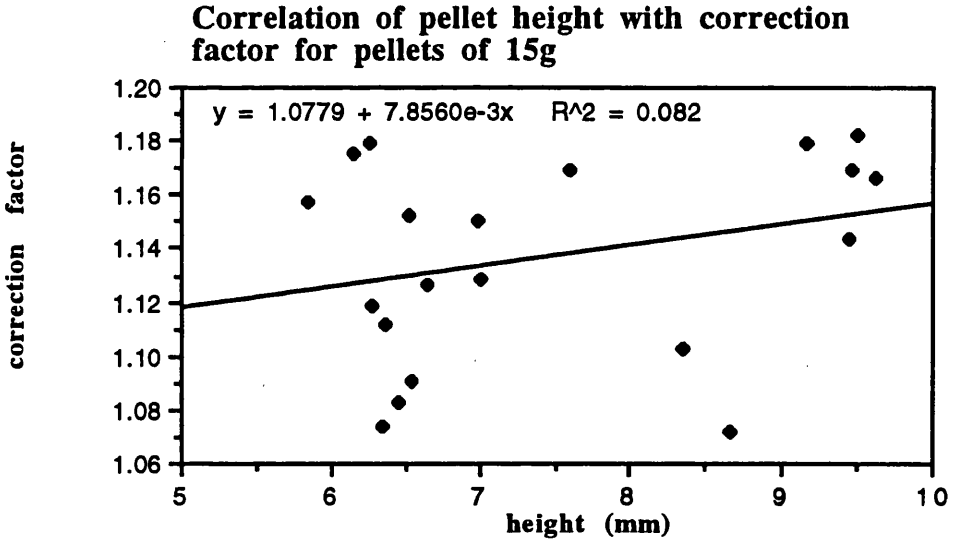

Figure 5.9 Correlation of pellet height and bulk density with correction factor for 20g pellets.

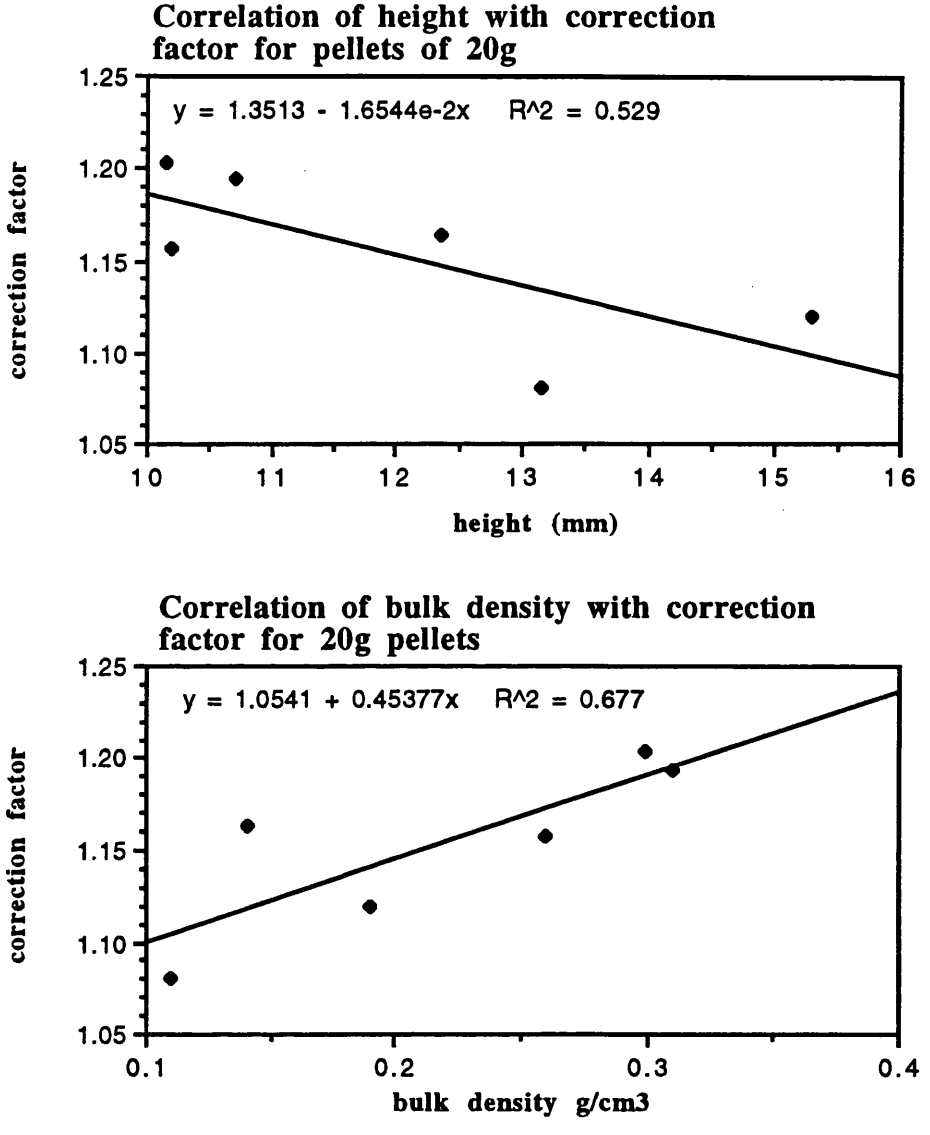

The correction factors calculated were used to correct the ^{210}Pb values recorded, and indicate that self absorption is a significant effect in soils with higher mineral content and bulk density, with the overall effect being less significant in pellets of lower weight (and therefore height).

5.3.3.6 ANALYSIS OF RADIONUCLIDE CONCENTRATIONS

Gamma spectra for individual pellets were recorded over three days, to give acceptable statistical uncertainties the count rates for ^{210}Pb (46.5 keV), ^{226}Ra (352 keV), ^{134}Cs (604.7 keV) and ^{137}Cs (661.6 keV) were corrected for background count rate, self absorption and decay since sampling. The final radionuclide concentration in the sample was then calculated using equation 5.7.

$$A = \frac{C \times 100}{E \times W} \tag{5.7}$$

where A is the sample radionuclide concentration in Bq kg^{-1}, C is the count rate, E is the % absolute detection efficiency and W is the sample weight in kg.

The error on the count rate (σ_S) derived by the software package included the errors on both the total peak area which includes the background (S + B) and the background B:

$$\begin{aligned} \sigma_S &= (S + B + B)^{1/2} \\ &= (S + 2B)^{1/2} \\ \%\sigma_{error} &= \frac{100(S + 2B)^{1/2}}{S} \end{aligned} \tag{5.8}$$

In calculating the radionuclide concentration this count rate was multiplied by the efficiency, which has an uncertainty associated with it, and this was taken into account using equation 5.9 to give the total sample error σ_t.

$$\%\sigma_t = \sqrt{\%\sigma^2_{error} + \%\sigma^2_{effic}} \tag{5.9}$$

The detection limit of the peaks recorded in the spectra was defined as three times the uncertainty on the Compton Continuum under the area of the spectrum encompassing the photopeak (i.e. 3σ, where $1\sigma = N^{1/2}$).

5.3.4 ANALYSIS OF THE METAL CONTENTS OF THE CORES

Concentrations of metals were measured by flame atomic absorption spectroscopy (FAAS), inductively coupled plasma mass spectroscopy (ICPMS) of acid digests of the samples and neutron activation analysis (NAA) of the solid peat samples (Table 5.14).

Table 5.14 Metals studied and the analytical techniques utilised in their detection.

FAAS		NAA		ICP-MS
Pb	Au	Co	Sb	^{206}Pb
Zn	Ag	Cr	Sc	^{207}Pb
Cu	As	Hf	Se	^{208}Pb
Mn	Br	Hg	Sm	
Al	Ba	La	Th	
Fe	Ce	Lu		

5.3.4.1 ACID DIGESTION OF PEAT SAMPLES

A standard method (HMSO, 1986) was used for the analysis of the metal contents of soils by digestion with a hydrochloric acid (HCl) - nitric acid (HNO_3) mixture. All reagents utilised were analytical grade and all glassware and storage bottles were cleaned before analysis using a 20% Decon solution, with several rinses of distilled water followed by 2M HNO_3 to minimise contamination. A temperature controlled Tecator Digestion Block System 40 (model 1016) was utilised to give controlled digestion. 40 samples and blanks could be digested simultaneously, with constant reflux to minimise any hazardous fumes.

1g of dried, ground peat was used for analysis, except in the most organic surface samples, where the mass of material was small and only 0.5g was utilised. The samples were accurately weighed out in triplicate into the reflux flasks. 7.5 ml of 6M HCl was added, followed by 2.5 ml concentrated HNO_3 and the flasks were connected to the reflux condenser and left to digest at room temperature overnight (or for at least 16 hours). The samples were then refluxed gently at 120^0 C for 2 hours before increasing the temperature to 125^0 C for 30 minutes. The digests were left to cool to room temperature before filtering through acid resistant Whatman cellulose filter papers into 25ml volumetric flasks. The filter papers were prewashed with 2M HNO_3. Each flask was rinsed with three successive 2 ml aliqouts of 2M HNO_3, adding the rinsings to the filtering samples. The filter and the residue were also washed five times with 1 ml aliquots of 2M HNO_3. 1 ml of potassium chloride solution was added as an ionisation suppressant, and the digest was made up to volume with 2M HNO_3. For each batch of digests, three blank determinations were also carried out. All samples and blanks were stored in polyethylene bottles at 4^0 C until analysis.

5.3.4.2 FAAS ANALYSIS OF THE DIGESTS

Atomic absorption spectrometry utilises the absorption of light energy of a specific wavelength by an atom when it becomes "excited". As the number of atoms in the light path increases, the amount of light absorbed will correspondingly increase, allowing quantitative determination of the amount of atoms present if specific light sources and the characteristic wavelengths of the atoms are utilised. An atomic absorption spectrometer has five main components, a hollow cathode lamp as the light source, the absorption cell where atoms of the sample are produced (either flame or furnace), a monochromator for light dispersion, a detector which measures the light intensity and amplifies the signal and a display unit which shows the reading.

A Perkin Elmer 1100B Atomic Absorption Spectrometer with v3.5 operating software was utilised with the "cookbook settings" and standard linear ranges of the elements being applied. The ranges and setting used are presented in Table 5.15. The spectrometer was calibrated with the relevant standard solutions to give the results in units of concentration. The standard solutions were prepared from Spectrosol standard reagents, which had 1000 ug ml^{-1} of analyte in 0.5M HNO_3. These were diluted to the required range with 2M HNO_3, and stored in polyelethylene bottles at 4^0 C between determinations.

In calibrating the machine, the auto mode was chosen which automatically selects the most appropriate line fitting equation depending on the number of standards used in the calibration. A reslope function was also present and was utilised during the runs.

Table 5.15 Specifications of the FAAS system.

Element	**Wavelength (nm)**	**Flame**	**Sensitivity Check**	**Linear Range (mg/l)**	**Limit of detection**
Pb	283.3	Air - Ac	20	0 - 20	0.2
Zn	213.9	Air - Ac	1.0	0 - 1	0.01
Mn	279.5	NO - Ac	2.5	0 - 3	0.03
Fe	248.3	NO - Ac	5	0 - 5	0.05
Cu	324.8	Air - Ac	4	0 - 5	0.05
Al	309.3	NO - Ac	50	0 - 150	1.5

5.3.4.3 ICP - MS ANALYSIS OF THE DIGESTS

ICP-MS was used to determine the stable lead isotope ratios for the samples. The technique of ICP-MS couples inductively coupled plasma (ICP) with a mass spectrometer (MS). An ICP is an ideal source of ions since it provides sufficiently high temperatures in a controlled, uncontaminated environment for the conditioning and excitation of liquid, solid and gaseous samples. A comprehensive outline of the principles of operation of the ICP-MS can be found in Sugden (1993).

A V.G. Plasmaquad ICP-MS was used to record the isotope ratios, with sample injection through nebulisation and an Ar gas supply. The specifications of the ICP-MS for the determination of lead isotopes are presented in Table 5.16. Considerable dilution of the digests was required to bring the solutions into the required concentration range, and care was taken to minimise contamination in the dilution step.

Table 5.16 Specifications of the ICP-MS system used for lead isotope determination.

Matrix	0.3M HNO_3
Linear Range	0 - 20 ng ml^{-1}
Limit of Detection	1 *pg* ml^{-1}
Dissolved Solid	0.1%

5.3.4.4 NEUTRON ACTIVATION ANALYSIS OF THE PEAT SAMPLES

PRINCIPLES OF INSTRUMENTAL NEUTRON ACTIVATION ANALYSIS

In this procedure, the samples and standards are simultaneously exposed to a flux of thermal neutrons, which activate a small number of the atoms forming radioactive species. ß / γ decay of the radioactive products gives rise to the emission of γ radiation, which can be detected using γ spectrometry (see section 5.3.3). The count rates of selected photopeaks in the γ spectrum of samples and standards are used to derive elemental concentrations in the samples since the energy of the photopeak is characteristic to that nuclide and the activity is proportional to the amount of the element present (assuming the counting geometry and therefore detector efficiency is constant):

$$\frac{\text{count rate of nuclide of element in sample}}{\text{count rate of nuclide of element in standard}} = \frac{\text{concentration of element in sample}}{\text{concentration of element in standard}} \quad (5.10)$$

INSTRUMENTATION

All irradiations were performed using the Scottish Universities Research and Reactor Centre (SURRC) UTR-300 research reactor which, at full power of 300kW, provides a neutron flux of around 3 x 10^{12} n cm^{-2} in the core area. The samples and standards were irradiated using the central vertical stringer (CVS) of the reactor for 6 hours.

The γ detection system used for analysis was an EG & G Ortec Gamma-X intrinsic Ge detector, which had a 10% relative efficiency and a resolution of 1.6 keV at 1333 keV. The detector was interfaced with an EG & G Adearn unit and an IBM-compatible PC which ran the EG & G software package MINIGAM II. This provided peak location, peak area calculation, and energy calibration of the sytsem. Element concentrations were calculated from the peak-search programme results with the aid of the SURRC activation analysis programm NAA. This programme takes the output file from the Ortec GAMMA 2 programme directly from disc, and performs equation 5.11. The programme corrects all observed count rates to a defined reference time, correcting for decay during counting and flux variations and incorporates an *a priori* error which allows for uncertainties in counting geometry, weight, etc. and systematic errors. The final results are expressed in mg kg^{-1}.

STANDARD AND SAMPLE PREPARATION AND ANALYSIS

The samples were irradiated for 6 hours alongside standards containing known weights of the elements of interest. The standards reproduced the geometry of the samples, thus removing the necessity for an efficiency calibration. The concentrations of the elements of interest were determined from equation 5.10, since the cross sections, decay constants, atomic weights, isotopic abundances, irradiation, decay and counting times and counting geometry were all identical for samples and standards.

To produce a multielement standard, Camac cellulose powder was used to provide a suitable matrix. The elements of interest were added as Spectrosol standard solutions and 1 ml of each of the 100 μg ml^{-1} solutions were mixed together and added carefully to 10 g of the cellulose powder, taking care to transfer all of the liquid. The only exception was Br, which was added separately. The cellulose mixture was then stirred for 2 hours before drying at 40^0 C. Once dry, the standard was mixed on an end-over-end shaker for 6 hours. The homogeneity and reproducibility was tested by analysis of nine aliqouts.

In the initial attempt to produce a standard in this way, it was evident that the homogeneity was not acceptable (Table 5.17). As well as the homogeneity being poor,

^{82}Br was not detectable. In the formulation of this standard, Br was not added separately, and may have evaporated off the mixture during the drying process. Thus in the formulation of the second sample, Br was added seperately being dried onto the cellulose at room temperature. In addition all of the other elements were added in this way before mixing on an end-over-end shaker. This substantially improved the reproducibility (Table 5.17). The complete data for these analyses can be found in Appendix 3.1.

Table 5.17 Standard deviation of replicate analyses of the nuclide content of the cellulose standards.

nuclide	keV	cps mg^{-1} standard 1	standard deviation	% error	cps mg^{-1} standard 2	standard deviation	% error
^{153}Sm	103	1.3569	0.0407	2.99	2.2700	0.0200	0.88
^{141}Ce	146	NM			0.1847	0.0022	1.19
^{177}Lu	209	0.3021	0.0807	26.71	0.3900	0.0054	1.38
^{75}Se	265	NM			0.1607	0.0033	2.05
^{203}Hg	279	NM			0.5792	0.0134	2.31
^{233}Pa	312	NM			1.3671	0.0235	1.72
^{60}Co	315	NM			0.2777	0.0022	0.79
^{198}Au	412	2.6819	0.1243	4.63	3.8800	0.0153	0.39
^{181}Hf	482	NM			1.1835	0.0210	1.77
^{131}Ba	496	0.1099	0.0476	42.49	0.1302	0.0019	1.46
^{76}As	559	0.0431	0.0400	92.81	0.1723	0.0035	2.03
^{122}Sb	564	0.1404	0.0196	13.96	0.1840	0.0037	2.01
^{110}Ag	658	NM			0.6506	0.0055	0.85
^{82}Br	777	0.0000	0.0000	0	0.4678	0.0079	1.69
^{46}Sc	889	NM			3.1858	0.0376	1.18
^{140}La	1597	0.0487	0.0209	42.92	0.1174	0.0017	1.45

The lack of values for some of the elements in standard 1 is because a long count was not carried out since it was evident from the short count that the homogeneity was not good. These nuclides are denoted by NM (not measured).

Approximately 0.3 g of each sample and standard were accurately weighed into clean, high purity polythene vials of 1 ml volume, taking care to maintain a uniform geometry in both the standards and samples. Corrections were made for neutron flux by attaching iron wire flux monitors (weighing approximately 0.03g, with 95% purity)

to the vials and assuming that the specific activity induced in the flux monitor for each sample is proportional to the neutron fluence experienced by the sample. The iron wires were counted in a standard geometry and the activity of ^{59}Fe calcuated at a defined reference time in each case. The individual and the average fluxes calculated from these results were used in the computer-based calculations of element concentration. The polyethylene vials, along with their flux monitors, were then individually wrapped in aluminium foil and labelled. Batches of 10 samples with 1 standard and 1 bulk reference peat were packaged together in aluminium foil and irradiated. In order to determine a wide range of elements two series of counts were utilised (see Table 5.19). This decay scheme also allowed the activity of the samples to be reduced to radiologically acceptable levels. The first series consisted of 30 minute counts, carried out 3-4 days after irradiation. The standard, reference peat and samples were counted at a distance of 10 cm from the detector to reduce dead time to below 5%. The second series of counts detects the longer lived nuclides, by allowing the short lived species to decay before counting. This was carried out approximately 28 days after irradiation, and the samples, standards and reference peats were counted for 3 hours by being placed directly on top of the detector, to maximise the counting efficiency.

Due to the lack of suitable certified reference materials, only an in-house reference material was run. This was a sample of bulk peat, which had previously been activated to determine the contents of the elements present, and was used to determine the reproducibility of the method. The bulk peat was first analysed ten times to assess its metal content, and then an aliquot was analysed with each batch of samples. The standard deviations of the replicate analyses of the bulk peat gives an estimate of the homogeneity of the material, with the standard deviations of the results from the between batch samples giving an estimate of the reproducibility of the method. These standard deviations are presented in Table 5.18, and the data can be found in Appendix 3.1.

The within-batch samples showed good reproducibility, making the bulk peat homogenous enough to be utilised as a reference material for all the elements shown. Ba, Sb, Ag and Au were not detected in the bulk peat.

Table 5.18 The standard deviations of replicate analyses of the bulk peat.

nuclide	mean mg kg^{-1} within batch	standard deviation	% error	mean mg kg^{-1} between batch	standard deviation	% error
Ta	2.00	0.094	4.69	2.0079	0.157	7.81
Hg	0.640	0.0222	3.47	0.6311	0.0832	13.18
Sm	2.19	0.095	4.33	2.1651	0.228	10.53
Ce	25.23	0.564	2.23	25.1035	5.443	21.71
Lu	1.84	0.0206	1.17	1.8446	0.224	12.14
Se	2.33	0.089	3.81	2.3267	0.238	10.23
Pa	1.39	0.081	5.80	1.3996	0.101	7.22
Co	4.14	0.126	3.01	4.1473	0.241	5.81
Hf	0.837	0.0132	1.58	0.8359	0.0203	2.43
As	0.856	0.121	14.1	0.8622	0.225	26.1
Br	23.41	0.329	1.41	23.3783	0.0820	3.51
Sc	2.02	0.157	7.77	2.0424	0.237	11.60
La	19.52	0.570	2.92	19.5164	2.71	13.89

The reproducibilities of the within-batch samples are significantly better than those for the between-batch samples. This indicates that there is a greater incidence of random error between each activation than within the same activation. As shows the highest errors, in both the within and between-batch determinations. This may be due to the low concentration of As in the bulk peat which is approaching the detection limit for the method.

Table 5.19 Elements determined by NAA, and their counting schemes.

Element	Nuclide	γ - ray energy (keV)	1/2 life
Short	**Count (30 min)**	**4 days after**	**irradiation**
As	^{76}As	559	1.09d
Au	^{198}Au	412	2.69d
Br	^{82}Br	777	1.47d
Ba	^{131}Ba	496	11.8d
La	^{140}La	1597	1.68d
Lu	^{177}Lu	208	6.71d
Sb	^{122}Sb	564	2.70d
Sm	^{153}Sm	103	1.95d
Long	**Count (3 hours)**	**28 days after**	**irradiation**
Ag	^{110m}Ag	658	249.8d
Co	^{60}Co	315	5.26y
Ce	^{141}Ce	145.4	33d
Hf	^{181}Hf	482	42.4d
Hg	^{203}Hg	279	46.6d
Sc	^{46}Sc	889.3	83.8d
Se	^{75}Se	265	119.8d
Th	^{233}Pa	311.9	27d

5.4 RESULTS AND DISCUSSION

5.4.1 THE PHYSICAL PROPERTIES OF THE CORES

The results for the moisture content, organic matter content (% loss on ignition), bulk density and pH of each core are presented in Figures 5.10 to 5.15

Figure 5.10 Physical Properties of Core 1.

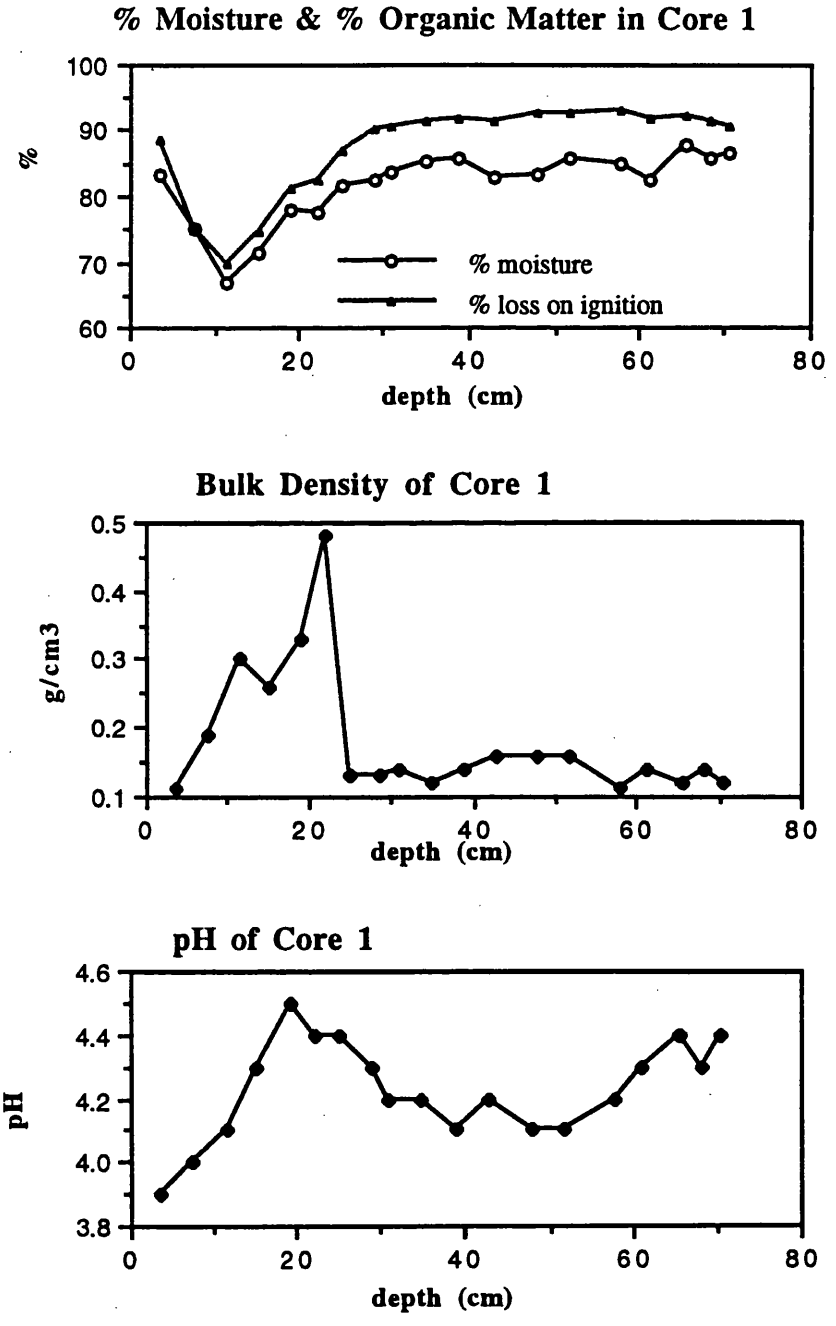

Figure 5.11 Physical properties of Core 2.

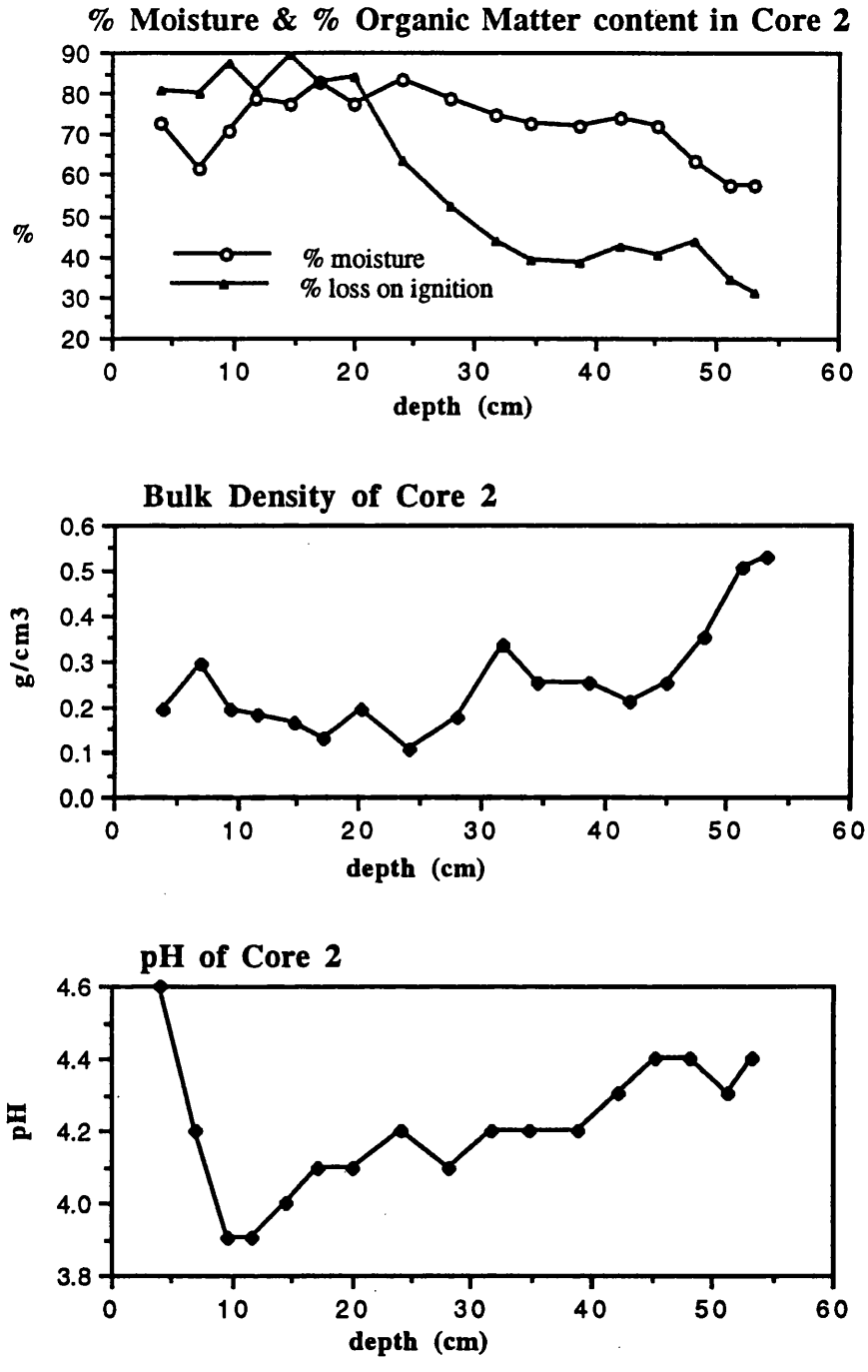

Figure 5.12 Physical properties of Core 3.

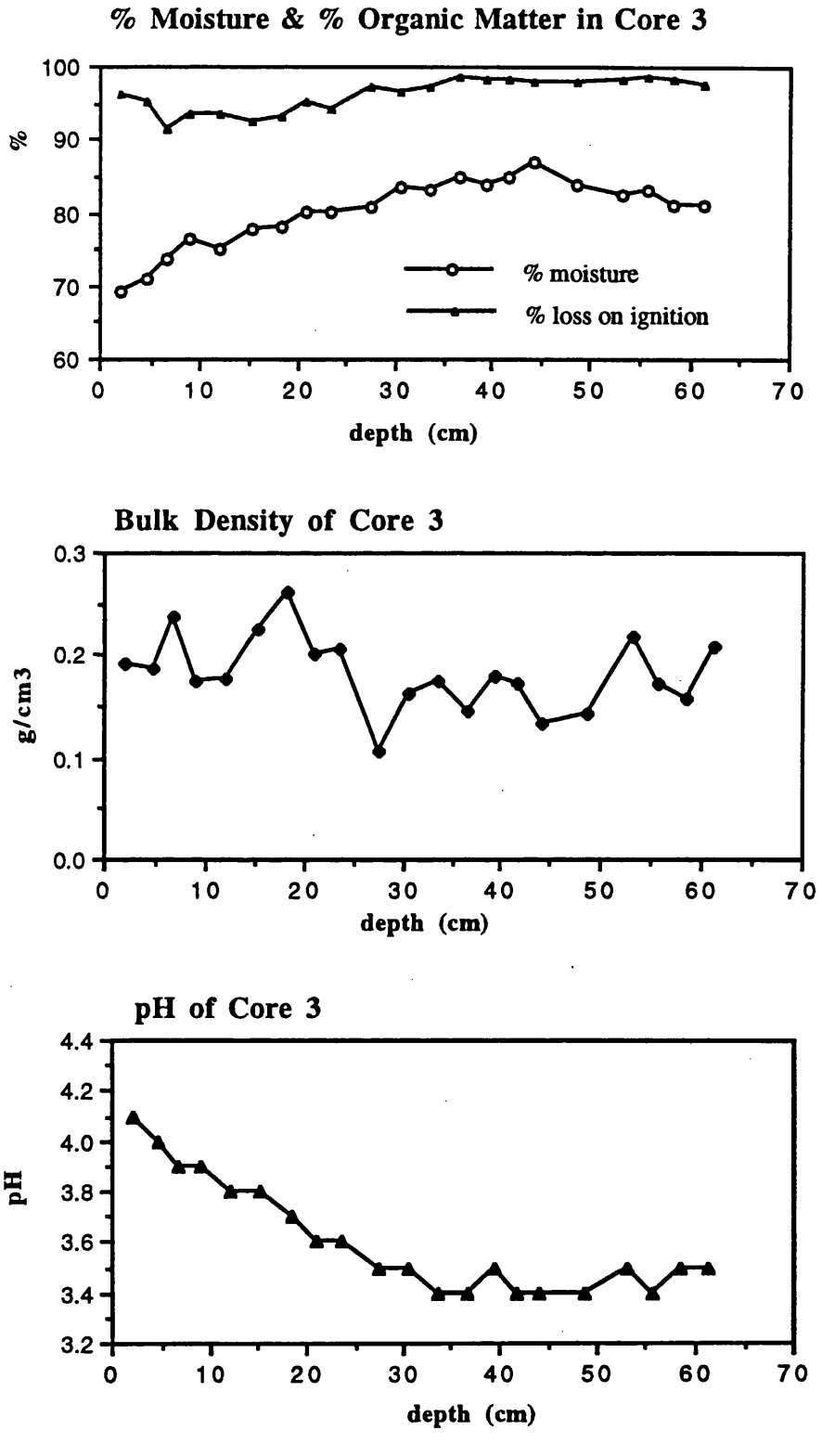

Figure 5.13 Physical properties of Core 4.

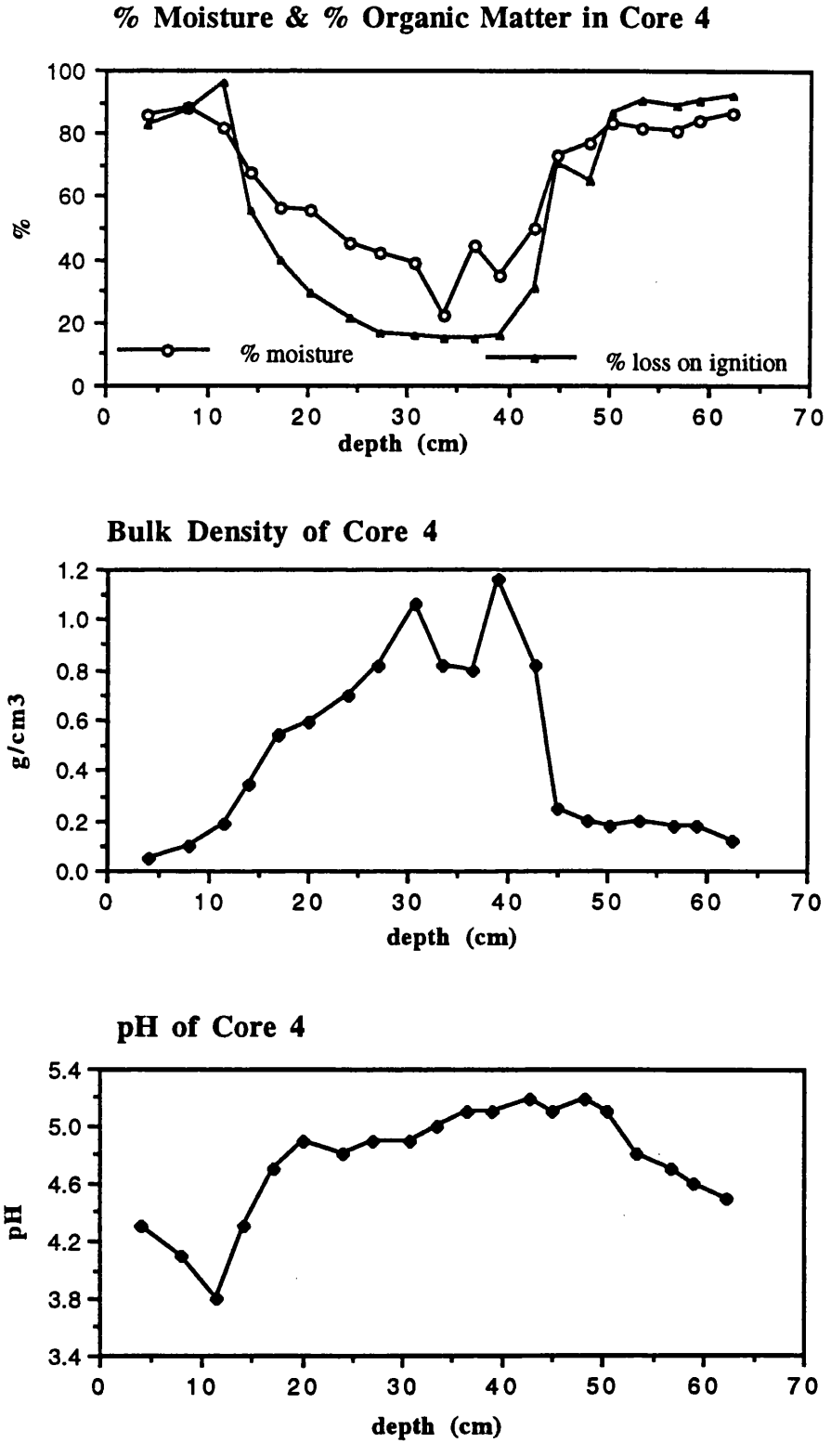

Figure 5.14 Physical properties of Core 5.

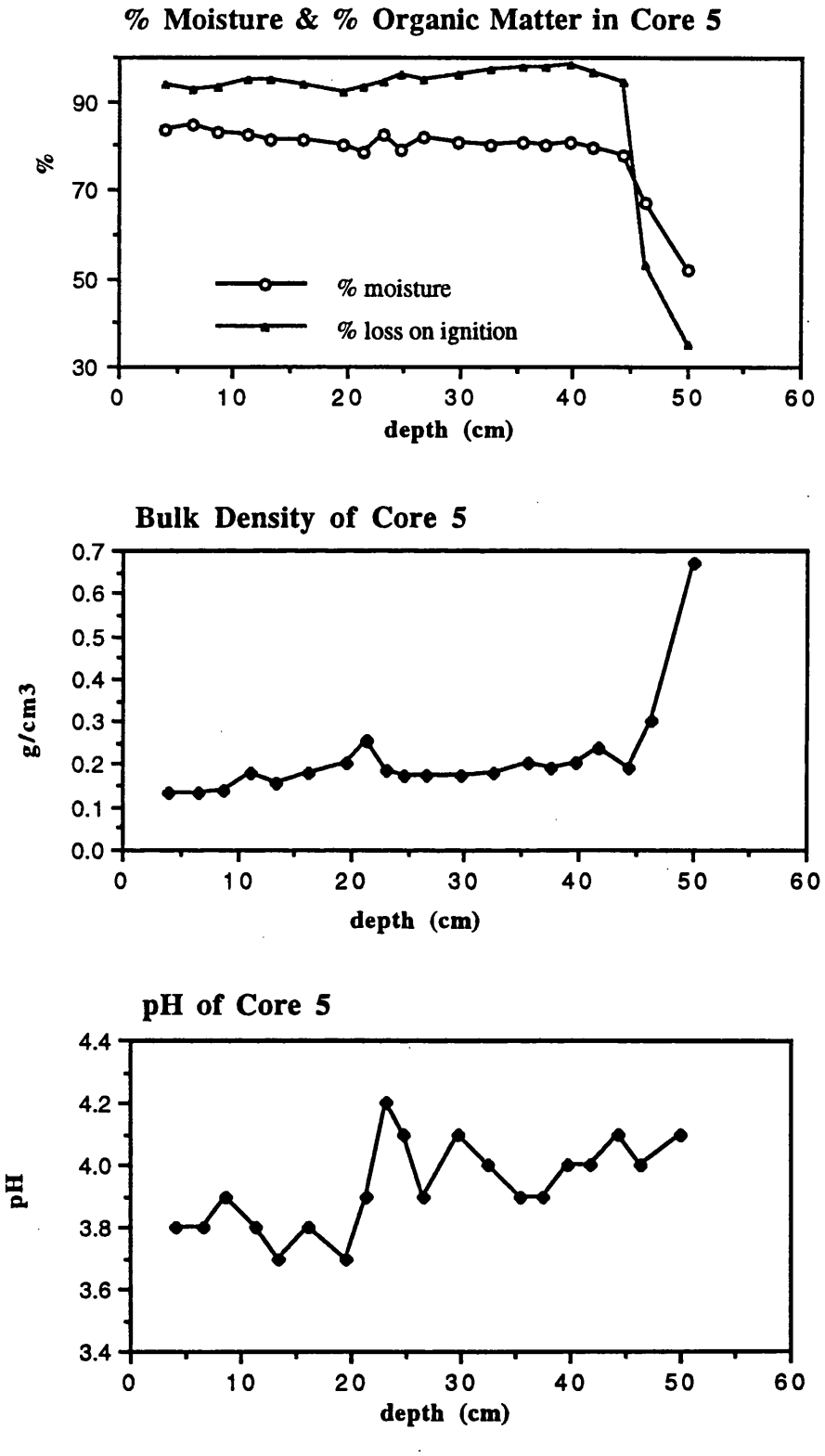

Figure 5.15 Physical properties of Core 6.

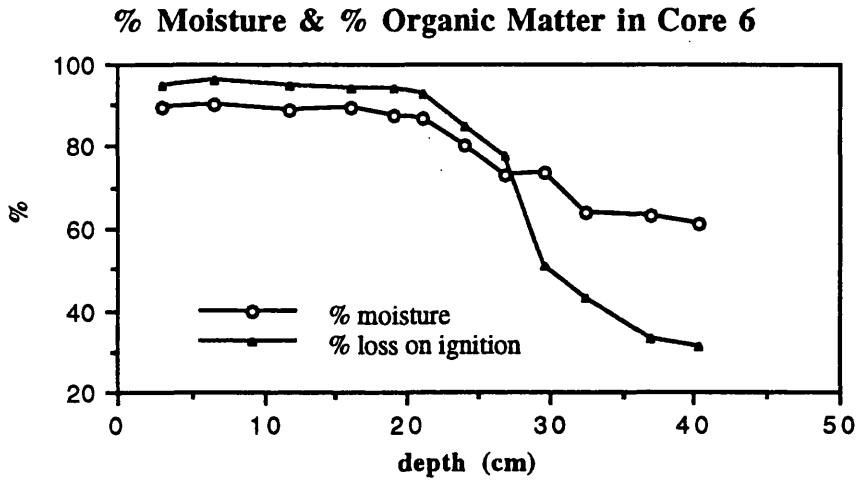

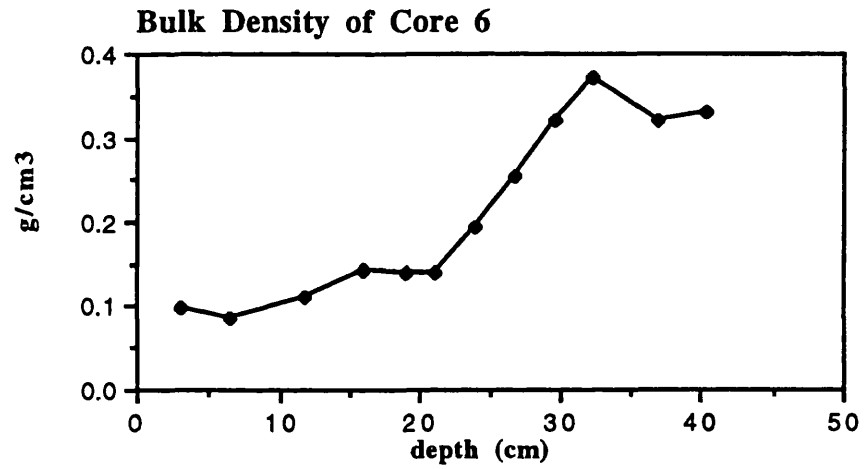

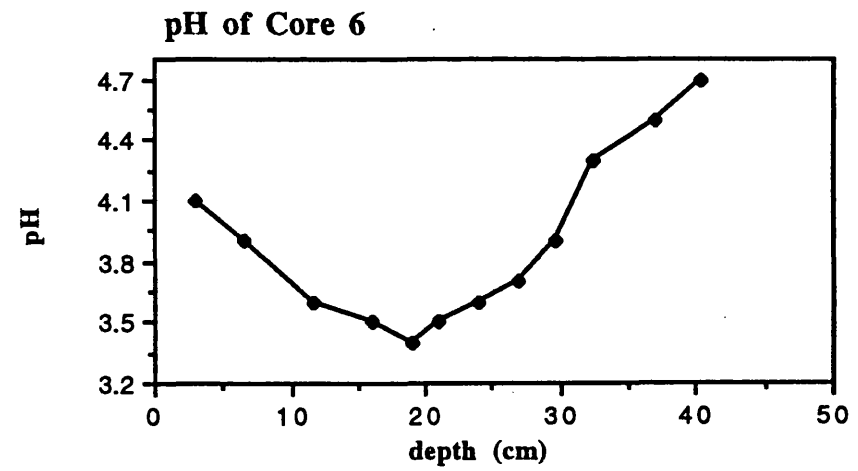

In all of the cores, the % moisture and % organic matter (L.O.I.) follow similar trends. In addition, in many cores a reduction in the values of the moisture and organic content was mirrored by a rise in bulk density values. In Cores 5 and 6 (Figures 5.14 and 5.15 respectively) this occurred at depth, when the bedrock was reached, and correspondingly the core became more mineral in nature. In Core 2 (Figure 5.11), there was a decrease in organic matter content, with an increase in bulk density at depth, as the gleyed mineral horizon was reached. In Core 1 (Figure 5.10), there was a sudden drop in organic matter content, with an increase in bulk density between 20 and 30 cm, indicating an increase in deposition of mineral material at this depth. With South Drumboy being a working hill farm, drainage channels have been inserted around the hill and Core 1 lay below a section of improved grassland where this had occurred. Accordingly, insertion of these may have caused disturbance giving an influx of mineral material into Core 1. Core 4 (Figure 5.13) also showed a pronounced mineral horizon, sandwiched between two organic horizons, which is again indicative of disturbance, perhaps due to the same reason. In addition, in Core 4, the pH values for the mineral horizon were significantly higher than for the organic horizons, rising to a value of 5.2.

The bulk density, % moisture and organic matter content reflect the botanical composition of the cores, as well as the above changes in composition. These herbaceous peats, show characteristic values of 0.12 - 0.16 g cm^{-3} for bulk density (Clymo, 1984). Had the peats been primarily formed from *Sphagnum* mosses, then the bulk density values would have been far lower (~ 0.05 g cm^{-3}) with higher % moisture.

Because of the possibility of compaction effects occurring, the bulk density should always be measured when measuring rates of peat accumulation (Jones & Gore, 1978) and accordingly the values will be utilised in later calculations. The bulk density has also been shown to correlate with degree of humification or decomposition (Clymo, 1984), and this can also cause inaccuracies when calculating peat accumulation rates. The difference in degree of organic matter content (%LOI), was also used in the calculation of γ detection efficiency (see section 5.3.3.5 and the following section).

5.4.2 THE CONTENTS AND DISTRIBUTIONS OF RADIONUCLIDES AND METALS WITHIN SOUTH DRUMBOY PEAT PROFILES

The activities of radionuclides in the peats are presented as specific activity (Bq kg^{-1}) versus cumulative weight (g cm^{-2}) which is used to compensate for the effects of any compaction processes in the peat (Clymo, 1990: El-Dahoushy, 1988: Swan *et al.*, 1982). Total inventories (Bq m^{-2}) were calculated, from which the average flux (calculated as inventory x λ, in units of Bq m^{-2} y^{-1}) of the radionuclides to the surface of the peat was derived. To calculate a chronology for the cores, the constant initial concentration (c.i.c.) model (Robbins, 1978) was used, as described in section 1.8.4.

In order to estimate the separate contributions of weapons testing and Chernobyl to the ^{137}Cs content, the decay corrected Chernobyl $^{134}Cs/^{137}Cs$ activity ratio was calculated. At the time of deposition, this ratio was approximately 0.55 (Clark & Smith, 1988), so the Chernobyl ^{137}Cs concentration A_t at the time of sampling (t) can be calculated from:

$$At\,^{137}Cs = \frac{At\,(^{134}Cs)\; e^{(0.33-0.023).t}}{0.55} \qquad (5.11)$$

The weapons-testing fallout inventory, decay corrected to the time of collection, was then determined by subtracting the estimated Chernobyl contribution from the total ^{137}Cs content of the section. All errors were calculated as in section 5.3.3.6, being fully propagated where necessary.

All metal and element profiles are plotted as concentration in mg kg^{-1} versus cumulative weight (g cm^{-2}), which for convenience is referred to as depth. Where appropriate, to calculate a depositional flux for each metal, the peat accumulation rate was multiplied by the individual section concentrations of that metal.

SOUTH DRUMBOY CORE 1

Core 1 was the lowest altitude core sampled on the easterly facing slope, and lay directly downslope from a section of improved grassland. As discussed in section 5.4.1 the peat showed an increased mineral content between 1 and 4 g cm^{-2}, as characterised by an increase in the bulk density and a decrease in the % loss on ignition. This was proposed to be an indicator of disturbance of the profile from the insertion of drainage channels further uphill.

The ^{210}Pb profile (Figure 5.16 & Table 5.20) did not show an exponential decrease in activity with depth as would be expected for a situation of uniform accumulation. Unsupported ^{210}Pb was detected only in the top three sections of the core to a depth of 4 g cm^{-2}, which represents the top of the more mineral layer, suggesting that the surface peat is a reasonably new horizon. However, the accumulation rate was calculated to be 0.015 g cm^{-2} y^{-1}, which is incompatible with recent disturbance, indicating that the data for this core must interpreted with caution. The ^{210}Pb inventory was calculated as 2157 Bq m^{-2}, giving an average flux of 66.9 Bq m^{-2} y^{-1}.

The radioacaesium data are presented in Tables 5.21 and 5.22. Of immediate note is the high concentration of ^{137}Cs in the surface section and like the ^{210}Pb, the majority of the radiocaesium is in the top three sections of the core, in the surface organic horizon (Figure 5.17). The ^{137}Cs inventory was 48953 Bq m^{-2}, comprising a Chernobyl inventory of 3841 Bq m^{-2} and a weapons-testing component of 45075 Bq m^{-2}. The ^{134}Cs inventory was 292 Bq m^{-2}. Thus, 92% of the ^{137}Cs inventory was attributable to weapons-testing ^{137}Cs and 96% of this weapons testing ^{137}Cs was contained within the surface section. With the presence of the mineral layer suggesting disturbance of the profile from insertion of drainage channels, this may also be affecting the ^{137}Cs profiles through promoting transport of ^{137}Cs through the channels. Since this effect is confined to the weapons-testing ^{137}Cs the disturbance must have occurred before the Chernobyl accident and is not a recent effect.

Although the majority of the radiocaesiumm was contained within the surface section some ^{137}Cs had penetrated to depths well beyond ^{210}Pb. ^{134}Cs had penetrated to a lesser extent, indicating that the effect is time dependent. The penetration of radiocaesium to depths dated before the onset of weapons-testing has previously been recorded (Maguire, 1994: Sugden, 1993: Mitchell *et al.*, 1992: Schell *et al.*, 1989: Clymo, 1979). Diffusive and advective processes have been proposed to be responsible and often lead to the loss of the peak in weapons-testing ^{137}Cs (Mitchell *et al.*, 1992: Schell *et al.*, 1989).

The Al concentrations in Core 1 (Figure 5.18) increased as the mineral content increased and this trend was mirrored by Ta, La, Sm, Se, Hf, Sc and Th (Appendix 3.3), with La and Ce being displayed here (Figure 5.19). These profiles also indicate minor fluctuations in mineral content at depth.

The Mn and Fe profiles (Figure 5.20) indicate that conditions become increasingly reducing with depth. Mn shows a significant decrease in concentration from the surface section, indicating that from this depth conditions are sufficently reducing to bring Mn oxides into solution through the reaction:

$$MnO_2 + 4H^+ + 2e^- = Mn^{2+} + 2H_2O$$

However, reduction does not give total loss of Mn, with between 10-20 mg kg^{-1} present to a depth of 9 g cm^{-2} beyond which total loss of Mn is observed as conditions become more reducing.

Fe does not show a surface reduction like Mn but instead shows loss from 9 g cm^{-2} further reinforcing that conditions become progressivly more reducing from this depth. Mn oxides are more sensitive to changes in Eh and consequently come into solution before Fe oxides (Alloway, 1990). The reduction of Fe oxides occurs through the following reaction:

$$Fe(OH)_3 + 3H^+ + e^- = Fe^{2+} + 3H_2O$$

The dissolution of Fe and Mn oxides can cause the release of metals co-precipitated with them (Jones, 1987: Alloway, 1990) and this may explain the pattern of the Zn and Cu profiles (Figure 5.22) which show peaks in concentration between 6-9 g cm^{-2} where conditions start to become more reducing.

In addition changes in the redox potential not only mediate the dissolution of Fe and Mn oxides, but can also mediate the reduction of sulphate to sulphite leading to the precipitation of metal sulphides (Alloway, 1990). FeS_2 is most readily formed with Mn participating to a lesser degree, especially where there is a high concentration of Fe^{3+} ions (Rowell, 1988). Cu and Zn have been proposed to form metal sulphides and this could also be occurring in Core 1. Walton Day *et al.* (1990) proposed that Cu was co-precipitated with FeS_2 rather forming CuS and this may also explain the pattern observed for Cu and Zn. Accumulation has been proposed to be an indication of the zone of water fluctuation, since the sulphides are continuously oxidised and mobilised, then reduced and precipitated (Damman, 1978).

Br (Figure 5.22) shows a slightly different relationship to Cu and Zn, with a peak in the surface organic layer, followed by reduction in concentration in the more mineral horizon and a bimodal peak between 7.5-10 g cm^{-2}. This bimodal peak at depth could be related to the fluctuation in the water table levels as discussed for Cu and Zn.

Pb, Co, Hg, As and Sb differ from the previous elements discussed by showing no increases in concentration or deposition at depth (Pb, Co and Hg are illustrated in Figure 5.23). All however show sub-surface maxima, which for Pb and Co occur in the second section and for As, Sb and Hg in the third section. The high surface concentrations of the metals indicate that they are of pollutant origin. Co also appears to show some redeposition at depth, giving a similar profile to Cu at depth.

The $^{206}Pb/^{207}Pb$ ratios (Figure 5.24) show a maximum of ~1.16 at 4 g cm^{-2}, decreasing to a value of ~1.10 towards the surface. Sugden (1993) in a similar study of ombrotrophic peat profiles also noted this effect and attributed it to the introduction of Pb with low ^{206}Pb content from car exhaust emissions. Pb which was deposited from industrial sources had a higher ratio of between 1.16-1.18 from the burning of fossil fuels. Thus the continuous decrease in $^{206}Pb/^{207}Pb$ ratio towards the surface indicates that car exhaust emissions are of increasing in importance in the top three sections. Below 4 g cm^{-2} the $^{206}Pb/^{207}Pb$ ratios show fluctuations which probably reflect variations in the mineral content at this depth.

However, interpretation of the pollutant metal profiles and the Pb-isotope ratios should be undertaken with caution due to the disturbance of the peat, which will also have disturbed these profiles.

Table 5.20 ^{210}Pb and ^{226}Ra specific activities and excess ^{210}Pb inventories for Core 1

depth cm	depth gcm^{-2}	total ^{210}Pb $Bq\ kg^{-1}$	^{226}Ra $Bq\ kg^{-1}$	excess ^{210}Pb $Bq\ kg^{-1}$	excess ^{210}Pb $Bq\ m^{-2}$
0-3.5	0-0.39	226.4 ± 7.6	4.4 ± 0.7	222.0 ± 19.2	855 ± 31.7
3.6-7.5	0.39-1.15	150.9 ± 4.9	11.5 ± 1.1	138.5 ± 11.2	1056 ± 41.7
7.5-11.5	1.15-2.35	24.6 ± 2.5	13.9 ± 1.3	10.7 ± 1.2	129 ± 35.8
11.5-15.2	2.35-3.31	15.3 ± 3.9	9.5 ± 0.8	5.8 ± 1.6	56.1 ± 14.3
15.2-19.2	3.31-4.63	8.3 ± 1.2	12.3 ± 1.0	0.00	0.00
19.2-22.2	4.63-6.07	5.9 ± 1.9	2.7 ± 0.4	3.2 ± 1.0	46.1 ± 14.4
22.2-25.1	6.07-6.44	11.1 ± 3.7	7.1 ± 0.8	4.0 ± 1.4	15.2 ± 5.32
25.1-28.8	6.44-6.93	BDL	12.3 ± 0.9	0.00	0.00

Figure 5.16 ^{210}Pb profiles for Core 1.

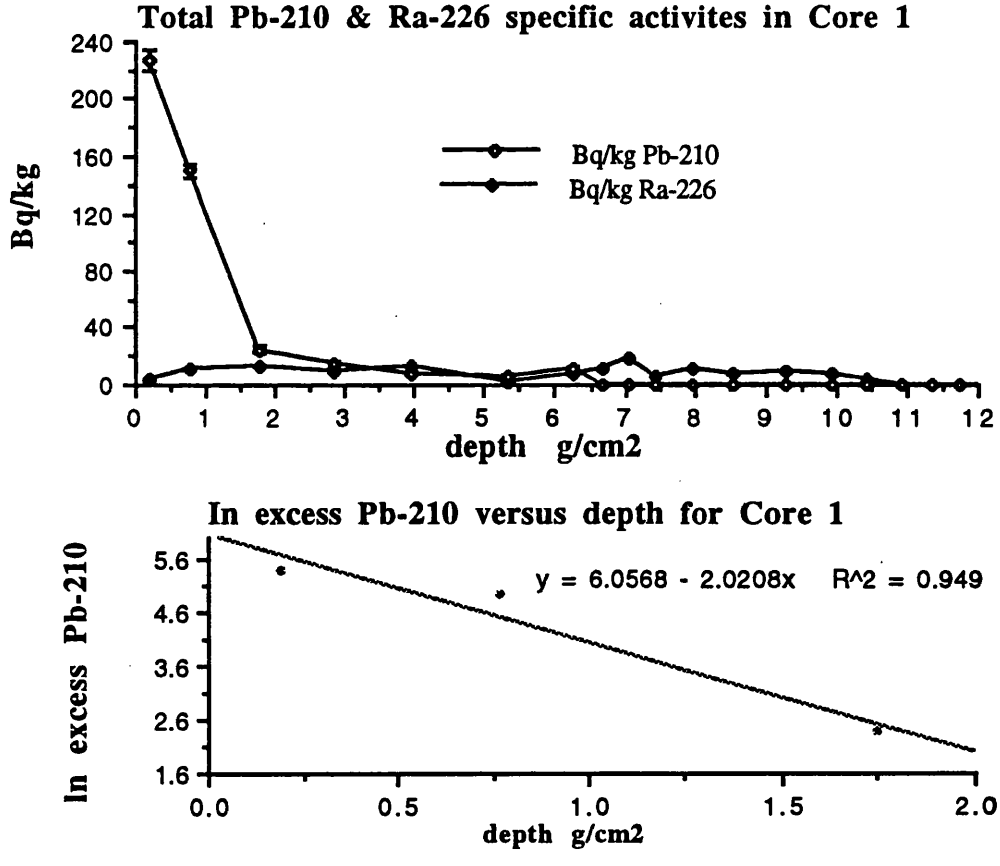

Table 5.21 ^{134}Cs and ^{137}Cs specific activites and inventories in Core 1.

depth g cm^{-2}	Total ^{137}Cs Bq kg^{-1}	Total ^{137}Cs Bq m^{-2}	^{134}Cs Bq kg^{-1}	^{134}Cs Bq m^{-2}
0-0.39	11798 ± 210	45400 ± 808	42.9 ± 1.6	165 ± 6.3
0.39-1.15	223 ± 3.9	1690 ± 30	14.6 ± 0.8	110 ± 5.8
1.15-2.35	32.1 ± 0.9	385 ± 12	2.3 ± 0.4	15.6 ± 2.5
2.35-3.31	19.8 ± 0.8	190 ± 8	0.00	0.00
3.31-4.63	17.8 ± 0.8	235 ± 11	0.00	0.00
4.63-6.07	13.9 ± 0.7	200 ± 10	0.00	0.00
6.07-6.44	20.5 ± 0.9	77 ± 4	0.00	0.00
6.44-6.93	27.7 ± 0.9	133 ± 5	0.00	0.00
6.93-7.21	18.1 ± 0.9	50 ± 3	0.00	0.00
7.21-7.69	12.7 ± 0.8	61 ± 4	0.00	0.00
7.69-8.25	7.6 ± 0.8	43 ± 5	0.00	0.00
8.25-8.89	5.1 ± 0.7	10 ± 1	0.00	0.00

Table 5.22 Chernobyl and weapons-testing ^{137}Cs specific activites and inventories in Core 1.

depth g cm^{-2}	Chernobyl ^{137}Cs Bq kg^{-1}	Chernobyl ^{137}Cs Bq m^{-2}	Weapons testing ^{137}Cs Bq kg^{-1}	Weapons testing ^{137}Cs Bq m^{-2}
0-0.39	574 ± 24	2210 ± 93	11224 ± 470	43200 ± 342
0.39-1.15	192 ± 11	1483 ± 83	27.4 ± 1.5	210 ± 12
1.15-2.35	17 ± 3	148 ± 26	14.7 ± 0.9	177 ± 14
2.35-3.31	0.00	0.00	19.8 ± 0.8	190 ± 7.5
3.31-4.63	0.00	0.00	17.8 ± 0.8	235 ± 10.3
4.63-6.07	0.00	0.00	13.9 ± 0.7	200 ± 9.6
6.07-6.44	0.00	0.00	20.5 ± 0.9	77.3 ± 3.7
6.44-6.93	0.00	0.00	27.7 ± 0.9	133 ± 4.8
6.93-7.21	0.00	0.00	18.1 ± 0.9	50.4 ± 2.5
7.21-7.69	0.00	0.00	12.7 ± 0.8	60.9 ± 3.9
7.69-8.25	0.00	0.00	7.6 ± 0.8	42.6 ± 4.7
8.25-8.89	0.00	0.00	5.2 ± 0.7	10.2 ± 1.3

Figure 5.17

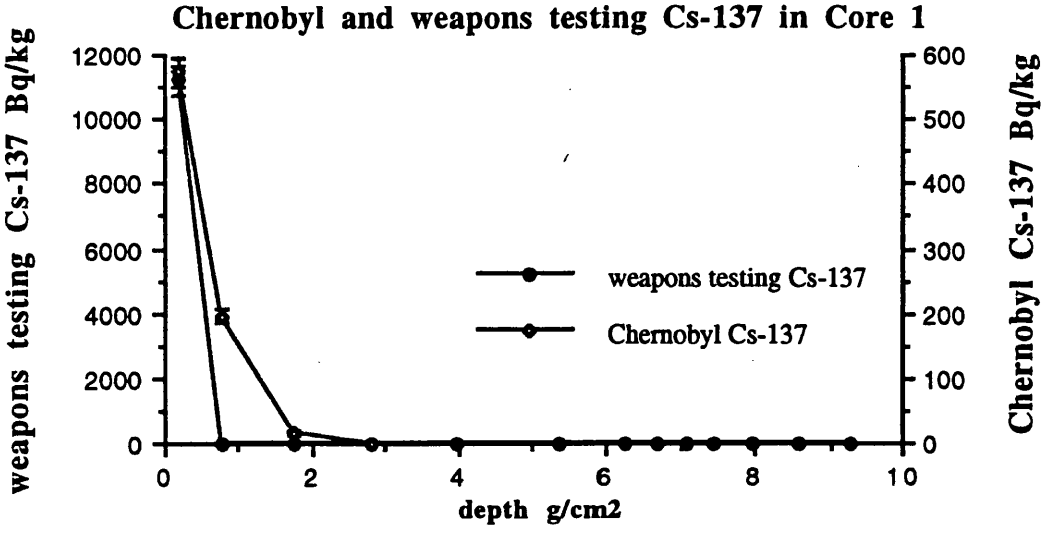

Figure 5.18

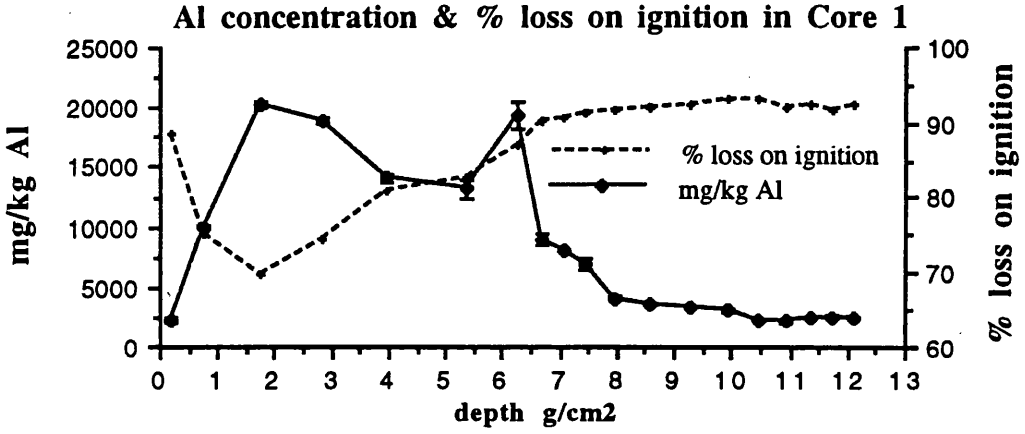

Figure 5.19 La and Ce concentrations in Core 1.

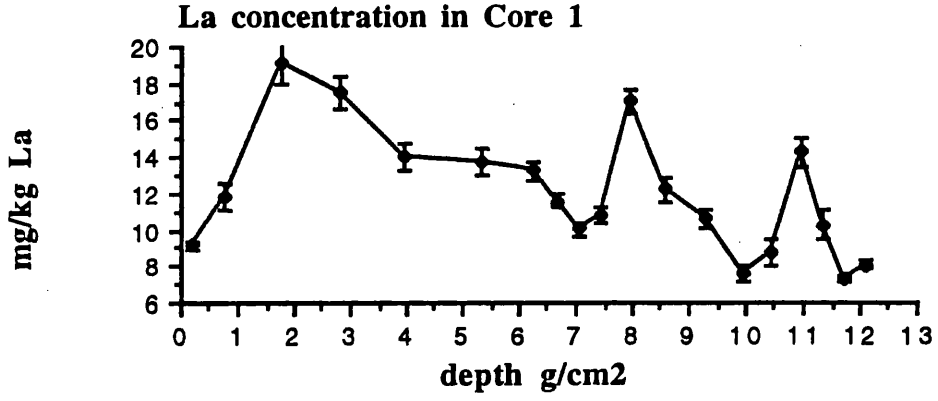

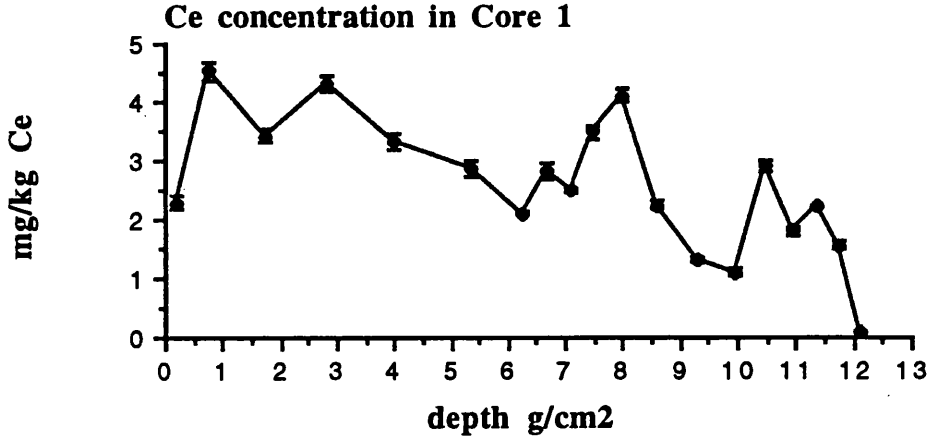

Figure 5.20 Mn and Fe concentrations in Core 1.

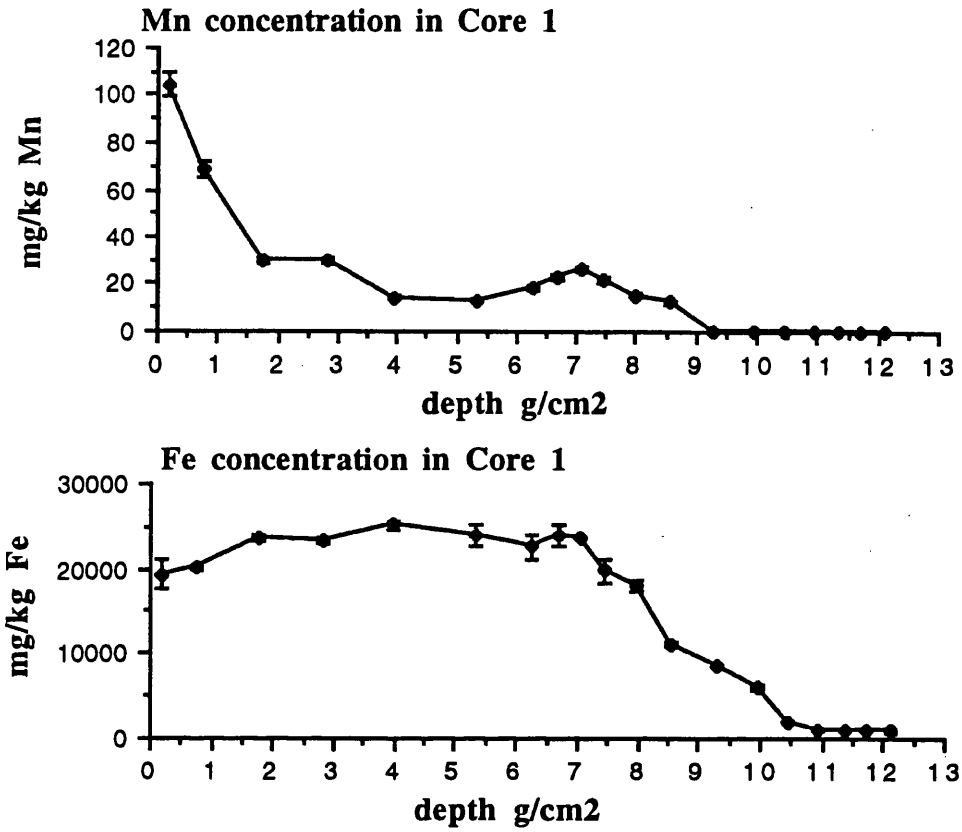

Figure 5.21 Cu and Zn concentrations in Core 1.

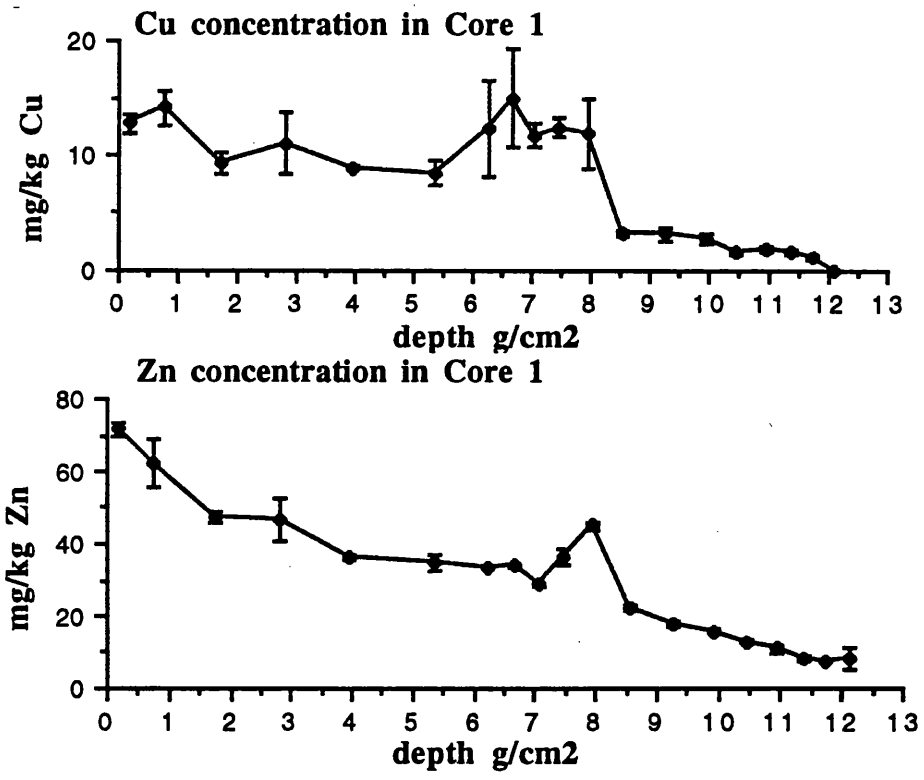

Figure 5.22

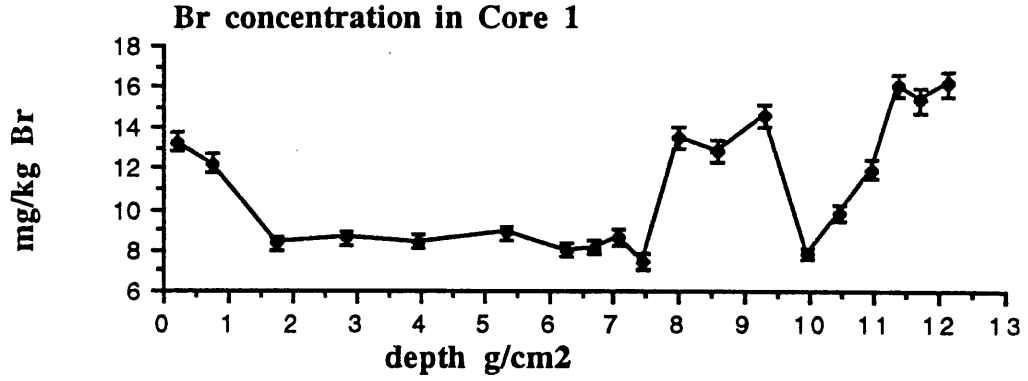

Figure 5.23 Pb, Co and Hg concentrations in Core 1.

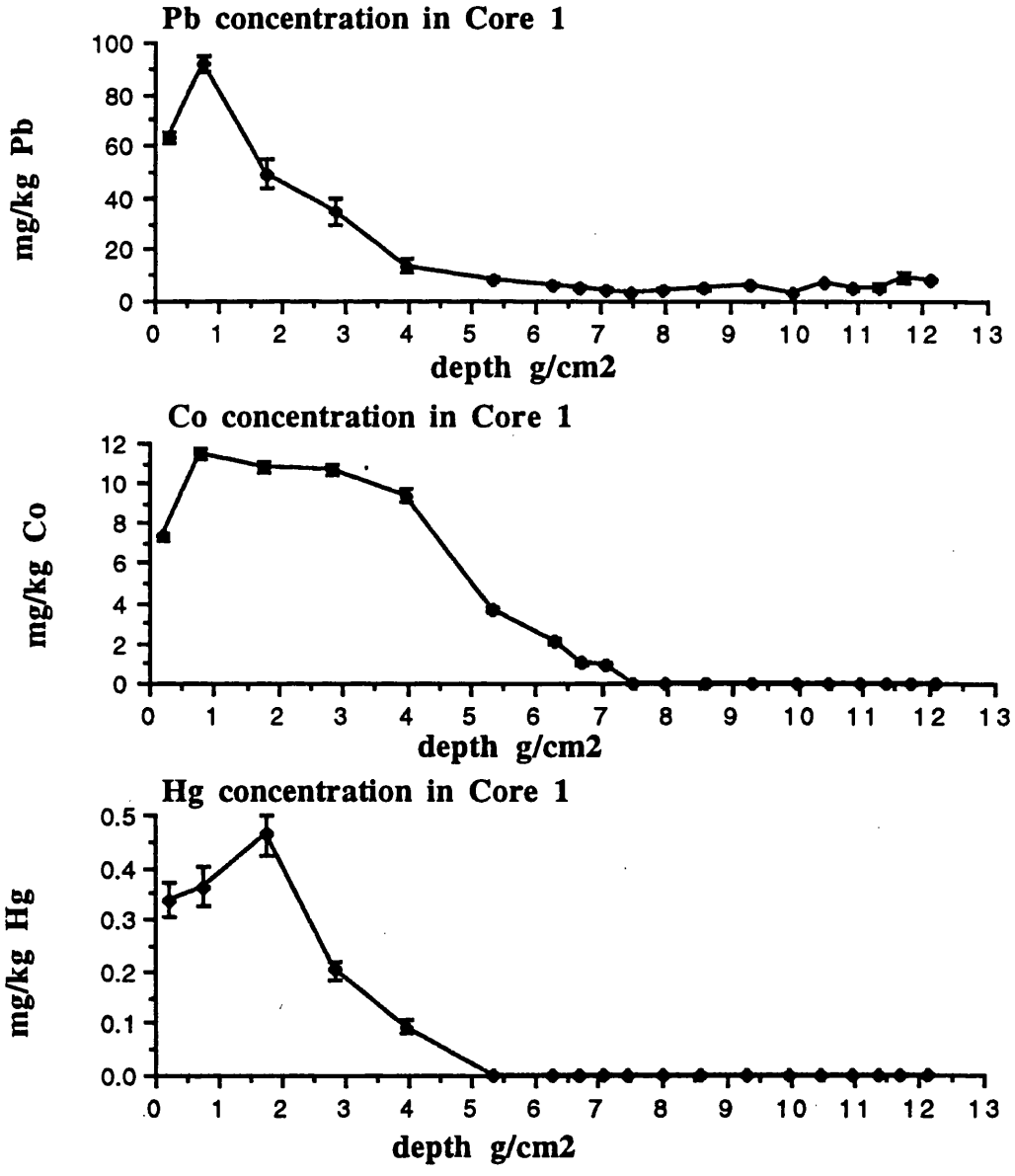

Figure 5.24

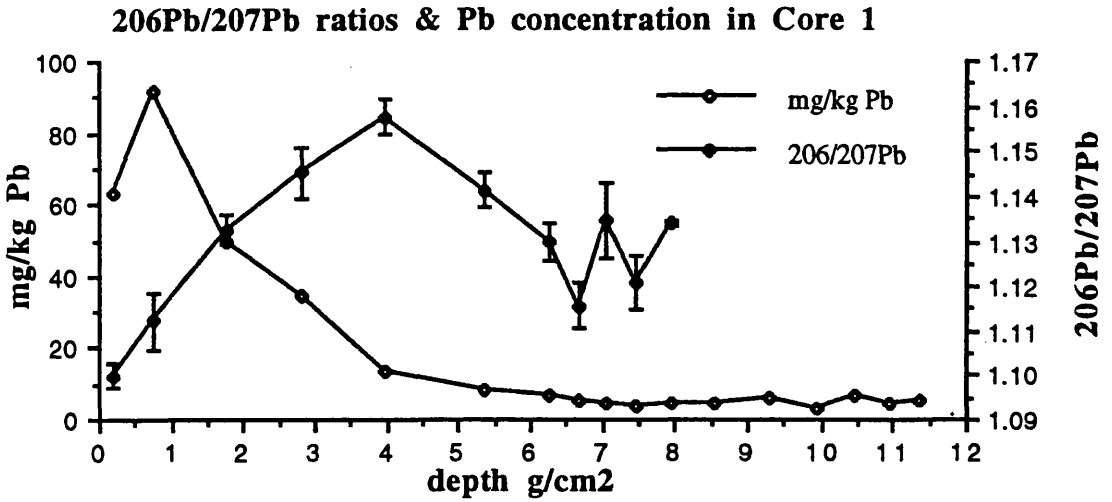
206Pb/207Pb ratios & Pb concentration in Core 1
mg/kg Pb
206/207Pb
mg/kg Pb
206Pb/207Pb
depth g/cm2
0
20
40
60
80
100
1.09
1.10
1.11
1.12
1.13
1.14
1.15
1.16
1.17
0
1
2
3
4
5
6
7
8
9
10
11
12

SOUTH DRUMBOY CORE 2

On sampling Core 2, it was observed that from 4.25 g cm^{-2} (20 cm) depth, a mineral horizon was present. Above the mineral horizon, overlying a compacted pan lay an organic horizon, giving a core which was effectively composed of two quite separate horizons.

As in Core 1, all of the unsupported ^{210}Pb was contained within the surface organic layer, in the first three sections, with no exponential relationship between unsupported ^{210}Pb and depth. In particular, 93% of the total ^{210}Pb inventory was contained within the surface section (Figure 5.25 & Table 5.23). With there being no linear relationship between ln (excess) ^{210}Pb and depth (Figure 5.25), no accumulation rate and therefore, no chronology, were calculated for Core 2. The total ^{210}Pb inventory was calculated as 1704 Bq m^{-2}, giving a flux of 52.8 Bq m^{-2} y^{-1}.

Radiocaesium penetrated further within the profile than ^{210}Pb, being present to 12 g cm^{-2} (Table 5.24) indicating that diffusive and advective processes are promoting vertical mobility within the core. Weapons-testing ^{137}Cs showed the greater penetration (Table 5.26 & Figure 5.26) than Chernobyl ^{137}Cs, which showed an exponential decrease through the profile, consistent with its recent input in conjunction with down-core movement. Weapons-testing ^{137}Cs did not show an exponential decrease, but instead showed a surface maximum and a major sub-surface peak between 3-7 g cm^{-2} (Figure 5.27). This occurred at the organic/mineral horizon, where there is a relatively imperveous compacted mineral pan. Accordingly, water may be flowing downslope along the surface of the pan, bringing ^{137}Cs which could then bind to the mineral material. The presence of mineral material in peat has previously been shown to reduce mobility of ^{137}Cs. Chronological integrity of the peak in weapons-testing ^{137}Cs was retained even though ^{137}Cs was penetrating to depths in the core which were dated before the onset of weapons testing (Schell *et al.*, 1989).

The ^{137}Cs inventory was 6207 Bq m^{-2}, comprising a Chernobyl inventory of 3918 Bq m^{-2} and a weapons-tesing inventory 2287 Bq m^{-2}. In Core 1, the inventory of weapons-testing ^{137}Cs was 45075 Bq m^{-2}, the majority of this being contained in the surface section. This was attributed to washing down of ^{137}Cs through drainage channels and this is supported by the evidence of downslope movement of ^{137}Cs along a mineral pan and with there being a far lower weapons-testing inventory in Core 2.

The Al profile (Figure 5.28) reflected the changes in mineral content in the Core, with Th, La, Sm, and Sc mirroring the effect. Only La is displayed (Figure 5.29) with the remainder of the data being found in Appendix 3.

Ta, Hf, Ce and Se show a slightly different effect, with Ce being displayed in Figure 5.30. These elements show a bimodal peak in concentration at the start of the mineral horizon, similar to the peaking observed for ^{137}Cs, but deeper within the core. This could reflect changes in mineralogy, or could be due to lateral flow through the profile. The mineral horizon (with the exception of the mineral pan) will have an increased permeability compared to the organic horizon, promoting flow of water laterally and vertically throughout the horizon.

The Mn and Fe profiles (Figure 5.31) indicate that quite different processes are occurring in the organic and mineral horizons. In the organic horizon, the Mn concentration drops off from the surface in an exponential manner, indicating that conditions are becoming increasingly reducing. Fe does not show any reduction in concentration until 3 g cm^{-2}, at the point of lowest Mn concentration, again indicating that Mn is being reduced before Fe. Both Fe and Mn show an increase in concentration at this point, as the mineral pan is approached with the increase continuing into the mineral horizon. The increase in Fe and Mn concentration could therefore be directly related to the increase in mineral content. In addition to the mineral content, the production of metal sulphides may be occurring, as previously discussed in Core 1.

Cu (Figure 5.32) shows a very similar profile to Mn, indicating that it is being affected by the same processes. Zn (Figure 5.32) shows a slightly different profile, with minimal reduction in concentration in the organic horizon and clear fluctuation in the mineral horizon. This fluctuation may represent changes in the water table level, causing continuous dissolution and redeposition of ZnS around the zone of fluctuation. Alternatively lateral flow through the core could be occurring, as already discussed for Ta, Hf, Ce and Se.

As with Core 1, Br (Figure 5.33) is associated with the organic matter, and shows a distinct peak at 3 g cm^{-2}, at the point when conditions have been demonstrated to become most reducing.

Pb, Co, Hg, As and Sb all show similar profiles, with Pb, Co and Hg being displayed in Figure 5.34. The high surface concentrations may be attributed to pollutant input. All metals show a peak in the second section, which may be representing a peak in pollutant output in the locality.

The $^{206}Pb/^{207}Pb$ ratios show a distinct reduction as conditions change from mineral to organic at 4 g cm^{-2} (Figure 5.35). However, in the organic horizon, the ratios show a decrease to surface values of ~1.13, indicating the increasing influence of car exhaust emissions on the Pb isotope ratios and Pb content.

The main differences between Core 1 and Core 2 were due to the the mineral horizon, which resulted in a totally different geochemical environment to the surface

organic horizon. In addition, the two horizons were seperated by a mineral pan which may have promoted downslope movement of peat water, leading to the observed peak in weapons-testing ^{137}Cs, and the redeposition of reduced Mn and Fe. This may also have facilitated downslope washing of weapons-testing ^{137}Cs, leading to the high inventory of ^{137}Cs in Core 1. Lateral flow of ^{137}Cs has been demonstrated to be more significant than vertical movement within the profile in soils of upland ecosystems (Coughtrey *et al.*, 1990). In addition, leaching of ^{210}Pb may have been promoted, leading to the observed profiles in both cores.

Thus, for Cores 1 and 2, interpretation of the chronology of pollutant metal deposition is complicated by disturbance of the peat, and also reduction and leaching processes.

Table 5.23 ^{210}Pb and ^{226}Ra specific activites and excess ^{210}Pb inventories for Core 2

depth cm	depth gcm^{-2}	total ^{210}Pb $Bq\ kg^{-1}$	^{226}Ra $Bq\ kg^{-1}$	excess ^{210}Pb $Bq\ kg^{-1}$	excess ^{210}Pb $Bq\ m^{-2}$
0-4.0	0-0.78	204.2± 8.90	0.00	204 ± 8.90	1583 ± 69
4.0-7.0	0.78-1.66	9.9 ± 0.97	0.00	9.9 ± 0.97	87.6 ± 8.7
7.0-9.5	1.66-2.15	6.8 ± 1.03	0.00	6.8 ± 1.03	33.2 ± 5.1
9.5-11.7	2.15-2.67	0.00	0.00	0.00	0.00
11.7-14.6	2.67-3.10	0.00	0.00	0.00	0.00
14.6-17.1	3.10-3.49	0.00	4.7 ± 0.84	0.00	0.00
17.1-20.1	3.49-4.25	0.00	0.9 ± 0.09	0.00	0.00
20.1-24.1	4.25-4.65	0.00	4.40± 0.36	0.00	0.00
24.1-28.1	4.65-5.29	0.00	10.4 ± 0.54	0.00	0.00
28.1-31.7	5.29-6.28	10.8 ± 1.7	9.9 ± 0.60	0.00	0.00
31.7-34.7	6.28-7.29	11.3 ± 2.0	10.9 ± 0.61	0.00	0.00
34.7-38.7	7.29-8.14	11.9 ± 2.0	12.2 ± 0.62	0.00	0.00

Figure 5.25 ^{210}Pb profiles for Core 2.

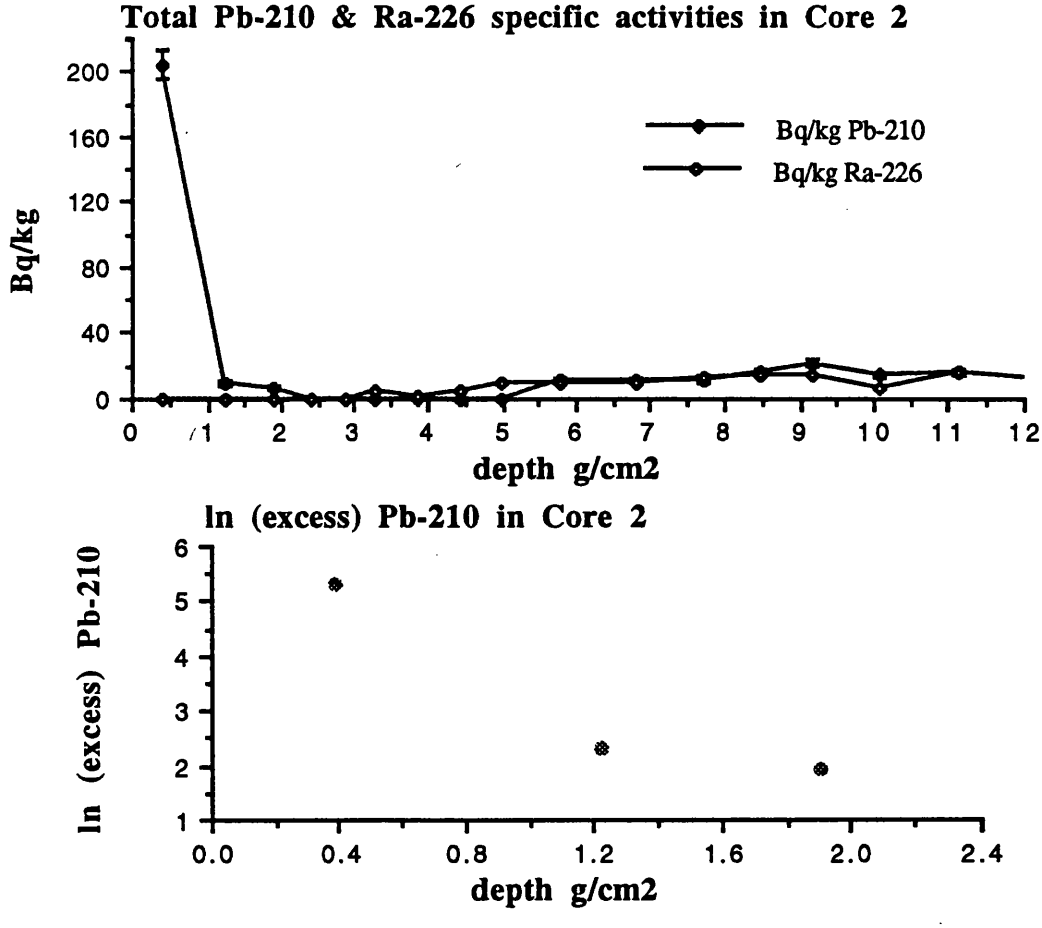

Table 5.24 ^{134}Cs and ^{137}Cs specific activities and inventories in Core 2.

depth g cm^{-2}	Total ^{137}Cs Bq kg^{-1}	Total ^{137}Cs Bq m^{-2}	^{134}Cs Bq kg^{-1}	^{134}Cs Bq m^{-2}
0-0.78	470 ± 8.7	3650 ± 67	32 ± 1.7	248 ± 13
0.78-1.66	104 ± 2.3	924 ± 20	4.7 ± 0.7	42 ± 6.3
1.66-2.15	24 ± 0.8	119 ± 3.8	0.6 ± 0.2	3.1 ± 1.7
2.15-2.67	12 ± 0.7	65 ± 3.7	0.00	0.00
2.67-3.10	16 ± 0.8	71 ± 3.4	0.00	0.00
3.10-3.49	40 ± 1.8	157 ± 7.0	0.00	0.00
3.49-4.25	36 ± 1.1	270 ± 7.9	0.00	0.00
4.25-4.65	37 ± 1.2	148 ± 4.6	0.00	0.00
4.65-5.29	28 ± 0.9	181 ± 5.9	0.00	0.00
5.29-6.28	27 ± 0.9	265 ± 8.8	0.00	0.00
6.28-7.29	18 ± 1.4	181 ± 14	0.00	0.00
7.29-8.14	8.2 ± 0.6	70 ± 5.3	0.00	0.00
8.14-8.80	2.3 ± 0.4	28 ± 2.8	0.00	0.00
8.80-9.56	2.9 ± 0.4	22 ± 3.2	0.00	0.00
9.56-10.61	3.5 ± 0.4	37 ± 4.1	0.00	0.00
10.61-11.62	2.9 ± 0.3	19 ± 3.7	0.00	0.00

Figure 5.26

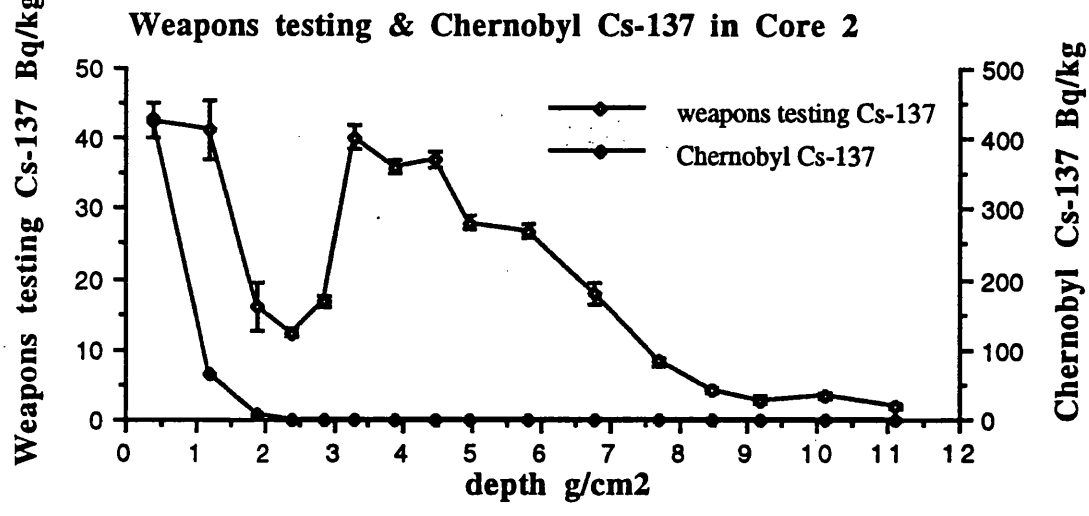

Table 5.25 Chernobyl and weapons-testing ^{137}Cs specific activities and inventories for Core 2.

depth g cm^{-2}	Chernobyl ^{137}Cs Bq kg^{-1}	Chernobyl ^{137}Cs Bq m^{-2}	Weapons testing ^{137}Cs Bq kg^{-1}	Weapons testing ^{137}Cs Bq m^{-2}
0-0.78	427.4 ± 23.7	3320 ± 183	42.5 ± 2.3	330 ± 18
0.78-1.66	63.2 ± 9.6	559 ± 85	41.2 ± 6.2	364 ± 55
1.66-2.15	8.5 ± 2.7	42 ± 14	16.1 ± 2.3	79 ± 11
2.15-2.67	0.00	0.00	12.4 ± 0.7	65 ± 3.7
2.67-3.10	0.00	0.00	16.7 ± 0.8	71 ± 3.4
3.10-3.49	0.00	0.00	40.3 ± 1.8	157 ± 7.0
3.49-4.25	0.00	0.00	36.0 ± 1.0	270 ± 7.9
4.25-4.65	0.00	0.00	37.1 ± 1.1	148 ± 4.6
4.65-5.29	0.00	0.00	27.9 ± 0.9	181 ± 5.9
5.29-6.28	0.00	0.00	26.9 ± 0.9	265 ± 8.8
6.28-7.29	0.00	0.00	17.9 ± 1.4	181 ± 14
7.29-8.14	0.00	0.00	8.2 ± 0.6	70 ± 5.3
8.14-8.80	0.00	0.00	4.3 ± 0.4	28 ± 2.8
8.80-9.56	0.00	0.00	2.9 ± 0.4	22 ± 3.2
9.56-10.61	0.00	0.00	3.5 ± 0.4	37 ± 4.1
10.61-11.62	0.00	0.00	1.9 ± 0.4	19 ± 3.7

Figure 5.27

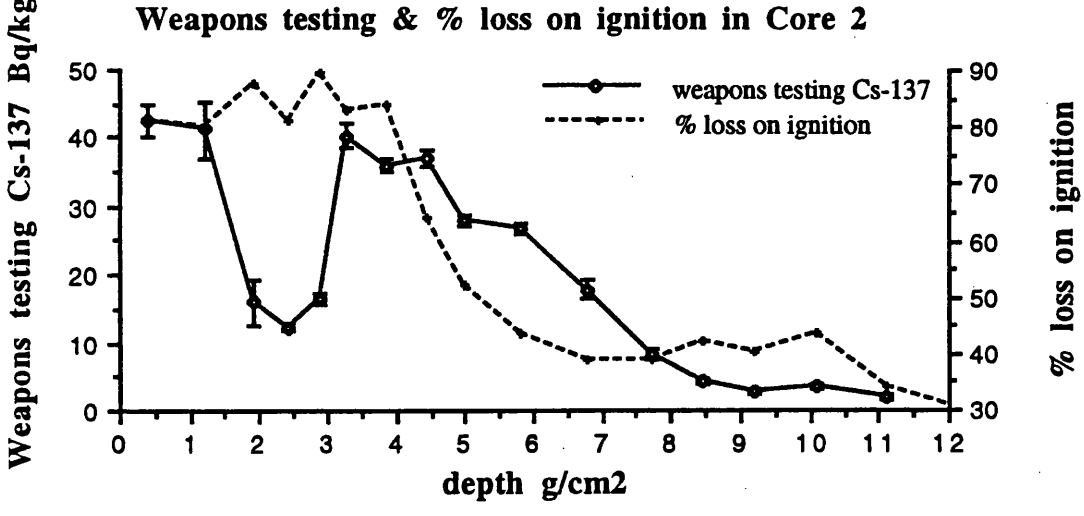

Figure 5.28

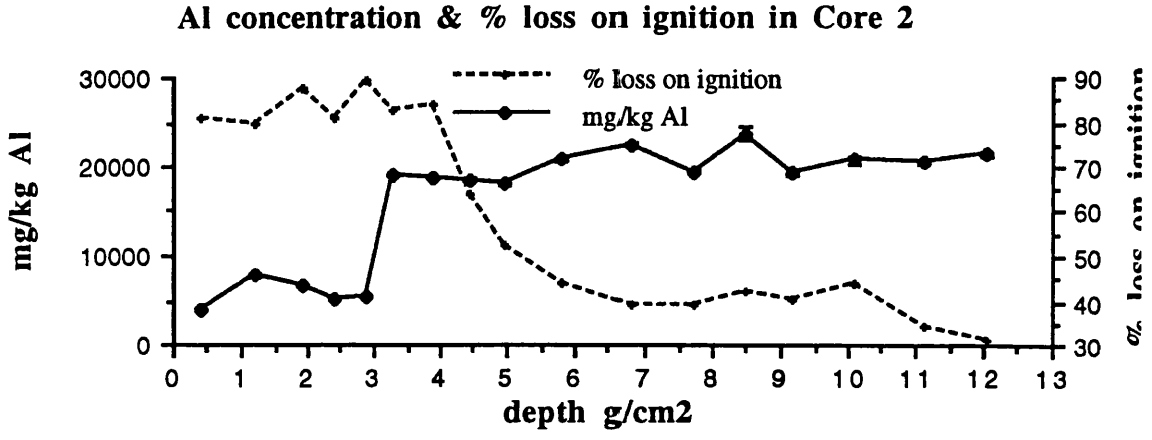

Figure 5.29

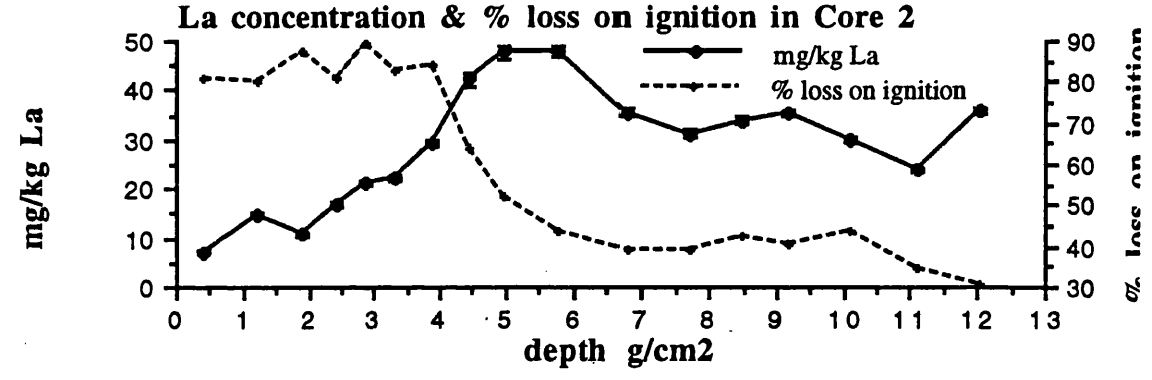

Figure 5.30

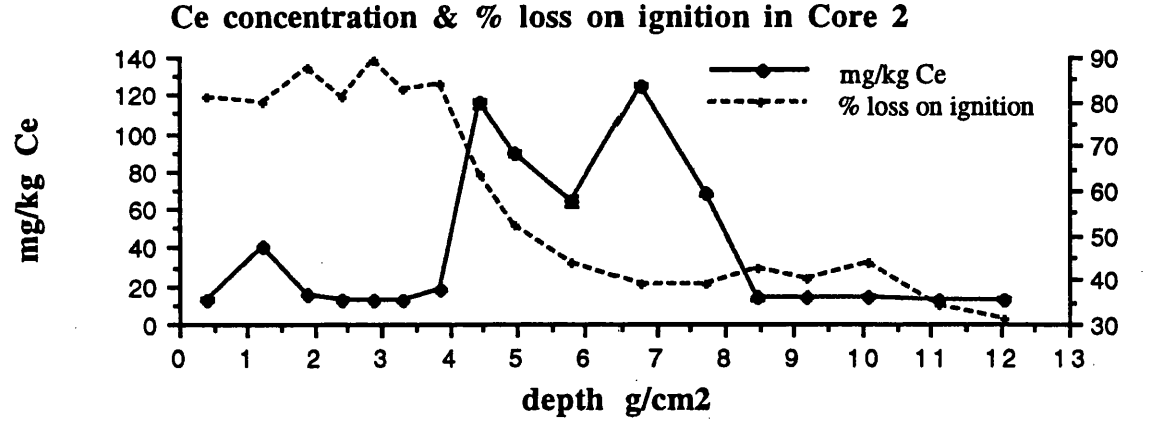

Figure 5.31 Mn and Fe concentrations in Core 2.

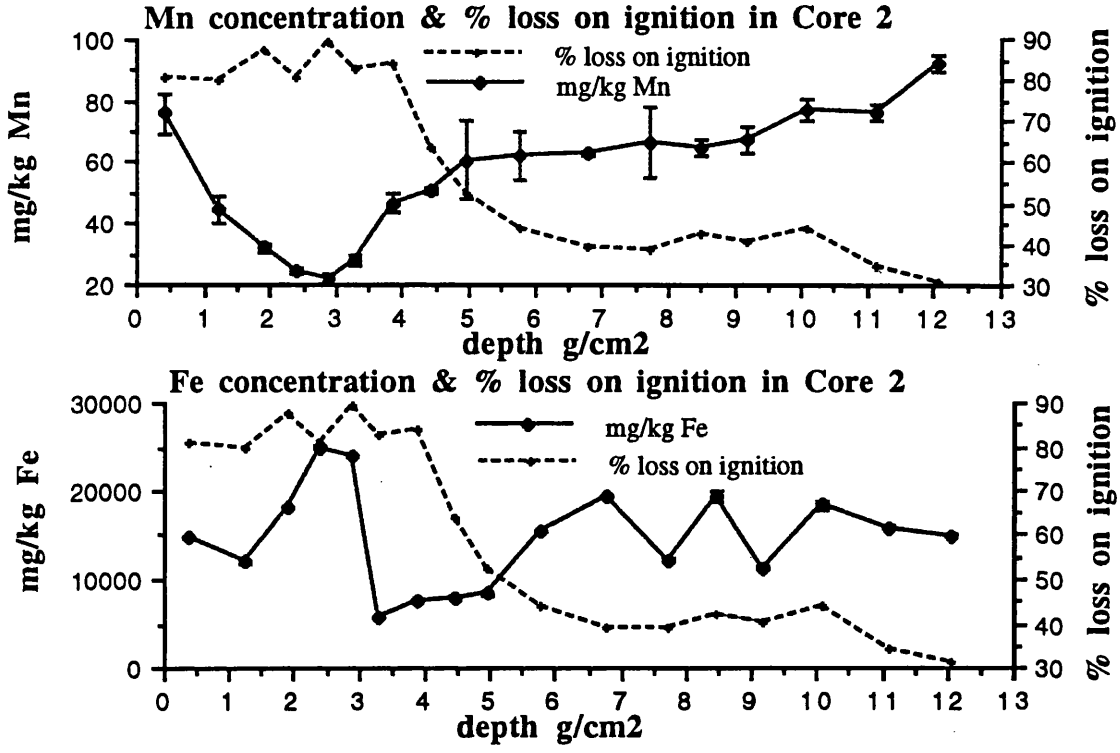

Figure 5.32 Cu and Zn concentrations in Core 2.

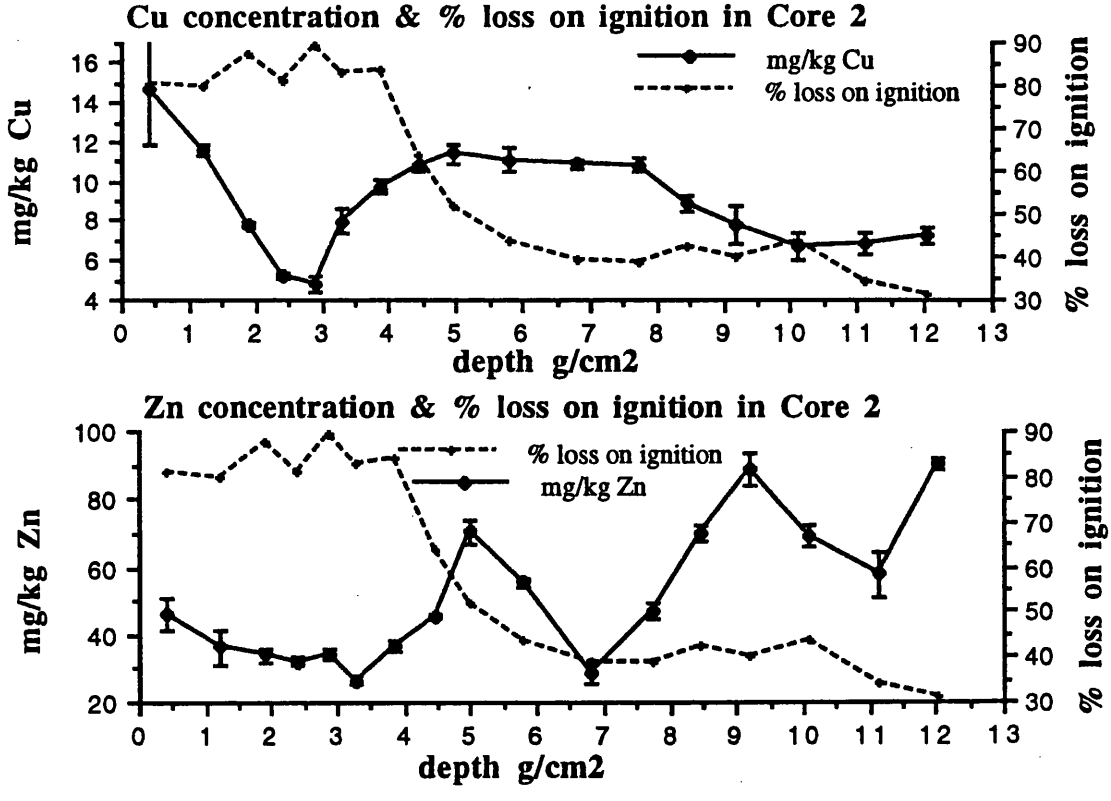

Figure 5.33

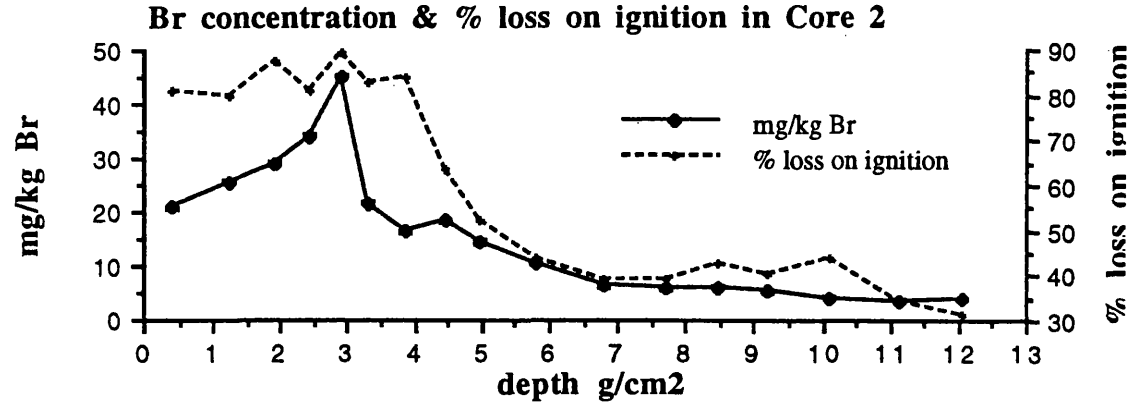

Figure 5.34 Pb, Co and Hg concentrations in Core 2.

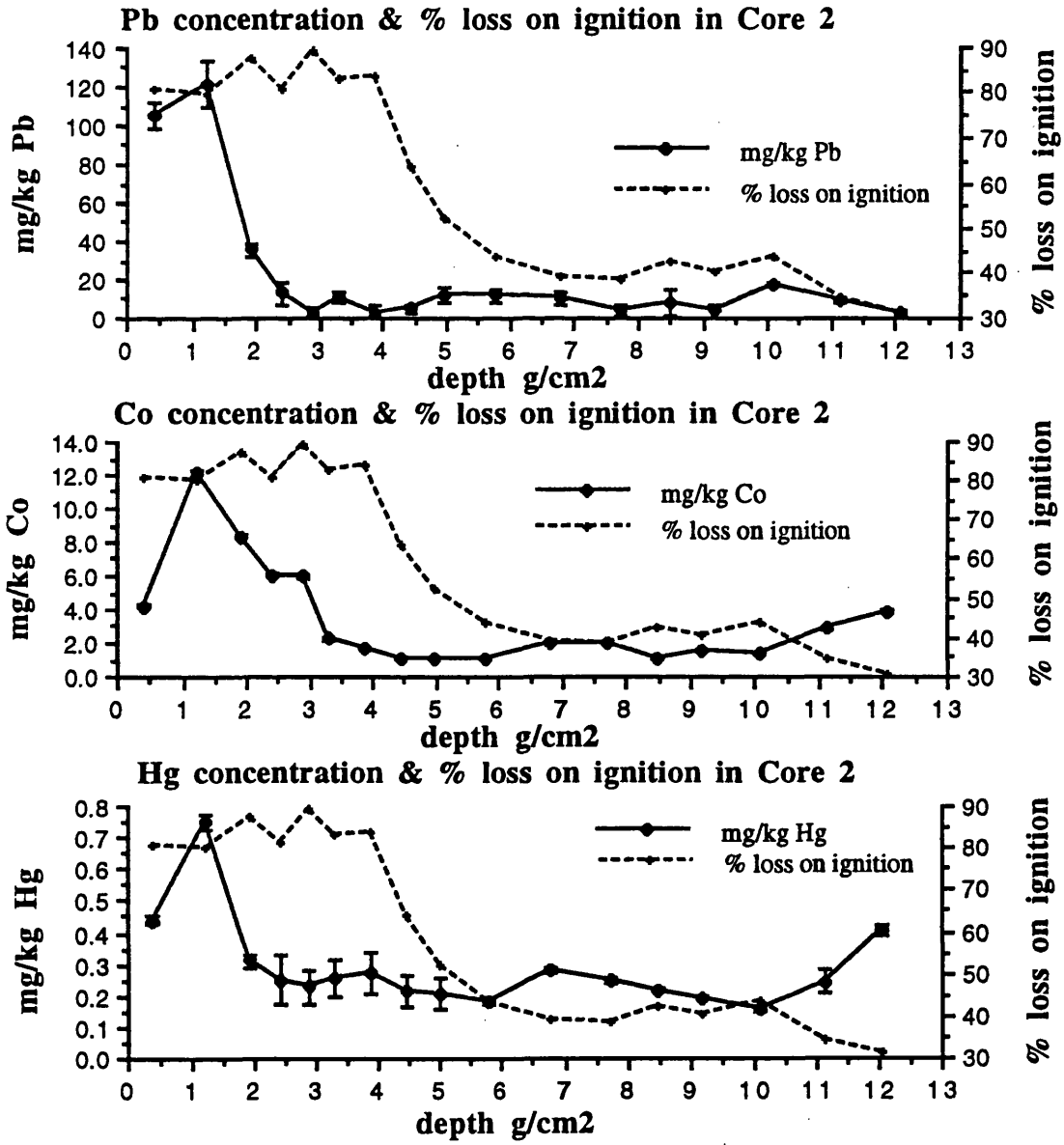

Figure 5.35

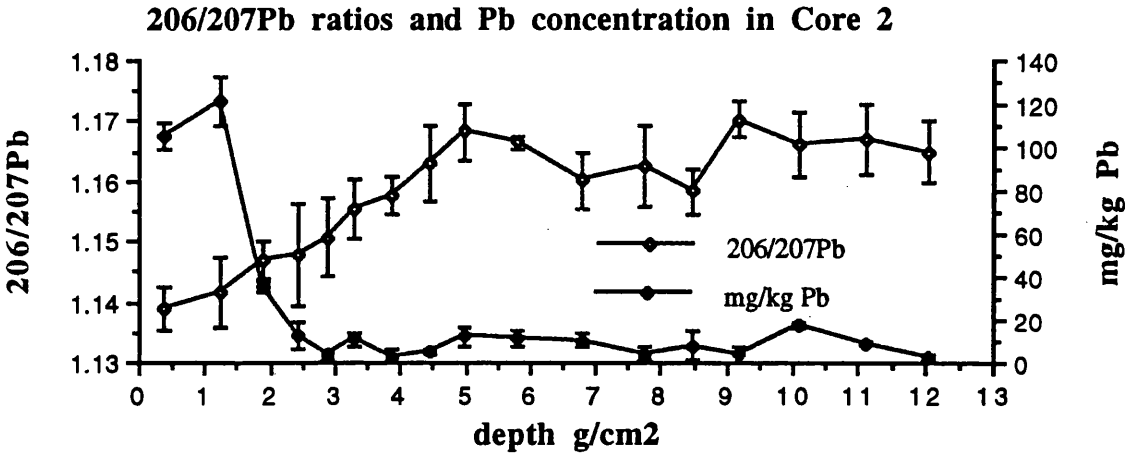
206/207Pb ratios and Pb concentration in Core 2
206/207Pb
mg/kg Pb
depth g/cm2
1.18
1.17
1.16
1.15
1.14
1.13
140
120
100
80
60
40
20
0
0 1 2 3 4 5 6 7 8 9 10 11 12 13
206/207Pb
mg/kg Pb

SOUTH DRUMBOY CORE 3

This core was sampled close to the summit of Drumboy Hill, on the westerly facing slope and shows quite different characteristics and metal profiles from the previous cores discussed. The % moisture, loss on ignition and the bulk density are all effectively uniform throughout the profile and indicate that this is a well humified, ombrotrophic peat. In the top three sections of the core there appears to be mixing of the peat, disturbing the ^{210}Pb profile (Figure 5.36). Mixing could be due to biological activity such as root growth or had the pH been higher earthworm activity could have been proposed. In addition, grazing sheep may be causing physical mixing of the surface sections. Whatever the explanation the mixing processes here are rapid and result in a reasonably constant ln (excess) ^{210}Pb activity over the mixed zone. Had mixing been slow the activity would not have been constant over the mixed zone but would have appeared as a change in accumulation rate. Below the mixing zone a normal radionuclide pattern was observed and an accumulation rate of 0.031g cm^{-2} y^{-1} was calculated from linear regression of the ln (excess) ^{210}Pb activity from the base of the mixed sections. The total inventory of ^{210}Pb was calculated as 3432 Bq m^{-2}, giving a flux of 106 Bq m^{-2} y^{-1} (Table 5.26).

The mixing processes also affect the metal and radiocaesium profiles. Chernobyl caesium was deposited over a short period of time and rapid mixing would result in mixing of the radiocaesium deposited at the peat surface through the mixing zone to the older peat at the base of the mixed zone. This effectively increases the apparent time elapsed since the deposition event. Heavy metals such as Pb, Cu, Hg, etc. have been deposited on peats over a longer period of time with variations in the metal fluxes to the peat surface over this time. Rapid mixing smooths out short variations in input over the mixing depth and displaces peak pollutant metal fluxes and the onset of the increase in pollutant inputs by the depth of the peat in the mixed zone, again increasing the apparent time elapsed since the deposition event. To compensate for this effect the chronology calculated for the metals and radionuclides begins at the base of the mixed zone and is not the actual date of the peat deposit.

Radiocaesium shows considerable penetration through the peat, to depths dated well before the advent of weapons testing (Table 5.27). Weapons-testing ^{137}Cs shows a slight peak in activity at 2 g cm^{-2} (Figure 5.37), which was dated as representing the period between 1964 and 1947 (Table 5.28). In Core 2, a peak in weapons-testing ^{137}Cs was also observed, occurring over an imperveous mineral pan indicating that the peak in ^{137}Cs was due to lateral flow. Thus, lateral flow could also be contributing to the peak in ^{137}Cs activity observed in Core 3. The total inventory of ^{137}Cs was

calculated as 11604 Bq m^{-2}, with a weapons-testing inventory of 3528 Bq m^{-2} and a Chernobyl inventory of 8076 Bq m^{-2}. The total inventory of ^{134}Cs was 497 Bq m^{-2}.

The Al concentration (Figure 5.38) is an order of magnitude lower than for Cores 1 and 2, reflecting the lower mineral content of this peat. However, at depth, as the % loss on ignition decreases the Al concentration also decreases. Ce, Ta, Hf, Se, Sc, Sm, La, and Th also show this effect, as illustrated by La and Ce (Figure 5.39). Unlike Al, these elements also show a peak in concentration at 1.5 g cm^{-2} indicating an increase in the mineral content at this point. Interestingly, this occurs in the same section as the peak in weapons-testing ^{137}Cs.

The Mn and Fe profiles (Figure 5.40) suggest that to a depth of 1.5 g cm^{-2}, conditions are only reducing enough to bring Mn into solution. Beneath 1.5 g cm^{-2} conditions are reducing enough to promote the dissolution of Fe. The Fe concentration throughout the profile is an order of magnitude lower than for Cores 1 and 2, reflecting the reduced mineral content of the peat.

Cu (Figure 5.41) shows a distinct peak in concentration at 2 g cm^{-2} and below 3 g cm^{-2} there is no Cu detected. With conditions becoming more reducing from 1.5 g cm^{-2} this peak could be due to deposition of CuS around the zone of water fluctuation. However, there is no observed deposition of FeS_2 which is more readily formed than CuS (Rowell, 1988). Accordingly the peak in Cu is more likely to be due to increases in pollutant input. Zn (Figure 5.41) does not show this distinct peak in deposition and instead shows a progressive decrease in concentration with depth. Jones (1987) attributed Zn mobility to it being co-precipitated with Mn and Fe oxides, whereas Cu was predominantly bound to organic matter. Zn mobility in surface sections has also been explained by it being an essential element for plant growth (Livett *et al.*, 1979: Shotyk *et al.*, 1990: Jones & Hao, 1993). However, Cu and Mn are also essential elements for plant growth.

Pb Co, Hg, As and Sb all show a distinct peak in concentration at 2 g cm^{-2}, as previously seen for Cu (Figure 5.43,Table 5.29 & Appendix 3). In addition Br (Figure 5.42) shows a peak in concentration at depth, giving a very similar profile to Pb. This may be an indication of the importance of car exhaust emissions on the Pb concentration, since Te Haar & Bayard (1971) observed that when car exhaust particles are emitted they mainly consist of $PbBr_2$, PbBrCl, Pb(OH)Br, $Pb(O)_2PbBr_2$, and $Pb(O)_2PbBrCl$. After around 18 hours, about 75% of the Br is lost from these particles. The Br/Pb ratio of soils has also been used to establish the relative importance of industry and car exhausts on the Pb content (Sturges & Harrison, 1986). However, the Br/Pb ratio of petrol can vary, and suitable background, or pre-industrial ratios must be established before the ratio can be used with any accuracy. But Br could

also be released from the burning of fossil fuels since bitumous coal has a Br content of 45 ppm (NBS SRM 1632a: Schell, 1987). With the peaking in concentration of the rare earth elements and metals occurring in the same section as the Br, the increased burning of fossil fuels is the most likely cause.

The $^{206}Pb/^{207}Pb$ ratios (Figure 5.44) decrease towards the surface of the core, as expected. Sugden (1993) recorded pre-1900 $^{206}Pb/^{207}Pb$ values of 1.17-1.18, which decreased to 1.14 during the course of the 20th century as Pb of low ^{206}Pb content was introduced into the atmosphere from car exhaust emissions. In Core 3, the reduction in $^{206}Pb/^{207}Pb$ ratio from 1.16 to 1.12 begins in the section dated 1947-1924 (Figure 5.44), consistent with the introduction of Pb as an additive to petrol in the 1920s. The Pb concentration peaks between 1964 and 1947, after which it decreases systematically with the $^{206}Pb/^{207}Pb$ ratios showing a continuous drop, indicating that car exhaust emissions are an increasingly important component to the Pb deposited.

Before 1900, the $^{206}Pb/^{207}Pb$ ratios have a value of around 1.18, upon which there are distinct peaks in the sections dated between 1848 and 1832 (1.24) and in the section dated as representing 1762 to 1741 (1.28). These increases are reflecting inputs of high ^{206}Pb content Pb into the atmosphere and may be due to the advent of industrial processes in the locality. However, the total concentration of Pb is not contaminating, being below the limit of detection of the analysis.

Table 5.26 ^{210}Pb and ^{226}Ra specific activites and excess ^{210}Pb inventories for Core 3.

depth cm	depth g cm^{-2}	total ^{210}Pb Bq kg^{-1}	^{226}Ra Bq kg^{-1}	excess ^{210}Pb Bq kg^{-1}	excess ^{210}Pb Bq m^{-2}
0 - 2.0	0.0-0.28	197.6 ± 4.4	1.2 ± 0.3	196.4 ± 21.2	546 ± 59
2.0 - 4.7	0.28-0.78	189.4 ± 11.0	5.9 ± 1.4	183.4 ± 23.3	949 ± 121
4.7-6.7	0.78-1.25	176.3 ± 8.6	10.0 ± 1.3	166.3 ± 21.3	831 ± 106
6.7-9.0	1.25-1.65	128.5 ± 10.9	6.9 ± 1.3	121.5 ± 21.4	520 ± 73
9.0-12.0	1.65-2.18	80.3 ± 4.3	13.7 ± 2.3	66.6 ± 13.9	438 ± 91
12.0-15.2	2.18-2.90	10.0 ± 3.2	9.7 ± 1.9	0.00	0.00
15.2-18.4	2.90-3.74	9.1 ± 3.2	9.2 ± 2.5	0.00	0.00
18.4-21.0	3.74-4.26	BDL	5.7 ± 1.0	0.00	0.00

Figure 5.36 ^{210}Pb profiles for Core 3.

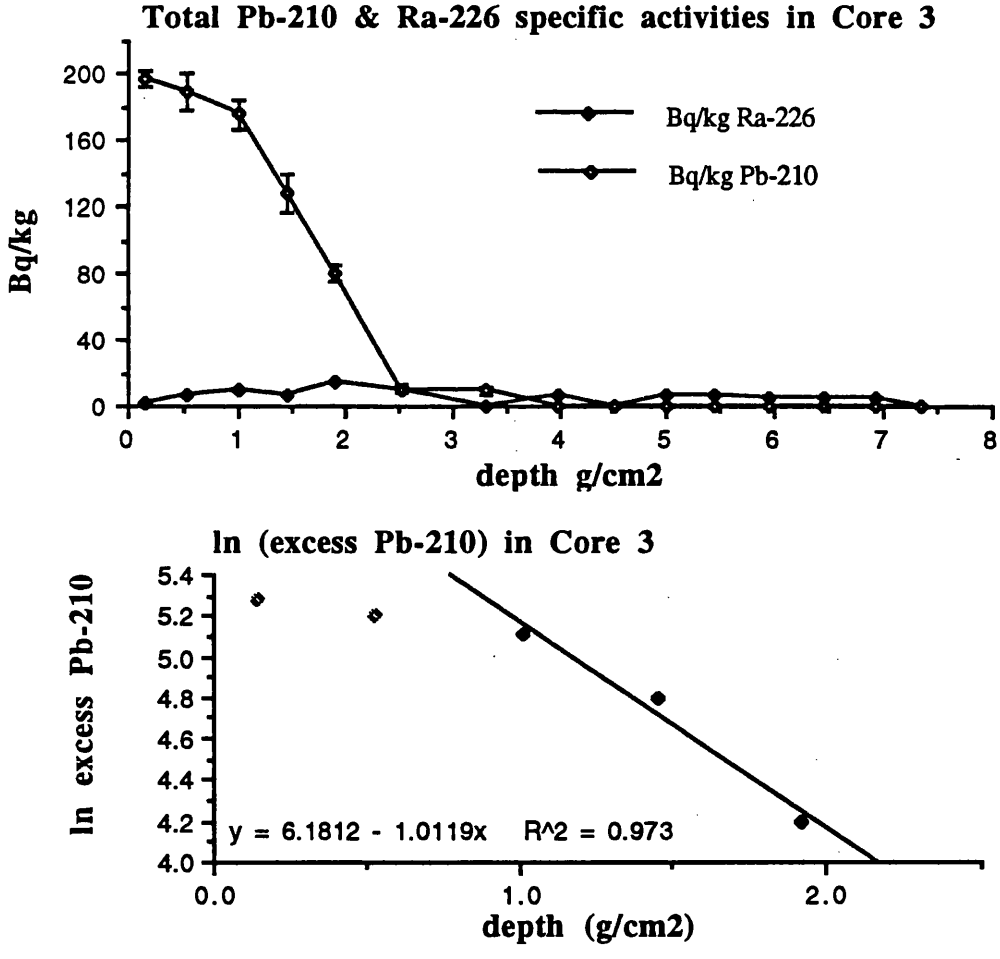

Table 5.27 ^{134}Cs and ^{137}Cs specific activites and inventories in Core 3.

depth g cm^{-2}	date	Total ^{137}Cs Bq kg^{-1}	Total ^{137}Cs Bq m^{-2}	^{134}Cs Bq kg^{-1}	^{134}Cs Bq m^{-2}
0.0-0.28	*mixed zone*	935 ± 18	4691 ± 90	37 ± 3	229 ± 13
0.28-0.78	*mixed zone*	820 ± 16	2264 ± 43	46 ± 3	102 ± 8
0.78-1.25	1993-1977	424 ± 8	1998 ± 38	22 ± 0.7	103 ± 4
1.25-1.65	1977-1964	122 ± 3	491 ± 11	8.8 ± 1.0	17 ± 3
1.65-2.18	1964-1947	236 ± 4	1248 ± 22	5.2 ± 0.9	47 ± 7
2.18-2.90	1947-1924	47 ± 2	388 ± 13	0.00	0.00
2.90-3.74	1924-1896	21 ± 1	179 ± 9	0.00	0.00
3.74-4.26	1896-1879	14 ± 1	72 ± 6	0.00	0.00
4.26-4.76	1879-1862	8.8 ± 0.9	45 ± 4	0.00	0.00
4.76-5.20	1862-1848	9.4 ± 1.0	40 ± 4	0.00	0.00
5.20-5.69	1848-1832	9.0 ± 0.9	44 ± 5	0.00	0.00
5.69-6.21	1832-1815	10.0 ± 0.8	53 ± 5	0.00	0.00
6.21-6.67	1815-1800	10.5 ± 0.9	48 ± 4	0.00	0.00
6.67-7.15	1800-1785	8.9 ± 0.9	43 ± 5	0.00	0.00

Table 5.28 Chernobyl and weapons testing ^{137}Cs specific activites and inventories in Core 3.

depth g cm^{-2}	date	Chernobyl ^{137}Cs Bq kg^{-1}	Chernobyl ^{137}Cs Bq m^{-2}	Weapons testing ^{137}Cs Bq kg^{-1}	Weapons testing ^{137}Cs Bq m^{-2}
0.0-0.28	*mixed zone*	740 ± 44	1662 ± 112	200 ± 15	637 ± 59
0.28-0.78	*mixed zone*	602 ± 45	3714 ± 247	195 ± 12	1004 ± 46
0.78-1.25	1993-1977	353 ± 12	1678 ± 60	70 ± 3	331 ± 12
1.25-1.65	1977-1964	84 ± 13	577 ± 136	37 ± 6	152 ± 25
1.65-2.18	1964-1947	143 ± 20	445 ± 43	93 ± 13	492 ± 68
2.18-2.90	1947-1924	0.00	0.00	47 ± 2	388 ± 13
2.90-3.74	1924-1896	0.00	0.00	21 ± 1	179 ± 9
3.74-4.26	1896-1879	0.00	0.00	14 ± 1	72 ± 6
4.26-4.76	1879-1862	0.00	0.00	8.8 ± 0.9	45 ± 4
4.76-5.20	1862-1848	0.00	0.00	9.4 ± 1.0	40 ± 4
5.20-5.69	1848-1832	0.00	0.00	9.0 ± 0.9	44 ± 5
5.69-6.21	1832-1815	0.00	0.00	10.0 ± 0.8	53 ± 5
6.21-6.67	1815-1800	0.00	0.00	10.5 ± 0.9	48 ± 4
6.67-7.15	1800-1785	0.00	0.00	8.9 ± 0.9	43 ± 5

Figure 5.37

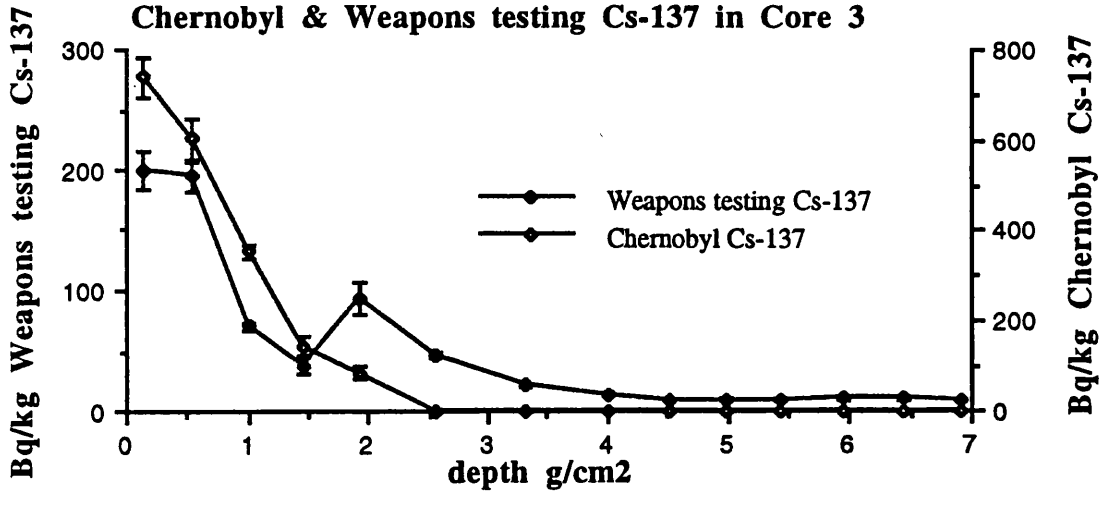

Figure 5.38

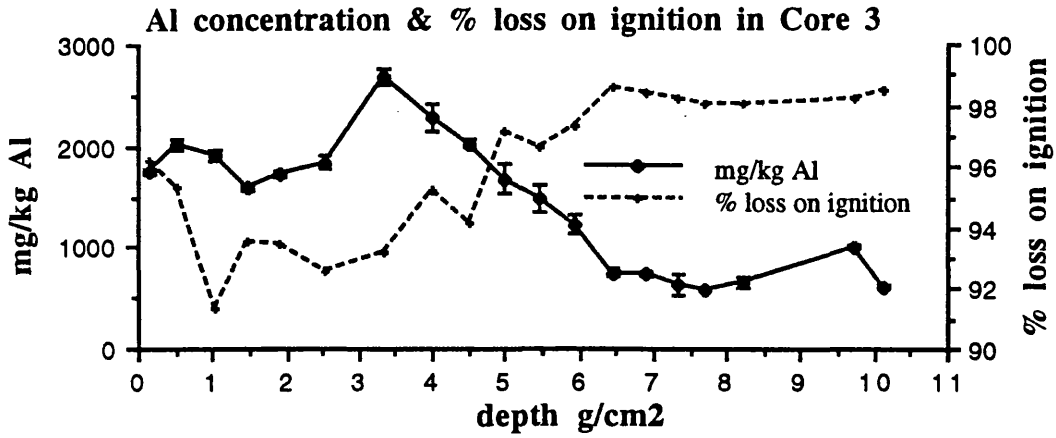

Figure 5.39 La and Ce concentrations in Core 3.

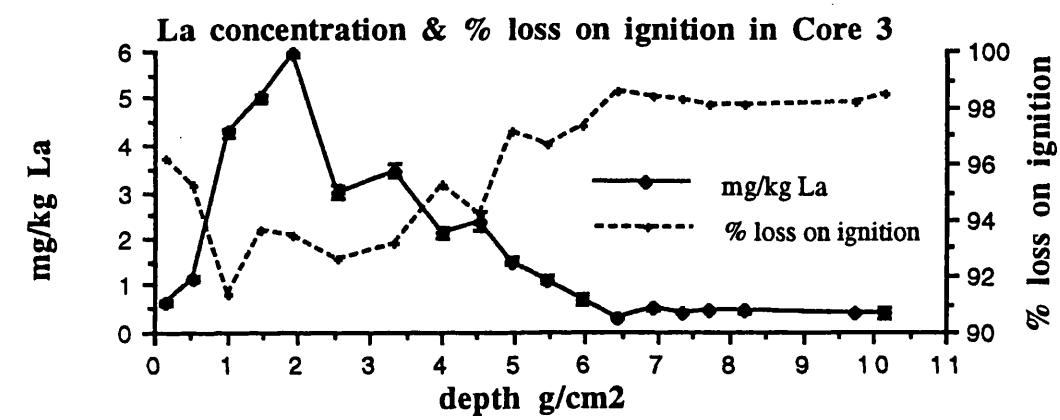

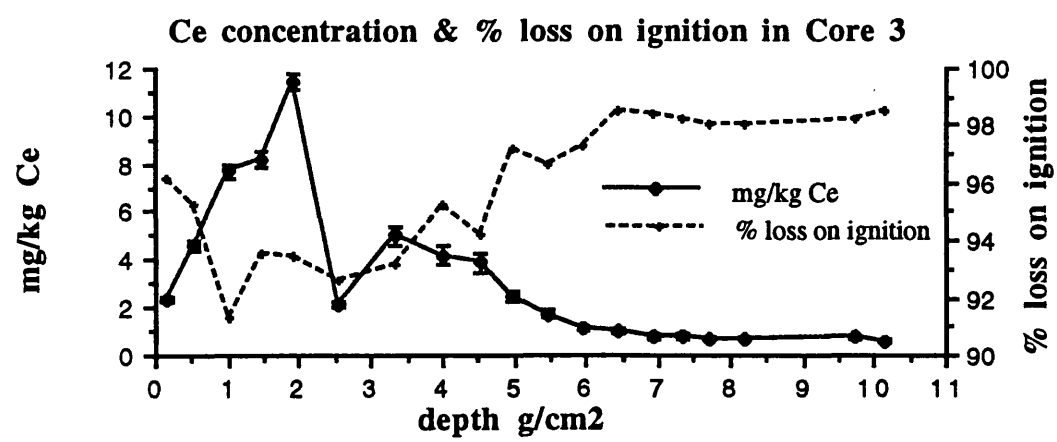

Figure 5.40 Mn and Fe concentrations in Core 3.

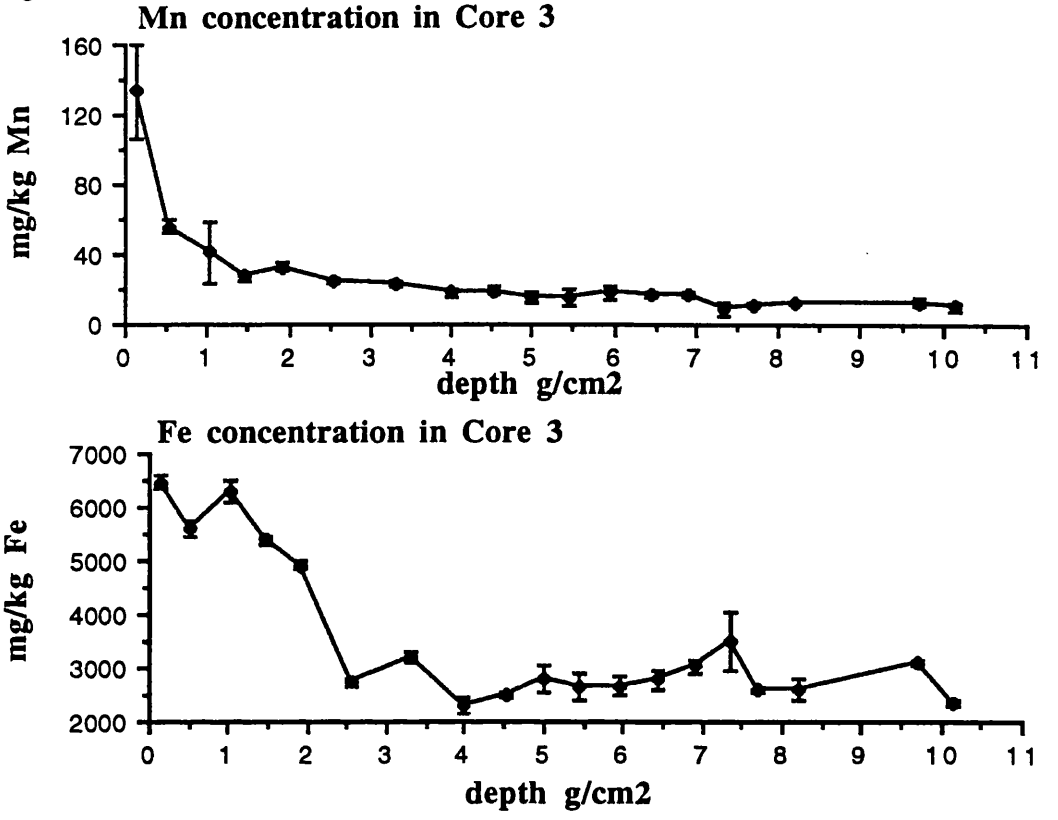

Figure 5.41 Cu and Zn concentrations in Core 3.

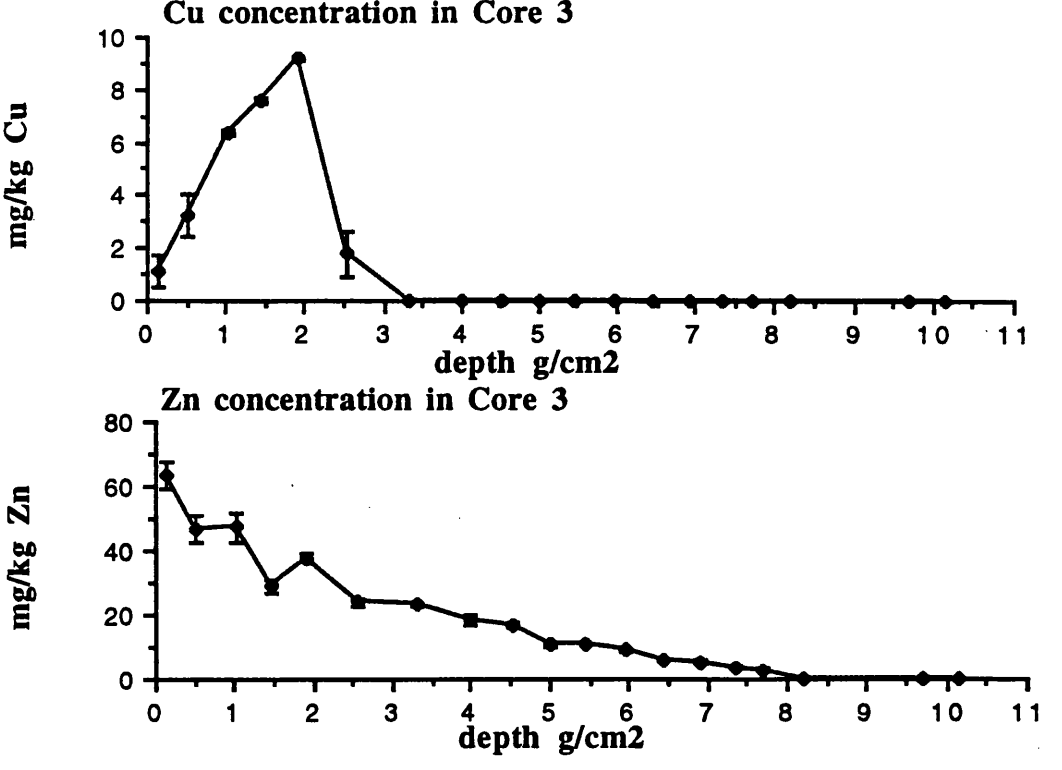

Figure 5.42

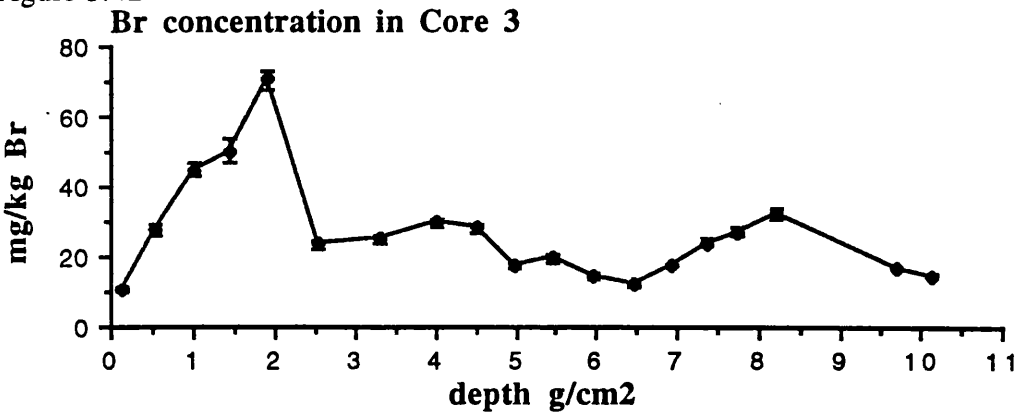

Figure 5.43 Pb, Co and Hg concentrations in Core 3.

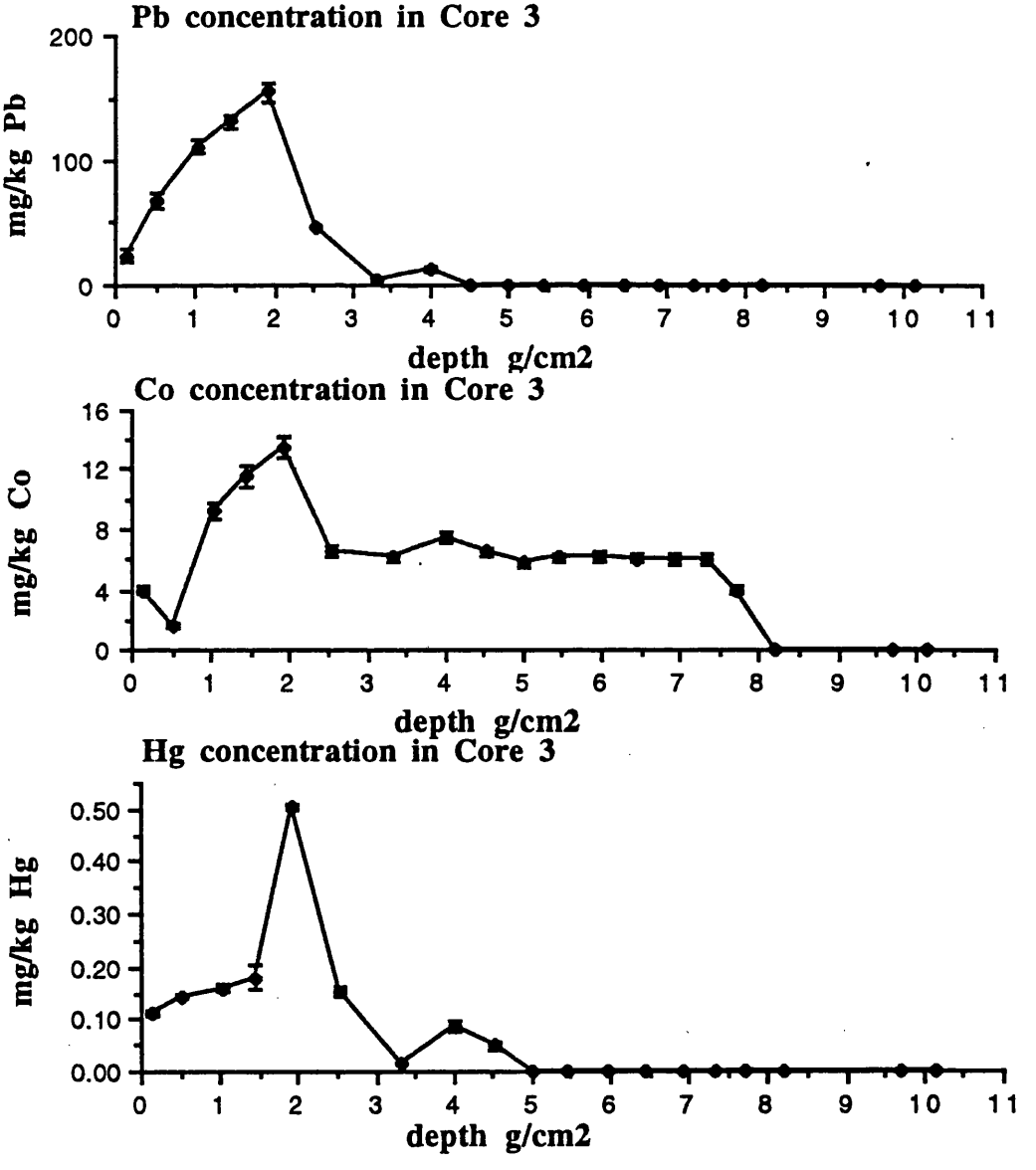

Figure 5.44 $^{206}Pb/^{207}Pb$ ratios for Core 3, and their relationship to the chronology.

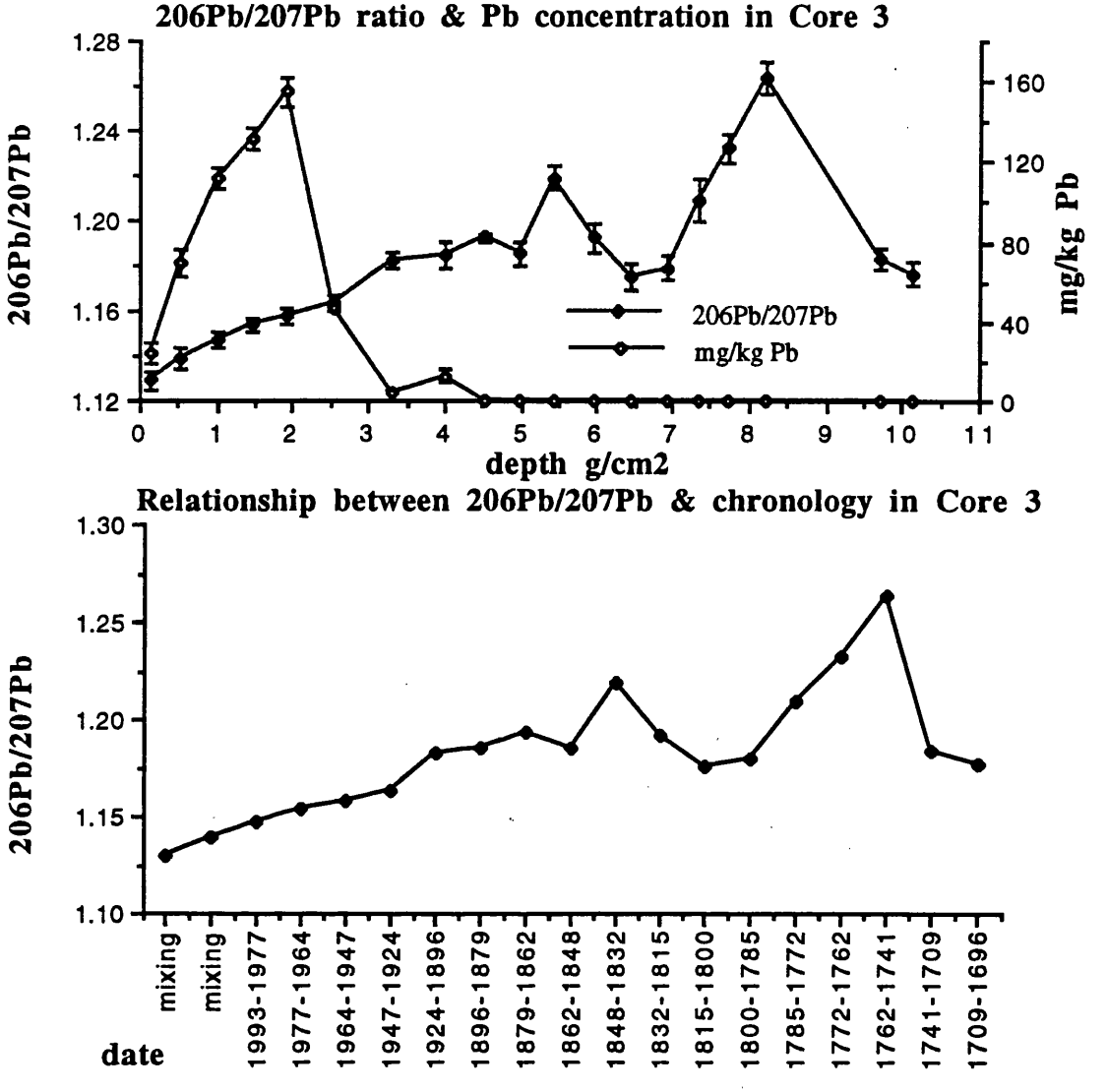

Table 5.29 Fluxes of Br, As, Sb, Co, Pb, Cu & Hg to Core 3 in mg m^{-2} y^{-1}.

depth g cm^{-2}	date	Br	As	Sb	Co	Pb	Cu	Hg
0.0-0.28	*mixed zone*	2.549	0.469	0.054	0.933	5.61	0.262	0.026
0.28-0.78	*mixed zone*	6.504	0.503	0.173	0.379	16.23	0.765	0.034
0.78-1.25	1993-1977	10.602	0.481	0.329	2.170	26.24	1.496	0.038
1.25-1.65	1977-1964	11.881	1.005	0.852	2.731	31.02	1.782	0.042
1.65-2.18	1964-1947	16.626	2.900	1.133	3.177	36.45	2.164	0.119
2.18-2.90	1947-1924	5.597	1.108	0.170	1.567	11.01	0.418	0.036
2.90-3.74	1924-1896	5.984	0.595	0.097	1.450	1.07	0.000	0.004
3.74-4.26	1896-1879	6.991	0.612	0.000	1.765	2.96	0.000	0.021
4.26-4.76	1879-1862	6.643	0.000	0.000	1.541	0.00	0.000	0.012

SOUTH DRUMBOY CORE 4

This core was sampled at the boundary of the farm where the land use changed from rough hill pasture to forestry. As noted in section 5.4.1 that Core 4 showed a pronounced mineral horizon, sandwiched between two organic horizons, with the pH values for the mineral horizon significantly higher than for the organic horizons. These results were attributed to disturbance of the peat and the metal and radionuclide profiles reinforce this conclusion.

The ^{210}Pb profile (Figure 5.45 and Table 5.30) shows a signficant peak at 25 g cm^{-2} which is also seen in the ^{137}Cs and ^{134}Cs profiles (Figure 5.46 & Table 5.31) indicating that this disturbance has occurred over the last 8 years.

The Al profile (Figure 5.47) reflects the changes in the mineral content, as do the La and Ce profiles (Figure 5.48). Sc, Sm, Se, Th, Hf, and Ta also showed this effect and the data can be found in Appendix 3. The $^{206}Pb/^{207}Pb$ ratios (Figure 5.50) show a similar relationship to Al and La, with a distinct increase in the mineral horizon.

Pb, Cu, and Br (Figure 5.49) all show similar profiles to ^{210}Pb, with As, Sb, Co and Hg showing similar relationships (data in Appendix 3). These profiles are all characterised by sub-surface maxima followed by concentrations below the detection limit in the mineral horizon and a peak in the bottom organic horizon at 25 g cm^{-2}.

The radionuclide and metal profiles all indicate that there has been profound disturbance of this site at some time over the last 8 years, with mineral matter having been deposited on the peat and subsequent burial of the mineral matter with fresh peat. Thus, effectively the bottom organic horizon would have been the original surface. This may be due to the insertion of draining channels which requires signficant amounts of gravel, or it could be due to the erection of fencing at the boundary of the farm. Whatever the cause it indicates that the use of such hill farms in this type of study should be undertaken with caution due to the possibility of disturbance of the site.

Table 5.30 ^{210}Pb and ^{226}Ra specific activities and excess ^{210}Pb inventories for Core 4.

depth cm	depth gcm^{-2}	total ^{210}Pb $Bq\ kg^{-1}$	^{226}Ra $Bq\ kg^{-1}$	excess ^{210}Pb $Bq\ kg^{-1}$	excess ^{210}Pb $Bq\ m^{-2}$
0-4.0	0.0-0.18	162 ± 9	6.3 ± 1.1	156 ± 11	287 ± 21
4.0-8.0	0.18-0.57	213 ± 13	2.7 ± 0.6	210 ± 19	818 ± 77
8.0-11.5	0.57-1.22	198 ± 10	4.6 ± 0.7	193 ± 19	1259 ± 127
11.5-14.1	1.22-2.12	36 ± 6	14.1 ± 1.8	22 ± 3	197 ± 22
14.1-17.1	2.12-3.75	0.00	41.6 ± 4.1	0.00	0.00
17.1-20.1	3.75-5.51	0.00	20.4 ± 1.7	0.00	0.00
20.1-24.1	5.51-8.29	0.00	19.6 ± 2.1	0.00	0.00
24.1-27.1	8.29-10.72	0.00	18.4 ± 2.0	0.00	0.00
27.1-30.7	10.72-14.54	0.00	24.3 ± 2.2	0.00	0.00
30.7-33.6	14.54-16.92	0.00	25.4 ± 2.2	0.00	0.00
33.6-36.5	16.92-19.23	0.00	22.2 ± 2.3	0.00	0.00
36.5-39.0	19.23-22.13	0.00	22.7 ± 2.1	0.00	0.00
39.0-42.7	22.13-25.15	25 ± 6	29.9 ± 2.3	0.00	0.00
42.7-44.9	25.15-25.70	255 ± 13	9.5 ± 1.1	245 ± 31	1346 ± 170
44.9-48.1	25.70-26.32	0.00	14.5 ± 2.2	0.00	0.00
48.1-50.3	26.32-26.72	0.00	17.5 ± 2.6	0.00	0.00

Figure 5.45

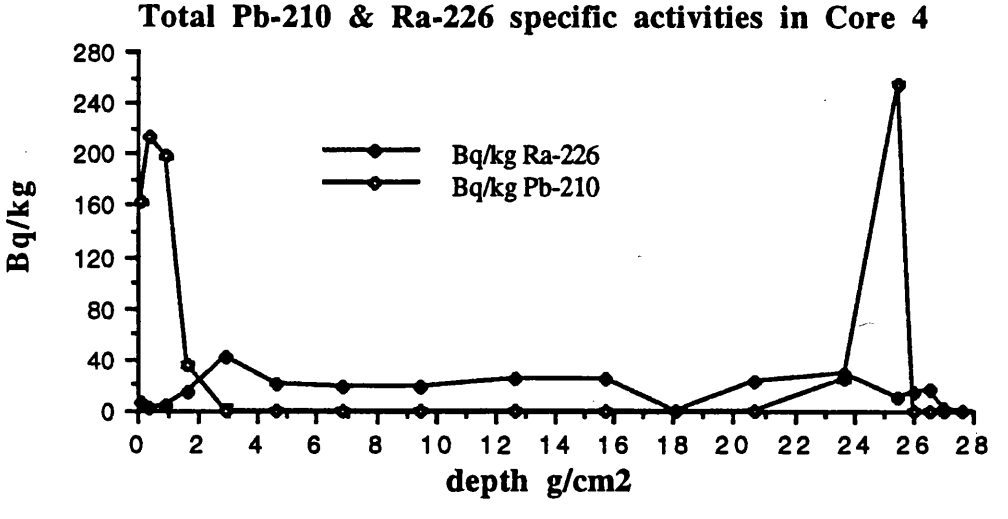

Table 5.31 ^{134}Cs and ^{137}Cs specific activities and inventories in Core 4.

depth g cm^{-2}	Total ^{137}Cs Bq kg^{-1}	Total ^{137}Cs Bq m^{-2}	^{134}Cs Bq kg^{-1}	^{134}Cs Bq m^{-2}
0.0-0.18	480 ± 9	883 ± 17	30 ± 3.	56 ± 6
0.18-0.57	431 ± 9	1676 ± 35	23 ± 1.6	90 ± 6
0.57-1.22	600 ± 12	3909 ± 78	30 ± 1.7	196 ± 11
1.22-2.12	52 ± 1.2	467 ± 11	BDL	BDL
2.12-3.75	24 ± 1.1	397 ± 17	0.00	0.00
3.75-5.51	11 ± 0.9	209 ± 16	0.00	0.00
5.51-8.29	7.9 ± 1.2	219 ± 34	0.00	0.00
8.29-10.72	5.8 ± 1.1	142 ± 27	0.00	0.00
10.72-14.54	5.9 ± 0.9	225 ± 35	0.00	0.00
14.54-16.92	3.1 ± 0.8	76 ± 20	0.00	0.00
16.92-19.23	4.2 ± 0.8	97 ± 24	0.00	0.00
19.23-22.13	6.1 ± 0.8	177 ± 22	0.00	0.00
22.13-25.15	4.6 ± 0.8	142 ± 25	0.00	0.00
25.15-25.70	234 ± 4.7	1283 ± 25	12 ± 1.0	65 ± 5
25.70-26.32	3.4 ± 1.1	22 ± 7	0.00	0.00
26.32-26.72	BDL	BDL	0.00	0.00

Figure 5.46

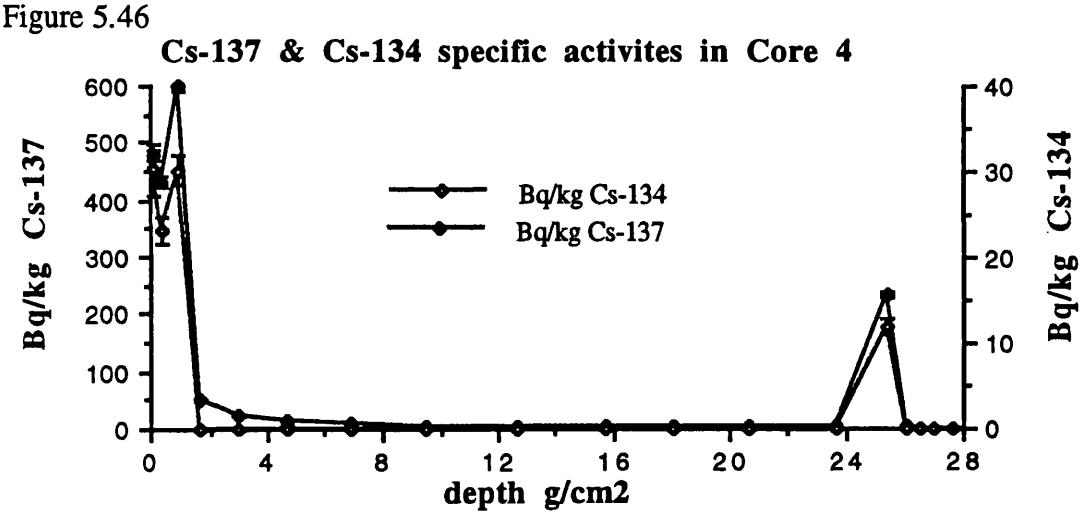

Figure 5.47

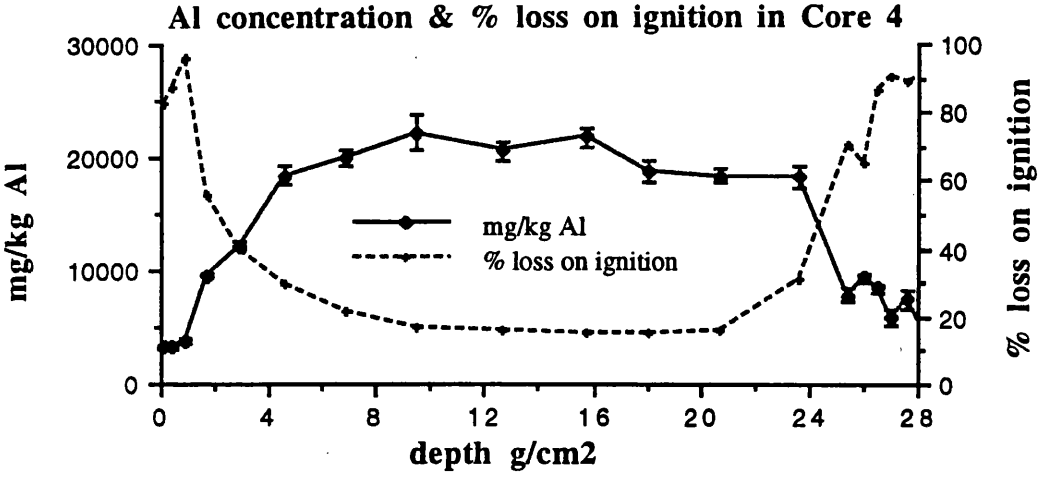

Figure 5.48 La and Ce concentrations in Core 4.

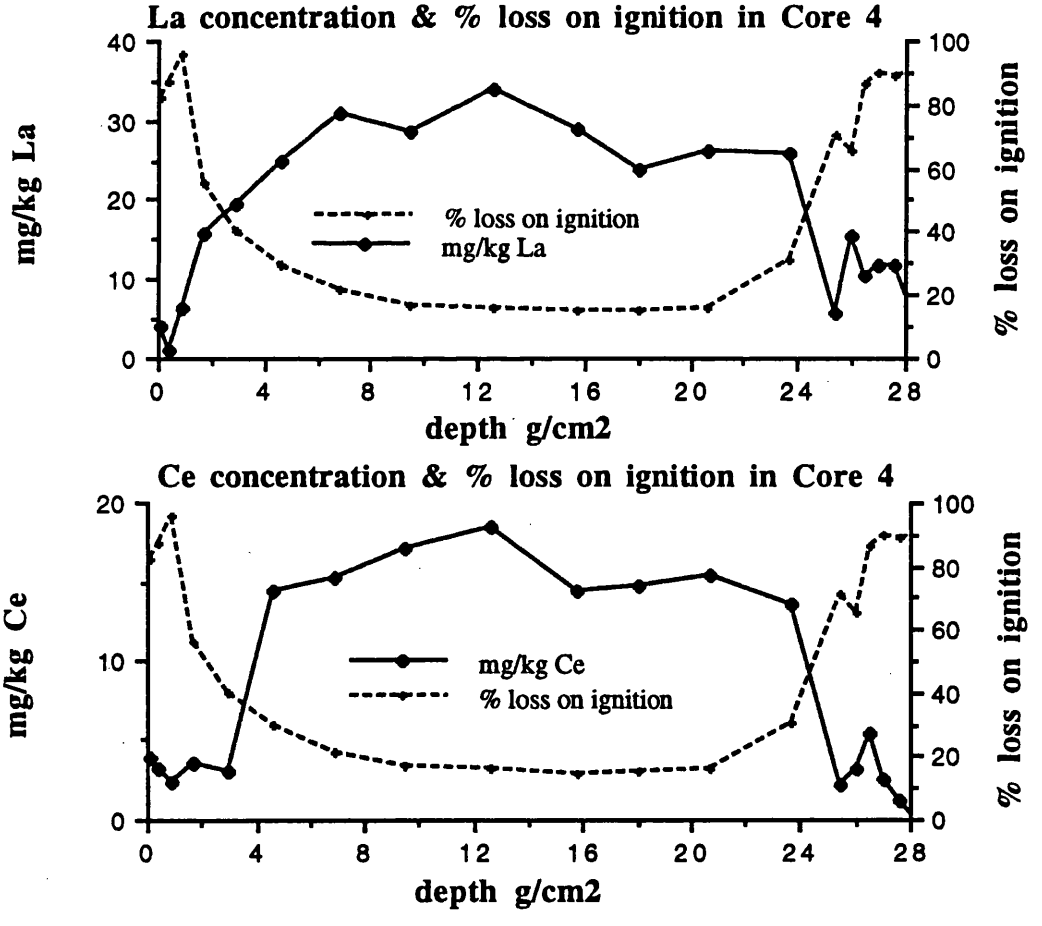

Figure 5.49 Pb, Cu, and Br concentrations in Core 4.

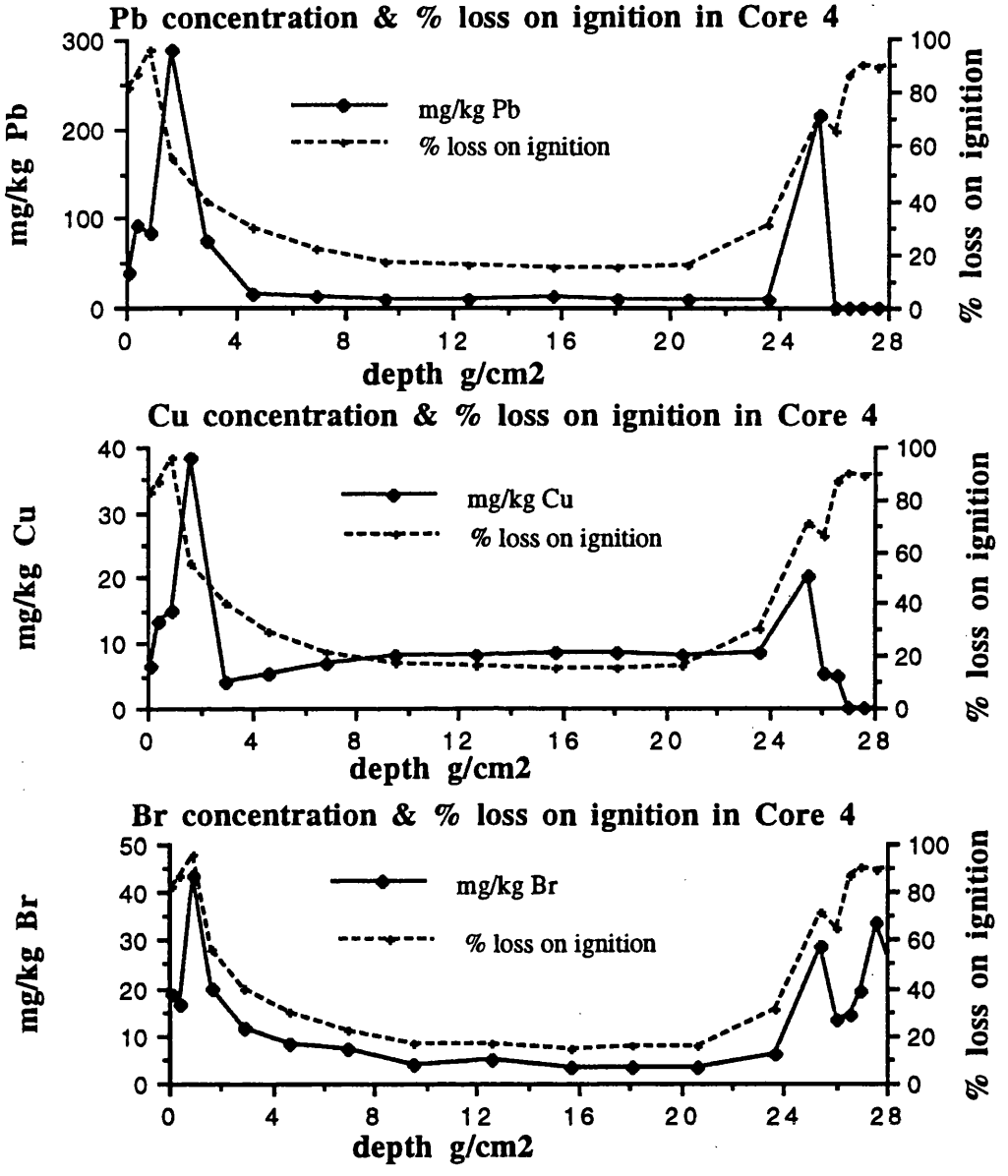

Figure 5.50

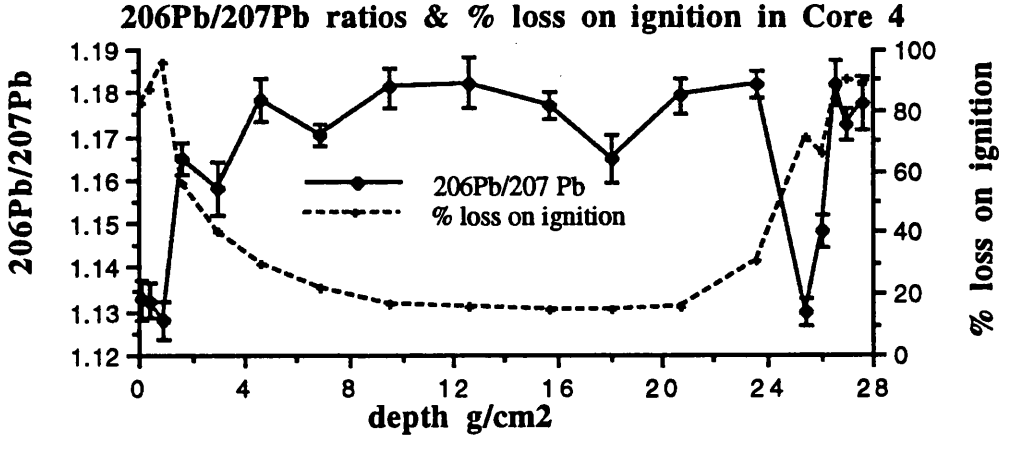

SOUTH DRUMBOY CORE 5

This core was collected directly downslope from Core 3, on the ridge of Drumboy Hill and was characterised by 50 cm of organic matter overlying bedrock. Accordingly, the influence of the bedrock was shown in section 5.4.1 by a decrease in % loss on ignition, an increase in bulk density and pH.

The ^{210}Pb profiles showed some evidence of mixing (Figure 5.51 & Table 5.32) in the first section. However, the effect is minimal and does not significantly affect the acumulation rate which was calculated to be 0.021 g cm^{-2} y^{-1}. The total inventory of ^{210}Pb was calculated as 2165 Bq m^{-2}, giving a flux of 67 Bq m^{-2} y^{-1}.

As with the core 3, radiocaesium penetrates to sections dated before the advent of weapons testing (Tables 5.33 & 5.34, Figure 5.52). ^{137}Cs is present to 9 g cm^{-2} with ^{134}Cs present to 3 g cm^{-2}. The total inventory of ^{137}Cs was 6437 Bq m^{-2}, comprising a Chernobyl inventory of 3933 Bq m^{-2} and a weapons-testing inventory of 2502 Bq m^{-2}. The total ^{134}Cs inventory was 245 Bq m^{-2}.

The Al profile (Figure 5.53) reflects the increase in mineral content as bedrock is approached. La and Ce (Figure 5.54) also show this effect, but also show sub-surface maxima. These maxima are seen in all the rare earth elements and the data can be found in Appendix 3. Sub-surface maxima in the profiles of these elements were also seen in Core 3 and proposed to be due to the burning of fossil fuels.

The Mn and Fe profiles (Figure 5.55) indicate that conditions are progressively reducing from the surface. The concentration of Mn is low throughout the core and decreases rapidly from the surface reflecting its sensitivity to changes in the redox potential. Fe also shows reduction in concentration from the surface with the effect being less pronounced. However, both Fe and Mn show an increase in concentration as bedrock is approached, with the increase occurring before the increase in concentrations of Al, La and Ce and drop in organic matter. However, the increases in Fe and Mn could be due to the influence of the bedrock, with Mn and Fe released from weathered minerals followed by diffusion and redeposition. Walton Day *et al.* (1990) observed that maxima in Fe, Mn and Co concentrations at the base of peat profiles were due to these metals being associated with a maximum in mineral matter content, resulting from a transition between the underlying inorganic sedimentary environment to an organic sedimentary environment within the peat. Mn and Fe could also be re-deposited due to the production of metal sulphides.

As in Core 3, Cu (Figure 5.56) shows a sub-surface maximum in concentration, which is not seen for Zn and which appears in the same section as the peak in the rare

earth elements. Both Cu and Zn show slight increases at the bottom of the core which can be attributed to weathering of the bedrock.

Br (Figure 5.56) also shows this sub-surface maximum in concentration, as also seen for Pb, Co, Hg, As and Sb (Figure 5.58 and Appendix 3). This mirrors Core 3, indicating that the processes which influenced the input of these elements into Core 3 may also have done so for Core 5. The peaks in fluxes of Cu, Pb, Br, Co, Hg, As, and Sb to Core 5 were dated as occurring between 1967 and 1951 (Table 5.35) agreeing well with the peaks in fluxes to Core 3 which were dated between 1964 and 1947 (Table 5.29). As with Core 3 the peaks in the concentrations of rare earth elements also occur in the same section as the maximum flux in the pollutant metals and this may be indicating the influx of atmospheric dust containing these pollutant metals, i.e. due to the burning of fossil fuels.

The $^{206}Pb/^{207}Pb$ ratios (Figure 5.59) show large increases in ratio between 1868 and 1744, indicating that there was an input of Pb low in ^{206}Pb around this time, which compares well with the peaks in Core 3 which occurred between 1845 and 1741. It should be noted that the accuracy of dates calculated from ^{210}Pb dating decreases with depth and cannot be assumed to be as reliable beyond 150 years. Between 1835 and 1951 the $^{206}Pb/^{207}Pb$ ratios are reasonably consistent around values of ~ 1.14. Only in the second section is there a drop in ratio to 1.12. These results are contrary to those observed in Core 3 and recorded by Sugden (1993) with no explanation being evident.

The increase in ratio in the surface section may be reflecting the decreased use of Pb in petrol. Previous research has indicated that Pb fluxes decreased by up to 80% between 1979 and 1983 due to the increased use of unleaded petrol (Eisenreich *et al.*, 1986).

Table 5.32 ^{210}Pb and ^{226}Ra specific activities and excess inventories in Core 5.

depth cm	depth gcm^{-2}	total ^{210}Pb $Bq\ kg^{-1}$	^{226}Ra $Bq\ kg^{-1}$	excess ^{210}Pb $Bq\ kg^{-1}$	excess ^{210}Pb $Bq\ m^{-2}$
0-4.0	0.0-0.54	212 ± 7	10.2 ± 0.3	202 ± 13	1081 ± 69
4.0-6.5	0.54-0.87	180 ± 6	7.9 ± 0.1	172 ± 11	573 ± 36
6.5-8.7	0.87-1.17	85 ± 4	3.2 ± 0.1	82 ± 9	235 ± 25
8.7-11.3	1.17-1.63	59 ± 4	12.8 ± 0.2	46 ± 6	211 ± 28
11.3-13.3	1.63-2.11	24 ± 3	3.4 ± 0.1	20 ± 3	65 ± 9
13.3-16.2	2.11-2.63	14 ± 2	10.4 ± 0.1	0.00	0.00

Figure 5.51 ^{210}Pb profiles for Core 5.

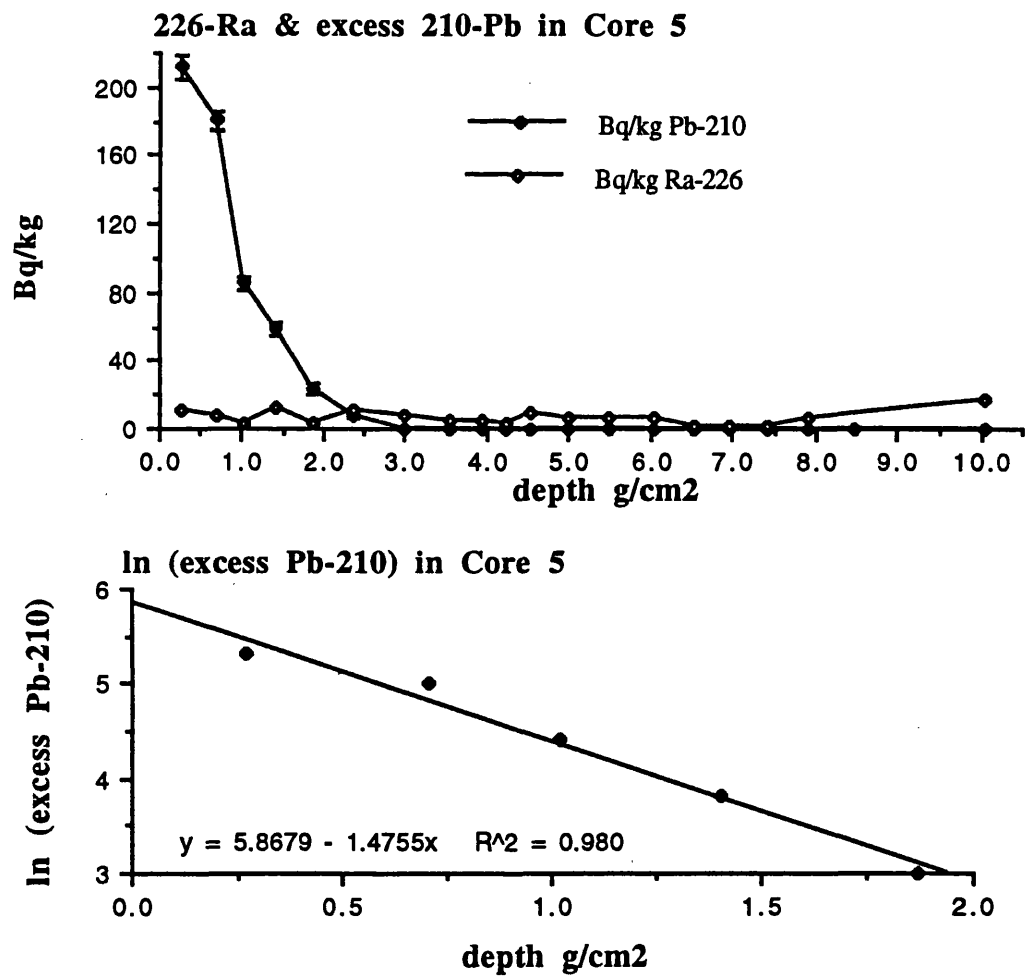

Table 5.33 ^{134}Cs and ^{137}Cs specific activities and inventories in Core 5.

depth g cm^{-2}	date	Total ^{137}Cs Bq kg^{-1}	Total ^{137}Cs Bq m^{-2}	^{134}Cs Bq kg^{-1}	^{134}Cs Bq m^{-2}
0.0-0.54	1993-1967	614 ± 4	3310 ± 23	25 ± 0.2	134 ± 11
0.54-0.87	1967-1951	342 ± 2	1140 ± 9	15 ± 0.1	50 ± 6
0.87-1.17	1951-1937	136 ± 2	420 ± 6	4.6 ± 0.1	14 ± 2
1.17-1.63	1937-1915	96 ± 1	440 ± 8	4.7 ± 0.1	22 ± 3
1.63-2.11	1915-1892	61 ± 2	292 ± 7	2.7 ± 0.1	13 ± 3
2.11-2.63	1892-1868	36 ± 1	186 ± 6	2.0 ± 0.1	10 ± 3
2.63-3.32	1868-1835	20 ± 0.9	139 ± 7	0.00	0.00
3.32-3.76	1835-1814	11 ± 0.8	48 ± 3	0.00	0.00
3.76-4.09	1814-1798	8.7 ± 0.9	29 ± 3	0.00	0.00
4.09-4.37	1798-1685	6.6 ± 0.7	18 ± 2	0.00	0.00
4.37-4.72	1685-1668	8.7 ± 1.0	30 ± 3	0.00	0.00
4.72-5.23	1668-1644	5.8 ± 0.9	30 ± 4	0.00	0.00
5.23-5.76		6.9 ± 0.7	36 ± 4	0.00	0.00
5.76-6.34		6.2 ± 0.7	36 ± 3	0.00	0.00
6.34-6.72		4.8 ± 0.7	18 ± 3	0.00	0.00
6.72-7.12		3.8 ± 0.5	17 ± 3	0.00	0.00
7.12-7.67		4.8 ± 0.7	24 ± 3	0.00	0.00
7.67-8.16		5.4 ± 0.7	27 ± 3	0.00	0.00
8.16-8.76		5.9 ± 0.6	33 ± 7	0.00	0.00

Table 5.34 Chernobyl and weapons-testing ^{137}Cs activities and inventories in Core 5.

depth g cm^{-2}	date	Chernobyl ^{137}Cs Bq kg^{-1}	Chernobyl ^{137}Cs Bq m^{-2}	Weapons testing Bq kg^{-1}	Weapons testing Bq m^{-2}
0.0-0.54	1993-1967	403 ± 32	2160 ± 170	214 ± 17	1150 ± 88
0.54-0.87	1967-1951	245 ± 27	817 ± 90	97 ± 11	324 ± 36
0.87-1.17	1951-1937	74 ± 13	228 ± 40	61 ± 10	187 ± 33
1.17-1.63	1937-1915	77 ± 12	352 ± 53	20 ± 3	91 ± 14
1.63-2.11	1915-1892	43 ± 11	205 ± 52	18 ± 5	87 ± 23
2.11-2.63	1892-1868	33 ± 7	171 ± 50	3 ± 0.6	15 ± 4
2.63-3.32	1868-1835	0.00	0.00	20 ± 0.9	139 ± 7
3.32-3.76	1835-1814	0.00	0.00	11 ± 0.8	48 ± 3
3.76-4.09	1814-1798	0.00	0.00	8.7 ± 0.9	29 ± 3
4.09-4.37	1798-1685	0.00	0.00	6.6 ± 0.7	18 ± 2
4.37-4.72	1685-1668	0.00	0.00	8.7 ± 1.0	30 ± 3
4.72-5.23	1668-1644	0.00	0.00	5.8 ± 0.9	30 ± 4
5.23-5.76		0.00	0.00	6.9 ± 0.7	36 ± 4
5.76-6.34		0.00	0.00	6.2 ± 0.7	36 ± 3
6.34-6.72		0.00	0.00	4.8 ± 0.7	18 ± 3
6.72-7.12		0.00	0.00	3.8 ± 0.5	17 ± 3
7.12-7.67		0.00	0.00	4.8 ± 0.7	24 ± 3
7.67-8.16		0.00	0.00	5.4 ± 0.7	27 ± 3
8.16-8.76		0.00	0.00	5.9 ± 0.6	33 ± 7

Figure 5.52

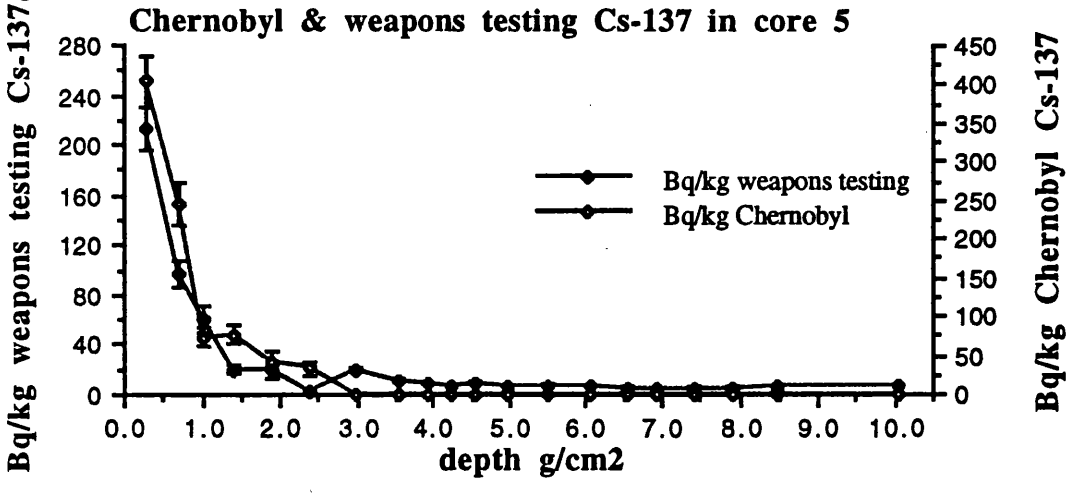

Figure 5.53

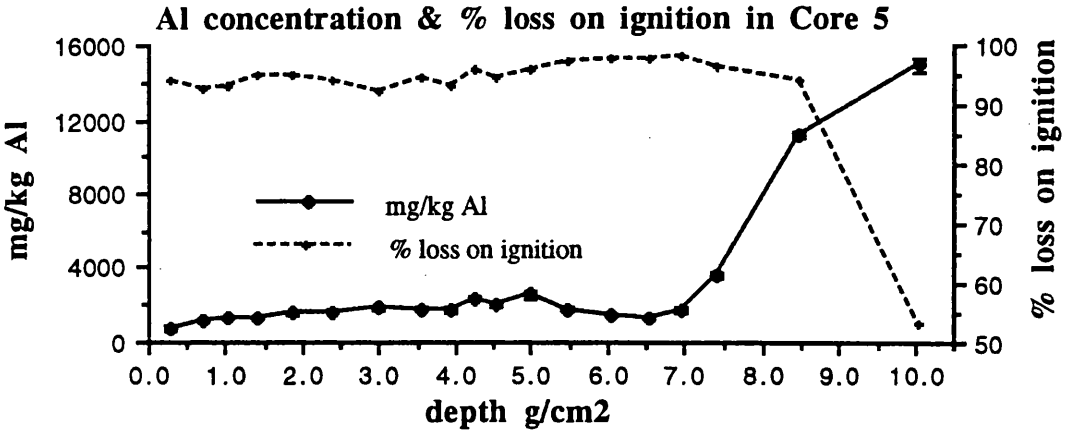

Figure 5.54 La and Ce concentrations in Core 5

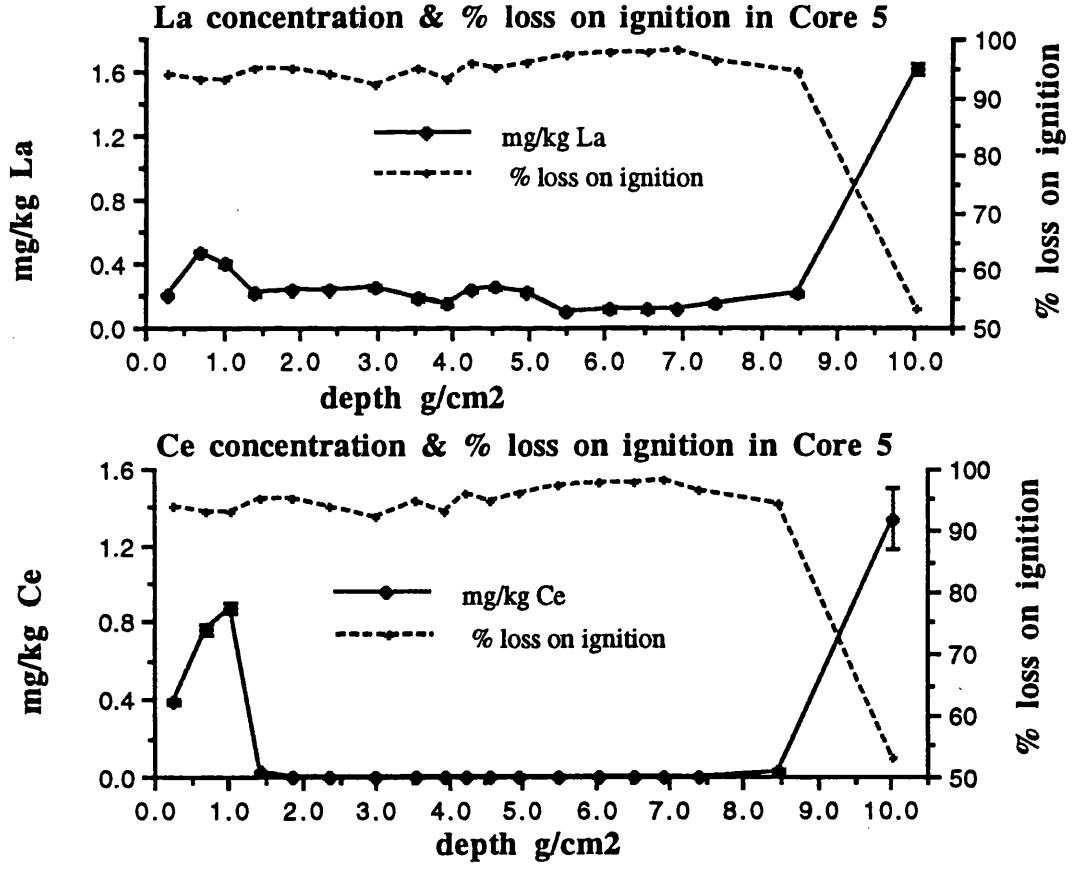

Figure 5.55 Mn and Fe concentrations in Core 5.

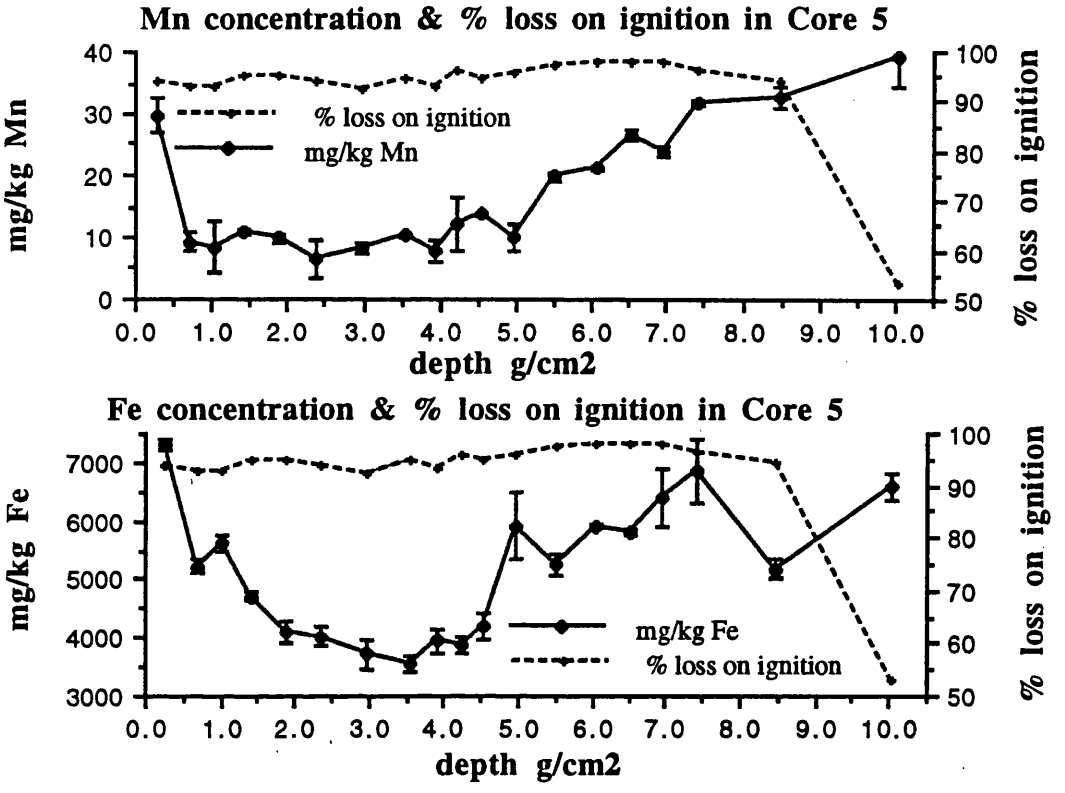

Figure 5.56 Cu and Zn concentrations in Core 5.

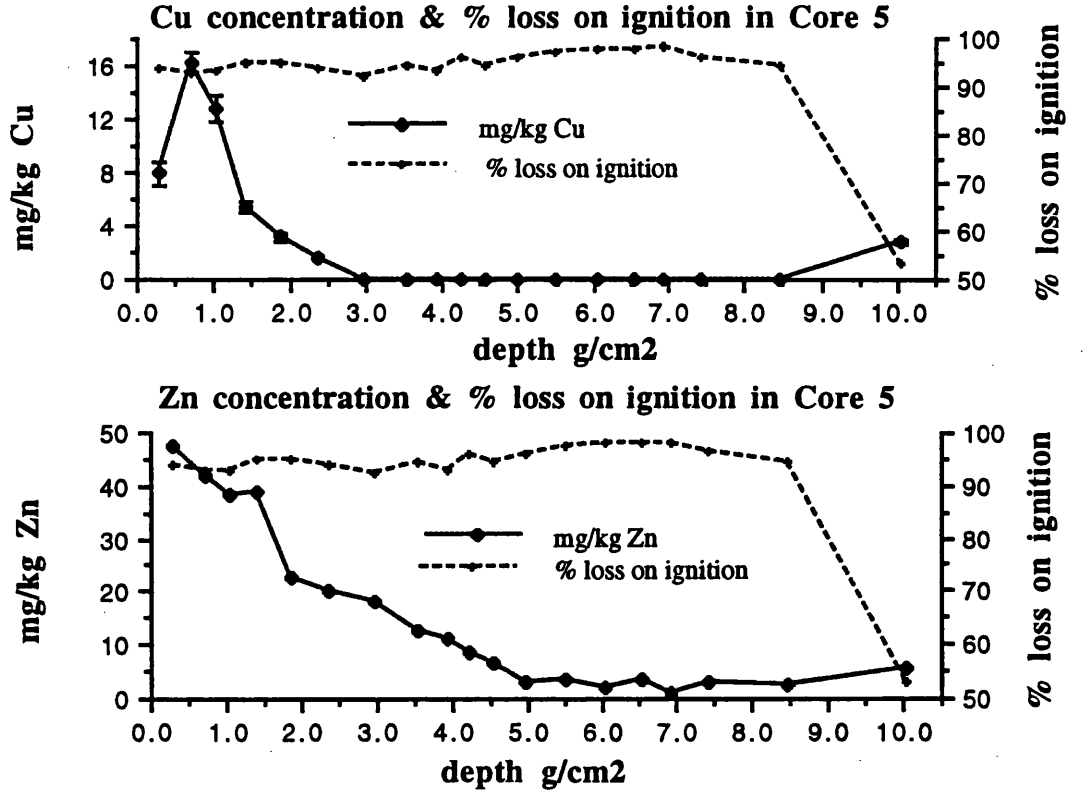

Figure 5.57

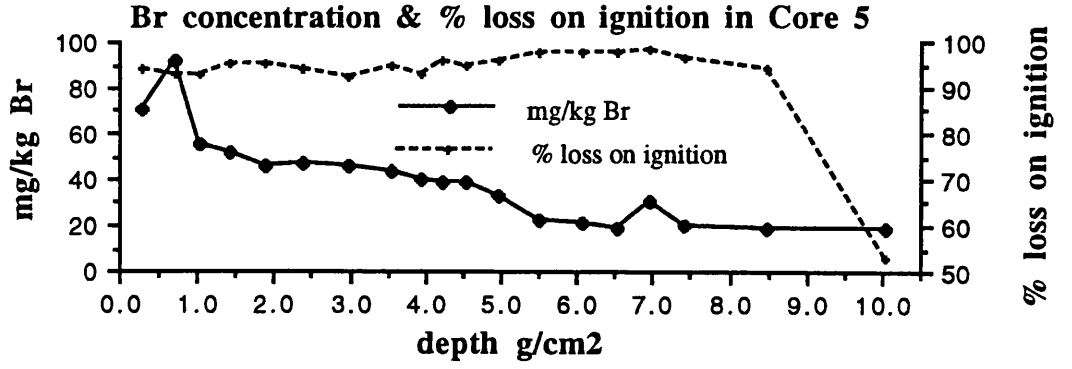

Figure 5.58 Pb, Co and Hg concentrations in Core 5.

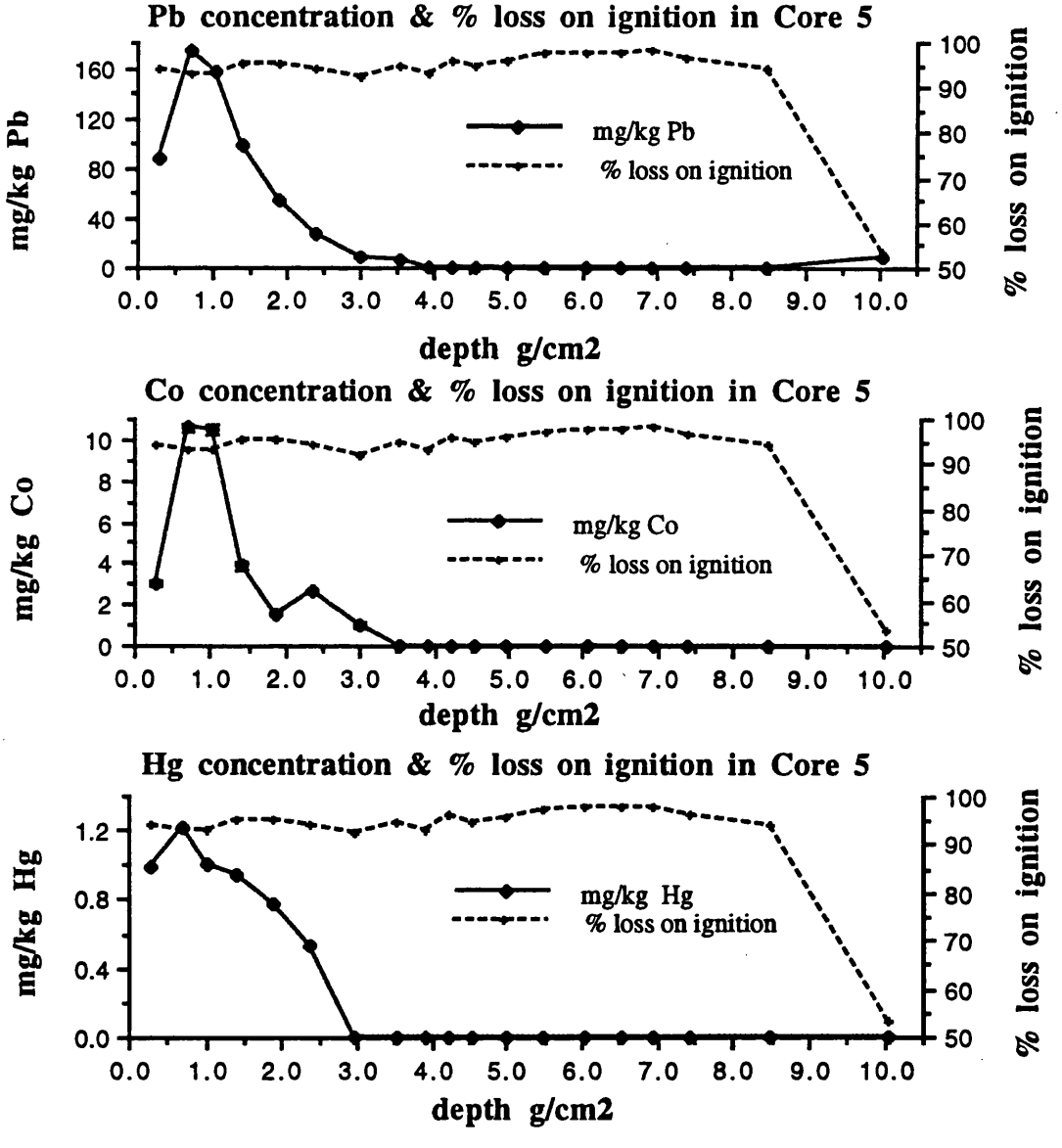

Figure 5.59 $^{206}Pb/^{207}Pb$ ratios for Core 5 and their relationship to the chronology.

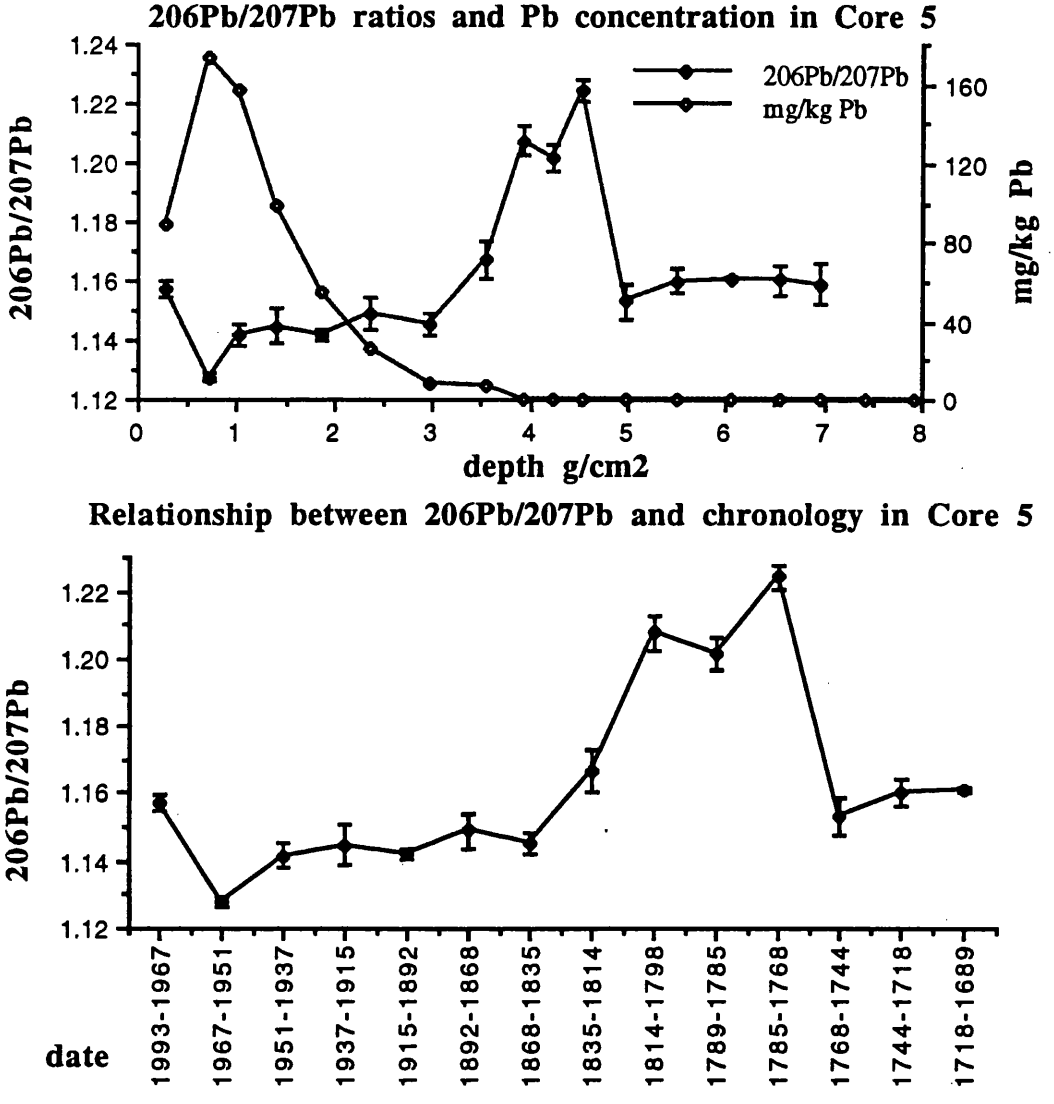

Table 5.35 Fluxes of Br, As, Sb, Hg, Pb, Cu & Co to Core 5, in mg m^{-2} y^{-1}.

depth g cm^{-2}	date	Br	As	Sb	Hg	Pb	Cu	Co
0.0-0.54	1993-1967	7.514	0.582	0.213	0.104	9.38	0.84	0.32
0.54-0.87	1967-1951	9.701	0.865	0.334	0.129	18.33	1.71	1.12
0.87-1.17	1951-1937	5.837	0.754	0.310	0.107	16.62	1.36	1.11
1.17-1.63	1937-1915	5.508	0.730	0.269	0.099	10.46	0.57	0.41
1.63-2.11	1915-1892	4.905	0.508	0.201	0.083	5.80	0.34	0.16
2.11-2.63	1892-1868	4.962	0.155	0.137	0.057	2.81	0.18	0.28
2.63-3.32	1868-1835	4.840	0.093	0.011	0.000	0.84	0.00	0.10
3.32-3.76	1835-1814	4.288	0.000	0.000	0.000	0.73	0.00	0.00
3.76-4.09	1814-1798	4.087	0.000	0.000	0.000	0.00	0.00	0.00

SOUTH DRUMBOY CORE 6

Core 6 was situated directly downslope from Core 5 and like Core 5 was characterised by a horizon of organic matter overlying bedrock. Consequently the % loss on ignition decreased systematically from 3 g cm^{-2}, as the mineral content rose.

The ^{210}Pb data and profiles (Figure 5.60 and Table 5.36) were similar to Core 3 in that mixing within the surface sections gave a non-linear relationship between ln (excess ^{210}Pb) and depth. Accordingly, the accumulation rate was calculated from the linear section of the graph, below the mixed section and an accumulation rate of 0.015 g cm^{-2} y^{-1} was calculated. The total inventory of ^{210}Pb was 2956 Bq m^{-2} which gave an average flux of 92 Bq m^{-2} y^{-1}.

The radiocaesium data and profile (Figure 5.61, and Tables 5.37 and 5.38) all show considerable penetration through the core and no peak in weapons-testing ^{137}Cs was observed. The total ^{137}Cs inventory was 5774 Bq m^{-2}, with a Chernobyl inventory of 3128 Bq m^{-2} and a weapons-testing inventory of 2646 Bq m^{-2}. The ^{134}Cs inventory was 194 Bq m^{-2}.

The Al concentration (Figure 5.62) shows a direct relationship to the rise in mineral content, as determined by the reduction in % loss on ignition. This effect is mirrored by the rare earth elements which are represented by the La and Ce profiles presented (Figure 5.63). Unlike Cores 3 and 5, no sub surface maxima were recorded.

Mn and Fe (Figure 5.64) show similar distributions to those seen in Core 5, which are essentially a drop in concentration from surface to a minimum at 3 g cm^{-2}, after which values increase as the mineral content rises. The main difference between Core 5 and Core 6 is that in Core 5 the increase in Fe and Mn occurred before the increase in mineral content. However, in Core 5 it was suggested that from the surface, conditions became progressively reducing, giving dissolution of Fe and Mn oxides which were then redeposited at depth through the production of metal sulphides. This could also apply for Core 6 since it was situated directly downslope from Core 5, and also overlies bedrock. Alternatively, the increase could be directly related to the increase in mineral content.

Cu, Zn and Br (Figure 5.65), Pb, Hg and Co (Figure 5.66) and As and Sb (Appendix 3) all show similar distributions within Core 6. In many ways these reflect the distributions seen in Core 3, where mixing processes had also acted to displace the peak in pollutant input down the profile. The metal profiles all suggest a peak in pollutant input which can be dated as occurring between 1976 and 1935 for As, Sb, Pb, Cu, Hg and Co and between 1993 and 1976 for Br and Zn (Table 5.39). Unlike Cores 3 and 5, there are only slight peaks in the concentrations of the rare earth

elements at depth, and often the peaks are not in the same section as the peaks in Pb, Co, Hg, As, Sb and Cu. In addition the peaks in Br and Pb occur in different sections.

The $^{206}Pb/^{207}Pb$ ratios show a reduction from values of ~1.16 at the turn of the century to surface values of ~1.12 (Figure 5.67). The onset of reduction begins between 1935 and 1907 which is consistent with the introduction of Pb as an anti-knock additive in petrol. Like Core 3, the section containing the peak in Pb concentration shows a values of ~1.15 indicating that car exhaust emissions show a contribution to the peak. However, like the Pb profiles the $^{206}Pb/^{207}Pb$ ratios may be affected by the mixing processes, since in Core 5 where no mixing processes affected the core, the peak in Pb concentration coincided with the lowest $^{206}Pb/^{207}Pb$ ratio. In Cores 3 and 5 there were large increases in the $^{206}Pb/^{207}Pb$ ratios to values of greater than ~1.21. This is not observed in Core 6. The greatest $^{206}Pb/^{207}Pb$ ratio recorded in Core 6 is ~1.19, which may be due to the increase in mineral content at depths. However, in Core 6 the Pb, ^{210}Pb and $^{206}Pb/^{207}Pb$ profiles are all consistent and indicate that Pb is not mobile within the peat and changes within the profile can be attributed to changes in atmospheric deposition.

Table 5.36 ^{210}Pb and ^{226}Ra specific activities and excess inventories in Core 6.

depth cm	depth gcm^{-2}	total ^{210}Pb $Bq\ kg^{-1}$	^{226}Ra $Bq\ kg^{-1}$	excess ^{210}Pb $Bq\ kg^{-1}$	excess ^{210}Pb $Bq\ m^{-2}$
0.0-3.0	0.0-0.30	236 ± 13	7.3 ± 0.14	229 ± 32	679 ± 93
3.0-6.5	0.30-0.60	202 ± 11	0.3 ± 0.01	202 ± 20	617 ± 61
6.5-9.5	0.60-0.99	193 ± 8	BDL	194 ± 10	750 ± 37
9.5-11.7	0.99-1.23	128 ± 6	0.48 ± 0.01	128 ± 18	315 ± 44
11.7-16.0	1.23-1.85	82 ± 4	6.2 ± 0.10	76 ± 8	468 ± 46
16.0-19.0	1.85-2.27	25 ± 2	2.8 ± 0.05	22 ± 3	91 ± 14
19.0-21.0	2.27-2.55	11 ± 2	2.1 ± 0.04	9 ± 2	36 ± 8
21.0-24.0	2.55-3.13	0.00	10.2 ± 0.17	0.00	0.00
24.0-26.8	3.13-3.84	0.00	9.4 ± 0.16	0.00	0.00
26.8-29.7	3.84-4.77	0.00	19.6 ± 0.33	0.00	0.00
29.7-32.4	4.77-5.77	0.00	16.9 ± 0.28	0.00	0.00
32.4-36.9	5.77-7.22	0.00	20.3 ± 0.34	0.00	0.00

Figure 5.60 ^{210}Pb profiles for Core 6.

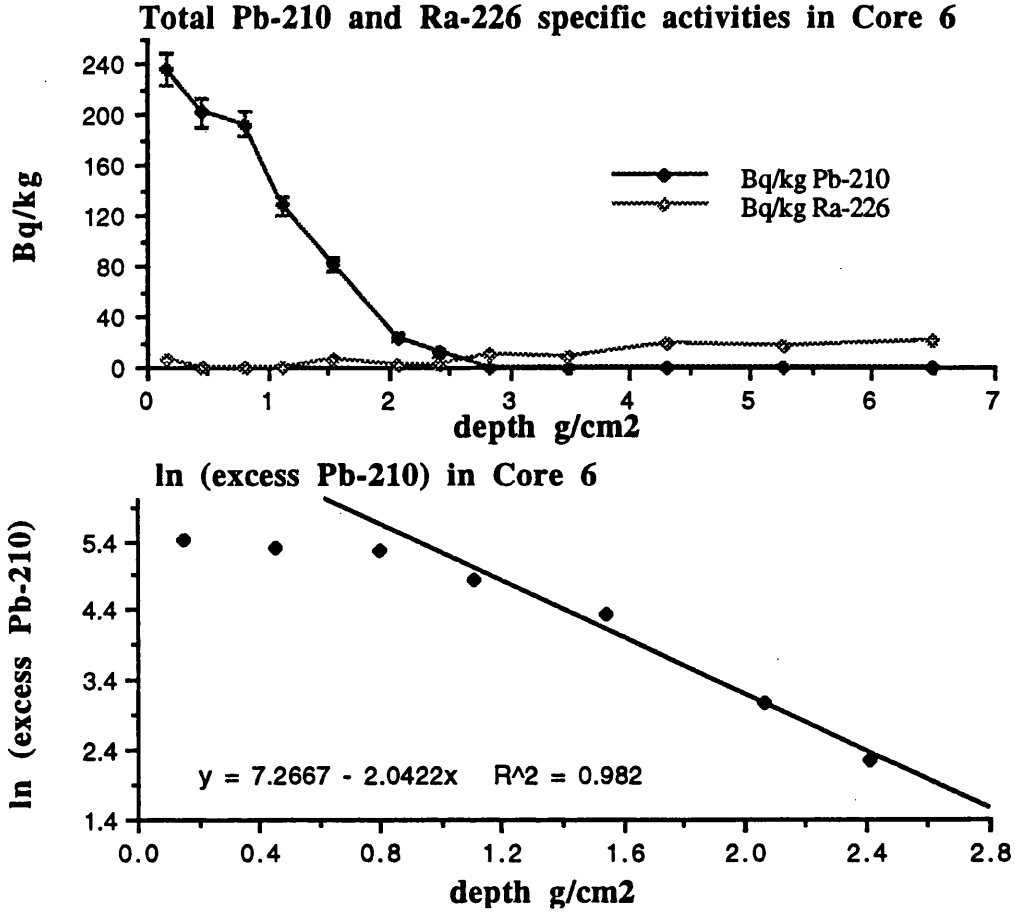

Table 5.37 ^{134}Cs and ^{137}Cs specific activities and inventories in Core 6.

depth g cm^{-2}	date	Total ^{137}Cs Bq kg^{-1}	Total ^{137}Cs Bq m^{-2}	^{134}Cs Bq kg^{-1}	^{134}Cs Bq m^{-2}
0.0-0.30	*mixed zone*	624 ± 12	1850 ± 110	27 ± 6	78 ± 17
0.30-0.60	*mixed zone*	437 ± 9	1330 ± 74	19 ± 2	56 ± 5
0.60-0.99	*mixed zone*	287 ± 6	1110 ± 47	11 ± 1	43 ± 4
0.99-1.23	1993-1976	149 ± 3	366 ± 20	6 ± 0.9	15 ± 5
1.23-1.85	1976-1935	67 ± 2	412 ± 25	0.00	0.00
1.85-2.27	1935-1907	39 ± 1.4	161 ± 20	0.00	0.00
2.27-2.55	1907-1889	35 ± 1.3	145 ± 31	0.00	0.00
2.55-3.13	1889-1850	33 ± 1.3	190 ± 45	0.00	0.00
3.13-3.84	1850-1803	29 ± 1.3	210 ± 57	0.00	0.00
3.84-4.77	1803-1740	0.00	0.00	0.00	0.00

Table 5.38 Chernobyl and weapons-testing ^{137}Cs specific activities and inventories in Core 6.

depth g cm^{-2}	date	Chernobyl ^{137}Cs Bq kg^{-1}	Chernobyl ^{137}Cs Bq m^{-2}	Weapons testing ^{137}Cs Bq kg^{-1}	Weapons testing ^{137}Cs Bq m^{-2}
0.0-0.30	*mixed zone*	428 ± 52	1267 ± 154	196 ± 24	579 ± 71
0.30-0.60	*mixed zone*	299 ± 28	914 ± 85	137 ± 13	418 ± 39
0.60-0.99	*mixed zone*	181 ± 13	702 ± 56	106 ± 8	410 ± 30
0.99-1.23	1993-1976	99 ± 14	245 ± 35	67 ± 2	121 ± 8
1.23-1.85	1976-1935	0.00	0.00	49 ± 7	412 ± 25
1.85-2.27	1935-1907	0.00	0.00	39 ± 2	161 ± 20
2.27-2.55	1907-1889	0.00	0.00	35 ± 2	145 ± 31
2.55-3.13	1889-1850	0.00	0.00	33 ± 1	190 ± 45
3.13-3.84	1850-1803	0.00	0.00	30 ± 1	210 ± 57
3.84-4.77	1803-1740	0.00	0.00	0.00	0.00

Figure 5.61

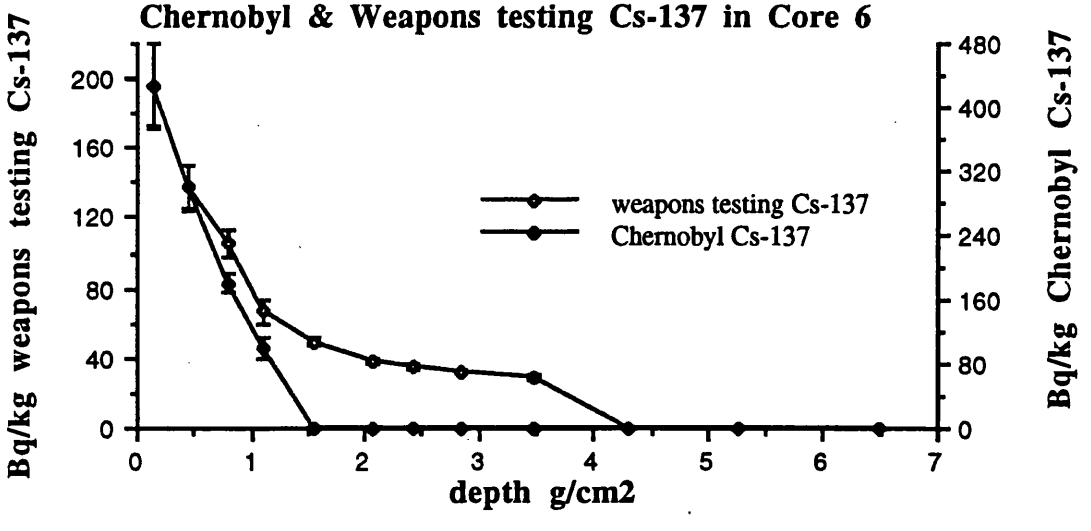

Figure 5.62

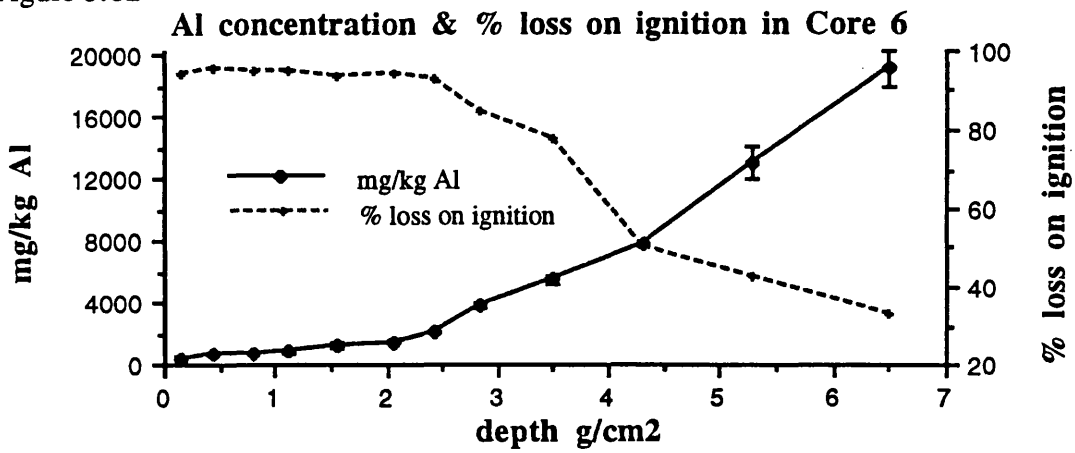

Figure 5.63 La and Ce concentrations in Core 6.

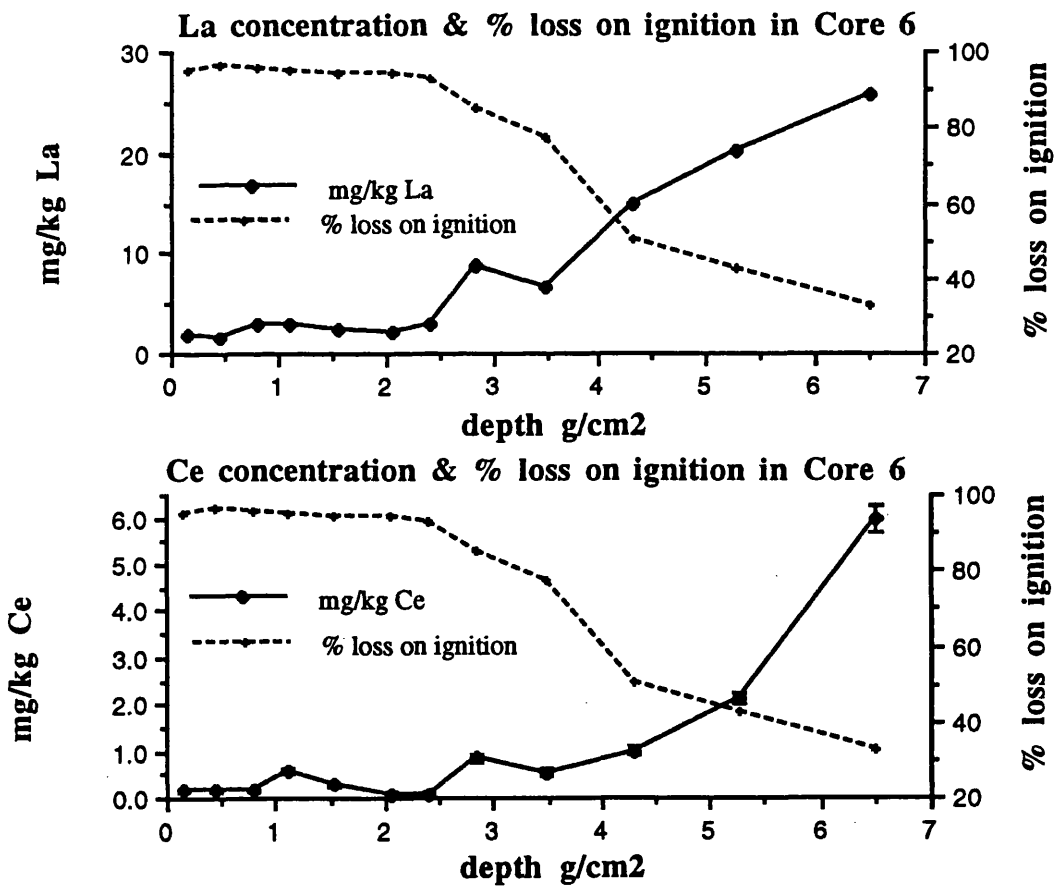

Figure 5.64 Mn and Fe concentrations in Core 6.

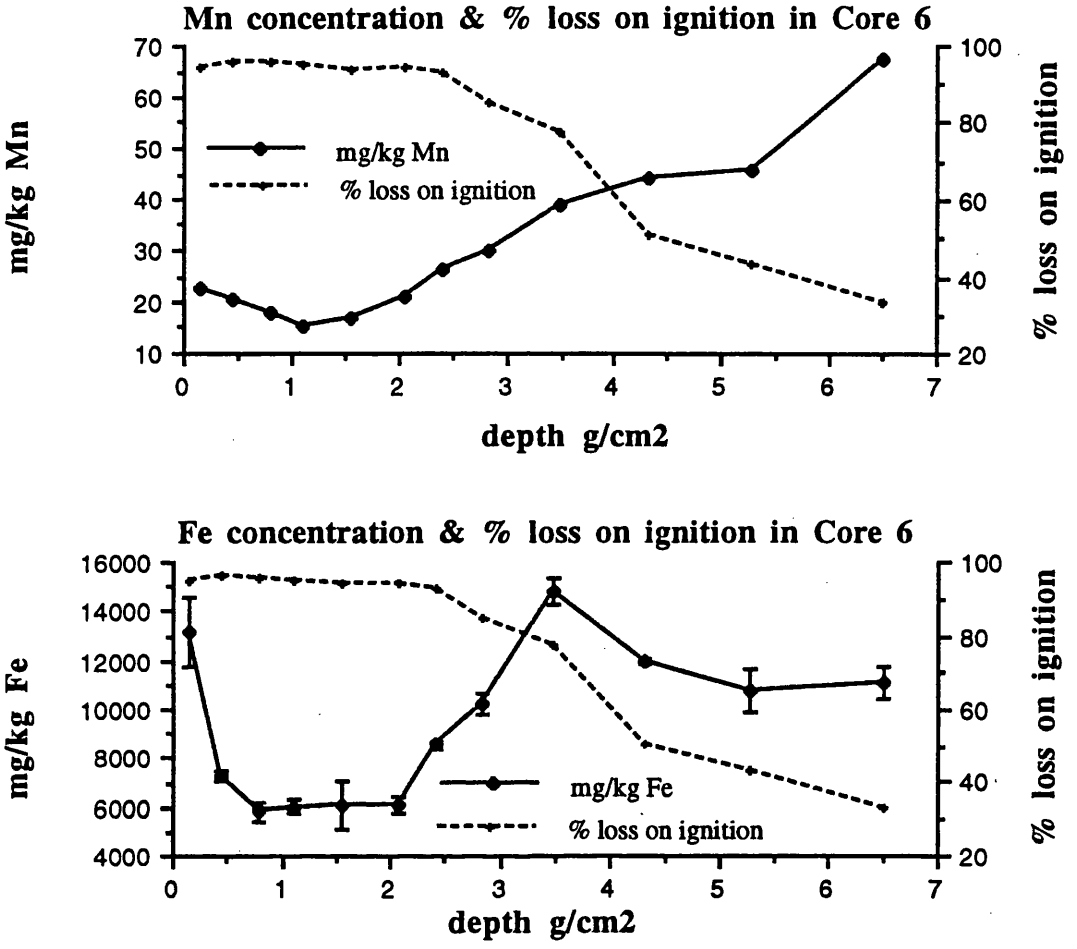

Figure 5.65 Cu, Zn and Br concentrations in Core 6.

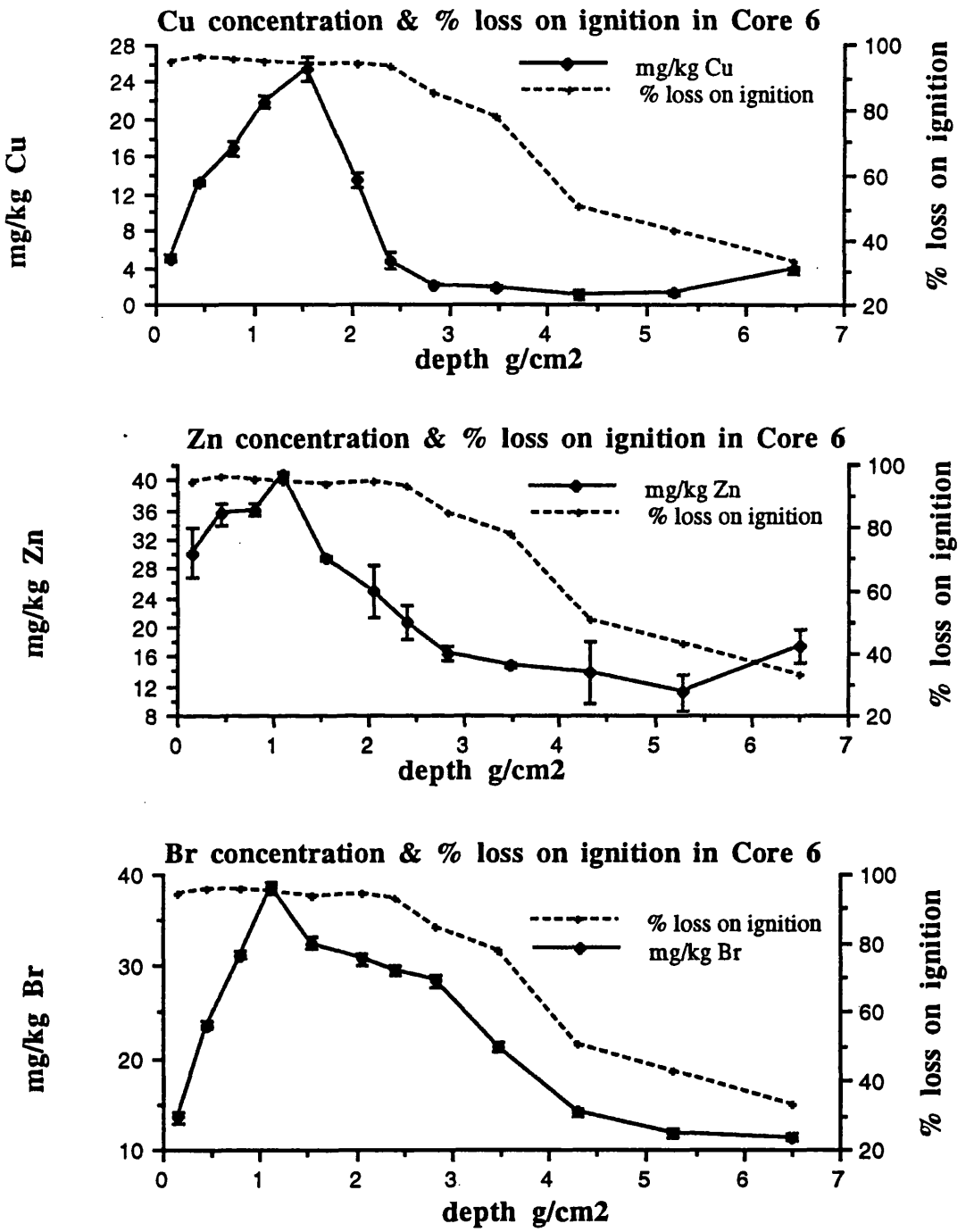

Figure 5.66 Pb, Co and Hg concentrations in Core 6.

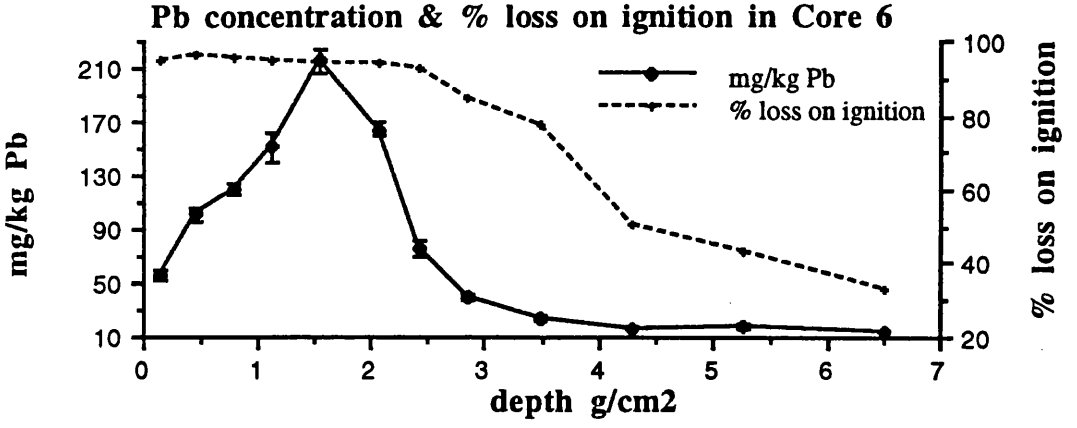

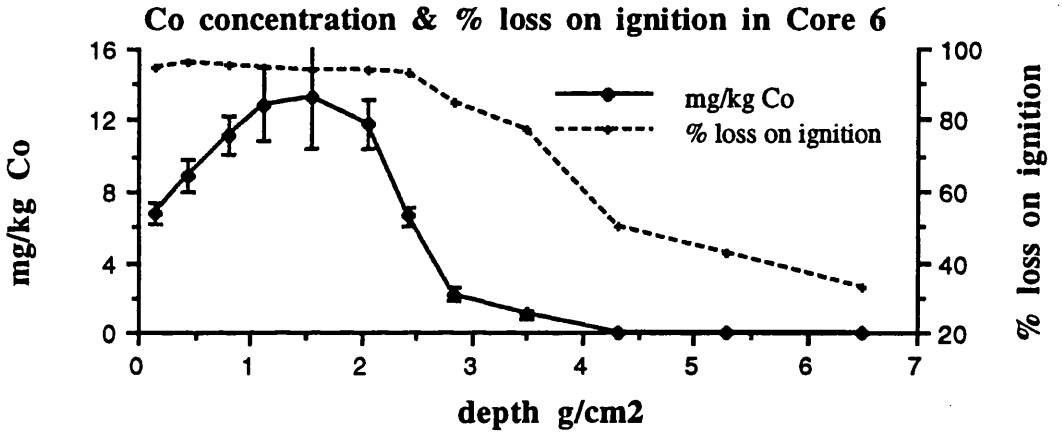

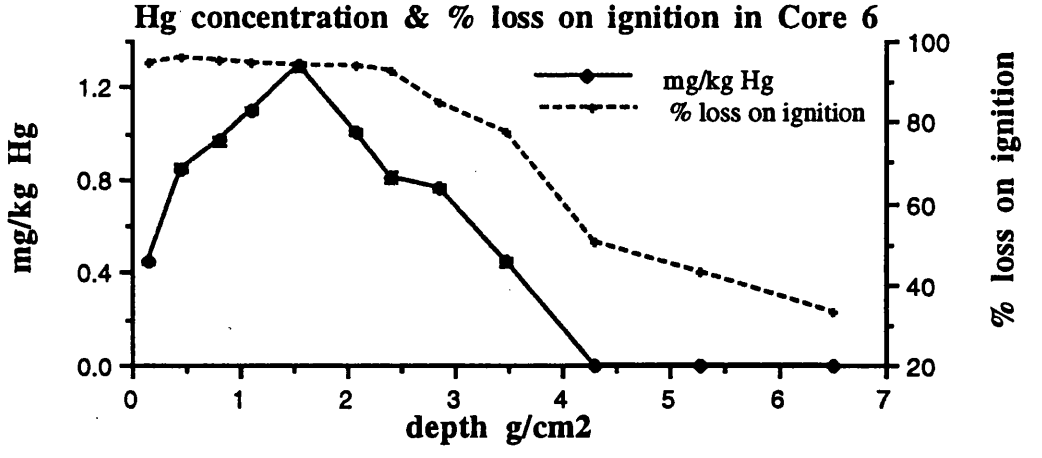

Figure 5.67 $^{206}Pb/^{207}Pb$ ratios in Core 6 and their relationship to the chronology.

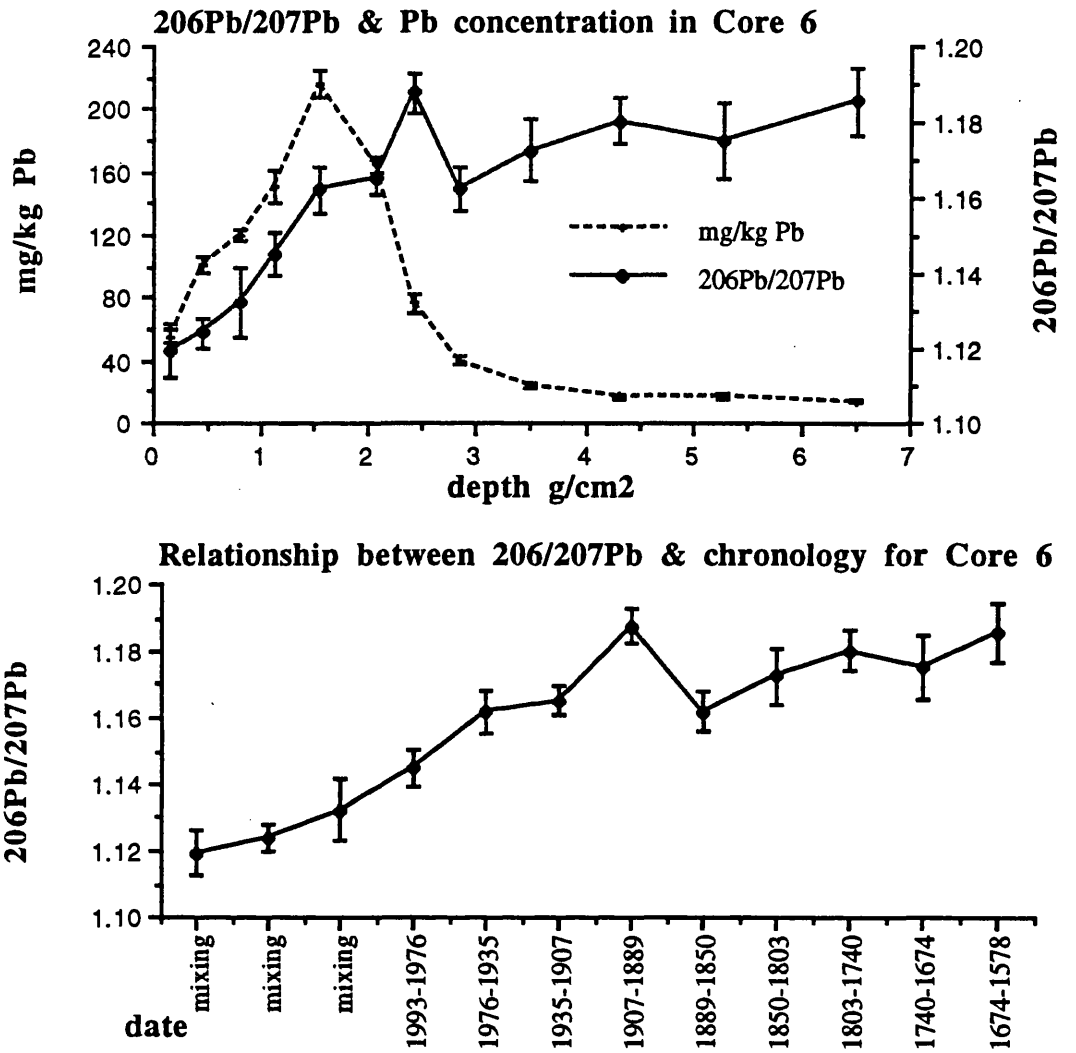

Table 5.39 Fluxes of Br, As, Sb, Pb, Cu, Hg & Co to Core 6, in mg m^{-2} y^{-1}.

depth g cm^{-2}	date	Br	As	Sb	Pb	Cu	Hg	Co
0.0-0.30	*mixed zone*	1.014	0.254	0.051	4.132	0.371	0.034	0.509
0.30-0.60	*mixed zone*	1.771	0.263	0.067	7.560	0.998	0.064	0.667
0.60-0.99	*mixed zone*	2.329	0.265	0.092	8.994	1.258	0.072	0.840
0.99-1.23	1993-1976	2.893	0.297	0.214	11.312	1.636	0.082	0.962
1.23-1.85	1976-1935	2.435	0.327	0.245	16.112	1.900	0.097	0.993
1.85-2.27	1935-1907	2.307	0.251	0.132	12.328	1.015	0.075	0.880
2.27-2.55	1907-1889	2.211	0.238	0.049	5.720	0.354	0.061	0.491
2.55-3.13	1889-1850	2.130	0.194	0.016	2.999	0.161	0.057	0.160
3.13-3.84	1850-1803	1.585	0.139	0.007	1.819	0.131	0.033	0.074
3.84-4.77	1803-1740	1.051	0.114	0.00	1.219	0.083	0.000	0.000
4.77-5.77	1740-1674	0.890	0.119	0.00	1.309	0.095	0.000	0.000
5.77-7.22	1674-1578	0.853	0.091	0.00	1.075	0.282	0.000	0.000

5.4.3 DISCUSSION OF THE RESULTS RECORDED AND THE RELATIONSHIPS BETWEEN THE SOUTH DRUMBOY CORES

One of the main aims of this thesis was to evaluate the validity of using ^{210}Pb as a dating mechanism in organic soils. The results for the South Drumboy cores clearly demonstrate that ^{210}Pb should be used with caution in situations where land management practices can result in the disturbance of profiles and accordingly the disturbance of ^{210}Pb profiles. Even though obviously disturbed areas were not sampled, this affected 3 out of the 6 cores studied with the most pronounced disturbance being noted in Core 4. The insertion of drainage channels on the easterly facing slope resulted in an increase in the total inventory and average flux of ^{210}Pb in Core 1, compared to Core 2, with the majority of the ^{210}Pb contained in the surface section (Table 5.40).

There was also a slight increase in inventory and flux values from Core 5 to Core 6, which may be indicating some lateral flow of ^{210}Pb. Lateral flow of ^{210}Pb in peat profiles has previously been suggested to occur (Maguire, 1994: El-Daoushy, 1988: Oldfield *et al.*, 1979) and often results in a reduction in the ^{210}Pb inventory of the profile up slope (Mitchell *et al.*, 1992). Urban *et al.* (1990) proposed that ^{210}Pb could be moving with dissolved organic matter, particularly where the peat is waterlogged and consequently reduced.

The highest inventory and flux values were recorded in Core 3, which was situated towards the summit of Drumboy Hill. This may be indicating that the flux of ^{210}Pb to these sites is affected by altitude with Core 3 receiving preferential deposition. Increased mist cover at higher altitudes has previously been reported to influence the deposition of ^{210}Pb (Olsen *et al,* 1985: Urban *et al.*, 1990).

The average flux values correspond well to previous measurements in ombrotrophic peat cores (Table 5.41). The values recorded by Sugden (1993) in a study of ombrotrophic peat cores from various sites around Scotland agree particularly well, with average flux values ranging from 71.3 - 150.0 Bq m^{-2} y^{-1}. The higher values were recorded in sites with higher rainfall.

Table 5.40 ^{210}Pb flux and inventory data for the South Drumboy profiles.

Site	Altitude m	Aspect	Inventory Bq m^{-2}	Flux Bq m^{-2} y^{-1}	Accumlation rate, g cm^{-2} y^{-1}
Core 1	237	east facing	2157	67	not calculated
Core 2	247	east facing	1704	53	not calculated
Core 3	267	summit of hill	3432	106	0.031
Core 5	257	south west facing	2165	67	0.021
Core 6	240	south west facing	2956	92	0.015
Core 4	247	west facing	3907	121	****

Table 5.41 Some previously reported ^{210}Pb fluxes to ombrotrophic peats at various locations.

Site	mm annual rainfall	Flux Bq m^{-2} y^{-1}	Reference
Kitte, Finland	*******	74.0	El-Daoushy & Tolonen, (1984)
Kippure, Ireland	1816	63.0	Mitchell *et al.*, (1992)
Clara, Ireland	818	58.0	Mitchell *et al.*, (1992)
North Uist, Scotland	1449	150.0	Sugden (1993)
Flanders Moss, Scotland	1320	108.0	Sugden (1993)
Easter Deans, Scotland	1013	71.3	Sugden (1993)

The radiocaesium profiles show considerable evidence of post-depositional movement. There is unequivocal evidence of lateral flow of weapons-testing ^{137}Cs between Core 2 and Core 1 (Table 5.42). This was attributed to the insertion of drainage channels upslope from Core 1 which mediated the flow of weapons-testing ^{137}Cs. Since Chernobyl ^{137}Cs was unaffected, the disturbance must have occurred before the Chernobyl accident. The total ^{137}Cs and Chernobyl ^{137}Cs inventories for the remainder of the cores do not immediately suggest that lateral flow may be occurring. However, the weapons:Chernobyl ^{137}Cs ratios increase as the altitude decreases and this may indicate movement of weapons-testing ^{137}Cs. In addition, as for ^{210}Pb, there is a slight increase in weapons-testing ^{137}Cs in Core 6, compared to Core 5. Colgan *et al.* (1990) observed an increase in the content of weapons-testing ^{137}Cs in the top 10 cm of organic soils as the altitude decreased, indicating lateral movement of ^{137}Cs. This effect was not reciprocated for Chernobyl derived ^{137}Cs. Coughtrey *et al.*, (1990) also observed that ^{137}Cs deposited after Chernobyl showed different distribution patterns in soils than weapons-testing ^{137}Cs.

Radiocaesium also shows considerable vertical mobility and in Cores 3, 5, and 6, ^{137}Cs was present in sections dated well before the onset of weapons-testing. The depths of penetration of radiocaesium are summarised in Table 5.43 and demonstrate that ^{137}Cs shows the greatest degree of mobility. This vertical movement of ^{137}Cs is well documented (Maguire, 1994: Sugden, 1993: Schell *et al.*, 1989: Oldfield *et al.*, 1979: Clymo, 1979). In particular, Mitchell *et al.*, (1992) observed that the mobility of ^{137}Cs within peat profiles was a factor of 2 higher than the mobility of ^{239}Pu or ^{241}Am. They also estimated a migration velocity of 8 cm y^{-1} for ^{134}Cs, based on its depth of penetration since the Chernobyl accident.

This vertical movement of radiocaesium has been attributed to diffusive and advection processes and as seen for the South Drumboy cores can result in the loss of the peak in ^{137}Cs, attributable to the peak in weapons-testing fallout (Mitchell *et al.*, 1992: Schell, 1987). However, vertical movement of radiocaesium in peat can occur via a variety of processes as well as diffusion and advection, such as active uptake by plants, transfer through root systems, capillary action and infiltration by rainwater (Frissel *et al.*, 1990: Horril *et al.*, 1990: Schell *et al.*, 1989: Clymo, 1983).

Previous studies have also suggested cycling of radiocaesium within surface sections of peat cores, resulting in the majority of the inventories occurring within these sections. Heaton *et al.* (1990) showed that approximately 73% of the total inventory of Chernobyl-derived radiocaesium remained in the top 10 cm of a Scottish peat profile, and this correlated well with the root distribution within the profile. Certain species of plant have been suggested to be more involved in the cycling

process. *Sphagnum* spp. which absorb radiocaesium by trapping aerosols and through soaking up ground water by capillary action and the vascular plant *Calluna vulgaris* both showed high soil:plant concentration factors (Horril *et al.*, 1990: Colgan *et al.*, 1990). Even though considerable penetration of radiocaesium is observed in the South Drumboy cores, each core still shows a high percentage of the total ^{137}Cs in the top 7 cm of the profile (Table 5.44).This effect is most pronounced for Chernobyl ^{137}Cs which showed little lateral flow and would be attributed more to the action of grasses and *Sphagnum* than *Calluna Vulgaris*, since these were the main species present.

The above mobility and bioavailability of Cs can be attributed to it being readily exchangeable in organic soils. In Chapter 3 it was observed that Cs^{+} bound to humic acid and peat through predominantly ionic linkages, unlike Pb^{2+} and Cu^{2+} which showed considerable evidence of covalency.

The radiocaesium inventories recorded for South Drumboy agree favourably with those recorded previously in similar studies (Table 5.45). However, the Chernobyl accident has affected the South Drumboy cores to a greater extent, resulting in greater inventories than those seen in Table 5.45. This is reflective of the high rainfall experienced in the west of Scotland as the Chernobyl plume passed over, leading to high levels of deposition of ^{137}Cs and ^{134}Cs (Smith & Clark, 1989).

Table 5.42 Summary of radiocaesium inventories for the South Drumboy cores, in Bq m^{-2}

Site	altitude	^{134}Cs	Total ^{137}Cs	Chernobyl ^{137}Cs	weapons testing ^{137}Cs	weapons: chernobyl
Core 1	237	164	27630	2110	25520	12.1
Core 2	247	162	3570	2180	1390	0.64
Core 3	267	379	8610	6150	2460	0.40
Core 5	257	114	3100	1880	1220	0.65
Core 6	240	102	2990	1646	1344	0.82

Table 5.43 Depths of penetration of radiocaesium within the South Drumboy cores.

Site	depth of core (cm)	depth of ^{134}Cs penetration (cm)	depth of ^{137}Cs penetration (cm)
Core 1	70	12	43
Core 2	60	10	32
Core 3	70	18	40
Core 5	50	16	50
Core 6	40	12	30

Table 5.44 The % of ^{137}Cs inventories within the top 7cm of the cores.

Site	% total ^{137}Cs	% Chernobyl ^{137}Cs	% weapons-testing ^{137}Cs
Core 1	97	94.9	97.2
Core 2	61.0	98.3	30.8
Core 3	60.1	64.2	37.2
Core 5	62.0	70.3	48.6
Core 6	53.2	66.4	53.8

Table 5.45 Some previously recorded radiocaesium inventories in peat cores in Bq m^{-2}.

Site	mm annual rainfall	total ^{137}Cs	Chernobyl ^{137}Cs	weapons testing ^{137}Cs
Kippure, Ireland Mitchell *et al.*, (1992)	1816	5482	1158	4364
Clara, Ireland Mitchell *et al.*, (1992)	818	2725	1993	880
North Uist, Scotland Sugden (1993)	1449	4186	3604	582
Flanders Moss, Scotland Sugden (1993)	1320	2653	2491	362
Easter Deans, Scotland Sugden (1993)	1013	1288	160	1120

Like the ^{210}Pb and radiocaesium results, remobilisation within the peat cores was also seen to affect the metal profiles, with the most pronounced changes again seen in Cores 1 and 2. Within these cores, conditions were sufficiently reducing to allow dissolution of Mn and Fe oxides, with redeposition at depth as metal sulphides. This also affected Cu, Zn and Co with Br also being affected in Core 1. Of interest are the differing behaviours of Cu and Pb. Cu was subject to remobilisation, associated with changes in redox conditions, whereas Pb did not show such changes. In Chapter 4, metal binding studies on unextracted peat showed that Cu was forming more stable complexes than in humic acid, whereas for Pb the humic acid and the peat showed similar stability constants. This was proposed to indicate that Cu could bind with materials other than humic acid in the unextracted peat, such as the mineral matter whereas Pb was predominantly binding with humic-type materials in peat. This provides further evidence of Cu being associated with the Mn and Fe oxides, resulting in the release of Cu as they come into solution with mobilisation and redeposition as metal sulphides at depth.

Lateral flow was also proposed to affect the metal profiles, especially in Core 2 where increases in the metals and weapons-testing ^{137}Cs were observed at the boundary of the change from organic to mineral horizon. As discussed, this could be mediated by flow of water along the surface of the mineral pan.

However, unlike the ^{210}Pb and radiocaesium results there was little evidence to suggest lateral flow from Core 2 to Core 1, although there was an increase in mineral matter at depth which was attributed to disturbance from the insertion of drainage channels. This resulted in sub-surface maxima in concentrations of Al and the rare earth elements. These cores do show high inventories of Mn, Fe, Zn, As, Hg, Co, Cu and Sb compared to Cores 3, 5 and 6 (Table 5.46) which may reflect their higher mineral content.

Table 5.46 Total inventories of Mn, Fe, Zn,Pb, Cu, As, Sb, Co, Hg and Br, in g m^{-2}.

Site	Mn	Fe	Zn	As	Hg	Co	Pb	Cu	Sb	Br
Core 1	1.430	1220	2.336	0.165	0.017	0.301	1.34	0.576	0.086	0.672
Core 2	5.851	1400	5.287	0.316	0.027	0.317	1.89	0.798	0.027	1.141
Core 3	1.678	269	1.243	0.120	0.015	0.362	2.04	0.107	0.043	1.832
Core 5	0.941	223	0.657	0.067	0.011	0.063	1.19	0.092	0.029	1.710
Core 6	1.331	370	0.788	0.077	0.015	0.140	2.04	0.226	0.023	1.797

Core 5 shows the lowest inventories for all metals and was previously observed to have reduced inventories of ^{210}Pb and weapons-testing ^{137}Cs, compared to Core 6. This would suggest that there is a loss of metals from the core and this may be due to its reducing environment causing dissolution of the Fe and Mn oxides, releasing metals which are co-precipitated with them. The $^{206}Pb/^{207}Pb$ ratios were also unusual, giving low ratios at depths dated well before the use of Pb as an anti-knock additive in petrol. Therefore, it can now be concluded that there is remobilisation and loss of metals and ^{210}Pb from Core 5, making it unsuitable for chronological studies on pollutant metal inputs.

Only Cores 3 and 6 can be used with any confidence to provide information on the changes in pollutant metal deposition over the last 200 years. In these cores Pb, Co, Hg, As, Sb, Cu and Br showed peaks in deposition in the same sections and in Core 3 the rare earth elements also showed peaks in this section. As previously discussed, this is indicative of increased burning of fossil fuels since these metals are present in coal (Table 5.47). The peaks in deposition were dated as occurring between 1964 and 1947 in Core 3 and 1976 and 1935 in Core 6.

Table 5.47 Trace element concentrations in coals used in power stations in the UK, in mg kg^{-1} (Health & Safety Commission, 1980).

Element	Mean value	Range
Sb	3	0.9-10
As	18	4-73
Be	1.8	0.4-3
Br	54	10-162
Cd	0.4	0.3-0.8
Cr	34	12-50
Ce	5	< 3-7
Pb	38	20-60
Mn	84	35-180
Mo	< 2	< 1-3
Ni	28	12-740
Se	2.8	1.8-4.4
U	1.3	0.5-2.3
V	76	30-154

The burning of fossil fuels may be due to industrial processes such as electricity generation. However, the major industries in North Ayrshire at that time were coal mining, whisky bottling and weaving and the increase in deposition of the metals is more likely to be due to domestic burning of fossil fuels. Goldberg *et al.* (1981) recorded steep rises in the content of heavy metals in lake sediments from Lake Michigan which began after 1920 and decreased continuously from 1960. A similar effect was also noted by Livett (1982) in ombrotrophic peat cores from Ringinglow Bog and the decrease in Pb deposition was directly related to the decrease in the primary consumption of coal. The increase in the metals contents in the South Drumboy cores can be seen to follow increases in the population of and number of households in the Burgh of Kilmarnock, which lies directly to the south west of South Drumboy farm (Table 5.48 and Figure 5.68).

However, as observed in Figure 5.68, as the Pb content of Core 1 decreases systematically from 15 g cm^{-2} (1969 - 1938) the number of households still increases. This can be attributed to the introduction of the Clean Air Acts of 1956 and 1968, which were aimed at reducing domestic and industrial emissions and were implemented by Local Authorities (Scorer, 1974). Domestic emissions were successfully reduced through encouraging householders to install approved appliances which used approved fuels and providing subsidies to promote implementation. Therefore the systematic reduction in the deposition of the metals and bromine can be attributed to successful implementation of these Acts.

Even though the total Pb content has decreased over the last 30 years, the $^{206}Pb/^{207}Pb$ ratios in Cores 3 and 6 indicated that car exhaust emissions were an increasingly important component, an effect previously noted by Sugden (1993) in ombrotrophic peats. However, the surface ratios for Cores 3 and 6 are lower than those observed by Sugden (1993), being 1.1291 and 1.1194 respectively. With the $^{206}Pb/^{207}Pb$ ratio of the petrol Pb additive in the UK being between 1.09 and 1.12 (Sugden, 1993), the ratios observed in the Cores 3 and 6 may be reflecting the proximity of the peats to the A77. In a study of the Pb content and isotopic composition of environmental materials in Scotland the $^{206}Pb/^{207}Pb$ ratios of surface soils close to roads were similar to those of petrol Pb additives (Bacon, 1993).

As can be observed from Table 5.49, the concentrations of metals recorded in the South Drumboy cores can not be regarded as contaminating, being below the trigger concentrations of heavy metals in polluted soils as determined by the ICRCL (1980). This may reflect the rural nature of the site, and higher levels of the metals may occur in soils closer to the populated areas. The values also compared well to similar studies on ombrotrophic peat cores (Table 5.50).

Table 5.48 The average populations and number of households for the Burgh of Kilmarnock between 1763 and 1991 (McKinlay *et al.*, 1841: Scottish Office, 1991).

Year	Population size	Number of households
1763	5, 000	*******
1792	6, 776	*******
1801	8, 079	*******
1811	10, 148	*******
1821	12, 769	*******
1831	18, 093	*******
1911	34, 728	7, 513
1921	35, 747	8, 280
1931	38, 681	9, 489
1951	42, 213	11, 713
1961	47, 509	15, 241
1971	48, 240	16, 195
1981	52, 077	18, 627
1991	44, 303	18, 074

Figure 5.68

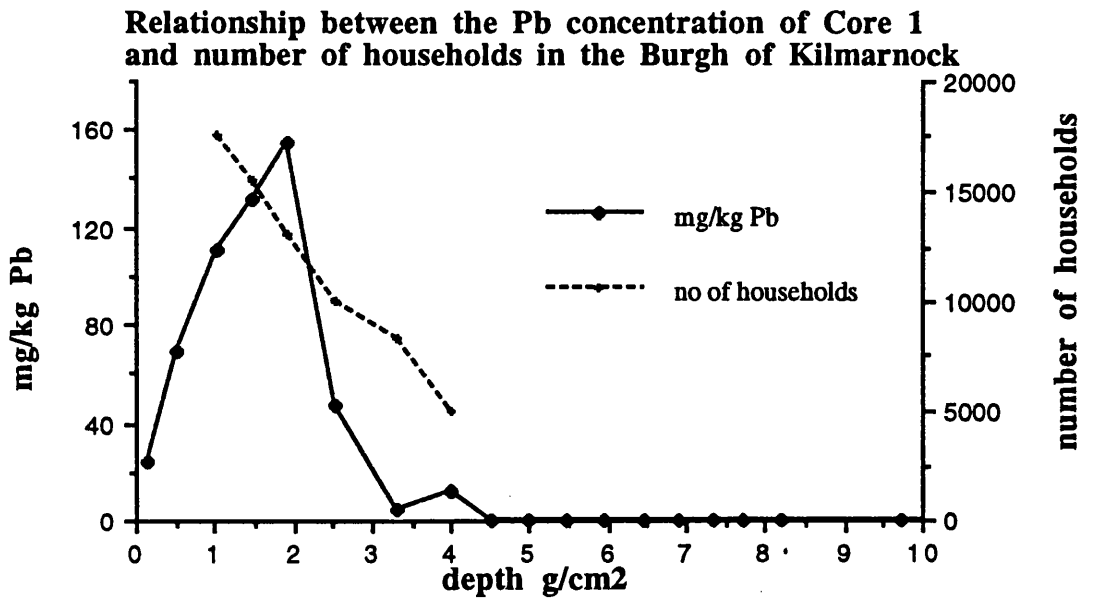

Table 5.49 Ranges in the concentrations of metals in the Drumboy Cores, in mg kg^{-1}

metal	range	ICRCL trigger concentrations (open space)
Pb	0 - 250	1500
Cu	0 - 30	140
As	0 - 13	40
Sb	0 - 6	500
Co	0 - 13	---
Hg	0 - 1	50

Table 5.50 Peak concentrations of Pb, Cu and Zn in ombrotrophic peats from various sites around Scotland, in mg kg^{-1}.

Site	Pb	Cu	Zn	Reference
Fladdabister	55	160	184	Livett *et al.* (1979)
Glenshieldaig	41	11	112	Livett *et al.* (1979)
Glen Torridon	53	16	100	Livett *et al.* (1979)
Flanders Moss	400	12	105	Sugden (1993)
Ringinglow Bog	204	24	118	Jones & Hao (1993)

5.5 CONCLUSIONS

With one of the main aims of the thesis being to evaluate the validity of dating peat profiles using ^{210}Pb it can be concluded that the method can only be utilised where it is clear that there has been no post-depositional mobility of ^{210}Pb, through lateral or vertical flow, or through past disturbance of the profile. This may seem an obvious conclusion, but in some cases disturbance of the profile can be difficult to assess and may affect profiles other than the one which has been disturbed. The effects of mixing of the profile should be taken into account in the calculation of the accumulation rate. It is also advisable to collect a group of peat cores, since the flux and inventory values from one core could give an ambiguous picture of ^{210}Pb deposition at a site. In calculating the activity of ^{210}Pb deposition, where the Z value of the peat changes significantly, the efficiency of the detection system should also be changed to incorporate this. Self absorption of ^{210}Pb may also affect the accuracy of the detection and should be assessed and taken into account.

The Chernobyl accident is still showing a significant contribution to the radiocaesium inventories and both Chernobyl and weapons-testing ^{137}Cs showed mobility within the profiles, being present at depths dated below the advent of weapons testing. Weapons-testing ^{137}Cs showed greater penetration and mobility within the profiles, as well as lateral flow between profiles. This was particularly prevalent in profiles which had been affected by disturbance and indicates that drainage of peats may be a route to decontamination of land affected by radiocaesium.

Post depositional mobility of Fe, Mn, Cu, Zn, Co and Br was observed in some of the cores studied and can be attributed to changes in the redox environment. By contrast Pb, Co, Hg, As and Sb were not affected by redox changes, nor did they exhibit the mobility which radiocaesium showed. Instead these elements, as well as Br when the redox environment allowed, showed peaks in deposition which can be attributed to burning of fossil fuels in the locality. Reductions in their concentrations towards the surface sections can be attributed to the introduction and implementation of the Clean Air Acts of 1956 and 1968.

In addition, the $^{206}Pb/^{207}Pb$ ratios indicated that even though the total Pb content has fallen over the last 30 years in Cores 3 and 6, car exhaust emissions had increasingly contributed to the Pb content over this period.

CHAPTER 6

FINAL CONCLUSIONS & SUGGESTIONS FOR FUTURE RESEARCH

When studying the literature and planning the research, it was evident that there were two main ways to approach the study and this thesis combined these through utilising both laboratory and field-based studies. This approach proved useful since they both gave results and conclusions which were similar and also provided many avenues for further research. However, it did also highlight how different the approaches are and as such further work needs to be carried out on combining them, to give further insight into the interaction of metals with humic substances.

From the studies on the nature and stability of metal binding in Chapters 3 and 4 it was evident that Pb, Cu and Cs all bind in quite different ways, to differing degrees of stability. The infra-red studies showed that Pb and Cu were able to form coordinate, covalent linkages with humic acid whereas Csshowed a predominately ionic linkage. In addition Cu showed a greater degree of covalency which may indicate that it was able to undergo more specific reactions with the functional groupings. The binding studies in Chapter 4 also suggested this, with Cu releasing more protons on interaction with functional groupings and also showing more curvilinearity in the Scatchard plots (both indicating a greater degree of conformational changes on binding).

These differences in behaviour were also seen in the peat profiles, where radiocaesium exhibited a high degree of mobility both vertically and laterally, consistent with its ionic, exchangeable nature. Conversely, Pb and Cu showed minimal mobility, which is consistent with complexation with organic matter.

As also mentioned above, the binding studies illustrated a difference in behaviour between Pb and Cu, which was also seen in the field studies. Cu showed a greater stability of binding to unextracted peat, compared to humic acid, whereas Pb showed similar formation constants for both humic acid and unextracted peat. This was proposed to suggest that Cu was able to bind to other fractions of the peat, such as the oxide fraction, in addition to the humic substances, whereas Pb was predominantly associated with the humic fraction. The field-based studies provided further evidence for this, since in some of the profiles studied Cu showed evidence of post-depositional mobility, mediated by redox changes. As conditions became more reducing the Mn and Fe oxides came into solution and were leached from the profile. Metals such as Cu, which are co-precipitated with them, can also be released and with the evidence provided from the binding studies it is likely that this may have resulted in the peaks in Cu concentration at depth in the peat profiles. Pb did not show this behaviour, with post-depositional mobility being minimal and related to disturbance of the peat profiles.

Both the laboratory and field studies showed that the extraction and fractionation of humic acid resulted in chemical and structural changes in the functional groupings, affecting the stability and nature of metal binding. In particular, extraction resulted in an increase in the nitrogen content, carboxyl content, total acidity and metal binding capacity of the material. Consequently, as discussed above, metal binding was affected. The main aim of the extraction and fractionation procedure is to reduce the heterogeneity of the material, but as observed from the studies presented here it did not meet this aim and could result in conclusions which have no bearing on how a metal or radionuclide will behave in the environment.

Therefore, laboratory-based metal-binding studies which aim to investigate the stability of metal binding should bear this in mind and adopt the methods to study binding with unextracted materials. This may have limitations since the methods will be measuring binding to all fractions of the soil and not just the humic fractions, but the advantages of not using an operationally-defined fraction surely outweighs this. In addition, future research should investigate further the development of non destructive methods of analysis such as ^{13}C NMR. Further research into metal-binding needs to be carried out on the competition of metals with binding sites, by reacting a variety of metals at one time, rather than the artificial one component studies carried out in this research. This was a major limitation when combining the results from the metal-binding studies with the metal profiles within the peat cores, since the constants and relationships produced represented a binding of one metal only to pre-treated peat at a defined pH and ionic strength.

The concept of combining the laboratory and field studies does need to be developed further to provide a more comprehensive picture of metal-soil relationships. Lysimeter studies may be one route, incorporating leaching of metal solutions through profiles and monitoring their uptake and extent of binding.

The field-based studies presented here involved taking a collection of cores and analysing for a wide variety of elements. Consequently, a plethora of data was generated, of which for the purpose of this thesis, only basic interpretation was carried out. In addition, three cores to the north of Glasgow were also collected which were not included. As a result the data will be analysed further in future publications, building on the conclusions presented here.

BIBLIOGRAPHY

Aaby B. & Jacobsen J. (1979). Changes in biotic conditions and metal deposition in the last millenium as reflected in ombrotrophic peat in Draved Mose, Denmark. *Geological Survey of Finland, Yearbook 1978,* Copenhagen, 5-43.

Adriano D.C. (1986). *Trace elements in the terrestial environment.* Springer-Verlag. New York.

Aiken G.R., McKight D.M., Wershaw R.L. & MacCarthy P. (1985). Introduction. In *Humic Substances in Soils, Sediments and Water. Geochemistry, Isolation & Characterisation*. (G.R. Aiken, D.M. McKnight, R.L. Wershaw, P. MacCarthy, eds.). Wiley Interscience, New York, pp 1-12.

Aitken M.J. (1990). Chapter 3: Radiocarbon 1. In *Science based dating in archaeology*. Longman Group Ltd.,U.K., pp56-76.

Alberts J.J., Filip Z. & Hertkorn N. (1992). Fulvics and humic acids isolated from groundwater: compositional characteristics and cation binding. *Journal of Contaminant Hydrology*, **11**, 317-330.

Allen S., Brown P., McKay G. & Flynn O. (1992). An evaluation of single resistance transfer models in the sorption of metal ions by peat. *Journal of Chemical Technology and Biotechnology*, **54** , 271-276.

Alloway B.J. (1990). Soil processes and the behaviour of metals. In *Heavy metals in soils,* (ed. B.J. Alloway), Blackie, London, pp 7-29.

Appleby P.G. & Oldfield F. (1978). The calculation of lead-210 dates assuming a constant rate of supply of unsupported ^{210}Pb to the sediment. *Catena,* **5**, 1-8.

Ault W.A., Senechal R.G. & Erlebach W.E. (1970). Isotopic composition as a natural tracer of lead in the environment. *Environmental Science and Technology*, **4**, 305-313.

Baes A.U. & Bloom P.R. (1988a). Exchange of alkaline earth cations in soil organic matter. *Soil Science*, **146**, 6-14.

Baes A.U. & Bloom P.R. (1988b). Effect of ionic strength on swelling and the exchange of alkaline earth cations in soil organic matter. *Soil Science*, **146**, 67-72.

Baes A.U. & Bloom P.R. (1989). DRIFT spectroscopy of humic and fulvic acid. *Journal of the Soil Science Society of America*, **53**, 695-700.

Backes C.A. & Tipping E. (1987). Aluminium complexation by an aquatic humic fraction under acidic conditions.*Water Research*, **21**, 211-216.

Bacon J.R. (1993). Characterisation of lead and other heavy metals in the Scottish upland environment using isotopic composition. In *Heavy Metals in the Environment*, 1, 282-284, Toronto.

Baldock J.A., Oades J.M., Waters A.G., Peng X., Vassalo A.M. & Wilson M.A., (1991). Aspects of the chemical structure of soil organic materials, as revealed by solid state C^{13} NMR spectroscopy. *Biogeochemistry*, **16** (1), 1-42.

Banerjee S.K. & Mukherjee S.K. (1972). Studies on the infra-red spectra of some divalent transitional metal humates. *Journal of the Indian Society of Soil Science*, **20**, 91-96.

Barber K.E. (1993). Peatlands as scientific archives of past biodiversity. *Biodiversity and Conservation*, **2**, 474-489.

Bellamy L.J. (1975). *The Infra red spectra of complex molecules.* J.Wiley & Sons, New York, pp 183-201.

Bennet B.G. (1990). Worldwide radiation exposure from the Chernobyl accident. In *Environmental contamination following a major nuclear accident,* vol. 2. IAEA-SM-306 94, Vienna, 251-260.

Bloom P.R. & McBride M.B. (1979). Metal ion binding and exchange with hydrogen ions in acid-washed peat. *Journal of the Soil Science Society of America* , **43**, 687-692.

Bonn B.A. & Fish W. (1991). Variability in the measurement of humic carboxyl content. *Environmental Science & Technology,* **25**, 232-240.

Bonn B.A. & Fish W. (1993). Measurement of electrostatic and site specific associations of alkali metal cations with humic acid. *Journal of Soil Science*, **44**, 335-346.

Bonnet R. & Cousins R.P.C. (1987). On the metal content and metal ion uptake of botanically specific peats and the derived humic acids. *Organic Geochemistry*, **11**, 497-503.

Bramryd T. (1980). The role of peatlands for the global carbon dioxide balance. *Proceedings of the 6th International Peat Congress*, pp 9-11.

Brennan R.F., Robson A.D. & Gartrell J.W. (1983). Reactions of copper with soil affecting its availablity to plants II. Effect of soil pH, sterilisation and organic matter on the availability of applied copper. *Australian Journal of Soil Research,* **1**, 153-63.

Bresnahan W.T., Grant C.L., & Weber J.H. (1978). Stability constants for the complexation of copper (II) with water and soil fulvic acids, measured by ion selective electrode. *Analytical Chemistry*, **50** (12), 1675-1679.

Broadbent F.E. & Bradford S. (1952). Cation exchange groupings in soil organic matter. *Soil Science,* **74**, 447-452.

Buffle J. (1988). *Complexation reactions in aquatic systems - an analytical approach.* Ellis Horwood Ltd, London.

Buffle J., Greter F.G.L. & Haerdi W. (1977). Measurement of complexation properties of humic and fulvic acids in natural waters with lead and copper ion selective electrodes. *Analytical Chemistry* , **49**, 216-221.

Buffle J., Langford C.H. & Gamble D.S. (1978). The use of ultrafiltration for the seperation and fractionation of organic ligands in freshwaters. *Analytica Chimica Acta*, **101**, 339-357.

Burkhart W. (1991). Radiation biology of the Lung. *Science of the Total Environment.*, **89**, 1-230.

Cabaniss S.E. (1991). Carboxylic acid content of a fulvic acid determined by potentiometry and aqueous Fourier Transform Infra Red Spectroscopy. *Analytica Chimica Acta* , **255**, 23-30.

Cabaniss S.E. & Shuman M.S. (1986). Combined ion selective electrode and fluorescence quenching detection for Cu^{2+} dissolved organic matter titrations. *Analytical Chemistry*, **58**, 398-401.

Cameron R.S., Thornton B.K., Swift E.S. & Posner A.M. (1972). Molecular weight and shape of humic acid from sedimentation and diffusion measurements on fractionated extracts. *Journal of Soil Science,* **23**, 394-408.

Campanella L. & Tomasseti M. (1990). Thermogravimetric and Infra Red analysis of different extracts of humic substances. *Thermochimica Acta* , **170**, 67-80.

Cheshire M.V., Berrow M.I., Goodman B.A. & Mundie C.M. (1977). Metal distribution and nature of some Cu, Mn and V complexes in humic and fulvic fractions of soil organic matter. *Geochimica et Cosmochimica Acta*, **41**, 1131-1138.

Chow T.J. & Johnstone M.S. (1965). Lead isotopes in gasoline and aerosols of the Los Angeles Basin, California. *Science*, **147**, 502-503.

Clark M.J. & Smith F.B. (1988). Wet and dry deposition of Chernobyl releases. *Nature*, **332**, 245-249.

Clymo R.S. (1963). Ion exchange in sphagnum and its relation to bog ecology. *Annals Botany*, **27**, 309-324.

Clymo R.S. (1983). Peat. In *Ecosystems of the World 4A: Mires, swamp, bog, fen and moor* (ed. Gore A.), pp 159-224, Elsevier, Amsterdam.

Clymo R.S. (1984). The limits to peat bog growth. *Proceedings of Royal Society of London*, **B303**, 605-654.

Clymo R.S. (1991). Peat Growth. In *Quaternary Landscapes* (eds. Shane L.K. & Cushing E.J.) University of Minnesota Press, pp 76-112.

Clymo R.S. & Mackay D. (1987). Upwash and downwash of pollen and spores in the unsaturated surface layer of sphagnum dominated peat. *New Phytologist*, **105**, 175-183.

Clymo R.S., Oldfield F., Appleby P.G., Pearson G.W., Ratnesar P. & Richardson N. (1990). The record of atmospheric deposition in a rainwater dependent peatland. *Philosophical Transactions of the Royal Society of London* , **B327**, 331-338.

Cole K.L., Ongstrom D.R., Futyma R.P. & Stottlemyer R. (1990). Past atmospheric deposition of metals in Northern Indiana measured in a peat core from Cowles Bog. *Environmental Science & Technology*, **24**, 543-549.

Colgan P.A., McGee E.J., Pearce J., Cruikshank J.G., Mulvany N.E., McAdam J.H. & Moss B.W. (1990). Behaviour of radiocaesium in organic soils - some preliminary results of soil-plant transfers from a semi-natural ecosystem in Ireland. In *Transfer of radionuclides in natural and semi-natural environments* (Eds. Desmet G., Nassimbeni P. & Belli M.) Elsevier, Amsterdam, 341-355.

Coppola M & Reiniger P. (1974). Influence of the chemical composition on the gamma-ray attenuation by soils. *Soil Science*, **117**, 331-335.

Coughtrey P.J., Kirkton J.A. & Mitchell N.G. (1990). Caesium distribution and cycling in upland pastures of N.Wales and Cumbria. In *Transfer of radionuclides in natural and semi-natural environments* (Eds. Desmet G., Nassimbeni P. & Belli M.). Elsevier, Amsterdam, 259-267.

Cutshall N.H., Larsen I.L. & Olsen C.R. (1983). Direct analysis of ^{210}Pb in sediment samples: self absorption corrections. *Nuclear Instruments & Methods*, **206**, 309-312.

Damman A.W.H. (1978). The distribution and movement of elements in ombrotrophic peat bogs. *Oikos*, **30**, 480-495.

Davidson C.I., Harrington J.R., Stephenson M.J., Monoghan M. C., Pudykiewcz J. & Schell W.R. (1987). Radioactive caesium from the Chernobyl accident in the Greenland ice sheet. *Science*, **237**, 633-634.

Davies B.E. & Jones L.H.P. (1988) Micronutrients and toxic elements, In *Russell's Soil Conditions and Plant Growth,* 11th edition. (ed. A.Wild), Wiley & Sons, New York, pp 780-815.

Davies R.I., Cheshire M.V. & Graham-Bryce I.I. (1969). Retention of low levels of copper by humic acid. *Journal of Soil Science*, **20**, 65-71.

Davis J.A. (1982). Complexation of trace metals by adsorbed natural organic matter. *Geochimica et Cosmochimica Acta*, **48**, 679-691.

Deina S., Gessa C., Manunza B., Rausa R. & Seeber R. (1990). Analytical and spectroscopic characteristics of humic acids extracted from sewage sludge, manure and worm compost. *Soil Science* **150** (1), 419-424.

Dissanayake C.B. (1983). Metal organic interactions in environmental pollution. *International Journal of Environmental Studies*, **22**, 25-42.

Dubach P. & Mehta N.C. (1963). The chemistry of soil humic substances. *Soils & Fertility* , **26**, 293-307.

Dumontet S., Levesque M. & Mathur S.P. (1990). Limited downward migration of pollutant metals in acidic virgin peat soils near a smelter. *Water, Air & Soil Pollution*, **49**, 329-342.

Dzombak D.A., Fish W. & Morel F.M. (1986). Metal-humate interactions. 1. Discrete ligand and continuous distribution models. *Environmental Science & Technology*, **20**, 669-675.

Eisenreich S.J., Metzer M., & Urban N.R. (1986). Response of atmospheric lead to decreased use of lead in gasoline. *Environmental Science and Technology*, **20**, 171-174.

El-Daoushy F. (1988). A summary on the lead-210 cycle in nature and related applications in Scandinavia. *Environment International*, **14**, 305-319.

El-Daoushy F., Tolonen K. & Rosenberg R. (1982). Lead-210 and moss increment dating of peat in two Finnish sphagnum hummocks. *Nature*, **296**, 429-431.

El-Daoushy F. & Tolonen K. (1984). Lead-210 and heavy metal contents in dated ombrotrophic peat hummocks from Finland. *Nuclear Instruments and Methods in Physics Research*, **223**, 392-399.

Ephraim J., Alegnet S., Mathuthu A., Bicking M., Malcolm R.L. & Marinsky J.A. (1986). A unified physicochemical description of the protonation and metal ion complexation equilibria of natural organic acids 2. Influence of polyelectreolytic properties and functional group heterogeneity on the protonation equilibria of fulvic acid. *Environmental Science & Technology*, **20**, 354-366.

Falck W.E. (1988). A review of modelling the interaction between natural organic matter and metal cations. *British Geological Technical Report*, **WE/88/49**.

Farmer J., Swan D.S. & Baxter M.S. (1980). Records and sources of metal pollutants in a dated Loch Lomond sediment core. *Science of the Total Environment*, **16**, 131-147.

Fitch A. & Stevenson F.J. (1984). Models for stability constants of metal complexes with humic substances. *Journal of Soil Science Society of America*, **48**, 1044-1050.

Fish W. & Morel F.M. (1985). Propogation of error in fuvic acid titration data: a comparison of three analytical methods. *Canadian Journal of Chemistry*, **63**, 1185-1193.

Fish W., Dzombak D.A. & Morel F.M. (1986). Metal humate interactions 2. Application and comparison of models. *Environmental Science & Technology*, **20**, 676-683.

Flaig W., Beutelspacher H. & Reitz E. (1975). Chemical composition and physical properties of humic substances. In *Soil Components: Volume 1. Organic components* (ed. Gjessing J.E.) Springer-Verlag, New York, pp 1-211.

Friedland A.J., Miller E.K., Siccama T.G., & Dunham S. (1993). The redistribution of lead in forest soils in response to changing atmospheric deposition rates. Proceedings of *Heavy Metals in the Environment*, **2**, 526-529, Toronto.

Frissel M.J., Noordijk H., & Van Bergeijk K.E. (1990). The impact of extreme environmental conditions, as occurring in natural ecosystems, on the soil-plant transfer of radionuclides. In *Transfer of radionuclides in natural and semi-natural environments* (eds. Desmet G., Nassimbeni P. & Belli M.), Elsevier, Amsterdam, pp 40-48.

Galloway J.N., Thornton J.D., Norton S.A., Volchok H.L. & McLean R.A.N. (1982). Trace metals in atmospheric deposition: a review and assessment. *Atmospheric Environment,* **16**, 1677-1700.

Gamayunov N.I. & Maslennikov B.I. (1992). Mechanism of the interaction of cations with the adsorptive complex of peat soil. *Pochvovedeniye*, **3**, 146-151.

Gamble D.S., Underdown A.W. & Langford C.H. (1980). Cu (II) titration of fulvic acid ligand sites with theoretical, potentiometric and spectrophotometric analysis. *Analytical Chemistry,* **52**, 1901-1908.

Gibbons D., Jones K.C. & Steinnes E. (1993). Deposition of heavy metals to Norwegian Ombrotrophic peat bogs. Proceedings of *Heavy Metals in the Environment,* **2**, 89-92,Toronto.

Glooschenko W.A., Holloway L., & Arafat N. (1986). The use of mires in monitoring the atmospheric deposition of heavy metals. *Aquatic Botany*, **25**, 179-190.

Goldberg E.D., Hodge V.F., Griffen J.J., Koide M. & Edgington D.M. (1981) The impact of fossil fuel combustion on the sediments of Lake Michigan. *Environmental Science & Technology*, **15**, 466-471.

Goodman B.A. & Cheshire M.V. (1976). The occurence of copper-porphoryn complexes in soil humic acids. *Journal of Soil Science*, **27**, 337-347.

Gore A.J.P. (1983). Introduction. In *Ecosystems of the World, 4A: General studies*. (A.J.P. Gore ed.) pp1-34., Elsevier, Amsterdam.

Gorres M. & Frenzel B. (1993). The Pb, Br, and Ti content in peat bogs as indicators for recent and past depositions. *Naturwissenschaften*, **80**, 333-335.

Gregor J.E., Powell H.J.K. & Town R.M. (1989). Metal fulvic acid complexing: evidence supporting an aliphatic carboxylate mode of coordination. *Science of the Total Environment,* **81/82**, 597-614.

Gregor H.P. (1955). The polyacrylic acid-copper complex. *Journal of Physical Chemistry*, **59**, 34-41.

Gregor J.E. & Powell H.J.K. (1987). Effects of extraction procedures on fulvic acid properties. *Science of the Total Environment,* **62**, 3-12.

Griffiths P.R. (1975). *Chemical analysis volume 43: Chemical Infra Red Fourier transform Spectroscopy.* J. Wiley & Sons, New York.

Hardman D.J., McEldowney S. & Waite S. (1993). Chapter 15: Environmental fate and effects of metals and radionuclides. In *Pollution: Ecology and Biotreatment.* pp233-260. Longman Group Ltd., U.K.

Harrison R.M. & Sturges W.T. (1983). The measurement and interpretation of Br/Pb ratios in airborne particles. *Atmospheric Environment*, **17**, 311-328.

Harrison R.M, Laxen D.P.H. & Wilson S.J. (1981). Chemical associations of lead, cadmium, copper and zinc. *Environmental Science and Technology*, **15**, 1378-1383.

Harrison R.M., Luhana L., & Smith D.J.T. (1993). Urban air pollution by heavy metals: sources and trends. Proceedings of *Heavy Metals in the Environment*, **1**, 81-84, Toronto.

Hatcher P.G., Breger I.A., Dennis L.W., & Maciel G.E. (1983). Solid state ^{13}C NMR of sedimentary humic substances: New revelations on their chemical composition. In *Aquatic and Terrestial Humic Materials* (eds. Christman R.F. & Gjessing E.T.), Ann Arbor Science, Ann Arbor, MI, pp 37-82.

Haworth R.D. (1971). The chemical nature of humic acid. *Soil Science,* **111**, 71-77.

Hayes M.B.H. & Swift R.S. (1978). The chemistry of soil organic colloids. In *The Chemistry of soil constituents.* (D.J. Greenland & M.B.H. Hayes, eds.). Wiley Interscience, New York, pp 179-230.

Hayes M.B.H. (1991). Concepts of the Origins, Composition, and Structures of humic substances. *Advances in soil organic matter research:the impact of agriculture on the environment.* (ed. W.S.Wilson) The Royal Society of Chemistry, pp 3-23.

Health & Safety Commission (1980). Study of Coal: evidence by the HSE to the Commission on Energy and the Environment concerning public health and amenity in the external environment. HMSO, London.

Heaton B., Mitchell R.D.J., Veresoglou D.S. & Killham K. (1990) Caesium dynamics in the peats and associated vegetation of Greece and Northern Scotland. In *Transfer of radionuclides in natural and semi-natural environments* (eds. Desmet G., Nassimbeni P. & Belli M.) Elsevier, Amsterdam, 669-675.

Helmer E.H., Urban N.R. & Eisenreich S.J. (1990). Aluminium geochemistry in peatland waters. *Biogeochemistry*, **9**, 247-276.

Hempfling R., Zech W. & Schulten H.R. (1988) Chemical components of the organic matter in forest soils 2: Moder profile. *Soil Science*, **146** (4), 262-276.

Hill B.M. & Siegel D.I. (1991). Groundwater flow and metal content of peat. *Journal of Hydrology*, **123**, 211-224.

Holdgate M.W. (1979). *A perspective of environmental pollution.* Cambridge University Press.

Hogg E.H. (1993). Decay potential of hummock and hollow sphagnum peats at different depths in a Swedish raised bog. *Oikos*, **66**, 269-278.

Holmgren A. Norden B.O. (1988). The characterisation of peat samples by diffuse reflectance FTIR spectroscopy. *Applied Spectroscopy*, **42** (2), 255-262.

Holtzclaw K.M. & Sposito G. (1978). Analytical properties of the soluble, metal complexing fractions in sludge-soil mixtures. *Journal of Soil Science Society of America*, **43**, 318-323.

Hopkins D.W. & Shiel R.S., (1991). Spectral characterisation of organic matter from soil with mor and mull humus forms. In *Advances in soil organic matter research: the impact of agriculture on the environment.* (ed. W.S.Wilson) The Royal Society of Chemistry, pp 71-78.

Horth H., Frimmel F.H., Hargitai L., Hennes E.C., Muller-Wegener U., Huc A.Y., Niemeyer J., Nissenbaum A., Sekoulov I., Tipping E., Weber J.H.\ & Zepp R.G. (1988). Environmental reactions and functions. In *Humic substances and their role in the environment.* (eds. Frimmel F.H. and Christman R.F.), Wiley Interscience, New York, pp. 245-256.

Horrill A.D., Kennedy V.H. & Harwood T.R. (1990). The concentrations of Chernobyl derived radionuclides in species characteristic of natural and semi-natural ecosystems. In *Transfer of radionuclides in natural and semi-natural environments* (eds. Desmet G., Nassimbeni P. & Belli M.). Elsevier, Amsterdam, pp 27-40.

Ikan R., Ioselip R., Rubinsztain Y., Aizenshtat Z., Miloslavsky I., Yariv S., Pugmire R., Anderson L.L., Woolfenden W.R., Kaplan I.R., Dorsey T., Peters K.E., Boon J.J., De Leeuw J.W., Ishiwatari R., Morinaga S., Yamamoto S., Macihara T., Muller-Vonmoos M. & Rub A. (1992). Chemical, isotopic, spectroscopic and geochemical aspects of natural and synthetic humic substances. *Science of the Total Environment,* **117/118**, 1-12.

Ingram J. (1978). Soil layers in mires: function and terminology. *Journal of Soil Science*, **29**, 224-227.

Ishiwatari R. (1975). Chemical nature of sedimentary humic acid. In *Humic Substances, Their Structure and Function in the Biosphere* (eds. Povoledo D. &. Golterman H.L.). Centre for Agricultural Publications and Documentation, Wageningen, pp 109-121.

Jensen A. & Jensen A. (1991). Historical deposition rates of mercury in Scandinavia estimated by dating and measurement of mercury in cores of peat bogs. *Water, Air & Soil Pollution,* **56**, 769-777.

Johnson L.C., Damman A.W.H. & Malmer N. (1990). *Sphagnum* macrostructure as an indicator of decay and compaction in peat cores from an ombrotrophic south Swedish peat bog. *Journal of Ecology*, **78**, 633-647.

Jones J.M. (1987). Chemical fractionation of Cu, Pb and Zn in ombrotrophic peat. *Environmental Pollution*, **48**, 131-144.

Jones J.M. & Hao J. (1992). Ombrotrophic peat as a medium for historical monitoring of heavy metal pollution. *Environmental Geochemistry & Health*, **15**, 67-74.

Joseph A.B. (1971). Sources of radioactivity and their characteristics. In *Radioactivity in the Marine Environment*, National Academy of Sciences, Washington, DC, 6-41.

Karlin E.F. & Bliss L.C. (1984). Variation in substrate chemistry along microtopographical and water chemistry gradients in peatlands. *Canadian Journal of Botany*, **62**, 142-153.

Kathren R.L. (1984). *Radioactivity in the Environment: Sources, Distribution and Surveillance*. Harwood Academic Publishers.

Keough J.R. & Pippen R.W. (1983). The movement of water from peatland into surrounding groundwater. *Canadian Journal of Botany*, **62**, 835-839.

Kemp W. (1991). Infra red Spectroscopy. In *Organic Spectroscopy*, 3rd edition, MacMillan Education Ltd, Hong Kong, pp 19-57.

Keller C. (1988). Radiochemical age determination. In *Radiochemistry*, Ellis Horwood Chichester, pp 193-199.

Khan S.U. & Schnitzer M. (1971). Further investigations on the chemistry of fulvic acid, a soil humic fraction. *Canadian Journal of Chemistry*, **49**, 2302-2315.

Kononova M.M. (1966). *Soil Organic Matter*. Pergamon, Elmsford, New York.

Kirkton J.A., Coughtrey P.J. & Mitchell N.G. (1990). Derivation of soil to plant concntration ratios for upland systems in the glasshouse and comparison with field and experimental measurements. In *Transfer of radionuclides in natural and semi-natural environments* (eds. Desmet G., Nassimbeni P. & Belli M.). Elsevier, Amsterdam, pp 267-275.

Krosshavn M. (1992). *A study of some chemical properties of soil organic matter: The influence of vegetational background and degree of humification on these properties, and the relationship between them.* Ph.D.Thesis, University of Trondheim, AVH.

Lantzy R.J. & Mackenzie F.T. (1979). Atmospheric trace metals: global cycles and assessment of mans impact. *Geochimica et Cosmochimica Acta*, **43**, 511-525.

Lee J.A. & Tallis J.H. (1973). Regional and historical aspects of lead pollution in Great Britain, *Nature*, **245**, 216-218.

Livens F.R. (1991). Chemical reactions of metals with humic material. *Environmental Pollution*, **70**, 183-208.

Livens F.R., Fowler D. & Horrill A.D. (1992). Wet and dry deposition of ^{131}I, ^{134}Cs, and ^{137}Cs at an upland site in Northern England. *Journal of Environmental Radioactivity*, **16**, 243-254.

Livett E.A. (1982). *The interaction of Heavy Metals with peat and vegetation of blanket bogs in Britain.* Ph.D. Thesis, University of Manchester.

Livett E.A., Lee J.A., & Tallis J.H. (1979). Lead, zinc and copper analysis of British Blanket Peats. *Journal of Ecology*, **67**, 865-891.

Livett E.A. (1988). Geochemical Monitoring of Atmospheric Heavy Metal Pollution: Theory and Applications. *Advances in Ecological Research*, **18**, 65-174.

MacCarthy P. (1976). A proposal to establish a reference collection of humic materials for interlaboratory comparisons. *Geoderma* , **16**, 179-181.

MacCarthy P. & Rice J.A. (1985). Spectroscopy of humic substances. In *Humic Substances in Soils, Sediments, and Water: Geochemistry, Isolation and Characterisation.* (eds. Aiken G.R., McKnight D.M., Wershaw R.L., MacCarthy P.). Wiley Interscience, New York, pp 527-559.

Macdonald P., Cook G.T., Baxter M.S. & Thomson J.T. (1992). The terrestial distribution of artificial radioactivity in South West Scotland. *Science of the Total Environment*, **111**, 59-83.

Mackinley J., Strang D. & Hamilton A. (1842). *The New Statistical Account of Ayrshire (Volume 5).* William Blackwood & Sons, Edinburgh.

McLaren R.G. & Crawford D.V. (1973). Studies on soil copper 2. The specific adsorption of copper by soils. *Journal of Soil Science,* **24**, 443-453.

Maguire S. (1993). Natural and anthropogenic radionuclides in organic and mineral soils. Ph.D. Thesis, University of Glasgow.

Maguire S, Pulford I.D., Cook G.T. & MacKenzie A.B. (1991). Use of infra-red spectroscopy to elucidate the role of functional groups in the binding of metals to humic acids. In *Heavy Metals in the Environment,* **1**, 88-91, Edinburgh.

Malcolm R.L. & MacCarthy P. (1991). The individuality of humic substances in diverse environments. *Advances in soil organic matter research: the impact of agriculture on the environment.* (ed. W.S.Wilson) The Royal Society of Chemistry, pp. 23-35.

Malmer N. & Holm E. (1984). Variations in C/N quotient of peat in relation to decomposition rate and age, determined with ^{210}Pb. *Oikos*, **43**, 171-182.

Mantoura R. & Riley J.P. (1977). Metal binding of organic macromolecules in soil 2. Characterisation of the maximum binding ability of the macromolecules. *Soil Science,* **23**, 188.

Marinsky J.A. & Ephraim J. (1986). A unified physicochemical description of the protonation and metal ion complexation equilibria of natural organic acids 1. Analysis of the influence of polyelectrolyte properties on protonation equilibria in ionic media: fundamental concepts. *Environmental Science & Technology,* **20**, 349-354.

Markert B. & Thornton I. (1990). Multielement analysis of an English peat bog soil. *Water, Air and Soil Pollution,* **49**, 113-123.

Marley N.A., Gaffney J.S., Orlandini K.A., Picew K.C. & Choppin G.R. (1992). Chemical characterisation of size fractionated humic and fulvic materials in aqueous samples. *Science of the Total Environment,* **113**, 159-177.

Martin M.H., Coughtrey P.J. & Ward P. (1979). Historical aspects of heavy metal pollution in the Gordano Valley. *Proceedings of the Bristol Naturalists Society,* **37**, 91-97.

Masini J.C. (1993). Evaluation of neglecting electrostatic interactions on the determination and characterisation of the ionisable sites in humic acid. *Analytica Chimica Acta*, **283**, 803-810.

Mathur S.P. & Farnham R.S. (1985). Geochemistry of humic substances in peat. *Humic Substances in Soils, Sediments, and Water: Geochemistry, Isolation and Characterisation.* (eds. Aiken G.R., McKnight D.M., Wershaw R.L. & MacCarthy P) Wiley Interscience, New York, pp 53-88.

Midgley D. & Torrance K. (1991). *Potentiometric Water Analysis (second edition).* J. Wiley & Sons, London.

Mierle G. & Ingram R. (1991). The role of humic substances in the mobilisation of Hg from watersheds. *Water, Air & Soil Pollution*, **56**, 349-357.

Miller E.K. & Friedland A.J. (1991). Recent reductions in the atmospheric lead flux to high elevation forests of the North Eastern USA. *Heavy Metals in the Environment*, **1**., 86-89, Edinburgh.

Mitchell P.I., Schell W.R., McGarry P., Ryan T.P., Sanchez-Cabeza J.A. & Vidal-Quadras A. (1992). Studies on the vertical distribution of ^{134}Cs, ^{137}Cs, ^{238}Pu, $^{239,240}Pu$, ^{241}Pu, ^{241}Am, & ^{210}Pb in ombrogenous mires at mid-latitudes. *Journal of Radioanalytical & Nuclear Chemistry, Articles*, **156(2)**, 361-387.

Moore P.D. & Bellamy D.J. (1974). *Peatlands*. Springer-Verlag, New York.

Morgan J.J. & Stumm W. (1991) Chemical processes in the environment, relevance of chemical speciation. In *Metals and their compounds in the environment.* (ed. Merian E.). VCH, Weinheim, pp 69-103.

Mortensen J.L. & Schwendinger R.B. (1963). Electrophoretic and spectroscopic characterisation of high molecular weight components of soil organic matter. *Geochimica et Cosmochimica Acta* , **27**, 201-208.

Mott C.J.B. (1988). Surface Chemistry of Soil Particles. In *Russell's Soil Conditions and Plant Growth,* 11th edition. (ed. Wild A.), Wiley & Sons, New York, pp 282-298.

Naeumann R. Steines E. & Guinn V.P. (1993). Feasibility of Instrumental Neutron Activation Analysis for trace element studies in natural soils. *Journal of Radioanalytical and Nuclear Chemistry Articles*, **168**, 61-68.

Nakamoto K (1986). *Infra-red and Raman spectra of Inorganic and Coordination compounds*, 4th edition, J. Wiley & Sons, London.

Niebor E. & Richardson D.H.S. (1980). The replacement of the term "heavy metals" by a biologically and chemically significant classification of metal ions. *Environmental Pollution*, **B1**, 3-26.

Niemeyer J. Chen Y., & Bollag J.M. (1992). The characterisation of humic acid, composts and peat by DRIFT. *Journal of Soil Science Society of America* , **56**, 135-140.

Njstaad O. Naeuman R. & Steinnes E. (1987). Variations in atmospheric trace element deposition studies by INAA of peat cores from ombrotrophic bogs. *Journal of Radioanalytical and Nuclear Chemistry Articles*, **114** (1), 69-75.

Nraigu J. (1989). Global inventory of natural and anthropogenic emissions of trace metals to the atmosphere. *Nature*, **279**, 409-411.

Nriagu J. (1991). Human influence on the global cycling of trace metals. In *Heavy Metals in the Environment*, **1**, 1-5, Edinburgh.

Nozaki Y., Demaster D.J., Lewis D.M., & Turekian K.K. (1978). Atmospheric Pb-210 fluxes determined from soil profiles. *Journal of Geophysical Research*, **83**, 4047-4051.

Ohlson M. & Dahlberg B. (1991). Rate of hummock and lawn communities on Swedish mires during the last 130 years. *Oikos*, **61**, 369-378.

Oldfield F. & Tolonen K. (1981). History of particulate atmospheric pollution from magnetic measurments in dated Finnish peat profiles. *Ambio*, **10**, 185-188.

Oldfield F., Appleby P.G., Cambray R.S., Eakins J.D., Barber K.E., Batterbee R.W., Pearson G.R. & Williams J.M. (1979). ^{210}Pb, ^{137}Cs & ^{239}Pu profiles in ombrotrophic peat. *Oikos*, **33**, 40-45.

Oldfield F., Appleby P.G., Crooks P., Hutchinson S. & Richardson N. (1989). Radioisotope dating of heavy metal deposition histories in sediments and peats: problems and approaches in their resolution. In *Heavy Metals in the Environment*, **1**, 457-459, Geneva.

Olsen E.R. (1985). Atmospheric fluxes and marsh soil inventories of ^{7}Be and ^{210}Pb. *Journal of Geophysical Research.* **90**(6) 10487-10495.

Ortiz de Serra M. & Schnitzer M. (1978). Extraction of humic acid by alkali and a chelating resin. *Canadian Journal of Soil Science*, **52**, 365-374.

Paim S., Linhares C.F., Mangrich A.S. & Martin J.P. (1990). Characterisation of fungal melanins and soil humic acids by chemical analysis and infra-red spectroscopy. *Biology & Fertility of Soils* , **10**, 72-76.

Pakarinen P. (1978). Distribution of heavy metals in the *sphagnum* layer of bog hummocks and hollows. *Annales Botanici Fennici*, **15**, 287-292.

Pakarinen P & Tolonen K (1977). Distribution of lead in Sphagnum fuscum profiles in Finland. *Oikos*, **23**, 69-73.

Parsons J.W. (1988). Isolation of Humic Substances from Soils and Sediments. In *Humic substances and their role in the environment.* (eds. Frimmel F.H &. Christman R.F.) Wiley Interscience, New York, pp.3-14.

Patterson C.C., Shirahat H., & Ericson J.E. (1987). Lead in ancient human bones and its relevance to historical developments of social problems with lead. *Science of the Total Environment*, **61**, 167-200.

Pearson G.W. (1986). Precise calendrical dating of known growth-period samples using a curve-fitting technique. *Radiocarbon*, **28**, 292-299.

Pearson R.G. (1963). Hard and Soft Acids and Bases. *Journal of the American Chemical Society*, **85**, 3533-3539.

Perdue E.M. (1985). Acidic functional groups of humic sunstances. In *Humic Substances in Soils, Sediments, and Water: Geochemistry, Isolation and Characterisation.* (eds. G.R. Aiken, D.M. McKnight, R.L. Wershaw, P MacCarthy). Wiley Interscience, New York, pp 493-526.

Perdue E.M. (1989). Effects of humic substances on metal speciation. *Advances in Chemistry,* **219**, 281-295.

Perdue E.M. & Lytle C.R. (1983). Distribution model for binding of protons and metal ions by humic substances. *Environmental Science & Technology*, **17**, 654-660.

Perdue E.M., Reuter J.H., & Ghosal M. (1980). The operational nature of acidic functional group analyses and its impact on mathematical descriptions of acid-base equilibria in humic substances, *Geochimica Cosmochimica Acta*, **44**, 1841-1851.

Piccolo A. (1989). Reactivity of added humic substances towards plant available heavy metals. *Science of the Total Environment*, **81/82**, 607-614.

Piccolo A. & Camici L. (1990). A comparison of two methods for the determination of total acidity in humic substances. *International Journal of Environmental & Analytical Chemistry,* **41**, 65-69.

Piccolo A. & Stevenson F.J. (1982). Infra red spectra of Cu, Pb and Ca complexes of soil humic substances. *Geoderma,* **27**, 195-202.

Posner A.M. (1964). Titration curves of humic acid. *Transactions of the 8th International Congress of Soil Science*, **2**, 161-174.

Renberg I., Persson M.W. & Emteryd O. (1994) Pre-industrial atmospheric lead contamination deected in Swedish lake sediments. *Nature* **368**, 323-326.

Robbins J.R. (1978). Geochemical and geophysical applications of radioactive lead. In *The Biogeochemistry of lead in the environment.* (ed. Nriagu J.O.), Elsevier, Amsterdam, pp 285-393.

Robbins J.R. & Herche L.R. (1993). Thirty years of ^{210}Pb dating; successes and problems. In *Heavy Metals in the Environment,* **2**, 202-203, Toronto.

Rowell D.L. (1988). Flooded and poorly drained soils. In *Russell's Soil Conditions and Plant Growth,* 11th edition. (ed. Wild A.), Wiley & Sons, New York, pp 899-927.

Ruhling A. & Tyler G. (1968). An ecological approach to the lead problem. *Botanical Notiser*, **121**, 321-342.

Ruhling A. & Tyler G. (1969). Ecology of heavy metals - a regional and historical study. *Botanical Notiser*, **122**, 248-259.

Saar R.A. & Weber J.H. (1979). Complexation of cadmium(II) with water and soil derived fulvic acids: effect of pH and fulvic acid concentration. *Canadian Journal of Chemistry,* **57**, 1263-1268.

Saar R.A. & Weber J.H. (1980). Lead (II) complexation by fulvic acid: how it differs from fulvic acid complexation of copper (II) and cadmium (II). *Geochimica et Cosmochimica Acta,* **44**, 1381-1384.

Sahu S. & Banerjee D.K. (1990). Complexation properties of typical soil and peat humic acids with copper (II) and cadmium (II). *International Journal of Environmental and Analytical Chemistry,* **42**, 35-44.

Salomons W. & Forstner U. (1984). Metals in the atmosphere. In *Metals in the Hydrocycle.* Springer-Verlag, Berlin, pp 99-137.

Salt C. & Mayes R.W. (1990). Seasonal patterns of Cs uptake into hill pasture vegetation. In *Transfer of radionuclides in natural and semi-natural environments* (eds. Desmet G., Nassimbeni P. & Belli M.), Elsevier, Amsterdam, pp 334-341.

Sanders J.R. (1980). The use of adsorption equations to describe copper complexing by humified organic matter. *Journal of Soil Science,* **31**, 633-641.

Santschi P.H. & Honeyman B.D., (1989). Radionuclides in the aquatic environment. *Radiation Physics & Chemistry-International Journal of Radiation Applications and Instruments, Part C,* **34**, 213-240.

Schell W.R. (1986). Deposited atmospheric chemicals. *Environmental Science and Technology,* **20**, 847-853.

Schell W.R. (1987). A historical perspective of atmospheric chemicals deposited on a mountain top peat bog in Pennsylvania. *International Journal of Coal Geology*, **8**, 147-173.

Schell W.R., Tobin M.J. & Massey C.D. (1989). Evaluation of trace metal deposition history and potential element mobility in selected cores from peat and wetland ecosystems. *The Science of the Total Environment*, **87/88**, 19-42.

Schell W.R. & Tobin M.J. (1990). Deposition and mobility of chemical elements in forest and wetland environments. In*Transfer of radionuclides in natural and semi-natural environments* (eds. Desmet G., Nassimbeni P. & Belli M.). Elsevier, Amsterdam, pp 118-129.

Schnitzer M. (1978). Humic Substances: Chemistry and reactions. In *Soil Organic Matter* (eds. Schnitzer M. & Khan S.U.). Elsevier, New York, pp 1-64.

Schnitzer M. & Gupta V.C. (1964). Some chemical characteristics of the organic matter extracted from the O and B_2 horizons of a grey wooded soil. *Soil Science Society of America, Proceedings*, **29**, 274-277.

Schnitzer M. & Khan S.U. (1972). *Humic Substances in the Environment.* Marcell Dekker, New York.

Schnitzer M. & Khan S.U. (1978). *Soil Organic Matter* . Elsevier, New York.

Schnitzer M. & Skinner S. (1968). Alkali versus acid extraction of soil organic matter. *Soil Science,* **105**, 392-396.

Schulten H.R. (1991). A chemical structure for humic substances. *Naturwissenschaften* , **78**, 311-313.

Scorer R.G. (1974). *Pollution in the air: problems, policies & priorities.* Routledge & Kegan Paul, London.

Segal M. & Morris C. (1991) The legacy of Chernobyl. *Chemistry in Britain*, **27**, 904-908.

Senesi N. & Calderoni G. (1987). Structural and chemical characteristics of Cu, Fe, & Mn complexes formed by paleosol humic acids. *Organic Geochemistry*, **13**, 1145-1151.

Sheppard M.I. & Thibault D.H. (1992). Migration of Tc, Np, U, Cs, & F in peat. *Journal of Environmental Quality* , **17**, 644-653.

Shirahata H., Elias R.W., Patterson C.C, & Koide M. (1980). Chronological variations in concentrations and isotopic compositions of anthropogenic atmospheric lead in sediments of a remote subalpine pond. *Geochimica et Cosmochimica Acta*, **44**, 149-162.

Shotyk W. (1988). Review of the inorganic geochemistry of peats and peatland waters. *Earth-science reviews*, **25**, 95-176.

Shotyk W., Nesbitt H. & Fyfe W. (1990). The behaviour of major and trace elements in vertical peat profiles. *International Journal of Coal Geology*, **15**, 163-190.

Shotyk W., Nesbitt H., & Fyfe W.S. (1992). Natural and anthropogenic enrichments of trace metals in peat profiles. *International Journal of Coal Geology*, **20**, 49-84.

Shuman M.S., Collins G.J., Fitzgerald P.J. & Olson D.L. (1983). Distribution of stability constants and dissociation rate constants among binding sites in estuarine copper-organic complexes. In *Aquatic and Terrestial Humic Materials* (eds.. Christman R.F. & Gjessing E.T.) Ann Arbor Science, Ann Arbor, MI, pp 349-370.

Siegel D.I. & Glaser P.H. (1987). Groundwater flow in a bog-fen complex, Lost River Peatland, Northern Minnesota. *Journal of Ecology*, **75**, 743-754.

Sikora S. & Stevenson F.J (1988) Silver complexation by humic substances. *Geoderma*, **42**, 353-361.

Smith F.B. & Clark M.J. (1989). The transport and deposition of airborne debris from the Chernobyl nuclear power plant accident with special emphasis on the consequences to the U.K. *Meterological Office Paper*, **42**, HMSO, London.

Socrates G. (1980). *Infra red characteristic group frequences.* J. Wiley & Sons, London.

Sposito G. (1982). The use of the Langmuir equation in the interpretation of adsorption phenomena 2. *Journal of Soil Science Society of America* , **46**, 1147.

Steelink C. (1985). Implications of Elemental Characteristics of Humic Substances. In *Humic Substances in Soils, Sediments, and Water: Geochemistry, Isolation and Characterisation.* (eds. Aiken G.R., McKnight D.M., Wershaw R.L., MacCarthy P) Wiley Interscience, New York, pp 457-475.

Steelink C. & Tollin G. (1967). Free radicals in soil. In *Soil biochemistry* (eds. Maclaren A.D. & Peterson G.H.) Marcell Dekker, New York, pp 147-169.

Stevenson F.J. (1976). Stability constants of Cu, Pb and Cd complexes with humic acids. *Journal of Soil Science Society of America,* **40**, 655-672.

Stevenson F.J. (1977). Metal complexes of humic acids. *Soil Science,* **123**, 10-17.

Stevenson F.J. (1982). *Humus Chemistry.* Wiley Interscience, New York.

Stevenson F.J. & Butler J.H.A. (1969). Chemistry of humic acids and related pigments. In *Organic Geochemistry* (eds. Eglinton G. & Murphy M.T.J.). Springer-Verlag, New York, pp 534-557.

Stevenson F.J. & Chen Y. (1991). Stability constants of copper(II)-humate complexes determined by modified potentiometric titration. *Journal of Soil Science Society of America,* **55**, 1586-1591.

Stevenson F.J. & Goh K.M. (1971). Infra-red spectra of humic acids and related substances. *Geochimica et Cosmochimica Acta* **35**, 471-483.

Stevenson F.J. & Goh K.M. (1974). IR-Spectra of humic acids. Elimination of interferences due to hygroscopic moisture. *Soil Science*, **117**, 34-41.

Stevenson F.J., Krastanov S.A. & Ardkani M.S. (1973). Formation constants of Cu complexes with humic and fulvic acids. *Geoderma*, **9**, 129-141.

Stevenson F.J., Fitch A. & Brar M.S. (1993). Stability constants of copper-humate complexes: comparison of select models. *Soil Science* , **155**, 77-91.

Sturges W.T. & Harrison R.M. (1986). The use of Br/Pb ratios in atmospheric particles to discriminate between vehicular and industrial lead sources in the vicinity of a lead works, Thorpe, West Yorkshire. *Atmospheric Environment*, **20**, 833-843.

Suess H.E. (1970). Bristlecone pine calibration time 5200BC to present. In *Radiocarbon dating*. (ed. Berger R. & Suess H.E.) University of California Press, Berkely, pp 777-784.

Sugden C.I. (1993). *Isotopic studies of the environmental chemistry of lead.* Ph.D. Thesis, University of Edinburgh.

Sugden C.I., Farmer J.G. & Mackenzie A.B. (1991). Lead and $^{206/207}$Pb proflies in ^{210}Pb-dated ombrotrophic peat cores from Scotland. In *Heavy Metals in the Environment*, **2**, 90-93, Edinburgh.

Swan D.S., Baxter M.S., McKinley I.G., & Jack W. (1982). Radiocaesium and Pb in Clyde Sea Loch sediments. *Estuarine, Coastal and Shelf Science*, **15**, 515-536.

Swift R.S. (1985). Fractionation of Soil Humic Substances. In *Humic Substances in Soils, Sediments, and Water: Geochemistry, Isolation and Characterisation.* (eds. Aiken G.R., McKnight D.M., Wershaw R.L. & MacCarthy P), Wiley Interscience, New York, pp 387-408.

Swift R.S., Thornton B.K., & Posner A.M. (1970). Spectral characteristics of a humic acid fraction with respect to molecular weight using an agar gel. *Soil Science,* **110**, 93-99.

Swift R.S. & Posner A.M. (1971). Gel chromatography of humic acid. *Journal of Soil Science,* **22**, 237-249.

Swift R.S. & Posner A.M. (1972). Autoxidation of humic acid under alkaline conditions. *Journal of Soil Science,* **2**, 381-393.

Tan K.H., Lobartini J.C., Himmelsbach D.S. & Asmussen L.E. (1991). The significance of solid state ^{13}C NMR spectroscopy of whole soil in the characterisation of humic matter. *Communication in Soil Science & Plant analysis*, **22**, 861-877.

Tao S. (1992). A fixed-*k* model for metal-humate binding. *Science of the Total Environment,* **117/118**, 139-144.

Thakur A.K., Munson P.J., Hunston D.L. & Robbard D. (1980). Characteristics of ligand binding systems by continuous affinity distributions of arbitary shape. *Analytical Biochemistry*, **103**, 240-254.

Thurman E.M. & Malcolm R.L. (1981). Preperative isolation of humic substances. *Environmental Science & Technology*, **15**, 463-466.

Thurman E.M. & Malcolm R.L. (1983). Structural study of humic substances: New approaches and methods. In *Aquatic and Terrestial Humic Materials* (eds. Christman R.F & Gjessing E.T.) Ann Arbor Science, Ann Arbor, MI, pp 1-23.

Tipping E. (1993). Modelling the competition between alkaline earth cations and trace metal species for binding by humic substances. *Environmental Science & Technology,* **27**, 520-529.

Tipping E. & Hurley M.A. (1988). A model of solid-solution interactions in acid organic soils, based in the complexation properties of humic substances. *Journal of Soil Science*, **39**, 505-519.

Tipping E. & Woof C. (1990). Humic substances in acid organic soils: modelling their release to the soil solution in terms of humic charge. *Journal of Soil Science*, **41**, 573-586.

Tipping E. & Woof C. (1991). The distribution of humic substances between the solid and aqueous phases of acid organic soils; a description based on humic heterogeneity and charge-dependent sorption equilibria. *Journal of Soil Science*, **42**, 437-448.

Tipping E. & Hurley M.A. (1992). A unifying model of cation binding by humic substances. *Geochimica et Cosmochimica Acta*, **56**, 3627-3641.

Tipping E., Backes C.A. & Hurley M.A. (1988). The complexation of protons, aluminium and calcium by aquatic humic substances: a model incorporating binding-site heterogeneity and macroionic effects. *Water Research*, **22**, 597-611.

Tipping E., Woof C. & Hurley M.A. (1991). Humic substances in acid surface waters; modelling aluminium binding, contribution to ionic charge-balance, and control of pH. *Water Research*, **25**, 425-435.

Tolonen K. & Oldfield F. (1986). The record of magnetic-mineral and heavy metal deposition at Regent Street Bog, Fredricton, New Brunswick, Canada. *Physics of the Earth and Planetory Interiors*, **42**, 57-66.

Tomar N.K, Yadav R.P. & Relan P.S. (1992). Characteristics of humic acid fulvic acids extracted with NaOH & NaOH-Na pyrophosphate mixture from soils of arid and subhumid regions 2. Spectroscopic properties. *Arid Soil Research & Rehabilitation*, **6**, 187-200.

Town R.M. & Powell H.K.J. (1993). Ion-selective electrode potentiometric studies on the complexation of copper(II) by soil-derived humic and fulvic acids. *Analytica Chimica Acta*, **279**, 221-223.

Tuschall J.R. Jnr. & Brezonik P.L. (1983). Application of continuous flow Ultrafiltration and competing ligand/differential spectrophotometry for measurement of heavy metal complexation by dissolved organic matter. *Analytica Chimica Acta*, **149**, 47-58.

Tuschall J.R. Jnr. & Brezonik P.L. (1984). Analytical methods for the measurement and interpretation of metal binding by aquatic humus and model compounds. In *Complexation of trace metals in natural waters*, (eds. Kramer C.J.M & Duinker J.C.), Martinus Nijhoff/ Dr. W. Junk Publishers, The Hague, pp 83-94.

Turner D.R., Varney M.S., Whitfield M., Mantoura R.F.C., & Riley J.P. (1986). Electrochemical studies of copper and lead complexation by fulvic acid. I. Potentiometric measurements and a critical comparison of metal binding models. *Geochimica et Cosmochimica Acta*, **50**, 289-297.

Underdown A.W., Langford C.H. & Gamble D.S. (1985). Light scattering studies of the relationship between cation binding and aggregation of a fulvic acid. *Environmental Science & Technology*, **19**, 132-136.

United Nations Scientific Committee on the Effects of Atomic Radiation (UNSCEAR, 1982). Ionising radiation: Sources and biological effects. *United Nations Publication*, **E.77.IX.8**, United Nations, New York.

Urban N.R., Eisenreich S.J., Grigal D.F. & Schurr K.T. (1990). Mobility and diagenesis of Pb and ^{210}Pb in peat. *Geochimica et Cosmochimica Acta*, **54**, 3329-3346.

Van Dijk H. (1971). Cation binding of humic acids. *Geoderma*, **5**, 53-61.

Vinkler P., Lakatos B. & Meisel J. (1976). IR spectroscopic investigations of humic substances and their metal complexes. *Geoderma*, **15**, 231-242.

Walton-Day K., Filipek L.H. & Papp C.S.E. (1990) Mechanisms for controlling Cu, Fe, Mn and Co profiles in peat in the Filson Creek Fen, Northeastern Minnesota. *Geochimica Cosmochimica Acta*, **54**, 2933-2966.

Warner B.G., Clymo R.S. & Tolonen K. (1993). Implications of peat accumulation at Pont Escuminac, New Brunswick. *Quaternary Research*, **39**, 245-248.

Wagner G.H. & Stevenson F.J. (1965). Structural arrangements functional groups soil humic acid as revealed by infra-red analysis. *Soil Science Society of America Proceedings*, **29**, 43-48.

Warwick P., Hall A. & Patterson M. (1991). Complexation of nickel with extracted and non-extracted humic and fulvic materials. *Radiochimica Acta*, **58/59**, 137-144.

Wershaw R.L., Pinkney D.J. & Booker S.E. (1977). Chemical structure of humic acid part 1: A generalised structural model. *Journal of Research of the U.S. Geological Survey*, **5**, 565-569.

Wheeler B.D. (1993). Botanical diversity in British mires. *Biodiversity and Conservation*, **2**, 490-512.

Williams D.H. & Fleming I. (1989). Infra red spectra. In *Spectroscopic methods in Organic Chemistry,* 4th edition, McGraw-Hill, London, pp 29-62.

Wilson D.E. & Kinney P. (1977). Effects of polymeric charge variations on the proton-metal ion equilibria of humic materials. *Limnology & Oceanography,* **22**, 281-289.

Wood J.C., Moschapedis S.E. & Elafson R.M. (1961). Studies in humic acid chemistry 1. Molecular weights of humic acids in sulfolane. *Fuel*, **40**, 193-201.

Zoller W.H., Gladney E.S. & Duce R.A. (1974). Atmospheric concentrations and sources of trace metals at the South Pole. *Science*, **183**, 199-210.

Zunino H. & Martin J.P. (1977). Metal binding of organic macromolecules in soil 2. *Soil Science,* **123** (3), 188-202.

APPENDIX 1

DATA & GRAPHS FROM CHAPTERS 2 & 3

A1.1 TOTAL ACIDITY DATA & CALCULATIONS

To calculate the total acidity the following calculation is used:

$$\frac{(\text{Blank - Sample titre}) \times \text{N Acid} \times 1000}{\text{mg Sample}} = \text{mmol}_c\ g^{-1}\ \text{Total acidity}$$

The titration data is presented here, along with all the calculations.

BLANK TITRATION DATA

pH	ml 0.1N HCl blank 1	pH	ml 0.1N HCl blank 2	pH	ml 0.1N HCl blank 3	pH	ml 0.1N HCl blank 4
12.27	40.00	12.07	40.00	12.07	40.00	12.27	40.00
12.16	42.80	11.95	42.89	11.95	41.99	12.16	41.80
12.09	43.80	11.77	45.54	11.77	44.18	12.09	42.80
11.90	46.00	11.69	46.24	11.69	45.00	11.98	44.12
11.78	47.00	11.55	46.98	11.55	46.00	11.90	45.00
11.70	47.57	11.37	47.66	11.37	46.98	11.78	46.00
11.42	49.00	11.07	48.24	11.07	48.00	11.70	46.57
11.21	49.44	10.68	48.81	10.68	48.60	11.21	48.60
11.02	49.74	10.19	49.12	10.19	48.95	11.02	48.97
10.66	49.94	9.61	49.50	9.80	49.08	10.66	49.40
8.80	50.48	8.80	49.57	9.61	49.18	8.80	49.92
8.60	50.56	8.40	49.59	8.08	49.24	8.60	49.98
8.40	50.62			7.94	49.30	8.40	49.98

pH	ml 0.1N HCl blank 5	pH	ml 0.1N HCl blank 6	pH	ml 0.1N HCl blank 7	pH	ml 0.1N HCl blank 8
12.64	35.00	12.52	35.00	12.53	40.00	12.55	30.16
12.52	38.12	12.31	40.00	12.22	45.00	12.31	35.31
12.40	40.82	11.90	45.00	11.62	48.81	12.11	40.08
12.11	43.26	11.54	48.00	11.22	49.43	11.80	43.17
11.92	45.89	11.11	50.00	10.91	49.81	11.41	45.09
11.50	47.74	10.83	50.34	10.51	50.02	10.82	46.33
10.81	48.38	10.61	50.52	10.22	50.11	10.70	46.44
10.52	48.68	10.22	50.72	9.81	50.19	10.40	46.56
10.11	48.78	9.60	50.85	9.60	50.28	9.91	46.71
9.80	48.86	9.30	50.89	9.11	50.35	9.70	46.76
9.60	48.89	8.90	50.92	8.80	50.41	9.30	46.82
8.90	48.91	7.50	51.02	8.70	50.46	7.80	46.90
8.40	48.89			8.10	50.51		

UNPROTONATED HUXTER PEAT TOTAL ACIDITY DATA

pH	ml 0.1N HCl HX1	pH	ml 0.1N HCl HX2	pH	ml 0.1N HCl HX3
11.90	40.00	11.27	40.00	11.93	40.00
11.78	42.21	11.20	43.31	11.74	43.00
11.16	47.78	11.14	48.02	11.09	48.00
11.02	48.40	10.91	48.61	10.84	48.70
10.87	48.80	10.63	49.02	10.28	49.40
10.59	49.30	10.40	49.21	9.84	49.60
10.39	49.50	9.89	49.30	9.83	49.64
10.18	49.65	9.66	49.42	9.72	49.67
9.83	49.80	9.21	49.54	9.60	49.70
9.44	49.90	8.98	49.60	9.45	49.72
9.27	49.97	8.34	49.66	9.16	49.78
8.88	50.00	7.39	49.72	8.78	49.84
8.40	50.04			7.97	49.89

pH	ml 0.1N HCl HX4	pH	ml 0.1N HCl HX5	pH	ml 0.1N HCl HX6
11.72	40.00	11.39	40.00	11.69	40.00
11.23	45.00	11.18	45.00	11.45	43.28
10.72	46.75	10.54	46.75	11.17	45.00
10.66	46.85	10.17	47.00	10.80	45.58
10.58	47.00	10.06	47.06	10.77	46.40
10.13	47.40	9.98	47.09	10.34	47.00
10.03	47.44	9.88	47.11	9.41	47.40
9.89	47.50	9.75	47.17	9.24	47.45
9.73	47.54	9.62	47.23	9.00	47.48
9.48	47.61	9.44	47.26	8.99	47.50
9.15	47.70	9.01	47.32	8.68	47.53
8.45	47.76	8.48	47.38	8.67	47.55
8.40	47.77	7.21	47.43	7.52	47.58

UNPROTONATED HUXTER PEAT RESULTS

sample	weight (mg)	normality HCl	blank titration used	end point blank (ml)	end point titre (ml)	total acidity $mmol_c\ g^{-1}$
HX1	54.4	0.099	1	50.62	50.04	1.06
HX2	56.9	0.099	1	50.62	49.66	1.67
HX3	54.8	0.099	1	50.62	49.88	1.34
HX4	78.9	0.100	2	49.59	47.77	2.31
HX5	61.7	0.100	2	49.59	47.39	3.57
HX6	63.8	0.100	2	49.59	47.56	3.19

UNPROTONATED LUNGA WATER PEAT TOTAL ACIDITY DATA

pH	ml 0.1N HCl LW1	pH	ml 0.1N HCl LW2	pH	ml 0.1N HCl LW3
11.92	40.00	12.04	40.00	11.78	41.00
11.67	43.00	11.74	43.98	11.57	43.20
11.47	44.53	11.63	44.98	11.31	44.70
11.21	45.67	11.48	45.98	11.03	44.90
10.75	46.65	11.37	46.58	10.81	45.40
10.67	46.72	11.28	46.98	10.49	45.90
10.40	47.00	11.17	47.58	10.41	46.15
9.85	47.13	10.94	47.98	10.27	46.40
9.73	47.17	10.75	48.28	10.09	46.70
9.51	47.21	10.36	48.60	9.84	46.90
9.36	47.26	9.86	48.70	9.35	47.04
8.97	47.31	9.22	48.80	8.97	47.11
8.64	47.34	8.63	49.00	8.63	47.14
7.96	47.38	7.04	49.08	7.66	47.18

pH	ml 0.1N HCl LW4	pH	ml 0.1N HCl LW5
11.75	40.00	11.48	40.00
11.56	42.00	11.44	41.10
11.27	43.78	11.20	42.50
11.22	44.26	10.92	43.86
11.18	44.49	10.81	44.38
10.96	44.88	10.73	45.14
10.84	45.00	10.38	45.39
10.70	45.20	10.26	45.48
10.22	45.60	10.18	45.55
9.88	45.80	9.88	45.70
9.16	45.86	9.22	45.80
8.77	45.92	8.95	45.83
8.52	45.99	8.70	45.86
7.76	46.01	7.94	45.91

UNPROTONATED LUNGA WATER PEAT RESULTS

sample	weight (mg)	normality HCl	blank titration used	end point blank (ml)	end point titre (ml)	total acidity $mmol_c\ g^{-1}$
LW1	60.9	0.099	1	50.62	47.36	5.30
LW2	59.3	0.099	1	50.62	49.00	2.70
LW3	65.2	0.100	2	49.59	47.15	3.74
LW4	100.7	0.100	2	49.59	45.90	3.66
LW5	83.0	0.100	2	49.59	45.89	4.46

PROTONATED HUXTER PEAT TOTAL ACIDITY DATA

pH	ml 0.1N HCl HX1	pH	ml 0.1N HCl HX2	pH	ml 0.1N HCl HX3
11.92	40.00	12.01	40.52	12.23	40.44
11.73	43.19	11.61	45.05	11.61	45.16
11.51	45.28	11.11	46.19	10.94	47.26
11.10	46.09	10.95	47.30	10.71	47.52
10.80	46.68	10.56	47.79	10.40	47.82
10.20	46.98	10.12	48.03	10.10	47.94
9.40	47.58	9.81	48.12	9.60	48.04
9.10	47.64	9.62	48.23	9.30	48.11
8.50	47.68	9.16	48.28	8.90	48.16
7.41	47.72	8.10	48.37	8.40	48.20

pH	ml 0.1N HCl HX4	pH	ml 0.1N HCl HX5
12.52	40.40	12.41	40.33
11.83	43.17	11.92	45.08
11.51	45.23	10.81	47.37
10.91	47.10	10.11	47.92
10.70	47.28	9.80	47.98
10.40	47.51	9.60	48.03
9.90	47.73	9.40	48.08
9.50	47.83	9.10	48.13
9.10	47.93	8.60	48.17
8.40	47.98	7.60	48.21

PROTONATED HUXTER PEAT RESULTS

sample	weight (mg)	normality HCl	blank titration used	end point blank (ml)	end point titre (ml)	total acidity $mmol_c\ g^{-1}$
HX1	54.4	0.1	6	50.95	47.69	5.99
HX2	58.0	0.1	6	50.95	48.35	4.48
HX3	52.2	0.1	6	50.95	48.22	5.23
HX4	52.3	0.1	6	50.95	47.98	5.68
HX5	56.0	0.1	6	50.95	48.18	4.89

PROTONATED LUNGA WATER PEAT TOTAL ACIDITY DATA

pH	ml 0.1N HCl LW1	pH	ml 0.1N HCl LW2	pH	ml 0.1N HCl LW3
12.43	30.00	12.34	30.00	12.35	30.00
12.25	35.00	12.14	35.00	12.12	35.00
11.91	40.00	11.85	41.09	11.91	38.00
11.73	42.00	10.71	45.00	11.80	40.00
10.90	45.00	10.40	45.25	11.10	44.00
10.40	45.38	9.90	45.44	10.90	45.00
9.90	45.52	9.60	45.50	10.40	45.28
9.50	45.61	9.30	45.56	9.60	45.48
8.90	45.72	8.80	45.61	8.80	45.54
7.90	45.76	7.80	45.66	7.90	45.55

pH	ml 0.1N HCl LW4	pH	ml 0.1N HCl LW5
12.36	30.00	12.35	30.00
12.14	35.00	12.14	35.00
11.93	40.00	11.83	40.00
11.18	45.00	10.81	45.00
10.60	45.68	10.60	45.20
10.40	45.78	10.40	45.33
10.10	45.94	10.11	45.49
9.70	46.08	9.70	45.60
9.10	46.18	9.20	45.68
7.90	46.28	7.60	45.78

PROTONATED LUNGA WATER PEAT RESULTS

sample	weight (mg)	normality HCl	blank titration used	end point blank (ml)	end point titre (ml)	total acidity $mmol_c\ g^{-1}$
LW1	50.5	0.1	5	48.89	45.75	6.22
LW2	51.8	0.1	5	48.89	45.65	6.25
LW3	58.0	0.1	5	48.89	45.54	5.78
LW4	51.6	0.1	5	48.89	46.00	6.49
LW5	54.8	0.1	5	48.89	45.77	5.69

UNPROTONATED HUXTER HUMIC ACID TOTAL ACIDITY DATA

pH	0.1N HCl HXHA1	pH	0.1N HCl HXHA 2	pH	0.1N HCl HXHA3
11.90	30.00	11.90	30.00	12.30	30.00
11.80	35.00	11.70	35.00	12.00	35.00
11.50	37.50	11.10	40.00	11.70	38.00
11.10	40.00	10.80	40.58	11.40	39.00
11.00	40.50	10.50	41.00	11.00	40.08
10.70	40.79	10.20	41.18	10.60	40.42
10.60	41.00	10.00	41.30	10.40	40.64
10.50	41.20	9.70	41.40	10.10	40.98
9.70	41.50	9.30	41.50	9.80	41.04
9.60	41.60	8.90	41.58	9.30	41.32
9.00	41.74	8.80	41.62	9.20	41.40
8.40	41.76	8.40	41.64	8.20	41.48

pH	0.1N HCl HXHA4	pH	0.1N HCl HXHA5
12.60	30.00	12.40	30.00
12.30	35.00	12.20	35.00
12.00	38.00	12.10	37.00
11.80	39.20	12.00	38.00
11.60	40.06	11.60	39.40
11.00	41.04	11.50	39.62
10.80	41.22	11.20	40.00
10.40	41.38	10.50	40.98
10.30	41.49	10.10	41.62
9.40	41.68	9.60	41.80
9.20	41.70	9.20	41.90
8.00	41.74	7.60	42.00

UNPROTONATED HUXTER HUMIC ACID RESULTS

sample	weight (mg)	normality HCl	blank titration used	end point blank (ml)	end point titre (ml)	total acidity $mmol_c\ g^{-1}$
HX1	53.3	0.11	3	43.90	41.76	4.42
HX2	80.5	0.11	3	43.90	41.64	3.09
HX3	77.4	0.10	4	44.51	41.47	3.93
HX4	58.1	0.10	4	44.51	41.73	4.78
HX5	62.8	0.10	4	44.51	41.98	4.03

UNPROTONATED LUNGA WATER HUMIC ACID TITRATION DATA

pH	0.1N HCl LWHA1	pH	0.1N HCl LWHA2	pH	0.1N HCl LWHA3
11.90	30.00	12.00	25.20	12.00	25.00
11.60	35.00	11.90	30.98	11.90	30.00
11.30	36.92	11.30	39.23	11.30	36.00
11.10	37.20	10.90	40.80	11.10	37.00
11.00	37.89	10.60	41.02	10.60	38.00
10.80	38.46	10.40	41.28	10.50	38.10
10.60	39.20	10.10	41.50	10.30	38.30
9.80	39.78	9.70	41.71	9.60	38.60
9.40	39.98	9.40	41.75	9.40	38.67
9.00	40.00	9.00	41.76	9.00	38.80
8.40	40.06	8.40	41.80	8.40	38.84

pH	0.1N HCl LWHA4	pH	0.1N HCl LWHA5
12.40	30.00	12.30	30.00
12.30	35.00	12.10	35.00
11.60	39.40	11.70	38.00
11.20	40.00	11.50	38.60
10.90	40.50	11.30	39.08
10.50	40.68	10.80	39.56
10.20	40.76	10.40	39.88
9.80	40.98	9.80	40.04
9.60	41.12	9.40	40.12
8.40	41.22	9.10	40.16
7.60	41.30	8.40	40.21

UNPROTONATED LUNGA WATER HUMIC ACID RESULTS

sample	weight (mg)	normality HCl	blank titration used	end point blank (ml)	end point titre (ml)	total acidity $mmol_c\ g^{-1}$
LW1	91.1	0.11	3	43.90	40.06	4.67
LW2	46.1	0.11	3	43.90	41.80	5.05
LW3	88.7	0.11	3	43.90	38.84	6.28
LW4	58.4	0.10	4	44.51	41.22	5.63
LW5	65.4	0.10	4	44.51	40.21	6.57

PROTONATED HUXTER HUMIC ACID TOTAL ACIDITY DATA

pH	ml 0.1N HCl HXHA1	pH	ml 0.1N HCl HXHA2	pH	ml 0.1N HCl HXHA3
12.31	35.00	12.42	35.00	12.28	30.10
12.14	40.00	12.11	40.40	12.19	35.24
11.92	43.00	11.70	42.20	11.81	37.08
11.31	45.00	10.90	43.11	11.42	40.00
11.10	45.82	10.60	44.08	10.90	41.47
10.80	46.04	10.10	45.02	10.70	42.37
10.40	46.41	9.70	45.18	10.20	42.65
9.60	46.48	9.10	45.24	9.80	42.78
8.80	46.50	8.80	45.31	9.40	42.88
7.60	46.53	7.80	45.35	7.20	43.01

pH	ml 0.1N HCl HXHA4	pH	ml 0.1N HCl HXHA5
12.23	30.00	12.24	30.00
12.11	35.00	12.12	35.00
11.74	40.00	11.82	40.00
11.20	42.12	11.41	41.65
11.13	42.28	11.11	42.82
10.80	42.79	10.90	43.94
10.70	43.02	9.80	44.58
10.40	43.26	9.60	44.68
9.80	43.46	9.40	44.72
7.51	43.68	8.10	44.76

PROTONATED HUXTER HUMIC ACID RESULTS

sample	weight (mg)	normality HCl	blank titration used	end point blank (ml)	end point titre (ml)	total acidity $mmol_c\ g^{-1}$
HX1	57.4	0.10	4	49.98	46.51	6.05
HX2	66.6	0.10	4	49.98	45.33	6.98
HX3	56.4	0.10	8	46.88	42.98	6.91
HX4	57.1	0.10	8	46.88	43.62	5.71
HX5	39.3	0.10	8	46.88	44.65	5.45

PROTONATED LUNGA WATER HUMIC ACID

pH	ml 0.1N HCl LWHA1	pH	ml 0.1N HCl LWHA2	pH	ml 0.1N HCl LWHA3
12.86	20.35	12.06	20.47	12.91	35.59
12.72	30.19	12.44	35.62	11.83	40.51
12.68	35.23	12.11	40.18	11.11	45.03
12.25	40.04	11.73	43.02	10.21	45.65
10.99	45.61	11.31	44.22	9.90	45.72
10.02	45.44	11.10	45.15	9.70	45.82
9.70	45.52	10.60	45.51	9.30	45.92
9.10	45.62	9.20	45.93	9.10	45.96
8.80	45.72	8.8	45.96	8.70	46.04
8.40	45.76	8.40	46.00	8.40	46.10

pH	ml 0.1N HCl LWHA4	pH	ml 0.1N HCl LWHA5	pH	ml 0.1N HCl LWHA6
12.72	30.06	12.55	35.17	12.64	30.35
12.63	35.42	12.38	40.36	12.53	35.18
12.37	40.19	11.72	43.84	12.25	40.47
11.81	43.94	11.33	45.02	11.63	44.21
11.51	45.02	11.09	45.32	11.20	45.13
10.41	46.11	10.81	45.51	10.71	45.52
10.10	46.21	10.40	45.71	10.20	45.75
9.80	46.29	9.80	45.88	9.60	45.92
9.50	46.38	9.50	46.01	8.80	46.05
8.40	46.48	8.40	46.17	8.40	46.11

PROTONATED LUNGA WATER HUMIC ACID RESULTS

sample	weight (mg)	normality HCl	blank titration used	end point blank (ml)	end point titre (ml)	total acidity $mmol_c\ g^{-1}$
LW1	57.8	0.10	4	49.98	45.76	7.30
LW2	57.9	0.10	4	49.98	46.00	6.87
LW3	51.1	0.10	4	49.98	46.10	7.53
LW4	58.5	0.10	7	50.47	46.48	6.82
LW5	58.9	0.10	7	50.47	46.17	7.30
LW6	60.3	0.10	7	50.47	46.11	7.23

A1.2 CARBOXYL CONTENT DATA & CALCULATIONS

To calculate the carboxyl content the following equation is used:

$$\frac{(\text{SAMPLE TITRE - BLANK TITRE}) \times \text{N BASE} \times 1000}{\text{mg HUMIC SUBSTANCE}} = \text{mmol}_c\ g^{-1}\ \text{COOH}$$

The data and the corresponding calculations are presented in the following sections.

BLANK TITRATION DATA

pH	ml 0.1N NaOH blank 1	pH	ml 0.1N NaOH blank 2	pH	ml 0.1N NaOH blank 3
8.06	0.00	8.31	0.00	7.40	0.00
8.33	0.05	8.70	0.05	7.60	0.05
8.71	0.11	8.90	0.11	7.80	0.09
9.13	0.18	9.17	0.15	8.00	0.15
9.24	0.22	9.33	0.21	8.40	0.28
9.49	0.27	9.65	0.26	9.60	0.41
9.86	0.35	9.74	0.29	9.80	0.46
9.92	0.39	9.99	0.34		

pH	ml 0.1N NaOH blank 4	pH	ml 0.1N NaOH blank 5	pH	ml 0.1N NaOH blank 6
7.40	0.00	7.80	0.00	7.31	0.00
8.60	0.28	8.22	0.05	8.42	0.21
9.02	0.32	8.41	0.11	8.80	0.25
9.20	0.37	8.60	0.16	9.30	0.34
9.40	0.41	9.10	0.29	9.50	0.40
9.60	0.44	9.80	0.44	9.80	0.43
9.80	0.48	9.90	0.46	9.90	0.45

UNPROTONATED HUXTER PEAT CARBOXYL CONTENT TITRATIONS

pH	ml 0.1N NaOH HX1	pH	ml 0.1N NaOH HX2	pH	ml 0.1N NaOH HX3
6.77	0.00	6.70	0.01	6.82	0.01
7.13	0.29	6.96	0.29	7.09	0.22
7.51	0.43	7.51	0.55	7.58	0.41
9.38	0.71	8.06	0.64	8.67	0.61
9.65	0.77	8.78	0.72	9.15	0.71
9.84	0.82	9.24	0.78	9.50	0.76
10.04	0.87	9.49	0.84	9.76	0.82
10.14	0.92	9.93	0.94	9.95	0.88

pH	ml 0.1N NaOH HX4	pH	ml 0.1N NaOH HX5	pH	ml 0.1N NaOH HX6
6.75	0.01	6.85	0.01	6.72	0.00
7.16	0.22	7.11	0.21	6.96	0.23
7.62	0.42	7.71	0.39	7.14	0.42
8.94	0.62	8.65	0.48	7.47	0.58
9.61	0.72	9.66	0.61	9.2	0.71
9.79	0.77	9.98	0.78	9.66	0.80
9.97	0.81	10.1	0.84	9.92	0.83

UNPROTONATED HUXTER PEAT CARBOXYL RESULTS

sample	weight (mg)	normality NaOH	blank titration used	end point blank (ml)	end point titre (ml)	carboxyl content $mmol_c\ g^{-1}$
HX1	64.1	0.0955	1	0.33	0.81	0.72
HX2	61.2	0.0955	1	0.33	0.89	0.87
HX3	63.2	0.0955	1	0.33	0.84	0.76
HX4	59.7	0.0955	2	0.31	0.79	0.77
HX5	52.3	0.0955	2	0.31	0.65	0.62
HX6	67.9	0.0955	2	0.31	0.81	0.70

UNPROTONATED LUNGA WATER PEAT CARBOXYL TITRATIONS

pH	ml 0.1N NaOH LW1	pH	ml 0.1N NaOH LW2	pH	ml 0.1N NaOH LW3
6.80	0.00	7.32	0.01	6.65	0.02
6.91	0.11	7.45	0.06	6.80	0.18
7.03	0.19	8.29	0.32	6.89	0.28
7.80	0.46	8.61	0.44	7.06	0.41
8.39	0.54	9.07	0.61	7.32	0.52
8.89	0.62	9.21	0.64	9.04	0.77
9.34	0.71	9.36	0.71	9.31	0.81
9.65	0.75	9.59	0.76	9.77	0.88
9.78	0.81	9.79	0.84	9.87	0.93
10.04	0.88	9.90	0.91	10.32	1.12

pH	ml 0.1N NaOH LW4	pH	ml 0.1N NaOH LW5	pH	ml 0.1N NaOH LW6
6.66	0.01	6.57	0.01	6.53	0.01
6.81	0.22	6.65	0.14	6.71	0.25
6.97	0.37	6.72	0.25	6.84	0.43
7.19	0.45	6.97	0.51	7.36	0.74
7.98	0.61	7.45	0.73	7.43	0.81
8.82	0.78	7.95	0.82	7.86	0.89
9.29	0.84	8.95	0.92	8.97	0.98
9.56	0.89	9.55	1.01	9.55	1.05
9.85	0.94	9.66	1.03	9.83	1.10
9.96	0.98	9.90	1.08	10.01	1.16

UNPROTONATED LUNGA WATER PEAT CARBOXYL RESULTS

sample	weight (mg)	normality NaOH	blank titration used	end point blank (ml)	end point titre (ml)	carboxyl content $mmol_c\ g^{-1}$
LW1	52.5	0.0955	1	0.33	0.79	0.84
LW2	52.0	0.0955	1	0.33	0.86	0.96
LW3	53.1	0.0955	1	0.33	0.87	0.97
LW4	55.2	0.0955	2	0.31	0.93	1.07
LW5	67.2	0.0955	2	0.31	1.06	1.07
LW6	64.9	0.0955	2	0.31	1.09	1.14

PROTONATED HUXTER PEAT CARBOXYL TITRATION DATA

pH	ml 0.1N NaOH HX1	pH	ml 0.1N NaOH HX2	pH	ml 0.1N NaOH HX3
6.62	0.01	6.73	0.02	6.82	0.04
7.26	0.55	7.31	0.35	6.94	0.11
7.82	0.70	7.92	0.54	7.08	0.22
8.83	0.85	8.94	0.64	7.28	0.32
9.58	0.96	9.41	0.69	7.65	0.42
9.90	1.01	9.80	0.72	9.46	0.58
10.1	1.12	9.98	0.92	9.87	0.64

pH	ml 0.1N NaOH HX4	pH	ml 0.1N NaOH HX5	pH	ml 0.1N NaOH HX6
6.82	0.00	6.72	0.04	6.72	0.04
7.03	0.18	7.00	0.28	7.20	0.42
7.32	0.34	7.27	0.43	7.94	0.57
8.33	0.49	8.18	0.52	8.33	0.66
9.40	0.59	8.67	0.62	9.16	0.72
9.80	0.65	9.94	0.76	10.10	0.78

PROTONATED HUXTER PEAT CARBOXYL RESULTS

sample	weight (mg)	normality NaOH	blank titration used	end point blank (ml)	end point titre (ml)	carboxyl content $mmol_c\ g^{-1}$
HX1	74.0	0.100	6	0.43	0.99	0.75
HX2	52.8	0.100	6	0.43	0.72	0.55
HX3	51.3	0.100	6	0.43	0.63	0.39
HX4	50.7	0.100	6	0.43	0.65	0.43
HX5	51.7	0.100	6	0.43	0.75	0.62
HX6	60.4	0.100	6	0.43	0.73	0.50

PROTONATED LUNGA WATER PEAT CARBOXYL TITRATION DATA

pH	ml 0.1N NaOH LW1	pH	ml 0.1N NaOH LW2	pH	ml 0.1N NaOH LW3
6.61	0.00	6.60	0.00	6.61	0.00
7.40	0.48	7.81	0.54	7.21	0.41
8.20	0.64	8.11	0.62	7.91	0.56
8.80	0.72	8.70	0.69	8.60	0.67
9.60	0.82	9.40	0.76	9.40	0.76
10.00	0.91	9.80	0.80	9.80	0.81

pH	ml 0.1N NaOH LW4	pH	ml 0.1N NaOH LW5	pH	ml 0.1N NaOH LW6
6.60	0.00	6.40	0.00	6.40	0.00
6.81	0.20	6.60	0.40	6.80	0.56
7.91	0.62	7.10	0.75	7.30	0.89
8.60	0.71	7.70	0.92	8.20	1.05
9.20	0.81	9.20	1.06	9.20	1.14
9.80	0.86	9.80	1.15	9.80	1.21

PROTONATED LUNGA WATER PEAT CALCULATIONS

sample	weight (mg)	normality NaOH	blank titration used	end point blank (ml)	end point titre (ml)	carboxyl content $mmol_c\ g^{-1}$
LW1	64.3	0.100	6	0.43	0.85	0.65
LW2	62.0	0.100	6	0.43	0.80	0.60
LW3	63.4	0.100	6	0.43	0.81	0.60
LW4	72.5	0.100	6	0.43	0.86	0.59
LW5	92.3	0.100	6	0.43	1.15	0.78
LW6	99.2	0.100	6	0.43	1.21	0.79

UNPROTONATED HUXTER HUMIC ACID CARBOXYL TITRATION DATA

pH	ml 0.1N NaOH HX1	pH	ml 0.1N NaOH HX2	pH	ml 0.1N NaOH HX3
6.51	0.00	6.51	0.00	6.52	0.00
7.64	1.01	7.32	0.81	7.71	1.21
8.35	1.16	7.50	0.92	8.18	1.29
9.05	1.26	9.30	1.26	9.11	1.41
9.22	1.31	9.50	1.31	9.35	1.45
9.61	1.36	9.60	1.34	9.62	1.49
9.80	1.42	9.80	1.39	9.80	1.53

pH	ml 0.1N NaOH HX4	pH	ml 0.1N NaOH HX5
6.61	0.00	6.55	0.00
7.45	1.02	7.41	1.02
7.98	1.13	8.12	1.12
8.28	1.25	8.73	1.21
9.24	1.31	9.25	1.27
9.46	1.36	9.43	1.35
9.80	1.42	10.20	1.45

UNPROTONATED HUXTER HUMIC ACID RESULTS

sample	weight (mg)	normality NaOH	blank titration used	end point blank (ml)	end point titre (ml)	carboxyl content $mmol_c\ g^{-1}$
HX1	58.1	0.100	3	0.46	1.42	1.55
HX2	54.0	0.100	3	0.46	1.39	1.62
HX3	67.0	0.100	4	0.48	1.53	1.47
HX4	58.8	0.100	4	0.48	1.42	1.50
HX5	62.6	0.100	4	0.48	1.39	1.37

UNPROTONATED LUNGA WATER HUMIC ACID CARBOXYL TITRATION DATA

pH	ml 0.1N NaOH LW1	pH	ml 0.1N NaOH LW2	pH	ml 0.1N NaOH LW3
6.40	0.00	6.40	0.00	6.40	0.00
6.60	0.55	6.70	0.78	6.61	0.41
6.90	0.74	7.00	1.20	6.92	0.91
7.10	1.01	7.20	1.34	7.40	1.25
7.50	1.24	7.41	1.51	7.80	1.41
8.40	1.33	8.30	1.73	8.40	1.52
8.80	1.51	8.80	1.81	8.90	1.61
9.30	1.61	9.20	1.88	9.30	1.69
9.60	1.66	9.70	1.98	9.60	1.81
9.80	1.73	9.80	2.02	9.80	1.87

pH	ml 0.1N NaOH LW4	pH	ml 0.1N NaOH LW5	pH	ml 0.1N NaOH LW6
6.50	0.00	6.51	0.00	6.51	0.00
6.61	0.31	6.71	0.35	6.61	0.12
6.91	0.71	7.11	0.81	6.82	0.48
7.51	1.11	7.82	1.02	7.31	1.02
8.31	1.27	8.40	1.09	8.01	1.21
8.50	1.36	8.70	1.14	9.20	1.36
8.90	1.41	9.10	1.22	9.50	1.41
9.60	1.47	9.80	1.41	9.70	1.45
9.80	1.50	10.00	1.62	9.80	1.50

UNPROTONATED LUNGA WATER HUMIC ACID RESULTS

sample	weight (mg)	normality NaOH	blank titration used	end point blank (ml)	end point titre (ml)	carboxyl content $mmol_c\ g^{-1}$
LW1	62.8	0.094	3	0.46	1.73	1.90
LW2	80.6	0.094	3	0.46	2.02	1.82
LW3	64.7	0.094	3	0.46	1.87	2.05
LW4	68.1	0.094	4	0.46	1.50	1.41
LW5	55.9	0.094	4	0.46	1.40	1.55
LW6	63.1	0.094	4	0.46	1.50	1.52

PROTONATED HUXTER HUMIC ACID TITRATION DATA

pH	ml 0.1N NaOH HX1	pH	ml 0.1N NaOH HX2	pH	ml 0.1N NaOH HX3
6.40	0.00	6.51	0.00	6.30	0.00
6.82	0.81	6.92	0.72	6.85	0.69
7.41	1.31	7.18	1.02	7.02	1.02
7.73	1.41	7.46	1.21	7.84	1.28
9.33	1.61	7.91	1.35	8.31	1.41
9.46	1.63	8.82	1.49	8.89	1.49
9.67	1.66	9.16	1.52	9.62	1.55
9.80	1.68	9.91	1.61	9.80	1.61

pH	ml 0.1N NaOH HX4	pH	ml 0.1N NaOH HX5
6.30	0.00	6.30	0.00
6.68	0.51	6.91	1.02
7.05	1.01	7.15	1.18
7.31	1.16	7.74	1.43
8.01	1.37	8.22	1.54
8.92	1.51	8.71	1.59
9.65	1.62	9.02	1.63
9.91	1.68	9.80	1.74

PROTONATED HUXTER HUMIC ACID RESULTS

sample	weight (mg)	normality NaOH	blank titration used	end point blank (ml)	end point titre (ml)	carboxyl content $mmol_c\ g^{-1}$
HX1	66.4	0.100	5	0.44	2.26	2.74
HX2	50.6	0.100	5	0.44	1.94	2.96
HX3	51.4	0.100	6	0.43	1.61	2.30
HX4	53.5	0.100	6	0.43	1.66	2.30
HX5	58.8	0.100	6	0.43	1.74	2.23

PROTONATED LUNGA WATER HUMIC ACID CARBOXYL TITRATION DATA

pH	ml 0.1N NaOH LW1	pH	ml 0.1N NaOH LW2
6.30	0.00	6.40	0.00
6.65	1.02	6.62	0.71
7.19	1.61	7.05	1.31
7.81	1.91	7.21	1.42
8.35	2.05	7.55	1.61
9.18	2.09	7.96	1.71
9.45	2.14	9.28	1.84
9.71	2.22	9.61	1.88
9.80	2.26	9.80	1.94

pH	ml 0.1N NaOH LW3	pH	ml 0.1N NaOH LW4	pH	ml 0.1N NaOH LW5
6.30	0.00	6.20	0.00	6.30	0.00
6.97	1.11	6.90	1.15	6.91	1.31
7.45	1.41	7.40	1.69	7.22	1.52
7.83	1.56	7.90	1.85	7.73	1.69
8.46	1.61	8.30	1.91	8.45	1.83
9.17	1.69	8.90	1.99	8.99	1.89
9.66	1.75	9.20	2.02	9.29	1.93
9.80	1.78	9.90	2.09	9.80	1.99

PROTONATED LUNGA WATER HUMIC ACID RESULTS

sample	weight (mg)	normality NaOH	blank titration used	end point blank (ml)	end point titre (ml)	carboxyl content $mmol_c\ g^{-1}$
LW1	66.4	0.100	5	0.44	2.26	2.74
LW2	50.6	0.100	5	0.44	1.94	2.96
LW3	52.0	0.100	6	0.43	1.78	2.60
LW4	60.1	0.100	6	0.43	2.08	2.75
LW5	58.5	0.100	6	0.43	1.99	2.67

A 1.3 SALICYLIC & PHTHALIC ACID TITRATION DATA & CALCULATIONS

SALICYLIC ACID DATA

ml KOH titration 1	pH	ml KOH titration 2	pH	ml KOH titration 3	pH
0.00	2.28	0.00	2.14	0.00	2.19
4.98	3.56	2.40	2.65	4.02	2.58
7.58	3.87	4.00	2.90	5.56	2.86
8.56	3.95	5.02	3.07	6.79	2.95
8.92	3.99	6.02	3.11	8.89	3.14
9.14	4.01	7.02	3.25	9.99	3.33
10.90	4.08	9.02	3.43	10.97	3.48
11.22	4.11	10.02	3.54	12.89	3.65
11.66	4.22	12.54	3.84	13.56	3.67
12.00	4.33	13.60	3.97	14.13	3.84
12.45	4.49	15.00	4.18	14.98	3.97
13.16	4.99	16.20	4.79	15.56	4.17
13.32	5.20	16.70	10.44	15.94	4.89
13.52	5.60	16.90	11.32	16.12	5.23
13.60	8.70	17.10	11.58	16.59	10.99
13.70	11.50	17.24	11.67	16.99	11.49
13.84	11.89	17.39	11.76	17.36	11.82
13.97	12.10	17.68	11.98	17.76	11.98
14.20	12.23	17.89	12.09	17.92	12.08

CALCULATION OF TOTAL TITRATABLE ACIDITY FOR SALICYLIC ACID

$$\frac{\text{end point (ml)} \times \text{normality}}{\text{weight (g)}} = \text{titratable acidity mmolc / g}$$

titration	weight (g)	normality	end point (ml)	titratable acidity $mmol_c\ g^{-1}$
1	0.7771	0.50	13.65	8.78
2	1.031	0.50	16.40	7.95
3	1.055	0.50	16.35	7.75

The mean value for the three titrations is 8.15$mmol_c\ g^{-1}$, and this was used to calculate the metal additions to salicylic acid.

PHTHALIC ACID DATA

ml KOH titration 1	pH	ml KOH titration 2	pH	ml KOH titration 3	pH
0.00	2.08	0.00	2.25	0.00	2.04
1.38	2.64	2.29	2.89	2.59	2.55
2.07	2.76	3.87	3.10	3.91	2.96
3.98	3.16	5.00	3.24	5.36	3.18
6.60	3.26	7.13	3.84	8.89	3.39
8.41	3.35	8.91	4.26	10.56	3.71
12.40	3.68	10.00	4.91	13.39	3.96
14.10	3.95	11.26	5.11	14.87	4.18
16.80	4.45	12.03	5.39	16.03	4.55
17.93	4.65	12.77	5.58	18.34	4.80
20.00	4.96	13.64	5.59	22.46	5.26
22.72	5.29	14.00	5.63	23.99	5.38
24.20	5.54	14.44	5.87	25.13	5.57
25.60	5.56	14.72	6.10	27.69	5.71
26.54	5.57	14.82	6.26	28.81	5.82
27.98	5.98	15.00	6.65	29.31	6.03
28.90	6.86	15.52	11.94	29.56	6.28
29.20	11.09	15.78	12.16	30.18	6.81
29.44	12.03	16.00	12.34	30.66	11.35
29.62	12.29	16.37	12.53	31.05	12.01
30.00	12.64	16.88	12.69	31.84	12.58
31.02	12.71	17.15	12.77	32.97	12.74

CALCULATION OF TOTAL TITRATABLE ACIDITY FOR PHTHALIC ACID

$$\frac{\text{end point (ml)} \times \text{normality}}{\text{weight (g)}} = \text{titratable acidity mmolc / g}$$

titration	weight (g)	normality	end point (ml)	titratable acidity $mmol_c\ g^{-1}$
1	1.0092	0.50	29.05	14.35
2	0.5230	0.50	15.26	14.59
3	1.0405	0.50	30.42	14.62

The mean value for the three titrations is 14.52 $mmol_c\ g^{-1}$ and this was used to calculate the metal additions to phthalic acid.

APPENDIX 2:

METAL BINDING DATA & GRAPHS FROM CHAPTER 4

A 2.1 FORMATION PLOTS FOR BJERRUM CALCULATIONS

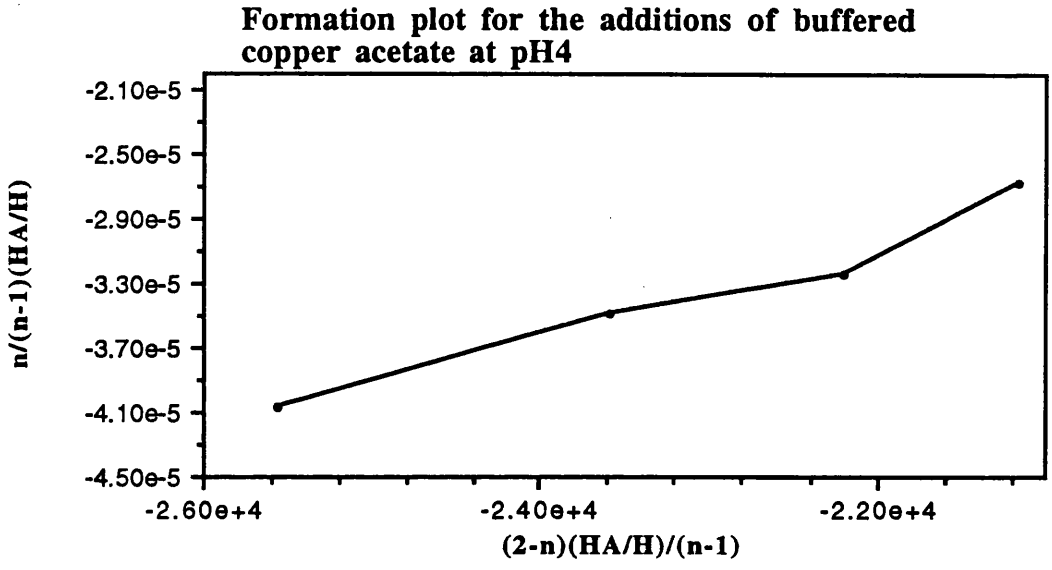

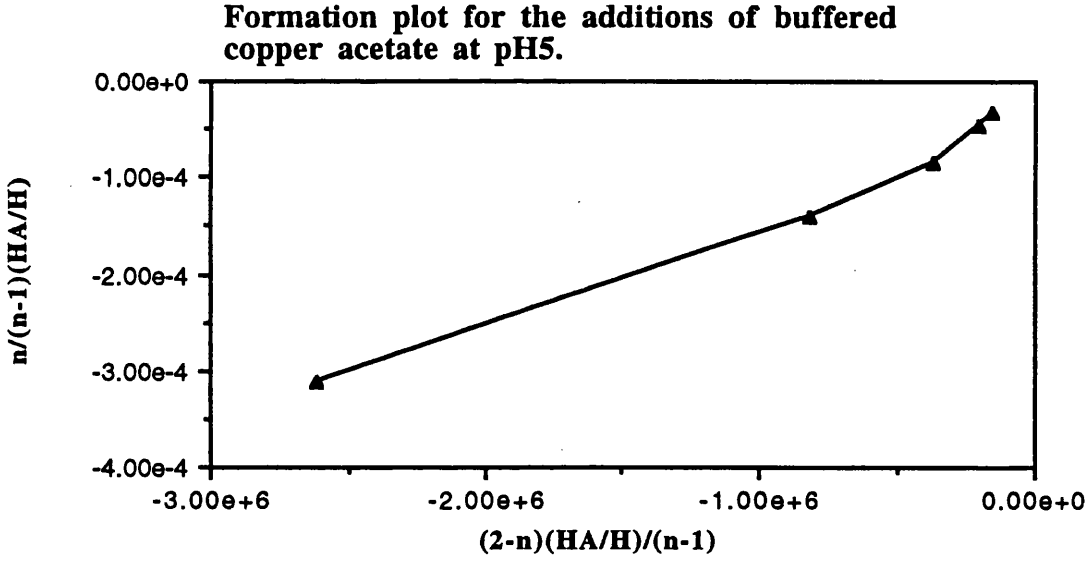

Formation plot for the additions of unbuffered copper chloride at pH4

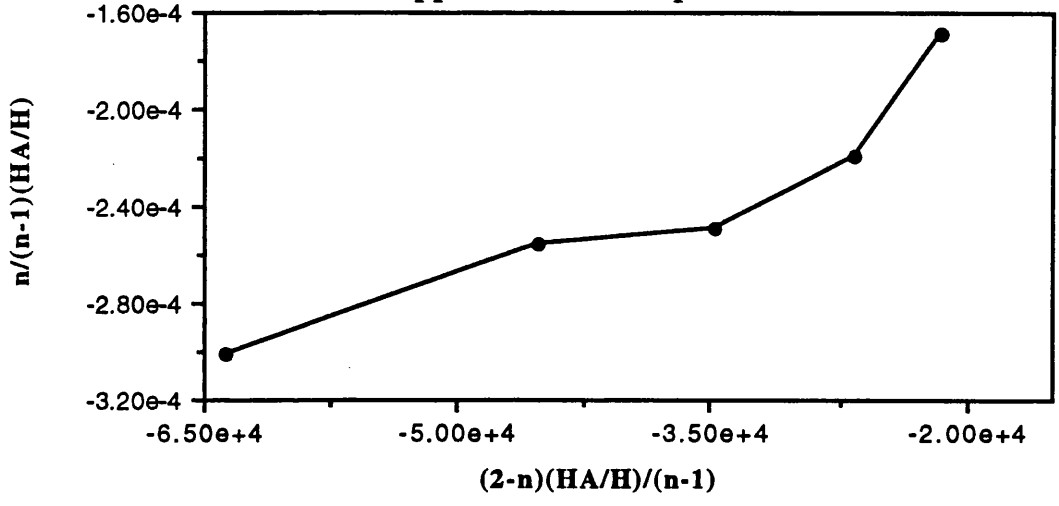

Formation plot for the additions of unbuffered copper chloride at pH5.

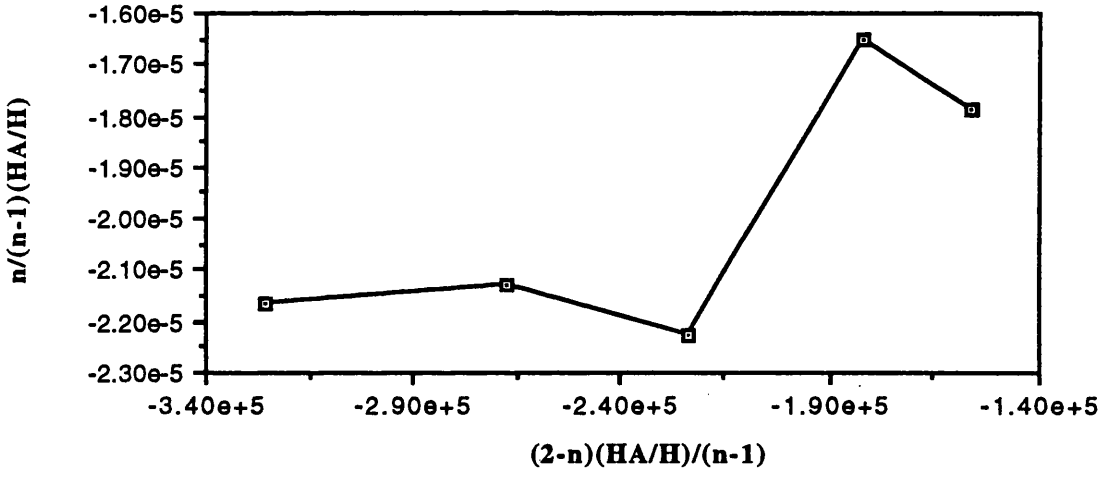

Formation plot for the additions of buffered lead acetate at pH4

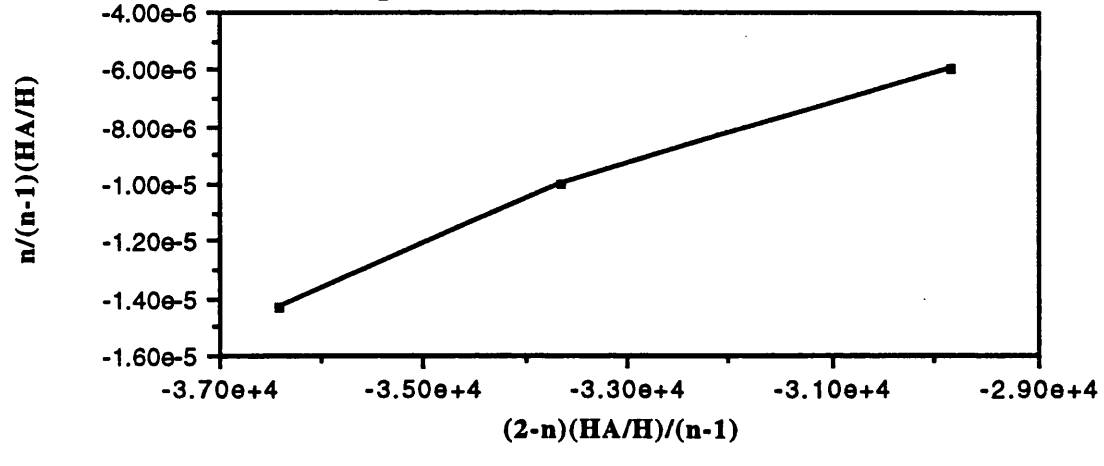

Formation plot for the additions of buffered lead acetate at pH5.

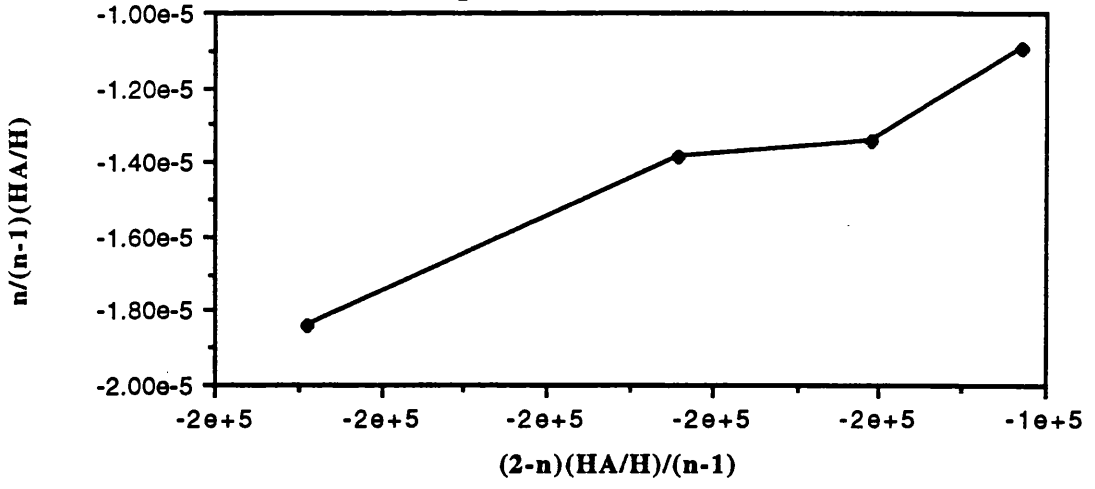

Formation plot for the additions of unbuffered lead nitrate at pH4

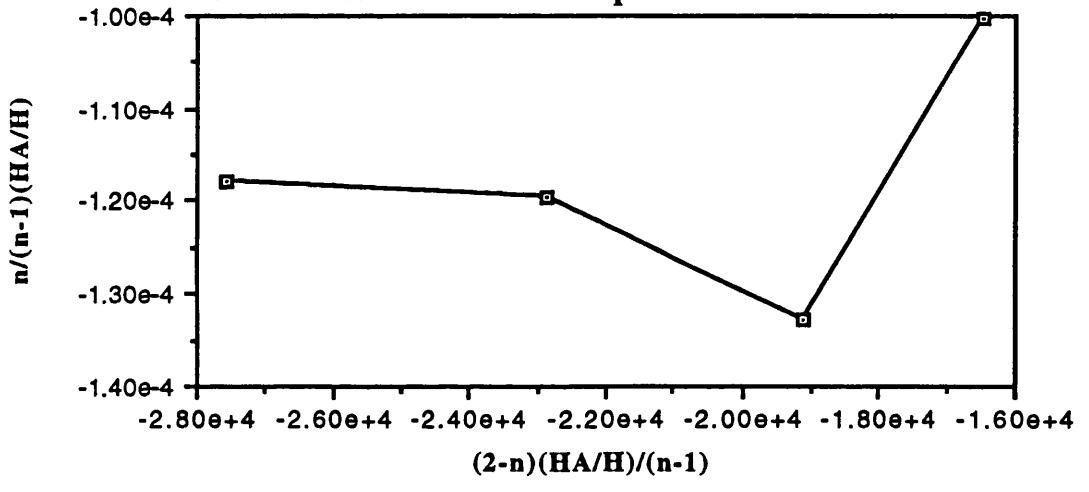

Formation plot for the additions of unbuffered lead nitrate at pH5.

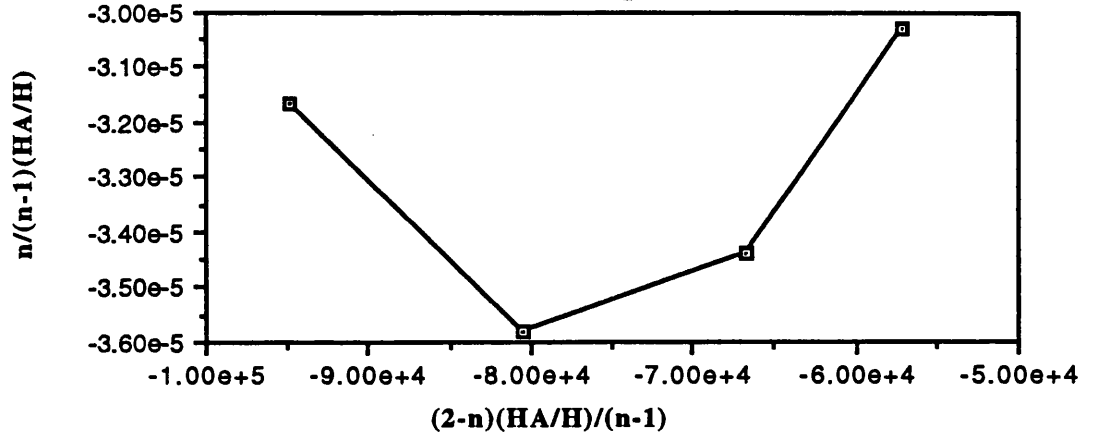

A 2.2 SCATCHARD & INCREMENTAL DATA & GRAPHS

A.2.2.1. Cu^{2+} BINDING TO UNEXTRACTED PEAT AT pH 4

Langmuir Isotherm for copper binding to unextracted peat at pH4.

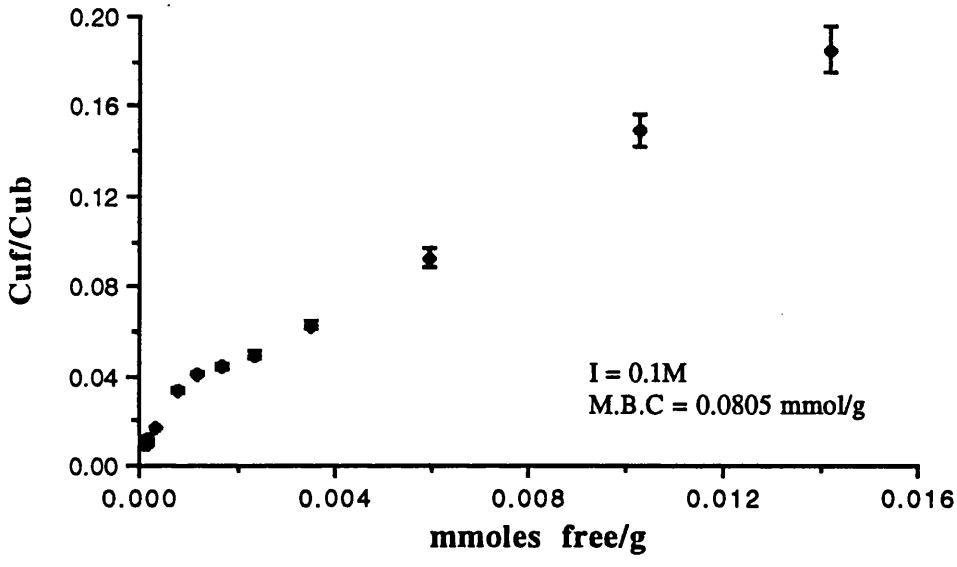

Two surface Langmuir isotherm for copper binding to unextracted peat at pH4.

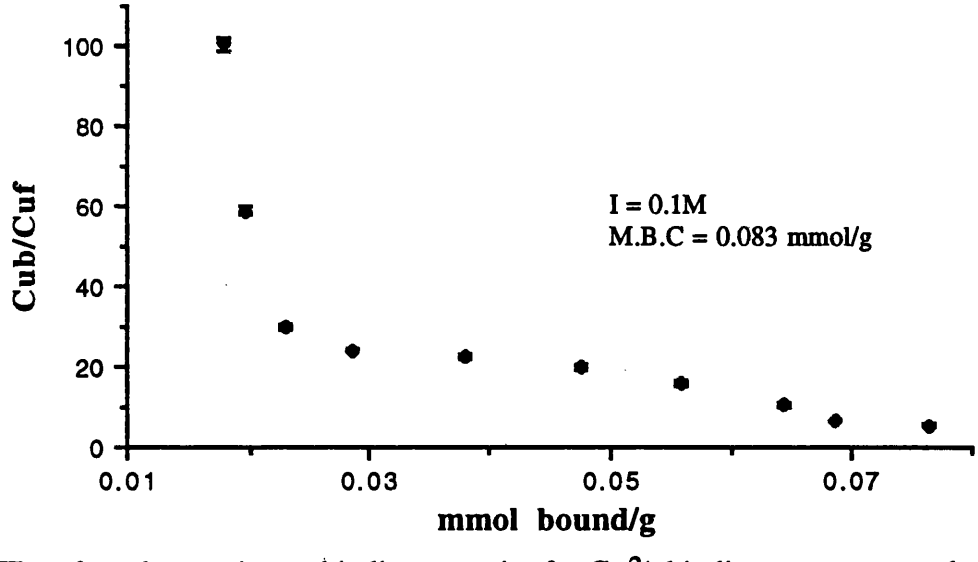

Therefore the maximum binding capacity for Cu^{2+} binding to unextracted peat at pH4 was calculated as 0.0817 mmol g^{-1}.

Scatchard plot for copper binding to unextracted peat at pH4

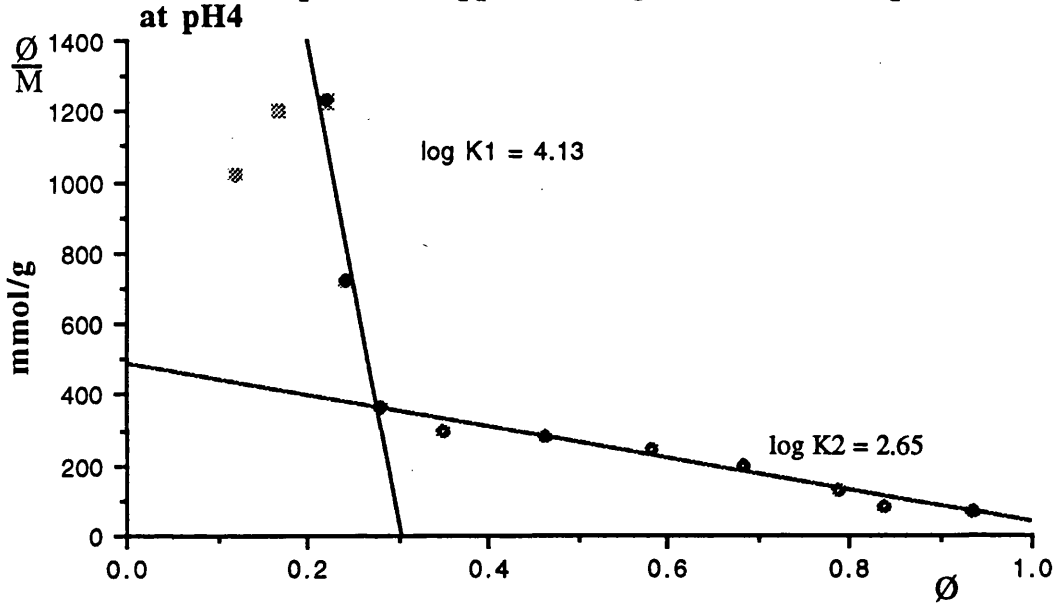

Formation Constants for Cu^{2+} binding to peat at pH 4.

Ø	log k_3	log k_4	Scatchard values
0.119	3.01	4.10	log K_1 = 4.13
0.168	3.08	4.17	
0.220	3.09	4.18	
0.241	2.86	3.95	log K_2 = 2.65
0.281	2.56	3.65	
0.350	2.47	3.56	
0.464	2.45	3.53	
0.583	2.39	3.48	
0.683	2.29	3.38	
0.787	2.29	3.21	
0.839	2.12	3.00	
0.934	1.91	2.91	

A.2.2.2. Cu^{2+} BINDING TO UNEXTRACTED PEAT AT pH 5

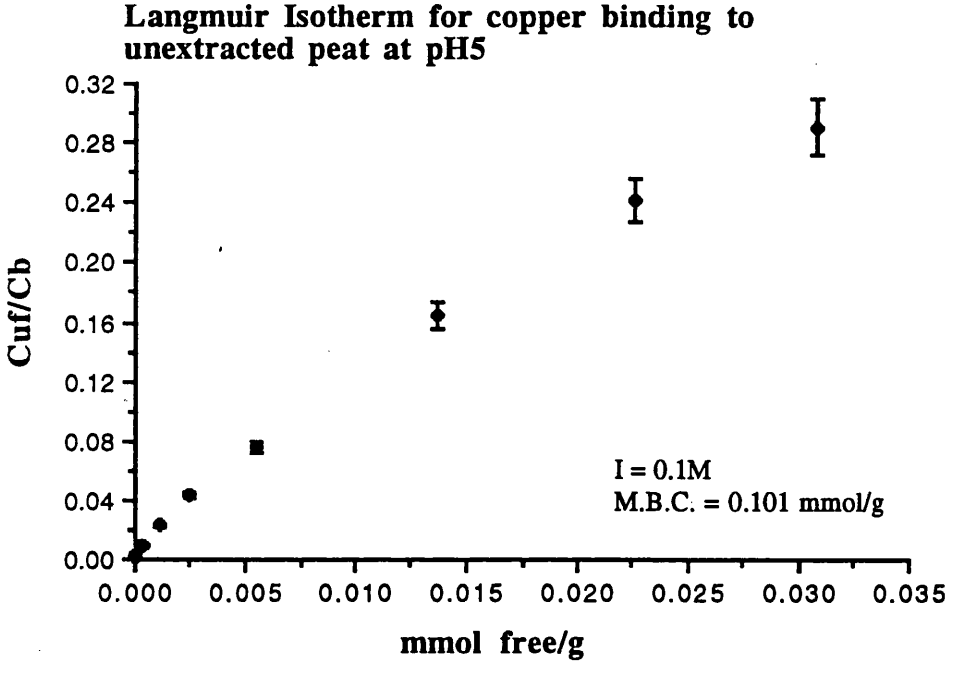

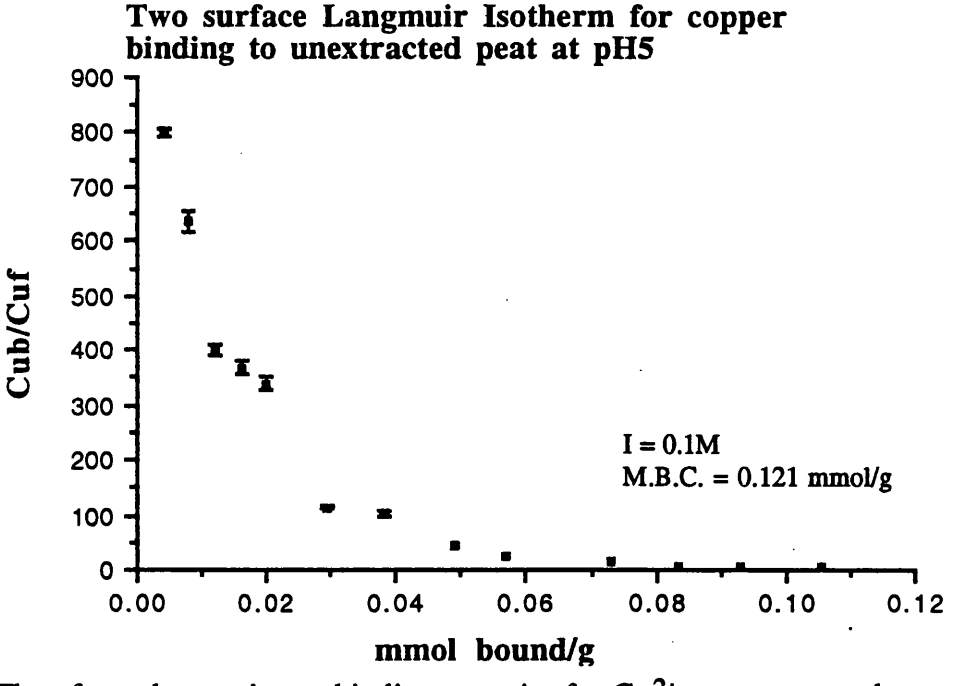

Therefore, the maximum binding capacity for Cu^{2+} to unextracted peat at pH 5 was calculated as 0.111 mmol g^{-1}.

Scatchard plot of copper binding to unextracted peat at pH5

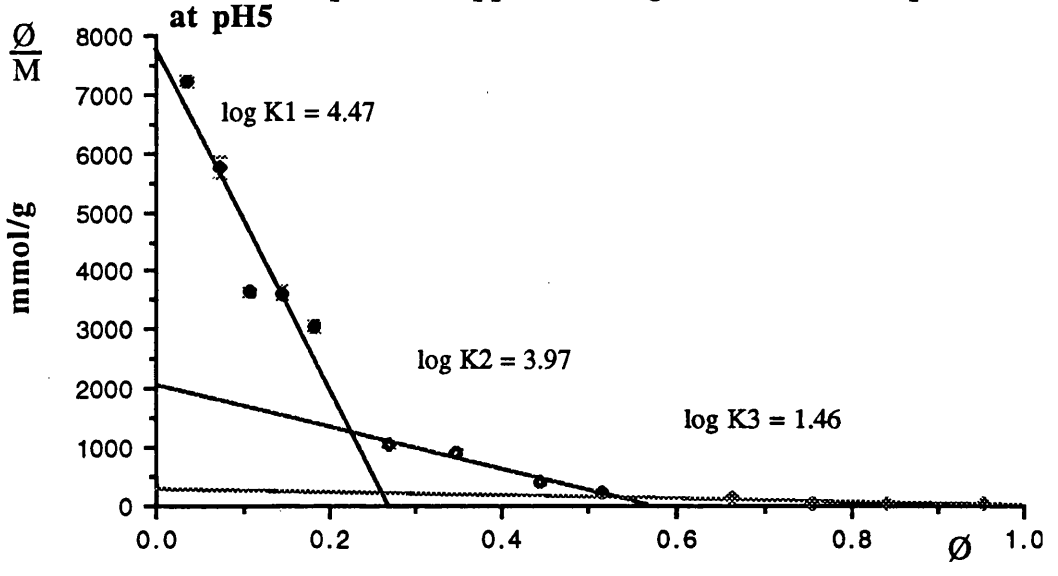

Formation Constants for Cu^{2+} binding to peat at pH5.

Ø	log k_3	log k_4	Scatchard values
0.0358	3.86	4.82	log K_1 = 4.47
0.0718	3.76	4.72	
0.1073	3.56	4.52	log K_2 = 3.97
0.1448	3.55	4.51	
0.1797	3.48	4.44	log K_3 = 1.46
0.2672	3.02	3.93	
0.3464	2.97	3.97	
0.4418	2.60	3.55	
0.5154	2.32	3.28	
0.6630	2.08	3.03	
0.7540	1.74	2.70	
0.8416	1.57	2.53	
0.9531	1.49	2.45	

A.2.2.3. Cu^{2+} BINDING TO HUMIC ACID AT pH 4.8

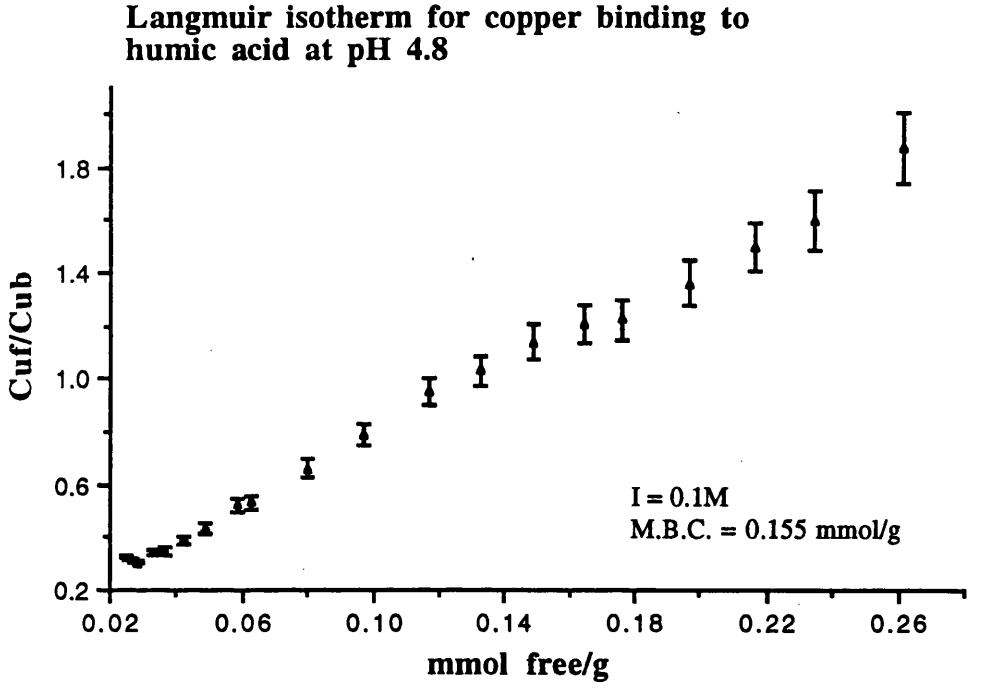

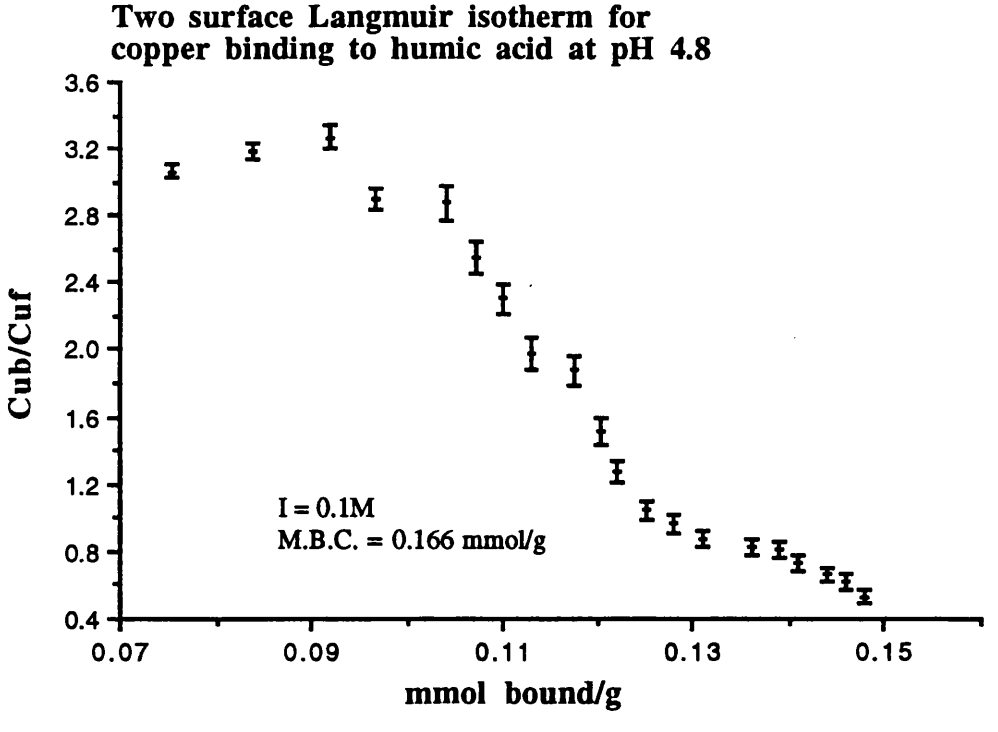

Therefore the maximum binding capacity of Cu^{2+} binding to humic acid at pH4.8 was calculated as 0.161 mmol g^{-1}.

Scatchard plot for copper binding to humic acid at pH4

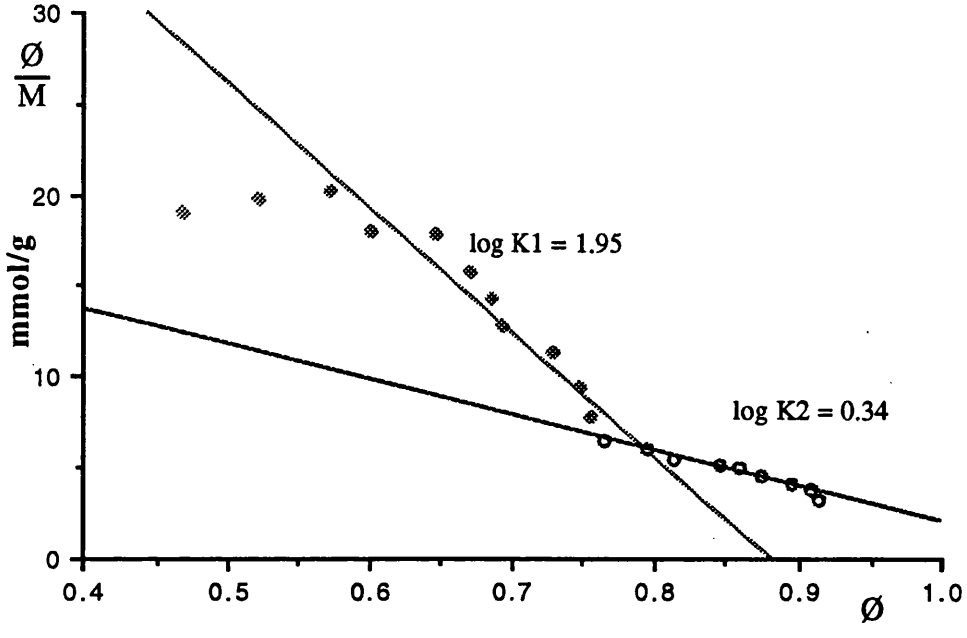

Formation Constants for Cu^{2+} binding to humic acid at pH 4.8

Ø	log k_3	log k_4	Scatchard values
0.468	1.28	2.07	log K_1 = 1.95
0.520	1.29	2.09	
0.571	1.31	2.10	log K_2 = 0.34
0.601	1.26	2.05	
0.670	1.21	1.95	
0.693	1.07	1.86	
0.748	0.97	1.69	
0.764	0.82	1.57	
0.814	0.74	1.51	
0.859	0.70	1.45	
0.874	0.62	1.38	
0.907	0.59	1.35	
0.914	0.52	1.31	

A.2.2.4. Cu^{2+} BINDING TO HUMIC ACID AT pH 5.12

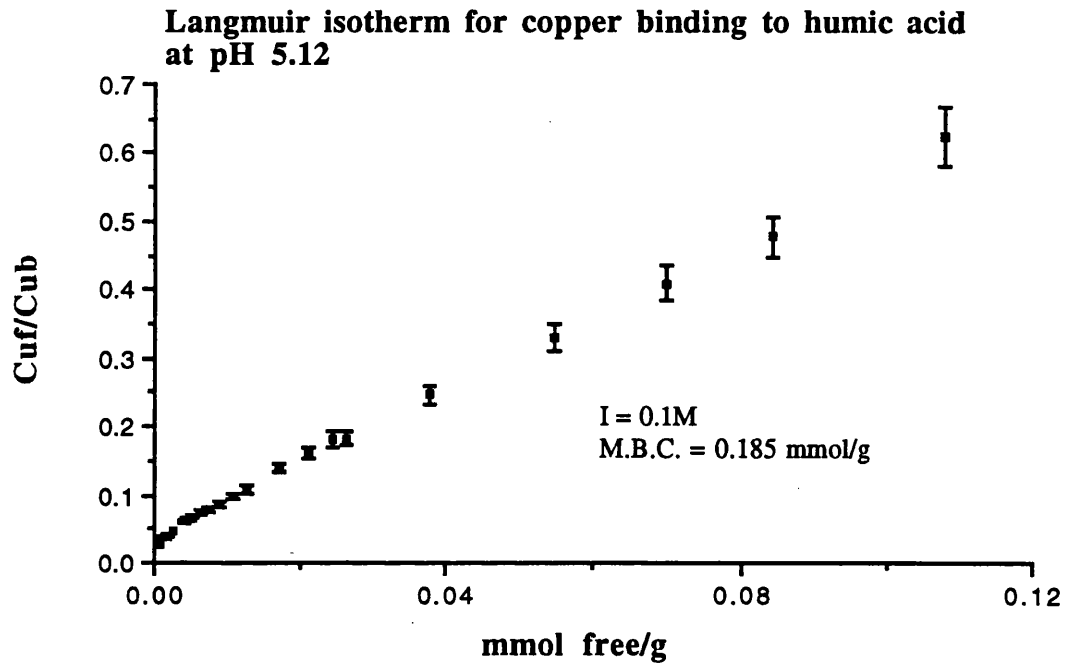

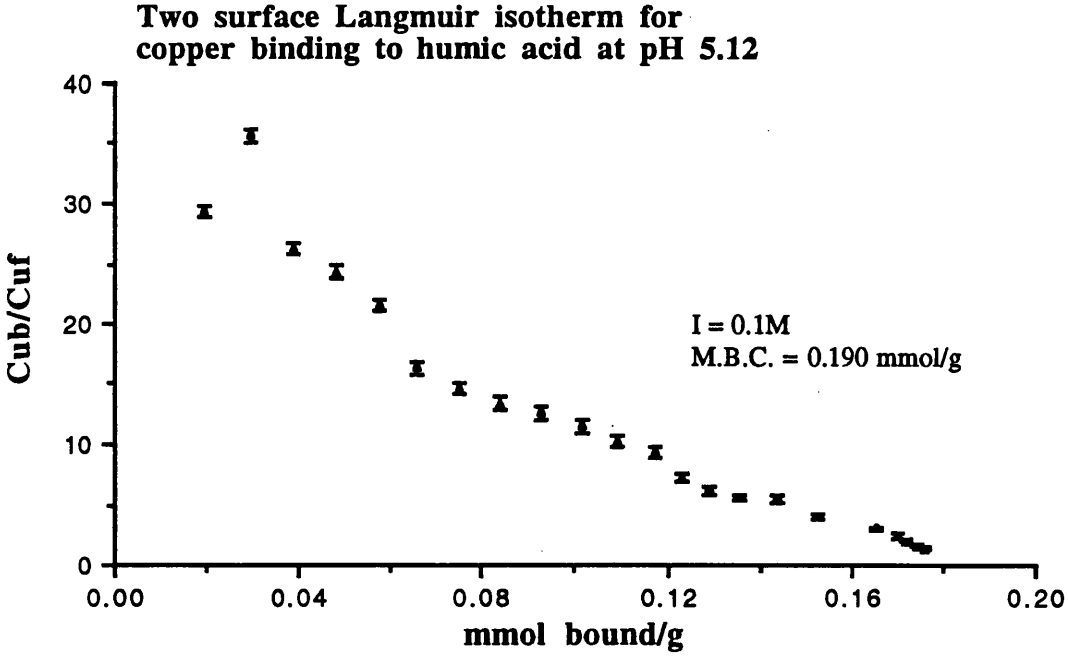

Therefore, the maximum binding capacity for Cu^{2+} binding to humic acid at pH 5.12 was calculated as 0.188 mmol g^{-1}.

Scatchard plot for copper binding to humic acid at pH 5.12

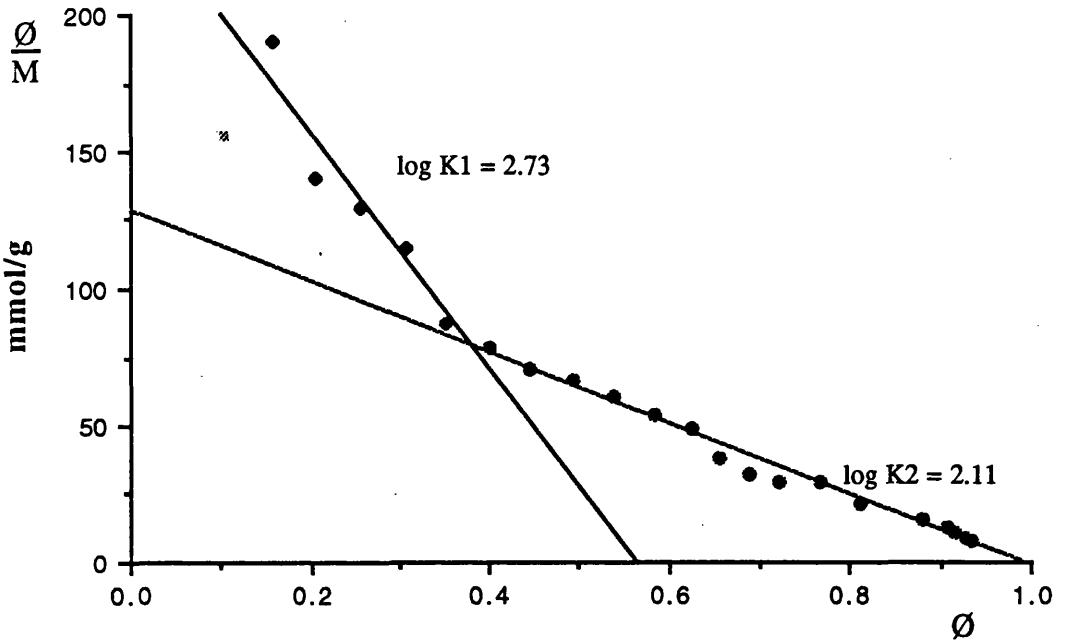

Formation Constants for Cu^{2+} binding to humic acid at pH 5.12.

Ø	log k_3	log k_4	Scatchard values
0.103	2.19	2.92	log K_1 = 2.72
0.155	2.27	3.00	
0.205	2.15	2.87	log K_2 = 2.11
0.255	2.11	2.84	
0.305	2.06	2.79	
0.351	1.94	2.67	
0.398	1.89	2.62	
0.493	1.83	2.55	
0.538	1.79	2.52	
0.581	1.74	2.46	
0.624	1.69	2.42	
0.654	1.58	2.31	
0.687	1.52	2.24	
0.721	1.47	2.20	
0.811	1.33	2.06	
0.880	1.21	1.93	
0.917	1.05	1.77	
0.928	0.93	1.66	
0.935	0.88	1.60	

A.2.2.5. Cu^{2+} BINDING TO HUMIC ACID AT pH 5.8

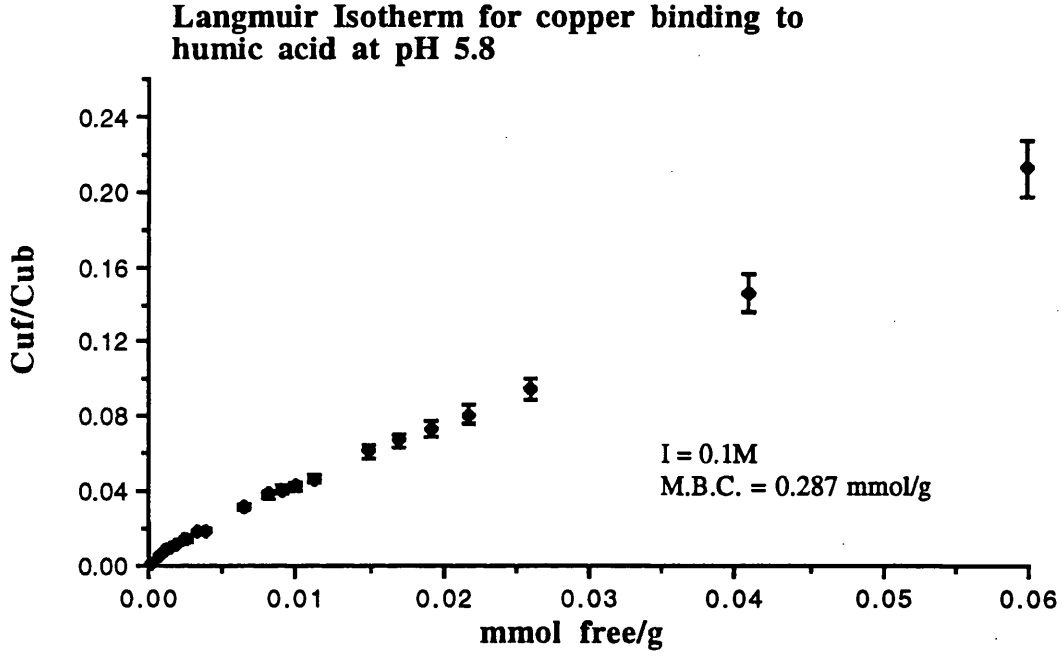

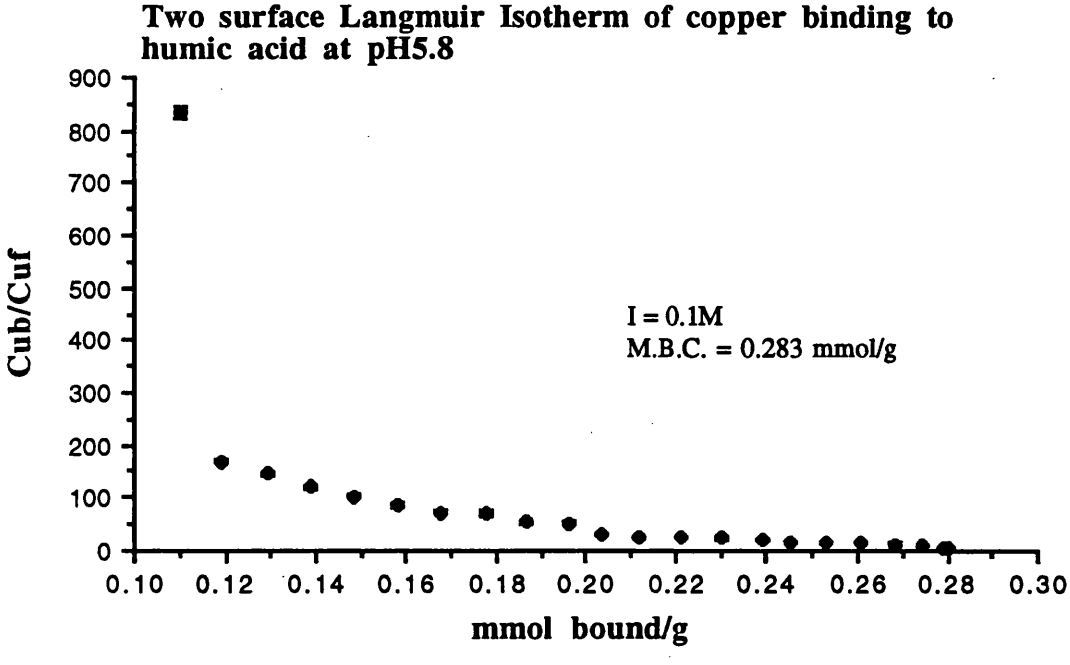

Therefore, the maximum binding capacity of Cu^{2+} binding to humic acid at pH 5.8 was calculated as 0.290 mmol g^{-1}

Scatchard plot for copper binding to humic acid at pH 5.8

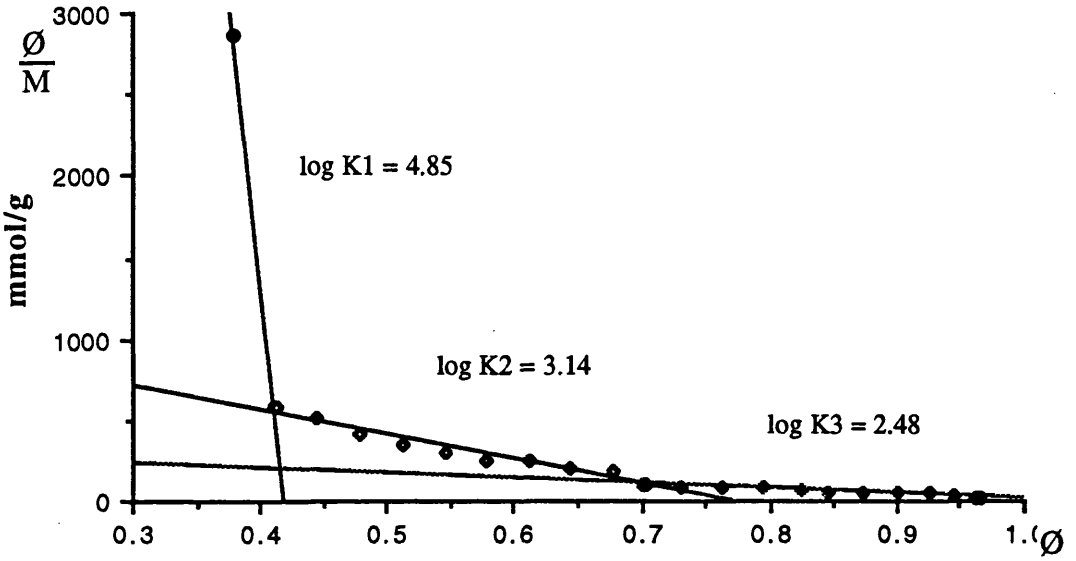

Scatchard plot for copper binding to humic acid at higher levels of metal addition at pH 5.8

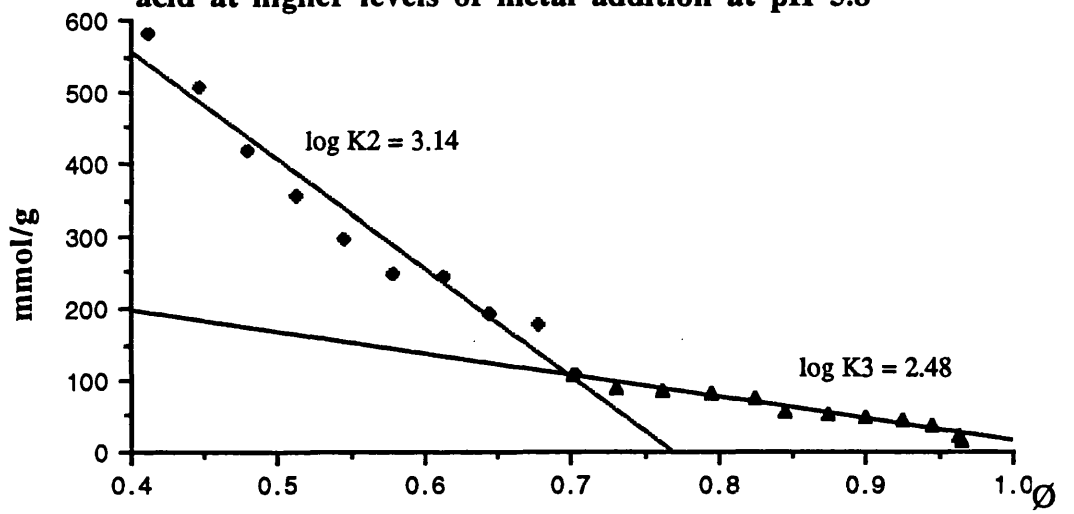

Formation Constants for Cu^{2+} binding to humic acid at pH 5.8.

Ø	log k_3	log k_4	Scatchard values
0.379	3.46	4.00	log K_1 = 4.85
0.411	2.76	3.30	
0.479	2.62	3.16	log K_2 = 3.14
0.512	2.55	3.09	
0.545	2.47	3.01	log K_3 = 2.48
0.612	2.38	2.92	
0.677	2.25	2.79	
0.702	2.03	2.57	
0.824	1.87	2.41	
0.873	1.71	2.25	
0.925	1.63	2.17	
0.963	1.37	1.91	
0.966	1.21	1.75	

A.2.2.6. Pb^{2+} BINDING TO UNEXTRACTED PEAT AT pH 4

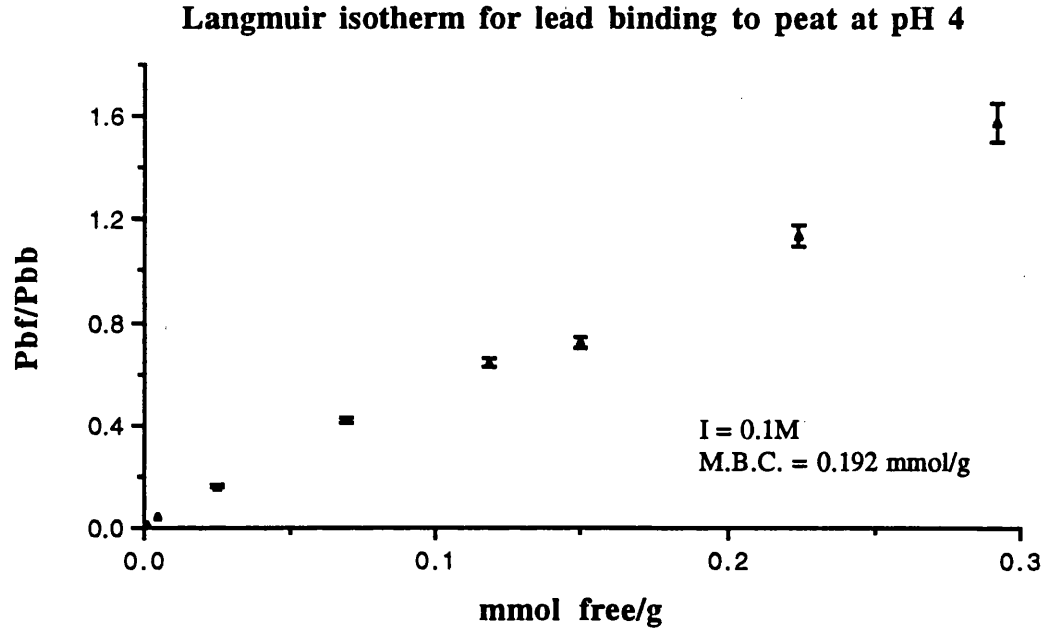

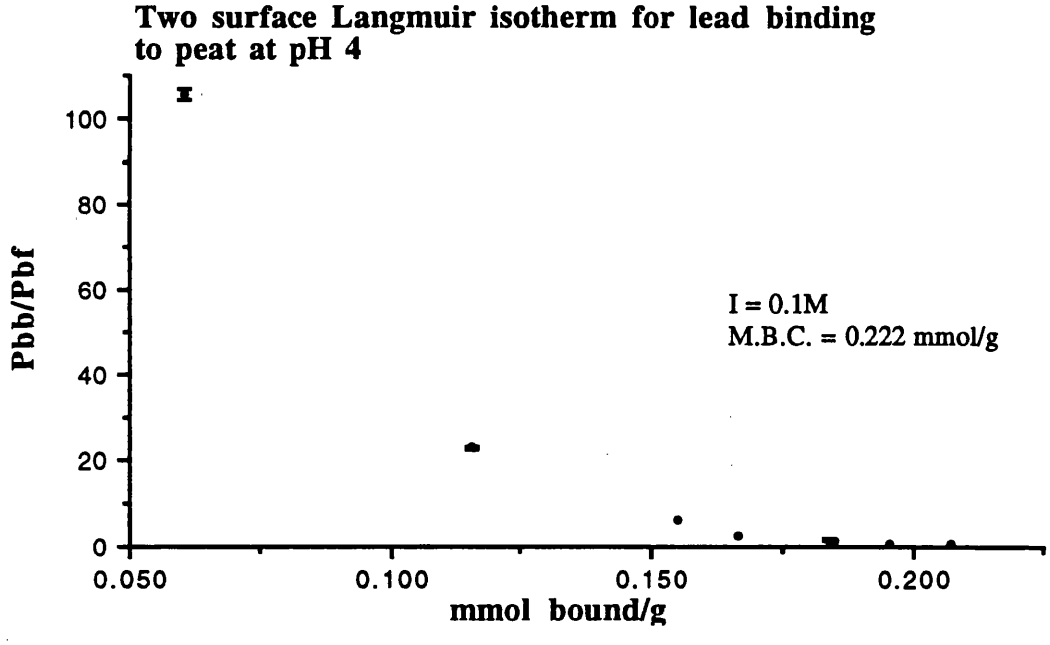

Therefore, the maximum binding capacity for Pb^{2+} binding to unextracted peat at pH 4 was calculated as 0.207 mmol g^{-1}.

Scatchard plot for lead binding to unextracted peat at pH4

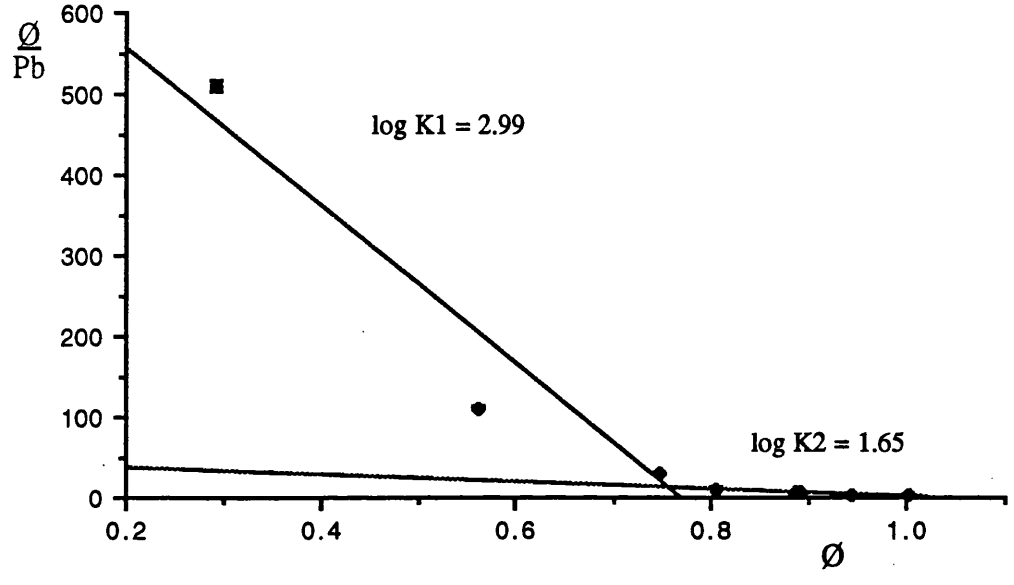

Formation Constants for Pb^{2+} binding to unextracted peat at pH4.

Ø	log k_3	log k_4	Scatchard values
0.293	2.71	3.39	log K_1 = 2.99
0.346	2.25	2.91	
0.559	2.05	2.73	log K_2 = 1.65
0.663	1.67	2.33	
0.749	1.48	2.16	
0.805	1.06	1.75	
0.888	0.88	1.56	
0.892	0.83	1.51	
0.912	0.71	1.43	
0.946	0.63	1.31	
1.00	0.49	1.17	

A.2.2.7. Pb^{2+} BINDING TO UNEXTRACTED PEAT AT pH 5

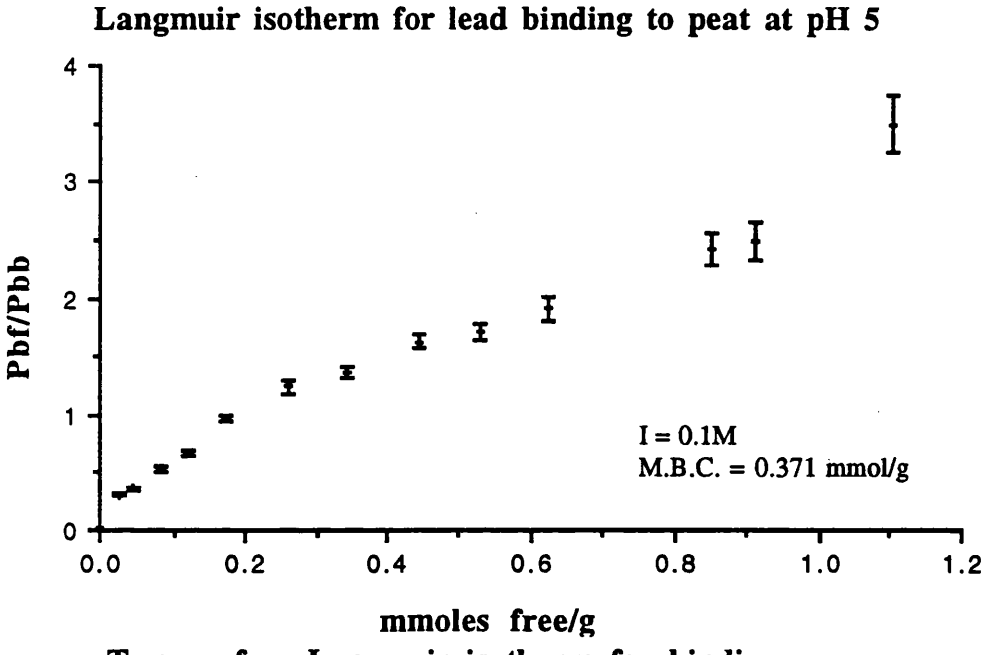

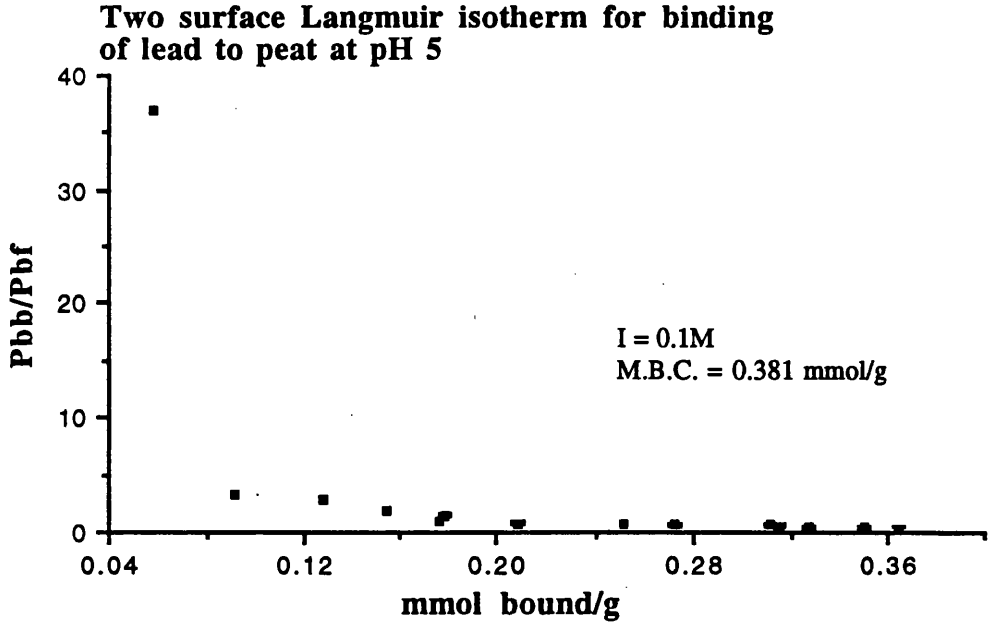

Therefore, the maximum binding capacity for Pb^{2+} binding to unextracted peat at pH 5 was calculated as 0.381 mmol g^{-1}.

Scatchard plot for lead binding to unextracted peat at pH5

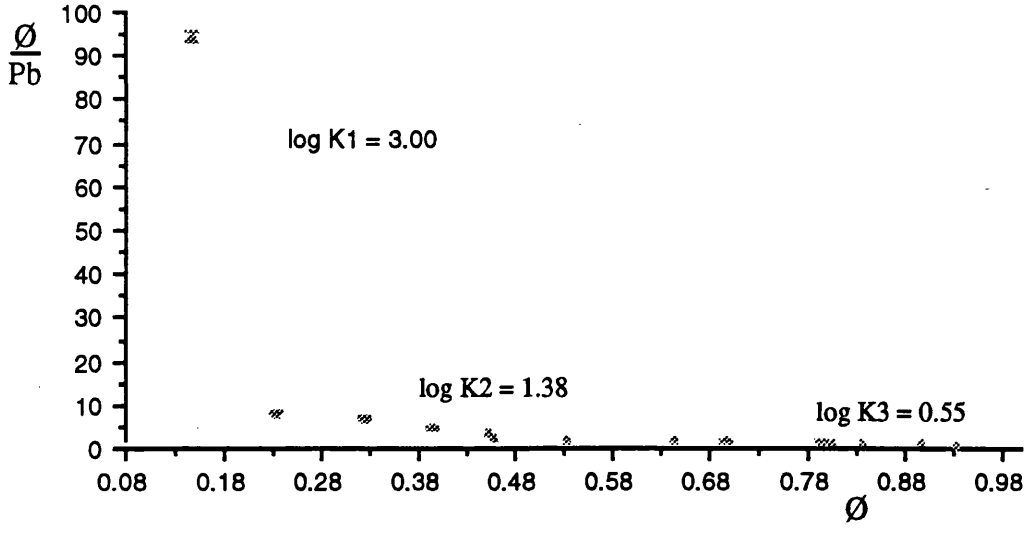

Scatchard plot for higher levels of addition of lead to unextracted peat at pH5

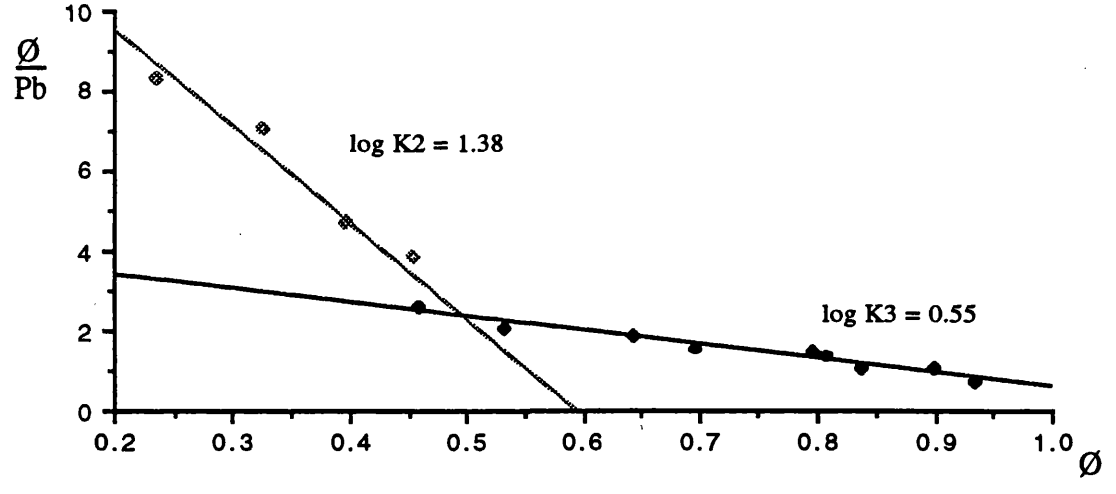

Formation Constants for Pb^{2+} binding to unextracted peat at pH 5.

Ø	log k_3	log k_4	Scatchard values
0.147	1.98	2.38	log K_1 = 3.00
0.234	0.92	1.33	
0.325	0.85	1.26	log K_2 = 1.38
0.395	0.68	1.08	
0.452	0.58	0.99	log K_2 = 0.55
0.533	0.31	0.72	
0.643	0.27	0.68	
0.696	0.20	0.60	
0.806	0.13	0.53	
0.836	0.02	0.43	
0.897	0.01	0.42	

A.2.2.8. Pb^{2+} BINDING TO HUMIC ACID AT pH 4.8

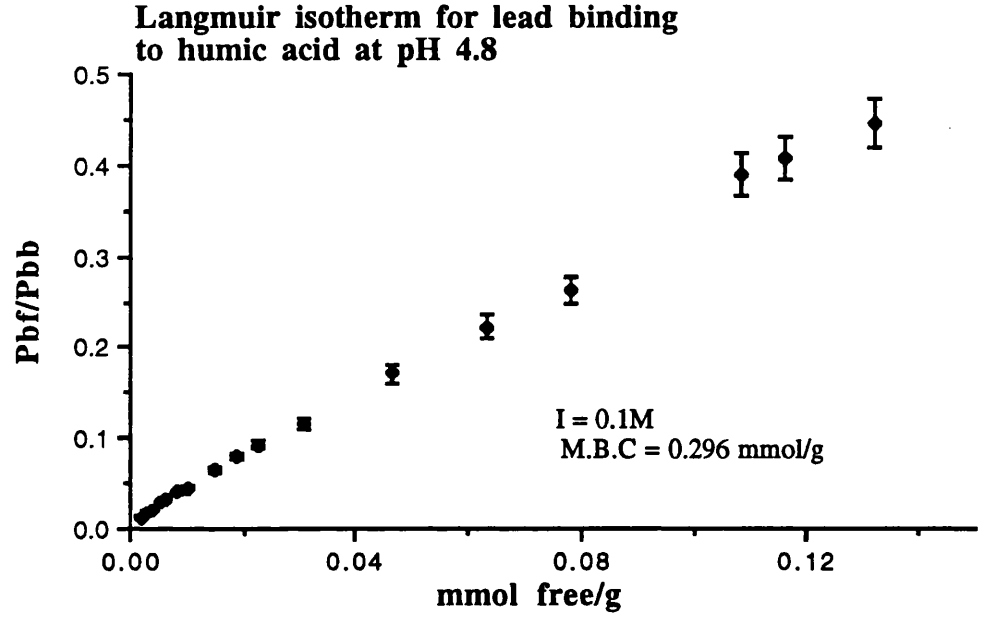

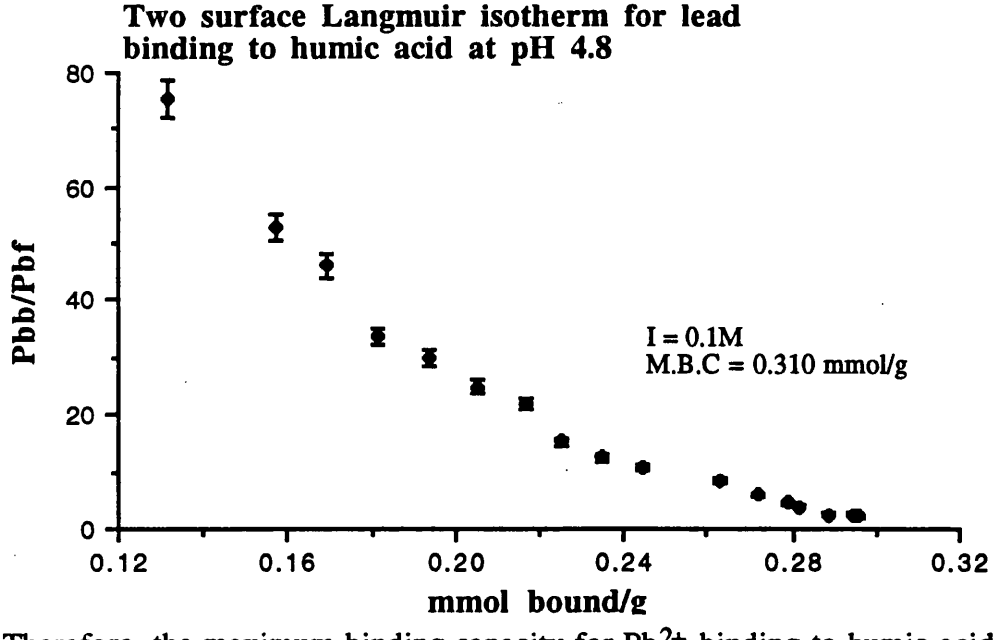

Therefore, the maximum binding capacity for Pb^{2+} binding to humic acid at pH 4.8 was calculated as 0.300 mmol g^{-1}.

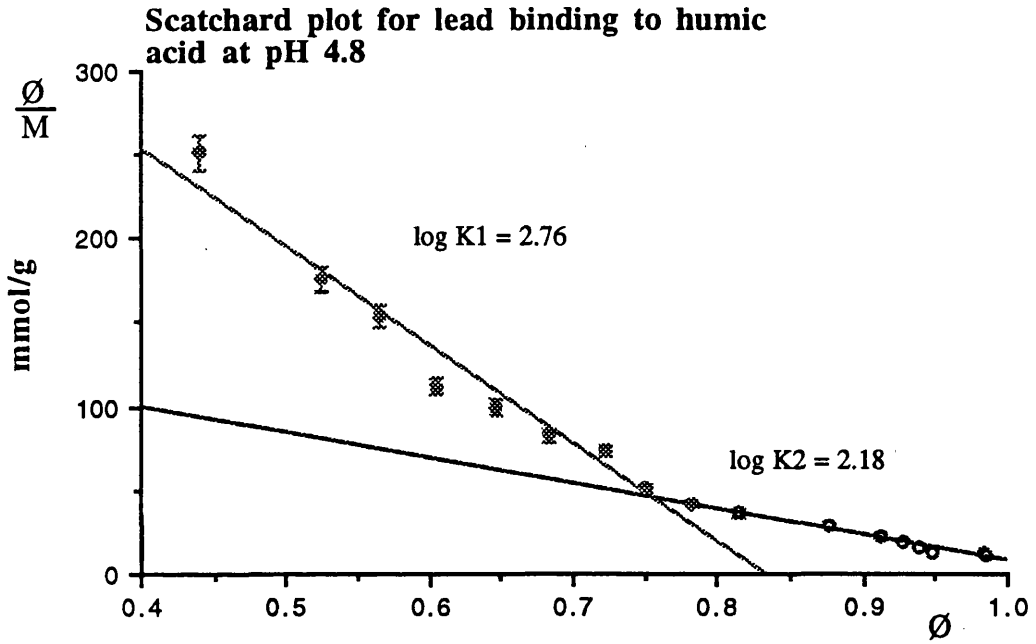

Formation Constants for Pb^{2+} binding to humic acid at pH 4.8.

Ø	log k_3	log k_4	Scatchard values
0.439	2.39	2.92	log K_1 = 2.76
0.523	2.25	2.77	
0.566	2.19	2.71	log K_2 = 2.19
0.604	2.05	2.57	
0.645	2.00	2.52	
0.684	1.92	2.47	
0.723	1.87	2.39	
0.751	1.71	2.23	
0.782	1.62	2.14	
0.814	1.56	2.08	
0.876	1.46	1.98	
0.912	1.29	1.81	
0.927	1.17	1.70	
0.938	1.10	1.53	
0.947	0.93	1.45	
0.982	0.91	1.43	
0.984	0.87	1.39	

A.2.2.9. Pb^{2+} BINDING TO HUMIC ACID AT pH 5.12

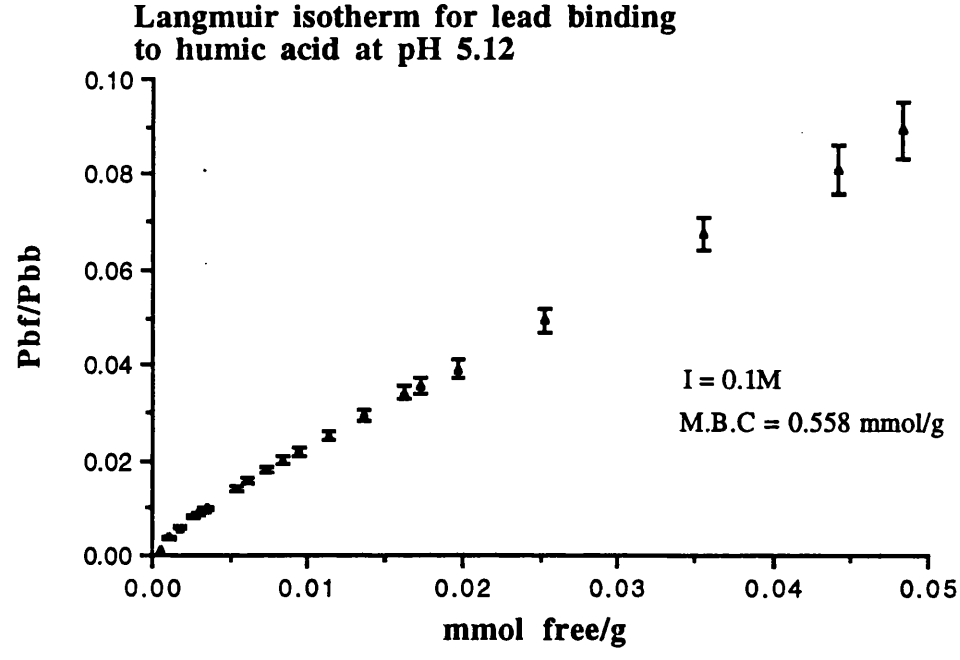

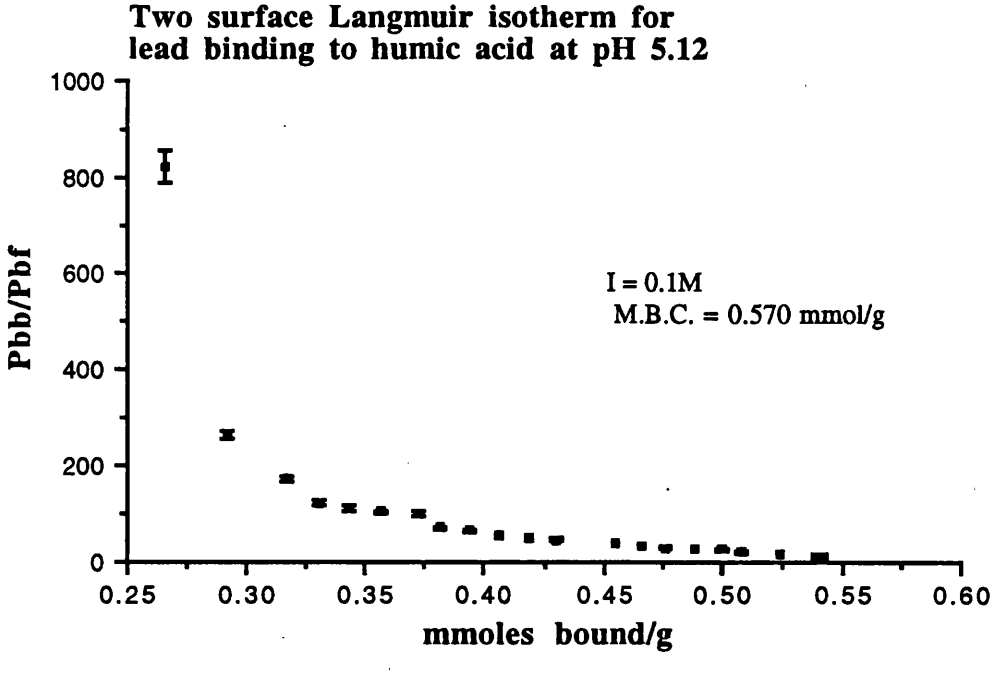

Therefore, the maximum binding capacity for Pb^{2+} binding to humic acid at pH5.11 was calculated as 0.564 mmol g^{-1}.

Scatchard plot of lead binding to humic acid at pH5.11

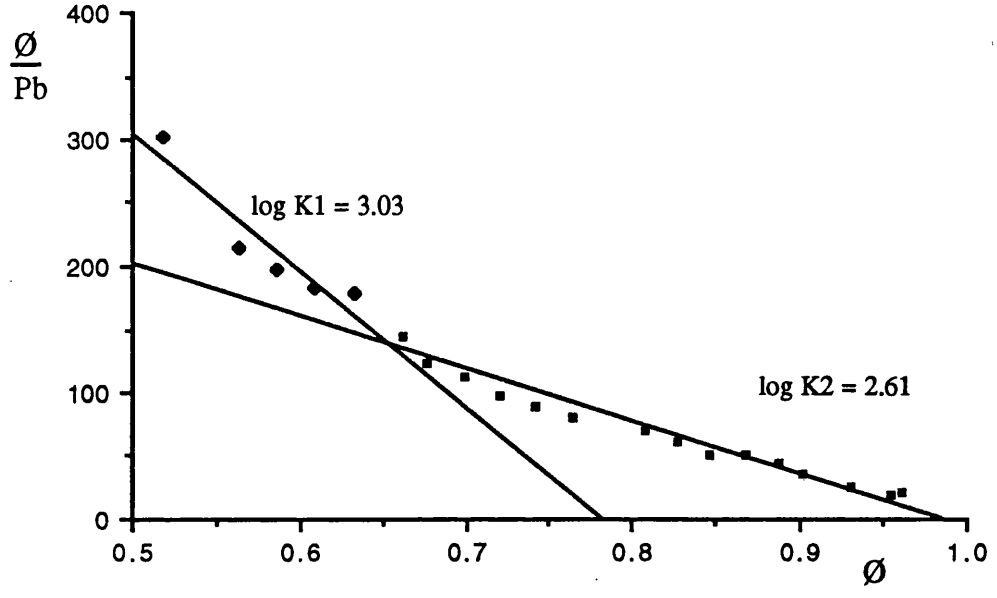

Formation Constants for Pb^{2+} binding to humic acid at pH 5.11.

Ø	log k_3	log k_4	Scatchard values
0.517	2.33	3.41	log K_1 = 3.03
0.562	2.30	2.58	
0.586	2.26	2.54	log K_2 = 2.61
0.609	2.25	2.51	
0.632	2.16	2.50	
0.661	2.09	2.34	
0.676	2.06	2.30	
0.698	1.99	2.24	
0.720	1.95	2.20	
0.742	1.91	2.16	
0.763	1.85	2.10	
0.807	1.78	2.03	
0.827	1.72	1.96	
0.868	1.66	1.90	
0.887	1.55	1.80	
0.901	1.41	1.67	
0.955	1.34	1.59	

A.2.2.10 Pb^{2+} BINDING TO HUMIC ACID AT pH 5.8

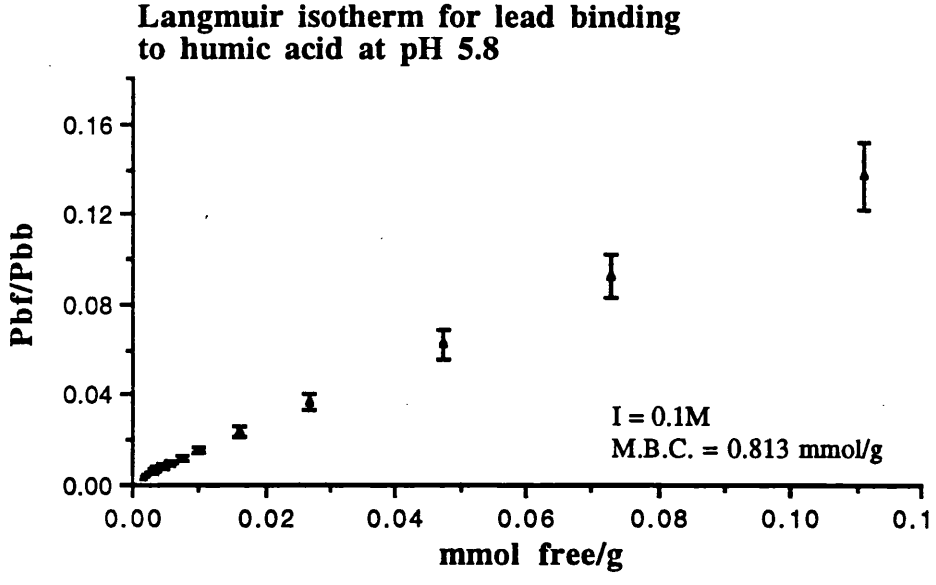

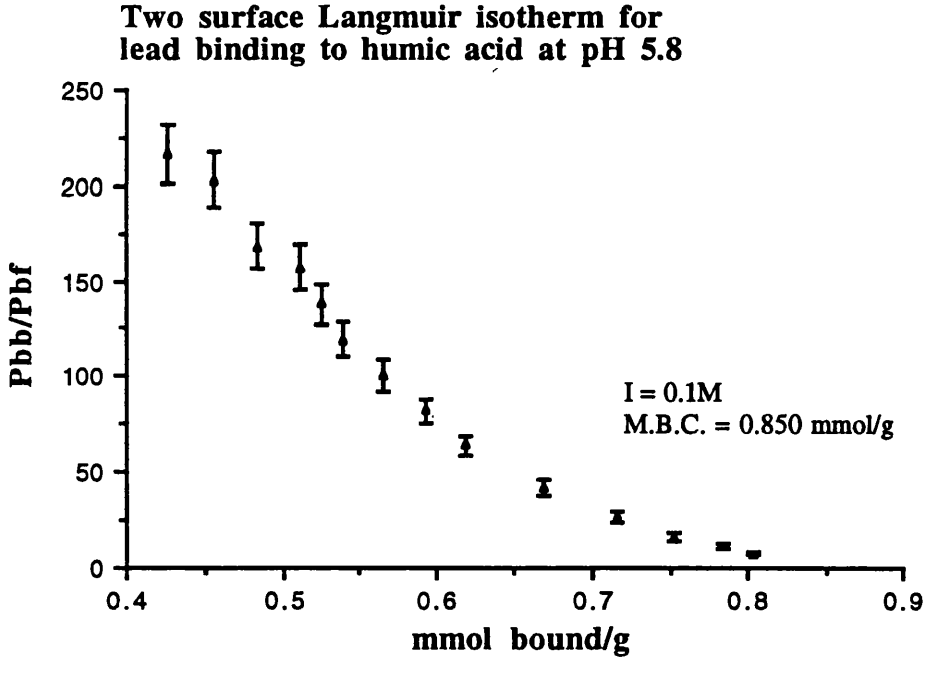

Therefore, the maximum binding capacity of Pb^{2+} to humic acid at pH 5.6 was calculated as 0.832 mmol g^{-1}.

Scatchard plot of lead binding to humic acid at pH5.6

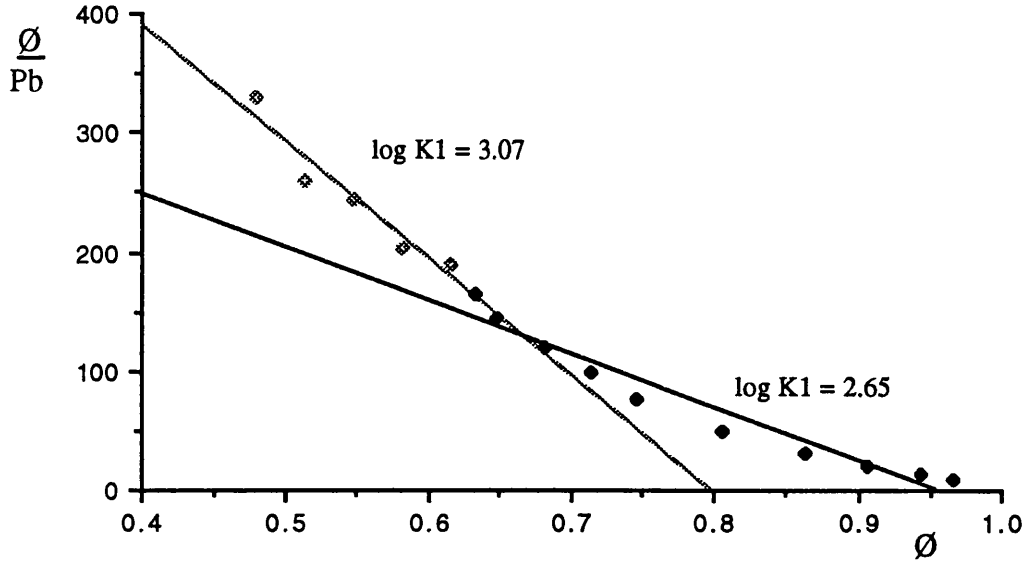

Formation Constants for Pb^{2+} binding to humic acid at pH 5.8

Ø	log k_3	log k_4	Scatchard values
0.4976	2.52	2.60	log K_1 = 3.07
0.5134	2.42	2.50	
0.5474	2.39	2.47	log K_2 = 2.65
0.5810	2.31	2.39	
0.6150	2.28	2.36	
0.6315	2.22	2.30	
0.6478	2.16	2.24	
0.6808	2.08	2.16	
0.7134	2.00	2.09	
0.7447	1.88	1.96	
0.8061	1.71	1.79	
0.8620	1.51	1.59	
0.9060	1.28	1.36	
0.9438	1.11	1.19	
0.9668	0.94	1.02	

APPENDIX 3

DATA FROM CHAPTER 5: RADIONUCLIDE & HEAVY METAL CONTENTS OF THE SOUTH DRUMBOY CORES

A.3.1 CELLULOSE STANDARD & REFERENCE PEAT REPRODUCIBILITY DATA.

CELLULOSE STANDARD 1

Nuclide	energy kev	mean of values	standard deviation	Bq mg^{-1}	% error	Bq mg^{-1}	% error	Bq mg^{-1}	% error	Bq mg^{-1}	% error
^{153}Sm	103	1.3569	0.0407	1.3795	0.98	1.3096	1.02	1.3796	0.89	1.3361	1.05
^{177}Lu	209	0.3021	0.0807	0.2804	1.39	0.2629	1.56	0.2726	1.42	0.2704	1.12
^{198}Au	412	2.6819	0.1243	2.7028	0.59	2.5648	0.83	2.6626	0.72	2.5984	0.79
^{131}Ba	496	0.1099	0.0476	0.0947	2.13	0.1170	2.31	0.0830	2.25	0.1142	1.88
^{76}As	559	0.0431	0.0400	0.0148	3.35	0.0437	3.64	0.1374	3.12	0.0641	3.88
^{122}Sb	564	0.1404	0.0196	0.1696	1.28	0.1378	1.55	0.1121	1.46	0.1413	1.38
^{82}Br	777	0.0000	0.0000	0.0000	0	0.0000	0	0.0000		0.0000	
^{140}La	1597	0.0487	0.0209	0.0691	2.43	0.0622	2.38	0.0303	2.23	0.0403	4.11

Nuclide	energy kev	Bq mg^{-1}	% error	Bq mg^{-1}	% error	Bq mg^{-1}	% error	Bq mg^{-1}	% error	Bq mg^{-1}	% error
^{153}Sm	103	1.3740	0.88	1.3442	0.93	1.3892	1.09	1.2868	0.97	1.4129	0.85
^{177}Lu	209	0.2833	1.16	0.5156	1.09	0.2868	1.08	0.2584	1.15	0.2881	1.32
^{198}Au	412	2.7204	0.49	2.6577	0.33	2.9317	0.31	2.5161	0.76	2.7824	0.84
^{131}Ba	496	0.0767	2.16	0.2275	1.84	0.0935	2.09	0.1158	1.56	0.0664	2.36
^{76}As	559	0.0138	3.86	0.0301	3.08	0.0186	3.64	0.0528	3.11	0.0123	4.64
^{122}Sb	564	0.1122	1.08	0.1325	1.12	0.1580	1.11	0.1444	1.68	0.1553	1.23
^{82}Br	777	0.0000		0.0000	0	0.0000		0.0000		0.0000	
^{140}La	1597	0.0767	3.56	0.0161	3.67	0.0650	3.68	0.0292	4.89	0.0496	2.98

CELLULOSE STANDARD 2

nuclide	energy keV	mean	standard deviation	Bq mg^{-1}	% error	Bq mg^{-1}	% error	Bq mg^{-1}	% error	Bq mg^{-1}	% error
^{153}Sm	103	2.2700	0.0200	2.2650	0.48	2.2869	0.41	2.2685	0.42	2.2823	0.51
^{141}Ce	146	0.1847	0.0022	0.1882	2.09	0.1837	1.99	0.1873	2.23	0.1841	1.08
^{177}Lu	209	0.3900	0.0540	0.4168	1.41	0.4038	1.31	0.4003	1.49	0.4112	1.62
^{75}Se	265	0.1607	0.0033	0.1583	1.56	0.1638	1.35	0.1594	2.11	0.1638	1.12
^{203}Hg	279	0.5792	0.0134	0.5840	1.83	0.5910	1.78	0.5940	2.12	0.5520	1.84
^{233}Pa	312	1.3671	0.0235	1.3570	0.89	1.3360	0.91	1.3890	0.89	1.3767	0.73
^{60}Co	315	0.2777	0.0022	0.2750	1.29	0.2780	1.23	0.2745	1.32	0.2816	1.11
^{198}Au	412	3.8800	0.0153	3.8980	0.31	3.8873	0.33	3.8765	0.42	3.8607	0.29
^{181}Hf	482	1.1835	0.0210	1.1600	1.21	1.1728	1.31	1.1537	1.1	1.2178	2.35
^{131}Ba	496	0.1302	0.0019	0.1344	1.97	0.1274	1.8	0.1305	2.13	0.1297	3.2
^{76}As	559	0.1723	0.0035	0.1720	1.91	0.1744	2.08	0.1695	2.05	0.1737	1.96
^{122}Sb	564	0.1840	0.0037	0.1869	1.55	0.1913	1.78	0.1936	1.71	0.1897	1.54
^{110m}Ag	658	0.6506	0.0055	0.6418	2.03	0.6475	2.11	0.6457	1.99	0.6518	2.11
^{82}Br	777	0.4678	0.0079	0.4715	0.71	0.4665	0.65	0.4677	0.49	0.4576	0.53
^{46}Sc	889	3.1858	0.0376	3.1542	0.41	3.1789	0.36	3.1668	0.23	3.2025	0.42
^{140}La	1597	0.1174	0.0017	0.1204	1.78	0.1170	1.71	0.1150	1.83	0.1170	1.68

nuclide	energy keV	Bq mg^{-1}	% error	Bq mg^{-1}	% error	Bq mg^{-1}	% error	Bq mg^{-1}	% error	Bq mg^{-1}	% error
^{153}Sm	103	2.2923	0.53	2.2414	0.42	2.2546	0.42	2.2946	0.42	2.2460	0.43
^{141}Ce	146	0.1859	1.67	0.1845	2.64	0.1849	2.17	0.1812	1.87	0.1827	1.94
^{177}Lu	209	0.4121	1.45	0.4057	1.55	0.4152	1.55	0.4063	1.48	0.4090	1.46
^{75}Se	265	0.1641	1.26	0.1648	1.65	0.1579	1.97	0.1564	2.13	0.1581	1.65
^{203}Hg	279	0.5820	1.66	0.5850	1.78	0.5670	2.12	0.5710	2.12	0.5870	1.95
^{233}Pa	312	1.3780	1.51	1.3910	0.9	1.3340	1.28	1.3930	1.16	1.3490	1.08
^{60}Co	315	0.2772	1.76	0.2783	1.16	0.2793	1.43	0.2786	1.32	0.2768	1.21
^{198}Au	412	3.8765	0.36	3.8868	0.32	3.8647	0.32	3.8971	0.28	3.8565	0.27
^{181}Hf	482	1.2056	1.19	1.1740	1.32	1.1970	1.47	1.1890	1.75	1.1820	2.02
^{131}Ba	496	0.1311	2.76	0.1302	3.12	0.1288	3.12	0.1292	4.12	0.1306	2.55
^{76}As	559	0.1782	1.89	0.1692	1.98	0.1686	1.98	0.1761	2.15	0.1686	2.32
^{122}Sb	564	0.1913	1.62	0.1888	1.81	0.1875	1.81	0.1987	1.88	0.1885	1.89
^{110m}Ag	658	0.6511	2.34	0.6608	2.06	0.6487	2.07	0.6533	2.15	0.6549	2.02
^{82}Br	777	0.4676	0.66	0.4735	0.66	0.4656	0.66	0.4828	0.88	0.4568	0.86
^{46}Sc	889	3.1528	0.26	3.1783	0.31	3.1828	0.29	3.2776	0.27	3.1783	0.36
^{140}La	1597	0.1190	1.81	0.1185	1.84	0.1165	1.84	0.1160	1.92	0.1180	1.81

REFERENCE PEAT DATA

WITHIN BATCH SAMPLES. All results are in mg kg^{-1}

nuclide	energy keV	BP1	% error	BP2	% error	BP3	% error	BP4	% error	BP5	% error
^{182}Ta	85	2.007	3.13	1.986	3.38	1.999	3.18	2.011	3.23	2.001	3.69
^{153}Sm	103	2.198	1.45	2.185	1.53	2.194	1.46	2.189	1.23	2.181	1.19
^{141}Ce	146	25.23	0.74	25.23	0.41	25.33	0.38	25.22	0.69	25.24	0.53
^{177}Lu	209	1.831	2.12	1.829	2.32	1.834	2.45	1.856	2.63	1.841	2.16
^{75}Se	265	2.338	3.13	2.341	3.19	2.335	3.59	2.331	3.69	2.344	3.79
^{203}Hg	279	0.601	4.56	0.640	4.89	0.626	5.46	0.670	5.12	0.660	5.02
^{233}Pa	312	1.401	4.12	1.401	3.88	1.399	3.79	1.399	2.99	1.398	2.46
^{60}Co	315	4.156	3.23	4.161	3.39	4.123	3.49	4.144	3.46	4.132	3.28
^{181}Hf	482	0.832	4.32	0.839	4.16	0.829	4.08	0.841	4.01	0.835	3.87
^{76}As	559	0.851	2.59	0.873	2.79	0.859	3.12	0.879	3.33	0.848	2.29
^{82}Br	777	23.41	0.98	23.38	0.87	23.42	0.87	23.40	0.83	23.38	0.87
^{46}Sc	889	2.012	2.68	2.021	3.69	2.009	3.79	2.015	4.12	2.011	4.32
^{140}La	1597	19.52	0.87	19.49	0.49	19.53	0.64	19.51	0.79	19.48	0.98

nuclide	energy keV	BP6	% error	BP7	% error	BP8	% error	BP9	% error	BP10	% error
^{182}Ta	85	2.009	3.89	2.013	3.46	1.987	3.29	2.005	3.88	1.998	3.69
^{153}Sm	103	2.191	1.82	2.198	1.31	2.189	1.11	2.187	1.56	2.215	1.45
^{141}Ce	146	25.24	0.64	25.23	0.56	25.25	0.64	25.11	0.46	25.35	0.64
^{177}Lu	209	1.855	2.49	1.839	2.71	1.831	2.45	1.828	2.73	1.895	2.09
^{75}Se	265	2.329	3.45	2.319	3.64	2.345	3.49	2.329	2.99	2.322	2.89
^{203}Hg	279	0.629	5.03	0.631	5.09	0.623	4.78	0.663	5.02	0.660	5.05
^{233}Pa	312	1.401	2.69	1.402	3.69	1.402	4.13	1.380	3.87	1.383	3.99
^{60}Co	315	4.146	3.59	4.137	3.46	4.131	3.88	4.126	3.56	4.134	3.66
^{181}Hf	482	0.831	3.59	0.829	3.64	0.818	3.59	0.855	3.44	0.863	3.56
^{76}As	559	0.852	3.79	0.838	4.01	0.855	3.87	0.855	2.99	0.849	3.13
^{82}Br	777	23.39	0.69	23.41	0.59	23.38	0.82	23.42	0.79	23.49	1.01
^{46}Sc	889	2.016	3.88	2.041	4.13	2.001	3.98	2.025	3.66	2.053	3.66
^{140}La	1597	19.51	0.87	19.49	0.89	19.51	0.79	19.53	0.57	19.68	0.46

BETWEEN BATCH SAMPLES. All results are in mg kg^{-1}

nuclide	energy keV	SDBP 3	% error	3BP3	% error	3BP1	% error	SDBP 4	% error	1BP1	% error	SDBP 1	% error	RBP3	% error	RBP4	% error
^{182}Ta	85	1.981	4.41	2.023	5.13	2.001	4.76	2.011	4.64	2.009	4.68	2.001	3.69	2.005	4.31	1.999	3.56
^{153}Sm	103	2.158	3.31	2.169	1.84	2.154	2.65	2.175	6.41	2.143	2.26	2.174	2.42	2.156	3.64	2.181	6.34
^{141}Ce	146	25.27	1.31	25.25	3.12	23.21	3.21	25.28	1.09	25.26	1.3	25.22	1.08	25.23	3.37	25.23	1.14
^{177}Lu	209	1.851	2.49	1.856	3.31	1.841	2.317	1.814	3.67	1.892	3.74	1.873	1.17	1.812	2.71	1.831	3.89
^{75}Se	265	2.319	2.13	2.331	2.22	2.323	1.98	2.315	2.67	2.340	3.92	2.366	2.588	2.338	116	2.259	2.16
^{203}Hg	279	0.637	4.95	0.588	4.62	0.632	5.38	0.600	5.17	0.699	4.62	0.648	5.19	0.499	4.53	0.514	5.89
^{233}Pa	312	1.401	2.45	1.378	2.58	1.401	3.26	1.408	2.35	1.398	2.38	1.419	2.19	1.399	2.56	1.387	2.34
^{60}Co	315	4.161	3.39	4.191	3.25	4.139	3.28	4.146	4.15	4.109	2.36	4.139	3.69	4.159	3.38	4.121	2.39
^{181}Hf	482	0.833	4.23	0.897	2.38	0.841	3.85	0.825	3.93	0.835	3.64	0.835	4.23	0.835	2.97	0.851	4.12
^{76}As	559	0.842	3.87	0.831	3.15	0.898	3.33	0.895	2.51	0.861	3.81	0.898	3.56	0.858	3.71	0.851	3.14
^{82}Br	777	23.39	3.59	23.38	2.01	23.41	1.187	23.34	4.65	23.39	5.01	23.41	5.03	23.35	2.59	23.41	4.32
^{46}Sc	889	2.022	3.49	2.016	2.62	2.044	3.22	2.056	3.23	2.031	2.7	2.088	2.11	2.033	2.58	2.00	2.35
^{140}La	1597	19.52	2.10	19.56	3.68	19.49	3.53	19.49	3.27	19.51	3.73	19.53	3.84	19.53	3.5	19.53	3.49

nuclide	energy keV	R19	% error	BHBP 2	% error	BHBP 1	% error	2BP1	% error	1BP4	% error	4BP2	% error
^{182}Ta	85	2.013	3.98	2.021	4.19	2.005	3.79	1.996	4.13	2.048	3.89	1.998	4.56
^{153}Sm	103	2.197	3.62	2.158	2.13	2.215	1.26	2.165	3.13	2.129	2.98	2.138	1.04
^{141}Ce	146	25.26	3.78	25.20	3.15	25.26	3.53	25.24	3.18	25.25	3.12	25.26	2.95
^{177}Lu	209	1.832	1.11	1.821	3.71	1.861	2.19	1.839	3.35	1.848	2.98	1.853	2.21
^{75}Se	265	2.332	1.61	2.349	1.79	2.319	1.64	2.322	1.62	2.325	3.15	2.336	2.69
^{203}Hg	279	0.633	5.35	0.567	4.89	0.712	5.32	0.759	4.74	0.574	4.89	0.775	4.89
^{233}Pa	312	1.401	2.10	1.401	1.69	1.399	4.31	1.401	3.18	1.390	3.59	1.411	2.69
^{60}Co	315	4.159	3.43	4.161	2.39	4.145	3.14	4.181	2.29	4.108	3.13	4.143	3.97
^{181}Hf	482	0.834	4.81	0.834	4.71	0.831	3.43	0.828	2.41	0.815	4.41	0.809	4.35
^{76}As	559	0.839	6.31	0.875	2.98	0.864	3.35	0.851	3.26	0.839	3.69	0.869	3.45
^{82}Br	777	23.39	3.52	23.42	3.84	23.39	3.01	23.12	3.12	23.49	2.59	23.40	2.91
^{46}Sc	889	2.028	3.41	2.059	2.43	2.069	3.13	2.027	2.45	2.064	1.98	2.055	2.31
^{140}La	1597	19.52	3.65	19.46	2.98	19.51	3.56	19.54	2.56	19.55	3.51	19.49	2.98

A3.2 METAL CONTENTS OF THE PEAT CORES

SOUTH DRUMBOY CORE 1

depth cm	depth g cm^{-2}	mg kg^{-1} Mn	% error Mn	mg kg^{-1} Zn	% error Zn	mg kg^{-1} Al	% error Al	mg kg^{-1} Cu	% error Cu	mgkg^{-1} Pb	% error Pb
0.0-3.5	0-0.39	104.3	5.02	71.7	2.70	2341.8	9.05	12.7	6.21	63.3	3.25
3.5-7.5	0.39-1.15	69.0	5.03	62.1	10.45	10006.3	1.35	14.1	10.72	91.7	3.51
7.5-11.5	1.15-2.35	29.6	5.08	47.3	2.51	20251.1	0.85	10.9	14.08	49.4	10.70
11.5-15.2	2.35-3.31	29.6	5.11	46.5	12.60	18871.4	1.42	9.3	9.86	34.8	14.65
15.2-19.2	3.31-4.63	13.9	5.02	36.2	1.58	14158.2	2.20	8.9	1.69	13.5	18.07
19.2-22.2	4.63-6.07	12.8	5.04	34.6	6.20	13259.9	5.77	8.4	12.36	8.5	2.64
22.2-25.1	6.07-6.44	18.2	5.64	33.3	0.39	19319.9	6.10	12.3	33.72	6.6	4.37
25.1-28.8	6.44-6.93	22.5	5.08	33.7	0.35	9031.5	5.38	14.9	27.99	5.3	11.68
28.8-30.8	6.93-7.21	26.5	5.01	28.6	0.59	8121.5	0.63	11.7	8.85	4.5	8.40
30.8-34.8	7.21-7.69	21.9	5.14	36.2	5.70	6926.4	6.97	12.4	6.50	3.5	11.24
34.8-38.8	7.69-8.25	15.3	5.05	44.9	2.44	4078.9	3.26	11.9	25.86	4.5	3.10
38.8-42.8	8.25-8.89	12.0	5.18	22.2	4.88	3597.1	2.91	3.2	8.02	4.8	5.00
42.8-47.8	8.89-9.69	0.00	0.00	17.9	4.63	3335.4	1.06	3.2	16.61	6.1	2.42
47.8-51.8	9.69-10.2	0.00	0.00	15.9	0.42	3042.9	4.91	2.7	16.83	3.2	2.04
51.8-56.2	10.2-10.7	0.00	0.00	12.9	3.40	2336.7	0.96	1.6	8.88	7.1	2.31
58.7-58.7	10.7-11.2	0.00	0.00	10.9	10.99	2149.5	0.88	1.9	11.81	4.9	18.75
58.7-62.2	11.2-11.5	0.00	0.00	8.3	10.02	2536.3	1.57	1.9	16.06	5.4	31.57
62.2-65.4	11.5-11.9	0.00	0.00	7.3	1.32	2558.6	2.38	1.2	23.83	9.1	24.80
65.4-68.2	11.9-12.3	0.00	0.00	8.1	32.97	2502.6	1.14	0.00	0.00	8.1	0.51

depth cm	depth g cm^{-2}	La mg kg^{-1}	% error La	mg kg^{-1} Fe	% error Fe	Sm mg kg^{-1}	% error Sm	mg kg^{-1} Br	% error Br	mg kg^{-1} Sc	% error Sc
0.0-3.5	0-0.39	9.17	6.63	19396.9	9.05	0.99	9.81	13.3	3.31	1.66	5.51
3.5-7.5	0.39-1.15	11.8	6.89	20089.7	1.35	1.83	8.06	12.2	3.65	4.08	6.13
7.5-11.5	1.15-2.35	19.1	5.99	23657.7	0.85	2.38	7.56	8.3	3.87	7.03	4.02
11.5-15.2	2.35-3.31	17.5	4.08	23291.7	1.42	2.81	7.31	8.5	3.43	6.56	4.13
15.2-19.2	3.31-4.63	14.0	3.99	25167.2	2.20	2.84	6.98	8.4	4.16	4.92	4.65
19.2-22.2	4.63-6.07	13.8	4.13	23963.7	5.77	2.14	6.79	8.8	4.31	4.05	5.64
22.2-25.1	6.07-6.44	13.2	3.76	22579.4	6.10	2.25	6.76	7.9	4.08	3.22	7.31
25.1-28.8	6.44-6.93	11.5	3.56	23909.8	5.38	2.32	5.46	8.1	4.55	2.99	8.13
28.8-30.8	6.93-7.21	10.0	4.16	23677.1	0.63	1.99	5.78	8.6	4.79	1.75	8.86
30.8-34.8	7.21-7.69	10.7	4.55	19811.3	6.97	1.71	5.13	7.4	4.89	2.11	7.41
34.8-38.8	7.69-8.25	17.0	4.78	17891.4	3.26	2.47	4.98	13.5	4.00	2.33	7.13
38.8-42.8	8.25-8.89	12.1	4.81	11092.4	2.91	2.61	4.16	12.8	4.13	2.16	7.08
42.8-47.8	8.89-9.69	10.6	4.66	8575.7	1.06	1.94	4.78	14.5	3.78	1.72	7.89
47.8-51.8	9.69-10.2	7.5	5.67	5981.0	4.91	1.53	3.89	7.8	3.99	1.39	7.93
51.8-56.2	10.2-10.7	8.8	8.34	1989.3	0.96	1.18	4.56	9.7	4.08	1.52	8.13
58.7-58.7	10.7-11.2	14.2	7.13	998.1	0.88	1.48	5.62	11.9	3.56	2.70	7.78
58.7-62.2	11.2-11.5	10.2	7.79	913.2	1.57	1.99	4.31	16.0	3.33	2.37	8.64
62.2-65.4	11.5-11.9	7.3	1.32	893.3	2.38	0.12	7.12	15.3	3.19	2.21	9.31
65.4-68.2	11.9-12.3	8.1	32.97	796.3	1.14	0.18	11.23	16.1	2.48	2.58	8.46

depth cm	depth g cm^{-2}	Th mg kg^{-1}	% error Th	Co mg kg^{-1}	% error Co	Se mg kg^{-1}	% error Se	Ce mg kg^{-1}	% error Ce	Hg mg kg^{-1}	% error Hg
0.0-3.5	0-0.39	1.03	5.36	7.34	3.34	2.65	7.56	2.30	4.59	0.334	9.81
3.5-7.5	0.39-1.15	2.97	4.13	11.45	2.12	3.80	4.32	4.53	3.34	0.364	10.52
7.5-11.5	1.15-2.35	4.53	3.33	10.85	2.59	6.09	4.56	3.42	3.58	0.466	8.19
11.5-15.2	2.35-3.31	3.98	4.26	10.64	2.69	6.80	4.12	4.32	3.12	0.202	8.52
15.2-22.2	3.31-4.63	2.60	5.68	9.42	3.98	5.64	4.09	3.31	4.12	0.102	15.33
22.2-25.1	4.63-6.07	2.82	5.55	3.66	4.05	4.91	3.22	2.86	4.65	0.000	0.00
25.1-28.8	6.07-6.44	1.99	6.79	2.12	4.15	3.38	2.89	1.11	3.88	0.000	0.000
28.8-30.8	6.44-6.93	1.14	6.88	1.01	5.33	2.98	3.56	2.80	4.76	0.000	0.000
30.8-34.8	6.93-7.21	0.42	9.13	0.98	9.98	2.73	4.89	2.51	4.88	0.000	0.000
34.8-42.8	7.21-7.69	0.58	10.05	0.00	0.00	3.41	4.96	3.48	3.35	0.000	0.000
42.8-47.8	7.69-8.25	0.54	11.08	0.00	0.00	3.28	3.33	4.11	2.89	0.000	0.000
47.8-51.8	8.25-8.89	0.59	12.25	0.00	0.00	4.24	3.35	2.25	3.68	0.000	0.000
51.8-56.2	8.89-9.69	0.21	12.99	0.00	0.00	2.09	3.97	1.30	3.77	0.000	0.000
58.7-58.7	9.69-10.2	0.19	13.69	0.00	0.00	2.22	4.56	1.11	4.99	0.000	0.000
58.7-62.2	10.2-10.7	0.19	13.45	0.00	0.00	2.28	4.58	2.90	4.78	0.000	0.000
62.2-65.4	10.7-11.2	1.51	8.64	0.00	0.00	3.32	5.13	1.56	3.21	0.000	0.000
65.4-68.2	11.2-11.5	0.11	8.33	0.00	0.00	0.35	4.12	0.10	6.58	0.000	0.000

depth gcm^{-2}	Sb mg kg^{-1}	% error Sb	As	% error As	Ta mg kg^{-1}	% error Ta	$^{208}Pb/^{207}Pb$	% error	$^{208}Pb/^{206}Pb$	% error	$^{206}Pb/^{207}Pb$	% error
0-0.39	2.91	3.13	2.35	7.57	1.21	5.68	2.5141	0.16	2.2861	0.39	1.0997	0.25
0.39-1.15	2.98	2.11	6.46	3.37	1.91	8.31	2.5091	0.37	2.2565	0.53	1.1120	0.58
1.15-2.35	3.15	2.03	6.86	3.25	3.37	5.46	2.5306	0.20	2.2340	0.26	1.1323	0.30
2.35-3.31	2.94	2.25	5.64	3.58	3.46	5.55	2.5537	0.18	2.2302	0.38	1.1451	0.49
3.31-4.63	2.23	2.19	2.75	6.46	1.48	5.89	2.5514	0.25	2.0690	0.32	1.1575	0.33
4.63-6.07	1.15	3.59	3.06	7.45	0.75	10.59	2.5433	0.36	2.2282	0.63	1.1414	0.36
6.07-6.44	0.84	5.55	1.95	7.78	0.98	10.05	2.5245	0.40	2.2346	0.55	1.1297	0.38
6.44-6.93	0.59	8.12	1.14	8.91	0.84	10.68	2.5096	0.40	2.2498	0.43	1.1155	0.45
6.93-7.21	0.28	9.97	0.86	9.35	0.65	12.25	2.5326	0.63	2.2321	0.45	1.1346	0.73
7.21-7.69	0.00	0.00	0.00	0.00	0.96	10.35	2.4999	0.33	2.2309	0.57	1.1206	0.55
7.69-8.25	0.00	0.00	0.00	0.00	1.61	11.35	2.5215	0.53	2.2234	1.00	1.1341	0.06
8.25-8.89	0.00	0.00	0.00	0.00	0.93	11.46						
8.89-9.69	0.00	0.00	0.00	0.00	0.64	11.88						
9.69-10.2	0.00	0.00	0.00	0.00	0.97	12.05	**********	*NOT*	*ANALYSED*	*****	**********	*****
10.2-10.7	0.00	0.00	0.00	0.00	1.26	12.87						
10.7-11.2	0.00	0.00	0.00	0.00	2.25	12.02						
11.2-11.5	0.00	0.00	0.00	0.00	0.34	14.56						

SOUTH DRUMBOY CORE 2

depth cm	depth g cm^{-2}	Mn mg kg^{-1}	% error Mn	Zn mg kg^{-1}	% error Zn	Al mg kg^{-1}	% error Al	Cu mg kg^{-1}	% error Cu	Pb mg kg^{-1}	% error Pb
0-4	0.0-0.78	76.1	8.58	46.1	10.22	3892.3	0.26	14.7	19.34	105.0	6.47
4-7.0	0.78-1.66	44.8	9.41	36.2	14.00	7739.0	0.39	11.5	2.29	121.1	9.56
7.0-9.5	1.66-2.15	31.9	4.28	33.9	4.95	6767.0	0.37	7.7	1.64	35.4	9.75
9.5-11.7	2.15-2.67	24.4	3.03	32.0	4.18	5045.6	0.27	5.2	2.06	12.6	47.25
11.7-14.6	2.67-3.10	21.7	8.58	34.0	4.43	5473.0	0.25	4.8	8.14	3.2	57.74
14.6-28.4	3.10-3.49	27.9	7.76	26.6	3.79	19184.1	0.17	7.9	8.03	10.6	30.17
28.4-31.7	3.49-4.25	46.7	6.58	36.6	4.88	18856.7	0.43	9.7	3.21	2.6	45.61
31.7-34.7	4.25-4.65	50.9	10.85	45.5	0.80	18572.0	0.73	10.7	1.80	4.9	34.67
34.7-38.7	4.65-5.29	60.8	10.67	70.3	5.18	18064.8	0.48	11.3	4.23	12.0	36.57
38.7-42.7	5.29-6.28	62.0	12.47	55.2	1.79	20841.2	0.68	11.1	5.39	11.5	32.39
42.7-45.2	6.28-7.29	63.0	8.72	28.5	9.47	22459.3	0.54	10.8	2.07	10.4	33.74
45.2-48.2	7.29-8.14	66.4	11.91	47.0	4.55	19482.8	0.70	10.7	3.25	4.0	78.47
48.2-51.2	8.14-8.80	64.9	4.57	69.9	3.62	23677.8	3.28	8.8	4.32	7.9	81.71
51.2-53.2	8.80-9.56	67.6	6.29	88.8	5.05	19454.1	1.71	7.8	11.76	3.6	86.56
53.2-55.7	9.56-10.6	76.8	4.75	68.8	4.54	20820.0	1.80	6.6	10.34	17.6	5.23
55.7-58.4	10.6-11.6	76.4	3.47	57.8	11.91	20536.8	0.50	6.8	8.55	9.1	8.13
58.4-60.4	11.6-12.5	92.2	2.69	90.7	1.77	21478.3	0.75	7.2	5.88	2.1	54.26

depth cm	depth g cm^{-2}	Sm mg kg^{-1}	% error Sm	La mg kg^{-1}	% error La	Fe mg kg^{-1}	% error Fe	Br mg kg^{-1}	% error Br	Sc mg kg^{-1}	%error Sc
0-4	0.0-0.78	0.78	4.11	7.15	2.66	14865.3	0.26	20.8	1.98	3.7	3.19
4-7.0	0.78-1.66	1.41	3.56	14.81	2.13	11981.1	0.39	25.6	0.63	5.7	3.88
7.0-9.5	1.66-2.15	0.94	4.12	10.83	2.25	18177.4	0.37	29.2	0.59	4.1	2.56
9.5-11.7	2.15-2.67	0.76	4.15	16.80	2.46	24942.4	0.27	34.1	0.68	2.0	1.86
11.7-14.6	2.67-3.10	2.03	3.46	21.16	2.58	23872.0	0.25	45.0	0.54	8.1	1.55
14.6-28.4	3.10-3.49	2.06	3.13	22.23	2.31	5654.5	0.17	21.6	1.12	8.6	2.59
28.4-31.7	3.49-4.25	2.79	2.87	29.42	2.19	7556.1	0.43	16.3	1.87	12.7	3.87
31.7-34.7	4.25-4.65	2.98	3.13	42.34	3.16	7972.2	0.73	18.2	1.45	19.5	2.34
34.7-38.7	4.65-5.29	4.29	2.55	47.59	2.88	8349.2	0.48	14.6	2.65	21.9	2.22
38.7-42.7	5.29-6.28	4.28	2.87	47.84	2.46	15410.7	0.68	10.6	2.89	22.0	2.13
42.7-45.2	6.28-7.29	3.45	2.56	35.50	1.87	19353.5	0.54	6.4	3.13	16.1	2.26
45.2-48.2	7.29-8.14	2.26	2.31	31.07	2.56	12229.0	0.70	5.8	2.79	13.4	3.26
48.2-51.2	8.14-8.80	3.33	2.11	33.91	1.99	19289.8	3.28	6.2	3.14	18.8	3.02
51.2-53.2	8.80-9.56	3.90	2.09	35.11	1.45	11352.3	1.71	5.2	3.08	18.0	2.87
53.2-55.7	9.56-10.6	2.92	2.58	29.95	2.03	18359.6	1.80	4.2	3.16	15.6	3.15
55.7-58.4	10.6-11.6	2.41	2.64	23.65	1.66	15847.2	0.50	3.7	2.99	12.5	3.56
58.4-60.4	11.6-12.5	3.47	3.11	35.78	1.54	14963.4	0.75	3.9	3.56	18.5	3.41

depth g cm^{-2}	Th mg kg^{-1}	% error Th	As mg kg^{-1}	% error As	Co mg kg^{-1}	%error Co	Hf mg kg^{-1}	% error Hf	Ta mg kg^{-1}	% error Ta	Hg mg kg^{-1}	%error Hg
0.0-0.78	0	0	7.17	1.87	4.2	1.87	1.46	2.87	2.99	1.87	0.44	3.56
0.78-1.66	0	0	10.80	2.05	12.17	1.45	4.19	3.15	4.97	2.25	0.75	3.19
1.66-2.15	0	0	9.14	1.55	8.38	1.29	1.33	3.25	1.79	2.46	0.31	2.87
2.15-2.67	0	0	4.47	1.89	6.01	1.34	0.83	3.98	0.92	2.69	0.25	2.88
2.67-3.10	0	0	2.33	1.76	5.97	1.55	2.78	3.16	1.86	2.33	0.23	3.16
3.10-3.49	0	0	1.83	2.16	2.25	1.87	4.35	3.45	2.17	2.15	0.26	3.59
3.49-4.25	6.39	2.13	3.02	2.18	1.67	1.09	4.72	3.22	3.01	2.58	0.27	3.41
4.25-4.65	10.37	1.45	2.88	2.08	1.13	1.15	7.32	3.15	15.14	1.87	0.21	3.06
4.65-5.29	15.07	1.13	2.95	1.87	1.06	1.87	11.39	2.78	23.25	2.03	0.21	5.46
5.29-6.28	14.79	1.23	3.61	1.45	1.14	0.86	10.64	2.55	20.31	1.45	0.18	8.87
6.28-7.29	6.85	1.05	1.97	1.68	1.98	2.36	11.32	2.56	21.53	1.33	0.28	12.55
7.29-8.14	8.01	1.46	1.84	1.31	2.01	2.45	6.38	2.48	4.32	1.16	0.24	13.13
8.14-8.80	14.75	1.58	3.06	1.21	1.13	2.13	6.31	2.38	4.46	1.05	0.19	13.69
8.80-9.56	15.98	2.19	2.48	1.56	1.54	2.58	8.68	2.22	4.74	1.19	0.16	0.00
9.56-10.6	11.7	2.46	1.87	1.87	1.35	2.79	8.15	3.09	3.24	1.24	0.18	0.00
10.6-11.6	9.6	3.16	1.25	1.46	2.86	2.31	9.02	2.68	5.39	2.55	0.24	0.00
11.6-12.5	16.55	1.87	2.49	1.55	3.88	2.15	11.18	2.22	10.15	2.01	0.41	0.00

depth g cm^{-2}	Sb mg kg^{-1}	% error Sb	Se mg kg^{-1}	% error Se	Ce mg kg^{-1}	% error Ce	$^{208}Pb/^{207}Pb$	% error	$^{208}Pb/^{207}Pb$	% error	$^{206}Pb/^{207}Pb$	% error
0.0-0.78	2.12	2.31	3.63	1.98	12.7	3.08	2.49	0.31	2.2353	0.38	1.1389	0.31
0.78-1.66	2.29	3.89	8.15	1.45	40.6	0.87	2.55	0.27	2.2336	0.44	1.1415	0.51
1.66-2.15	0.88	4.16	3.8	1.32	15.3	2.13	2.50	0.28	2.1416	0.46	1.1668	0.30
2.15-2.67	0.35	5.99	2.33	1.78	13.3	2.22	2.55	0.25	2.2228	0.89	1.1478	0.74
2.67-3.10	0.00	0.00	3.65	1.77	12.3	2.08	2.55	0.43	2.2168	0.47	1.1507	0.57
3.10-3.49	0.00	0.00	4.5	1.46	12.4	2.34	*********	*****	*sample*	*not*	*analysed*	*****
3.49-4.25	0.00	0.00	5.78	1.33	18.4	0.99	2.56	0.09	2.2095	0.23	1.1578	0.28
4.25-4.65	0.00	0.00	10.53	2.09	115.6	2.13	2.57	0.36	2.2116	0.49	1.1630	0.53
4.65-5.29	0.00	0.00	9.36	1.57	89.7	2.05	2.57	0.22	2.1992	0.24	1.1683	0.41
5.29-6.28	0.00	0.00	8.83	2.31	64.1	3.11	2.57	0.38	2.2064	0.33	1.1665	0.09
6.28-7.29	0.00	0.00	5.66	2.16	124.9	0.75	2.57	0.51	2.2114	0.61	1.1602	0.40
7.29-8.14	0.00	0.00	5.05	2.56	68.0	0.94	2.57	0.20	2.2096	0.48	1.1625	0.58
8.14-8.80	0.00	0.00	7.16	2.09	13.3	1.87	2.57	0.38	2.2193	0.52	1.1584	0.32
8.80-9.56	0.00	0.00	7.28	1.46	13.9	2.05	2.58	0.22	2.2001	0.14	1.1704	0.26
9.56-10.6	0.00	0.00	7.73	2.08	14.6	2.66	2.58	0.34	2.2081	0.50	1.1662	0.47
10.6-11.6	0.00	0.00	6.42	1.59	12.1	2.89	2.57	0.58	2.2059	0.55	1.1670	0.49
11.6-12.5	0.00	0.00	9.48	2.33	13.1	2.73	2.57	0.19	2.2051	0.43	1.1650	0.45

SOUTH DRUMBOY CORE 3

depth cm	depth gcm^{-2}	mg kg^{-1} Mn	% error Mn	mg kg^{-1} Al	% error Al	mg kg^{-1} Cu	% error Cu	mg kg^{-1} Zn	% error Zn	mg kg^{-1} Pb	% error Pb
0-2.0	0.0-0.14	133.4	19.90	1751.2	2.05	1.11	6.49	63.2	6.81	23.78	6.49
2.0-4.7	0.14-0.53	56.0	6.82	2012.0	2.49	3.24	3.29	46.7	8.54	68.78	3.30
4.7-6.7	0.53-1.01	40.9	42.53	1915.5	3.20	6.31	3.61	47.2	9.63	111.20	3.58
6.7-9.1	1.01-1.45	27.4	7.65	1588.3	1.44	7.55	1.43	28.8	6.55	131.43	1.43
9.1-12.1	1.45-1.92	32.7	6.78	1731.4	1.42	9.17	4.14	37.8	2.88	154.56	4.67
12.1-15.2	1.92-2.54	24.2	6.99	1844.8	27.85	1.77	4.86	23.8	4.15	46.67	0.64
15.2-18.4	2.54-3.32	23.7	6.37	2684.0	2.67	0	0	23.0	2.91	4.52	19.03
18.4-21.0	3.32-3.99	18.2	12.60	2284.3	6.17	0	0	18.5	9.87	12.53	21.71
21.0-23.5	3.99-4.52	19.1	13.98	2029.7	1.93	0	0	16.6	6.01	0	0
23.5-27.5	4.52-4.99	15.3	22.11	1681.2	8.85	0	0	10.4	6.19	0	0
27.5-30.5	4.99-5.45	15.5	28.83	1486.7	9.08	0	0	10.8	2.12	0	0
30.5-33.5	5.45-5.95	18.1	22.32	1232.2	7.05	0	0	8.8	1.47	0	0
33.5-36.7	5.95-6.44	16.2	9.60	754.6	6.42	0	0	5.8	4.75	0	0
36.7-39.4	6.44-6.91	17.0	11.77	735.4	4.13	0	0	5.3	6.35	0	0
39.4-41.7	6.91-7.34	8.5	41.22	630.7	15.91	0	0	3.7	19.37	0	0
41.7-44.2	7.34-7.71	11.4	6.46	582.2	1.32	0	0	2.7	12.21	0	0
44.2-48.7	7.71-8.20	12.0	1.58	668.4	7.58	0	0	0	0	0	0
48.7-55.7	8.20-9.71	12.8	13.92	1020.2	1.77	0	0	0	0	0	0
55.7-58.4	9.71-10.1	10.3	20.46	616.1	2.15	0	0	0	0	0	0

depth cm	depth gcm^{-2}	mg kg^{-1} Fe	% error Fe	mg kg^{-1} Se	% error Se	mg kg^{-1} Sm	% error Sm	mg kg^{-1} Co	% error Co	mg kg^{-1} Sc	% error Sc
0-2.0	0.0-0.14	6473.9	2.05	0.97	3.36	0.32	1.56	3.95	7.29	1.45	13.93
2.0-4.7	0.14-0.53	5594.8	2.49	1.33	3.35	0.89	5.64	1.60	7.31	2.80	12.64
4.7-6.7	0.53-1.01	6321.1	3.20	2.10	1.98	1.38	2.48	9.20	5.87	3.25	7.07
6.7-9.1	1.01-1.45	5385.3	1.44	2.70	3.32	1.22	11.40	11.57	5.55	2.80	10.77
9.1-12.1	1.45-1.92	4914.2	1.42	3.74	1.54	1.74	1.32	13.46	5.00	5.27	6.56
12.1-15.2	1.92-2.54	2745.0	27.85	0.89	5.64	0.48	0.0	6.63	4.99	1.38	11.21
15.2-18.4	2.54-3.32	3204.5	2.67	1.53	3.23	1.05	0.0	6.14	4.36	1.25	13.64
18.4-21.0	3.32-3.99	2293.2	6.16	1.33	3.31	0.82	0.0	7.44	4.69	0	0
21.0-23.5	3.99-4.52	2486.5	1.93	1.26	3.92	0.34	0.0	6.53	4.69	0	0
23.5-27.5	4.52-4.99	2815.3	8.85	0.96	4.39	0.28	0.0	5.82	5.01	0	0
27.5-30.5	4.99-5.45	2648.0	9.08	1.03	3.59	0.0	0.0	6.19	4.58	0	0
30.5-33.5	5.45-5.95	2670.5	7.05	0.49	4.23	0.0	0.0	6.21	4.46	0	0
33.5-36.7	5.95-6.44	2793.9	6.42	0.41	4.15	0.0	0.0	6.11	4.52	0	0
36.7-39.4	6.44-6.91	3029.9	4.13	0.70	4.09	0.0	0.0	6.09	5.21	0	0
39.4-41.7	6.91-7.34	3501.8	15.91	0.70	4.33	0.0	0.0	6.12	5.69	0	0
41.7-44.2	7.34-7.71	2583.8	1.32	0.89	4.23	0.0	0.0	3.98	5.57	0	0
44.2-48.7	7.71-8.20	2581.9	7.57	0.54	5.35	0.0	0.0	0.00	0.00	0	0
48.7-55.7	8.20-9.71	3087.7	1.77	0.64	4.93	0.0	0.0	0.00	0.00	0	0
55.7-58.4	9.71-10.1	2373.5	2.15	0.56	4.94	0.0	0.0	0.00	0.00	0	0

depth cm	depth gcm^{-2}	mg kg^{-1} Hg	% error Hg	mg kg^{-1} La	% error La	mg kg^{-1} Br	% error Br	mg kg^{-1} Hf	% error Hf	mg kg^{-1} Ce	% error Ce
0-2.0	0.0-0.14	0.112	4.51	0.64	5.31	10.8	4.21	0.260	2.86	2.31	2.32
2.0-4.7	0.14-0.53	0.145	3.05	1.14	5.13	27.5	5.08	0.365	2.21	4.60	2.12
4.7-6.7	0.53-1.01	0.160	3.52	4.27	3.31	44.9	4.43	0.642	2.32	7.70	2.48
6.7-9.1	1.01-1.45	0.184	3.01	5.00	3.34	50.3	4.88	0.570	2.34	8.18	4.32
9.1-12.1	1.45-1.92	0.506	4.29	5.96	3.33	70.4	4.57	0.815	3.74	11.41	2.19
12.1-15.2	1.92-2.54	0.153	5.66	2.98	3.76	23.7	4.54	0.232	2.18	2.12	5.03
15.2-18.4	2.54-3.32	0.016	9.26	3.45	4.82	25.3	4.47	0.946	2.45	5.00	5.48
18.4-21.0	3.32-3.99	0.088	11.16	2.13	3.14	29.6	4.53	0.769	2.36	4.16	6.33
21.0-23.5	3.99-4.52	0.049	15.53	2.37	3.86	28.1	4.56	0.602	3.15	3.90	5.76
23.5-27.5	4.52-4.99	0.000	0.00	1.50	3.03	17.8	4.6	0.517	3.32	2.46	5.51
27.5-30.5	4.99-5.45	0.000	0.00	1.08	4.01	19.7	4.67	0.398	3.65	1.69	5.97
30.5-33.5	5.45-5.95	0.000	0.00	0.68	5.31	14.7	4.77	0.258	3.99	1.10	5.32
33.5-36.7	5.95-6.44	0.000	0.00	0.30	5.84	11.9	4.83	0.193	3.06	1.00	5.58
36.7-39.4	6.44-6.91	0.000	0.00	0.49	5.01	17.8	4.61	0.105	3.12	0.81	5.08
39.4-41.7	6.91-7.34	0.000	0.00	0.42	5.94	24.0	4.48	0.124	5.45	0.90	4.37
41.7-44.2	7.34-7.71	0.000	0.00	0.45	6.19	27.1	4.51	0.235	5.46	2.69	5.32
44.2-48.7	7.71-8.20	0.000	0.00	0.43	6.99	32.3	4.57	0.301	3.13	2.90	5.59
48.7-55.7	8.20-9.71	0.000	0.00	0.40	7.06	16.6	4.11	0.256	8.14	0.94	5.68
55.7-58.4	9.71-10.1	0.000	0.00	0.39	5.65	14.9	4.21	0.316	9.31	0.61	4.91

depth g cm^{-2}	As mg kg^{-1}	% error As	Sb mg kg^{-1}	% error Sb	$^{206}Pb/^{207}Pb$	% error	$^{208}Pb/^{206}Pb$	% error	$^{208}Pb/^{207}Pb$	% error
0.0-0.14	1.99	10.34	0.229	11.23	1.1291	0.35	2.1712	0.26	2.4802	0.32
0.14-0.53	2.13	8.32	0.734	13.38	1.1388	0.42	2.1636	0.32	2.4863	0.26
0.53-1.01	2.04	9.78	1.392	6.46	1.1472	0.31	2.1682	0.20	2.4883	0.28
1.01-1.45	4.25	3.13	3.611	5.25	1.1537	0.26	2.1607	0.33	2.4928	0.26
1.45-1.92	12.29	1.22	4.801	4.87	1.1581	0.32	2.1686	0.22	2.4838	0.15
1.92-2.54	4.70	4.76	0.719	4.99	1.1636	0.33	2.1446	0.37	2.4954	0.10
2.54-3.32	2.52	5.64	0.409	6.90	1.1828	0.29	2.1354	0.14	2.5257	0.38
3.32-3.99	2.59	7.76	0.00	0.00	1.1846	0.49	2.1219	0.37	2.5137	0.28
3.99-4.52	0.00	0.00	0.00	0.00	1.1926	0.14	2.0972	0.24	2.5011	0.26
4.52-4.99	0.00	0.00	0.00	0.00	1.1857	0.44	2.0994	0.40	2.4893	0.56
4.99-5.45	0.00	0.00	0.00	0.00	1.2193	0.43	2.0584	0.10	2.5098	0.41
5.45-5.95	0.00	0.00	0.00	0.00	1.1925	0.51	2.0753	0.25	2.4905	0.51
5.95-6.44	0.00	0.00	0.00	0.00	1.1753	0.54	2.1070	0.40	2.4765	0.62
6.44-6.91	0.00	0.00	0.00	0.00	1.1793	0.45	2.0531	0.32	2.4891	0.38
6.91-7.34	0.00	0.00	0.00	0.00	1.2094	0.77	2.0722	0.44	2.5060	0.78
7.34-7.71	0.00	0.00	0.00	0.00	1.2324	0.52	2.0405	0.33	2.5258	0.64
7.71-8.20	0.00	0.00	0.00	0.00	1.2632	0.57	2.0094	0.29	2.5382	0.44
8.20-9.71	0.00	0.00	0.00	0.00	1.1835	0.36	2.0358	0.42	2.4936	0.45
9.71-10.1	0.00	0.00	0.00	0.00	1.1770	0.42	2.1118	0.40	2.4857	0.49

SOUTH DRUMBOY CORE 4

depth cm	depth gcm^{-2}	mg kg^{-1} Mn	% error Mn	mg kg^{-1} Al	% error Al	mg kg^{-1} Cu	% error Cu	mg kg^{-1} Pb	% error Pb	mg kg^{-1} Fe	% error Fe
0-4.0	0.0-0.09	132.3	2.49	3246.2	4.07	6.3	5.59	37.6	5.50	13273.1	4.07
4.0-8.0	0.09-0.38	192.8	5.25	3343.8	6.31	13.3	7.39	91.6	5.96	8648.4	6.31
8.0-12.0	0.38-0.89	72.0	9.22	3835.0	7.41	14.8	6.61	82.7	5.68	5040.0	7.16
12.0-14.1	0.89-1.67	38.3	6.16	9552.5	1.17	38.3	2.09	287.7	2.84	19578.0	1.17
14.1-17.1	1.67-2.93	39.7	8.93	12239.9	2.96	4.1	5.61	72.9	4.21	26241.8	2.96
17.1-20.1	2.93-4.62	87.9	8.36	18413.7	4.80	5.3	8.69	15.1	2.14	25518.9	3.71
20.1-24.1	4.62-6.89	133.7	1.52	19997.9	3.58	6.8	7.56	11.1	8.04	41971.0	3.55
24.1-27.1	6.89-9.50	126.5	5.22	22219.7	4.57	8.1	8.37	8.7	9.77	54721.8	5.68
27.1-30.1	9.50-12.63	164.5	7.09	20658.7	4.11	8.1	11.63	8.9	9.57	48582.1	4.19
30.1-33.6	12.63-15.72	136.2	6.73	21791.1	3.58	8.3	11.63	11.0	13.21	44185.0	3.38
336.-36.5	15.72-18.07	124.1	2.25	18769.2	4.61	8.4	15.30	9.7	12.33	44597.4	4.12
36.5-39.0	18.07-20.68	114.4	8.73	18390.8	3.30	8.2	10.83	10.3	10.20	42023.0	4.30
39.0-42.7	20.68-23.65	92.4	7.78	18287.7	5.21	8.5	9.11	8.4	18.41	38304.6	4.18
42.7-44.9	23.65-25.43	48.2	7.99	7911.3	4.93	20.0	1.15	212.7	1.60	14485.2	5.86
44.9-48.1	25.43-26.01	32.0	3.15	9481.4	3.52	5.2	15.88	0.0	0.00	11327.1	3.57
48.1-50.3	26.01-26.52	20.1	4.14	8493.6	4.15	5.0	21.87	0.0	0.00	15420.9	5.64
50.3-53.3	26.52-27.00	18.2	2.73	5994.2	12.62	0.0	0.00	0.0	0.00	15884.4	9.62
53.3-56.8	27.00-27.62	28.0	7.52	7542.4	11.04	0.0	0.00	0.0	0.00	18591.9	10.14
56.8-59.1	27.62-28.11	30.8	2.58	5304.2	10.17	0.0	0.00	0.0	0.00	18278.4	8.64
59.1-62.4	28.11-28.50	37.1	2.81	4702.6	9.39	0.0	0.00	0.0	0.00	17747.2	9.18

depth cm	depth gcm^{-2}	mg kg^{-1} Zn	% error Zn	mg kg^{-1} Br	% error Br	mg kg^{-1} Sc	% error Sc	mg kg^{-1} La	% error La
0-4.0	0.0-0.09	45.71	4.01	18.77	1.91	1.91	3.11	4.09	4.51
4.0-8.0	0.09-0.38	60.43	5.78	16.27	1.05	2.65	3.59	1.17	4.87
8.0-12.0	0.38-0.89	42.36	3.41	43.16	2.13	4.47	4.16	6.26	3.33
12.0-14.1	0.89-1.67	27.57	0.52	20.03	2.59	7.02	2.55	15.73	2.02
14.1-17.1	1.67-2.93	26.29	3.99	11.71	2.11	7.60	2.33	19.53	2.25
17.1-20.1	2.93-4.62	26.63	8.06	8.22	3.13	12.73	2.59	24.90	2.19
20.1-24.1	4.62-6.89	29.35	1.85	7.38	2.99	14.39	2.45	31.03	2.35
24.1-27.1	6.89-9.50	71.63	5.78	3.71	3.56	12.08	2.31	28.57	2.44
27.1-30.1	9.50-12.63	50.15	10.37	5.00	4.13	14.67	2.88	33.79	2.43
30.1-33.6	12.63-15.72	42.14	8.45	3.22	4.44	11.90	3.13	28.75	2.21
336.-36.5	15.72-18.07	16.86	11.16	3.06	3.38	10.97	3.16	23.82	1.87
36.5-39.0	18.07-20.68	61.27	16.79	3.03	4.01	13.08	3.22	26.38	1.59
39.0-42.7	20.68-23.65	46.22	30.01	6.25	4.02	11.29	2.87	25.85	1.43
42.7-44.9	23.65-25.43	47.35	17.76	28.60	1.11	3.06	4.12	5.66	3.38
44.9-48.1	25.43-26.01	18.12	8.23	13.36	1.87	7.20	4.25	15.62	4.21
48.1-50.3	26.01-26.52	12.01	0.36	14.23	1.56	6.21	4.36	10.26	4.45
50.3-53.3	26.52-27.00	8.30	26.90	19.35	1.45	5.21	4.27	11.64	3.39
53.3-56.8	27.00-27.62	14.42	7.94	33.31	1.66	4.70	3.97	11.74	3.46
56.8-59.1	27.62-28.11	13.13	4.85	25.36	1.48	2.75	4.08	7.01	4.45
59.1-62.4	28.11-28.50	7.57	25.14	29.61	1.51	2.85	4.55	6.37	4.46

depth cm	depth gcm^{-2}	mg kg^{-1} Hg	% error Hg	mg kg^{-1} Th	% error Th	mg kg^{-1} Sm	% error Sm	mg kg^{-1} Co	% error Co
0-4.0	0.0-0.09	0.25	3.36	0.00	0.00	0.13	3.68	6.65	2.25
4.0-8.0	0.09-0.38	0.02	5.65	0.00	0.00	0.11	3.45	3.17	3.18
8.0-12.0	0.38-0.89	0.03	6.13	0.00	0.00	0.22	3.44	3.85	3.55
12.0-14.1	0.89-1.67	0.05	8.15	0.00	0.00	0.19	3.75	9.38	3.35
14.1-17.1	1.67-2.93	0.05	9.33	0.00	0.00	0.18	4.05	1.73	2.19
17.1-20.1	2.93-4.62	0.16	5.56	0.00	0.00	0.22	4.11	1.99	2.25
20.1-24.1	4.62-6.89	0.17	5.69	0.00	0.00	0.62	4.21	2.65	2.89
24.1-27.1	6.89-9.50	0.10	8.39	10.41	3.33	0.50	4.25	2.29	2.46
27.1-30.1	9.50-12.63	0.07	10.05	16.70	3.61	0.57	4.36	2.52	2.56
30.1-33.6	12.63-15.72	0.10	6.13	9.13	3.58	0.66	4.58	1.85	2.74
336.-36.5	15.72-18.07	0.12	5.46	5.94	3.97	0.51	4.55	1.18	2.58
36.5-39.0	18.07-20.68	0.13	5.58	6.31	4.05	0.49	4.13	1.85	2.98
39.0-42.7	20.68-23.65	0.14	4.35	5.83	4.11	0.46	5.08	1.61	2.96
42.7-44.9	23.65-25.43	0.83	3.32	1.71	4.28	0.18	5.16	13.0	0.87
44.9-48.1	25.43-26.01	0.77	5.13	3.53	4.05	0.20	5.46	6.10	2.49
48.1-50.3	26.01-26.52	0.73	3.13	1.32	4.38	0.22	5.33	5.18	3.69
50.3-53.3	26.52-27.00	0.69	3.35	1.25	4.49	0.27	4.31	5.56	4.35
53.3-56.8	27.00-27.62	0.62	3.69	2.06	4.43	0.28	4.16	2.23	5.97
56.8-59.1	27.62-28.11	0.47	3.46	1.70	5.03	0.29	4.25	1.00	8.63
59.1-62.4	28.11-28.50	0.47	3.47	0.25	9.15	0.36	4.29	1.98	9.36

depth gcm^{-2}	mg kg^{-1} Sb	% error Sb	mg kg^{-1} As	% error As	mg kg^{-1} Se	% error Se	mg kg^{-1} Ce	% error Ce	mg kg^{-1} Ta	% error Ta	mg kg^{-1} Hf	% error Hf
0.0-0.09	0.242	5.38	2.86	4.11	0.13	3.13	3.90	3.56	1.11	5.33	1.73	4.12
0.09-0.38	0.653	4.35	2.13	3.87	1.30	3.58	3.27	3.69	2.90	4.15	1.54	4.55
0.38-0.89	2.379	5.26	7.44	2.13	5.70	3.99	2.40	3.46	4.63	2.89	1.63	4.87
0.89-1.67	2.871	3.37	15.41	1.11	12.11	2.13	3.49	4.13	23.35	2.12	11.56	1.31
1.67-2.93	1.329	6.13	10.00	1.05	14.76	2.25	3.10	5.58	31.02	2.55	17.51	1.68
2.93-4.62	0.116	9.13	6.65	3.13	14.85	2.68	14.42	4.23	33.85	2.68	19.22	1.45
4.62-6.89	0.000	0.00	5.69	3.55	18.74	2.71	15.22	4.28	37.38	3.66	21.59	1.98
6.89-9.50	0.000	0.00	4.32	4.13	12.38	2.89	17.06	3.99	32.28	2.56	16.80	2.64
9.50-12.63	0.000	0.00	3.97	6.46	14.84	2.66	18.40	3.66	38.69	3.89	20.14	2.48
12.63-15.72	0.000	0.00	3.71	9.11	16.24	3.16	14.45	5.69	79.29	3.88	19.64	2.31
15.72-18.07	0.000	0.00	0.00	0.00	14.52	3.55	14.82	6.33	20.13	3.46	18.34	2.46
18.07-20.68	0.000	0.00	0.00	0.00	16.35	3.09	15.43	6.79	20.30	3.51	10.56	2.89
20.68-23.65	0.000	0.00	0.00	0.00	15.12	3.65	13.62	6.12	19.05	3.19	8.76	3.16
23.65-25.43	3.13	2.45	9.89	2.56	5.54	1.77	2.18	3.22	5.15	0.89	2.82	1.11
25.43-26.01	0.000	0.00	0.00	0.00	13.15	2.32	3.16	6.97	5.52	3.69	2.01	3.69
26.01-26.52	0.000	0.00	0.00	0.00	12.93	3.38	5.36	6.32	7.14	4.68	2.00	8.67
26.52-27.00	0.000	0.00	0.00	0.00	11.12	4.19	2.58	7.13	2.21	3.57	1.92	11.56
27.00-27.62	0.000	0.00	0.00	0.00	5.09	4.55	1.13	7.77	0.02	11.35	0.12	13.59
27.62-28.11	0.000	0.00	0.00	0.00	3.23	6.66	0.14	9.79	0.05	14.35	0.09	14.98
28.11-28.50	0.000	0.00	0.00	0.00	0.19	10.25	1.54	10.55	0.06	20.56	0.10	13.87

depth cm	depth gcm^{-2}	$^{206}Pb/^{207}Pb$	%error	$^{208}Pb/^{206}Pb$	%error	$^{208}Pb/^{207}Pb$	%error
0-4.0	0.0-0.09	1.1327	0.42	2.1697	0.26	2.4577	0.57
4.0-8.0	0.09-0.38	1.1324	0.35	2.1781	0.36	2.4664	0.33
8.0-12.0	0.38-0.89	1.1277	0.38	2.1680	0.32	2.4449	0.43
12.0-14.1	0.89-1.67	1.1649	0.30	2.1453	0.28	2.4991	0.18
14.1-17.1	1.67-2.93	1.1579	0.52	2.1454	0.36	2.4841	0.50
17.1-20.1	2.93-4.62	1.1784	0.43	2.1334	0.48	2.5140	0.40
20.1-24.1	4.62-6.89	1.1703	0.21	2.1372	0.22	2.5013	0.33
24.1-27.1	6.89-9.50	1.1814	0.39	2.1279	0.60	2.5138	0.48
27.1-30.1	9.50-12.63	1.1822	0.50	2.1324	0.40	2.5211	0.46
30.1-33.6	12.63-15.72	1.1773	0.27	2.1290	0.17	2.5065	0.21
336.-36.5	15.72-18.07	1.1647	0.48	2.1506	0.18	2.5049	0.41
36.5-39.0	18.07-20.68	1.1794	0.34	2.1412	0.51	2.5119	0.32
39.0-42.7	20.68-23.65	1.1823	0.26	2.1389	0.48	2.4996	0.42
42.7-44.9	23.65-25.43	1.1298	0.27	2.1682	0.34	2.4502	0.58
44.9-48.1	25.43-26.01	1.1483	0.31	2.1508	0.41	2.4782	0.63
48.1-50.3	26.01-26.52	1.1823	0.42	2.1459	0.51	2.4813	0.42
50.3-53.3	26.52-27.00	1.1728	0.33	2.1468	0.33	2.4905	0.32
53.3-56.8	27.00-27.62	1.1778	0.52	2.1411	0.34	2.4998	0.55

SOUTH DRUMBOY CORE 5

depth cm	depth g cm^{-2}	Mn mg kg^{-1}	% error Mn	Al mg kg^{-1}	% error Al	Cu mg kg^{-1}	% error Cu	Pb mg kg^{-1}	% error Pb	Fe mg kg^{-1}	% error Fe
0-4.0	0.0-0.26	29.8	10.05	705.0	13.76	7.94	10.95	88.5	5.5	7312.4	13.76
4.0-6.5	0.26-0.70	9.3	16.43	1145.9	2.19	16.13	4.84	172.9	1.86	5207.9	2.19
6.5-8.7	0.70-1.02	8.4	48.62	1311.2	2.39	12.82	7.72	156.8	2.14	5599.0	2.39
8.7-11.3	1.02-1.40	10.8	2.86	1264.2	1.09	5.36	6.53	98.7	2.31	4720.6	1.09
11.3-13.3	1.40-1.87	10.0	6.41	1551.6	4.61	3.16	9.18	54.7	2.94	4106.1	4.61
13.3-16.2	1.87-2.37	6.5	14.96	1621.6	3.87	1.69	4.14	26.5	8.26	4030.2	3.87
16.2-19.6	2.37-2.98	8.4	10.74	1832.4	6.35	0	0	7.9	14.09	3715.1	6.35
19.6-21.3	2.98-3.54	10.3	2.24	1806.7	3.41	0	0	6.9	21.16	3552.6	3.41
21.3-23.1	3.54-3.92	7.7	22.61	1757.5	5.07	0	0	0.0	0	3955.4	5.07
23.1-24.7	3.92-4.23	12.1	25.67	2370.4	3.48	0	0	0.0	0	3861.9	3.48
24.7-26.7	4.23-4.54	13.9	16.55	2065.6	5.81	0	0	0.0	0	4197.5	5.81
26.7-29.7	4.54-4.97	9.9	21.76	2577.9	9.61	0	0	0.0	0	5914.4	9.61
29.7-32.6	4.97-5.49	19.8	3.28	1771.0	3.48	0	0	0.0	0	5253.1	3.48
32.6-35.5	5.49-6.05	21.2	2.76	1429.3	0.64	0	0	0.0	0	5908.7	0.64
35.5-37.5	6.05-6.53	26.4	3.41	1323.0	0.77	0	0	0.0	0	5815.3	0.77
37.5-39.7	6.53-6.94	23.9	3.34	1299.3	7.72	0	0	0.0	0	6393.8	0.77
39.7-44.4	6.94-7.42	31.7	1.58	1725.7	8.13	0	0	0.0	0	6853.2	0.82
44.4-46.4	7.42-8.46	39.1	1.25	11186.3	3.36	0	0	0.0	0	6587.1	3.36
46.4-50.0	8.46-10.0	61.1	3.87	14915.9	1.05	2.79	6.45	7.4	14.38	6769.3	1.05

depth cm	depth g cm^{-2}	Zn mg kg^{-1}	% error Zn	Br mg kg^{-1}	% error Br	Sc mg kg^{-1}	% error Sc	Co mg kg^{-1}	% error Co	La mg kg^{-1}	% error La
0-4.0	0.0-0.26	47.30	19.23	70.9	0.99	0.69	4.12	3.05	4.51	0.2	3.56
4.0-6.5	0.26-0.70	41.87	3.72	91.9	1.12	1.25	3.02	10.57	2.31	0.47	2.31
6.5-8.7	0.70-1.02	38.15	4.59	55.1	1.15	1.38	3.15	10.51	2.58	0.4	2.58
8.7-11.3	1.02-1.40	38.97	5.03	51.9	1.18	0.5	3.08	3.86	3.69	0.22	3.69
11.3-13.3	1.40-1.87	22.94	5.14	46.3	1.31	0.53	2.11	1.56	5.61	0.24	4.56
13.3-16.2	1.87-2.37	20.35	3.05	46.8	1.75	0.56	2.52	2.65	2.34	0.24	3.96
16.2-19.6	2.37-2.98	17.93	4.85	45.7	1.81	0.6	2.45	0.99	10.08	0.25	5.78
19.6-21.3	2.98-3.54	12.8	5.31	40.5	2.89	0.52	2.64	0	0	0.18	7.51
21.3-23.1	3.54-3.92	11.08	7.58	38.6	2.45	0.36	3.73	0	0	0.14	7.13
23.1-24.7	3.92-4.23	8.61	3.48	39.1	3.18	0.71	2.55	0	0	0.23	6.59
24.7-26.7	4.23-4.54	6.58	26.75	33.4	1.65	0.84	2.65	0	0	0.24	6.67
26.7-29.7	4.54-4.97	3.28	30.55	22.4	5.33	0.93	2.41	0	0	0.21	6.89
29.7-32.6	4.97-5.49	3.51	20.8	21.0	5.13	0.48	2.19	0	0	0.1	8.13
32.6-35.5	5.49-6.05	1.83	20.77	19.0	5.45	0.58	2.03	0	0	0.12	8.25
35.5-37.5	6.05-6.53	3.69	34.21	30.8	5.98	0.96	1.99	0	0	0.11	8.34
37.5-39.7	6.53-6.94	1.25	44.01	20.5	5.12	0.52	2.56	0	0	0.12	8.31
39.7-44.4	6.94-7.42	3.00	12.22	18.8	5.88	0.71	2.31	0	0	0.15	7.59
44.4-46.4	7.42-8.46	5.43	15.12	18.8	5.67	0.72	2.49	0	0	0.21	6.32
46.4-50.0	8.46-10.0	14.5	7.92	13.6	5.91	6.47	2.87	0	0	1.61	2.13

depth cm	depth g cm^{-2}	Sm mg kg^{-1}	% error Sm	Hg mg kg^{-1}	% error Hg	Ta mg kg^{-1}	% error Ta	Th mg kg^{-1}	% error Th	Se mg kg^{-1}	% error Se
0-4.0	0.0-0.26	0.58	4.12	0.19	5.31	0.52	11.89	0.000	0.000	0.1	5.55
4.0-6.5	0.26-0.70	3.4	2.58	0.22	4.68	1.1	12.31	0.094	19.8	0.31	4.48
6.5-8.7	0.70-1.02	2.92	2.99	0.12	8.25	1.1	12.31	0.394	19.8	0.56	4.31
8.7-11.3	1.02-1.40	0.32	6.13	0.10	11.35	0.07	21.58	0.017	22.5	0.02	6.89
11.3-13.3	1.40-1.87	0.19	6.79	0.098	11.58	0.01	17.94	0.009	25.4	0	21.54
13.3-16.2	1.87-2.37	0.1	16.64	0.054	25.31	0.02	18.65	0.000	0.000	0	0
16.2-19.6	2.37-2.98	0	0	0	0	0	0	0.000	0.000	0	0
19.6-21.3	2.98-3.54	0	0	0	0	0	0	0.000	0.000	0	0
21.3-23.1	3.54-3.92	0	0	0	0	0	0	0.000	0.000	0	0
23.1-24.7	3.92-4.23	0	0	0	0	0	0	0.000	0.000	0	0
24.7-26.7	4.23-4.54	0	0	0	0	0	0	0.000	0.000	0	0
26.7-29.7	4.54-4.97	0	0	0	0	0	0	0.000	0.000	0	0
29.7-32.6	4.97-5.49	0	0	0	0	0	0	0.000	0.000	0	0
32.6-35.5	5.49-6.05	0	0	0	0	0	0	0.042	29.3	0	0
35.5-37.5	6.05-6.53	0	0	0	0	0	0	0.060	21.5	0	0
37.5-39.7	6.53-6.94	0	0	0	0	0	0	0.135	18.8	0	0
39.7-44.4	6.94-7.42	0	0	0	0	0	0	0.421	11.2	0	0
44.4-46.4	7.42-8.46	1.04	10.59	0	0	0.1	17.33	0.543	10.0	0.03	9.68
46.4-50.0	8.46-10.0	0.87	12.24	0	0	5.98	7.44	3.18	5.46	9.79	2.18

depth g cm^{-2}	As mg kg^{-1}	% error As	Sb mg kg^{-1}	% error Sb	$^{206}Pb/^{207}Pb$	% error	$^{208}Pb/^{207}Pb$	% error	$^{208}Pb/^{206}Pb$	% error
0.0-0.26	5.49	3.36	0.201	2.15	1.1573	0.22	2.5348	0.30	2.1902	0.14
0.26-0.70	8.16	3.19	0.315	2.08	1.1277	0.14	2.1581	0.29	2.2329	0.27
0.70-1.02	7.11	3.35	0.292	2.69	1.1417	0.31	2.5353	0.30	2.2207	0.19
1.02-1.40	6.89	3.48	0.254	2.54	1.1449	0.49	2.5350	0.19	2.2143	0.46
1.40-1.87	4.79	3.94	0.186	3.13	1.1221	0.17	2.5262	0.25	2.2513	0.27
1.87-2.37	1.46	4.65	0.129	3.38	1.1489	0.46	2.5453	0.23	2.2155	0.28
2.37-2.98	0.88	8.36	0.105	5.19	1.1453	0.30	2.5354	0.13	2.2138	0.36
2.98-3.54	0.00	0.00	0.000	0.000	1.1669	0.55	2.5480	0.60	2.1836	0.54
3.54-3.92	0.00	0.00	0.000	0.000	1.2076	0.42	2.5585	0.34	2.1188	0.16
3.92-4.23	0.00	0.00	0.000	0.000	1.2016	0.38	2.5639	0.29	2.1338	0.53
4.23-4.54	0.00	0.00	0.000	0.000	1.2243	0.30	2.5805	0.19	2.1078	0.41
4.54-4.97	0.00	0.00	0.000	0.000	1.1532	0.48	2.5307	0.46	2.1945	0.50
4.97-5.49	0.00	0.00	0.000	0.000	1.1604	0.36	2.5393	0.20	2.1883	0.41
5.49-6.05	0.00	0.00	0.000	0.000	1.1612	0.36	2.5461	0.26	2.2050	0.62
6.05-6.53	0.00	0.00	0.000	0.000	1.1605	0.40	2.5498	0.36	2.1964	0.32
6.53-6.94	0.00	0.00	0.000	0.000	1.1595	0.59	2.5586	0.37	2.2067	0.53

depth cm	depth g cm^{-2}	Ce mg kg^{-1}	% error Ce	Hf mg kg^{-1}	% error Hf	Th mg kg^{-1}	% error Th
0-4.0	0.0-0.26	0.39	3.58	0.05	7.57	0.035	18.31
4.0-6.5	0.26-0.70	0.77	3.67	0.08	10.08	0.055	19.85
6.5-8.7	0.70-1.02	0.88	3.19	0.22	8.34	0.048	22.45
8.7-11.3	1.02-1.40	0.03	8.19	0	10.12	0.034	19.87
11.3-13.3	1.40-1.87	0	21.22	0	21.96	0.025	25.37
13.3-16.2	1.87-2.37	0	0	0	0	0	0
16.2-19.6	2.37-2.98	0	0	0	0	0	0
19.6-21.3	2.98-3.54	0	0	0	0	0	0
21.3-23.1	3.54-3.92	0	0	0	0	0	0
23.1-24.7	3.92-4.23	0	0	0	0	0	0
24.7-26.7	4.23-4.54	0	0	0	0	0	0
26.7-29.7	4.54-4.97	0	0	0	0	0	0
29.7-32.6	4.97-5.49	0	0	0	0	0	0
32.6-35.5	5.49-6.05	0	0	0	0	0	29.34
35.5-37.5	6.05-6.53	0	0	0	0	0	21.46
37.5-39.7	6.53-6.94	0	0	0	0	0	18.76
39.7-44.4	6.94-7.42	0	0	0	0	0	11.21
44.4-46.4	7.42-8.46	0.03	12.86	0.06	15.18	0.01	9.99
46.4-50.0	8.46-10.0	1.34	8.68	1.22	5.64	0.09	5.46

SOUTH DRUMBOY CORE 6

depth cm	depth g cm^{-2}	Mn mg kg^{-1}	% error Mn	Al mg kg^{-1}	% error Al	Cu mg kg^{-1}	% error Cu	Pb mg kg^{-1}	% error Pb	Zn mg kg^{-1}	% error Zn
0-3.0	0.0-0.30	22.9	5.82	402.0	10.74	4.95	4.55	55.2	7.65	30.1	8.99
3.0-6.5	0.30-0.60	20.6	1.38	682.8	3.36	13.35	1.92	101.0	4.42	35.3	3.97
6.5-9.5	0.60-0.99	18.0	2.33	706.4	6.43	16.81	4.97	120.2	2.79	36.0	2.51
9.5-11.7	0.99-1.23	15.2	4.49	806.7	4.66	21.88	3.04	151.2	7.08	40.7	1.12
11.7-16.1	1.23-1.85	17	6.42	1221.9	16.03	25.41	5.43	215.4	3.98	29.3	1.39
16.1-19.1	1.85-2.27	21.2	5.09	1409.3	5.19	13.57	5.82	164.8	3.04	24.8	9.13
19.1-21.1	2.27-2.55	26.3	7.19	2092.3	1.89	4.73	11.50	76.5	8.17	20.5	11.21
21.1-24.1	2.55-3.13	30.1	7.87	3889.8	4.54	2.16	6.57	40.1	6.16	16.3	6.18
24.1-26.7	3.13-3.84	38.7	6.02	5530.3	3.97	1.76	17.46	24.3	8.63	14.8	8.13
26.7-29.7	3.84-4.77	44.1	4.46	7808.0	2.92	1.10	27.46	16.3	4.56	13.7	20.13
29.7-32.4	4.77-5.77	45.6	2.73	13100.9	7.85	1.26	17.46	17.5	9.63	11.0	21.56
32.4-36.9	5.77-7.22	67.4	8.49	19079.6	5.70	3.77	9.49	14.4	1.95	17.4	13.14

depth cm	depth g cm^{-2}	Fe mg kg^{-1}	% error Fe	Br mg kg^{-1}	% error Br	La mg kg^{-1}	% error La	Sc mg kg^{-1}	% error Sc	Co mg kg^{-1}	% error Co
0-3.0	0.0-0.30	13192.27	10.74	13.56	1.98	1.77	2.32	0.98	11.22	6.80	9.16
3.0-6.5	0.30-0.60	7256.66	3.36	23.68	1.21	1.64	3.58	1.03	9.81	8.91	10.15
6.5-9.5	0.60-0.99	5813.79	6.43	31.14	1.25	2.83	3.64	1.28	5.34	11.22	8.68
9.5-11.7	0.99-1.23	6000.69	4.66	38.67	1.68	2.93	3.13	1.55	8.19	12.87	9.79
11.7-16.1	1.23-1.85	6113.45	6.03	32.56	1.88	2.33	6.31	1.52	6.68	13.27	8.64
16.1-19.1	1.85-2.27	6107.43	5.19	30.84	2.15	2.14	3.58	1.35	7.31	11.77	7.46
19.1-21.1	2.27-2.55	8573.72	1.89	29.56	1.88	2.96	5.44	1.11	6.15	6.57	7.15
21.1-24.1	2.55-3.13	10213.31	4.54	28.48	2.25	8.85	6.68	2.35	5.97	2.14	16.97
24.1-26.7	3.13-3.84	14787.41	3.97	21.19	2.35	6.55	3.12	3.62	5.13	0.99	26.69
26.7-29.7	3.84-4.77	11984.28	2.92	14.05	3.67	14.94	3.08	5.58	4.99	0.00	0.00
29.7-32.4	4.77-5.77	10759.33	7.85	11.90	3.89	20.18	3.35	8.66	4.13	0.00	0.00
32.4-36.9	5.77-7.22	11113.84	5.70	11.41	4.12	25.86	2.02	11.54	4.08	0.00	0.00

depth cm	depth g cm^{-2}	As mg kg^{-1}	% error As	Sm mg kg^{-1}	% error Sm	Hg mg kg^{-1}	% error Hg	Ta mg kg^{-1}	% error Ta	Se mg kg^{-1}	% error Se
0-3.0	0.0-0.30	3.39	3.21	1.13	5.13	0.075	8.67	0.50	11.67	0.026	14.31
3.0-6.5	0.30-0.60	3.51	3.55	1.32	4.98	0.15	8.16	0.72	14.34	0.034	14.02
6.5-9.5	0.60-0.99	3.55	4.31	1.42	6.13	0.17	8.45	0.88	11.59	0.041	12.28
9.5-11.7	0.99-1.23	3.96	4.58	2.06	5.88	0.19	7.12	0.27	10.35	0.058	10.58
11.7-16.1	1.23-1.85	4.37	3.56	1.21	8.16	0.25	6.68	0.20	12.89	0.012	15.64
16.1-19.1	1.85-2.27	3.35	3.57	0.96	19.05	0.18	6.97	0.15	12.12	0.010	15.83
19.1-21.1	2.27-2.55	3.18	2.89	0.82	17.33	0.11	17.59	0.13	13.38	0.009	16.22
21.1-24.1	2.55-3.13	2.59	2.12	0.83	16.89	0.076	15.35	0.24	13.05	0.017	16.19
24.1-26.7	3.13-3.84	1.86	4.35	0.49	19.33	0.045	36.22	0.36	14.18	0.021	16.08
26.7-29.7	3.84-4.77	1.53	4.67	1.08	12.15	0.000	0.00	1.05	6.67	0.19	6.38
29.7-32.4	4.77-5.77	1.59	5.18	2.07	7.13	0.000	0.00	2.06	6.34	1.45	5.46
32.4-36.9	5.77-7.22	1.22	5.88	3.35	6.69	0.000	0.00	3.34	6.28	4.35	5.18

depth cm	depth g cm^{-2}	Sb mg kg^{-1}	% error Sb	$^{208}Pb/^{206}Pb$	% error	$^{208}Pb/^{207}Pb$	% error	$^{206}Pb/^{207}Pb$	% error
0-3.0	0.0-0.30	0.68	3.16	2.1604	0.62	2.4182	0.34	1.1194	0.62
3.0-6.5	0.30-0.60	0.89	4.15	2.1448	0.50	2.4123	0.39	1.1240	0.35
6.5-9.5	0.60-0.99	1.23	2.89	2.1346	0.86	2.4170	0.23	1.1323	0.83
9.5-11.7	0.99-1.23	2.87	3.79	2.1332	0.58	2.4424	0.18	1.1450	0.48
11.7-16.1	1.23-1.85	3.27	2.64	2.1227	0.46	2.4662	0.20	1.1618	0.55
16.1-19.1	1.85-2.27	1.77	4.15	2.1226	0.47	2.4732	0.15	1.1652	0.39
19.1-21.1	2.27-2.55	0.66	7.15	2.0747	0.53	2.4639	0.19	1.1876	0.43
21.1-24.1	2.55-3.13	0.21	9.98	2.0961	0.58	2.4355	0.58	1.1620	0.50
24.1-26.7	3.13-3.84	0.09	10.97	2.1090	0.80	2.4726	0.25	1.1725	0.73
26.7-29.7	3.84-4.77	0.00	0.00	2.1089	0.55	2.4891	0.30	1.1803	0.51
29.7-32.4	4.77-5.77	0.00	0.00	2.1153	0.74	2.4855	0.21	1.1751	0.84
32.4-36.9	5.77-7.22	0.00	0.00	2.1060	0.76	2.4965	0.17	1.1855	0.74

depth cm	depth g cm^{-2}	Ce mg kg^{-1}	% error Ce	Hf mg kg^{-1}	% error Hf	Th mg kg^{-1}	% error Th
0-3.0	0.0-0.30	0.15	14.39	0.22	8.36	0.00	0.00
3.0-6.5	0.30-0.60	0.15	15.88	0.31	5.51	0.00	0.00
6.5-9.5	0.60-0.99	0.16	17.78	0.50	10.05	0.00	0.00
9.5-11.7	0.99-1.23	0.57	8.14	0.10	8.42	0.00	0.00
11.7-16.1	1.23-1.85	0.28	7.35	0.10	11.31	0.00	0.00
16.1-19.1	1.85-2.27	0.08	10.08	0.05	11.89	0.00	0.00
19.1-21.1	2.27-2.55	0.09	10.35	0.03	13.05	0.00	0.00
21.1-24.1	2.55-3.13	0.85	10.18	0.06	13.37	0.00	0.00
24.1-26.7	3.13-3.84	0.55	15.34	0.07	13.59	0.02	18.34
26.7-29.7	3.84-4.77	0.98	7.78	0.29	12.68	0.02	17.43
29.7-32.4	4.77-5.77	2.12	5.13	0.91	11.07	0.03	19.34
32.4-36.9	5.77-7.22	5.96	4.87	1.11	12.13	0.32	12.25